Design and Synthesis of Functionally Selective Kappa Opioid Receptor Ligands

By

Stephanie Nicole Johnson

Submitted to the graduate degree program in Medicinal Chemistry and the Graduate Faculty of the University of Kansas in partial fulfillment of the requirements for the degree of Masters in Science.

_____

Chairperson: Dr. Thomas E. Prisinzano

_____

Dr. Apurba Dutta

_____

Dr. Jeffrey P. Krise

Date Defended: May 2, 2017

The Thesis Committee for Stephanie Nicole Johnson

certifies that this is the approved version of the following thesis:

Design and Synthesis of Functionally Selective Kappa Opioid Receptor Ligands

_____

Chairperson: Dr. Thomas E. Prisinzano

Date approved: May 4, 2017

Abstract

The ability of ligands to differentially regulate the activity of signaling pathways coupled to a receptor potentially enables researchers to optimize therapeutically relevant efficacies, while minimizing activity at pathways that lead to adverse effects. Recent studies have demonstrated the functional selectivity of kappa opioid receptor (KOR) ligands acting at KOR expressed by rat peripheral pain sensing neurons. In addition, KOR signaling leading to antinociception and dysphoria occur via different pathways. Based on this information, it can be hypothesized that a functionally selective KOR agonist would allow researchers to optimize signaling pathways leading to antinociception while simultaneously minimizing activity towards pathways that result in dysphoria.

In this study, our goal was to alter the structure of U50,488 such that efficacy was maintained for signaling pathways important for antinociception (inhibition of cAMP accumulation) and minimized for signaling pathways that reduce antinociception. Thus, several compounds based on the U50,488 scaffold were designed, synthesized, and evaluated at KORs. Selected analogues were further evaluated for inhibition of cAMP accumulation, activation of extracellular signal-regulated kinase (ERK), and inhibition of calcitonin gene-related peptide release (CGRP).

The data obtained demonstrates that modification of the structure of U50,488 changed the signaling pathway regulation. Specifically, we identified three functionally selective KOR ligands **(4b, 9u,** and **9ac)** that inhibit cAMP accumulation, similar to U50,488, but, unlike U50,488, do not activate ERK. In addition, the ability to inhibit CGRP release showed monotonic concentration-response curves, indicating that a pathway leading to nociception is not activated. These data suggest that the efficacy for specific signaling pathways can be finely tuned by structural modifications to a given ligand.

Table of Contents

Abstract **iii**
Table of Contents **iv**
List of Figures **v**
List of Schemes **vi**
List of Tables **vii**
I. Background **1**
Historical Aspects of Opioids **1**
Identification of the Opioid Receptors **2**
G-Protein Coupled Receptors **5**
Receptor Pharmacology Towards the Theory of Functional Selectivity **6**
Functional Selectivity of the Kappa Opioid Receptor **11**
U50,488 as a Probe to Identify Functionally Selective KOR Ligands **14**
References **18**
II. Rationale and Specific Aims **39**
References **42**
III. Results and Discussion **45**
Specific Aim #1: Design, Synthesis, and Evaluation of KOR Activity of U50,488 Analogues **45**
Synthesis of Proposed U50,488 Analogues **49**
Analogues with Modification to the Pyrrolidine Group **49**
Homologation of the *N*-Alkyl Group of U50,488 **50**
Modification to the Aromatic Group and Linker Region **51**
Analogues with Modifications to the Cyclohexane Ring **52**
In Vitro Evaluation of the KOR Activity of Analogues **53**
Specific Aim #2: *Ex Vivo* Measurements of Signal Pathway-Dependent Efficacy **56**
Specific Aim #3: *Ex Vivo* Measurement of CGRP Release **58**
Synthesis and *In Vitro* Analysis of Enantiopure Analogues **59**
Summary of Results **62**
References **63**
IV. Conclusions **65**
V. Experimental Data **70**
References **87**
Appendix A: ^{1}H and ^{13}C NMR Spectra **88**
Appendix B: HPLC Chromatograms/Chiral HPLC Chromatograms **244**

List of Figures

Figure 1.1. Structures of the main alkaloids found in opium. **1**

Figure 1.2. Structure of heroin. **2**

Figure 1.3. Amino acid sequences of the endogenous opioid peptides. **3**

Figure 1.4. Structures of prototypical opioid ligands. **3**

Figure 1.5. Structures of the five most commonly prescribed narcotics. **4**

Figure 1.6. Depiction of a prototypical 7-transmembrane receptor. **5**

Figure 1.7. Depiction of GCPR signaling. **6**

Figure 1.8. Representation of receptors as molecular switches. **7**

Figure 1.9. Representation of the two-state model of receptor activation. **7**

Figure 1.10. Responses of various types of ligands. **8**

Figure 1.11. Diverse functional consequences of two different ligands mediated via a single receptor. **9**

Figure 1.12. Salvinorin A and its analogues which differentially regulate signaling pathways. **12**

Figure 1.13. KOR agonists which differentially regulate signaling pathways. **13**

Figure 1.14. Summary of U50,488 analgesic SARs. **14**

Figure 1.15. Dose response curves for U50,488 inhibition of PGE_2-induced thermal allodynia in the rat hindpaw. **15**

Figure 1.16. Inhibition of PGE_2-stimulated cAMP accumulation by U50,488 and salvinorin A. **15**

Figure 1.17. Activation of ERK and JNK by U50,488 in primary cultures of peripheral sensory neurons. **16**

Figure 1.18. The descending limb of the dose-response curve for U50,488 and salvinorin A in primary cultures of peripheral sensory neurons. **17**

Figure 2.1. Structure of U50,488. **39**

Figure 3.1. Proposed analogues with modifications to the pyrrolidine. **45**

Figure 3.2. Proposed analogues with modifications to the *N*-alkyl group. **46**

Figure 3.3. Proposed analogues with modified aryl groups. **47**

Figure 3.4. Proposed analogues with modifications to the linker region. **48**

Figure 3.5. Proposed analogues with modifications to the cyclohexane ring. **49**

Figure 3.6. Depiction of the GPCR signaling pathway of the DiscoveRx cAMP functional assay. **53**

Figure 3.7. KOR ligands that were evaluated *ex vivo.* **57**

Figure 3.8. Inhibition of cAMP accumulation for KOR analogues. **57**

Figure 3.9. ERK phosphorylation of select KOR ligands. **58**

Figure 3.10. Inhibition of GCRP release for select U50,488 analogues. **58**

Figure 3.11. Proposed enantiopure analogues. **59**

List of Schemes

Scheme 3.1. Synthesis of U50,488 analogues with substituted pyrrolidine group. **49**

Scheme 3.2. Synthesis of U50,488 analogues with modified *N*-alkyl substituents. **50**

Scheme 3.3. Synthesis of U50,488 analogues with modified aryl groups and modified linker regions. **51**

Scheme 3.4. Synthesis of analogue with aromatic core. **52**

Scheme 3.5. Synthesis of analogue with ethylene core. **52**

Scheme 3.6. Synthesis of analogues with a 1-phenethyl core. **52**

Scheme 3.7. Synthesis of enantiopure analogues. **60**

List of Tables

Table 3.1. KOR activity of analogues with one region of U50,488 is modified. **53**

Table 3.2. KOR activity of enantiopure analogues. **61**

I. Background

Historical Aspects of Opioids

Opium, or poppy tears, refers to the dried latex produced by the opium poppy, *Papaver somniferum*.[1] This particular strain is the evolution of centuries of cultivation and breeding that originated with a wild strain, *Papaver setigerum*.[1] Today, *Papaver somniferum* is the only species used to produce opium.[1] Carbon-14 dating indicates that the opium poppy has been used since as early as 4200 BC.[1] The earliest findings of cultivation of opium dates back to 3400 BC in Mesopotamia.[2-4] There, Sumerians referred to the poppy as *Hul Gil*, which translates to the "joy plant".[1-3,5] Eventually, use of the poppy to treat pain and other ailments spread to every major civilization in ancient Europe and Asia.[2,5-8]

Western medicine continued to uncover the positive potential of opium.[9] In spite of the addictive nature, there was no better substitute to opium, and its use prevailed.[9] During the 19th century, the use of analgesics transitioned from opium to opioids with gradually stronger effects.[2] Specifically, there are four main alkaloids in opium, as follows: morphine, codeine, thebaine, and papaverine[5] **(Figure 1.1)**. In 1803, Sir William Seturner isolated and

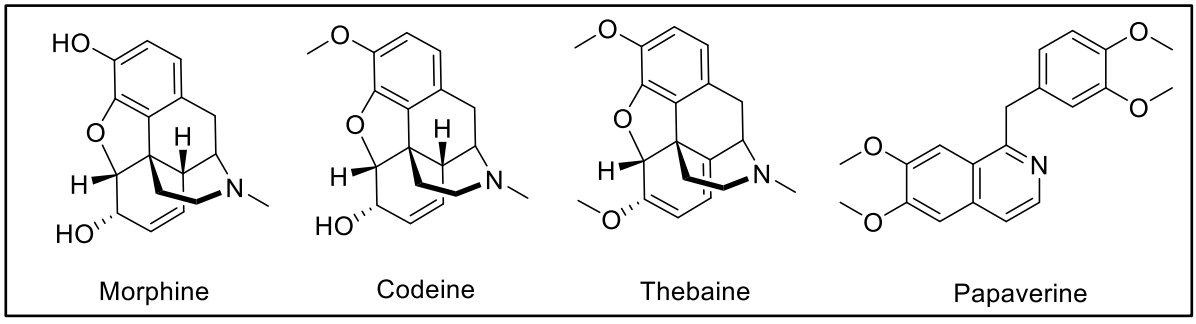

Figure 1.1. Structures of the main alkaloids found in opium.

identified the alkaloid morphine, named after Morpheus, the Greek god of dreams.[2-4] Shortly following, Pierre Robiquet isolated codeine in 1832,[10] Thiboumery and Pelletier identified thebaine in 1835,[11] and Merck extracted papaverine in 1848.[12] Successful isolations of these opiates paved the way for chemists who would improve upon these compounds.[2]

In 1874, C. R. Alder Wright synthesized the earliest opiate, diacetylmorphine, more commonly known as heroin **(Figure 1.2)**.[13] The hypothesis was that by acetylating morphine, they would produce a drug like codeine, which is pharmacologically similar to morphine, but less potent and less addictive.[14] Bayer Pharmaceutical Company then started the production of heroin in 1898 on a commercial scale.[14] Bayer named the drug "heroin", based on the German *heroisch*, which means "heroic", and proclaimed that this new compound had less habit-forming potential than morphine.[14] From 1898 to 1920, the drug was erroneously marketed as a non-addictive substitute for morphine.[14] By the 1920s, however, evidence of heroin's risks prompted recall of the drug.[13] The failure of this "heroic" drug to cure morphine addiction instigated the search for non-addictive opioids.[2]

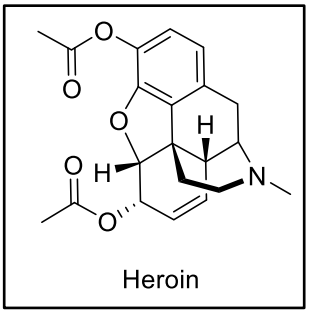

Figure 1.2. Structure of heroin.

Identification of the Opioid Receptors

Although morphine had been used as a potent analgesic since its isolation by Seturner, the idea of opioid receptor was not proposed until 1954 when Beckett and Casy suggested, based on their structure-activity relationships (SAR) for antinociceptive activity, that a specific receptor for opiate drugs must exist.[15] In order to prove this theory, Goldstein *et al.*[16] suggested that radiolabeled drugs would demonstrate the existence of multiple receptors and allow for their characterization. Unfortunately, their efforts failed because they did not have radioligands with high specific activities.[16] In 1973, however, Pert and Snyder,[17] Simon *et al.*,[18] and Terenius[19] succeeded almost simultaneously in showing that there are stereospecific opiate binding sites in the central nervous system. Opioid receptors were found to have a nonuniform distribution, suggesting that these receptors might be the targets of endogenous peptides.[3] Shortly thereafter, several endogenous peptides were discovered with high affinity

for brain opioid receptors: the enkephalins,[20] β-endorphin,[21] and dynorphin,[22] as depicted in **Figure 1. 3**.

Leu-Enkephalin	Tyr-Gly-Gly-Phe-Leu
Met-Enkephalin	Tyr-Gly-Gly-Phe-Met
β-Endorphin	Tyr-Gly-Gly-Phe-Met-Thr-Ser-Glu-Lys-Ser-Gln-Thr-Pro-Leu-Val-Thr-Leu-Phe-Lys-Asn-Ala-Ile-Ile-Lys-Asn-Ala-Tyr-Lys-Lys-Gly-Glu
Dynorphin A	Tyr-Gly-Gly-Phe-Leu-Arg-Arg-Ile-Arg-Pro-Lys-Leu-Lys-Trp-Asp-Asn-Gln

Figure 1.3. Amino acid sequences of the endogenous opioid peptides.

By the mid-1960s, it was becoming apparent that opiate drugs were likely to exert their actions at specific receptor sites, and that there were likely to be multiple such sites.[3] The first conclusive evidence for multiple opioid receptors was provided in 1976 by Martin et al.[22] Specifically, researchers analyzed the neurophysiological and behavioral properties of several opiate compounds and looked for "cross tolerance" (i.e. the ability of a drug to prevent withdrawal symptoms after removal of the second drug from an animal tolerant to it). The results of these experiments suggested the existence of three types of receptors. Specifically, the opioid receptor subtypes are as follows: the δ (delta) receptor, named after the mouse vas deferens tissue preparation (the prototypical agonist for this receptor is *N*-allylnormetazocine);[23] the μ (mu) receptor, named after its well-known agonist, morphine; and κ (kappa), named after ketocyclazocine, the agonist first used to characterize it.[24-25] The structures of the prototypical agonists for the delta and kappa receptors are shown in **Figure 1.4**.

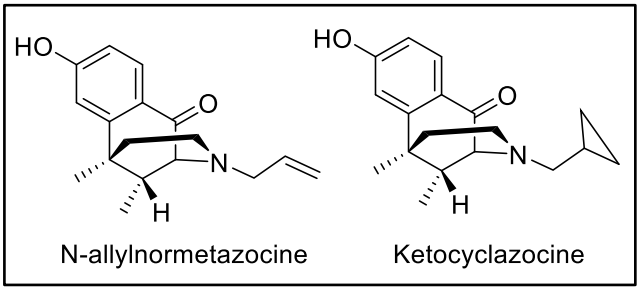

Figure 1.4. Structures of prototypical opioid ligands.

The functional roles each of the receptor subtypes will be described herein. To begin, the delta opioid receptor (DOR) mediates the analgesic effects of delta agonists.[26] It also plays a role in gastrointestinal motility, mood and behavior, as well as cardiovascular regulation.[26]

Of the three opioid receptor families, the mu opioid receptor (MOR) subtype is the most extensively studied.[15-19] Morphine alkaloids and many of their synthetic derivatives are selective agonists at the MOR.[26] The most commonly used narcotic agents include morphine, codeine, hydrocodone, oxycodone, and fentanyl,[27] the structures of which are shown in **Figure 1.5**. These compounds are some of the most potent analgesics used in the clinic.[27]

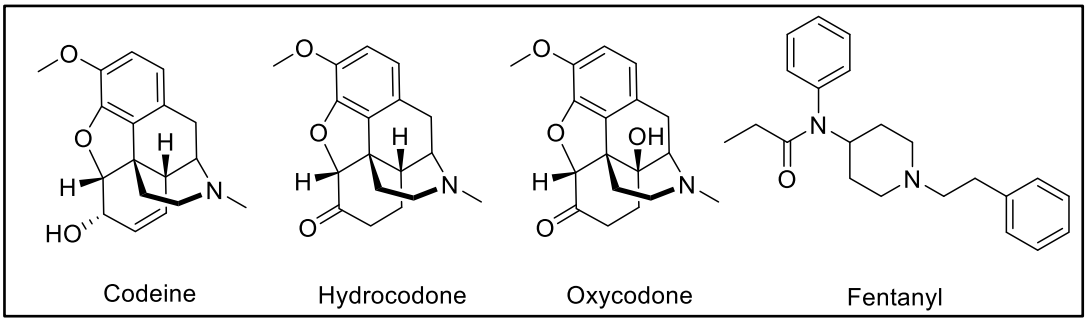

Figure 1.5. Structures of the five most commonly prescribed narcotics.

While they are a popular choice for the treatment of severe pain, unfortunately they have several dose-limiting side effects, including respiratory depression, constipation, tolerance, and dependence.[28] Thus, when the kappa opioid receptor (KOR) subtype was first distinguished, there was tremendous interest in developing analgesics that would provide pain relief without activating the reward pathways stimulated by morphine-like mu opioids.[29-44] A non-addictive opioid has been a holy grail of medicinal chemistry ever since morphine was first isolated from opium in 1804.[27] Selective kappa agonists were developed and were shown to reduce the rewarding effect of co-administered addictive drugs and lack many of the dose-limiting side effects of current opioid analgesics.[28,44] However, these drugs were quickly found to produce different problems, including dysphoria, diuresis, and constipation.[28]

Although pharmacological differences amongst the opioid receptor subtypes have been described since the early 1970s, the subtypes were not cloned and purified until the 1990s. The first opioid receptor to be cloned was the DOR.[45-46] This was accomplished simultaneously and independently by Keiffer *et al.*[45] and Evans *et al.*[46] Shortly after, the KOR

was isolated and cloned by Meng *et al.*[47] and the MOR was cloned by Wang *et al.*[48] The data confirmed what scientists already believed, that opioid receptors are in fact members of the G protein-coupled receptor (GPCR) family.[45-48]

G-Protein Coupled Receptors (GPCRs)

All of the opioid ligands exert their effects via the opioid receptors, which are GPCRs.[3] GPCRs are seven-transmembrane cell surface receptors which are responsible for regulating a variety of physiological events.[49] Specifically, GPCRs are the largest and most diverse family of cell surface receptors.[50] It is estimated that 50% of the currently marketed drugs directly target GPCRs or their downstream effectors.[49] GPCRs share a common structure composed of seven hydrophobic transmembrane segments with an extracellular amino acid terminus and an intracellular carboxyl terminus **(Figure 1.6)**.[50] Although there is variation regarding the structure of GPCRs, there are two main requirements for classification. First of all, the protein must have seven sequence stretches of about 25 to 35 consecutive residues that have a high degree of hydrophobicity.[49] These sequences represent the seven α-helices that span the plasma membrane in a counter-clockwise manner, which enable an extracellular ligand to exert a specific effect.[49] Secondly, the receptor must be able to interact with a G-protein.[49] The portions of a GPCR with the greatest variation are the carboxyl terminus, the intracellular loops, and the amino terminus.[51] In contrast to the structural and functional similarity of GPCRs, GPCR ligands have tremendous variation, which include subatomic particles (photons), ions, small organic molecules, lipids, nucleotides, peptides,

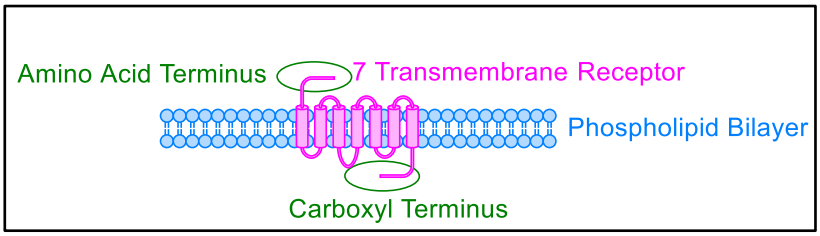

Figure 1.6. Depiction of a prototypical 7-transmembrane receptor.

and proteins.[49]

Despite the variations in the receptors and ligands, the cellular signaling of GPCRs is largely conserved.[52] A representative depiction of GPCR signaling is shown in **Figure 1.7**. Upon activation by a ligand, the GPCR will undergo a conformational change which activates an associated G protein by exchanging GDP for GTP.[52] This leads to dissociation of the αβγ-complex into the α subunit with the bound GTP and the βγ subunit.[52] Both of these moieties then become free to act upon their downstream effectors and thereby initiate unique intracellular signaling responses.[52] Thus, science has demonstrated that GPCRs are a large, versatile class of plasma membrane receptors.[49-52] However, despite their central role in biomedical research, scientists are still gaining insight into the mechanistic details underlying receptor activation.[52-54]

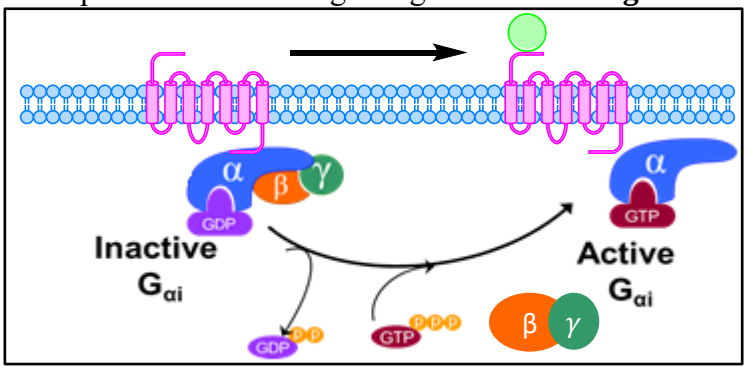

Figure 1.7. Depiction of GPCR signaling.

Receptor Pharmacology Towards the Theory of Functional Selectivity

The concept of drug receptors began as an abstract idea, which then led to models that considered receptors as pharmacological switches, which laid the foundation for the more mechanistically driven models of receptors in use today.[53-54] At the turn of the 20th century, different groups postulated the existence of control points on cells that responded to chemicals.[55] Historically, scientists believed that GPCRs acted as molecular switches, which posited that GCPRs could exist in two different conformations: the inactive state, functionally and physically uncoupled from the G protein and the active state which was associated with a G protein, resulting in its activation **(Figure 1.8)**.[55-56] A.J. Clark, who is largely considered

the father of modern receptor pharmacology, was the first to suggest that a unimolecular

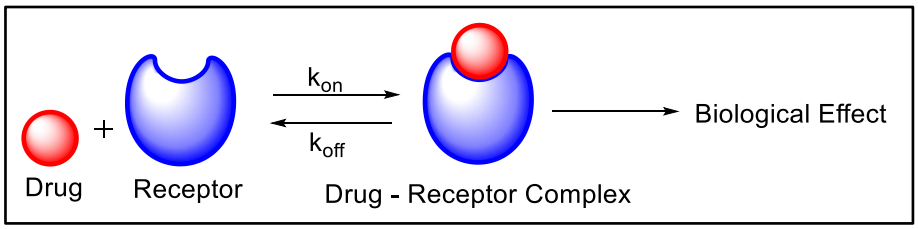

Figure 1.8. Representation of receptors as molecular switches.

interaction occurs between a drug and a substance on the cell.[57] Extending this theory, R. P. Stephenson postulated the existence of a theoretical parameter called "stimulus" when he observed different potencies for compounds that had similar receptor affinities.[58] This concept of efficacy allowed for powerful agonists that could produce maximal tissue response by activating only a portion of the available receptors; the remaining portion being referred to as "spare".[58] However, upon discovering that an agonist is not necessarily required to toggle receptors, this theory was replaced by a more complex model that accounts for multiple conformations assumed by the receptor.[59] This model, referred to as the two-state model of GPCR activation was developed in the mid-1990s.[60] In this paradigm, GPCRs isomerize between an inactive (R) state and an active (R*) state, as shown in **Figure 1.9**.[59] The affinity of the agonist for each of the two states is governed by the dissociation equilibrium constants, K_A and K_{A^*}.[59] This contrasts with the

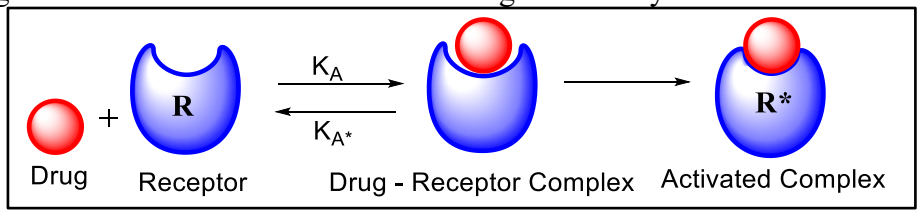

Figure 1.9. Representation of the two-state model of receptor activation.

aforementioned receptor theory which defines agonist affinity by a single constant.[58] In addition, the efficacy of an agonist is dependent on K_A and K_{A^*}, which allows for determination of the degree to which an agonist displaces receptors towards the active state.[59] This concept is referred to as "intrinsic efficacy" and can be described as a measure of the stimulus per receptor molecule produced by a ligand.[61] This concept has led to the

classification of receptor ligands as full agonists, partial agonists, antagonists, or inverse agonists, as depicted in **Figure 1.10**.[61] According to this notion, full agonists possess sufficiently high intrinsic efficacy, such that they maximally stimulate all cellular responses linked to a given receptor.[61] Partial agonists possess lower degrees of intrinsic efficacy leading to submaximal responses.[61] Antagonists possess no intrinsic efficacy, but occupy the receptor to block the effects of agonists.[61] This idea has also lead to the assumption in pharmacology that the ability of the ligand to impart stimulus once that ligand is bound to the receptor is an inherent property of the ligand-receptor complex.[61] Therefore, a full agonist would be expected to activate all of the signaling pathways linked to a receptor to the same degree as the endogenous ligand for that receptor.[61]

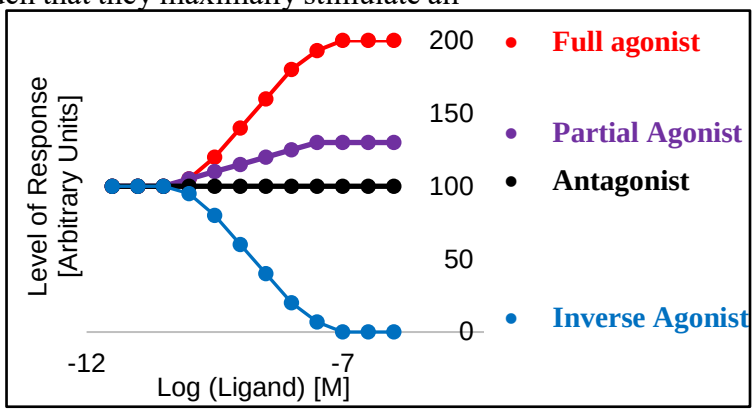

Figure 1.10. Responses of various types of ligands.

The notion that intrinsic efficacy is system-independent forms a major underlying premise in drug discovery today – that the pharmacological characteristics of a drug tested in an experimental model system can be extrapolated to all systems.[61] In the past decade, however, data has emerged in which certain ligands were shown to have quite diverse functional consequences mediated via a single receptor.[61] At first, these observations were simply dismissed as artifacts. However, as more data has been amassed, it is becoming clear that "intrinsic efficacy" as a system-independent constant, is probably not correct.[61] Thus, in order to rationalize these observations, the concept of functional selectivity was introduced.

Functional selectivity, also known as biased agonism, is the ability of ligands to differentially regulate the activity of specific signaling pathways coupled to a receptor.[62] As shown in **Figure 1.11**, two drugs (represented as A and B) bind to the same receptor, yet have different efficacies for various pathways (efficacy for a particular pathway represented by the size of the arrow). As depicted below, Drug A is more efficacious for PLA_2 and ERK than for activation of PLC and B-arr. On the other hand, Drug B has greater efficacy for PLC and β-arr. and produces less activation of ERK and PLA_2. Essentially, the hypothesis is that

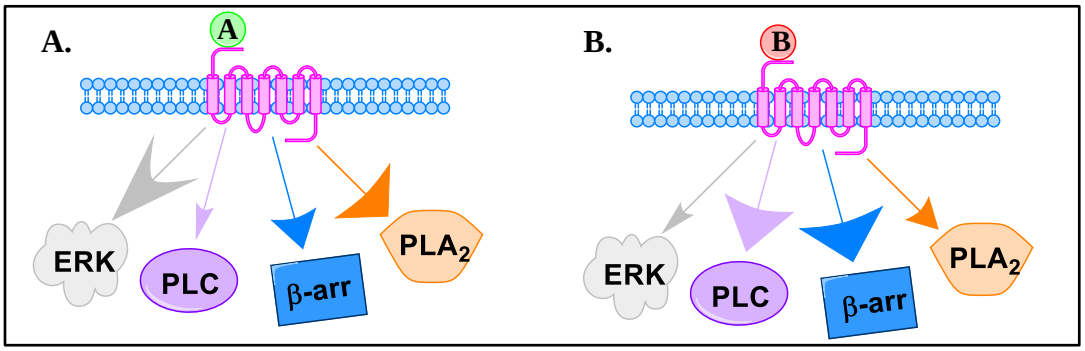

Figure 1.11. Diverse functional consequences of two different ligands mediated via a single receptor. Efficacy is represented by the size of the arrow. **A.** Drug A is more efficacious for PLA_2 and ERK, than for PLC and β-Arr. **B.** Drug B acts at the same receptor, but has greater efficacy towards PLC and β-Arr, than for PLA_2 and ERK.

ligands induce unique, ligand-specific receptor conformations that result in differential activation of signal transduction pathways associated with a particular receptor.[62] This differential activation may be expressed as differences in intrinsic activity at one signaling pathways versus another that are not due to differences in affinity at the mediating receptor.[62]

Two of the earliest studies reporting biased signaling showed that the capacities of agonists bound to α-2 adrenergic (α_2AR)[63] and cannabinoid receptors[64] preferentially couple to $G_{\alpha s}$ or $G_{\alpha i}$, which leads to different efficacies for cyclic AMP (cAMP) production. Subsequently, studies showed that different pathways can be triggered following activation of a single α_2AR subtype with the same type of ligand.[65] In addition, research regarding the β_2-adrenergic receptor (β_2AR) showed that G proteins also play a role in functional selectivity, possibly by inducing specific conformations of GPCRs to which they are

coupled.[66] These studies reiterated the significance of GPCRs, namely that they can be considered "modular" entities that are capable of responding to distinct ligands with specific signaling outcomes depending on their specific sets of partners.[55,67-68]

Today, there is a plethora of observations of functional selectivity including, but not limited to the following: Angiotensin II type I A receptors,[69-70] 5-HT_2 serotonin receptors,[71-76] mu opioid receptors,[77-79] β_2-adrenergic receptors,[80-83] V2 vasopressin receptors [84-86] D_{2L} and D_1 dopamine receptors,[87-98] and of particular interest, kappa opioid receptors (KORs).[29,99,100]

In order to highlight the potential implications of functional selectivity in drug design, angiotensin II Type 1A (AT_1) receptors will briefly be examined. Ligands that target AT_1 receptors are one of the most well understood classes of functionally selective ligands.[69-70,101-103] These receptors play a key role in cardiovascular and renal regulation of blood pressure, along with a spectrum of other conditions, including endothelial dysfunction and atheroma, cardiac hypertrophy, atrial fibrillation, nephropathy, insulin resistance, and cancer.[70,102] Clinically, these molecules are especially interesting due to their multi-functionality. Ligands that target AT_1 receptors function via two main signaling pathways: (a) the canonical G protein-dependent activation and (b) the G protein-independent recruitment of β-arrestin-scaffolded signaling complexes.[102,104-105] The G-protein mediated pathways have been shown to be deleterious by leading to increased myocyte size, apoptosis, and heart failure.[104-105] The G-protein independent pathways that involve recruitment of β-arrestin, however, have been shown to promote cardioprotective signaling in response to stress.[69,104-111] Many of the angiotensin-receptor blockers (ARBs) approved to treat heart failure block both G-protein and β-arrestin signaling.[69,101-103] Fortunately, in 2002, a synthetically generated biased ligand known as SII (Sar1, Ile4, Ile8) was shown to be functionally selective in that it recruits β-arrestin without inducing any G protein activity.[112-114] *In vivo* treatment confirms that SII is

able to selectively antagonize harmful cardiac signaling while simultaneous potentiating beneficial pathways.[115-116] Thus, SII is currently considered the gold-standard β-arrestin-biased AT_1 analog.[117]

Although the concept of functional selectivity has not been largely incorporated in the pharmaceutical industry, the implications are extensive.[62] Functional selectivity potentially enables researchers to optimize therapeutically relevant efficacies, while minimizing activity at pathways that lead to adverse effects.

Functional Selectivity of the Kappa Opioid Receptor

The therapeutic promise of kappa agonists in the treatment of pain has recently revived by studies showing that KORs exist as dynamic, multi-conformational protein complexes that can be directed by specific ligands towards distinct signaling pathways.[62] In 2007, Chavkin *et al.*[118] began experiments that would help them understand how c-Jun-*N*-terminal kinase (JNK) activation by certain KOR ligands disrupts KOR signaling. They found that the long duration of action of certain KOR antagonists was not a result of KOR downregulation, but rather that these ligands were exerting their effects via activation of JNK.[62,118] Based on this information, they proposed that low-efficacy ligands that bind to the KOR without activating JNK may be short-acting antagonists.[62,118] In 2010, Chavkin *et al.*[119] published their results, which showed that the KOR demonstrates ligand-directed selectivity.[62,119] Specifically, their study shows that the dysphoric effects require activation of G-protein receptor kinase, arrestin recruitment, and subsequent p38 mitogen activated protein kinase (MAPK) activation, whereas their analgesic effects do not.[29,62,119] On the basis of this concept, an analgesic KOR agonist that does not activate MAPK would not produce the associated dysphoria.[29,62,119,120]

Ligand-specific receptor conformations suggest that small modifications of ligand structures can have profound effects on signaling profiles.[121-122] For example, in regards to opioid agonists, small structural changes to the KOR agonist, salvinorin A, have resulted in differentially regulated signaling pathways for the ligands depicted in **Figure 1.12**.[100,124-125]

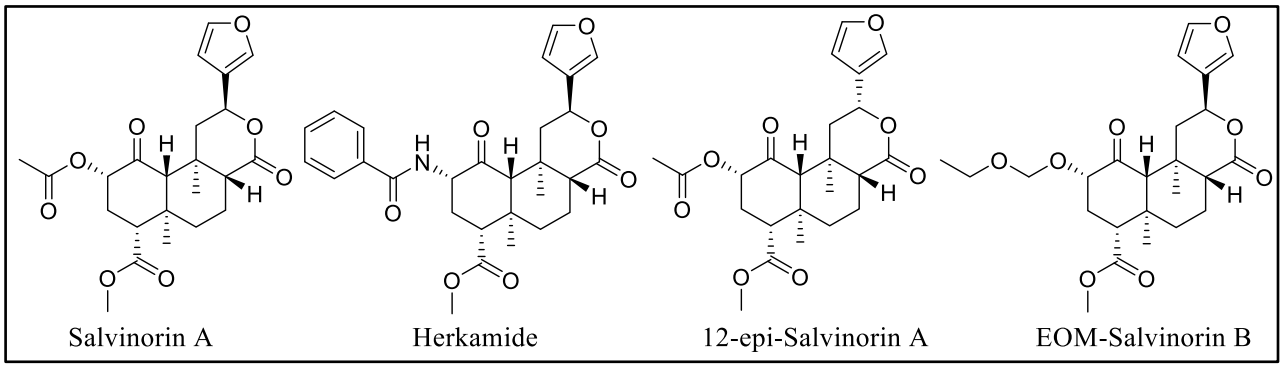

Figure 1.12. Salvinorin A and its analogues which differentially regulate signaling pathways.[100,124-125]

First of all, in 2008, research in the Prisinzano lab showed that replacement of the 2-acetoxy group of herkinorin, a MOR agonist based on the salvinorin A scaffold, with benzamide (yielding herkamide) results in greater β-arrestin 2 recruitment.[124] Following this discovery, in 2012, 12-epi-salvinorin A was shown to have reduced activity for G protein activation, while retaining full activity for β-arrestin 2 recruitment.[125] In addition, Berg et al.[100] established in 2015 that the ethoxymethyl derivative of salvinorin A (EOM-salvinorin B) had similar efficacy to G protein activation, but did not activate JNK as salvinorin A did. Interestingly, EOM-salvinorin B activated ERK to an extent similar to that of U50,488.[100] Nonetheless, the mechanism by which EOM-salvinorin B activated ERK differed from that of U50,488.[100]

In addition, other functionally selective KOR ligands have been described in literature, which are shown in **Figure 1.13**. First of all, in 2013, researchers discovered the biased agonism of 6'-Guaninonaltridole (6'-GNTI).[126-127] 6'-GNTI is a potent partial agonist at the KOR for the G protein activation pathway, yet is an antagonist for recruiting β-arrestins.[126-127] Secondly, a series of triazole and isoquinolinone analogues were identified

which produced a pronounced variation in bias between G protein signaling and ERK1/2 activation, i.e. these analogues are full agonists in G protein signaling and they are able to recruit β-arrestin2, although at a greatly diminished potency.[128-130] Additionally, researchers have discovered that nalfurafine is a G protein biased ligand with bias towards ERK1/2 activation.[131-132] Unfortunately, nalfurafine lacks receptor selectivity and its binding affinity for KOR is only between 2 and 15-fold higher than for the mu opioid receptor (MOR). [131-132]

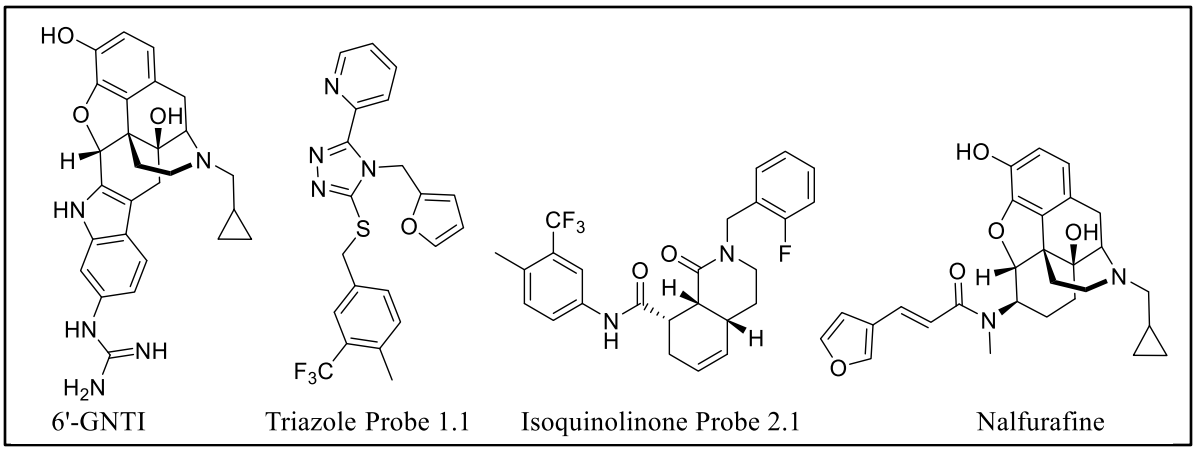

Figure 1.13. KOR agonists which differentially regulate signaling pathways.[126-132]

Accordingly, these results demonstrate that small structural changes may lead to a KOR agonist that does not activate ERK or JNK.[100] As highlighted above, studies have shown that small structural changes to the KOR agonist, salvinorin A, have resulted in differentially regulated signaling pathways.[100,124-125] In addition, research utilizing several different scaffolds have afforded functionally selective molecules. Consequently, additional KOR agonist scaffolds should be investigated in order to determine if structural changes result in functionally selective molecules.

U50,488 as a Probe to Identify Functionally Selective KOR Ligands

U50,488 is a KOR agonist that is a member of the arylacetamide class of compounds.[120] It was first discovered in 1982 by the Upjohn Company and was of particular interest because unlike MOR ligands, it does not cause respiratory depression or constipation, and does not activate reward pathways.[120] Following the discovery of this molecule, many researchers focused their efforts on improving selectivity of this molecule for the KOR over the MOR and DOR, as well as improving potency.[125, 133-170] Notably, these efforts included work by Glaxo,[100, 121-122] SmithKline Beecham,[135-139] Sankyo,[140] Parke-Davis,[141-143] DuPont Merck,[144-145] and Hoechst Marion Roussel.[146-147] Despite successful efforts in regards to the selectivity and potency of U50,488 analogues, the clinical testing of a majority of these molecules was discontinued due to dose limiting dysphoria.[148] There are four generalizations that can be made regarding the SAR of the arylacetamide class. First, the *trans* configuration is necessary for KOR agonistic activity, and the S,S configuration results in the greatest activity.[171-172] Secondly, there is an "eastern methylene group" effect, simply meaning that the methylene group adjacent to the carbonyl is necessary for KOR selectivity.[171] Third, substitution of the cyclohexane ring in either position para to the nitrogens produced, in many cases, potent MOR agonists.[171-172] Fourth, fusion of a benzene ring onto the cyclohexane ring produces an active KOR agonist.[171] A figure summarizing these overall structure-activity relationships (SARs) for U50,488 are presented in **Figure 1.14.**

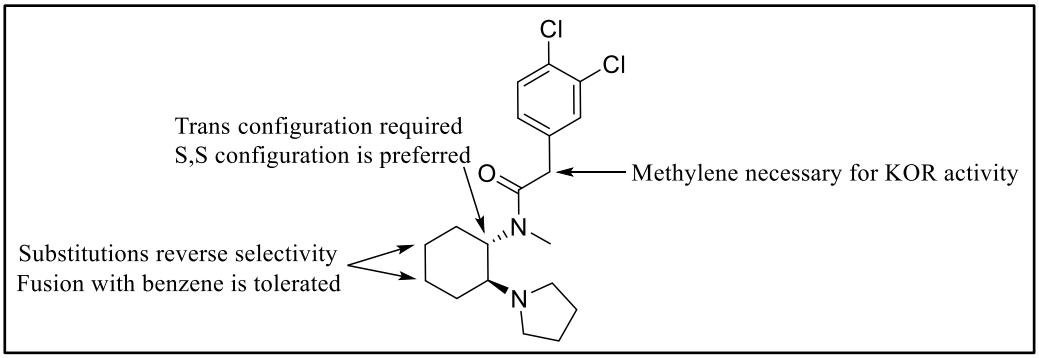

Figure 1.14. Summary of U50,488 analgesic SARs.

In order to better understand the regulation of KORs, Berg et al.[99] used (-)-U50,488 in primary cultures of sensory neurons in a rat model of thermal allodynia. The data indicated that pretreatment with bradykinin (BK), which is an inflammatory mediator, was necessary for (-)-U50,488 to inhibit thermal allodynia. Contrarily, BK pretreatment was not required for, nor modified, the stimulation of the extracellular signal-regulated kinases (ERK) pathway by (-)-U50,488.[99] This suggests that the adenylyl cyclase pathway, and not the ERK pathway, plays a role in mediating the anti-allodynic effect of (-)-U50,488.[99] In addition, Berg *et al.*[99] noted that the duration of the antiallodynic effect of (-)-U50,488 was inversely related to its dose, as shown in **Figure 1.15**. This suggests that in addition to the allodynic effects, this KOR ligand may initiate competing pronociceptive mechanisms.[99] These results prompted further investigation regarding the inverted U-shaped dose response curve of (-)-U50,488.

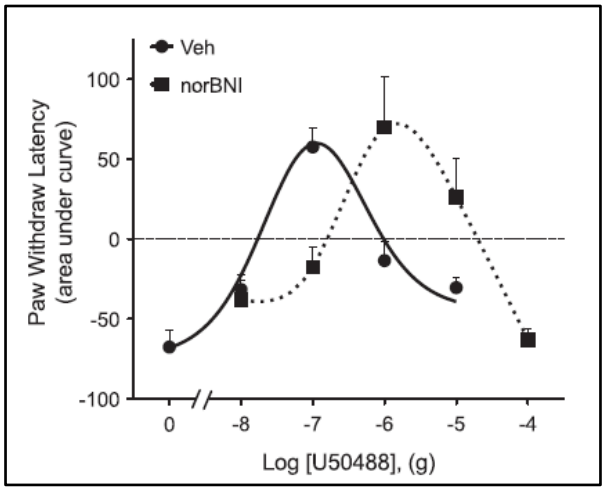

Figure 1.15. Dose response curves for (-)-U50,488 inhibition of PGE_2-induced thermal allodynia in the rat hindpaw.[99]

In order to study the regulation of KOR signaling in peripheral sensory neurons, cellular cAMP accumulation, ERK phosphorylation, and JNK were measured for the KOR selective agonists (-)-U50,488 and salvinorin A.[100] In addition, opioid agonist-mediated changes in paw withdrawal latency (PWL) to a thermal stimulus were measured with a plantar test apparatus.[100] The *in vitro* results show that (-)-U50,488 and salvinorin A inhibit PGE_2-stimulated adenylyl cyclase activity with similar efficacies, as shown in **Figure 1.16**.[100] Despite

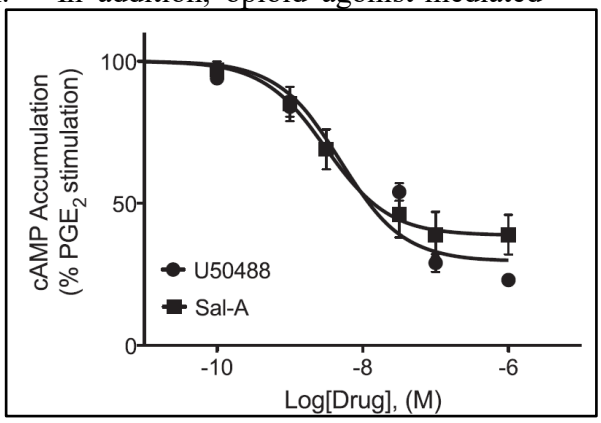

Figure 1.16. Inhibition of PGE_2-stimulated cAMP accumulation by (-)-U50,488 and salvinorin A.[100]

the similarity in cAMP inhibition, (-)-U50,488 and salvinorin A differ in their ability to regulate ERK and JNK. As shown in **Figure 1.17 (A)**, (-)-U50,488, but not salvinorin A, activated ERK in a nor-BNI sensitive manner (measured as a production of pERK). On the contrary, as depicted in **Figure 1.17 (B)**, salvinorin A, but not (-)-U50,488 activated JNK, as measured by Western Blot.[100]

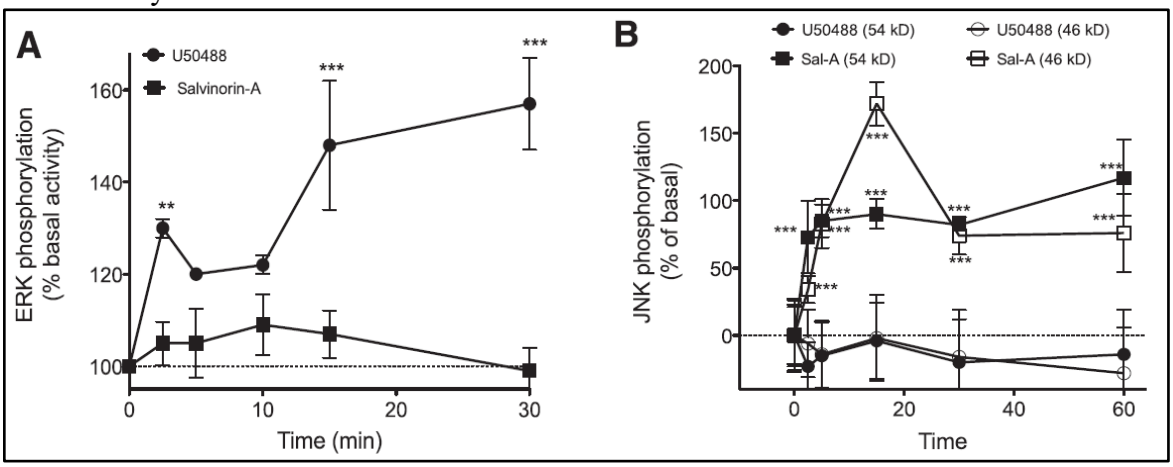

Figure 1.17. Activation of ERK **(A)** and JNK **(B)** by (-)-U50,488 and salvinorin A in primary cultures of peripheral sensory neurons.[100]

In regards to the *in vivo* data, the PWL upon co-administration of nor-BNI and varying doses of (-)-U50,488 produced a rightward shift of the dose-response curve, indicating that both phases of the curve are mediated via the KOR.[100] The roles of ERK and JNK on the descending phase of the dose-response curve for (-)-U50,488 were further examined.[100] Specifically, to study the role of ERK, the selective mitogen-activated protein kinase kinase ½ inhibitor, U0126, was injected into the rat hindpaw 15 minutes before i.pl. injection of a dose of (-)-U50,488 or salvinorin A, respectively.[100] Similarly, to study the role of JNK, the selective JNK inhibitor, SP600125, was injected prior to a dose of (-)-U50,488 or salvinorin A.[100] As depicted in **Figure 1.18 (A)**, the response to (-)-U50,488 was significantly enhanced by U0126, while SP600125 showed no effect.[100] Conversely, as depicted in **Figure 1.18 (B)**, the response to salvinorin A was enhanced by SP600125, while U0126 showed no effect.[100] These results show that the downward phase of the dose-response curves (DRCs) for

(-)-U50,488 and salvinorin A are differentially sensitive to kinase inhibitors.[100] The differential, ligand-dependent signaling of KOR agonists to ERK and JNK, elicited by (-)-U50,488 and salvinorin A, respectively, provides evidence of the functional selectivity of KOR ligands in peripheral sensory neurons.

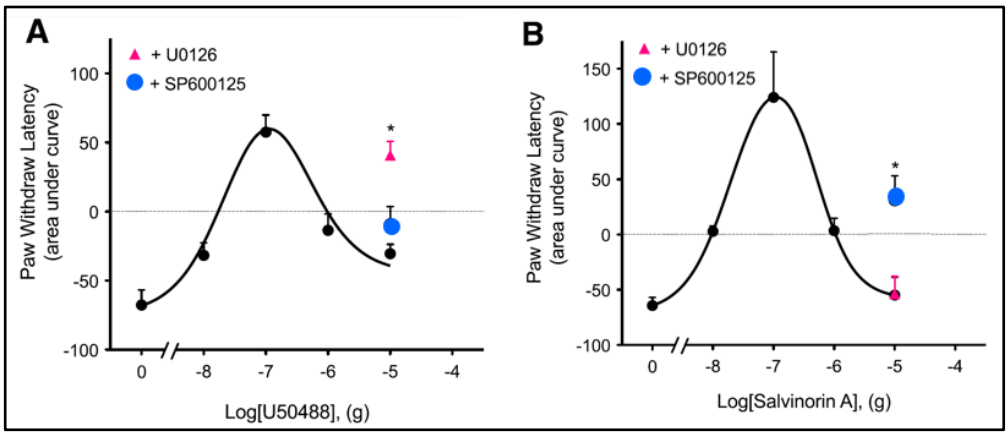

Figure 1.18. The descending limb of the dose-response curve for (-)-U50,488 and salvinorin A in primary cultures of peripheral sensory neurons.[100]

In summary, recent studies have demonstrated the functional selectivity of KOR ligands in rat peripheral pain sensing neurons.[99,100] In addition, researchers have demonstrated that receptor signaling leading to antinociception and dysphoria occur via different pathways.[29,62,119] Currently, there is a wealth of research and literature data in regards to the arylacetamide class of compounds.[120-172] Despite this abundance of knowledge, to-date, no medicinal chemistry campaign has been launched in order to identify functionally selective ligands based on the U50,488 scaffold. Consequently, there exists a gap in the knowledge regarding the potential of known arylacetamides to be functionally selective KOR agonists. Based on the information provided above, it can be hypothesized that a functionally selective KOR agonist, based on the U50,488 scaffold, would allow researchers to optimize signaling pathways leading to antinociception while simultaneously minimizing activity towards pathways that result in dysphoria. If successful, this has the potential to lead to new drugs with improved therapeutic profiles for the treatment of pain.

References

1. US Drug Enforcement Agency. **1993**, www.dea.gov.
2. Rosenblum, A.; Marsch, L.A.; Joseph, H.; Portenoy, R.K. Opioids and the Treatment of Chronic Pain: Controversies, Current Status, and Future Directions. *Exp. Clin. Pyschopharmacol.* **2008**, *16(5),* 405.
3. Brownstein, M.J. A Brief History of Opiates, Opioid Peptides, and Opioid Receptors. *Proc. Natl. Acad. Sci.* **1993**, *90*, 5391.
4. Martins, R.T.; Almedia, D.B.; Monteiro, F.M.; Kowacs, P.A.; Ramina, R. Opioid Receptors to Date. *Rev. Dor. Sao Paulo.* **2012**, *13(1),* 75.
5. Booth, M. *Opium: A History*, New York: St. Martin's Press, **1986**.
6. Schiff, P.L. Opium and its Alkaloids. *Am. J. of Pharm. Educ*. **2002**, *66*, 186.
7. Askitopoulou, H.; Ramoutsaki, I.A.; Konsolaki, E. Archaeological Evidence on the Use of Opium in the Minoan World. *International Congress Series*. **2002**, *1292*, 23.
8. Dikotter, F.; Laaman, L.; Xun, Z. *Narcotic Culture: A History of Drugs in China.* Chicago: University of Chicago Press, **2004**.
9. Flascha, C. On Opium: Its History, Legacy, and Cultural Benefits. Prospect Journal [Online] **2011**.
10. Wisniak, J. Pierre-Jean Robiquet. *Educ. Quim.* **2013**, *24*, 139.
11. Leeke, H. *The Pharmaceutical Review*. **1892**, *11*, 201.
12. Meldrum, M.L. A Capsule History of Pain Management. *JAMA,* **2003**, *290(18),* 2470.
13. Nicolau, K.C.; Montagnon, T. *Molecules That Changed the World.* **2008**. Germany: Wiley-VCH.
14. Alcabes, P. Medication Nation. The American Scholar. [Online] **2016**.

15. Beckett, A. H.; Casy, A.F. Synthetic Analgesics: Stereochemical Considerations. *J. Pharm. Pharmacol.* **1954**, *6(12),* 986.

16. Goldstein, A.; Tachibana, S.; Lowney, L.I.; Hunkapiller, M.; Hood, L. Dynorphin-(1-13), An Extraordinarily Potent Opioid Peptide. *Proc. Natl. Acad. Sci,* **1979**, *76*, 6666.

17. Pert, C.B.; Snyder, S.H. Opiate Receptor: Demonstration in Nervous Tissue. *Science.* **1973**, *179,* 1011.

18. Simon, E.J.; Hiller, J. M.; Edelman, I. Stereospecific Binding of the Potent Narcotic Analgesic [^{3}H]Etorphine to Rat-Brain Homogenate. *Proc. Nat. Acad. Sci.* **1973**, *70(7),* 1947.

19. Terenius, L. Stereospecific Interaction Between Narcotic Analgesics and a Synapse Plasma Membrane Fraction of Rat Cerebral Cortex. *Acta Pharmacol. Toxicol.* **1973**, *32,* 317.

20. Hughes, J.; Smith, T.W.; Kosterlitz, H.W.; Fothergill, L.A.; Morgan, B.A.; Morris, H.R. Identification of Two Related Pentapeptides from the Brain with Potent Opiate Agonist Activity. *Nature.* **1975**, *258,* 577.

21. Cox, B.M.; Goldstein, A.; Li, C.H. Opioid Activity of a Peptide, Beta-Lipotropin-(61,91), Derived from Beta-Lipotropin. *Proc. Natl. Acad. Sci.* **1976**, *73,* 1821.

22. Martin, W.R.; Eades, C.G.; Thompson, J.A.; Huppler, R.E.; Gilbert, P.E. *J.* The Effects of Morphine- and Nalorphine- Like Drugs in the Nondependent and Morphine-Dependent Chronic Spinal Dog. *Pharmacol. Exp. Ther*. **1976**, *197*, 517.

23. Lord, J.A.H.; Waterfield, A.A.; Hughes, J.; Kosterlitz, H.W. Endogenous Opioid Peptides: Multiple Agonists and Receptors. *Nature,* **1977**, *267*, 495.

24. Feng, Y.; He, X.; Yang, Y.; Chao, D.; Lazarus, L.H.; Xia, Y. Current Research on Opioid Receptor Function. *Curr. Drug Targets*. **2012**, *13(2),* 230.

25. Gilbert, P.E.; Martin, W.R. Sigma Effects of Nalorphine in the Chronic Spinal Dog. *Drug Alcohol Depend*. **1976**, *6*, 373.

26. Reinscheid, R.K.; Nothacker, H.P.; Bourson, A.; Ardati, A.; Henningsen, R.A.; Bunzow, J.R.; Grandy, D.K.; Langen, H.; Monsma F.J.; Civelli, O. The Therapeutic Potential of κ-Opioids for Treatment of Pain and Addiction. *Science,* **1995**, *270,* 792.

27. National Institute on Drug Abuse. **2016.** www.drugabuse.gov.

28. Rudgley, R. The Lost Civilizations of the Stone Age. New York, NY: Free Press. **1999**.

29. Chavkin, C. The Therapeutic Potential of κ-Opioids for the Treatment of Pain and Addicition. *Neuropsychopharmacology Reviews*. **2011**, *36*, 369.

30. Kosterlitz, H.W.; Leslie, F.M. Comparison of the Receptor Binding Characteristics of Opiate Agonists Interacting with μ- or κ- Receptors. *Br. J. Pharmac*. **1978**, *64*, 607.

31. Tyers, M.B. A Classification of Opiate Receptors that Mediate Antinociception in Animals. *Br. J. Pharmac*. **1980**, *69,* 503.

32. Ward, S.J.; Portoghese, P.S.; Takemori, A.E. Pharmacological Characterization *in Vivo* of the Novel Opiate,β-Funaltrexamine. *J. Pharmacol. Exp. Ther.* **1982**, *220,* 494.

33. Tung, A.S.; Yaksh, T.L. *In vivo* Evidence for Multiple Opiate Receptors Mediating Analgesia in the Rat Spinal Cord. *Brain Research.* **1982**, *247,* 75.

34. Pilcher, C.W.; Browne, J. Environmental Crowding Modifies Responding to Noxiuos Stimuli and the Effects of Mu- and Kappa-Agonists. *Life Sci.* **1982**, *31*, 1213.

35. Grossman, A.; Clement-Jones, V. Opiate Receptors: Enkephalins and Endorphins. *Clin. Endocrinol. Metab*. **1983**, *12,* 31.

36. Kamerling, S.G.; Martin, W.R.; Wu, K.M.; Wettstein, J.G.Medullary Kappa Hyperalgesic Mechanisms II. The Effects of Ethylketazocine Administered into the Fourth Cerebral Ventricle of the Conscious Dog. *Life Sci.* **1983**, *33*, 1839.

37. Nabeshima, T.; Yamada, K.; Kameyama, T. Contribution of Different Opioid Systems to Footshock-Induced Analgesia and Motor Supression. *Eur. J. Pharmacol.* **1983**, *92*, 199.

38. Upton, N.; Sewell, R.D.; Spencer, P.S. Analgesic Actions of μ- and κ-Opiate Agonists in Rats. *Arch. Int. Pharmacodyn. Ther.* **1983**, *262,* 199.

39. Herz, A. Multiple Opiate Receptors and Their Functional Significance. *J. Neural. Transm. Suppl.* **1983**, *18,* 227.

40. Wu, K.M.; Martin, W.R.; Kamerling, S.G.; Wettstein, J.G. Possible Medullary Kappa Hyperalgesic Mechanism. *Life Sci.* **1983**, *33*, 1831.

41. Przewlocki, R.; Stala, L.; Greczek, M.; Shearman, G.T.; Przewlocka, B.; Herz, A. Analgesic Effects of Mu-, Delta-, and Kappa-Opiate Agonists and, in Particular, Dynorphin at the Spinal Level. *Life Sci.* **1983**, *33,* 649.

42. Bhargava, H.N.; Pandey, R.N.; Matwyshyn, G.A. Effects of Prolyl-Leucyl-Glycinamide and Cyclo(Leucyl-Clycine) on Morphine-Induced Antinociception and Brain Mu, Delta, and Kappa Opiate Receptors. *Life Sci.* **1983**, *32,* 2096.

43. Ward, S.J.; Takemori, A.E. Relative Involvement of Mu, Kappa, and Delta Receptor Mechanisms in Opiate-Mediated Antinociception in Mice. *J. Pharmacol. Exp. Ther.* **1983**, *224,* 525.

44. Shippinberg, T.S.; Herz, A.; Spanagel, R.; Kubik, R.B.; Stein, C. Conditioning of Opioid Reinforcement: Neuroanatomical and Neurochemical Substrates. *Annals. N. Y. Acad. Sci.* **1992**, *654*, 348.

45. Kieffer, B.L.; Befort, K.; Gaveriaux-Ruff, C.; Hirth, C.G. The Delta Receptor: Isolation of cDNA by Expression Cloning and Pharmacological Characterization. *Proc. Natl. Acad. Sci.* **1992**, *89*, 12048.

46. Evans, C.J.; Keith, D.E.; Morrison, H.; Magendzo, K.; Edwards, R H. Cloning of a Delta Opioid Receptor by Functional Expression. *Science.* **1992**, *258*, 1952.

47. Meng, F.; Xie, G.X.; Thompson, R.C.; Mansour, A.; Goldstein, A.; Watson, S.J.; Akil, H. Cloning and Pharmacological Characterization of a Rat Kappa Opioid Receptor. *Proc. Natl. Acad. Sci.* **1993**, *90*, 9954.

48. Wang, J.B.; Johnson, P.S.; Persico, A.M.; Hawkins, A.L.; Griffin, C.A.; Uhl, G.R. Human Mu Opiate Receptor. cDNA and Genomic Clones, Pharmacological Characterization and Chromosomal Assignment. *FEBS Lett.* **1994**, *338*, 217.

49. Fredriksson, R.; Lagerstrom, M.C.; Lundin, L.G.; Schioth, H.B. The G-Protein-Coupled Receptors in the Human Genome Form Five Main Families. *Mol. Pharmacol.* **2003**, *63*, 1256.

50. Filmore, D. It's a GPCR World. *Mod. Drug Disc.* **2004**, 24.

51. Kobilka, B.K. G Protein Coupled Receptor Structure and Activation. *Biochim. Biophys. Acta.* **2007**, *1769*, 794.

52. Tuteja, N. Signaling Through G Protein Coupled Receptors. *Plant Signaling and Behavior.* **2009**, *4,* 942.

53. Kenakin, T. The Evolution of Receptors: From On-Off Switches to Microprocessors. John Wiley & Sons. **2010**.

54. De Lean, A.; Stadel, J.M.; Lefkowitz, R.J. A Ternary Complex Model Explains the Agonist-Specific Binding Properties of Adenylate Cyclase-Coupled β-Adrenergic Receptor. *J. Biol. Chem.* **1980**, *255(15),* 7108.

55. Goupil, E.; Laporte, S.A.; Hebert, T.E. Functional Selectivity in GPCR Signaling: Understanding the Full Spectrum of Receptor Conformation. *Mini Rev. Med. Chem.* **2012**, *12,* 817.

56. Hoffmann, C.; Zum, A.; Bunemann, M; Lohse, M.J. Conformational Changes in G-Protein-Coupled Receptors-The Quest for Functionally Selective Conformations is Open. *Br. J. Pharmacol.* **2008**, *153,* 358.

57. Clark, A.J. *Heffter's Handbuch Der Experimentellen Pharmakologie*. Berlin: Springer. **1937**.

58. Stephenson, R.P. A Modification of Receptor Theory. *Br J Pharmacol.* **1956**, *11,* 379.

59. Seifert, R. Functional Selectivity of G-Protein-Coupled Receptors: From Recombinant Systems to Native Human Cells. *Biochem. Pharm.* **2013**, *86*. 853.

60. Leff, P. The Two-State Model of Receptor Activation. *Trends Pharmacol. Sci.,* **1995**, *16(3),* 89.

61. Urban, J.D.; Clarke, W.P.; Zastrow, M.V.; Nichols, D.E.; Kobilka, B.; Weinstein, H.; Javitch, J.A.; Roth, B.L.; Christopoulos, A.; Sexton, P.M.; Miller, K.J.; Spedding, M.; Mailman, R.B. Functionally Selectivity and Classical Concepts of Quantitative Pharmacology. *J. Pharm. Exp. Ther.,* **2007**, *320(1),* 1.

62. Bruchas, M.R.; Chavkin, C. Kinase Cascades and Ligand-Directed Signaling at the Kappa Opioid Receptor. *Neuropyschopharmacology,* **2010**, *210(2)*, 137.

63. Eason, M.G.; Jacinto, M.T.; Liggett, S.B. Contribution of Ligand Structure to Activation of α_2-Adrenergic Receptor Subtype Coupling to G_s. *Mol. Pharmacol.* **1994**, 45(4), 696.

64. Bonhaus, D.W.; Chang, L.K.;Kwan, J.; Martin, G.R. Dual Activation and Inhibition of Adenyl Cyclase by Cannabinoid Receptor Agonists: Evidence for Agonist-Specific Trafficking of Intracellular Responses. *J. Pharmacol. Exp. Ther.* **1998**, *287(3),* 884.

65. Kukkonen, J.P.; Jansson, C.C.; Akerman, K.E. Agonist Trafficking of G(i/o)-Mediated α_2-Adrenoreceptor Responses in HEL 92.1.7 Cells. *Br. J. Pharmacol.* **2001**, *132(7),* 1477.

66. Watson, C.; Chen, G.; Irving, P.; Way, J.; Chen, W.J.; Kenakin, T. The Use of Stimulus-Biased Assay Systems to Detect Agonist-Specific Receptor Active States. *Mol. Pharmacol.* **2000**, *58(6),* 1230.

67. Kenakin, T. Biased Agonism. *F1000 Biol. Rep*. **2009**, *1*, 87.

68. Kenakin, T. Functional Selectivity Through Protean and Biased Agonism. *Mol. Pharmacol.* **2007**, *72(6),* 1393.

69. Noor, N.; Patel, C.B.; Rockman, H.A. β-Arrestin: A Signaling Molecule and Potential Therapeutic Target for Heart Failure. *J. Mol. Cell. Cardiol.* **2011**, *51(4),* 534.

70. Sanni, S.J.; Hansen, J.T.; Bonde, M.M.; Speerschneider, T.; Christensen, G.L.; Munk, S.; Gammeltoft, S.; Hansen, J.L. β- Arrestin 1 and 2 Stabilize the Angiotensin II Type I Receptor in Distinct High-Affinity Conformations. *Br. J. Pharmacol.* **2010**, *161*, 1476.

71. Berg, K.A.; Maayani, S.; Goldfarb, J.; Scaramellini, C.; Leff, P.; Clarke, W.P. Effector Pathway-Dependent Relative Efficacy at Serotonin Type 2A and 2C Receptors. *Mol. Pharmacol.* **1998**, *54*, 94.

72. Berg, K.A.; Maayani, S.; Goldfarb, J.; Clarke, W.P. Pleiotropic Behavior of 5-HT2A Receptor Agonists. *Ann. N. Y. Acad. Sci.* **1998**, *861*, 104.

73. Stout, B.D.; Clarke, W.P.; Berg, K.A. Rapid Desensitization of Serotonin Receptor System. *J. Pharmacol. Exp. Ther.* **2002**, *302*, 957.

74. Visiers, I.; Hassan, S.A.; Weistein, H. Differences in Conformational Propeties of the Second Intracellular Loop (IL2) in HTC(2C) Receptors Modified by RNA Editing Can Account for G Protein Coupling Efficiency. *Protein. Eng*. **2001**, *14*, 409.

75. Cussac, D.; Newman-Tancredi, A.; Duqueyroix, D.; Pasteau, V.; Millan, M.J. Differential Activation of G_q/11 and G_i Proteins at the 5-Hydroxytryptamine Receptors Revealed by Antibody Capture Assays: Influence of Receptor Reserve and Relationship to Agonist Directed Trafficking. *Mol. Pharmacol.* **2002**, *62*, 578.

76. De Deurwaerdere, P.; Navailles, S.; Berg, K.A.; Clarke, W.P.; Spampinato, U. Constitutive Activity of the Serotonin2C Receptor Inhibits *In vivo* Dopamine Release in the Rat Striatum and Nucleus Accumbens. *J. Neurosci.* **2004**, *24,* 3235.

77. Keith, D.E.; Murray, S.R.; Zaki, P.A.; Chu, P.C.; Lissin, D.V.; Kang, L.; Evans, C.J.; von Z.M. Morphine Activates Opioid Receptors Without Causing Their Rapid Internalization. *J. Biol. Chem.* **1996**, *271*, 19021.

78. Whistler, J.L.; Chuang, H.H.; Chu, P.; Jan, L.Y.; von Zastrow, M. Functional Dissociation of Mu Opioid Receptors Signaling an Endocytosis: Implications for the Biology of Opioid Tolerance and Addiction. *Neuron.* **1999**, *23,* 737.

79. Alvarez, V.A.; Arttamangkul, S.; Dang, V.; Salem, A.; Whistler, J.L. von Zastrow, M.; Grandy, D.K.; Williams, J.T. Mu Opioid Receptors: Ligand-Dependent Activity of Potassium Conductance Desensitization and Internalization. *J. Neurosci*. **2002**, *22,* 5769.

80. Benovic, J.L.; Staniszewski, C.; Mayor, F.; Caron, M.G.; Lefkowitz, R.J. Beta-Adrenergic Receptor Kinase. Activity of Partial Agonist for Stimulation of Adenylate Cyclase Correlates with the Ability to Promote Receptor Phosphorylation. *J. Biol. Chem.* **1988**, *263,* 3893.

81. Trester-Zedlitz, M.; Burlingame, A.; Kobilka, B.; von, Z.M. Mass Spectrometric Analysis of Agonist Effects on Posttranslational Modifications of the Beta-2-Adrenoceptor in Mammalian Cells. *Biochemistry.* **2005**, *44,* 6133.

82. Hausdorf, W.P.; Campbell, P.T.; Ostrowski, J.; Yu, S.S.; Caron, M.G.; Lefkowitz, R.J. A Small Region of the Beta-Adrenergic Receptor is Selectively Involved in its Rapid Regulation. *Proc. Natl. Acad. Sci.* **1991**, *88,* 2979.

83. Tran, T.M.; Friedman, J.; Qunaibi, E.; Baameur, F.; Moore, R.H.; Clark, R.B. Characterization of Agonist Stimulation of cAMP-Dependent Protein Kinase and G Protein-Coupled Receptor Kinase Phosphorylation of the Beta2-Adrenergic Receptor Using Phosphoserine-Specific Antibodies. *Mol. Pharmacol.* **2004**, *65,* 196.

84. Feldman, B.J.; Rosenthal, S.M.; Vargas, G.A.; Fenwick, R.G.; Huang, E.A.; Matsuda-Abedini, M; Lustig, R.H.; Mathias, R.S.; Portale, A.A.; Miller, W.L. Nephrogenic Syndrome of Inappropriate Antidiuresis. *N. Engl. J. Med.* **2005**, *352*, 1884.

85. Rosenthal, W.; Antaramian, A.; Gilbert, S.; Birnbaumer, M. Nephrogenic Diabetes Insipidus. A V2 Vasopressin Receptor Unable to Stimulate Adenylyl Cyclase. *J. Biol. Chem*. **1993**, *268,* 13030.

86. Barak, L.S.; Oakley, R.H.; Laporte, S.A.; Caron, M.G. Constitutive Arrestin-Mediated Desensitization of a Human Vasopressin Receptor Mutant Associated with Nephrogenic Diabetes Insipidus. *Proc. Natl. Acad. Sci.* **2001**, *98,* 93.

87. Charifson, P.S.; Bowen, J.P.; Wyrick, S.D.; Hoffman, A.J.; Cory, M.; McPhail, A.T.; Mailman, R.B. Conformational Analysis of Molecular Modeling of 1-Phenyl-4-phenyl-, and 1-Benzyl-1,2,3,4-tetrahydroisoquinolines as D_1 Dopamine Receptor Ligands. *J. Med. Chem.* **1989**, *32,* 2050.

88. Mottola, D.M.; Laiter, S.; Watts, V.J.; Tropsha, A.; Wyrick, S.D.; Nichols, D.E.; Mailman, R.B. Conformational Analysis of D1 Dopamine Receptor Agonists: Pharmacophore Assessment and Receptor Mapping. *J. Med. Chem.* **1996**, *39*, 285.

89. Qandil, A.M.; Lewis, M.M.; Janssen, A.; Leonard, S.K.; Mailman, R.B.; Nichols, D.E. Synthesis and Pharmacological Evaluation of Substituted Naphth[1,2,3-de]isoquinolines (dinapsoline analogues) as D_1 and D_2 Dopamine Receptor Ligands. *Bioorg. Med. Chem.* **2003**, *11,* 1451.

90. Lovenberg, T.W.; Brewster, W.K.; Mottola, D.M.; Lee, R.C.; Riggs, R.M.; Nichols, D.E.; Lewis, M.H.; Mailman, R.B. Dihydrexidine, A Novel Selective High Potency Full Dopamine D-1 Receptor Agonist. *Eur J. Pharmacol.* **1989**, *166,* 111.

91. Brewster, W.K.; Nichols, D.E.; Riggs, R.M.; Mottola, D.M.; Lovenberg, T.W.; Lewis, M.H.; Mailman, R.B. *Trans*-10,11-dihydroxy-5,6,6a,7,8,12b-hexahydrobenzo[a-]phenanthridine: A Highly Potent Selecitve Dopamine D1 Full Agonist. *J. Med. Chem.* **1990**, *33,* 1756.

92. Mottola, D.M.; Brewster, W.K.; Cool, L.L.; Nichols, D.E.; Mailman, R.B. Dihydrexidine, A Novel Full Efficacy D_1 Dopamine Receptor Agonist. *J. Pharmacol. Exp. Ther.* **1992**, *262,* 383.

93. Kilts, J.D.; Connery, H.S.; Arrington, E.G.; Lewis, M.M.; Lawler, C.P.; Oxford, G.S.; O'Malley, K.L.; Todd, R.D.; Blake, B.L.; Nichols, D.E. Functionally Selectivity of Dopamine Receptor Agonist. II. Actions of Dihydrexidine in D2L Receptor-Transfected MN9D Cells and Pituitary Lactotrophs. *J. Pharmacol. Exp. Ther.* **2002**, *301,* 1179.

94. Lawler, C.P.; Watts, V.J.; Booth, R.G.; Southerland, S.B.; Mailman, R.B. A Selective Antagonist for Post-Synaptic Dopamine D2 Receptors. *Soc. Neurosci. Abstr.* **1994**, Abstracts 20, 525

95. Mailman, R.B.; Nichols, D.E.; Lewis, M.M.; Blake, B.L.; Lawler, C.P. Functional Effects of Novel Dopamine Ligands: Dihydrexidine and Parkinson's Disease as a First Step, in *Dopamine Receptor Subtypes: From Basic Research to Clinical Application.* IOS Stockton Press, Washington, DC, **1998**.

96. Mailman, R.B.; Nichols, D.E.; Tropsha, A. Molecular Drug Design and Dopamine Receptors, in *The Dopamine Receptors*. Humana Press, Totowa, NJ, **1997**.

97. Smith, H.P.; Nichols, D.E.; Mailman, R.B.; Lawler, C.P. Locomotor Inhibition, Yawning and Various Chewing Induced by a Novel Dopamine D2 Post-Synaptic Receptor Agonist. *Eur. J. Pharmacol.* **1997**, *323*, 27.

98. Gay, E.A.; Urban, J.D.; Nichols, D.E.; Oxford, G.S.; Mailman, R.B. Functional Selectivity of the D2 Receptor Ligands in a Chinese Hamster Ovary hD2L Cell Line: Evidence for Induction of Ligand-Specific Receptor States. *Mol. Pharmacol*. **2004**, *66,* 97.

99. Berg, K.A.; Rowan, M.P.; Sanchez, T.A.; Silva, M.; Patwardhan, A.M.; Milam, S.B.; Hargreaves, K.M.; Clarke, W.P. Regulation of κ-Opioid Receptor Signaling in Peripheral Sensory Neurons in Vitro and in Vivo. *J. Pharmacol. Exp. Ther.* **2011**, *338*, 92.

100. Jamshidi, R.J.; Jacobs, B.A.; Sullivan, L.C.; Chavera, T.A.; Saylor, R.M.; Prisinzano, T.E.; Clarke, W.P.; Berg, K.A. Functional Selectivity of Kappa Opioid Receptor Agonists in Peripheral Sensory Neurons. *J. Pharmacol. Exp. Ther.* **2015**, *355,* 174.

101. Patel, C.B.; Noor, N.; Rockman, H.A. Functional Selectivity in Adrenergic and Angiotensin Signaling Systems. *Mol. Pharmacol.* **2010**, *78,* 983.

102. Aplin, M.; Christensen, G.L.; Hansen, J.L. Pharmacological Perspectives of Functional Selectivity by the Angiotensin II Type I Receptor. *Trends Cardiovasc. Med.* **2008**, *18*, 305.

103. Aplin, M.; Bonde, M.M.; Hansen, J.L. Molecular Determinants of Angiotensin II Type I Receptor Functional Selectivity. *J. Mol. Cell. Cardiol.* **2009**, *46,* 15.

104. Lefkowitz, R.J.; Shenoy, S.K. Transduction of Receptor Signals by Beta-Arrestins. *Science.* **2005**, *308*, 512.

105. Rajagopal, K.; Lefkowitz, R.J.; Rockman, H.A. When 7 Transmembrane Receptors are not G Protein-Coupled Receptors. *J Clin Invest.* **2005**, *115*, 2971.

106. Lefkowitz, R.J.; Rajagopal, K.; Whalen, E.J. New Roles for Beta-Arrestins in Cell Signaling: Not Just for Seven-Transmembrane Receptors. *Mol. Cell*. **2006**, *24*, 643.

107. Moore, C.A.; Milano, S.K.; Benovic, J.L. Regulation of Receptor Trafficking by GRKs and Arrestins. *Annu. Rev. Physiol.* **2007**, *69*, 451.

108. Wu, N.; Hanson, S.M.; Francis, D.J.; Vishnivetskiy, S.A.; Thibonnier, M.; Klug, C.S. Arrestin Binding to Calmodulin: A Direct Interaction Between Two Ubiquitous Signaling Proteins. *J. Mol. Biol.* **2006**, *364*, 955.

109. Xiao, K.; McClatchy, D.B.; Shukla, A.K.; Zhao, Y.; Chen, M.; Shenoy, S.K. Functional Specialization of Beta-Arrestin Interactions Revealed by Proteomic Analysis. *Proc. Natl. Acad. Sci.* **2007**, *104*, 12011.

110. Mangmool, S.; Shukla, A.K.; Rockman, H.A. Beta-Arrestin-Dependent Activation of Ca[2+]/Calmodulin Kinase II After Beta(1)-Adrenergic Receptor Stimulation. *J. Cell. Biol*. **2010**, *189*, 573.

111. Couchonnal, L.F.; Anderson, M.E. The Role of Calmodulin Kinase II in Myocardial Physiology and Disease. *Physiology (Bethesda).* **2008**, 151.

112. Wei, H.; Ahn, S.; Shenoy, S.K.; Karnik, S.S.; Hunyady, L.; Luttrell, L.M. Indepdent Beta-Arrestin 2 and G Protein-Mediated Pathway for Angiotensin II Activation of Extracellular-Signal Regulated Kinase 1 and 2. *Proc. Natl. Acad. Sci.* **2003**, *100,* 10782.

113. Ahn, S.; Shenoy, S.K.; Wei, H.; Lefkowitz, R.J. Differential Kinase and Spatial Patterns of Beta-Arrestin Dependent, G Protein-Independent ERK Activation by the Angiotensin II Receptor. *J. Biol. Chem.* **2004**, *279*, 35518.

114. Holloway, A.C.; Qian, H.; Pipolo, L.; Ziogas, J.; Miura, S.; Karnik, S. Side Chain Substitutions with Angiotensin II Reveal Different Requirements for Signaling, Internalization, and Phosphorylation of Type 1A Angiotensin Receptors. Mol. Pharmacol. 2002, 61, 768.

115. Aplin, M.; Christensen, G.L.; Schneider, M.; Heydorn, A.; Gammeltoft, S.; Kjolbye, A.L. The Angiotensin Type 1 Receptor Activates Extracellular Signal-Regulated Kinase 1 and 2 by G Protein-Dependent and -Independent Pathways in Cardiac Myocytes and Langendroff-Perfused Parts. *Basic Clin. Pharmacol. Toxicol.* **2007**, *100*, 289.

116. Rajagopal, K.; Whalen, E.J.; Violin, J.D.; Stiber, J.A.; Rosenberg, P.B.; Premont, R.T. Beta-Arrestin2-Mediated Ionotropic Effects of the Angiotensin II Type 1A Receptor in Isolated Cardiac Myocytes. *Proc. Natl. Acad. Sci.* **2006**, *103*, 16284.

117. Valero, T.R.; Sturchler, E.; Jafferjee, M.; Rengo, G.; Magafa, V.; Cordopatis, P.; McDonald, P.; Koch, W.J.; Lymperopoulos, A. Structure-Activity Relationship Study

of Angiotensin II Analogs in Terms of β-Arrestin-Dependent Signaling to Adolsterone Production. *Pharmacol. Res. Perspect.* **2016**, *4,* 226.

118. Bruchas, M.R.; Yang, T.; Schreiber, S.; DeFino, M.; Kwan, S.C.; Li, S.; Chavkin, C. Long-Acting κ Opioid Antagonists Disrupt Receptor Signaling and Produce Noncompetitive Effects by Activating c-Jun *N*-terminal Kinase. *J. Biol. Chem.* **2007**, *282*, 29803.

119. Melief, E.J.; Miyatake, M.; Bruchas, M.R.; Chavkin, C. Ligand-Directed c-Jun *N*-terminal Kinase Activation Disrupts Opioid Receptor Signaling. *Proc. Natl. Acad. Sci.* **2010**, *107*, 11608.

120. Szmuszkovicz, J.; Von Voigtlander, P.F. Benzeneacetamide Amines: Structurally Novel Non-Mu Opioids. *J. Med. Chem.* **1982**, *25,* 1125.

121. Chen, X.; Sassano, M.F.; Zheng, L.; Setola, V.; Chen, M.; Bai, X.; Frye, S.V.; Wetsel, W.C.; Roth, B.L.; Jin, J. Structure-Functional Selectivity Relationship Studies of β-arrestin-biased Dopamine D_2 Receptor Agonists. *J. Med. Chem.* **2012**, *55,* 7141.

122. Shonberg, J.; Herenbrink, C.K.; Lopez, L.; Christopolous, A.; Scammells, P.J.; Capuano, B.; Lane, J.R. A Strucutre-Activity Analysis of Biased Agonism at the Dopamine D_2 Receptor. *J. Med. Chem.* **2013**, *56*, 9221.

123. Beguin, C.; Potuzak, J.; Xu, W.; Liu-Chen, L.Y.; Streicher, J.M.; Groer, C.E.; Bohn, L.M.; Carlezon, W.A.; Cohen, B.M. Differential Signaling Properties at the Kappa Opioid Receptor of 12-epi-salvinorin A and Its Analogues. *Bioorg. Med. Chem. Lett*. **2012**, *22*, 1023.

124. Tidgewell, K.; Groer, C.E.; Harding W.W.; Lozama, A.; Schmidt, M.; Marquam, A.; Hiemstra, J.; Partilla, J.S.; Dersch, C.M.; Rothman, R.B.; Bohn, L.M.; Prisinzano, T.E.

Herkinorin Analogues with Differential Beta-Arrestin-2 Interactions. *J. Med. Chem.* **2008**, *51*, 2421.

125. Scopes, D.I.C.; Hayes, D.E.; Bays, D.; Belton, J.; Brain, D.S.; Brown, D.B.; Judd, D.B.; McElroy, A.B.; Meerholz, C.A.; Naylor, A. New κ-Receptor Agonists Based on a 2-[(alkylamino)methyl]piperidine Nucleus. *J Med. Chem.* **1992**, *35*, 490.

126. Rives, M.L.; Rossillo, M.; Chen, L.Y.; Javitch, J.A. 6'-Guanidinonaltrindole (6'-GNTI) Is a G Protein-biased κ-Opioid Receptor Agonist that Inhibits Arrestin Recruitment. *J. Biol. Chem.* **201**2, *287,* 27050.

127. Schmid, C.L.; Streicher, J.M.; Groer, C.E.; Munro, T.A.; Zhou, L.; Bohn, L.M. Functional Selectivity of 6'-Guanidinonaltrindole (6'-GNTI) at κ-Opioid Receptors in Striatal Neurons. *J. Biol. Chem*. **2013***, 288,* 22837.

128. Lovell, K.M.; Frankowski, K.J.; Stahl, E.L.; Slauson, S.R.; Yoo, E.; Prisinzano, T.E.; Aube, J.; Bohn, L.M. Structure-Activity Relationship Studies of Functionally Selective Kappa Opioid Receptor Agonists that Modulate ERK ½ Phosphorylation While Preserving G Protein over βArrestin2 Signaling Bias. *ACS Chem. Neurosci*. **2015**, *6,* 1411.

129. Zhou, L.; Lovell, K.M.; Frankowski, K.J.; Slauson, S. R.; Philips, A.M.; Streicher, J.M.; Stahl, E.; Schmid, C.L.; Hodder, P.; Madoux, F.; Cameron, M.D.; Prisinzano, T.E.; Aube, J.; Bohn, L.M. Development of Functionally Selective, Small Molecule Agonists at Kappa Opioid Receptors. *J. Biol. Chem*. **2013**, *288,* 36703.

130. Brust, T.F.; Morgenweck, J.; Kim, S.A.; Rose, J.H.; Locke, J.L.; Schmid, C.L.; Zhou, L.; Stahl, E.L.; Cameron, M.D.; Scarry, S.M.; Aube, J.; Jones, S.R.; Martin, T.J.; Bohn, L.M. Biased Agonists of the Kappa Opioid Receptor Supress Pain and Itch without Causing Sedation or Dysphoria. *Sci. Signal.* **2016**, *9*, ra117.

131. Schattauer, S.S.; Kuhar, J.R.; Song, A.; Chavkin, C. Nalfurafine is a G-Protein Biased Agonists Having Significantly Greater Bias at the Human Than Rodent Form of the Kappa Opioid Receptor. *Cell. Signal*. **2017**, *32,* 59.

132. Inan, S.; Dun, N.J.; Cowan, A. Nalfurafine Prevents 5'-Guanidinonaltrindole- and Compound 48/80-Induced Spinal c-fos Expression and Attenuates 5'-Guanidinonaltrindole-Elicited Scratching Behavior in Mice. *Neuroscience.* **2009**, *163,* 23.

133. Hayes, A.G.; Birch, P.J.; Hayward, N.J.; Sheehan, M.J.; Rogers, H.; Tyers, M.B.; Judd, D.B.; Scopes, D.I.C.; Naylor, A. A Series of Novel, Highly Potent and Selective Agonists for the κ-Opioid Receptor. *Br. J. Pharmacol*. **1990**, *191*, 994.

134. Naylor, A.; Judd, J.B.; Lloyd, J.E.; Scopes, D.I.C.; Hayes, A.G.; Birch, P.J. A Potent New Class of κ-Receptor Agonist: 4-Subsituted 1(-arylacetyl)-2-[(dialkylamino)methyl]piperazines. *J. Med. Chem*. **1993**, *36*, 2075.

135. Vecchietti, V.; Giordani, A.; Girdina, G.; Colle, R.; Clarke, G.D. (2S)-1-(arylacetyl)-2-(aminomethyl)piperidine Derivatives: Novel, Highly Selective Kappa Opioid Analgesics. *J. Med. Chem.* **1991**, *34*, 397.

136. Vecchietti, V.; Clarke, G.D.; Colle, R.; Dondio, G.; Giardina G.; Petrone, G.; Sbacchi, M. Substituted 1-(aminomethyl)-2-(arylacetyl)-1,2,3,4-tetrahydroisoquinolines: A Novel Class of Very Potent Antinociceptive Agents with Varying Degrees of Selectivity for Kappa and Mu Opioid Receptors. *J. Med. Chem*. **1992**, *35*, 2970.

137. Vecchietti, V.; Clarke, G.D.; Colle, R.; Giardina, G.; Petrone, G.; Sbacchi, M. (1S)-1-(aminomethyl)-2-(arylacetyl)-1,2,3,4-tetrahydroisoquinoline and Heterocycle-Condensed Tetrahydropyridine Derivatives: Members of a Novel Class of Very Potent Kappa Opioid Analgesics. *J. Med. Chem.* **1991**, *34*, 2624.

138. Giardina, G.; Clarke, G.D.; Dondio, G.; Petrone, G.; Sbacchi, M.; Vecchietti, V. Selective κ-Opioid Agonists: Synthesis and Structure-Activity Relationships of Piperidines Incorporating an Oxo-Containing Acyl Group. *J. Med. Chem.* **1994**, *37,* 3482.

139. Colle, R.; Clarke, G.D.; Dondio, G.; Giardina, G.; Petrone, G.;Sbacchi, M.; Vecchietti, V. Enantiospecificity of Kappa Receptors: Comparison of Racemic Compounds and Active Enantiomers in Two Novel Series of Kappa Agonist Analgesics. *Chirality,* **1992**, *4*, 8.

140. Fujibayashi, K.; Kubota, K.; Saito, K. Effects of R-84760, A Selective Kappa-Opioid Receptor Agonist, on Nociceptive Reflex in Isolated Neonatal Rat Spinal Cord. *Eur. J. Pharmacol*. **1998**, *343,* 171.

141. Halfpenny, P.R.; Horwell, D.C.; Hughes, J.; Humblet, C.; Hunter, J.C.; Neuhaus, D.; Rees, D.C. Highly Selective κ Opioid Analgesics. *J. Med. Chem*. **1991**, *34,* 190.

142. Tortella, F.C.; Rose, J.; Robles, L.; Moreton, J.E.; Hughes, J.; Hunter, J.C. EEG Spectral Analysis of the Neuroprotective Kappa opioids in Enadoline and PD117302. *J. Pharmacol. Exp. Ther.* **1997**, *282,* 286.

143. Sabin, V.; Horwell, D.C.; McKnight, A.T.; Broqua, P. *Trans N*-Methyl-*N*-[2-(1-pyrrolidinylcyclohexyl] cycloprop-2-ene-1-carboxamides: Novel Lipophilic Kappa Opioid Agonists. *Bioorg. Med. Chem. Letts*. **1997**, *7,* 291.

144. Rajagopalan, P.; Scribner, R.M.; Pennev, P.; Schmidt, W.K.; Tam, S.W.; Steinfels, G.F.; Cook, L. DuP 747: A New, Potent, Kappa Opioid Analgesic. Synthesis and Pharmacology1. *Bioorg. Med. Chem. Letts*. **1992**, *2*, 715.

145. Rajagopalan, P.; Scribner, R.M.; Pennev, P.; Mattie, P.L.; Kezar, H.S.; Cheng, C.Y.; Cheeseman, R.S.; Ganti, V.R.; Johnson, A.L.; Wuonola, M.A. DuP 747: SAR Study. *Bioorg. Med. Chem. Letts.* **1992**, *2*, 721.

146. Hamon, G.; Celemence, F.; Fortin, M.; Martret, O.L.; Jouquey, S.; Vincent, J.C.; Petit, F.; Bichet, D.G. Effects of Subchronic Administration of Niravoline, A Novel Aquaretic Compound, On Water and Electrolyte Renal Excretion in Cirrhotic Rats. *Brit. J. Pharmacol*. **1995**, *114*, 310.

147. Bamana, I.; Nagao, S. Effects of Niravoline (RU 51599), A Selective Kappa-Opioid Receptor Agonist on Intracranial Pressure in Gradually Expanding Extradural Mass Lesion. *J. Neurotrama*. **1998**, *15,* 117.

148. Barber, A.; Gottschlich, R. Central and Peripheral Nervous System. Novel Developments with Selective, Non-Peptidic Kappa-Opioid Receptor Agonists. *Exp. Opin. Invest. Drugs*. **1997**, *6*, 1351.

149. Pechulis, A.D.; Archer, S.; Wentland, M.P.; Colasurdo, A.M.; Bidlack, J.M. Arylacetamide Kappa-Selective Opioid Ligands. *Bioorg. Med. Chem. Letts.* **1997**, *7*, 2271.

150. Cheng, C.Y.; Wu, S.C.; Hsin, L.W.; Tam, S.W. Selective Reversible and Irreversible Ligands for the κ Opioid Receptor. *J. Med. Chem*. **1992**, *35*, 2243.

151. Cheng, C.Y.; Lu, H.Y.; Lee, F.M.; Tam, S.W. Synthesis of (1'2'-*trans*)-3-phenyl-1-[2'-(*N*-pyrrolidinyl)cyclohexyl]pyrrolid-2-ones as Kappa Selective Opiates. *J. Pharmac. Sci.* **1990**, *29*, 758.

152. Cheng, C.Y.; Lu, H.Y.; Lee, F.M. *N*-Methyl-*N*-[*trans*-2-(1-pyrrolidinyl)cyclohexyl]-1-phenylcyclopropanecarboxylic amides – Analogues of U50488 with Much Reduced Opiate Affinity and Loss of κ Selectivity. *J. Med. Chem*. **1991**, *26,* 125.

153. Zhao, S.; Freeman, J.P.; VonVoigtlander, P.F.; Howe, W.J.; Szmuszkovicz, J. Structure-Activity Relationship Pertaining to the North-West Region of the Kappa Opioid Agonist, U50,488. *Bioorg. Med. Chem. Letts.* **1994**, *4*, 2139.

154. Zhao, S.; Freeman, J.P.; VonVoigtlander, P.F.; Smith, M.W.; Szmuszkovicz, J. Phenalene Analogs of the Kappa Opiate Agonist U50,488. *Bioorg. Med. Chem. Letts.* **1993**, *12,* 2641.

155. D'Andrea, S.V.; Michalson, E.T.; Freeman, J.P.; Chidester, C.G.; Szmuszkovicz, J. *Trans*-3,4-Diaminopiperidines. Azacyclohexane Congeners of Kappa Agonist U-50488. *J. Org. Chem.* **1991**, *56,* 3133.

156. Zhao, S.; Freeman, J.P.; Chidester, C.G.; VonVoigtlander, P.F.; Mizsak, S.A.; Szmuszkovicz, J. Regioselective and Stereoselective Syntheses of 1,2,3-triaminocyclohexane Derivatives. *J. Org. Chem.* **1993**, *58*, 4043.

157. Cappelli, A.; Anzini, M.; Vomero, S.; Menziana, M.C.; De Benedetti, P.G.; Sbacchi, M.; Clarke, G.D.; Mennuni, L. Synthesis, Biological Evaluation, and Quantitative Receptor Docking Simulations of 2-[(Acylamino)ethyl]-1,4-benzodiazepines as Novel Tifluadom-like Ligands with High Affinity and Selectivity for κ-Opioid Receptors. *J. Med. Chem.* **1996**, *39*, 860.

158. Guyon, C.; Fardin, V.; Carruette, A.; Garret, C.; Plau, B.; Taurand, G. AFMC International Medicinal Chemistry Symposium/AIMECS. **1995**.

159. Brandt, W.; Drosihn, S.; Haurand, M.; Holzgrabe, U. Search for the Pharmacophore in Kappa-Agonistic Diazabicyclo[3.3.1]nonan-9-one-1,5-diesters and Arylacetamides. *Nachtsheim. Arch. Pharm. Med. Chem.* **1996**, *329*, 311.

160. Kogel, B.; Christoph, T.; Friderichs, E.; Hennies, H.H.; Matthiesen, T.; Schneider, J.; Holzgrabe, U. HZ2, A Selective Kappa-Opioid Agonist. *CNS Drug Reviews*. **1998**, *4,* 54.

161. Kolesnikov, Y.; Jain, S.; Wilson, R.; Pasternak, G.W. Peripheral K_1-Opioid Receptor-Mediated Analgesia in Mice. *Eur. J. Pharmacol*. **1996**, *310*, 141.

162. Catheline, G.; Guilbaud, G.; Kayser, V. Peripheral Component in the Enhanced Antinociceptive Effect of Systemic U-69,593, A Kappa Opioid Receptor Agonist in Mononeuropathic Rats. *Eur. J. Pharmacol*. **1998**, *357,* 171.

163. Rogers, H.; Birch, P.J.; Harrison, S.M.; Palmer, E.; Manchee, G.R.; Judd, D.B.; Naylor, A.; Scopes, D.I.C.; Hayes, A.G. GR94839, A Kappa-Opioid Agonist with Limited Access to the Central Nervous System, Has Antinociceptive Activity. *Br. J. Pharmacol*. **1992**, *106*, 783.

164. Gottschlich, R.; Ackermann, K.A.; Barber, A.; Bartoszyk, G.D.; Greiner, H.E. EMD 61 753 As A Favourable Representative of Structurally Novel Arylacetamido-Type K Opiate Receptor Agonists. *Bioorg. Med. Chem. Letts.* **1994**, *4,* 677.

165. Barber, A.; Bartoszyk, G.D.; Bender, H.M.; Gottschlich, R.; Greiner, H.E.; Harting, J.; Mauler, F.; Minck, K.O.; Murray, R.D.; Simon, M. A Pharmacological Profile of the Novel, Peripherally-Selective κ-Opioid Receptor Agonist, EMD 61753. *Br. J. Pharmacol.* **1994**, *113*, 1317.

166. Gottschlich, R.; Krug, M.; Barber, A.; Devant, R.M. Kappa-Opioid Activity of the Four Stereoisomers of the Peripherally Selective Kappa-Agonists, EMD 60,400 and EMD 61, 753. *Chirality*. **1994**, *6*, 685.

167. Wiley, R.A.; Rich, D.H. Peptidomimetics Derived from Natural Products. *Med. Res. Rev*. **1993**, *3*, 327.

168. Rich, D.H. Effect of Hydrophobic Collapse on Enzyme-Inhibitor Interactions. Implications for the Design of Peptidomimetics. *Perspectives in Medicinal Chemistry*. VCH, New York, **1993**.

169. Barber, A.; Bartoszyk, G.D.; Greiner, H.E.; Mauler, F.; Murray, R.D.; Seyfried, C.A.; Simon, M.; Gottschlich, R.; Harting, J.; Lues, I. Central and Peripheral Actions of the Novel Kappa-Opioid Receptor Agonist, EMD 60400. *Br. J. Pharmacol*. **1994**, *111*, 843.

170. Chang, A.C.; Cowan, A.; Takemori, A.E.; Portoghese, P.S. Aspartic Acid Conjugates of 2-(2,3-Dichlorophenyl)-*N*-methyl-*N*-[(1S)-1-(3-aminophenyl)-2-(1-pyrrolidinyl) ethyl] acetamide: κ Opioid Receptors Agonists with Limited Access to the Central Nervous System. *J. Med. Chem*. **1996**, *39*, 4478.

171. Birch, P.J.; Hayes, A.G.; Johnson, M.R.; Lea, T.A.; Murray, P.J.; Rogers, H.; Scopes, D.I.C. Preparation and Evaluation of Some Hydrophilic Phenylacetyl-piperazines as Peripherally Selective κ-Opioid Receptor Agonists. *Bioorg. Med. Chem. Letts*. **1992**, *2*, 1275.

172. Feuerstein, T.J.; Seeger, W. Modulation of Acetylcholine Release in Human Cortical Slices: Possible Implications for Alzheimer's Disease. *Pharmacol. Ther*. **1997**, *74*, 333.

II. Rationale and Specific Aims

Ligand efficacy for specific signaling pathways can be finely tuned by structural modifications of a ligand.[1-2] In addition, the KOR demonstrates ligand-directed selectivity.[3] Specifically, researchers have shown that the dysphoric effects require activation of G-protein receptor kinase, arrestin recruitment, and subsequent p38 mitogen activated protein kinase (MAPK) activation, whereas their analgesic effects do not.[3] On the basis of this concept, an analgesic KOR agonist that does not activate MAPK would not produce the associated dysphoria.[3] Our central hypothesis is that the structure of U50,488 can be refined to produce ligands with high efficacy for inhibition of cAMP accumulation and low efficacy for ERK and JNK signaling.

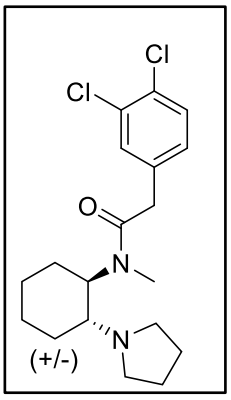

Figure 2.1. Structure of U50,488.

Specifically, we chose to use U50,488 as a scaffold, rather than salvinorin A due to the straightforward synthesis and cost effectiveness of U50,488 analogues. To begin, many analogues of U50,488 have been previously described in the literature dating back to the discovery of the arylacetamide class of KOR agonists.[4-18] However, these were investigated before studies demonstrating that KORs exist as dynamic, multi-conformational protein complexes that can be directed by specific ligands towards distinct signaling pathways.[19] Thus, there is a wealth of knowledge regarding the synthesis of U50,488 analogues that can be utilized in order to study the effects of structural changes on signaling pathways. In addition, as depicted previously by the structure of salvinorin A **(Figure 1.12)** it is evident that salvinorin A is a much more complex molecule with seven chiral centers, whereas U50,488 has only two **(Figure 2.1)**. Thus, the chemistry utilized in order to modify salvinorin A must involve mild reaction conditions, so as to avoid degradation of the molecule in other areas.

In regards to the cost associated with the synthesis, it is much less expensive to generate analogues of U50,488. For example, purchasing 100 mg of salvinorin A or (-)-U50,488 from Sigma Aldrich costs $1,500 and $930, respectively.[20] In comparison, the prices for the stoichiometric reagents necessary for synthesis of U50,488 are as follows: cyclohexene oxide ($56.50 for 500mL), pyrrolidine ($82.10 for 500mL), methanesulfonyl chloride ($31.20 for 100mL), aqueous methylamine solution ($51.80 for 1 L), and 3,4-dichlorophenylacetic acid ($63.20 for 25g).[20] Thus, in regards to costs, it is evident that it is relatively inexpensive to synthesize large quantities of U50,488 analogues, using cheap, commercially available starting materials. In order to test our central hypothesis, we proposed the following:

Specific Aim 1: Design and synthesize analogues of U50,488 and evaluate, *in vitro,* how modifications affect KOR activity. In order to better understand the relationship between structure and functional selectivity for U50,488 analogues, several sites were modified, as follows: the pyrrolidine group, the *N*-alkyl substituent, the linker region, the aryl group, and the cyclohexane ring. Although modifications to these regions have been explored in regards to analogues with increased affinity and potency, the effects on functional selectivity had not been investigated. In addition, we hypothesized that changes to more than one portion of the molecule would result in additive KOR activity. In order to test this hypothesis, we prepared analogues incorporating changes to two of the sites listed above. From the SAR trends elucidated for these analogues, we then identified compounds for further investigation. Our hypothesis is that ligands with activity inconsistent with our SAR trends may be promoting a unique receptor conformation with the ability to differentially regulate signaling pathways. Lastly, we prepared enantiopure ligands for the analogues which produced monotonic CRCs, as identified by specific aim #3.

Specific Aim #2: Evaluate *ex vivo* efficacy, including inhibition of cAMP accumulation and stimulation of ERK. Selected analogues identified in specific aim #1 then proceeded to *ex vivo* measurements of their efficacy to activate $G_{\alpha i}$ and ERK. For each ligand, full concentration response curves (CRCs) measuring inhibition of PGE_2-stimulated cAMP accumulation and stimulation of ERK was completed. The analogues with signaling profiles with maintained or enhanced efficacy at $G_{\alpha i}$ signaling and reduced efficacy at ERK signaling were then tested for their efficacy to inhibit the release of calcitonin gene-regulated peptide (CGRP).

Specific Aim #3: Evaluate *ex vivo* inhibition of CGRP release. Analogues with efficacy similar to (-)-U50,488, for signaling pathways leading to antinociception, and reduced efficacy for signaling pathways leading to nociception, were then assessed for their ability to inhibit calcitonin gene-regulated peptide (CGRP). CGRP is a neuropeptide released by the nerve endings of activated nociceptors and its neurosecretion can be used as an index of the overall, integrated activity of nociceptor ability.[13] As such, this assay provides a translational measure for antinociception, i.e. the action of drugs to alter CGRP has high fidelity with their effects in the behavioral assay.

Thus, by accomplishing the aims outlined above, we intend to show that structural modifications to the U50,488 scaffold will alter ligand efficacy for specific signaling pathways. We anticipate that these molecules will be useful biological probes for studying KOR-mediated antinociception. Ultimately, our long-term goal is that these ligands may lead to new drugs with improved therapeutic profiles for the treatment of pain.

References

1. Chen, X.; Sassano, M.F.; Zheng, L.; Setola, V.; Chen, M.; Bai, X.; Frye, S.V.; Wetsel, W.C.; Roth, B.L.; Jin, J. Structure-Functional Selectivity Relationship Studies of β-arrestin-biased Dopamine D_2 Receptor Agonists. *J. Med. Chem.* **2012**, *55,* 7141.
2. Shonberg, J.; Herenbrink, C.K.; Lopez, L.; Christopolous, A.; Scammells, P.J.; Capuano, B.; Lane, J.R. A Strucutre-Activity Analysis of Biased Agonism at the Dopamine D_2 Receptor. *J. Med. Chem.* **2013**, *56*, 9221.
3. Bruchas, M.R.; Chavkin, C. Kinase Cascades and Ligand-Directed Signaling at the Kappa Opioid Receptor. *Neuropyschopharmacology,* **2010**, *210(2)*, 137.
4. Scopes, D.I.C.; Hayes, D.E.; Bays, D.; Belton, J.; Brain, D.S.; Brown, D.B.; Judd, D.B.; McElroy, A.B.; Meerholz, C.A.; Naylor, A. New κ-Receptor Agonists Based on a 2-[(alkylamino)methyl]piperidine Nucleus. *J Med. Chem.* **1992**, *35*, 490.
5. Hayes, A.G.; Birch, P.J.; Hayward, N.J.; Sheehan, M.J.; Rogers, H.; Tyers, M.B.; Judd, D.B.; Scopes, D.I.C.; Naylor, A. A Series of Novel, Highly Potent and Selective Agonists for the κ-Opioid Receptor. *Br. J. Pharmacol*. **1990**, *191*, 994.
6. Naylor, A.; Judd, J.B.; Lloyd, J.E.; Scopes, D.I.C.; Hayes, A.G.; Birch, P.J. A Potent New Class of κ-Receptor Agonist: 4-Subsituted 1(-arylacetyl)-2-[(dialkylamino)methyl]piperazines. *J. Med. Chem*. **1993**, *36*, 2075.
7. Vecchietti, V.; Giordani, A.; Girdina, G.; Colle, R.; Clarke, G.D. (2S)-1-(arylacetyl)-2-(aminomethyl)piperidine Derivatives: Novel, Highly Selective Kappa Opioid Analgesics. *J. Med. Chem.* **1991**, *34*, 397.
8. Vecchietti, V.; Clarke, G.D.; Colle, R.; Dondio, G.; Giardina G.; Petrone, G.; Sbacchi, M. Substituted 1-(aminomethyl)-2-(arylacetyl)-1,2,3,4-tetrahydroisoquinolines: A

Novel Class of Very Potent Antinociceptive Agents with Varying Degrees of Selectivity for Kappa and Mu Opioid Receptors. *J. Med. Chem*. **1992**, *35*, 2970.

9. Vecchietti, V.; Clarke, G.D.; Colle, R.; Giardina, G.; Petrone, G.; Sbacchi, M. (1S)-1-(aminomethyl)-2-(arylacetyl)-1,2,3,4-tetrahydroisoquinoline and Heterocycle-Condensed Tetrahydropyridine Derivatives: Members of a Novel Class of Very Potent Kappa Opioid Analgesics. *J. Med. Chem.* **1991**, *34*, 2624.
10. Giardina, G.; Clarke, G.D.; Dondio, G.; Petrone, G.; Sbacchi, M.; Vecchietti, V. Selective κ-Opioid Agonists: Synthesis and Structure-Activity Relationships of Piperidines Incorporating an Oxo-Containing Acyl Group. *J. Med. Chem.* **1994**, *37,* 3482.
11. Colle, R.; Clarke, G.D.; Dondio, G.; Giardina, G.; Petrone, G.;Sbacchi, M.; Vecchietti, V. Enantiospecificity of Kappa Receptors: Comparison of Racemic Compounds and Active Enantiomers in Two Novel Series of Kappa Agonist Analgesics. *Chirality,* **1992**, *4*, 8.
12. Fujibayashi, K.; Kubota, K.; Saito, K. Effects of R-84760, A Selective Kappa-Opioid Receptor Agonist, on Nociceptive Reflex in Isolated Neonatal Rat Spinal Cord. *Eur. J. Pharmacol*. **1998**, *343,* 171.
13. Halfpenny, P.R.; Horwell, D.C.; Hughes, J.; Humblet, C.; Hunter, J.C.; Neuhaus, D.; Rees, D.C. Highly Selective κ Opioid Analgesics. *J. Med. Chem*. **1991**, *34,* 190.
14. Tortella, F.C.; Rose, J.; Robles, L.; Moreton, J.E.; Hughes, J.; Hunter, J.C. EEG Spectral Analysis of the Neuroprotective Kappa opioids in Enadoline and PD117302. *J. Pharmacol. Exp. Ther.* **1997**, *282*, 286.

15. Sabin, V.; Horwell, D.C.; McKnight, A.T.; Broqua, P. *Trans N*-Methyl-*N*-[2-(1-pyrrolidinylcyclohexyl] cycloprop-2-ene-1-carboxamides: Novel Lipophilic Kappa Opioid Agonists. *Bioorg. Med. Chem. Letts*. **1997**, *7*, 291.
16. Rajagopalan, P.; Scribner, R.M.; Pennev, P.; Schmidt, W.K.; Tam, S.W.; Steinfels, G.F.; Cook, L. DuP 747: A New, Potent, Kappa Opioid Analgesic. Synthesis and Pharmacology1. *Bioorg. Med. Chem. Letts*. **1992**, *2*, 715.
17. Rajagopalan, P.; Scribner, R.M.; Pennev, P.; Mattie, P.L.; Kezar, H.S.; Cheng, C.Y.; Cheeseman, R.S.; Ganti, V.R.; Johnson, A.L.; Wuonola, M.A. DuP 747: SAR Study. *Bioorg. Med. Chem. Letts.* **1992**, *2*, 721.
18. Hamon, G.; Celemence, F.; Fortin, M.; Martret, O.L.; Jouquey, S.; Vincent, J.C.; Petit, F.; Bichet, D.G. Effects of Subchronic Administration of Niravoline, A Novel Aquaretic Compound, On Water and Electrolyte Renal Excretion in Cirrhotic Rats. *Brit. J. Pharmacol*. **1995**, *114*, 310.
19. Bamana, I.; Nagao, S. Effects of Niravoline (RU 51599), A Selective Kappa-Opioid Receptor Agonist on Intracranial Pressure in Gradually Expanding Extradural Mass Lesion. *J. Neurotrama*. **1998**, *15*, 117.
20. Sigma Aldrich. **2017**, www.sigmaaldrich.com.

III. Results and Discussion

In order to investigate the functional selectivity of KOR agonists, several compounds based on the U50,488 scaffold were synthesized and evaluated. Selected analogues were further evaluated for inhibition of PGE_2-stimulated cAMP accumulation and activation of ERK in CHO cells transiently transfected with rat KORs. In addition, the ligands were assessed for their ability to inhibit calcitonin gene-related peptide (CGRP) release, as a translational measure for antinociception.

Specific Aim 1: Design and synthesize analogues of U50,488 and evaluate, *in vitro,* how modifications affect KOR activity. To provide a more thorough representation of the how structural modification of U50,488 affects activity at the KOR, several analogues were designed.

First of all, in regards to modification of the pyrrolidine group, several analogues were proposed **(Figure 3.1)**. In order to evaluate steric effects, we aimed to increase the size of the pyrrolidine ring by one and two methylene units **(4a-4b)**. The rationale is that by increasing the size of the pyrrolidine ring, we will identify if the pyrrolidine binds in a tight pocket in the receptor or if increasing lipophilicity increases KOR activity. Next, in order to gain information regarding how introduction of a second heteroatom affects KOR activity, we planned to substitute the pyrrolidine with morpholine and *N*-methylpiperazine, respectively **(4c-4d)**. We envisioned that if an H-bond donor were present in the active site, then the morpholine analogue would have increased activity. Also, we chose a *N*-methyl piperazine substituent to determine how introduction of

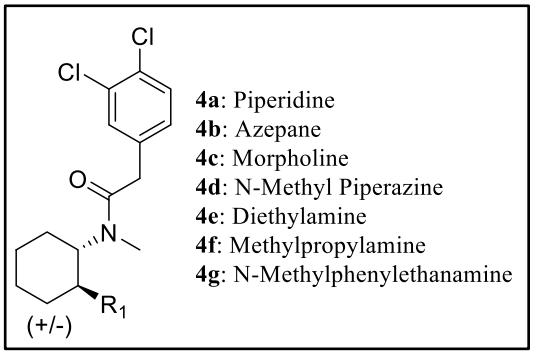

Figure 3.1. Proposed analogues with modifications of the pyrrolidine group.

a second heteroatom, which does not have H-bonding potential, affects KOR activity. To further probe the steric effects of this region, we proposed non-cyclic derivatives with varying degrees of alkylation **(4e-4g)**. Specifically, we chose diethylamine and methypropylamine to mimic the size of the pyrrolidine group, in order to investigate the effects of conformational flexibility of this region. In addition, we also chose to substitute *N*-methylphenylethanamine in order to determine, as mentioned above, if the receptor binding region for this portion of the molecule tolerates larger substituents. We hypothesize that if the binding region is a small, specific, pocket, then the *N*-methylphenylethanamine analogue will eliminate KOR activity.

Secondly, in regards to modification of the *N*-alkyl substituent, we designed two analogues **(Figure 3.2)**. Specifically, we evaluated homologation to an ethyl and benzyl group **(7a-7b)**. First, we chose homologation to an ethyl group to determine if the smallest change in the steric hindrance at this position is tolerated. We also decided to investigate the effect on KOR activity for substitution to a benzyl group to assess not only if larger substitutions were tolerated, but also if the addition of an aromatic ring would increase KOR activity. We hypothesized that if an aromatic amino acid was near the binding pocket for this particular substituent, then the addition of a benzyl group may allow favorable pi-stacking interactions, resulting in increased KOR activity.

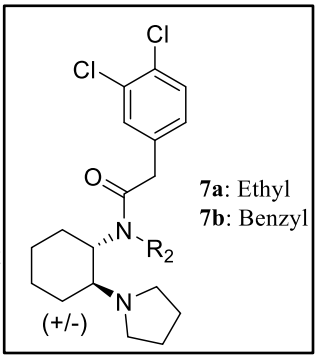

Figure 3.2. Proposed analogues with modifications of the *N*-alkyl group.

Third, we envisioned several analogues with modifications to the 3,4-dichlorophenyl ring **(Figure 3.3)**. Based on previous SAR studies, we knew that 3,4-dichlorosubstitutents result in potent KOR activity.[3-7] However, a systematic analysis of the effects of KOR activity on analogues with a single substituent or a change in substitution patterns has not been investigated. Thus, we proposed to examine the steric and electronic effects associated with

various substitutions **(9a-9q)**. The electronic differences in the substitutions spanned from strongly electron withdrawing groups, such as the nitro moiety **(9j-9k)**, to electron donating groups, such as the methoxy moiety **(9p-9q)**. In addition, previous studies have shown that a benzo[b]thiophene and benzo[b]furan are potent KOR agonists.[8] Therefore, we planned to synthesize analogues with a 4-Phenyl, 2-Napthyl, and 3-Napthyl group **(9r-9t)** to see if these analogues were also tolerated, or if the heteroatom in the analogues described above is interacting with the receptor to increase activity. To conclude our substitutions to the aryl group, we decided to investigate changes in substitution patterns for the halogens **(9u-9y)** to determine if alternate patterns are tolerated. As mentioned above, effects of changing the substitution patterns of U50,488 have not been thoroughly investigated. Therefore, we proposed to evaluate whether various dichloro- patterns were tolerated, whether a difluoro- analogue resulted in equivalent potency, and the effects of substituting a fluoro- for one of the chloro- groups. We hypothesize that the 2,4-substitution pattern, and replacement of the chloro- groups with fluoro- will not significantly change the KOR activity.

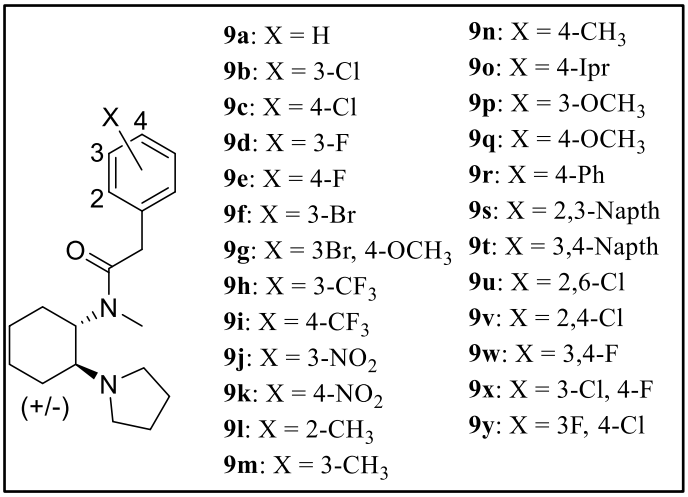

Figure 3.3. Proposed analogues with modified aryl groups.

Next, we proposed to investigate the role of the linker between the amide and aryl group **(Figure 3.4)**. Specifically, we designed analogues in which the linker region was extended by one or two methylene units **(9aa-9ab)**. We hypothesized that if the binding pocket for the aryl group is a deep pocket, then by extending the linker region, we may be able to gain more favorable interactions. However, if the binding pocket is a relatively tight

fit for the aryl group, then extension of the linker region will not be tolerated. In addition, in order to assess how the addition of a heteroatom affects the KOR activity, we designed an analogue incorporating an oxygen in the linker region **(9ac)**. The rationale is that if the oxygen is in the proximity of a H-bond donor in the receptor pocket, then we will observe increased KOR activity as a result. Then, to evaluate the effects of conformational constraint of U50,488, we proposed analogues incorporating a cyclopropane and cyclopentane group **(9ad-9ae)**, respectively. Thus, if we are able to lock the conformation of the molecule in its preferred position, we expect increased KOR activity. However, if conformational flexibility is preferred, we expect a loss of KOR activity.

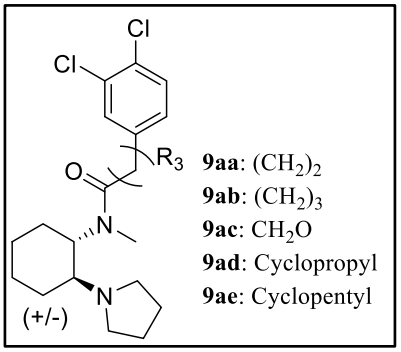

Figure 3.4. Proposed analogues with modifications to the linker region.

Finally, we planned to evaluate how KOR activity is affected by replacement of the cyclohexane ring **(Figure 3.5)**. To begin, we designed an analogue where the cyclohexane core was replaced with an aromatic ring to assess the effects of a planar backbone which alters the basicity of the amine **(12)**. A majority of KOR agonists require a basic nitrogen for their activity. However, certain analogues, such as salvinorin A, do not. Therefore, we proposed to synthesize this compound to determine if decreasing the basicity of the amine alters the KOR activity. In addition, the cyclohexane group was replaced with an ethylene linker to assess the effects of conformational flexibility of the molecule **(14)**. Much like conformational constraint via a cyclopropyl or cyclopentyl group, we anticipated that if conformational flexibility of U50,488 was preferred, we would see an increase in KOR

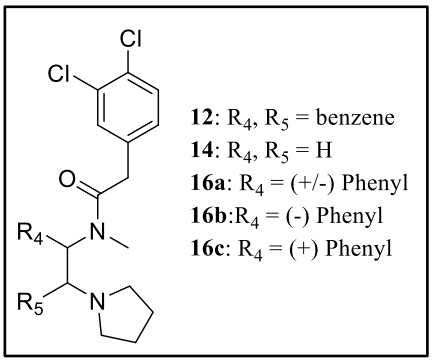

Figure 3.5. Proposed analogues with modifications to the cyclohexane ring.

activity with cleavage of the cyclohexane ring; whereas, if the cyclohexane ring is locking the molecule in the preferred conformation, then cleavage would result in a loss of KOR. Finally, previous studies[9] have shown that a non-fused phenyl ring results in potent KOR activity. Therefore, we synthesized this analogue adjacent to the amide in order to test the steric requirements for this particular position, as well as the preferred absolute configuration for this group **(16a-16c)**.

Synthesis of Proposed U50,488 Analogue

Analogues with Modification to the Pyrrolidine Group

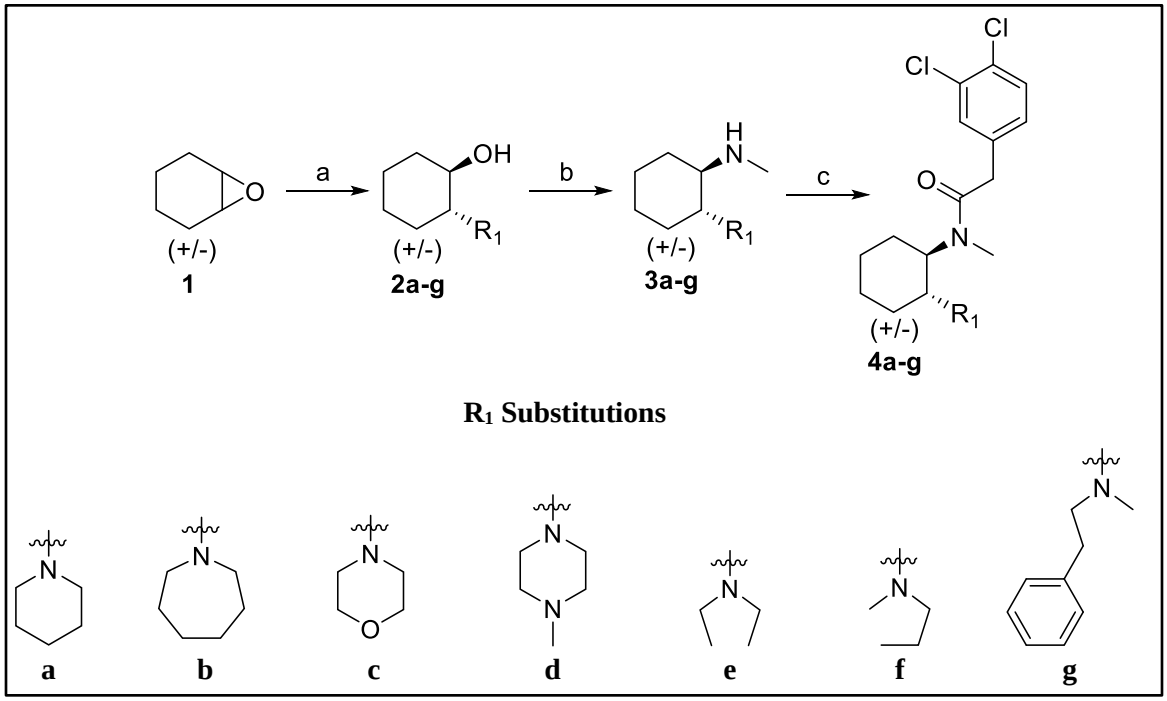

Scheme 3.1. Synthesis of U50,488 analogues with substituted pyrrolidine group. Reagents and conditions: a) R_1, EtOH, 80°C, Overnight; b) MsCl, Et_3N, 0°C, 2 hours; $MeNH_2$, RT, Overnight; c) 3,4-dichlorophenylacetic acid, HOBt, DIPEA, EDCI, RT, 4 hours.

The first step of the synthesis involves the reaction of cyclohexene oxide **(1)** and the amine (piperidine, morpholine, *N*-methyl piperazine, azepane, diethylamine, methylpropylamine, or *N*-methyl-2-phenylethanamine) at reflux, overnight **(Scheme 3.1)**. This yields a 2-substituted cyclohexanol **(2a-2g)** in quantitative yields with no additional purification necessary. Cyclohexanols **(2)** were then reacted with methanesulfonyl chloride

(MsCl) in the presence of triethylamine (Et_3N). Addition of methylamine then generates a racemic mixture of the corresponding diamine **(3a-3q)**. Finally, treatment of the appropriate diamine **(3a-3q)** with 3,4-dichlorophenylacetic acid, utilizing HOBt, DIPEA, and EDCI in DMF, at room temperature, gives the desired aryl acetamides **(4a-4g)**.

Homologation of the N-Alkyl Group of U50,488

Compounds **7a** and **7b** were prepared as shown in **(Scheme 3.2)**. To begin, the aminocyclohexanol **(5)**[1] was reacted with MsCl in the presence of Et_3N, followed by ethylamine and benzylamine, respectively, to form the racemic diamine intermediate **(6a-6b)**. Treatment of **(6a-6b)** with 3,4-dichlorophenylacetic acid, utilizing Et_3N and the catalyst, PyBrop, at 0°C to deliver the desired products **(7a-7b)**.

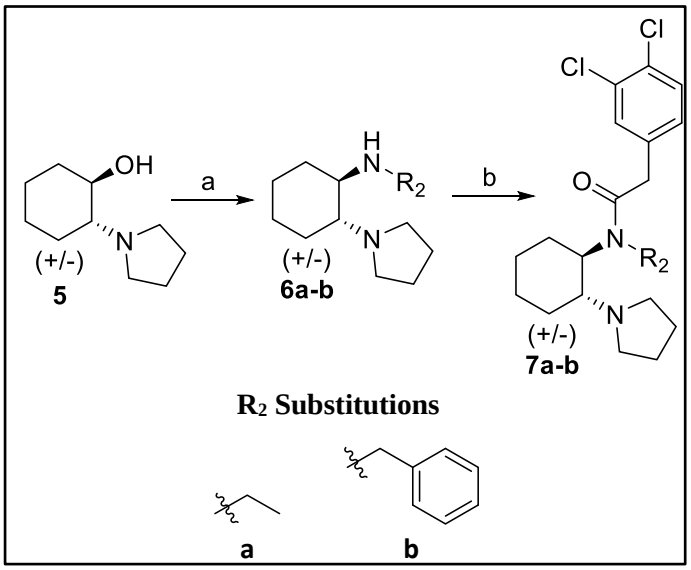

Scheme 3.2. Synthesis of U50,488 analogues with modified *N*-alkyl substituents. Reagents and conditions: a) MsCl, Et_3N, 0°C, 2 hours; R_2NH_2, RT, Overnight; b) 3,4-dichlorophenylacetic acid, Et_3N, PyBrop, 0°C, 1 hour.

Analogues with Modification to the Aromatic Group and Linker Region

The next series of analogues involved substitutions of the aryl group and modification of the linker region **(Scheme 3.3)**. The racemic diamine **(8)**[1] was reacted with various acids and acid chlorides utilizing three coupling methods to afford **9a-9ae**. The first coupling method involved the treatment of **8** with the appropriate acid, utilizing HOBt, DIPEA, and EDCI in DMF, at room temperature. The second method reacted **8** with the corresponding

acid chloride at 0ºC. The third method, catalyzes the reaction between the appropriate acid and **8**, using PyBrop and Et_3N at 0ºC.

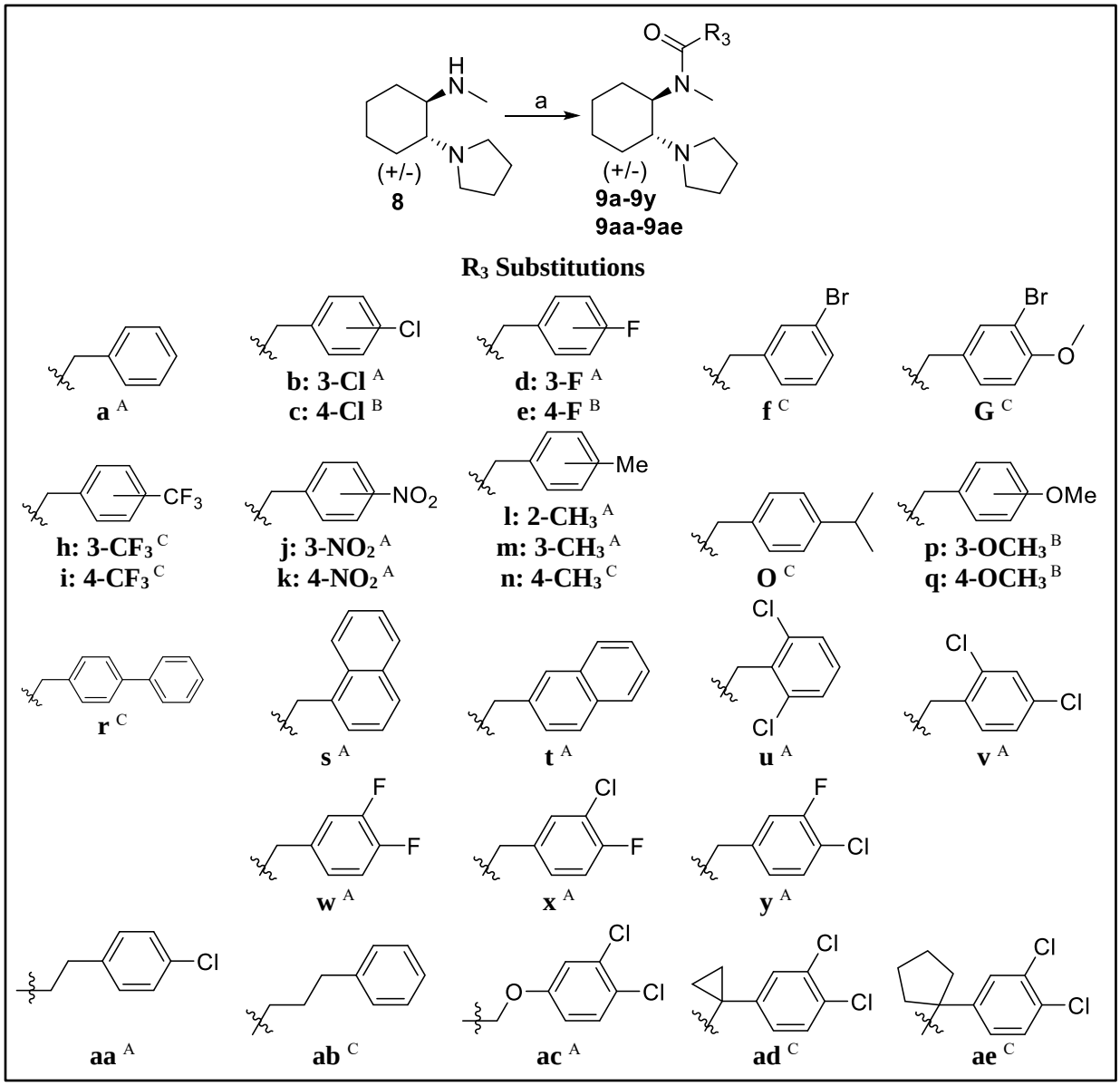

Scheme 3.3. Synthesis of U50,488 analogues with modified aryl groups (**a-y**) and modified linker regions (**aa-ae**). Reagents and conditions: a) Pyrrolidine, EtOH, 80ºC, Overnight; b) MsCl, Et_3N, 0ºC, 2 hours; $MeNH_2$, RT, Overnight; c) Method A: R_3COOH, HOBt, DIPEA, EDCI, RT, Method B: R_3COCl 0ºC, Method C: R_3COOH, Et_3N, PyBrop, 0ºC.
[A]Analogues prepared by Method A.
[B]Analogues prepared by Method B.
[C]Analogues prepared by Method C.

Analogues with Modification to the Cyclohexane Ring

Synthesis of the first analogue, with the cyclohexane core as an aromatic ring began with commercially available 2-(pyrrolidine-1-yl)aniline **(10)**, which was reacted with 3,4-dichlorophenylacetic acid utilizing HOBt, DIPEA, and EDCI in DMF at room temperature **(Scheme 3.4)**. This resulted in the intermediate **(11)**, which was used to prepare the final compound **(12)** via the action of NaH and MeI.

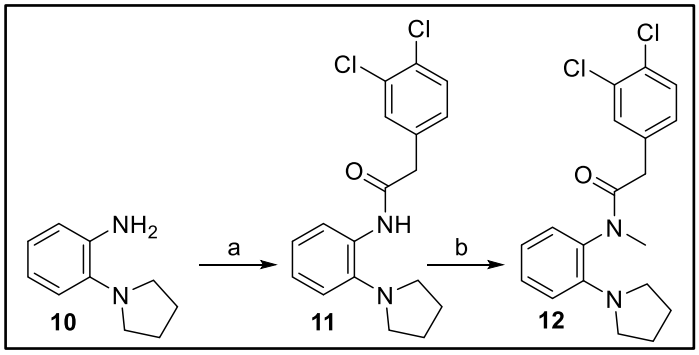

Scheme 3.4. Synthesis of analogue with aromatic core. Reagents and conditions: a) 3,4-dichlorophenylacetic acid, HOBt, DIPEA, EDCI, RT; b) NaH, MeI, RT.

The cyclohexane ring was then replaced with an ethylene group **(Scheme 3.5)**. Synthesis began from *N*-methyl-2-(pyrrolidine-1-yl)ethan-1-amine **(13)**. Upon condensation with 3,4-dichlorophenylacetic acid utilizing HOBt, DIPEA, and EDCI in DMF at room temperature, the aryl acetamide **(14)** was formed.

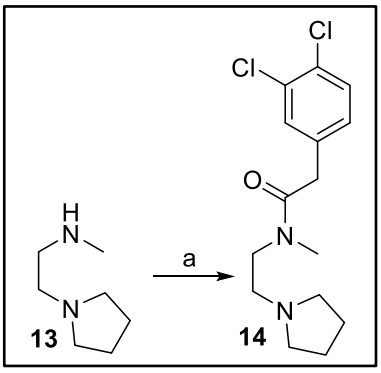

Scheme 3.5. Synthesis of U50,488 analogue with ethylene core. Reagents and conditions: a) 3,4-dichlorophenylacetic acid, HOBt, DIPEA, EDCI, RT.

Lastly, an analogue with a 1-phenethyl core was synthesized **(Scheme 3.6)**. Synthesis initiated from either the racemic starting material **(15a)**, or the two enantiopure molecules **(15b-15c)**, respectively, of *N*-Methyl-1-phenyl-2-(1-pyrrolidinyl)ethylamine. Reaction with 3,4-dichlorophenylacetic acid with HOBt, DIPEA, and EDCI in DMF at room temperature yielded the desired products **(16a-16c)**.

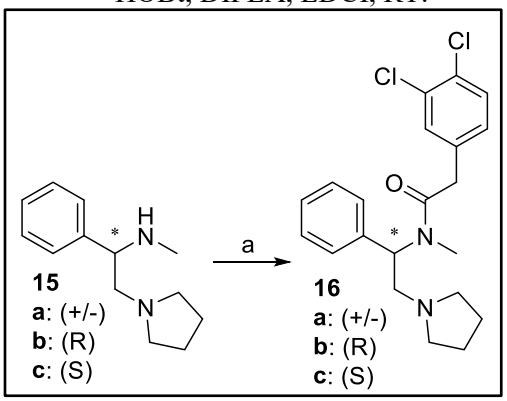

Scheme 3.6. Synthesis of analogues with a 1-phenethyl core. Reagents and conditions: a) 3,4-dichlorophenylacetic acid, HOBt, DIPEA, EDCI, RT.

In Vitro Evaluation of the KOR Activity of Analogues

KOR activity was determined via a DiscoveRx HitHunter® cAMP Assay, as depicted in **Figure 3.6**. This *in vitro* measure of receptor activation utilizes CHO cells overexpressing the KOR. Forskolin is used to induce the production of cAMP. Activation of the receptor via KOR agonists results in the release of $G_{\alpha i}$ which inhibits the production of cAMP. The levels of cAMP can then be quantified via luminescence using a plate reader.[2] The resulting dose-response data was then normalized to vehicle and forskolin only control values and analyzed using nonlinear regression with GraphPad Prism v6.07.

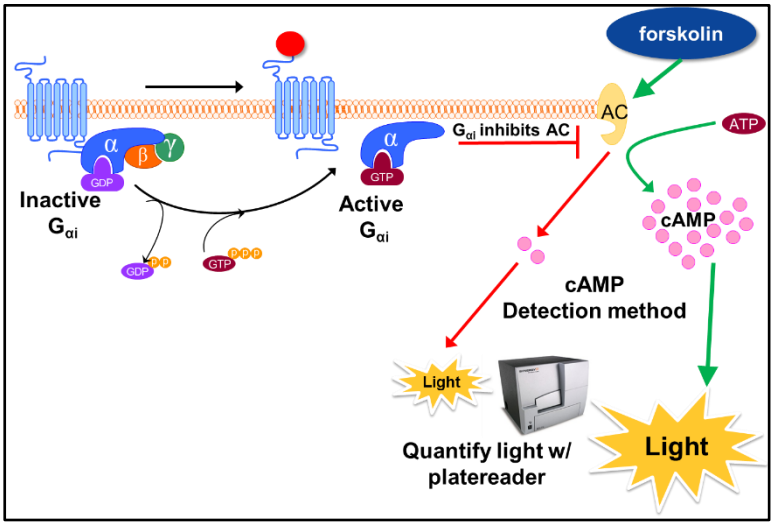

Figure 3.6. Depiction of the GPCR signaling pathway of the DiscoveRx cAMP functional assay.

Compound #	$EC_{50} \pm$ SEM nM	Compound #	$EC_{50} \pm$ SEM nM	Compound #	$EC_{50} \pm$ SEM nM
(-)-U50,488	**0.12 ± 0.02**	**9f**	0.62 ± 0.05	**9u**	0.46 ± 0.21
4a	24 ± 6.0	**9g**	2.8 ± 0.5	**9v**	1.9 ± 0.7
4b	4.0 ± 1.0	**9h**	1.1 ± 0.3	**9w**	1.5 ± 0.7
4c	> 10,000	**9i**	1.8 ± 0.8	**9x**	0.16 ± 0.03
4d	> 10,000	**9j**	1.6 ± 0.1	**9y**	0.35 ± 0.09
4e	39 ± 2.0	**9k**	3.0 ± 0.7	**9aa**	> 10,000
4f	0.75 ± 0.04	**9l**	5.0 ± 1.0	**9ab**	> 10,000
4g	210 ± 60	**9m**	7.0 ± 2.0	**9ac**	1.2 ± 0.6
7a	24 ± 1	**9n**	8.0 ± 3.0	**9ad**	> 10,000
7b	> 10,000	**9o**	8.0 ± 2.0	**9ae**	> 10,000
9a	30 ± 10	**9p**	16 ± 4	**12**	> 10,000
9b	3.3 ± 0.2	**9q**	100 ± 20	**14**	> 10,000
9c	4.0 ± 1.0	**9r**	> 10,000	**16a**	0.007 ± 0.002
9d	7.0 ± 1.0	**9s**	0.32 ± 0.08	**16b**	0.14 ± 0.02
9e	4.2 ± 1.0	**9t**	20 ± 7	**16c**	0.005 ± 0.001

Table 3.1. KOR activity of analogues in which one region of U50,488 is modified.

The KOR activity for each of the analogues in which the pyrrolidine group is modified is shown in **Table 3.1**. Replacement of the pyrrolidine with 6-membered analogues (piperidine **(4a)**, morpholine **(4c)**, *N*-methyl piperazine **(4d)**) results in decreased potency, compared to (-)-U50,488. Specifically, the incorporation of a second heteroatom (morpholine **(4c)**, *N*-methyl piperazine **(4d)**) results in complete loss of KOR activity. Based on these trends, we hypothesize that the binding pocket for the pyrrolidine group is a small and unable to accommodate larger cyclic groups. In addition, it appears that this pocket does not have an H-bond donor in close enough proximity to bind with the morpholine. Interestingly, replacement of the pyrrolidine with azepane **(4b)**, however, is better tolerated. We rationalize this observation based on the azepane ring remaining in a puckered conformation. This conformation more closely resembles the conformation of pyrrolidine than the possible conformations of the cyclohexane ring (boat or chair conformations). In regards to non-cyclized compounds, the data supports our hypothesis above that the binding pocket is small. Consequently, the small, alkyl amines we designed (diethylamine **(4e)** and methylpropylamine **(4f)**) are much better tolerated than the bulky amine, *N*-ethyl-2-phenylethanamine **(4g)**.

Next, the resulting KOR activity for analogues of the *N*-alkyl group will be examined. According to the data, homologation from a methyl to an ethyl group **(7a)** decreases the potency, compared to (-)-U50,488 by 200-fold, indicating that there is likely an unfavorable steric clash in the binding site. Further validation of this hypothesis is provided by substitution with a benzyl group **(7b)**, which eliminates KOR activity.

In regards to the KOR activity of the aryl group, an unsubstituted phenyl **(9a)** results in decreased potency, as expected based on previous SAR trends.[3-4] Further confirming previous studies, it is evident that electron withdrawing groups (EWGs), such as Br, Cl, F,

CF_3, and NO_2 **(9b-9f, 9h-9k)**, are preferred in both the meta and para positions of the aryl ring. Correspondingly, the compounds with aliphatic groups, such as CH_3 and $CH(CH_3)_2$ **(9l-9o)**, or electron donating groups (EDGs), such as OCH_3 **(9p-9q)**, are less potent than the corresponding substitutions with EWGs.[6-8] Specifically, one analogue **(9g)** incorporating both an EWG (Br) and an EDG (OCH_3) has activity more closely matching the molecule with only the corresponding EWG [compare **9g** (3-Br,4-OCH_3), **9f** (3-Br), and **9q** (4-OCH_3)]. This observation demonstrates that the presence of a single EWG can overcome a large portion of the KOR activity loss caused by an EDG. In addition, we analyzed the effect of KOR activity on analogues with a single substituent. In regards to the EWG and neutral analogues, there is not a clear trend for preference of the meta or para position. However, upon examination of the EDGs, the meta substituted OCH_3 group is greater than 6-fold more potent than the corresponding para substituent. Next, in regards to the steric effects of bulky substitutions, a 4-phenyl substitution results in a complete loss of KOR activity **(9r).** Conversely, a 2-napthyl substituent **(9s)** leads to potent KOR activity; whereas a 3-napthyl substituent **(9t)** leads to activity closely matching that of an unsubstituted phenyl group. This result could indicate that there is an additional hydrophobic binding pocket that the 2,3-napthyl substituted analogue can access, which results in greater KOR activity. Finally, in regards to various substitution patterns for the halogens, we originally hypothesized that replacement of the chloro- groups with fluoro- groups would not significantly change KOR activity. In addition, we hypothesized that the 2,4-dichloro- analogue would have greater activity than the 2,6-dichloro- analogue. We observed that the 2,4-dichloro- analogue **(9v)** and the 3,4-difluoro-analogue **(9w)** are slightly more potent than the corresponding substitutions in only one position. We also observed similar potencies for the 2,6-dichloro- substitution pattern **(9u)**, the 3-Cl,4-F analogue **(9x)**, and the 3-F,4-Cl analogue **(9y)**. Specifically, the

potency of the 2,6-dichloro substituent **(9u)** was greater than we hypothesized. We propose this could be caused by the ortho substituents locking the molecule into a favorable conformation.

In regards to analogues with a modified linker region, the KOR activity shows that extension of the linker by one or two methylene units is not tolerated **(9aa-9ab)**. This result can be rationalized by a shallow binding pocket for the aryl group, which is further validated by **9r**, as described above. The addition of an oxygen atom, however, is tolerated **(9ac)**. We hypothesize that this could be the result of an additional H-bonding interaction. Next, the data shows that conformational constraint of U50,488 analogues via a cyclopropyl or cyclopentyl group leads to a complete loss of KOR activity **(9ad-9ae)**, signifying that some degree of flexibility of the molecules is preferred.

Finally, the KOR activity for analogues with changes to the cyclohexane ring was determined. The data shows that replacement with an aromatic ring leads to complete loss of KOR activity **(12)**, likely due to the altered basicity of the amine. In addition, cleavage of the backbone to an ethylene linker results in a loss of KOR activity **(14)**. As expected, based on literature precendence,[9] the racemic 1-phenethyl derivative resulted in a nearly 20-fold increase in potency **(16a)**, compared to (-)-U50,488. Subsequent synthesis of the enantiopure analogues, **(16b-16c)** and determination of their KOR activity, shows that the (S) derivative **(16c)** is the eutomer, with the highest potency of any of analogue tested.

Specific Aim #2: Evaluate *ex vivo* efficacy, including inhibition of cAMP accumulation and stimulation of ERK. Select analogues, as depicted in **Figure 3.7**, were further evaluated for *ex vivo* efficacy. These analogues were prioritized for *ex vivo* testing because their KOR activity was inconsistent with the SAR trends we observed. For example, substitution of the pyrrolidine ring with six-membered analogues resulted in decreased potency compared to

(-)-U50,488. However, substitution with an azepane ring was tolerated **(4b)**. Also, regarding changes in the substitution pattern, a 2,6-dichloro substituted aryl group resulted in approximately a 3-fold decrease in potency **(9u)**, compared to (-)-U50,488; whereas, a 2,4-dichloro substituted aryl group decreased potency by nearly 16-fold.

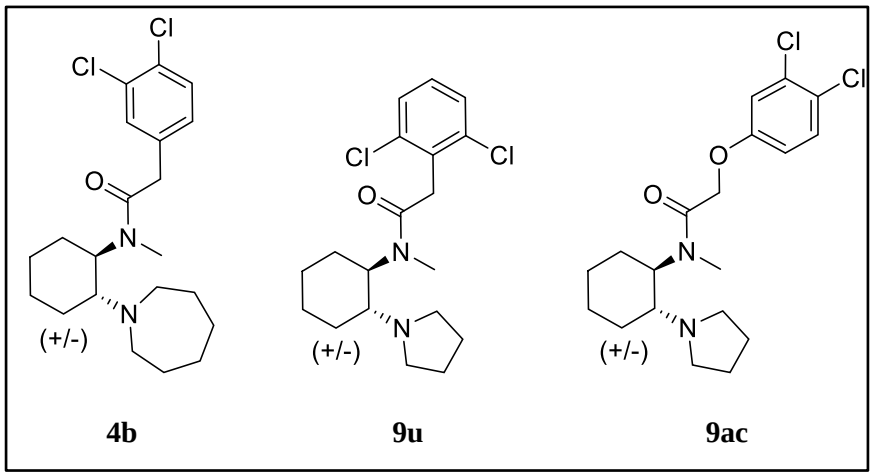

Figure 3.7. KOR ligands that were evaluated *ex vivo*.

Lastly, additional alkyl spacers and conformational constraint of U50,488 resulted in a loss of KOR activity. However, the addition of an oxygen spacer was tolerated **(9ac)**. Our hypothesis is that ligands with activity inconsistent with our SAR trends may be promoting a unique receptor conformation with the ability to differentially regulate signaling pathways. Specifically, these analogues were tested for their ability to activate $G_{\alpha i}$ and ERK signaling in primary cultures of adult rat peripheral sensory neurons. $G_{\alpha i}$ and ERK activation are indices for antinociception and nociception, respectively.

In regards to the ability to inhibit AC activity, the analogues have similar activity compared to (-)-U50,488 **(Figure 3.8)**. It is known that this pathway is responsible for leading to antinociceptive effects. Therefore, based on this data, we anticipate that compounds **4b**, **9u**, and **9ac** will have similar analgesic effects as compared to (-)-U50,488.

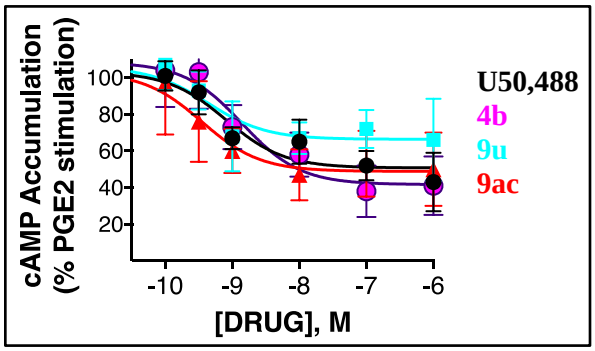

Figure 3.8. Inhibition of cAMP accumulation for KOR analogues.

Unlike (-)-U50,488, however, the analogues tested do not activate ERK **(Figure 3.9)**. Since activation of ERK ultimately leads to dysphoric effects, we expect that these ligands will cause decreased incidence of dysphoria. These results indicate that all three of the compounds have signaling profiles that differ from that of (-)-U50,488.

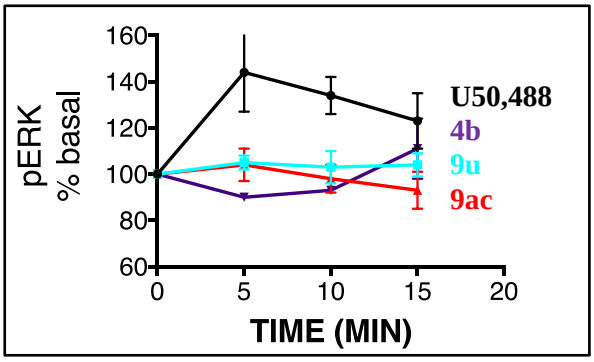

Figure 3.9. ERK phosphorylation of select KOR ligands.

Thus, the three analogues described above all have maintained efficacy for pathways leading to nociception (cAMP accumulation assay), and reduced efficacy for signaling pathways leading to nociception (ERK phosphorylation assay). Therefore, each of the ligands will proceed for evaluation of their ability to inhibit CGRP release.

Specific Aim #3: Evaluate *ex vivo* inhibition of CGRP release. Based on the success of the ligands, as described above, **4b**, **9u**, and **9ac** were assessed for their ability to inhibit calcitonin gene-related peptide release (CGRP). CGRP is a neuropeptide released by the nerve endings of activated nociceptors and its neurosecretion can be used as an index of the overall, integrated activity of nociceptor ability. As such, this assay provides a translational measure for antinociception, i.e. the action of drugs to alter CGRP has high fidelity with the effects in the behavioral assay.

In regards to the concentration-response curve (CRC) **(Figure 3.10)**, the ligands tested produce monotonic CRCs, as opposed to the inverted-U CRC displayed by (-)-U50,488. However, in contrast to the

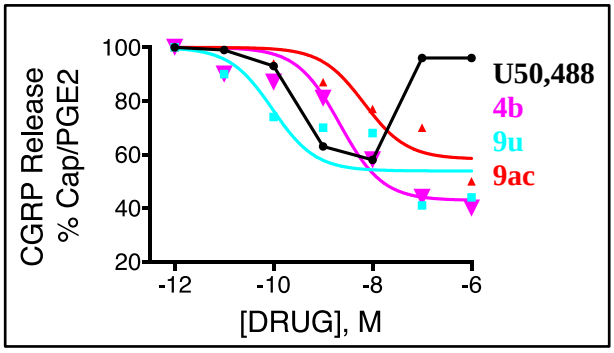

Figure 3.10. Inhibition of GCRP release for select U50,488 analogues.

inhibition of cAMP accumulation, the potency of the ligands differs, as follows: **9u** > **9ac** > **4b**. The difference in the CGRP release amongst the three ligands is important because it indicates that they may be differentially regulating alternative pathways leading to nociception i.e. these ligands may be activating different MAPKs.

Synthesis and *In Vitro* Analysis of Enantiopure Analogues

Based on the success of the functionally selective KOR ligands described above, synthesis of enantiopure ligands was initiated in order to determine the eutomer for each of the *trans*-isomers of the functionally selective ligands **(Figure 3.11)**. Structurally, these ligands differ in three regions of the molecule: the pyrrolidine group, linker region, and aryl group. Thus, it was envisioned that ligands incorporating more than one of the modifications above would result in additive changes to KOR activity. Therefore, in order to determine if additive changes result in additive KOR activity, we also initiated synthesis of enantiopure isomers incorporating changes to two regions of U50,488, as shown in **Figure 3.11**.

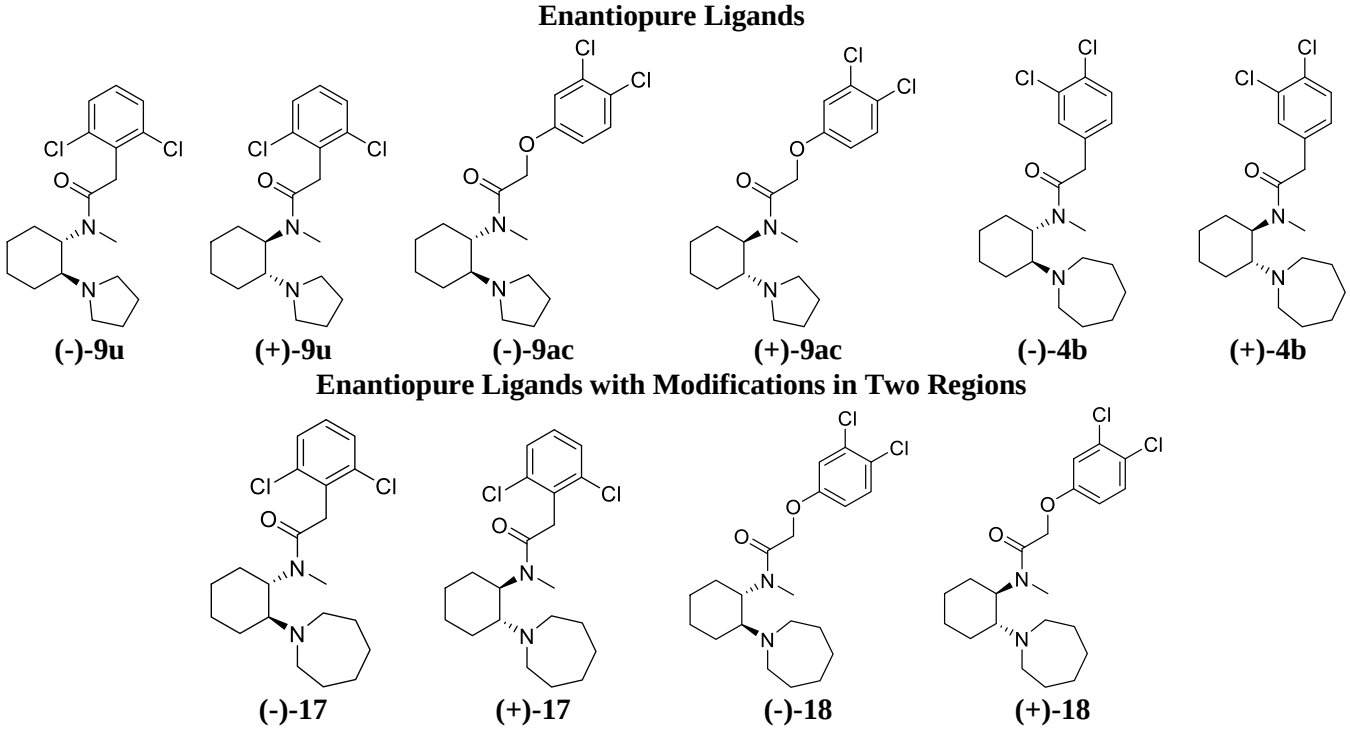

Figure 3.11. Proposed enantiopure analogues.

The chemistry related to these analogues begins as described previously with **(8)** **(Scheme 3.6)**.[10] The racemic diamine **8** and 2,3-di-p-toluoyl-D-tartaric acid, or 2,3-di-p-toluoyl-L-tartaric acid, respectively, were dissolved separately in 400 mL methanol at 60ºC. The solutions were then mixed and allowed to cool to room temperature, and were further cooled to 0ºC. The solid was then filtered and recrystallized three times from methanol. The parent amine was then regenerated by partitioning between dichloromethane (DCM) and aqueous (20%) KOH. Fractional crystallization with 2,3-di-p-toluoyl-D-tartaric acid yielded the (-)-(S,S) enantiomer; whereas 2,3-di-p-toluoyl-L-tartaric acid yielded the (+)-(R,R) enantiomer. Racemic diamine **3b** was resolved into its enantiomerically pure form, as described above, except methanol was replaced with ethanol as the crystallization solvent. The four enantiomeric diamines were then used to prepare the optically active compounds outlined below via reaction with the corresponding acid chloride in DCM.

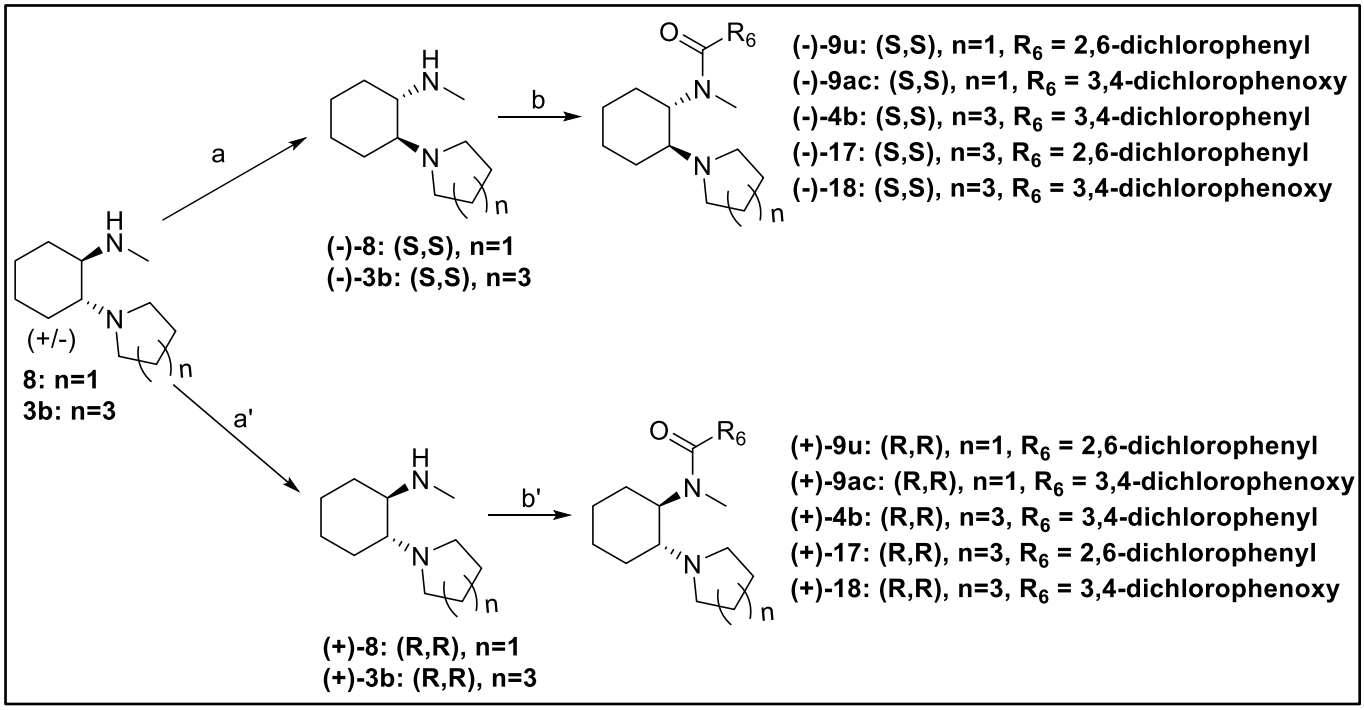

Scheme 3.7. Synthesis of enantiopure analogues. Reagents and conditions: a) (i) 2,3-di-p-toloyl-D-tartartic acid or 2,3-di-p-toloyl-L-tartartic acid, respectively (ii) KOH; b) R_6CH_2COCl, 0ºC.

The KOR activity of the compounds, determined via a DiscoveRx cAMP functional assay, are presented in **Table 3.2**. It should be noted that this data is preliminary (n=2 for all compounds except **(+)-18**, where n=1). Based on the activity, however, the activity of the (-)-enantiomers closely matches the activity observed from the racemic mixtures. The (+)-enantiomers, however, are less potent than the (-)-enantiomers and the racemic mixture, in all cases.

Compound #	$EC_{50} \pm$ SEM nM
(-)-U50,488	**0.12 ± 0.02**
(+/-)-9u	0.46 ± 0.21
(-)-9u	0.36 ± 0.04
(+)-9u	15 ± 4
(+/-)-9ac	1.2 ± 0.6
(-)-9ac	0.9 ± 0.2
(+)-9ac	11 ± 6
(+/-)-4b	4.0 ± 1.0
(-)-4b	4 ± 3
(+)-4b	9.5 ± 0.7
(-)-17	0.8 ± 0.2
(+)-17	18 ± 9
(-)-18	9 ± 4
(+)-18	46 ± 0

Table 3.2. KOR activity of racemic and enantiopure analogues.

Next, in regards to the molecules with modifications in two regions, **(-)-17** is more potent than the corresponding analogue with modification of the pyrrolidine to an azepane **(-)-4b**, but is less potent than the analogue incorporating a 2,6-dichlorophenyl substituent **(-)-9u**. The other analogues, however, all have decreased potency compared to the analogues incorporating only one of the modifications, i.e. **(+)-17** is less potent than either **(+)-4b** or **(+)-9u**; **(-)-18** is less potent than either **(-)-4b** or **(-)-9ac**; **(+)-18** is less potent than either **(+)-4b** or **(+)-9ac**. For the analogues we tested, these results indicate that changes to more than one portion of the molecule do not result in additive changes to KOR activity, but rather decrease potency compared to analogues incorporating only one modification (with the exception of **(-)-21**).

Summary of Results

Thus, in summary, we have designed several compounds, incorporating modifications to five regions of U50,488, including the pyrrolidine group, *N*-alkyl substituent, the linker region, the aryl group, and the cyclohexane ring. Upon successful synthesis of these analogues, the KOR activity was evaluated.

Based on these SARs we observed, we prioritized three molecules, **4b**, **9u**, and **9ac** for subsequent *ex vivo* evaluation of cAMP accumulation and stimulation of ERK. The results indicate that each of these molecules have signaling profiles that differ from that of (-)-U50,488. We then evaluated *ex vivo* inhibition of CGRP release as a translational measure for antinociception. The data showed that the ligands produce monotonic CRCs, as opposed to the inverted-U CRC produced by (-)-U50,488. However, the potency of the ligands differs: **9u** > **9ac** > **4b.**

Finally, the success of these ligands prompted further investigation into the stereochemical preference for each of these ligands, as well as the effects of analogues incorporating changes to two of the sites listed above. The preliminary data suggests that the (-)-enantiomer is the eutomer in all cases. Finally, incorporating two changes to the molecules, as outlined above, results in decreased potency in all but one analogue (except **(-)-17**).

References

1. Smith, V.C.; Cleghorn, L.A.T.; Woodland, A.; Spinks, D.; Hallyburton, I.; Collie, I. T.; Mok, N.Y.; Norval, S.; Brenk, R.; Fairlamb, A.H.; Frearson, J.A.; Read, K.D.; Gilbert, I.H.; Wyatt, P.G. Optimisation of the Anti-Trypanosoma *brucei* Activity of the Opioid Agonist U50488. *Chem. Med. Chem.* **2011**, *6*, 1832.
2. Fontana, G.; Savona, G.; Rodríguez, B.; Dersch, C. M.; Rothman, R. B.; Prisinzano, T. E. Synthetic Studies of Ceoclerodane Diterpenoids from *Salvia splendens* and Evaluation of Opioid Receptor Affinity. *Tetrahedron.* **2008**, *64,* 10041.
3. Szmuszkovicz, J.; Von Voigtlander, P.F. Benzeneacetamide Amines: Structurally Novel Non-Mu Opioids. *J. Med. Chem.* **1982**, *25,* 1125.
4. Zhao, S.; Freeman, J.P.; VonVoigtlander, P.F.; Howe, W.J.; Szmuszkovicz, J. Structure-Activity Relationship Pertaining to the North-West Region of the Kappa Opioid Agonist, U50,488. *Bioorg. Med. Chem. Letts.* **1994**, *4*, 2139.
5. Zhao, S.; Freeman, J.P.; VonVoigtlander, P.F.; Smith, M.W.; Szmuszkovicz, J. Phenalene Analogs of the Kappa Opiate Agonist U50,488. *Bioorg. Med. Chem. Letts.* **1993**, *12,* 2641.
6. D'Andrea, S.V.; Michalson, E.T.; Freeman, J.P.; Chidester, C.G.; Szmuszkovicz, J. *Trans*-3,4-Diaminopiperidines. Azacyclohexane Congeners of Kappa Agonist U-50488. *J. Org. Chem.* **1991**, *56,* 3133.
7. Zhao, S.; Freeman, J.P.; Chidester, C.G.; VonVoigtlander, P.F.; Mizsak, S.A.; Szmuszkovicz, J. Regioselective and Stereoselective Syntheses of 1,2,3-triaminocyclohexane Derivatives. *J. Org. Chem.* **1993**, *58*, 4043.
8. Halfpenny, P.R.; Horwell, D.C.; Hughes, J.; Humblet, C.; Hunter, J.C.; Neuhaus, D.; Rees, D.C. Highly Selective κ Opioid Analgesics. *J. Med. Chem*. **1991**, *34,* 190.

9. Cheng, C.Y.; Wu, S.C.; Hsin, L.W.; Tam, S.W. Selective Reversible and Irreversible Ligands for the κ Opioid Receptor. *J. Med. Chem.* **1992**, *35,* 2243.

10. Clark, C.R.; Halfpenny, P.R.; Hill, R.G.; Horwell, D.C.; Hughes, J.; Jarvis, T.C.; Rees, D.C.; Schofield, D. Highly Selective κ Opioid Analgesics. *J. Med. Chem.* **1988**, *31,* 831.

IV. Conclusions

Thus, by accomplishing the aims outlined herein, we have shown that structural modifications to the U50,488 scaffold alters ligand efficacy for specific signaling pathways. Specifically, we have identified three functionally selective KOR ligands, **3b**, **9u**, and **9ac**, with efficacy similar to that of (-)-U50,488, which do not activate ERK. We anticipate that these molecules will be useful in designing better biological probes for studying KOR-mediated antinociception.

We have designed several compounds, incorporating modifications to five regions of U50,488, including the pyrrolidine group, *N*-alkyl substituent, the linker region, the aryl group, and the cyclohexane ring. Upon successful synthesis of these analogues, the KOR activity was evaluated.

To begin, in regards to modification of the pyrrolidine group, we observed that 6-membered analogues and non-cyclic bulky amines resulted in decreased potency. Further, analogues which incorporate a second heteroatom result in a complete loss of KOR activity. On the contrary, replacement with azepane and small, non-cyclic amines are tolerated. Thus, we hypothesize that the pyrrolidine group fits into a somewhat small binding pocket that does not have H-bond donors in close enough proximity to allow additional interactions with incorporation of second heteroatom. In addition, we propose the azepane substituent is better tolerated than the 6-memebered analogues because it adopts a puckered conformation that much more closely resembles the envelope conformation of a five-membered ring.

In regards to modification of the *N*-alkyl substituent, homologation to an ethyl or benzyl group results in a decrease of KOR, likely indicating that there is a steric clash in the binding site by addition of these aliphatic and aromatic groups.

Next, pertaining to the aryl group, we confirmed previous SAR studies showing that EWGs are preferred in both the meta and para positions. Accordingly, small aliphatic groups and EDGs result in decreased potency compared to the corresponding substitutions with EWGs. In addition, there is no clear preference for a substituent to be in the meta vs para position, except for with the case of OCH_3, which results in a 6-fold decrease in potency when in the meta position. Our data has also shown that a 4-Ph substitution results in a loss of KOR activity, while a 2,3-napthyl is well tolerated, and a 3,4-napthyl leads to KOR similar to that of an unsubstituted phenyl group. Our hypothesis is that the hydrophobic binding pocket has somewhat of a "bent" shape, making it ideal to accommodate a 2,3-napthyl group rather than a 3,4-napthyl group. Along this same model, the hydrophobic pocket would not accommodate a 4-Ph substituent, which corresponds to the trends we observed. Next, in investigation of various substitution patterns, we observed similar potencies of the 2,6-dichloro analogue, the 3-Cl,4-F analogue, and the 3-F,4-Cl analogue. In addition, the 2,4-dichloro analogue and the 3,4-difluoro analogue are slightly more potent that what we have observed for the corresponding substitutions in only one position. We were surprised to learn that the 2,6-dichloro analogue is well tolerated. We hypothesize that these ortho substituents hold the analogue in a much more rigid conformation, in which it preferentially remains in the pharmacologically active form.

In addition, we evaluated the effects of KOR activity when the linker region was modified. First, extension of the linker by one or two methylene units resulted in a loss of KOR activity, which can be rationalized by a shallow binding pocket. Interestingly, the addition of an oxygen atom in the linker region is tolerated. We hypothesize that the oxygen atom may be forming a H-bond with the receptor in order to afford this activity. Lastly, conformational constraint of U50,488 via a cyclopropyl or cyclopentyl group is not tolerated,

indicating that some degree of flexibility is preferred, or that these groups lock U50,488 into an unfavorable conformation.

Lastly, we evaluated KOR activity when the cyclohexane ring was altered. The data indicates that replacement with an aromatic group leads to a loss of KOR activity, signifying that the basic nitrogen is necessary for activity. Next, cleavage of the backbone to an ethylene linker also leads to a loss of KOR activity. Lastly, based on literature precedence, we synthesized analogues with a 1-phenethyl backbone (racemic and enantiopure). These derivatives resulted in a nearly 20-fold increase in potency, compared to (-)-U50,488. Specifically, the (S) enantiomer yields the highest potency of any analogues tested.

Thus, based on the SARs trends described above, we prioritized three molecules, **4b**, **9u**, and **9ac** for subsequent *ex vivo* testing. Specifically, these analogues were prioritized, as detailed above, because their KOR activity was inconsistent with the SAR trends we observed. These ligands were evaluated in an assay of cAMP accumulation and stimulation of ERK. The results show that each of the ligands inhibit AC activity similar to that of (-)-U50,488, but, unlike (-)-U50,488, do not activate ERK. Therefore, these results indicate that each of these molecules have signaling profiles that differ from that of (-)-U50,488. Consequently, since **4b**, **9u**, and **9ac** have maintained efficacy for pathways leading to antinociception, and decreased efficacy for pathways leading to nociception, all ligands were further evaluated for CGRP release.

CGRP release was evaluated as a translational measure for antinociception. The data from this assay showed that the ligands produce monotonic CRCs, as opposed to the inverted-U CRC produced by (-)-U50,488. However, the potency of the ligands differs: **9u** > **9ac** > **4b.** The difference in the CGRP release amongst the three ligands is important because it

indicates that they may be differentially regulating alternative pathways leading to nociception i.e. these ligands may be activating different MAPKs.

Finally, the success of these ligands prompted further investigation into the stereochemical preference for each of the functionally selective ligands described above, as well as the effects of analogues incorporating changes to two of the sites listed above. The preliminary data shows that the activity of the (-)-enantiomers closely matches the activity of the racemic mixtures. In addition, the (-)-enantiomers have the greatest potency for the KOR, but also, the presence of the (+)-enantiomers in the racemic mixtures appears to have little effect on the overall KOR activity. In order to rationalize this data, we propose that the (+)-enantiomers do not activate pathways leading to nociception.

In regards to the analogues which incorporate modifications in two regions, we observed, similarly to the results above, that the (-)-enantiomer is the eutomer in all cases. In addition, incorporating two changes to the molecules, as outlined above, results in decreased potency in all but one analogue (except **(-)-17**). Thus, for the molecules tested (except **(-)-17**), we can conclude that changes to more than one portion of U50,488 do not result in additive changes in KOR activity, but rather decrease the overall KOR activity.

In the future, the compounds that we have identified as functionally selective KOR ligands, **3b**, **9u**, and **9ac,** will be evaluated for off-target affinity for binding to mu and delta opioid receptors. Analogues with an affinity of greater than 500 nM for the mu and delta receptors will then be tested *in vivo* in a rat model of thermal allodynia. Specifically, paw withdrawal latency will be measured at various doses of the above ligands. In this assay, we anticipate monotonic dose response curves for inhibition of PGE_2-induced thermal allodynia, similar to the results obtained by the *ex vivo* assay measuring inhibition of CGRP. Thus, we anticipate that ligands identified above, which have high efficacy for $G_{\alpha i}$ signaling, and do

not activate ERK will have monotonic DRCs with strong antinociceptive efficacy in the rat model of PGE_2-induced thermal allodynia.

V. Experimental Data

General Experimental Procedures. All reactions were performed in glassware dried in an oven at 120°C overnight and cooled under a stream of argon. Solvents were obtained from a dry solvent system that dried solvent by passage through two columns of alumna and degassed by extensive argon sparging. Flash column chromatography (FCC) was performed on silica gel (4-60 μm) from Sorbent Technologies. Reactions and chromatography was monitored by thin-layer chromatography (TLC) on 0.25 mm Analtech GHLF silica gel plates and visualized by UV light (254 nm) and phosphomolybdic TLC stain. ^{1}H and ^{13}C NMR spectra were acquired on a 500 MHz Bruker AVIII spectrometer equipped with a cryogenically-cooled carbon observe probe. High resolution mass spectroscopy (HRMS) analyses were carried out on a Waters LCT Premiere Time of Flight detector with a photodiode array UV detector. Purification was carried out via FCC or Mass Directed Fractionation on an Agilent 1200 instrument with a photodiode array detector attached to an Agilent 6120 quadrupole mass spectrometer. HPLC was conducted using a Waters Acquity BEH C18 equipped with a Waters XBridge C18 column (19 × 150 mm, 5μm), at a flow rate of 20 mL/min, over 3.5 minutes. Specific rotations were recorded on a Rudolph Autopol III ($\lambda = 589$ nm) at 20 °C using a polarimeter cell with a path length of 1 dm. Compounds tested in biological assays were identified as having a purity of ≥ 95% via HPLC. Commercially available reagents were used directly without further purification.

General Procedure for Amino-alcohol Formation: Cyclohexene oxide (1 mL, 10 mmol) and appropriate amine (12 mmol) in EtOH were refluxed overnight and concentrated. The product was formed in quantitative yield and was used without further purification.

General Procedure for Diamine Formation: Methanesulfonyl chloride (MsCl) (1 mL, 12 mmol) was added dropwise to an ice-cold solution of the appropriate amino-alcohol and Et_3N (4.40 mL, 30 mmol) in anhydrous Et_2O (10 mL). The reaction mixture was stirred for 30 minutes and methylamine (41% aqueous solution, 5 mL) was added. The reaction was then allowed to warm to room temperature, with vigorous stirring, overnight. The biphasic mixture was separated, and the aqueous layer was further extracted with Et_2O (150 mL). The combined organics were dried over Na_2SO_4 and concentrated in vacuo. The crude reaction mixture was utilized without purification. As such, the yields are calculated based on the amount of crude reaction mixture used.

General Procedure for Amide Formation:

Method A: Diamine (1 equiv), acid (2 equiv), HOBt (2 equiv), and DMF were added to a dry round bottom flask. DIPEA (2 equiv) and EDCI (2 equiv) were then added, and the reaction was stirred at room temperature for 4 hours. After completion of the reaction, the mixture was concentrated and the resulting gum was partitioned between EtOAc and saturated aqueous $NaHCO_3$. The organic layer was then dried over Na_2SO_4 and concentrated. The samples were purified using mass-directed reverse phase HPLC.

Method B: Acid chloride (1.1 equiv) was added dropwise to an ice-cold solution of diamine (1 equiv) in anhydrous DCM. The reaction was allowed to warm to room temperature. After 2 hours, the reaction was washed with saturated aqueous $NaHCO_3$. The organic layer was then dried over Na_2SO_4, concentrated and purified by mass-directed reverse phase HPLC or FCC.

Method C: Diamine (1 equiv), acid (1 equiv), Et_3N (0.4 mL/mol), and PyBrop (1.2 equiv) were added to a dry round bottom flask. The flask was purged with argon and the cooled to 0^oC. Anhydrous DCM was then added to the flask, and the mixture was stirred for 1 hour.

After 1 hour, the reaction was washed with H_2O, dried over Na_2SO_4, and concentrated. The product was purified via mass-directed reverse phase HPLC or FCC.

Compounds **2a-2e, 2g, 3a-3e, 3g, 4a-4d, 4g, 5, 6a-6b, 7a-7b, 8, 9a-9w, 9aa-9ae, 11, 14,** and **16a-16c** were found to be in agreement with previously reported values.[1-3]

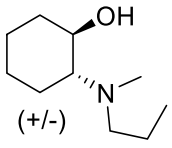

***trans*-(+/-)-2-(Methyl(propyl)amino)cyclohexanol (2f).** Prepared according to the general procedure for aminoalcohol formation to give the title compound in quantitative yield. The resulting viscous red oil was used without further purification. ^{1}H NMR (500 MHz, Chloroform-*d*) δ 4.72 (d, *J* = 2.5 Hz, 1H), 3.96 (d, *J* = 2.5 Hz, 1H), 3.46 – 3.31 (m, 1H), 3.10 (s, 5H), 2.84 (dd, *J* = 6.2, 4.9 Hz, 4H), 2.32 (s, 2H), 2.17 – 2.06 (m, 1H), 2.06 – 1.97 (m, 1H), 1.89 – 1.77 (m, 2H), 1.44 – 1.31 (m, 1H), 1.31 – 1.10 (m, 5H). ^{13}C NMR (126 MHz, $CDCl_3$) δ 88.52, 80.56, 69.55, 53.24, 37.21, 28.72, 27.29, 24.11. HRMS [M+H]: 172.1696 (calcd), 172.1706 (found).

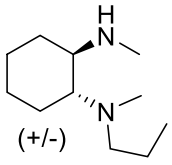

***trans*-(+/-)-*N*-Methyl-2-(Methyl(propyl)amino)cyclohexanamine (3f).** Prepared from **2f** according to the general procedure for diamine formation to give the title compound. The resulting viscous red oil was subsequently used without further purification. The presence of the product was confirmed via HRMS. [M+H]: 185.2012 (calcd), 185.2014 (found).

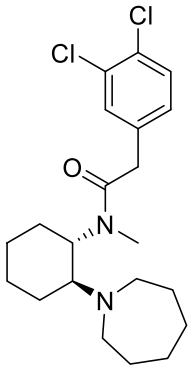

(1S,2S)-(2-(3,4-Dichlorophenyl)-*N*-methyl-*N*-(2-(azepan-1-yl)cyclohexyl) acetamide ((-)-4b). Prepared according to the general procedure for amide formation (method B) from **(-)-3b** (238 mg, 1.1 mmol) and 3,4-dichlorophenylacetyl chloride (491 mg, 2.2 mmol) in 98% yield. ^{1}H NMR (500 MHz, Chloroform-*d*) δ 7.41 (s, 1H), 7.37 (d, *J* = 6.6 Hz, 1H), 7.23 (d, *J* = 8.8 Hz, 2H), 4.90 (s, 1H), 4.33 (s, 1H), 3.92 (s, 1H), 3.70 (s, 2H), 3.08 (d, *J* = 54.7 Hz, 6H), 2.25 (s, 2H), 1.68 (tt, *J* = 103.0, 53.2 Hz, 17H). ^{13}C NMR (126 MHz, $CDCl_3$) δ 173.14, 135.76, 132.11, 131.81, 130.65, 130.22, 129.66, 67.32, 56.49, 48.52, 40.95, 30.12, 28.28, 28.17, 24.86, 24.75, 24.55, 23.92. HRMS [M+H]: 397.1808 (calcd), 397.1808 (found). Melting point: 162°C (dec). HPLC t_R = 1.48 min; purity = 98.1%, using a gradient of 85% - 100% acetonitrile/pH 9.8 aqueous ammonium hydroxide as the mobile phase. $[\alpha]^{20}_{D}$ (MeOH) = – 31.8° (c = 0.011 g/mL).

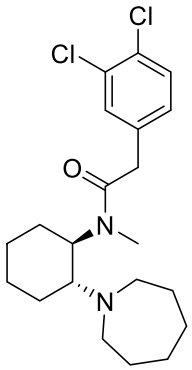

(1R,2R)-(2-(3,4-Dichlorophenyl)-*N*-methyl-*N*-(2-(azepan-1yl)cyclohexyl) acetamide ((+)-4b). Prepared according to the general procedure for amide formation (method B) from **(+)-3b** (231 mg, 1.1 mmol) and 3,4-dichlorophenylacetyl chloride (491 mg, 2.2 mmol) in 94% yield. ^{1}H NMR (500 MHz, Chloroform-*d*) δ 7.44 – 7.32 (m, 2H), 7.23 (d,

J = 8.8 Hz, 1H), 4.90 (s, 1H), 4.33 (s, 1H), 3.81 (d, J = 110.9 Hz, 3H), 3.08 (d, J = 55.4 Hz, 6H), 2.36 (d, J = 108.0 Hz, 3H), 2.05 – 1.26 (m, 13H). ^{13}C NMR (126 MHz, $CDCl_3$) δ 173.14, 135.76, 132.11, 131.82, 130.65, 130.23, 129.68, 67.36, 56.50, 48.56, 40.98, 30.13, 28.29, 28.18, 24.88, 24.77, 24.55, 23.95. HRMS [M+H]: 397.1808 (calcd), 397.1810 (found). Melting point: 153°C (dec). HPLC t_R = 1.54 min; purity = 98.0%, using a gradient of 75% - 95% acetonitrile/pH 9.8 aqueous ammonium hydroxide as the mobile phase. $[\alpha]^{20}_D$ (MeOH) = + 30.9° (c = 0.015 g/mL).

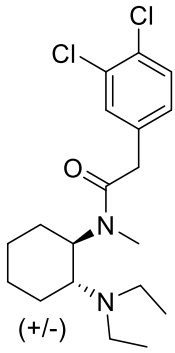

***trans*-(+/-)-2-(3,4-Dichlorophenyl)-*N*-methyl-*N*-(2-(diethylamino)cyclo hexyl)acetamide (4e).** Prepared according to the general procedure for amide formation (method A) from **3e** (172 mg, 0.55 mmol) and 3,4-dichlorophenylacetic acid (247 mg, 1.0 mmol) in 42% yield. Melting point: 55–56°C. ^{1}H NMR (500 MHz, DMSO-d_6) δ 7.56 (dd, J = 5.5, 8.2 Hz, 1H), 7.50 (d, J = 2.0 Hz, 1H), 7.24 (ddd, J = 2.1, 8.3, 13.9 Hz, 1H), 3.85 – 3.56 (m, 2H), 2.83 (s, 2H), 2.68 (s, 1H), 2.61 – 2.53 (m, 1H), 2.25 (ddq, J = 6.8, 13.4, 40.5 Hz, 2H), 1.85 – 1.00 (m, 8H), 0.88 (dt, J = 7.1, 16.5 Hz, 6H). ^{13}C NMR (126 MHz, DMSO) δ 169.42, 137.97, 131.63, 131.00, 130.56, 130.28, 129.25, 60.25, 59.15, 57.64, 53.09, 43.50, 43.06, 29.89, 27.62, 25.66, 25.46, 25.19, 23.90, 14.96, 14.84. HRMS [M+H]: 371.1652 (calcd), 371.1642 (found). HPLC t_R = 1.37 min; purity = 97.2%, using a gradient of 85% - 100% acetonitrile/pH 9.8 aqueous ammonium hydroxide as the mobile phase.

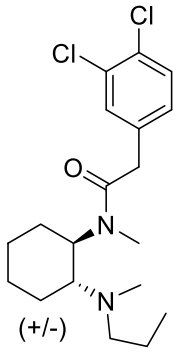

***trans*-(+/-)-2-(3,4-Dichlorophenyl)-*N*-methyl-*N*-(2-(Methyl(propyl)amino) cyclohexyl)acetamide (4f).** Prepared according to the general procedure for amide formation (method A) from **3f** (119 mg, 0.55 mmol) and 3,4-dichlorophenylacetic acid (231 mg, 1.0 mmol) in 20% yield. ^{1}H NMR (500 MHz, DMSO-d_6) δ 7.56 (dd, J = 2.4, 8.2 Hz, 1H), 7.47 (d, J = 2.1 Hz, 1H), 7.23 (ddd, J = 2.0, 8.3, 13.6 Hz, 1H), 3.90 – 3.46 (m, 2H), 2.79 (s, 2H), 2.70 – 2.62 (m, 1H), 2.40 – 2.08 (m, 2H), 2.05 (s, 2H), 1.89 – 0.98 (m, 7H), 0.69 (t, J = 7.3 Hz, 2H). ^{13}C NMR (126 MHz, DMSO) δ 169.49, 137.81, 131.35, 131.09, 130.63, 130.04, 129.31, 63.90, 63.04, 57.50, 55.18, 53.16, 36.33, 29.76, 27.27, 25.57, 25.27, 21.33, 11.90. HRMS [M+H]: 371.1652 (calcd), 371.1616 (found). HPLC t_R = 1.46 min; purity = 100.0%, using a gradient of 85% - 100% acetonitrile/pH 9.8 aqueous ammonium hydroxide as the mobile phase.

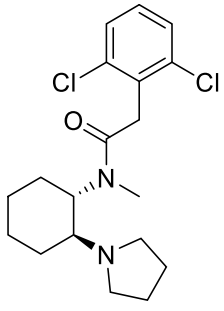

(1S,2S)-(2-(2,6-Dichlorophenyl)-*N*-methyl-*N*-(2-(pyrrolidin-1-yl)cyclo hexyl)acetamide ((-)-9u). Prepared according to the general procedure for amide formation (method B) from **(-)-8** (203 mg, 1.1 mmol) and 2,6-dichlorophenylacetyl chloride (491 mg, 2.2 mmol) in 56% yield. ^{1}H NMR (500 MHz, Chloroform-d) δ 7.31 (d, J = 8.0 Hz, 2H), 7.14 (dd, J = 8.5, 7.6 Hz, 1H), 4.45 (d, J = 107.7 Hz, 2H), 3.98 (d, J = 16.6 Hz, 1H), 3.90 – 3.39

(m, 2H), 3.25 (s, 3H), 3.14 – 2.79 (m, 2H), 2.13 (d, J = 45.0 Hz, 3H), 1.85 (dd, J = 39.7, 13.7 Hz, 5H), 1.56 – 1.14 (m, 3H). ^{13}C NMR (126 MHz, $CDCl_3$) δ 136.12, 132.84, 127.86, 99.97, 37.19, 29.70, 29.31, 24.54, 23.83. HRMS [M+H]: 369.1495 (calcd), 369.1521 (found). HPLC t_R = 1.30 min; purity = 97.1%, using a gradient of 85% - 100% acetonitrile/pH 9.8 aqueous ammonium hydroxide as the mobile phase. $[\alpha]^{20}_D$ (MeOH) = – 10.1° (c = 0.010 g/mL).

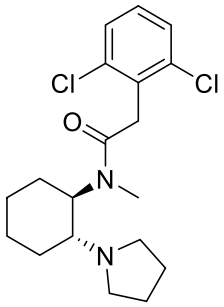

(1R,2R)-(2-(2,6-Dichlorophenyl)-*N*-methyl-*N*-(2-(pyrrolidin-1-yl)cyclohexyl)acetamide ((+)-9u). Prepared according to the general procedure for amide formation (method B) from **(+)-8** (200 mg, 1.1 mmol) and 2,6-dichlorophenylacetyl chloride (494 mg, 2.2 mmol) in 49% yield. ^{1}H NMR (500 MHz, Chloroform-*d*) δ 7.31 (d, J = 8.0 Hz, 2H), 7.14 (dd, J = 8.5, 7.7 Hz, 1H), 4.45 (d, J = 107.6 Hz, 2H), 4.04 – 3.94 (m, 1H), 3.87 (s, 1H), 3.25 (s, 3H), 3.15 – 2.73 (m, 2H), 2.38 – 2.01 (m, 2H), 1.96 – 1.78 (m, 4H), 1.56 – 1.20 (m, 2H). ^{13}C NMR (126 MHz, $CDCl_3$) δ 136.12, 132.84, 128.54, 127.86, 37.22, 29.30, 24.53, 24.34, 23.84. HRMS [M+H]: 369.1495 (calcd), 369.1493 (found). HPLC t_R = 1.29 min; purity = 96.7%, using a gradient of 85% - 100% acetonitrile/pH 9.8 aqueous ammonium hydroxide as the mobile phase. $[\alpha]^{20}_D$ (MeOH) = + 9.9° (c = 0.007 g/mL).

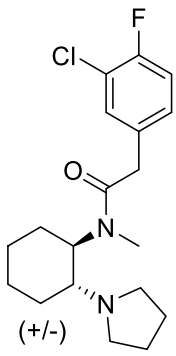

***trans*-(+/-)-(2-(3-chloro-4-fluorophenyl)-*N*-methyl-*N*-(2-(pyrrolidin-1-yl) cyclohexyl)acetamide (9x).** Prepared according to the general procedure for amide formation (method A) from **5** (105 mg, 0.55 mmol) and 3-chloro-4-fluorophenylacetic acid (216 mg, 1.1 mmol) in 18% yield. ^{1}H NMR (500 MHz, DMSO-d_6) δ 7.51 – 7.30 (m, 2H), 7.24 (tdd, *J* = 8.5, 4.8, 2.2 Hz, 1H), 3.85 – 3.50 (m, 2H), 2.81 (s, 3H), 2.70 (s, 1H), 2.65 – 2.53 (m, 2H), 1.91 – 1.37 (m, 8H), 1.37 – 1.03 (m, 2H). ^{13}C NMR (126 MHz, DMSO) δ 169.92, 164.12, 155.36, 134.60, 131.25, 130.06, 116.80, 58.14, 47.17, 29.59, 25.44, 23.90, 22.90. HRMS [M+H]: 353.1791 (calcd), 353.1806 (found). HPLC t_R = 1.26 min; purity = 97.0%, using a gradient of 85% - 100% acetonitrile/pH 9.8 aqueous ammonium hydroxide as the mobile phase.

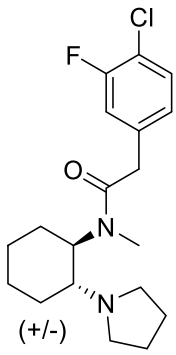

***trans*-(+/-)-(2-(3-fluoro-4-chlorophenyl)-*N*-methyl-*N*-(2-(pyrrolidin-1-yl) cyclohexyl)acetamide (9y).** Prepared according to the general procedure for amide formation (method A) from **5** (101 mg, 0.55 mmol) and 3-fluoro-4-chlorophenylacetic acid (213 mg, 1.1 mmol) in 15% yield. ^{1}H NMR (500 MHz, Chloroform-*d*) δ 7.49 (td, *J* = 8.1, 3.3 Hz, 1H), 7.26 (ddd, *J* = 28.6, 10.6, 2.0 Hz, 1H), 7.14 – 7.02 (m, 1H), 3.85 – 3.54 (m, 2H), 2.77 (s, 2H),

2.59 – 2.29 (m, 7H), 1.85 – 0.97 (m, 9H). ^{13}C NMR (126 MHz, $CDCl_3$) δ 174.18, 163.12, 161.17, 143.26, 135.38, 131.48, 122.25, 63.92, 62.62, 52.49, 51.59, 34.37, 30.30, 29.89, 28.78, 28.55, 27.44. HRMS [M+H]: 353.1791 (calcd), 353.1789 (found). HPLC t_R = 2.29 min; purity = 97.7%, using a gradient of 85% - 100% acetonitrile/pH 9.8 aqueous ammonium hydroxide as the mobile phase.

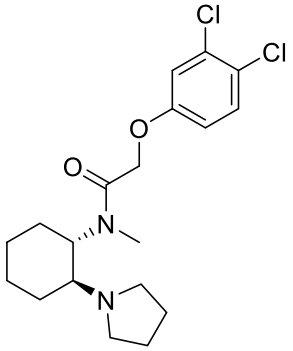

(1S,2S)-2-(3,4-Dichlorophenoxy)-*N*-methyl-*N*-((2-(pyrrolidin-1-yl)cyclohexyl)acetamide ((-)-9ac). Prepared according to the general procedure for amide formation (method B) from **(-)-8** (215 mg, 1.1 mmol) and 3,4-dichlorophenoxyacetyl chloride (520 mg, 2.2 mmol) in 53% yield. ^{1}H NMR (500 MHz, Chloroform-*d*) δ 7.34 (d, *J* = 3.0 Hz, 1H), 7.31 (d, *J* = 8.9 Hz, 1H), 7.08 (dd, *J* = 8.9, 2.9 Hz, 1H), 5.37 (d, *J* = 15.4 Hz, 1H), 4.81 (d, *J* = 15.4 Hz, 2H), 3.95 (dq, *J* = 13.6, 7.0, 6.6 Hz, 1H), 3.55 (ddt, *J* = 18.1, 11.8, 5.0 Hz, 1H), 3.22 (d, *J* = 17.6 Hz, 1H), 3.07 (s, 4H), 2.99 (dt, *J* = 14.7, 7.5 Hz, 1H), 2.26 (ddq, *J* = 35.0, 15.2, 7.6, 6.8 Hz, 2H), 2.13 – 2.01 (m, 1H), 1.89 (ddt, *J* = 38.0, 33.1, 8.6 Hz, 4H), 1.53 – 1.22 (m, 3H). ^{13}C NMR (126 MHz, $CDCl_3$) δ 169.67, 157.44, 132.71, 130.52, 124.14, 117.07, 114.91, 66.96, 60.91, 52.19, 48.07, 29.37, 24.84, 24.44, 24.32, 24.12. HRMS [M+H]: 385.1444 (calcd), 385.1417 (found). Melting point: 187–189°C. HPLC t_R = 1.40 min; purity = 98.8%, using a gradient of 85% - 100% acetonitrile/pH 9.8 aqueous ammonium hydroxide as the mobile phase. $[\alpha]^{20}_D$ (MeOH) = – 16.6° (c = 0.010 g/mL).

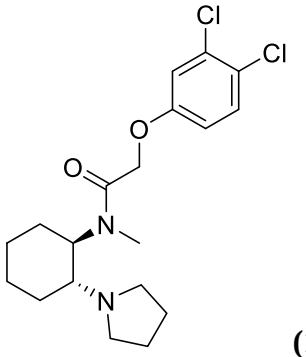

(1R,2R)-2-(3,4-Dichlorophenoxy)-*N*-methyl-*N*-((2-(pyrrolidin-1-yl)cyclohexyl)acetamide ((+)-9ac). Prepared according to the general procedure for amide formation (method B) from **(+)-8** (210 mg, 1.1 mmol) and 3,4-dichlorophenoxyacetyl chloride (520 mg, 2.2 mmol) in 43% yield. ^{1}H NMR (500 MHz, Chloroform-*d*) δ 7.34 (d, *J* = 3.4 Hz, 1H), 7.31 (d, *J* = 8.9 Hz, 1H), 7.08 (d, *J* = 8.9 Hz, 1H), 5.37 (d, *J* = 15.5 Hz, 1H), 4.94 – 4.67 (m, 2H), 3.95 (s, 1H), 3.55 (d, *J* = 18.2 Hz, 1H), 3.06 (d, *J* = 8.9 Hz, 4H), 3.00 (s, 2H), 2.34 – 2.13 (m, 2H), 2.13 – 2.02 (m, 1H), 2.02 – 1.72 (m, 4H), 1.52 – 1.15 (m, 2H). ^{13}C NMR (126 MHz, $CDCl_3$) δ 169.67, 157.44, 132.72, 130.53, 117.06, 114.90, 66.97, 60.89, 52.18, 48.05, 29.38, 24.83, 24.44, 24.30, 24.11. HRMS [M+H]: 385.1444 (calcd), 385.1420 (found). Melting point: 174–175°C. HPLC t_R = 1.37 min; purity = 98.7%, using a gradient of 85% - 100% acetonitrile/pH 9.8 aqueous ammonium hydroxide as the mobile phase. $[\alpha]^{20}_{D}$ (MeOH) = + 17.7° (c = 0.009 g/mL).

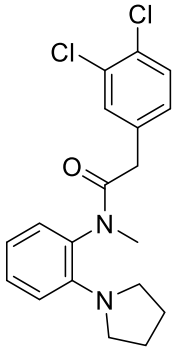

2-(3,4-Dichlorophenyl)-*N*-methyl-*N*-(2-(pyrrolidin-1-yl)phenyl)acetamide (12). Prepared from **15** (208 mg, 0.57 mmol) via the action of NaH (60% weight, 0.72 mmol) and MeI (0.04mL, 0.66 mmol) in 20% yield. ^{1}H NMR (500 MHz, Chloroform-*d*) δ 7.29 (d,

J = 8.2 Hz, 1H), 7.25 – 7.21 (m, 1H), 7.09 (d, *J* = 2.1 Hz, 1H), 6.96 – 6.88 (m, 2H), 6.82 (dd, *J* = 8.3, 1.4 Hz, 1H), 6.76 (td, *J* = 7.5, 1.4 Hz, 1H), 3.40 (s, 2H), 3.30 – 3.10 (m, 7H), 2.00 – 1.75 (m, 4H). ^{13}C NMR (126 MHz, $CDCl_3$) δ 170.93, 145.74, 135.52, 131.88, 131.30, 129.90, 129.78, 129.01, 128.83, 118.26, 115.90, 49.73, 41.00, 39.59, 37.84, 30.96, 25.43. HRMS [M+H]: 363.1026 (calcd), 363.1029 (found). HPLC t_R = 2.76 min; purity = 97.7%, using a gradient of 85% - 100% acetonitrile/pH 9.8 aqueous ammonium hydroxide as the mobile phase.

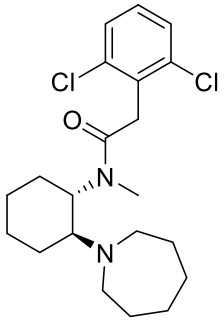

(1S,2S)-2-(2,6-Dichlorophenyl)-*N*-methyl-*N*-((2-(azepan-1-yl)cyclo hexyl)acetamide ((-)-17). Prepared according to the general procedure for amide formation (method B) from **(-)-3b** (230 mg, 1.1 mmol) and 2,6-dichlorophenylacetyl chloride (493 mg, 2.2 mmol) in quantitative yield. ^{1}H NMR (500 MHz, Chloroform-*d*) δ 7.32 (d, *J* = 8.0 Hz, 2H), 7.15 (t, *J* = 8.0 Hz, 1H), 4.93 (s, 1H), 4.46 (s, 1H), 4.00 (s, 1H), 3.38 – 3.05 (m, 4H), 2.99 (s, 1H), 2.44 (d, *J* = 64.6 Hz, 3H), 1.89 (d, *J* = 50.5 Hz, 7H), 1.66 (s, 2H), 1.60 (s, 8H), 1.44 (d, *J* = 32.2 Hz, 3H). ^{13}C NMR (126 MHz, $CDCl_3$) δ 136.26, 132.84, 128.61, 127.89, 65.87, 37.59, 30.32, 27.44, 24.92, 24.60, 24.31, 15.29. HRMS [M+H]: 397.1808 (calcd), 397.1801 (found). Melting point: 121°C (dec). HPLC t_R = 1.42 min; purity = 99.9%, using a gradient of 85% - 100% acetonitrile/pH 9.8 aqueous ammonium hydroxide as the mobile phase. $[\alpha]^{20}_D$ (MeOH) = – 16.3° (c = 0.010 g/mL).

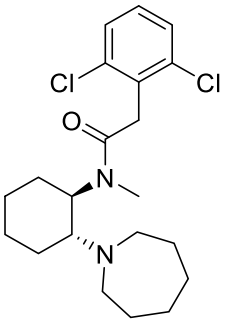

(1R,2R)-2-(2,6-Dichlorophenyl)-*N*-methyl-*N*-((2-(azepan-1-yl)cyclo hexyl)acetamide ((+)-17). Prepared according to the general procedure for amide formation (method B) from **(+)-3b** (240 mg, 1.1 mmol) and 2,6-dichlorophenylacetyl chloride (493 mg, 2.2 mmol) in 98% yield. ^{1}H NMR (500 MHz, Chloroform-*d*) δ 7.32 (d, *J* = 8.0 Hz, 2H), 7.15 (t, *J* = 8.0 Hz, 1H), 4.94 (s, 1H), 4.46 (s, 1H), 4.00 (s, 1H), 3.38 – 2.85 (m, 5H), 2.44 (d, *J* = 65.9 Hz, 3H), 1.89 (d, *J* = 48.3 Hz, 6H), 1.62 (s, 5H), 1.39 (d, *J* = 56.9 Hz, 3H). ^{13}C NMR (126 MHz, $CDCl_3$) δ 170.98, 136.26, 132.85, 128.61, 127.89, 99.97, 67.35, 65.87, 37.57, 30.35, 27.45, 24.99, 24.78, 24.60, 24.33, 15.29. HRMS [M+H]: 397.1808 (calcd), 397.1811 (found). Melting point: 149°C (dec). HPLC t_R = 1.45 min; purity = 98.0%, using a gradient of 85% - 100% acetonitrile/pH 9.8 aqueous ammonium hydroxide as the mobile phase. $[\alpha]^{20}_{D}$ (MeOH) = + 16.5° (c = 0.009 g/mL).

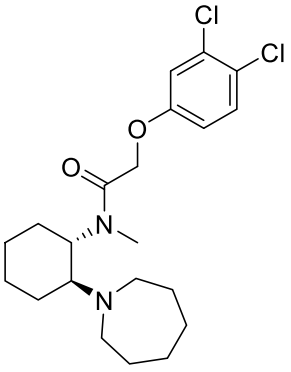

(1S,2S)-2-(3,4-Dichlorophenoxy)-*N*-methyl-*N*-((2-(azepan-1-yl) cyclohexyl)acetamide ((-)-18). Prepared according to the general procedure for amide formation (method B) from **(-)-3b** (231 mg, 1.1 mmol) and 3,4-dichlorophenoxyacetyl chloride (522 mg, 2.2 mmol) in 99% yield. ^{1}H NMR (500 MHz, Chloroform-*d*) δ 7.36 (s, 1H), 7.33 – 7.28 (m, 1H), 7.11 (d, *J* = 8.5 Hz, 1H), 5.44 (s, 1H), 4.84 (d, *J* = 35.5 Hz, 2H),

3.83 (d, *J* = 117.3 Hz, 2H), 3.03 (d, *J* = 68.7 Hz, 6H), 2.25 (d, *J* = 40.1 Hz, 2H), 2.07 – 1.71 (m, 5H), 1.62 (s, 4H), 1.45 (s, 3H). ^{13}C NMR (126 MHz, $CDCl_3$) δ 169.94, 157.53, 132.66, 130.46, 124.06, 117.33, 115.16, 67.38, 48.18, 29.89, 28.28, 28.17, 24.89, 24.76, 24.65, 24.49, 23.80. HRMS [M+H]: 413.1757 (calcd), 413.1764 (found). Melting point: 138°C (dec). HPLC t_R = 1.51 min; purity = 99.6%, using a gradient of 85% - 100% acetonitrile/pH 9.8 aqueous ammonium hydroxide as the mobile phase. $[\alpha]^{20}_D$ (MeOH) = – 21.3° (c = 0.012 g/mL).

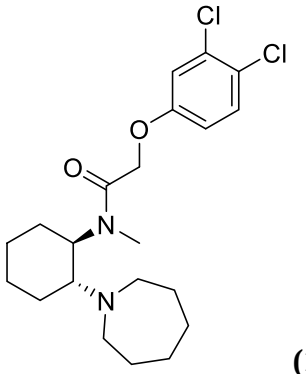

(1R,2R)-2-(3,4-Dichlorophenoxy)-*N*-methyl-*N*-((2-(azepan-1-yl) cyclohexyl)acetamide ((+)-18). Prepared according to the general procedure for amide formation (method B) from **(+)-3b** (236 mg, 1.1 mmol) and 3,4-dichlorophenoxyacetyl chloride (522 mg, 2.2 mmol) in quantitative yield. ^{1}H NMR (500 MHz, Chloroform-*d*) δ 7.36 (s, 1H), 7.30 (d, *J* = 7.8 Hz, 1H), 7.11 (d, *J* = 8.4 Hz, 1H), 5.44 (s, 1H), 4.84 (d, *J* = 39.2 Hz, 2H), 3.83 (d, *J* = 118.5 Hz, 2H), 3.03 (d, *J* = 70.4 Hz, 6H), 2.63 – 2.08 (m, 3H), 2.08 – 1.53 (m, 7H), 1.45 (s, 3H). ^{13}C NMR (126 MHz, $CDCl_3$) δ 169.94, 157.53, 132.66, 130.46, 124.06, 117.32, 115.16, 67.37, 48.21, 29.91, 28.28, 28.17, 24.94, 24.78, 24.67, 24.49, 23.80. HRMS [M+H]: 413.1757 (calcd), 413.1783 (found). Melting point: 152°C (dec). HPLC t_R = 1.51 min; purity = 99.1%, using a gradient of 85% - 100% acetonitrile/pH 9.8 aqueous ammonium hydroxide as the mobile phase. $[\alpha]^{20}_D$ (MeOH) = + 20.9° (c = 0.007 g/mL).

Cell Lines and Cell Culture. Cells were cultured as previously described.[4] The HitHunter Chinese hamster ovary cells (CHO-K1) stably expressing the human κ-opioid receptor (OPRK1, catalogue no. 95-0088C2) were purchased from DiscoverX Corp. (Fremont, CA) and maintained in F-12 media with 10% fetal bovine serum (Life Technologies, Grand Island, NY), 1% penicillin/streptomycin/L-glutamine (Life Technologies), and 800 μg/mL geneticin (Mirus Bio, Madison, WI). The media of the PathHunter cells was supplemented with an additional 250 μg/mL hygromycin B (Mirus Bio). All cells were grown at 37 °C and 5% CO_2 in a humidified incubator.

Forskolin-Induced cAMP Accumulation. Assays proceeded as previously described.[4] On day 1, ∼80% confluent KOR-CHO cells were detached from culture plates using nonenzymatic cell dissociation buffer (Life Technologies) and counted using a hemocytometer. Cells were plated at 10,000 cells/well in 20 μL of Cell Plating Reagent 2 (DiscoveRx) in 384-well tissue culture plates and incubated at 37°C overnight. On day 2, stock solutions of all compounds were generated by dissolution in 100% DMSO (Alfa Aesar, Ward Hill, MA) to 10 mM. Stock solutions were used to make 10 serial dilutions in 100% DMSO at 100× final compound concentrations, and 100× compound concentrations were diluted in assay buffer [Hank's Buffered Salt Solution (HBSS, Life Technologies) with 10 mM HEPES (Life Technologies)] containing forskolin (DiscoveRx) to yield 5× compound concentrations, 100 μM forskolin, and 5% DMSO in assay buffer. The DiscoveRx HitHunter cAMP Assay was used according to manufacturer's instructions. Briefly, media was removed from cells, and cells were washed with 10 μL of assay buffer. Assay buffer containing antibody reagent (20 μL/ well) was added to cells. A 5 μL potion of 5× compound/forskolin solution were added to cells (final concentrations were 1× compound, 20 μM forskolin, and

1% DMSO). Cells were incubated at 37 °C and 5% CO2 for 30 min, followed by incubation with detection reagents according to manufacturer's instructions at room temperature protected from light overnight. On day 3, luminescence was quantified using a Synergy 2 plate reader with Gen5 software (BioTek, Winooski, VT). Data were normalized to vehicle and forskolin only control values and analyzed using nonlinear regression with GraphPad Prism v6.07.

Primary Sensory Neuron Cultures. Primary cultures of rat trigeminal ganglion neurons were prepared as described previously.[5-6] Cells were maintained in culture for 6 days before experimentation. For all experiments, cells were refed with serum-free Dulbecco's modified Eagle's medium without nerve growth factor on day 5 and used for experiments on the sixth day of culture (i.e., after a 24-hour serum/nerve growth factor free period).

Measurement of Cellular cAMP Accumulation. Opioid agonist-induced inhibition of PGE2-stimulated adenylyl cyclase activity was measured as described previously.[5-6] In brief, TG cultures in 48-well plates were washed twice with HBSS containing 20 mM HEPES, pH 7.4 (wash buffer). Cells were pre-equilibrated in 250 µl of wash buffer per well for 30 min at 37°C. Cells were then incubated with KOR agonists (various concentrations) in the presence of the phosphodiesterase inhibitor rolipram (100 µM) for 15 min at 37°C. A maximal concentration of PGE2 (1 µM) was added, and cells were incubated for a further 15 min. As appropriate, BK (10 µM) was added during the pre-equilibration period, 15 min before the KOR agonists. Incubations were terminated by aspiration of the wash buffer and addition of 500 µl of ice-cold absolute ethanol. The ethanol extracts from individual wells were dried under a gentle air stream and reconstituted in 100 µl of 50 mM sodium acetate, pH 6.2. The cAMP content of each 100-µl sample was determined by radioimmunoassay (RIA).

Measurement of ERK1/2 Activation. KOR agonist–mediated activation of ERK in peripheral sensory neurons was measured as described previously.[5-6] Cells were washed twice with HBSS containing 20 mM HEPES, pH 7.4 (wash buffer) and pre-equilibrated in 250 µl of wash buffer per well for 30 min at 37°C. Cells were then incubated with a KOR agonist (100 nM) in the absence or presence of nor-BNI (3 nM) for 0 to 15 min at 37°C. BK (10 µM) or vehicle was added during the pre-equilibration period 15 min before the KOR ligand. Incubations were terminated by aspiration of buffer and addition of 50 µl of lysis buffer supplied with the SureFire phospho-extracellular signal-regulated kinase (pERK) assay kit (PerkinElmer Life and Analytical Sciences). Samples were processed according to the manufacturer's directions. The fluorescence signal from pERK was measured in duplicate using a Fluostar microplate reader (BMG Labtech GmbH, Offenburg, Germany) with AlphaScreen settings.

Measurement of Calcitonin Gene-Related Peptide Release. Opioid agonist-induced inhibition of BK/PGE_2-stimulated calcitonin gene-related peptide (CGRP) release from TG cultures was measured as described previously.[5] Cells were washed twice in release buffer (HBSS supplemented with 10.9 mM HEPES, 4.2 mM sodium bicarbonate, 10 mM dextrose, and 0.1% bovine serum albumin, pH 7.4) and then pretreated with vehicle (Veh) or BK (10 µM). Fifteen minutes later, cells were treated with opioid ligands or vehicle (15 min), followed by PGE_2/BK (1 µM/10 µM) or vehicle for an additional 15 min. Levels of CGRP obtained from the supernatant (500 µl) were measured with radioimmunoassay.

Data Analysis. All statistical tests were performed using GraphPad Prism software v6.07 (La Jolla, CA, USA). One-way ANOVAs were used to compare data from multiple treatment groups. Two-way ANOVAs were used to test for significant effects of two factors. For the

dose response experiment, non-linear regression analysis was used to calculate the potency (EC_{50}) and the efficacy (*Emax*), with data normalized to salvinorin A, a full KOR agonist. A p value of ≤ 0.05 was used to define significance. When significant differences were found for one- and two-way ANOVAs Bonferroni post-hoc tests were used. All values presented are means ± the standard error of the mean (S.E.M.).

References

1. Smith, V.C.; Cleghorn, L.A.T.; Woodland, A.; Spinks, D.; Hallyburton, I.; Collie, I. T.; Mok, N.Y.; Norval, S.; Brenk, R.; Fairlamb, A.H.; Frearson, J.A.; Read, K.D.; Gilbert, I.H.; Wyatt, P.G. Optimisation of the Anti-Trypanosoma *brucei* Activity of the Opioid Agonist U50488. *Chem. Med. Chem.* **2011**, *6*, 1832.
2. Azizi, N.; Saidi, M.R. Highly Chemoselective Addition of Amines to Epoxides in Water. *Org. Lett.* **2005**, *7*, 3649.
3. DeCosta, B.R.; Rothman, R.B.; Bykov, V.; Band, L.; Pert, A.; Jacobsen, A.E.; Rice, K.C. Probes for Narcotic Receptor Mediated Phenomena. Synthesis and Evaluation of a Series of *trans*-3,4-dichloro-*N*-methyl-*N*-[2-(1-pyrrolidinyl)cyclohexyl) benzeneacetamide (U50,488) Related Isothiocyanate Derivatives as Opioid Receptor Affinity Ligands. *J. Med. Chem.* **1990**, *33*, 1171.
4. Riley, A. P.; Groer, C. E.; Young, D.; Ewald, A. W.; Kivell, B. M.; Prisinzano, T. E. Synthesis and Kappa-Opioid Receptor Activity of Furansubstituted salvinorin A Analogues. J. Med. Chem. 2014, 57, 10464.
5. Berg, K.A.; Rowan, M.P.; Sanchez, T.A.; Silva, M.; Patwardhan, A.M.; Milam, S.B.; Hargreaves, K.M.; Clarke, W.P. Regulation of κ-Opioid Receptor Signaling in Peripheral Sensory Neurons in Vitro and in Vivo. *J. Pharmacol. Exp. Ther.* **2011**, *338*, 92.
6. Jamshidi, R.J.; Jacobs, B.A.; Sullivan, L.C.; Chavera, T.A.; Saylor, R.M.; Prisinzano, T.E.; Clarke, W.P.; Berg, K.A. Functional Selectivity of Kappa Opioid Receptor Agonists in Peripheral Sensory Neurons. *J. Pharmacol. Exp. Ther.* **2015**, *355*, 174.


SJ-1-111.1.fid
PROTON CDCl3
OH
N
A (s)
4.16
B (td)
3.35
J(9.80, 4.64)
C (ddd)
2.66
J(10.81, 7.05, 3.37)
D (d)
2.32
J(10.29)
E (m)
2.13
F (m)
1.64
G (m)
1.20
1.00
0.99
2.02
1.78
2.07
8.63
2.91
f1 (ppm)

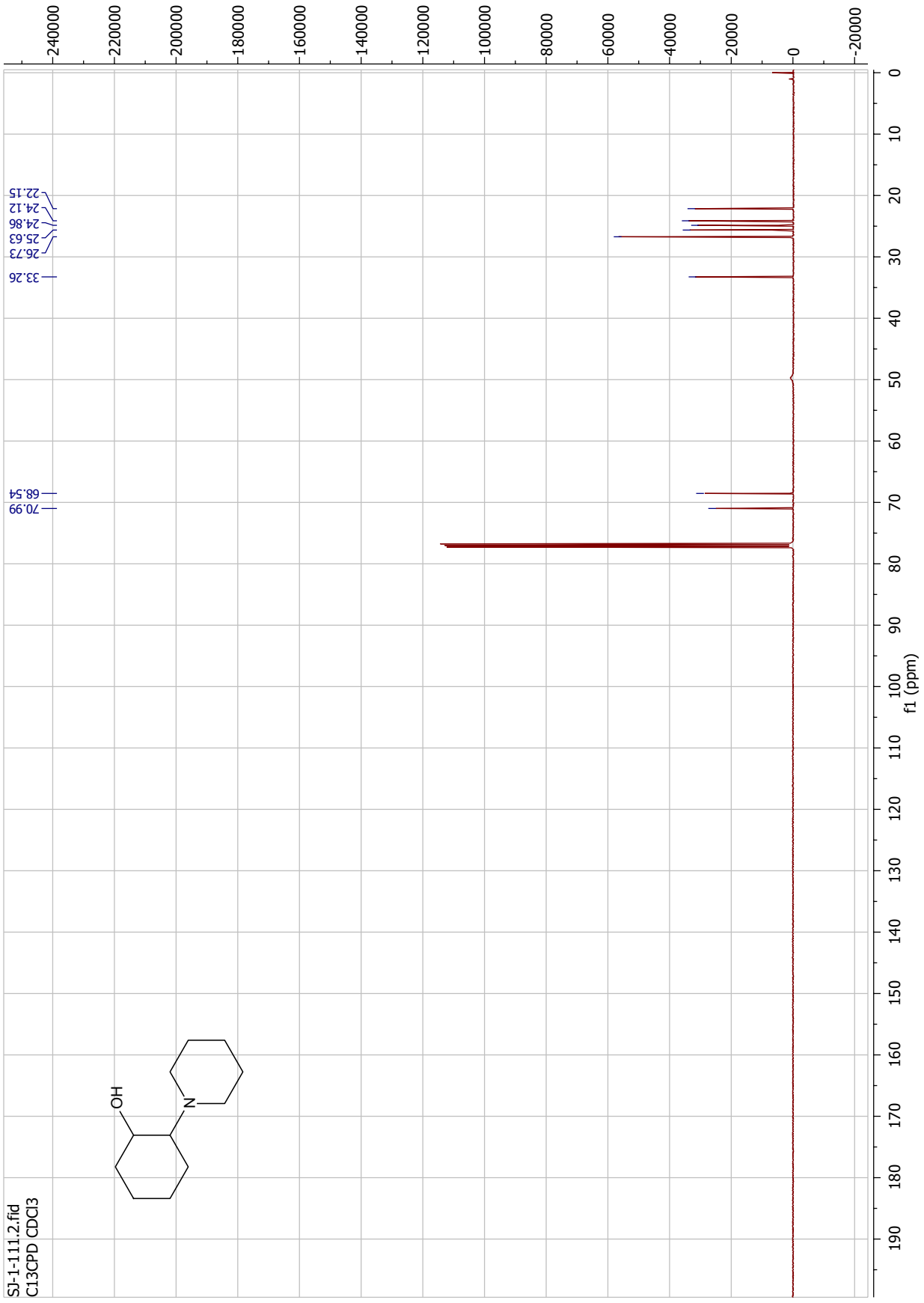
SJ-1-111.2.fid
C13CPD CDCl3
22.15
24.12
24.86
25.63
26.73
33.26
68.54
70.99
OH
N
f1 (ppm)

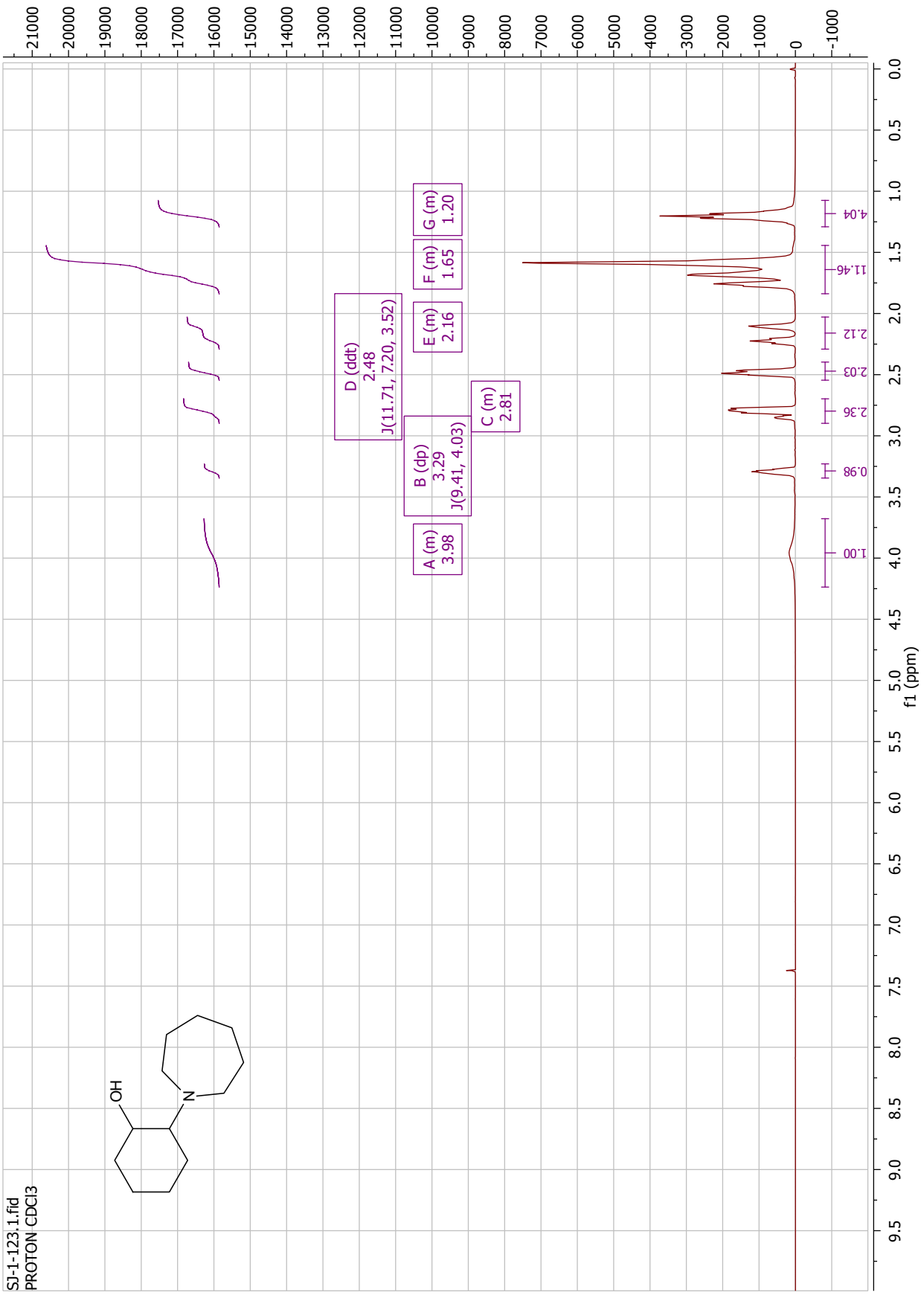
SJ-1-123.1.fid
PROTON CDCl3
OH
N
A (m)
3.98
B (dp)
3.29
J(9.41, 4.03)
C (m)
2.81
D (ddt)
2.48
J(11.71, 7.20, 3.52)
E (m)
2.16
F (m)
1.65
G (m)
1.20
4.04
11.46
2.12
2.03
2.36
0.98
1.00
f1 (ppm)

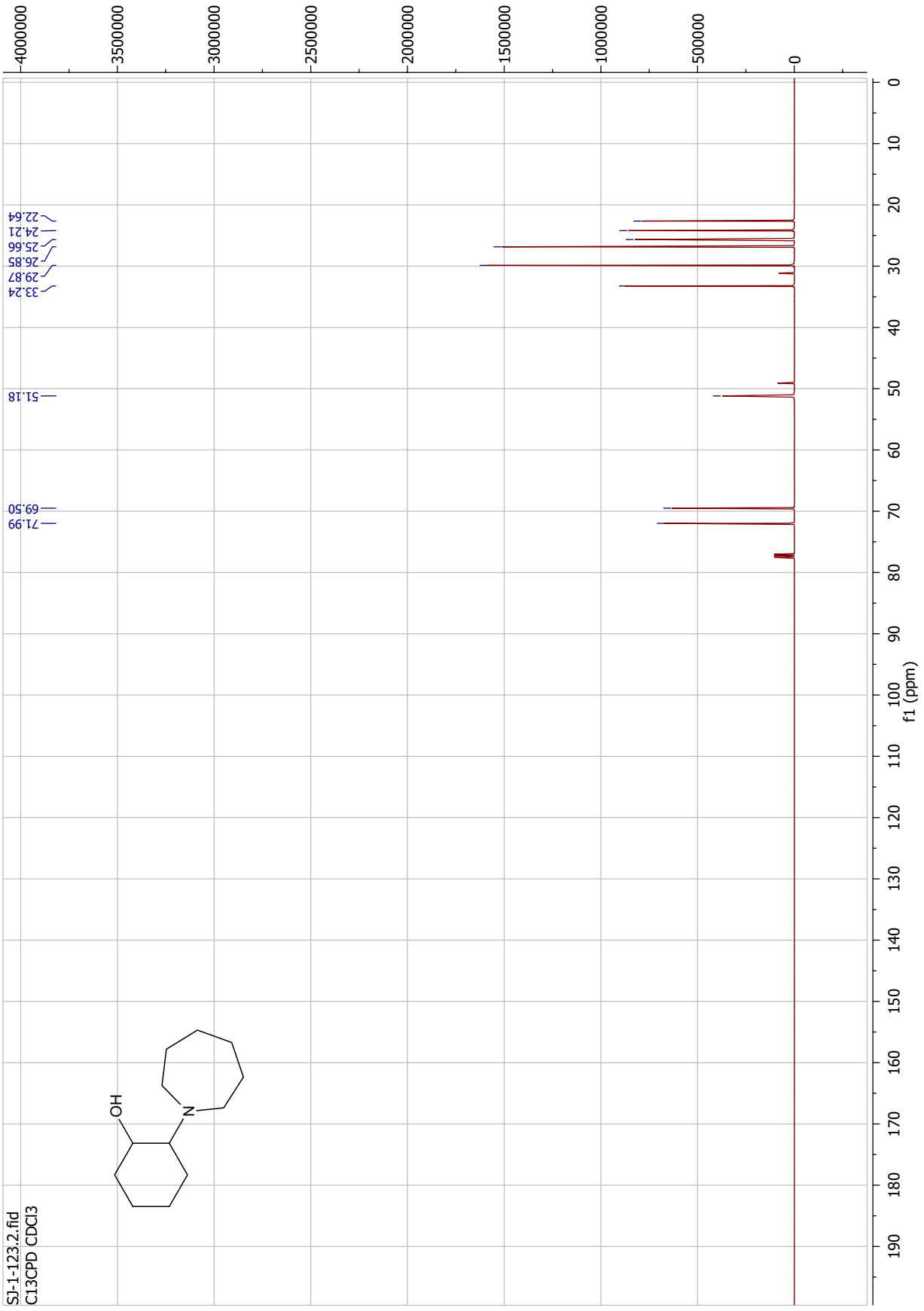
SJ-1-123.2.fid
C13CPD CDCl3
OH
N
22.64
24.21
25.66
26.85
29.87
33.24
51.18
69.50
71.99
f1 (ppm)

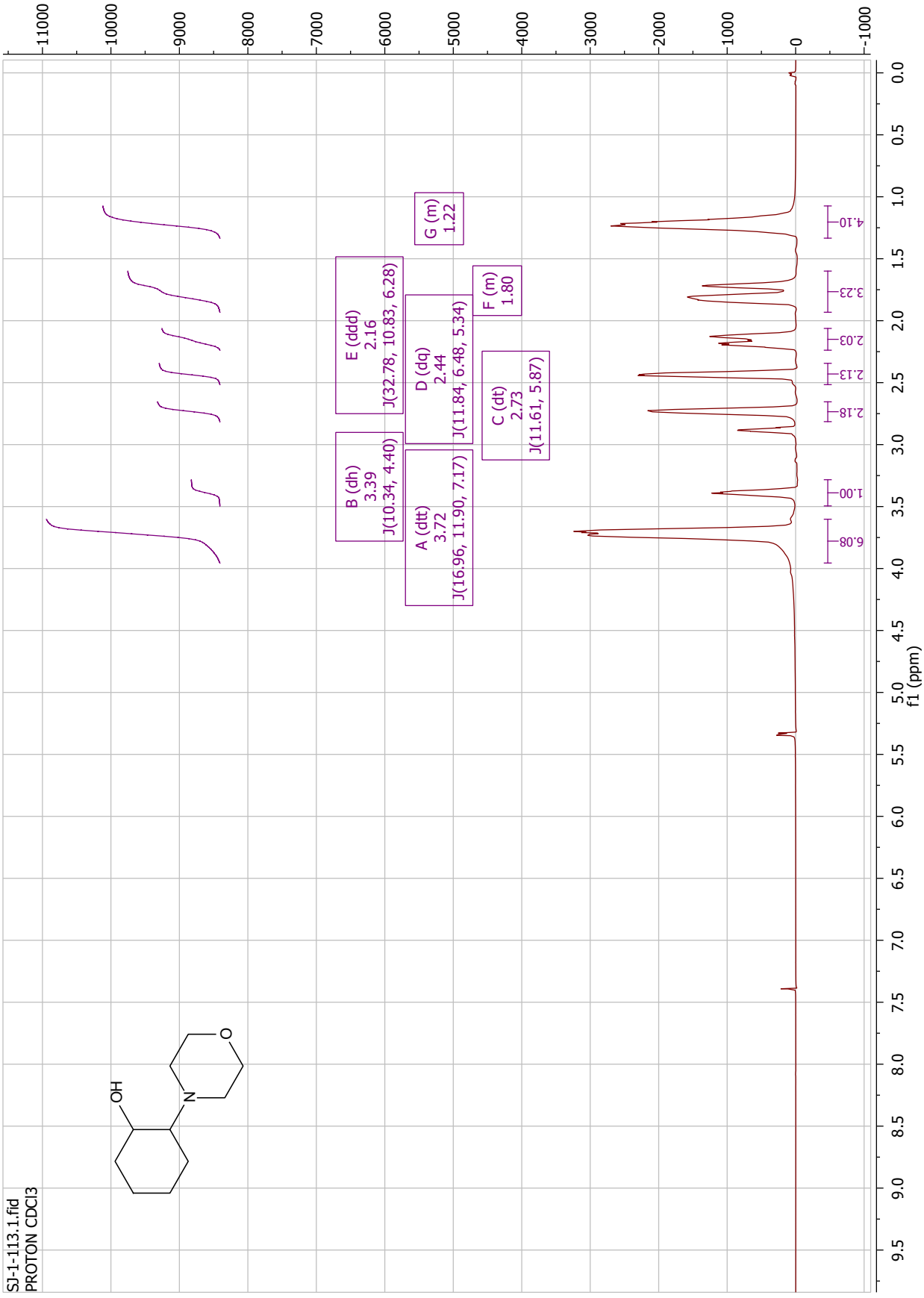
SJ-1-113.1.fid
PROTON CDCl3
OH
N
O
A (dtt)
3.72
J(16.96, 11.90, 7.17)
B (dh)
3.39
J(10.34, 4.40)
C (dt)
2.73
J(11.61, 5.87)
D (dq)
2.44
J(11.84, 6.48, 5.34)
E (ddd)
2.16
J(32.78, 10.83, 6.28)
F (m)
1.80
G (m)
1.22
6.08
1.00
2.18
2.13
2.03
3.23
4.10
f1 (ppm)

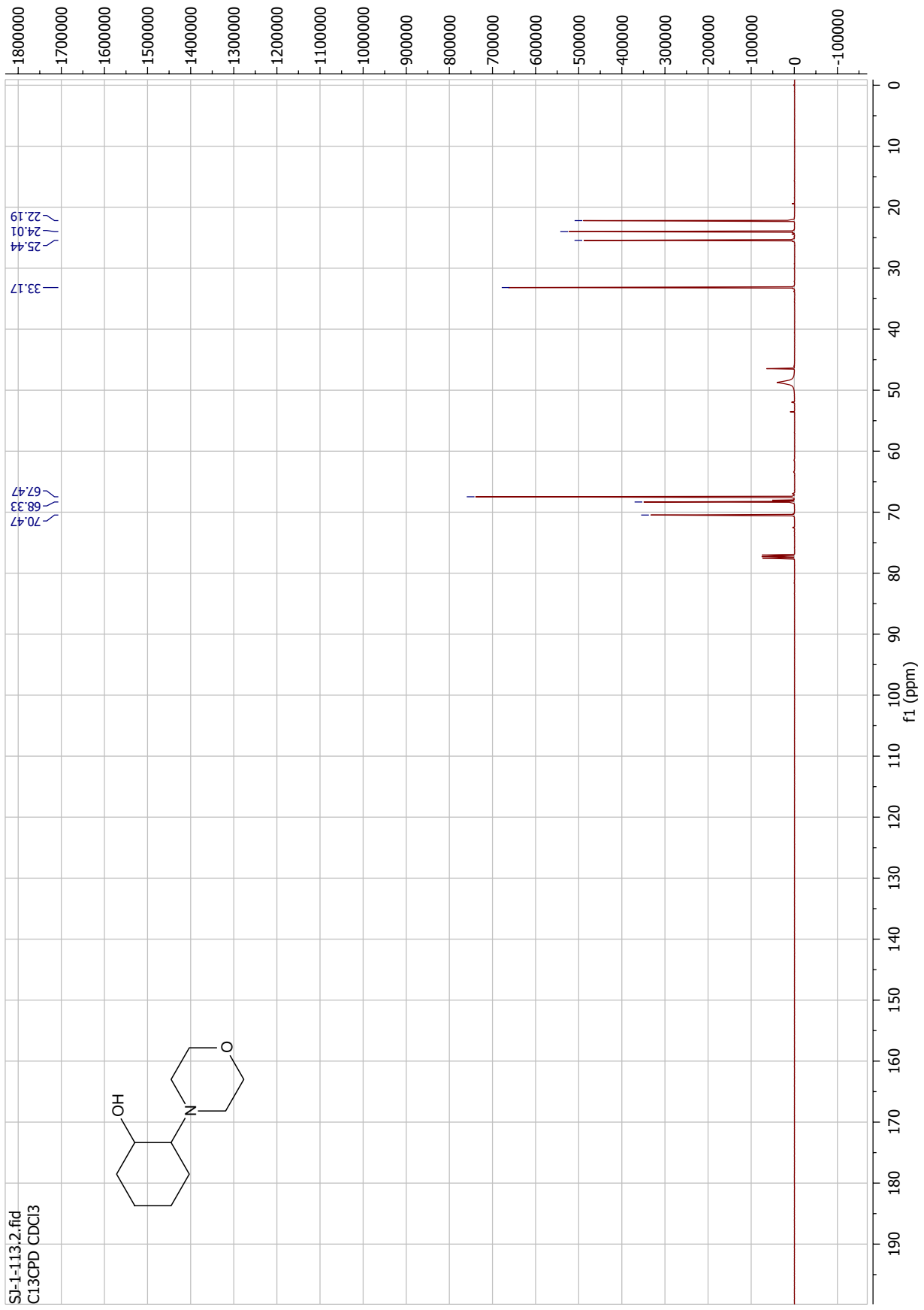
SJ-1-113.2.fid
C13CPD CDCl3
OH
N
O
22.19
24.01
25.44
33.17
67.47
68.33
70.47
f1 (ppm)

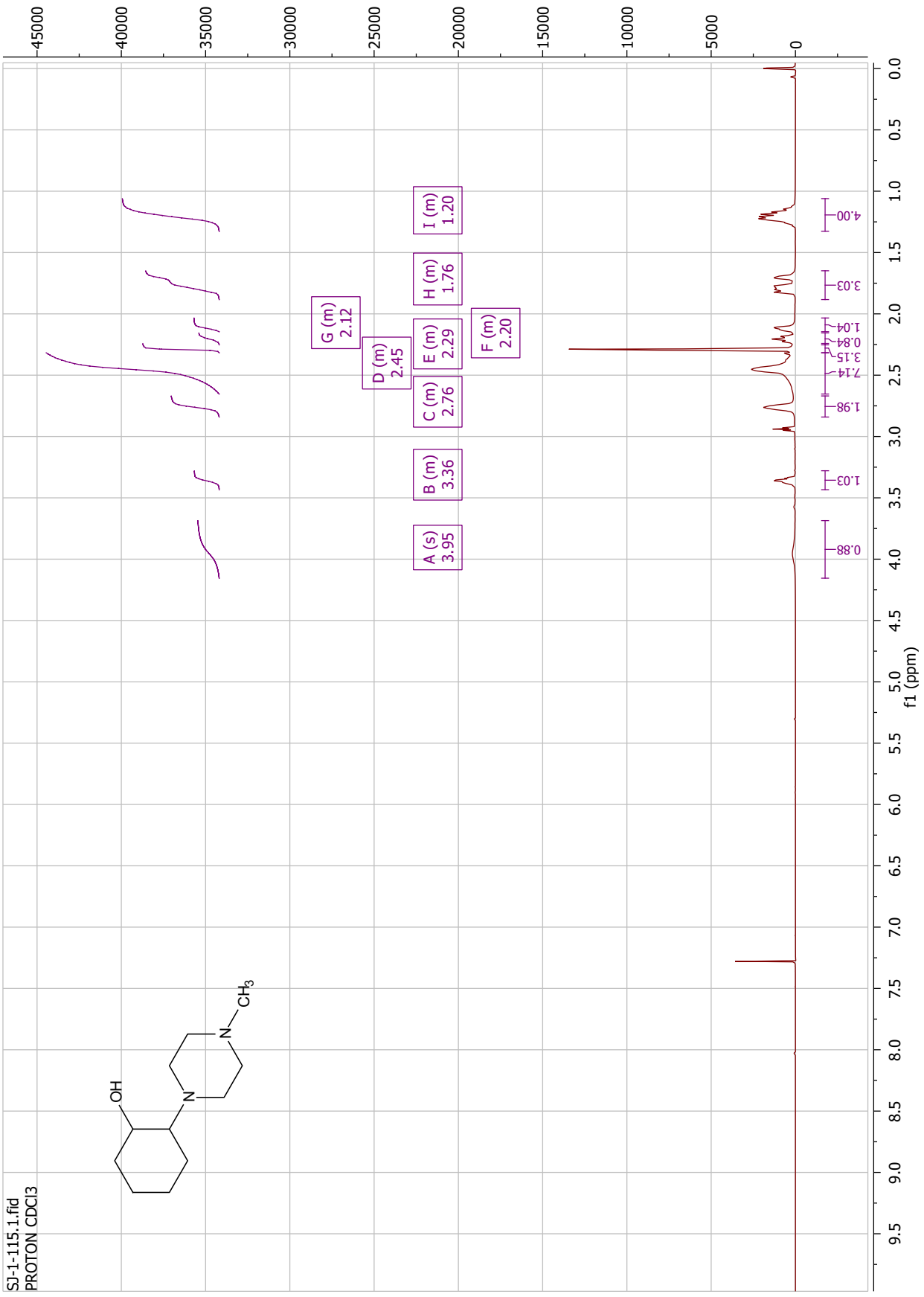
SJ-1-115.1.fid
PROTON CDCl3
A (s) 3.95
B (m) 3.36
C (m) 2.76
D (m) 2.45
E (m) 2.29
F (m) 2.20
G (m) 2.12
H (m) 1.76
I (m) 1.20
4.00
3.03
1.04
0.84
3.15
7.14
1.98
1.03
0.88
OH
N
N
CH3
f1 (ppm)

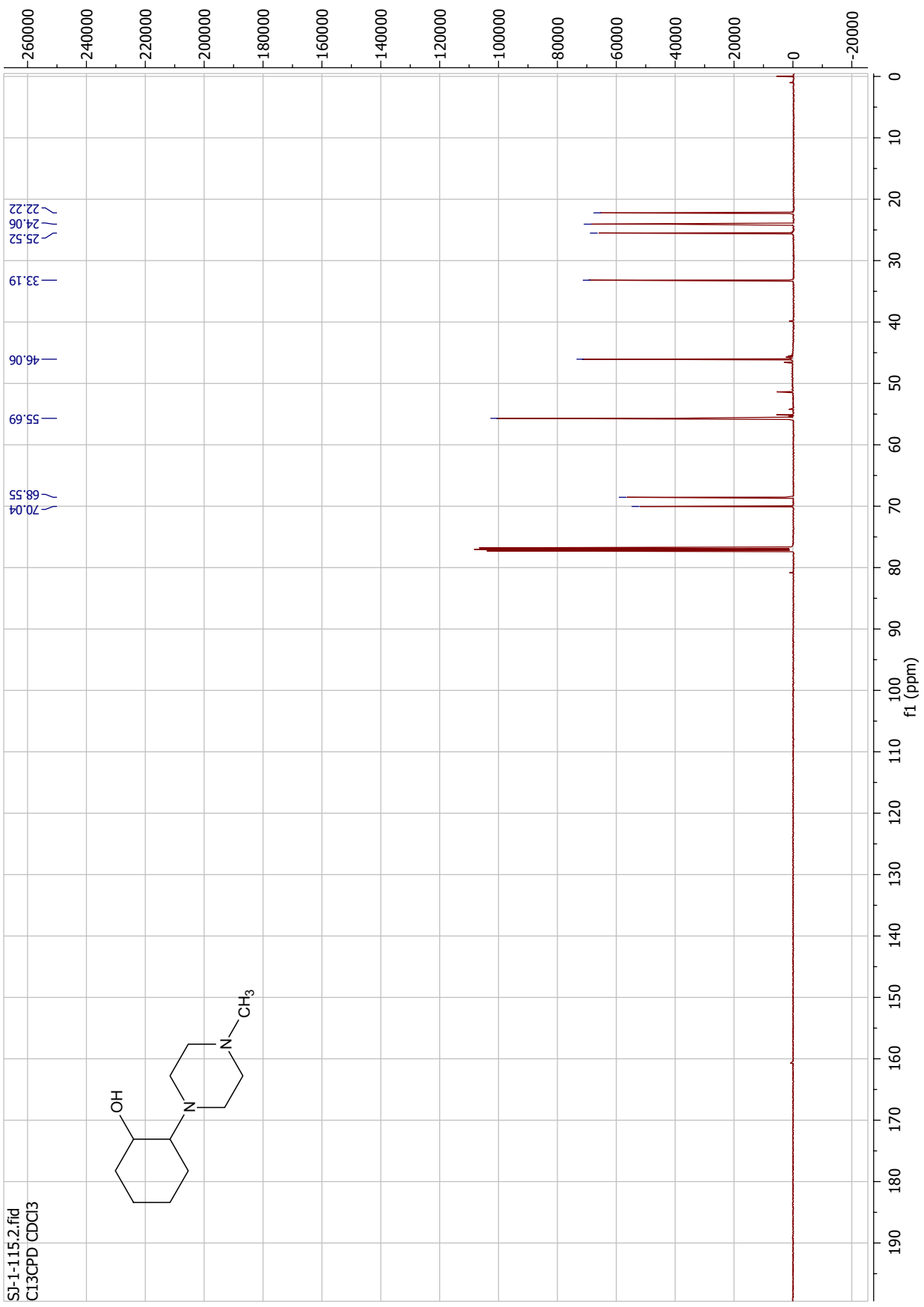
SJ-1-115.2.fid
C13CPD CDCl3
22.22
24.06
25.52
33.19
46.06
55.69
68.55
70.04
OH
N
N
CH3
f1 (ppm)

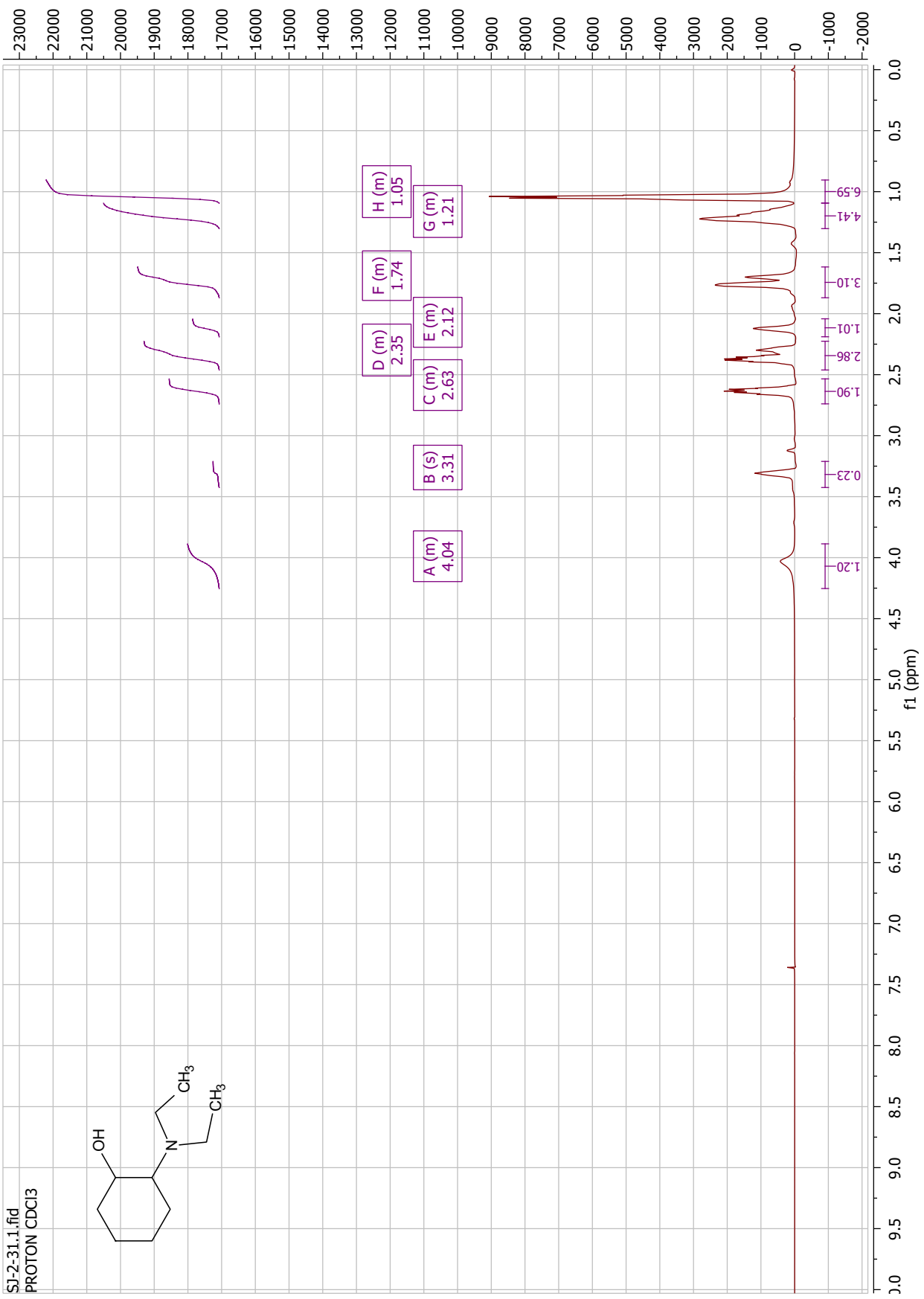
SJ-2-31.1.fid
PROTON CDCl3
OH
N
CH3
CH3
A (m) 4.04
B (s) 3.31
C (m) 2.63
D (m) 2.35
E (m) 2.12
F (m) 1.74
G (m) 1.21
H (m) 1.05
6.59
4.41
3.10
1.01
2.86
1.90
0.23
1.20
f1 (ppm)

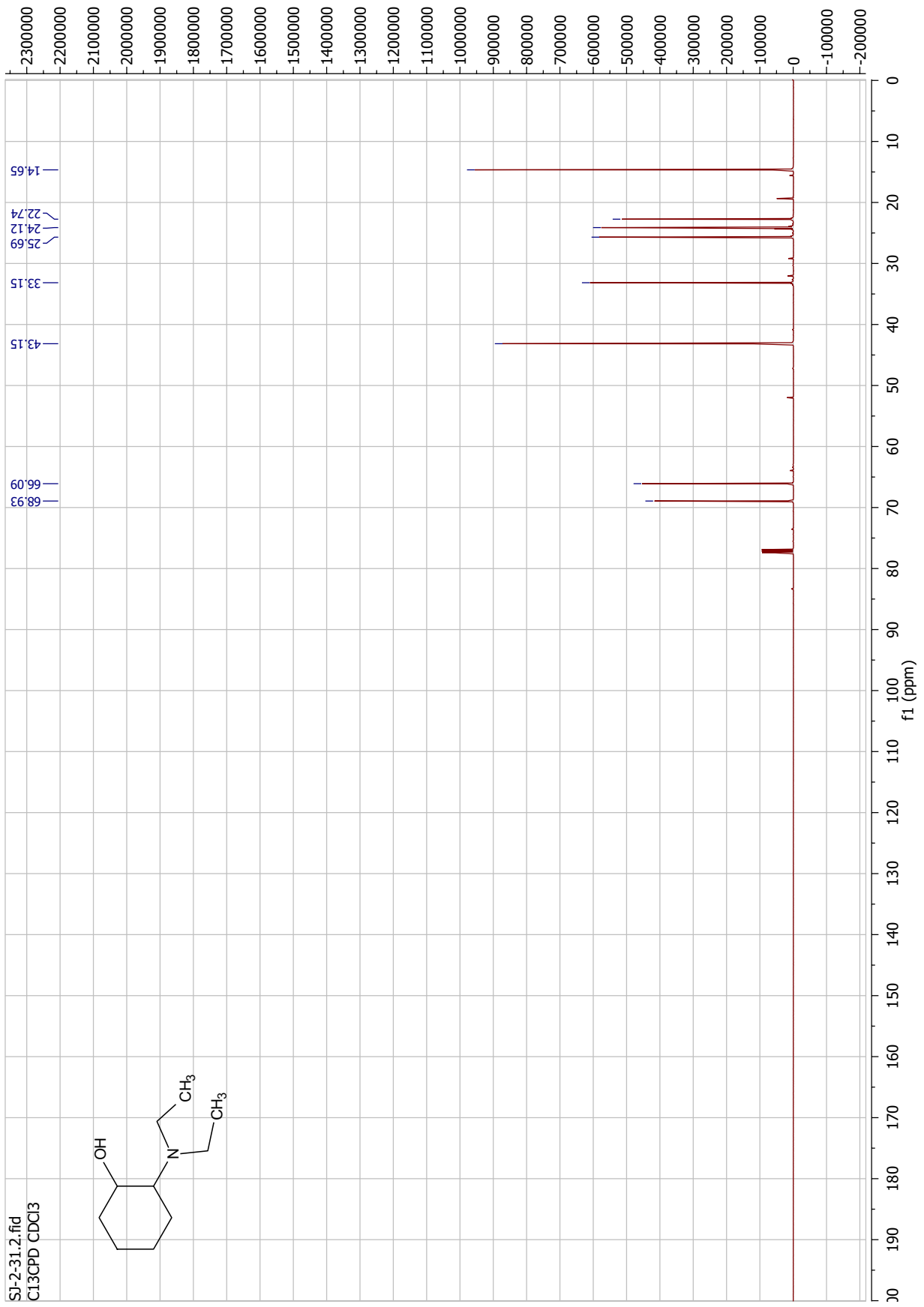
SJ-2-31.2.fid
C13CPD CDCl3
14.65
22.74
24.12
25.69
33.15
43.15
66.09
68.93
OH
N
CH3
CH3
f1 (ppm)

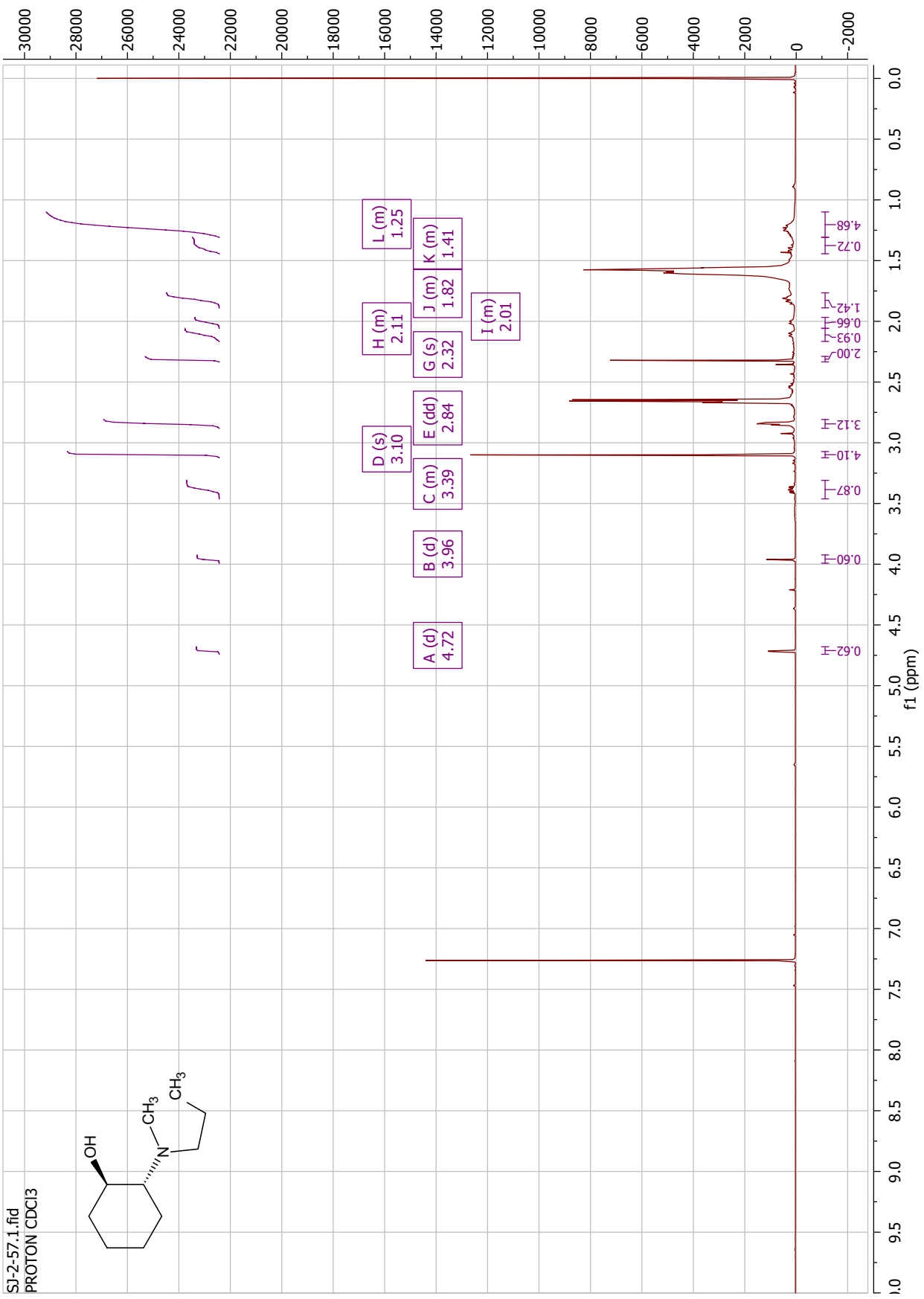
SJ-2-57.1.fid
PROTON CDCl3
OH
N
CH3
CH3
A (d) 4.72
B (d) 3.96
C (m) 3.39
D (s) 3.10
E (dd) 2.84
G (s) 2.32
H (m) 2.11
I (m) 2.01
J (m) 1.82
K (m) 1.41
L (m) 1.25
4.68
0.72
1.42
0.66
0.93
2.00
3.12
4.10
0.87
0.60
0.62
f1 (ppm)

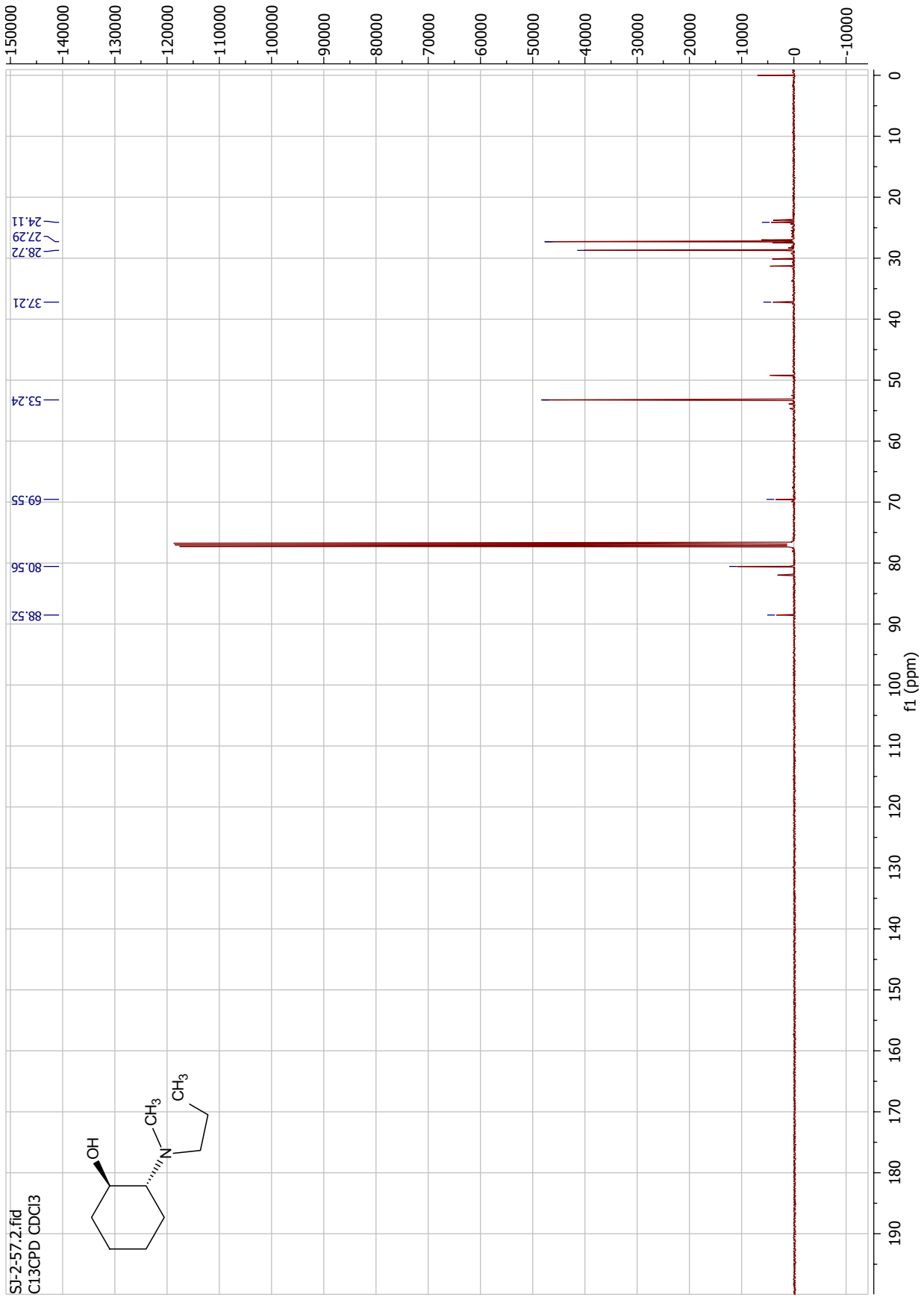
SJ-2-57.2.fid
C13CPD CDCl3
24.11
27.29
28.72
37.21
53.24
69.55
80.56
88.52
f1 (ppm)
OH
N
CH3
CH3

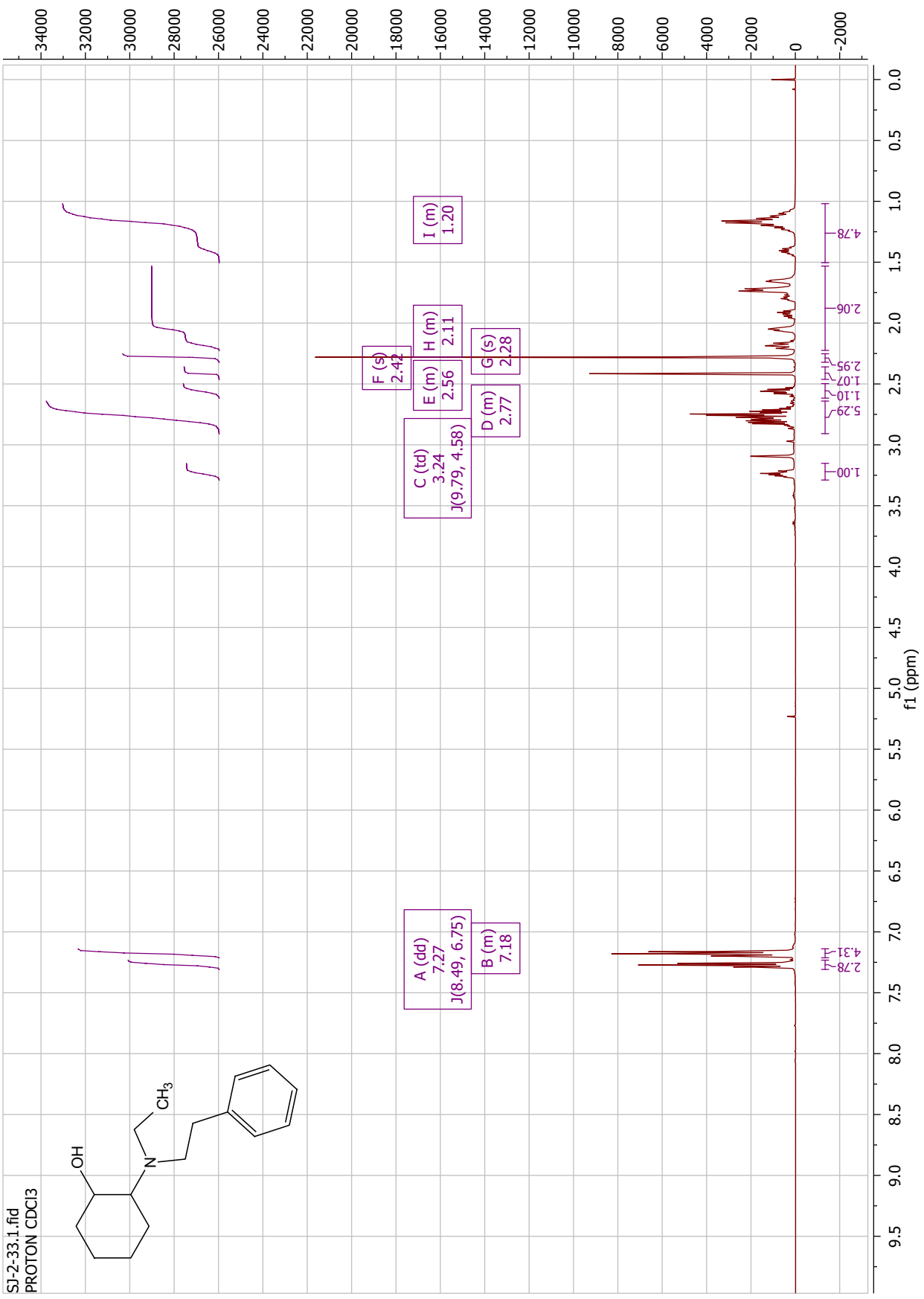
SJ-2-33.1.fid
PROTON CDCl3
OH
N
CH3
A (dd)
7.27
J(8.49, 6.75)
B (m)
7.18
C (td)
3.24
J(9.79, 4.58)
D (m)
2.77
E (m)
2.56
F (s)
2.42
G (s)
2.28
H (m)
2.11
I (m)
1.20
4.78
2.06
2.95
1.07
1.10
5.29
1.00
2.78
4.31
f1 (ppm)

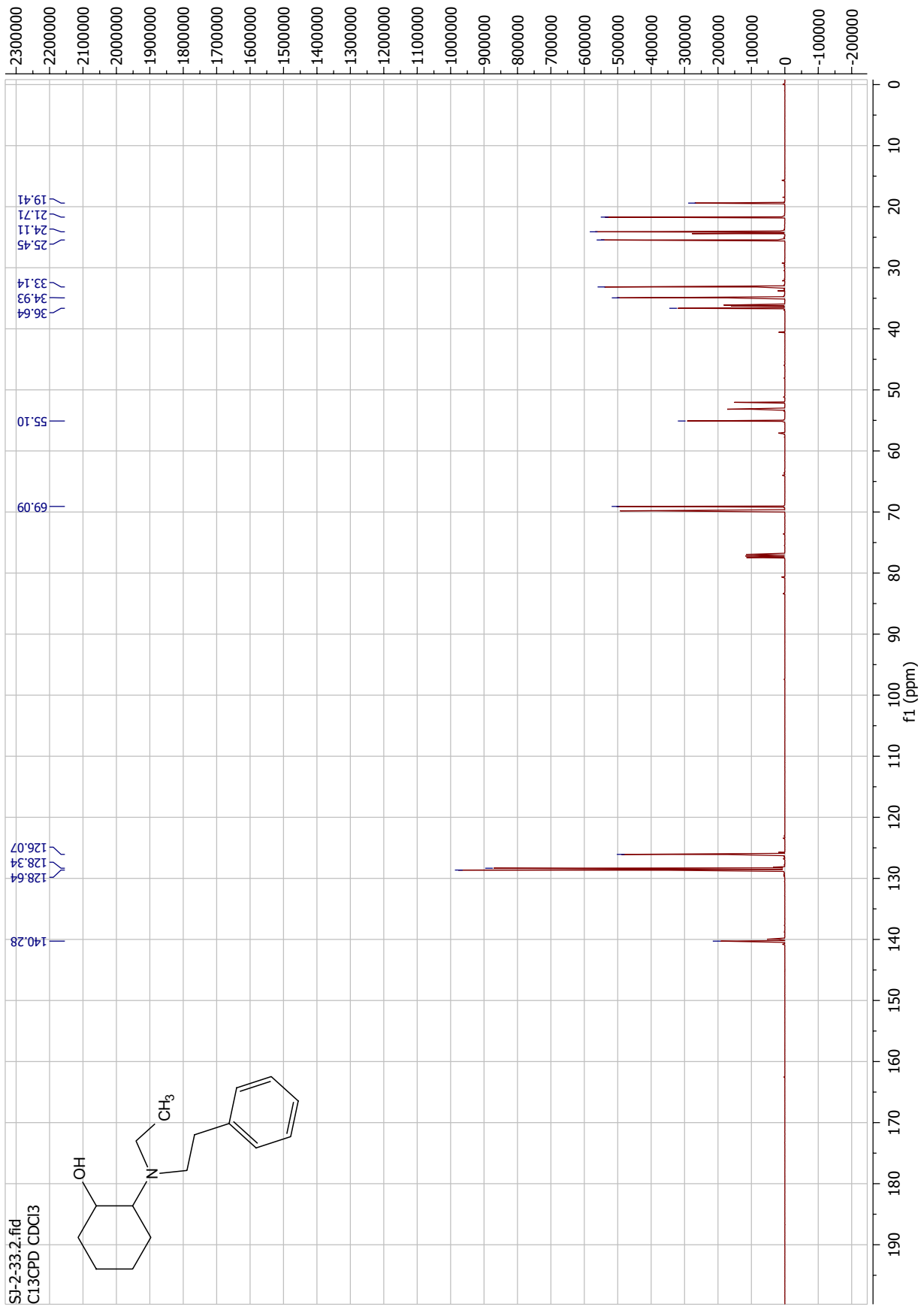
SJ-2-33.2.fid
C13CPD CDCl3
OH
N
CH3
19.41
21.71
24.11
25.45
33.14
34.93
36.64
55.10
69.09
126.07
128.34
128.64
140.28
f1 (ppm)

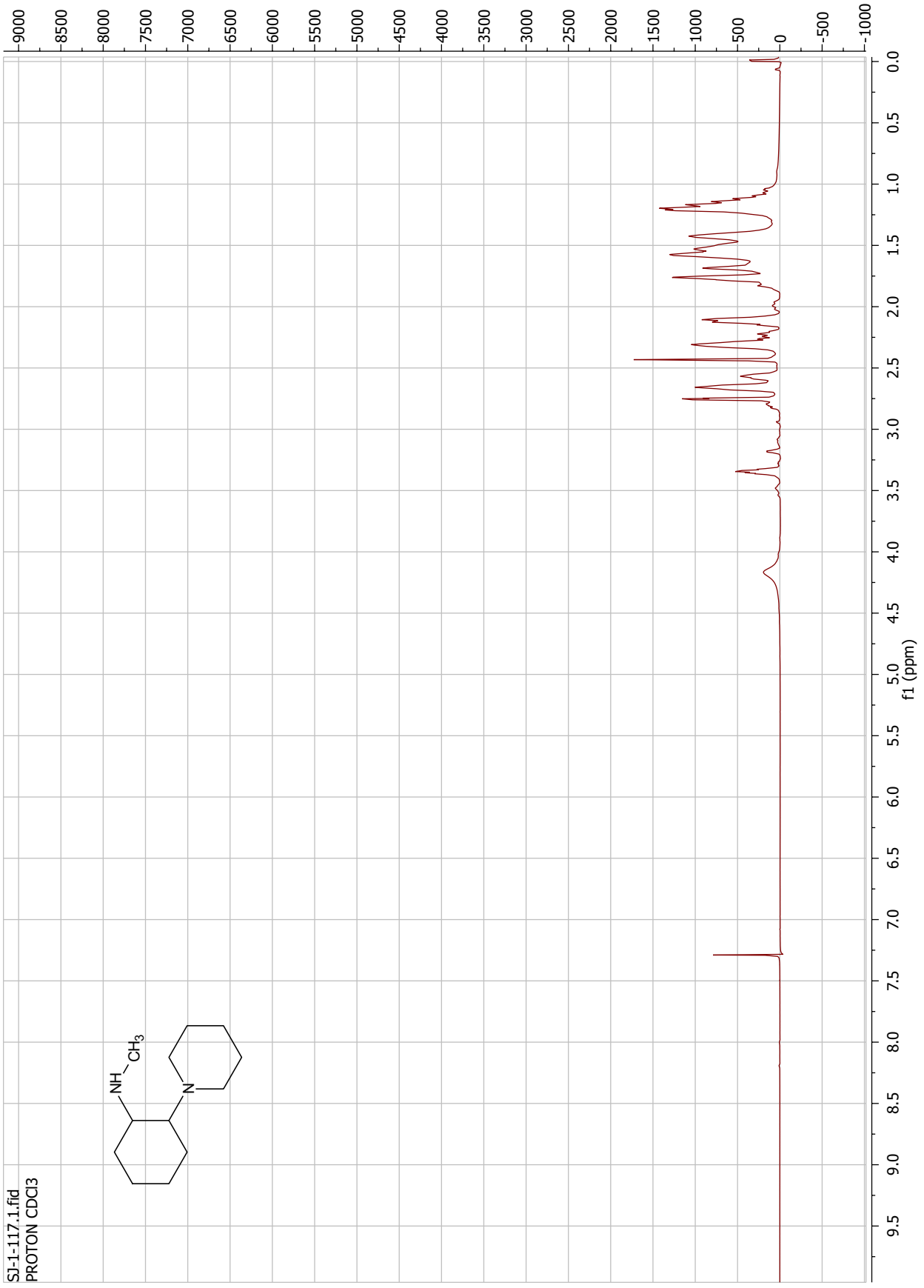
SJ-1-117.1.fid
PROTON CDCl3
NH
CH3
N
f1 (ppm)

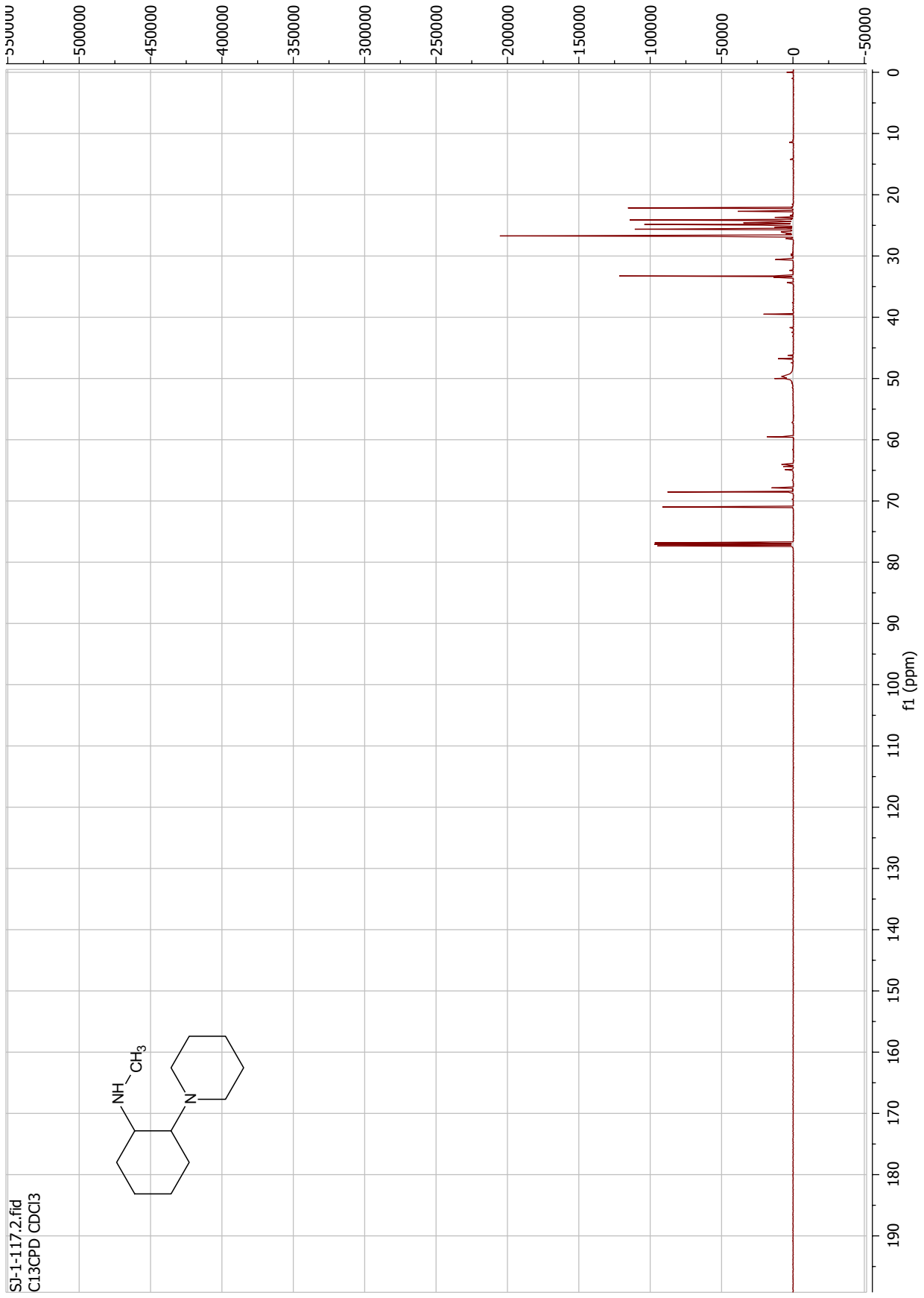
SJ-1-117.2.fid
C13CPD CDCl3
NH
CH3
N
f1 (ppm)

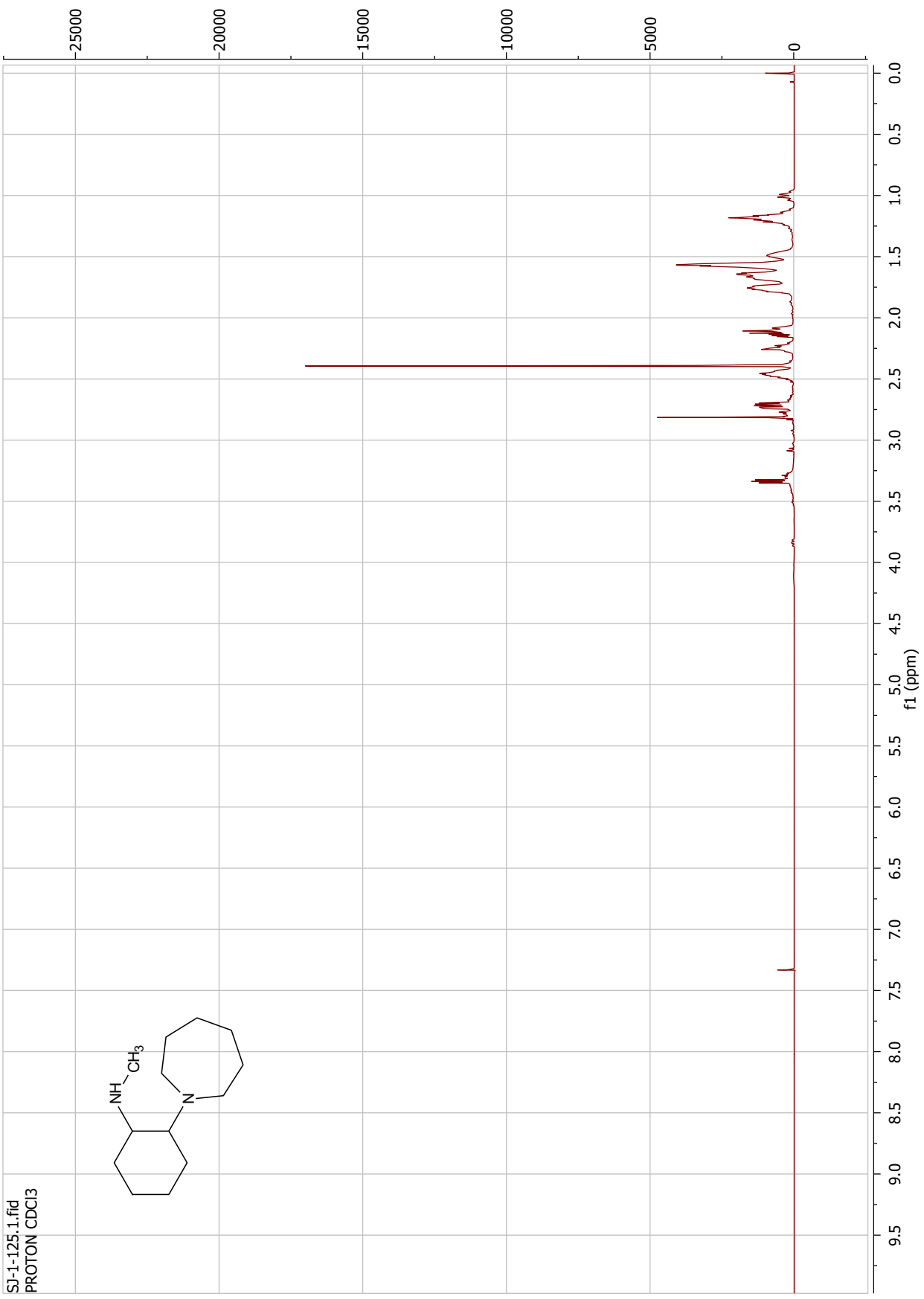
SJ-1-125.1.fid
PROTON CDCl3
NH
CH3
N
25000
20000
15000
10000
5000
0
0.0
0.5
1.0
1.5
2.0
2.5
3.0
3.5
4.0
4.5
5.0
5.5
6.0
6.5
7.0
7.5
8.0
8.5
9.0
9.5
f1 (ppm)

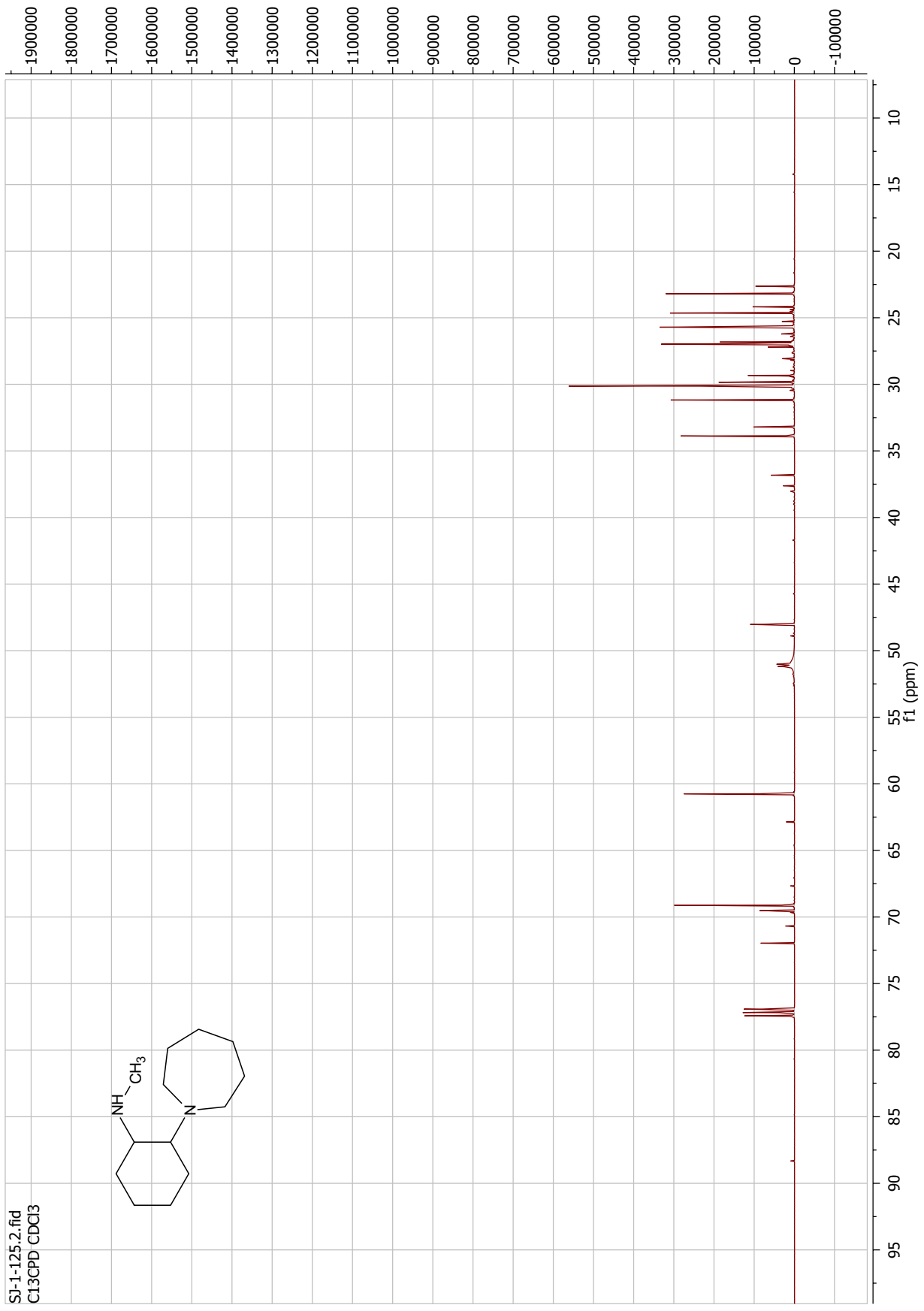
SJ-1-125.2.fid
C13CPD CDCl3
NH
CH3
N
f1 (ppm)

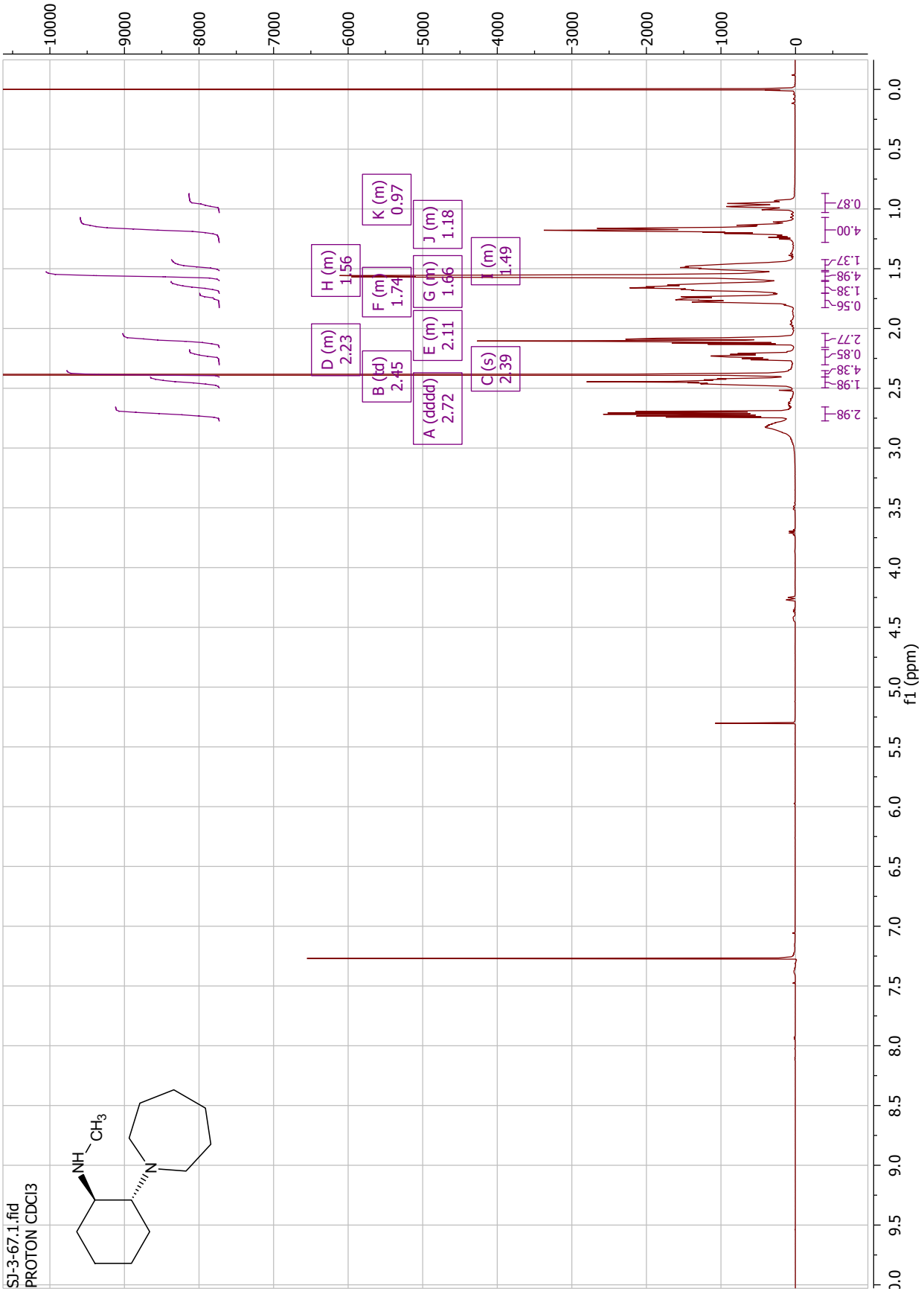
SJ-3-67.1.fid
PROTON CDCl3
NH
CH3
N
A (dddd) 2.72
B (td) 2.45
C (s) 2.39
D (m) 2.23
E (m) 2.11
F (m) 1.74
G (m) 1.66
H (m) 1.56
I (m) 1.49
J (m) 1.18
K (m) 0.97
0.87
4.00
1.37
4.98
1.38
0.56
2.77
0.85
4.38
1.98
2.98
f1 (ppm)

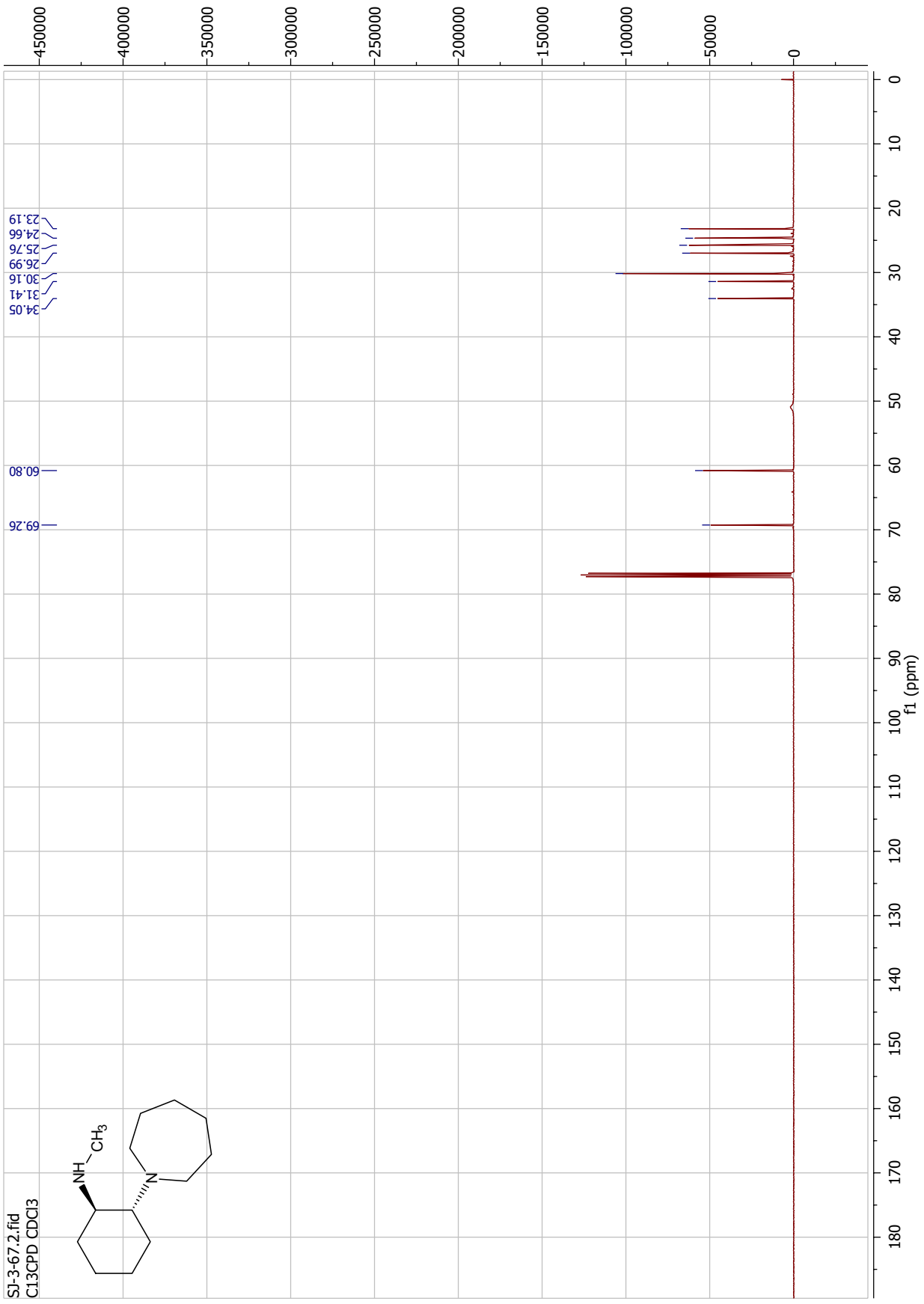
S1-3-67.2.fid
C13CPD CDCl3
NH
CH3
N
23.19
24.66
25.76
26.99
30.16
31.41
34.05
60.80
69.26
f1 (ppm)

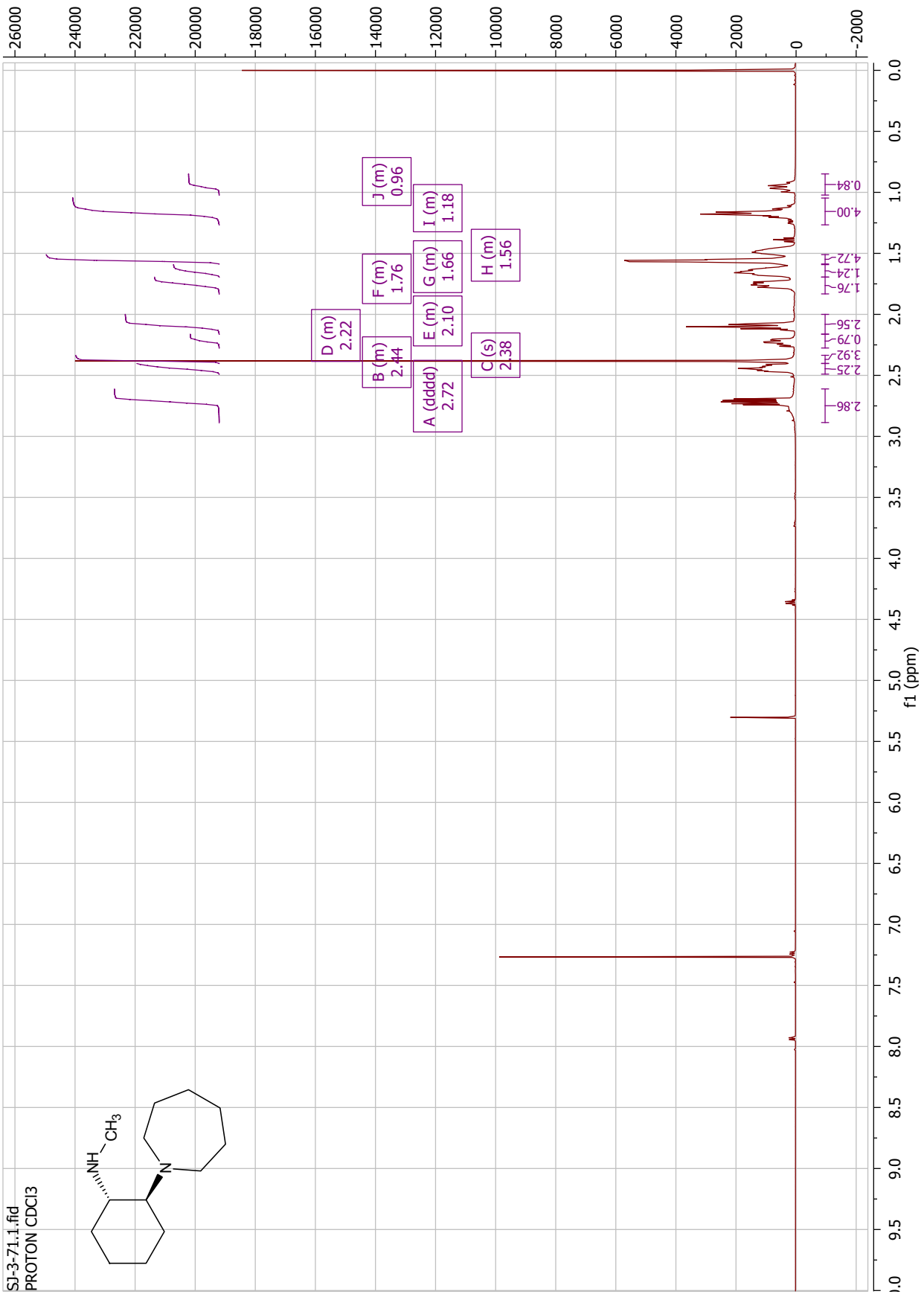
SJ-3-71.1.fid
PROTON CDCl3
A (dddd) 2.72
B (m) 2.44
C (s) 2.38
D (m) 2.22
E (m) 2.10
F (m) 1.76
G (m) 1.66
H (m) 1.56
I (m) 1.18
J (m) 0.96
0.84
4.00
4.72
1.24
1.76
2.56
0.79
3.92
2.25
2.86
f1 (ppm)

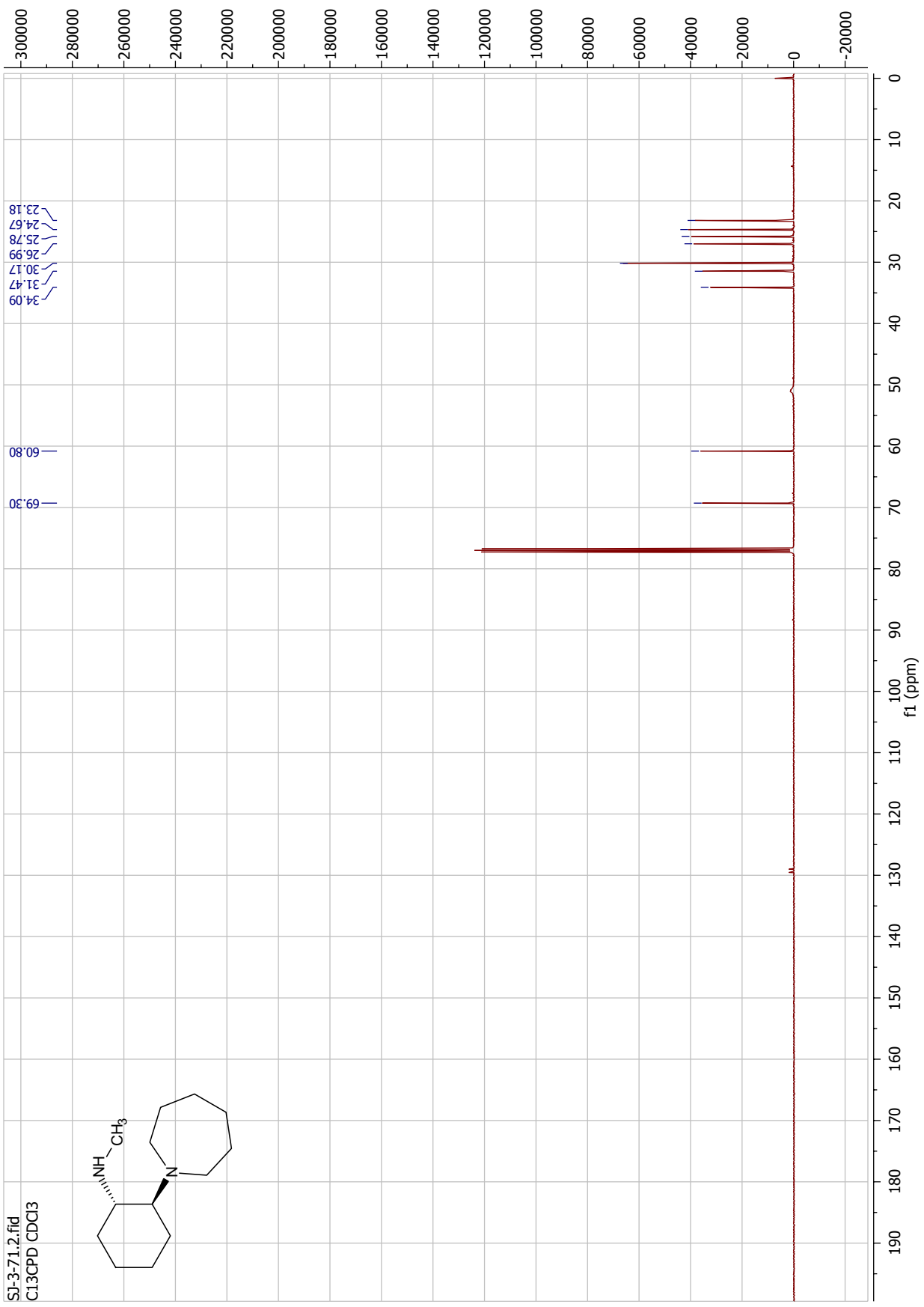
S1-3-71.2.fid
C13CPD CDCl3
NH
CH3
N
23.18
24.67
25.78
26.99
30.17
31.47
34.09
60.80
69.30
f1 (ppm)

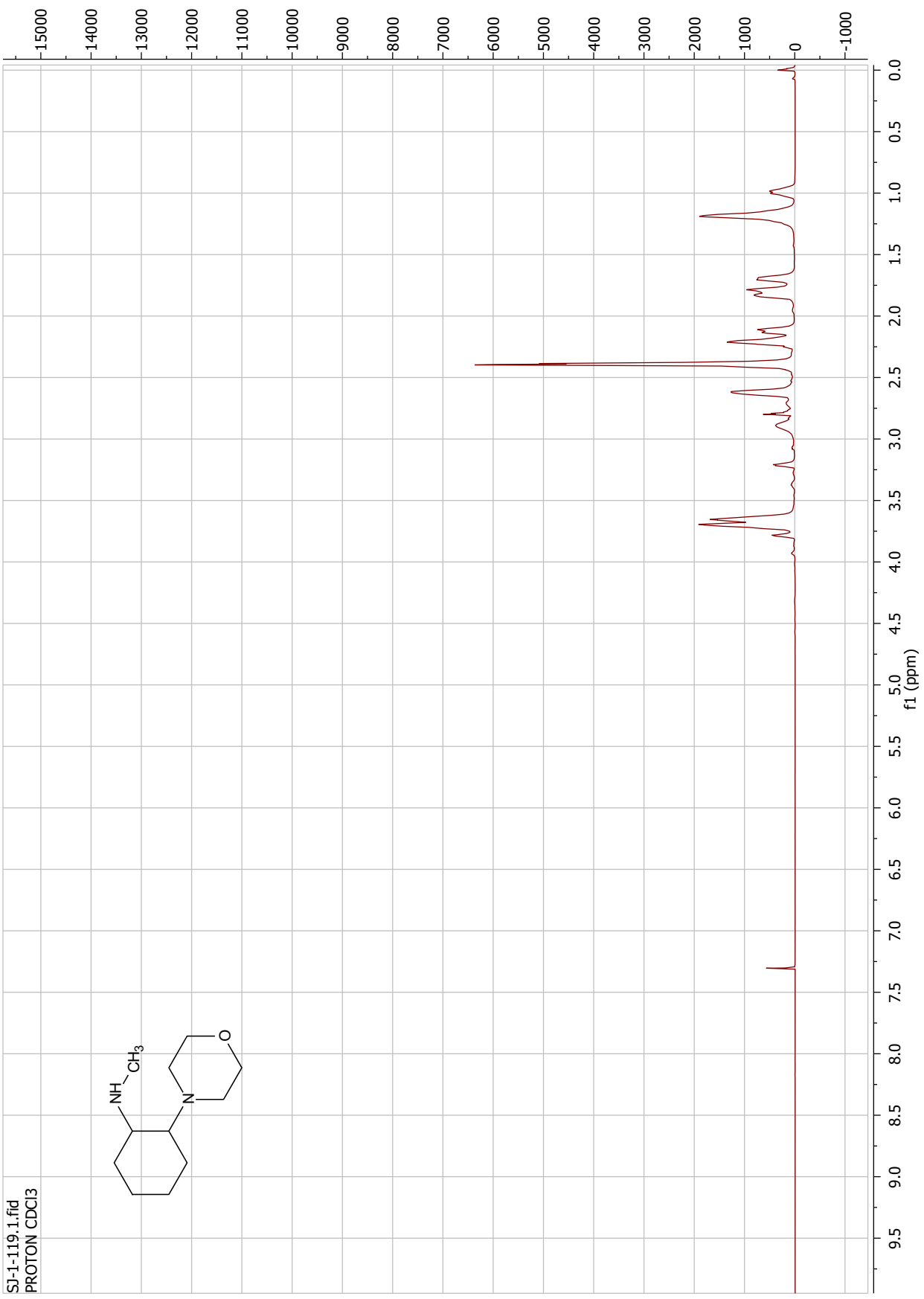
SJ-1-119.1.fid
PROTON CDCl3
NH
CH3
N
O
f1 (ppm)

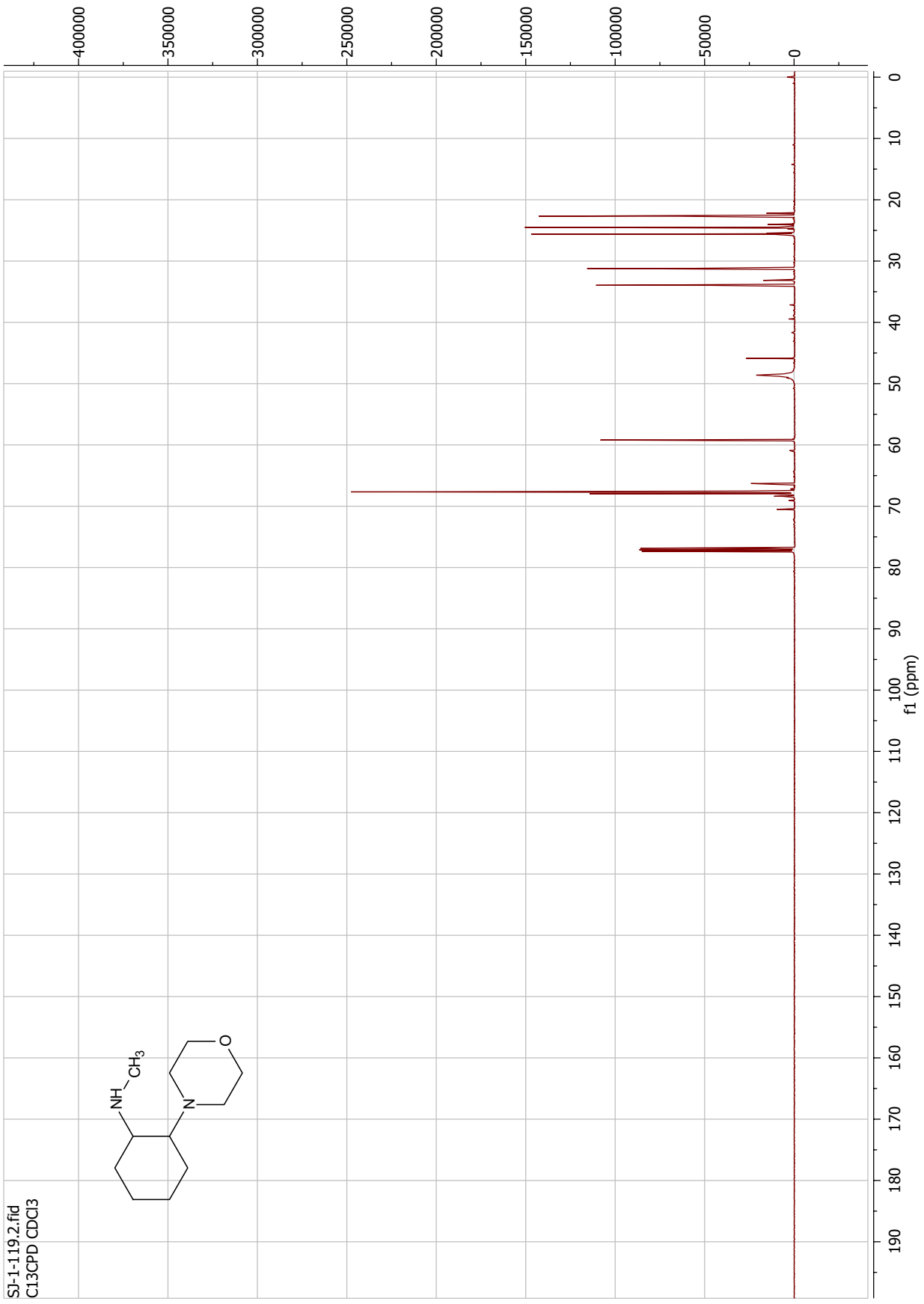
SJ-1-119.2.fid
C13CPD CDCl3
NH
CH3
N
O
f1 (ppm)

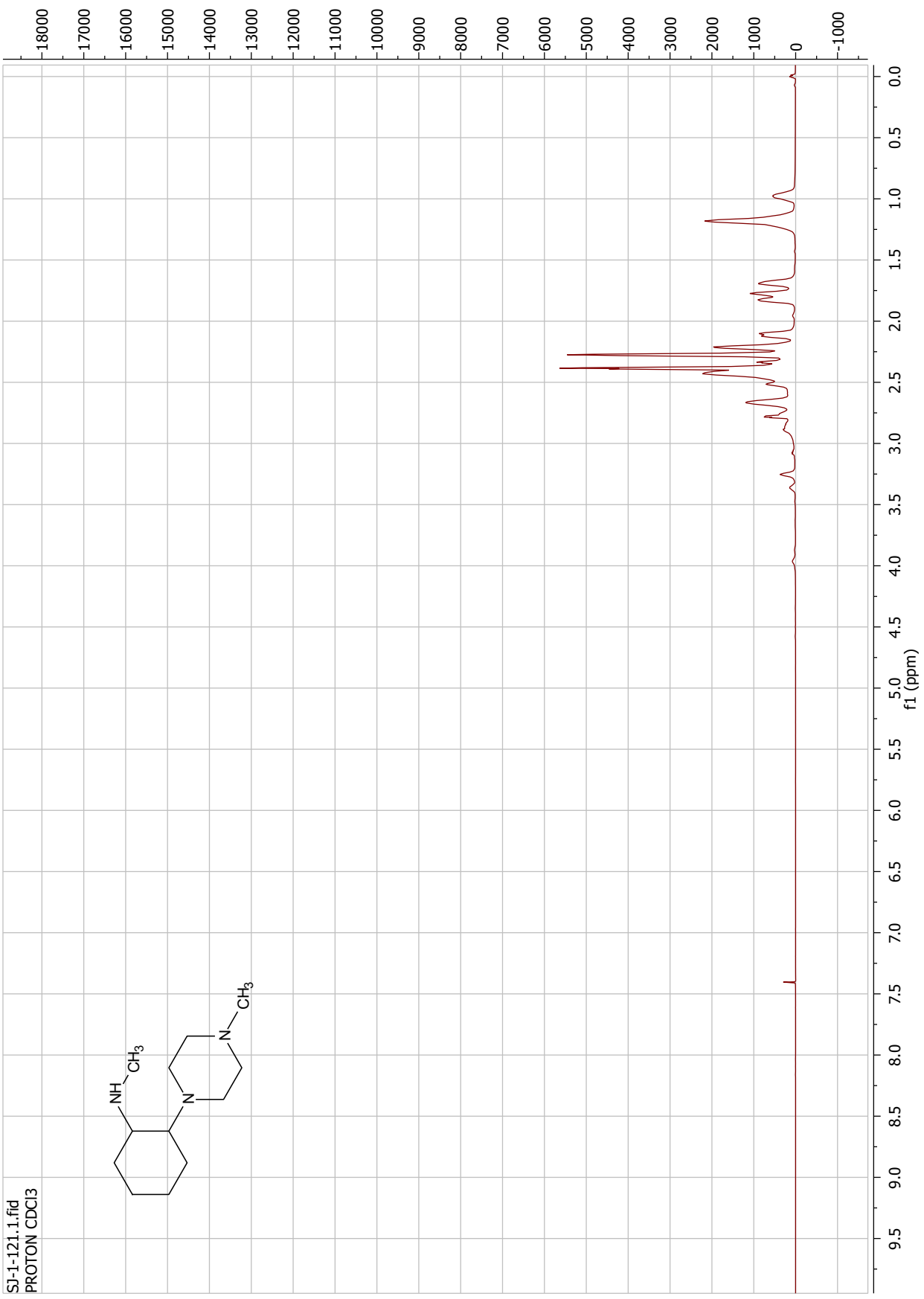
SJ-1-121.1.fid
PROTON CDCl3
NH
CH3
N
N
CH3
f1 (ppm)

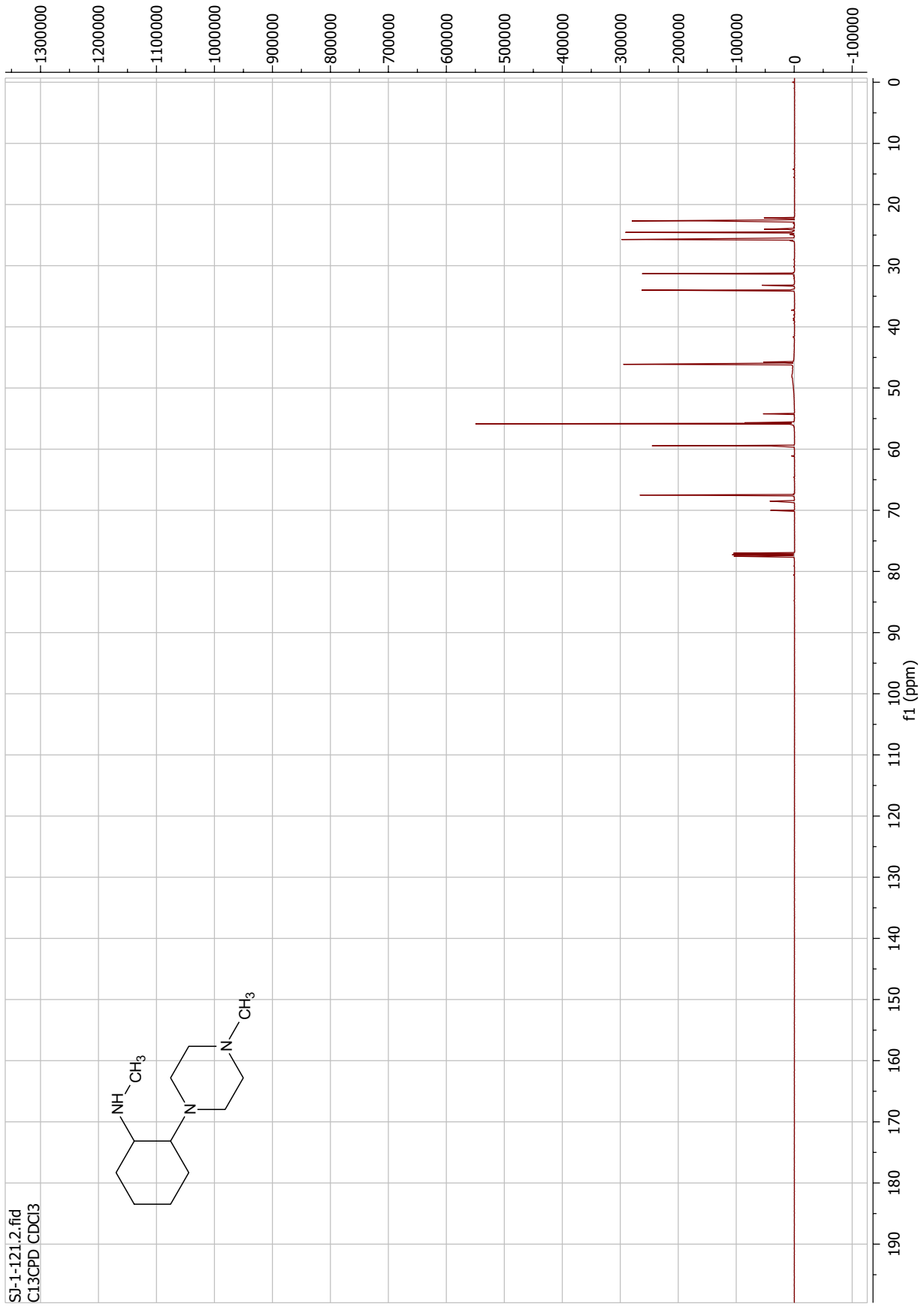
SJ-1-121.2.fid
C13CPD CDCl3
NH
CH3
N
N
CH3
1300000
1200000
1100000
1000000
900000
800000
700000
600000
500000
400000
300000
200000
100000
0
-100000
0
10
20
30
40
50
60
70
80
90
100
110
120
130
140
150
160
170
180
190
f1 (ppm)

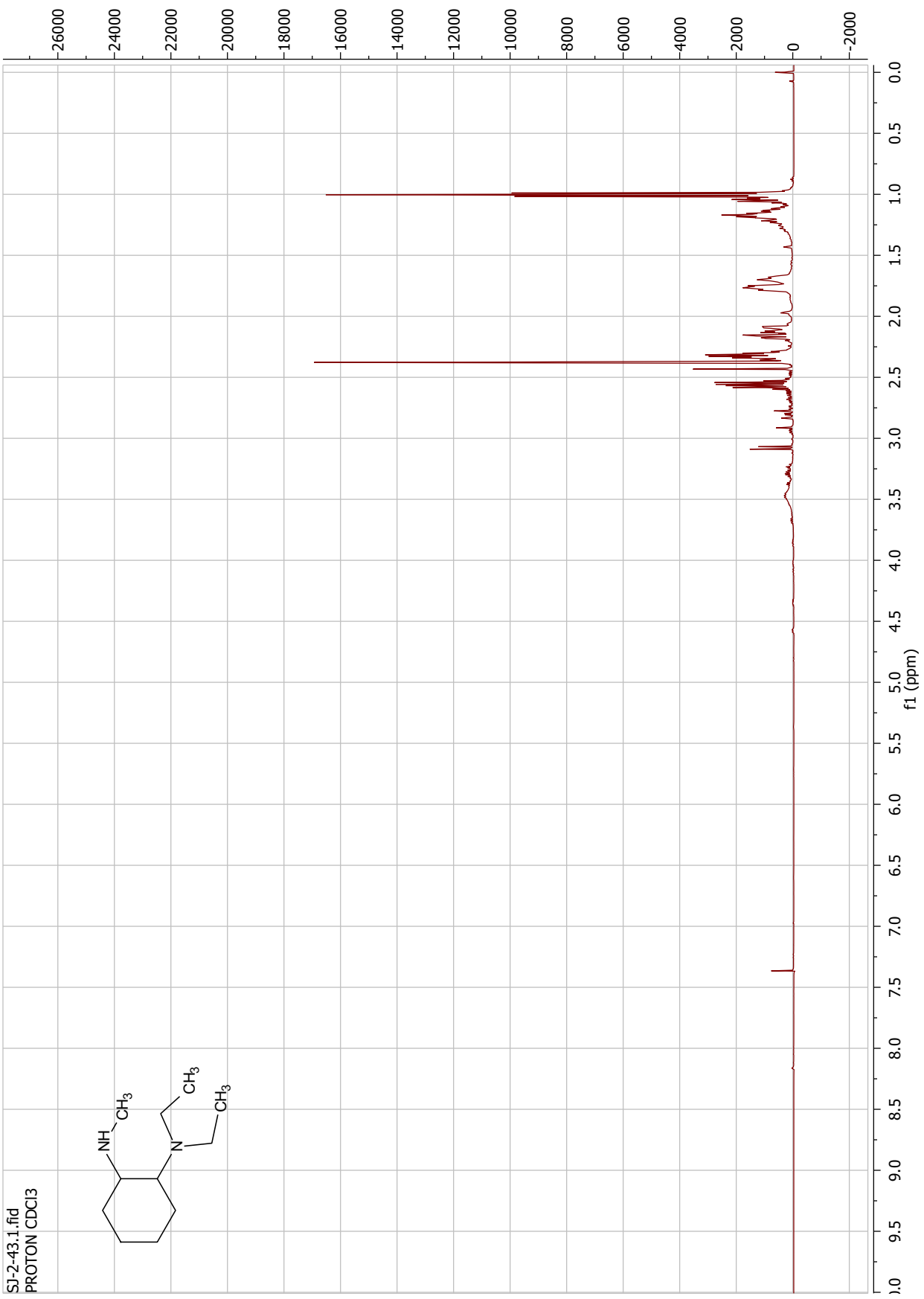
SJ-2-43.1.fid
PROTON CDCl3
NH
CH3
N
CH3
CH3
f1 (ppm)

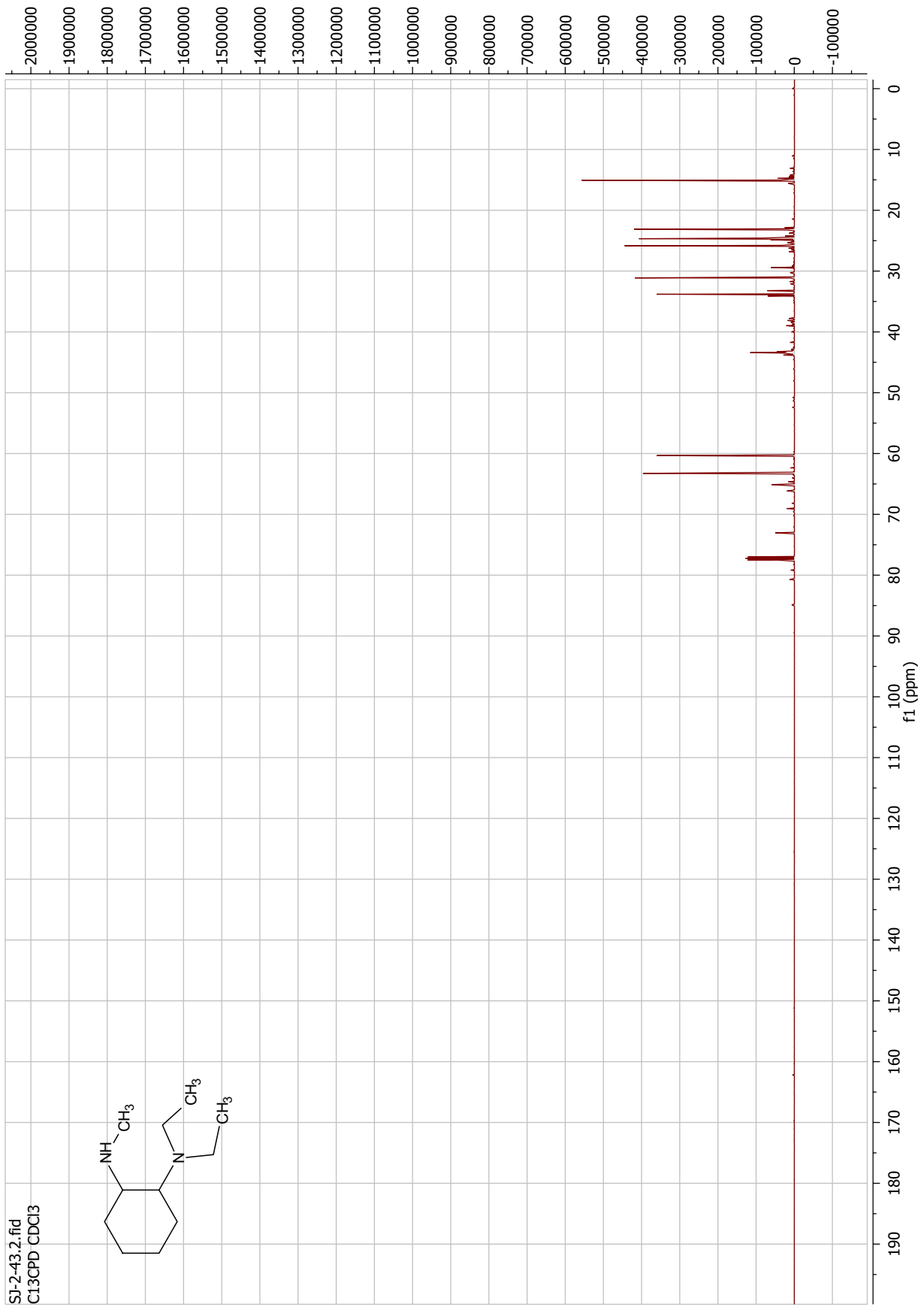
SJ-2-43.2.fid
C13CPD CDCl3
NH
CH3
N
CH3
CH3
f1 (ppm)

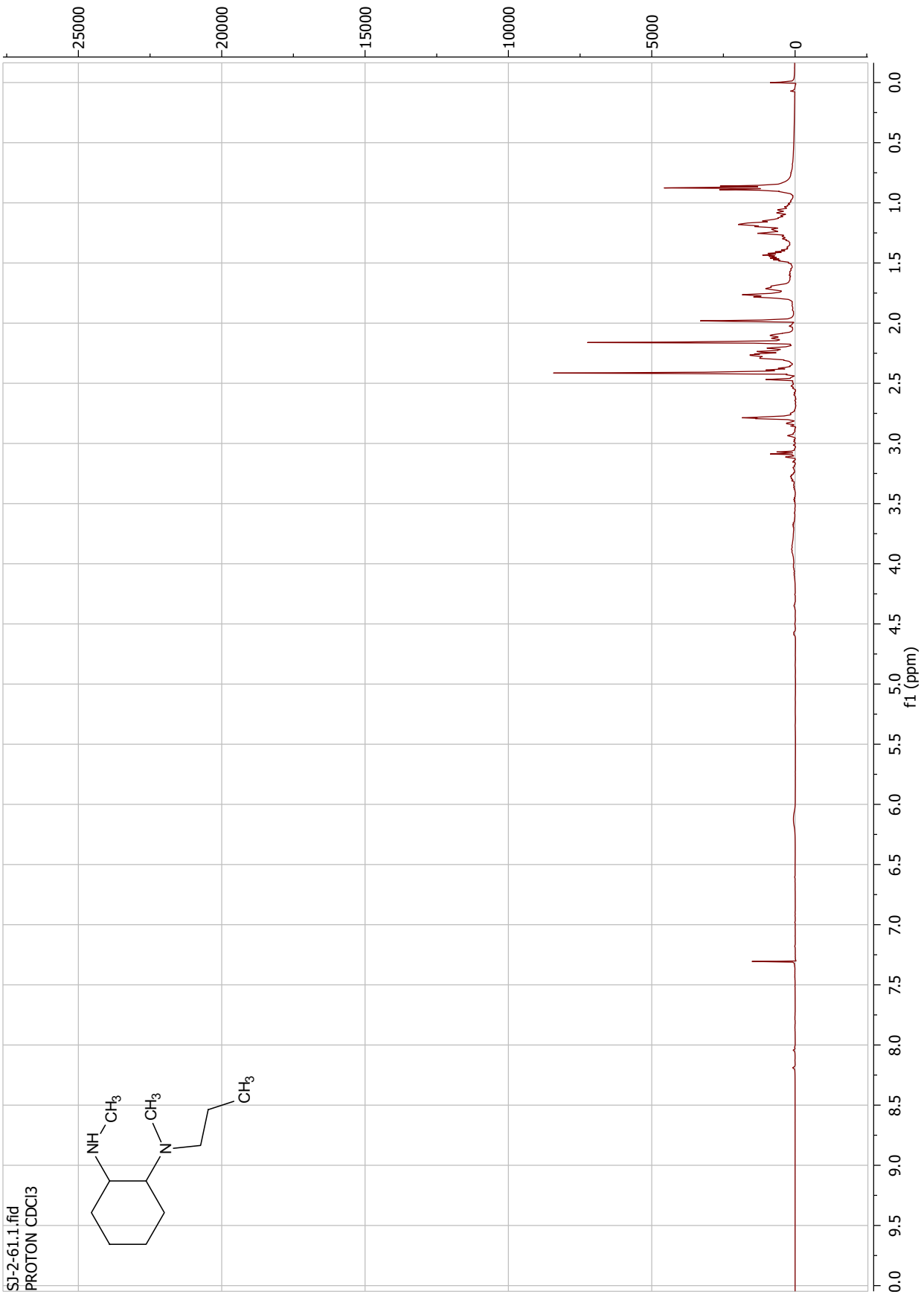
SJ-2-61.1.fid
PROTON CDCl3
NH
CH3
CH3
N
CH3
25000
20000
15000
10000
5000
0
0.0
0.5
1.0
1.5
2.0
2.5
3.0
3.5
4.0
4.5
5.0
5.5
6.0
6.5
7.0
7.5
8.0
8.5
9.0
9.5
0.0
f1 (ppm)

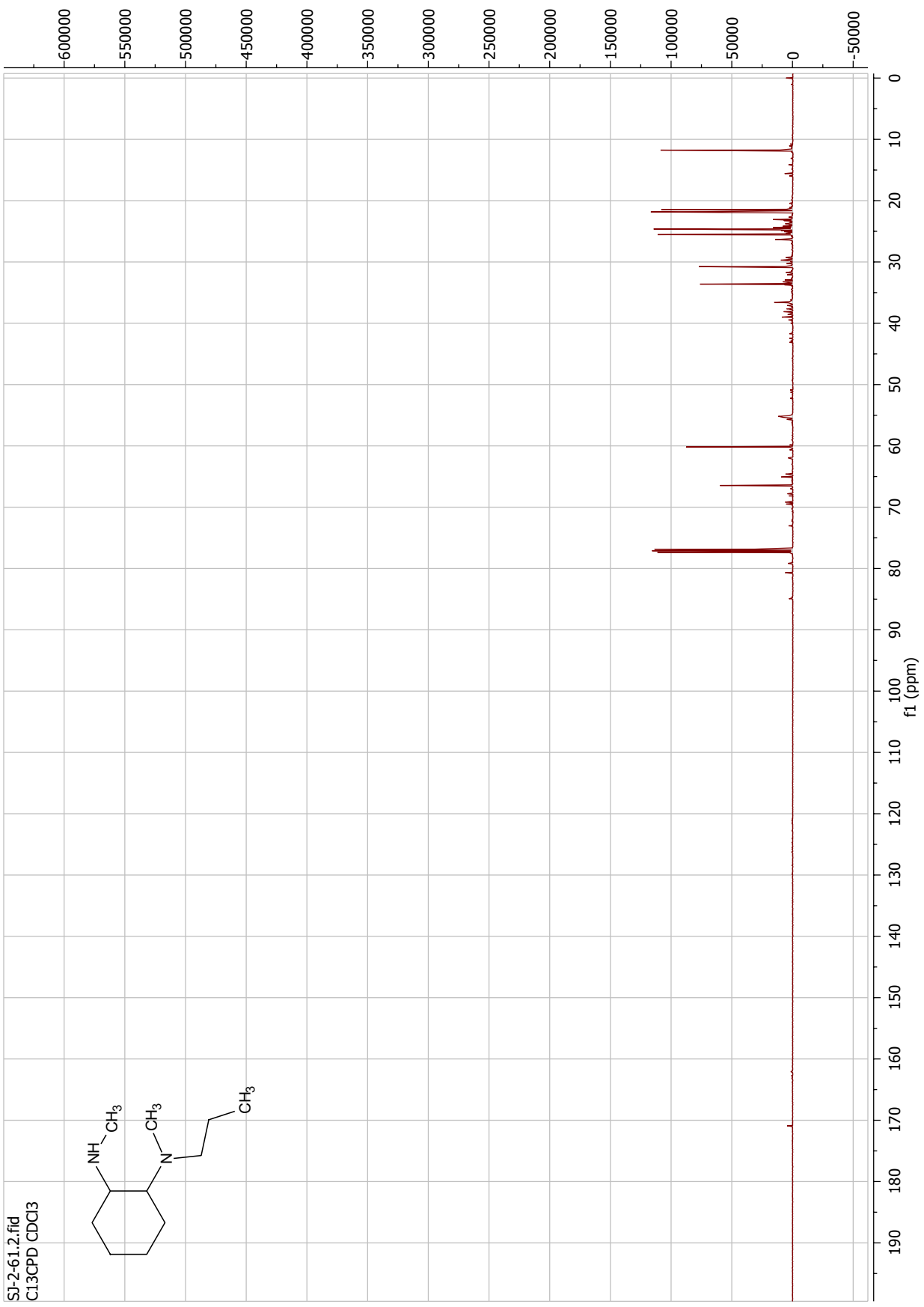
SJ-2-61.2.fid
C13CPD CDCl3
NH
CH3
CH3
N
CH3
600000
550000
500000
450000
400000
350000
300000
250000
200000
150000
100000
50000
0
-50000
0
10
20
30
40
50
60
70
80
90
100
110
120
130
140
150
160
170
180
190
f1 (ppm)

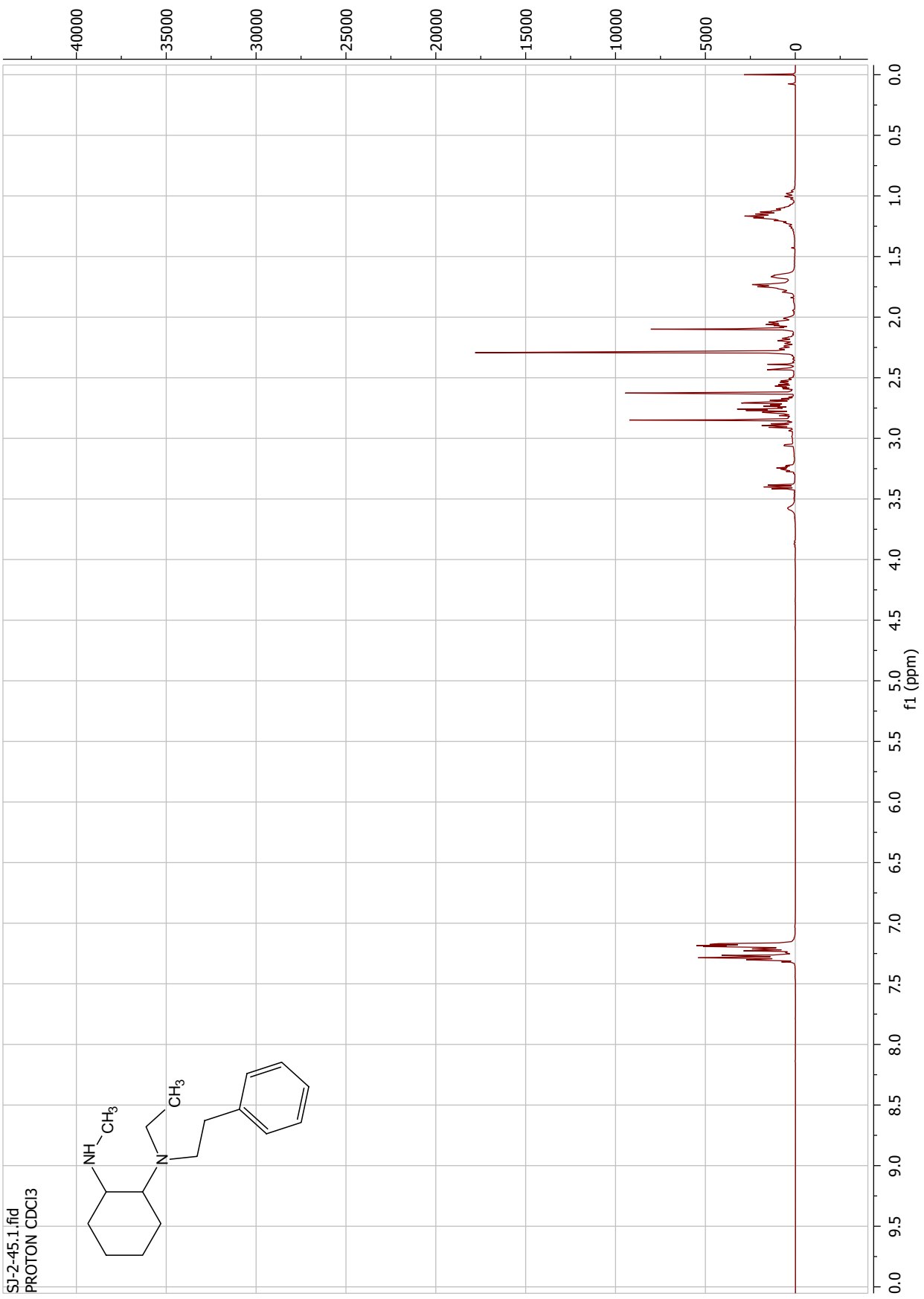
SJ-2-45.1.fid
PROTON CDCl3
NH
CH3
N
CH3
40000
35000
30000
25000
20000
15000
10000
5000
0
0.0
0.5
1.0
1.5
2.0
2.5
3.0
3.5
4.0
4.5
5.0
5.5
6.0
6.5
7.0
7.5
8.0
8.5
9.0
9.5
0.0
f1 (ppm)


SJ-2-45.2.fid
C13CPD CDCl3
NH
CH3
N
CH3
f1 (ppm)


SJ-1-169.1.fid
PROTON CDCl3
A (m) 7.38
B (m) 7.15
C (dd) 3.65 J(7.06, 4.29)
D (d) 2.82 J(3.30)
E (m) 2.61
F (m) 2.29
G (s) 2.18
H (m) 1.79
I (s) 1.56
J (d) 1.39 J(40.34)
K (m) 1.19
0.83
1.75
1.49
2.53
1.58
3.23
0.89
2.99
4.47
7.00
1.90
f1 (ppm)

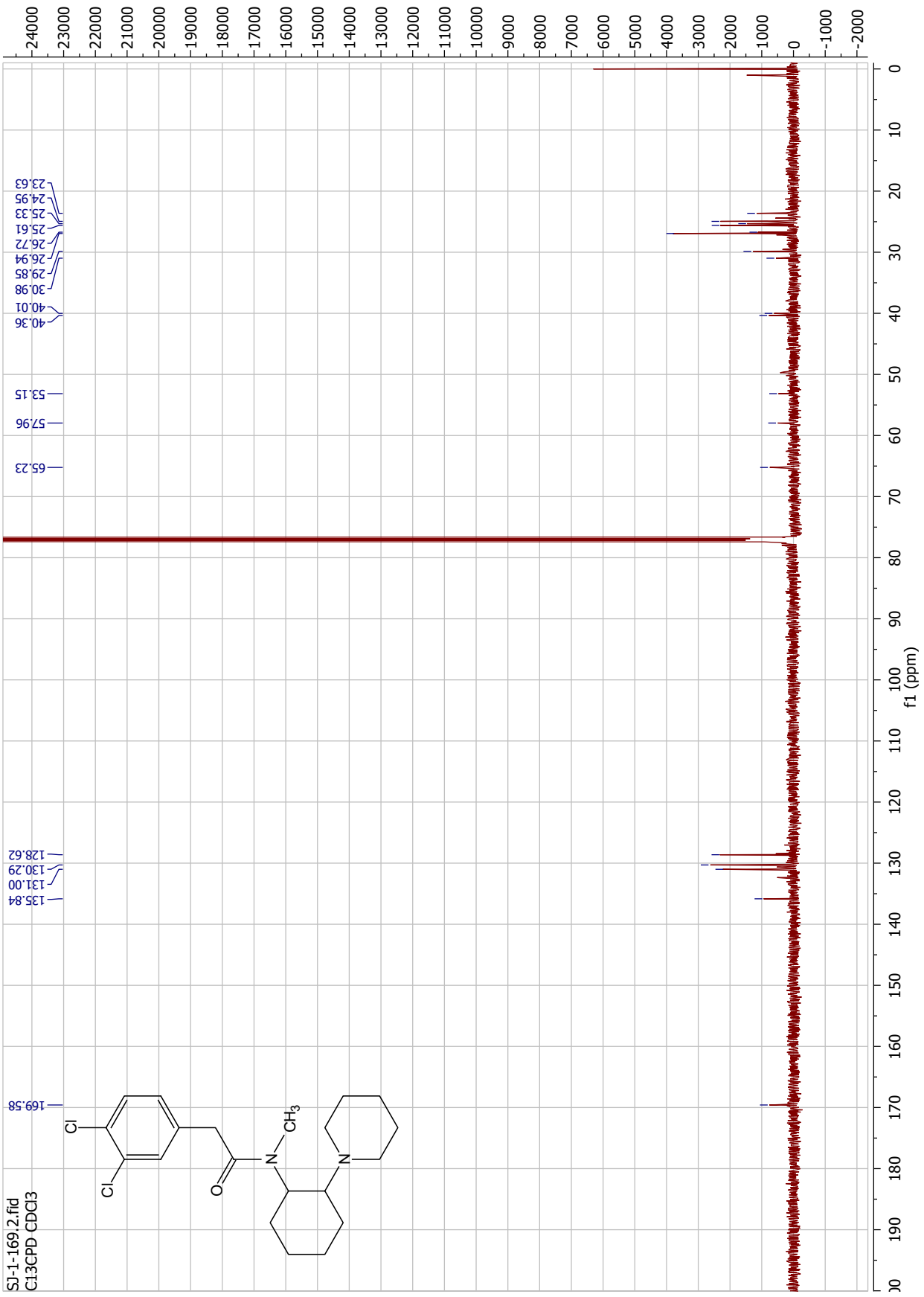
SJ-1-169.2.fid
C13CPD CDCl3
169.58
135.84
131.00
130.29
128.62
65.23
57.96
53.15
40.36
40.01
30.98
29.85
26.94
26.72
25.61
25.33
24.95
23.63
Cl
Cl
O
N
CH3
N
f1 (ppm)

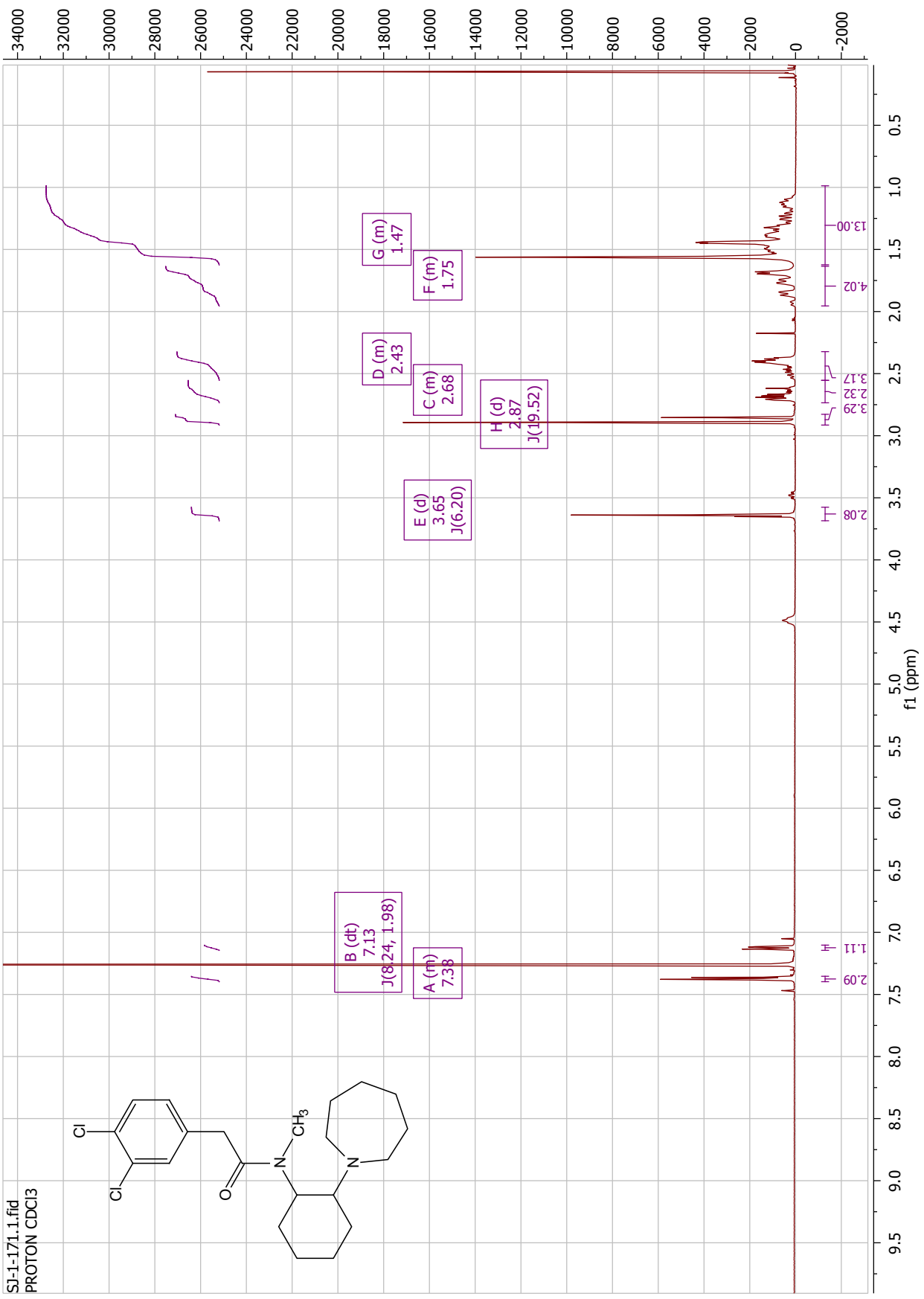
SJ-1-171.1.fid
PROTON CDCl3
A (m)
7.38
B (dt)
7.13
J(8.24, 1.98)
D (m)
2.43
C (m)
2.68
E (d)
3.65
J(6.20)
H (d)
2.87
J(19.52)
G (m)
1.47
F (m)
1.75
2.09
1.11
2.08
3.29
2.32
3.17
4.02
13.00
f1 (ppm)

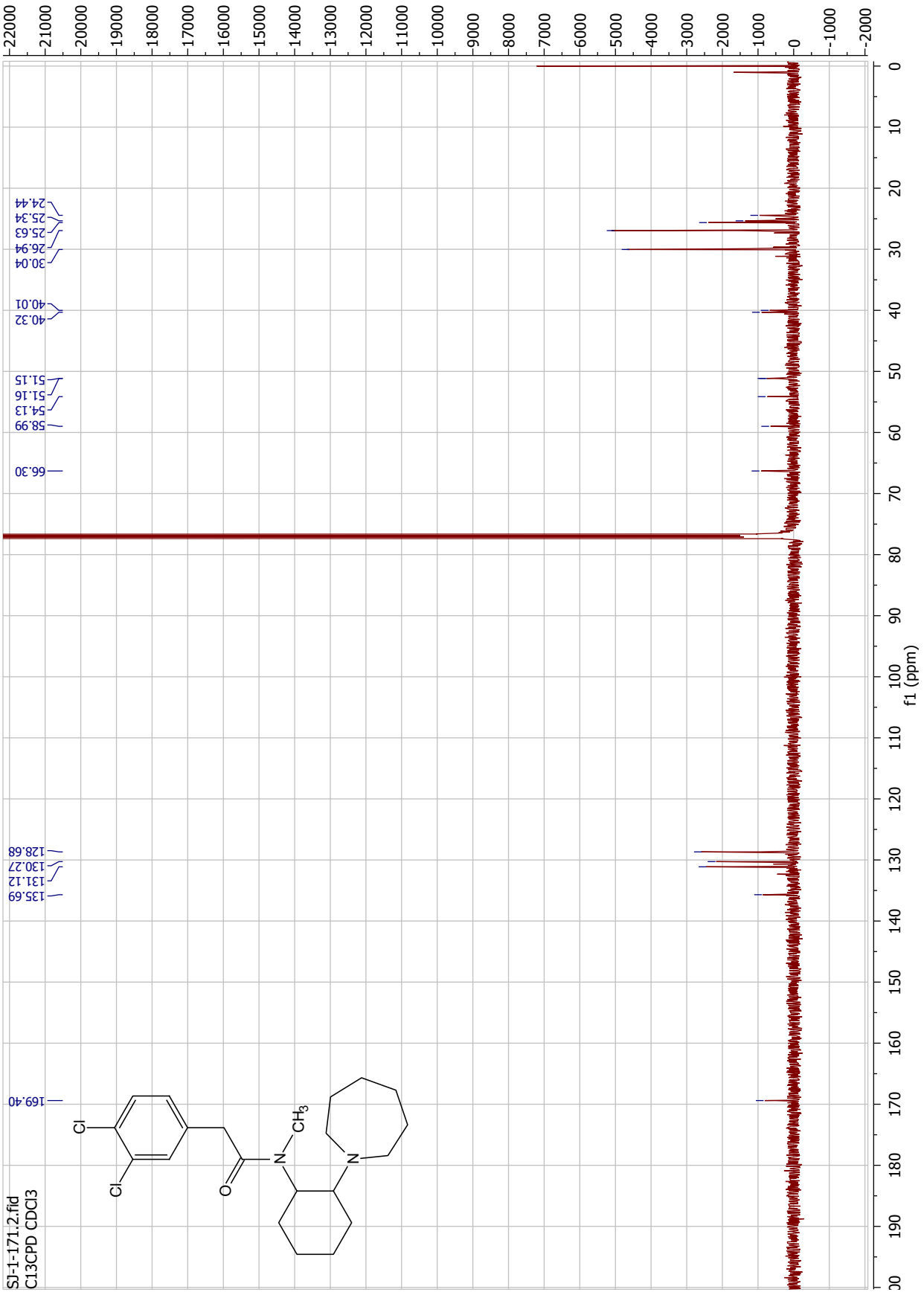
SJ-1-171.2.fid
C13CPD CDCl3
169.40
135.69
131.12
130.27
128.68
66.30
58.99
54.13
51.16
51.15
40.32
40.01
30.04
26.94
25.63
25.34
24.44
Cl
Cl
O
N
CH3
N
f1 (ppm)

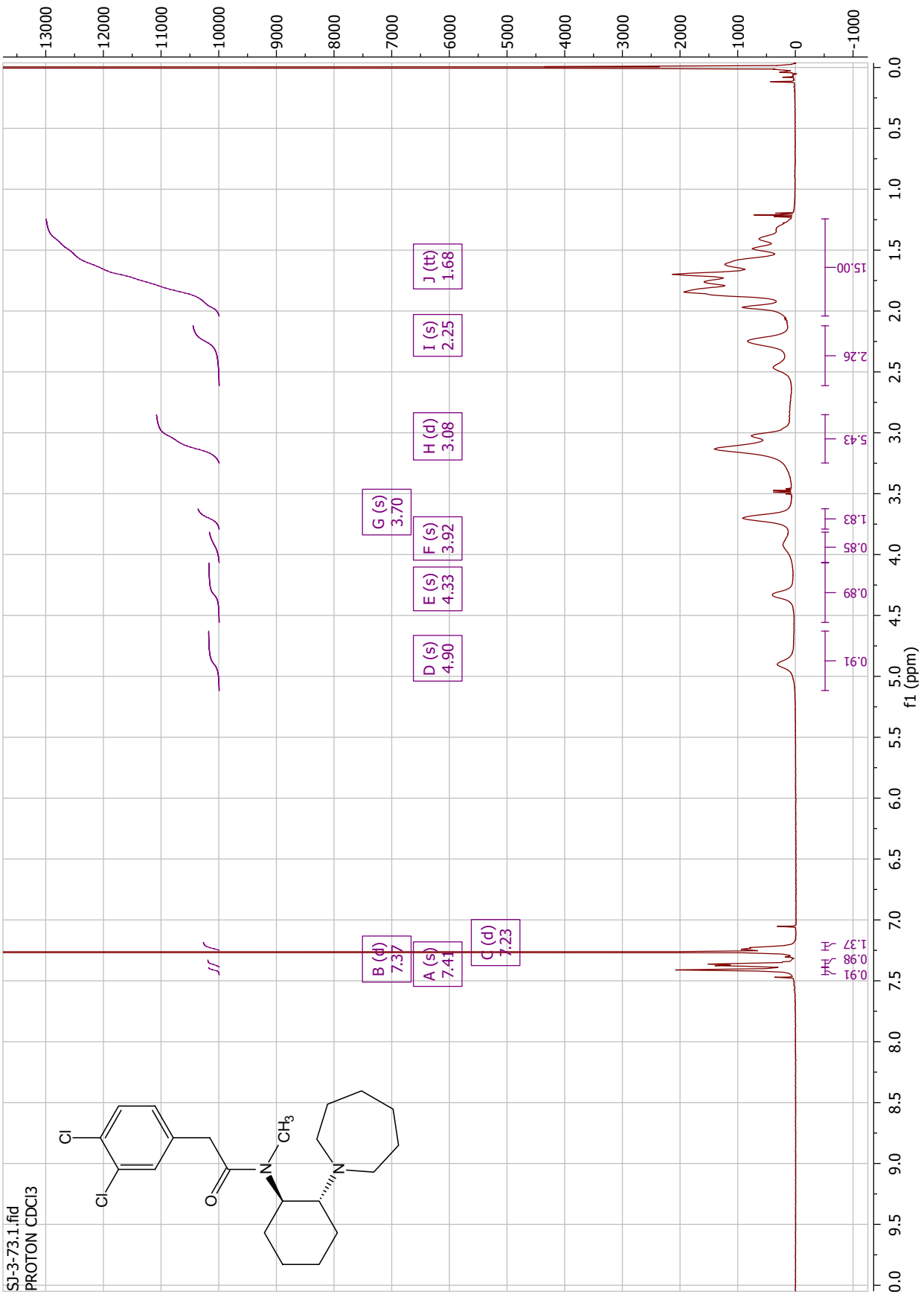
SJ-3-73.1.fid
PROTON CDCl3
B (d) 7.37
A (s) 7.41
C (d) 7.23
D (s) 4.90
E (s) 4.33
F (s) 3.92
G (s) 3.70
H (d) 3.08
I (s) 2.25
J (tt) 1.68
15.00
2.26
5.43
1.83
0.85
0.89
0.91
1.37
0.98
0.91
f1 (ppm)

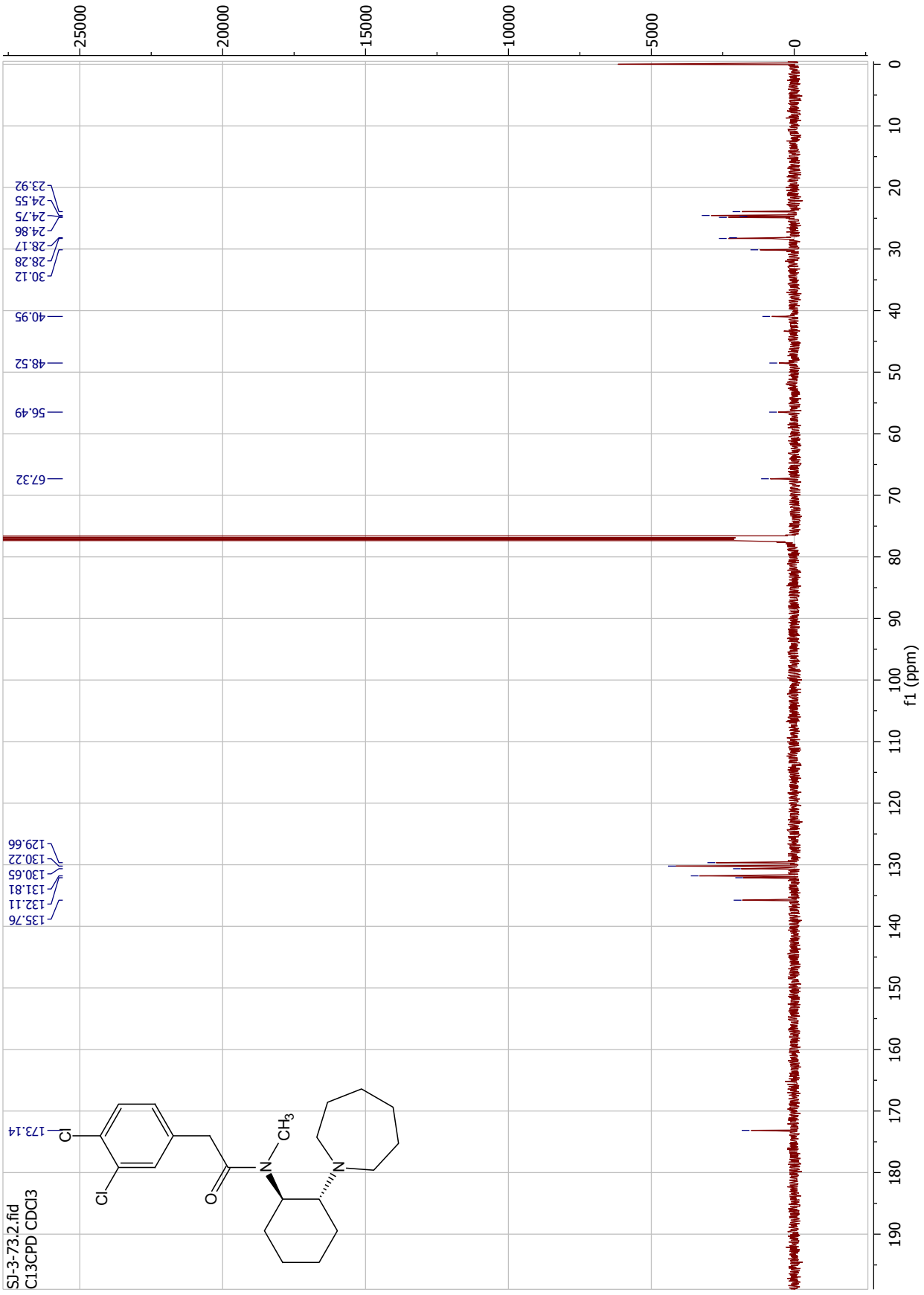
SJ-3-73.2.fid
C13CPD CDCl3
173.14
135.76
132.11
131.81
130.65
130.22
129.66
67.32
56.49
48.52
40.95
30.12
28.28
28.17
24.86
24.75
24.55
23.92
Cl
Cl
O
N
CH3
N
f1 (ppm)

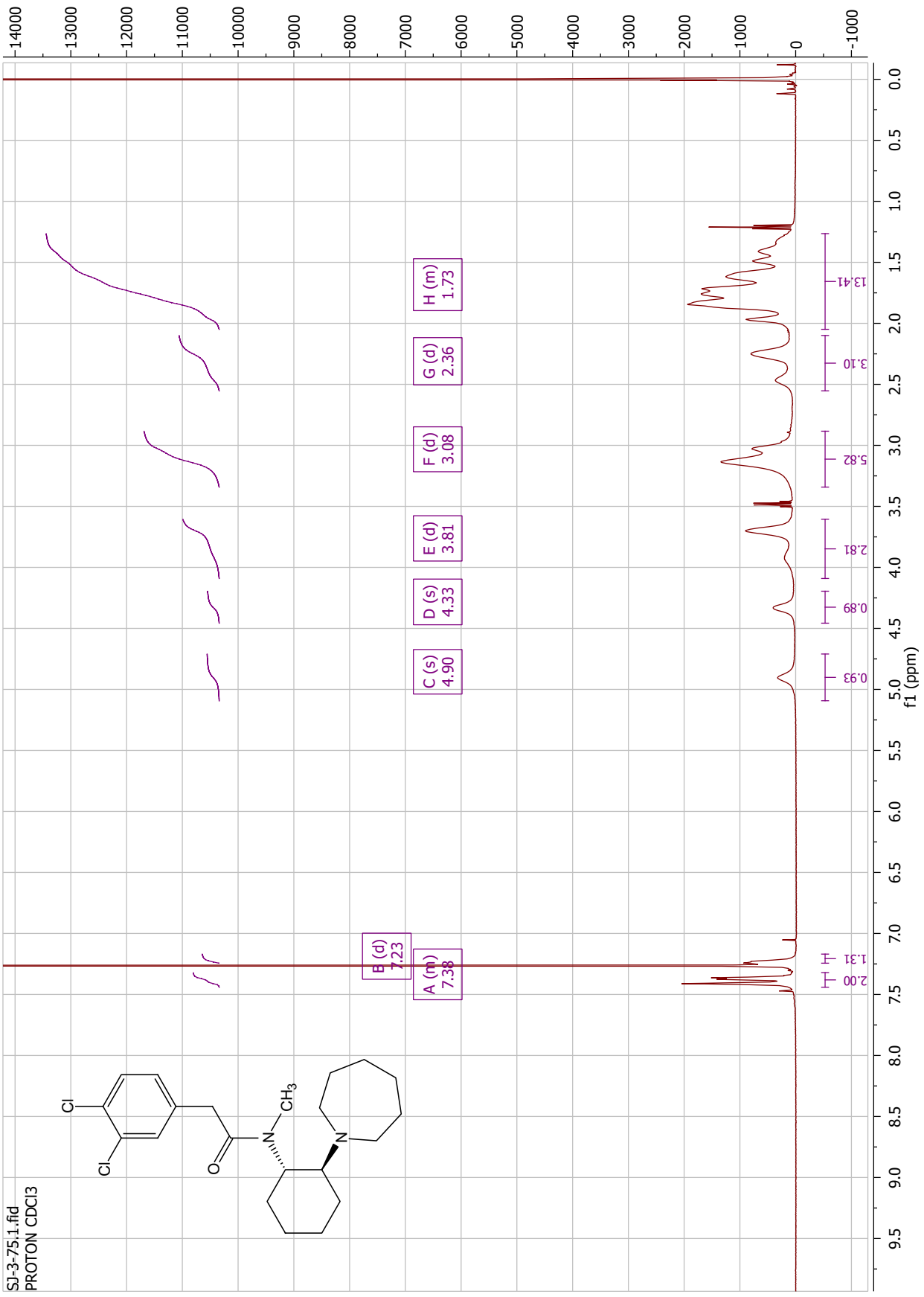
SJ-3-75.1.fid
PROTON CDCl3
A (m) 7.38
B (d) 7.23
C (s) 4.90
D (s) 4.33
E (d) 3.81
F (d) 3.08
G (d) 2.36
H (m) 1.73
2.00
1.31
0.93
0.89
2.81
5.82
3.10
13.41
f1 (ppm)

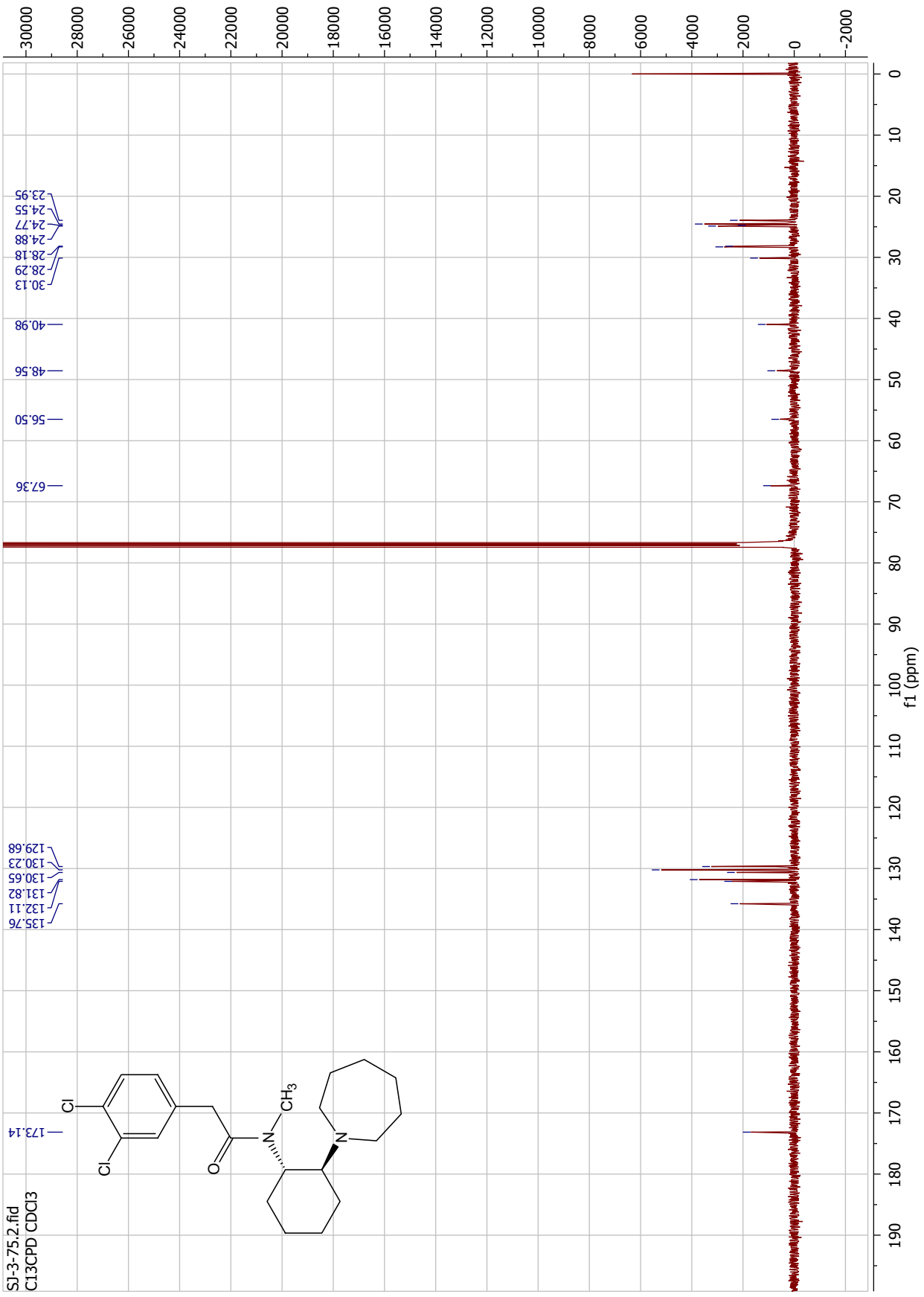
SJ-3-75.2.fid
C13CPD CDCl3
173.14
135.76
132.11
131.82
130.65
130.23
129.68
67.36
56.50
48.56
40.98
30.13
28.29
28.18
24.88
24.77
24.55
23.95
Cl
Cl
O
N
CH3
N
f1 (ppm)

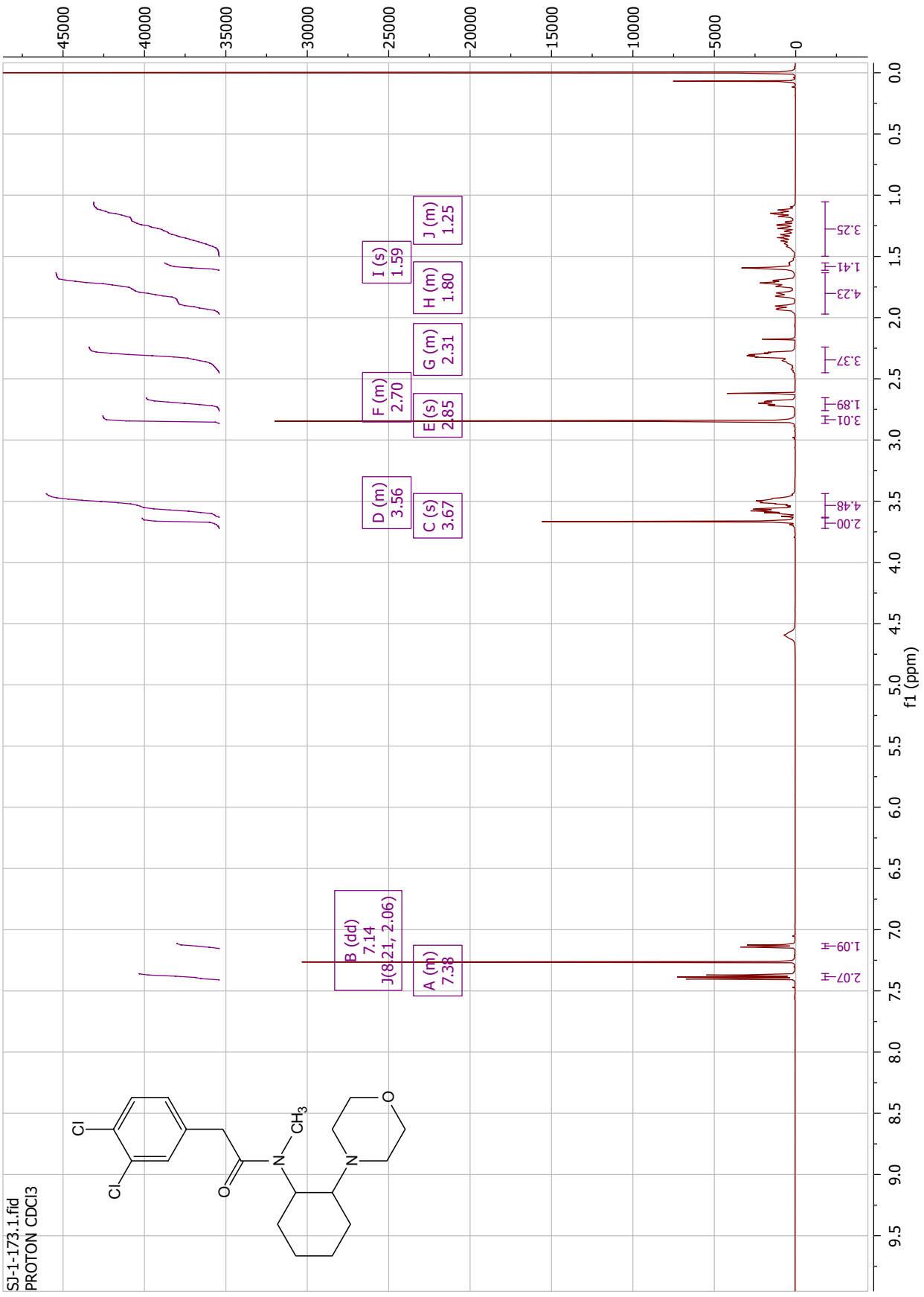
SJ-1-173.1.fid
PROTON CDCl3
A (m) 7.38
B (dd) 7.14 J(8.21, 2.06)
C (s) 3.67
D (m) 3.56
E (s) 2.85
F (m) 2.70
G (m) 2.31
H (m) 1.80
I (s) 1.59
J (m) 1.25
2.00
4.48
1.09
2.07
3.01
1.89
3.37
4.23
1.41
3.25
f1 (ppm)

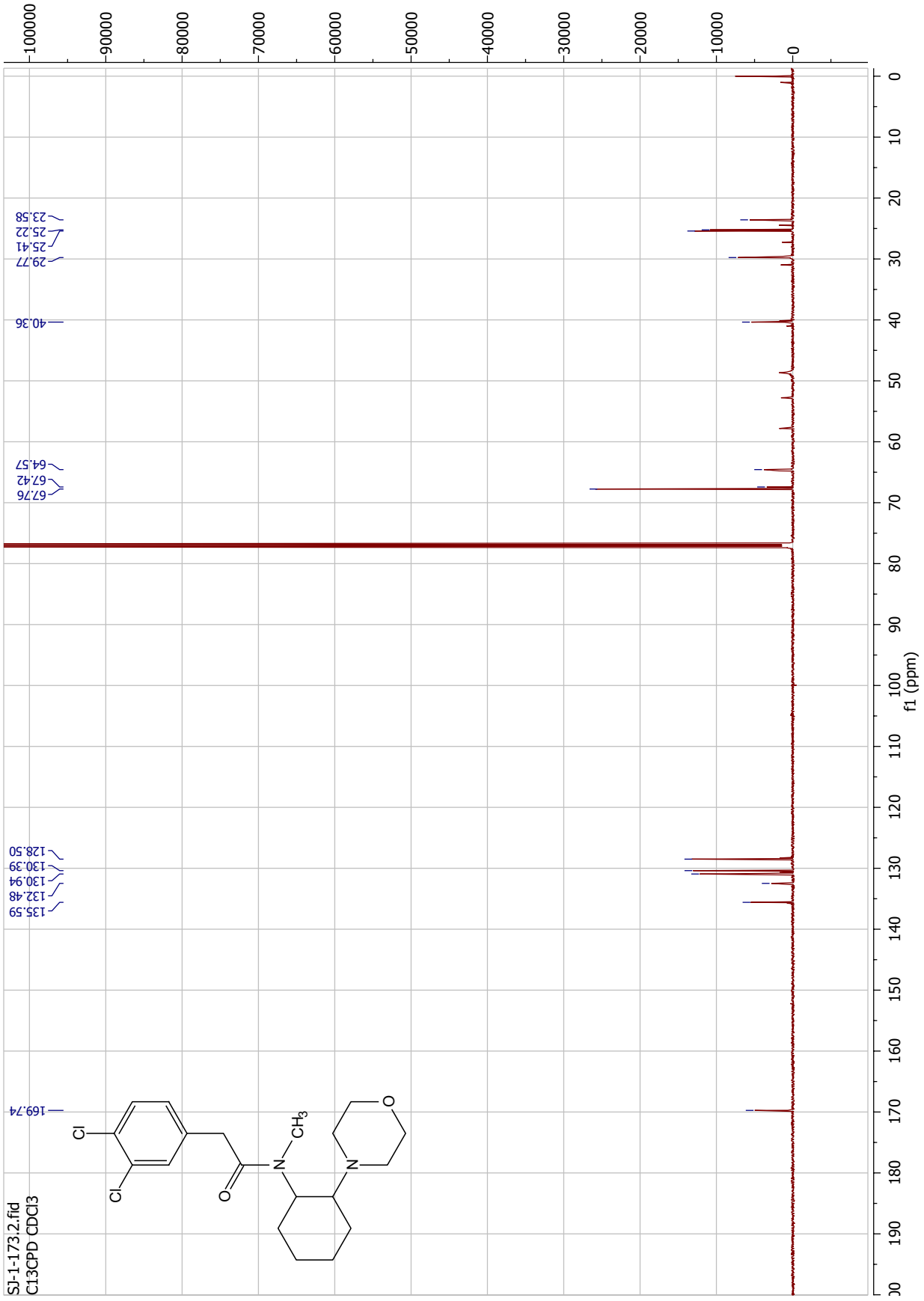
S3-1-173.2.fid
C13CPD CDCl3
169.74
135.59
132.48
130.94
130.39
128.50
67.76
67.42
64.57
40.36
29.77
25.41
25.22
23.58
Cl
Cl
O
N
CH3
N
O
f1 (ppm)

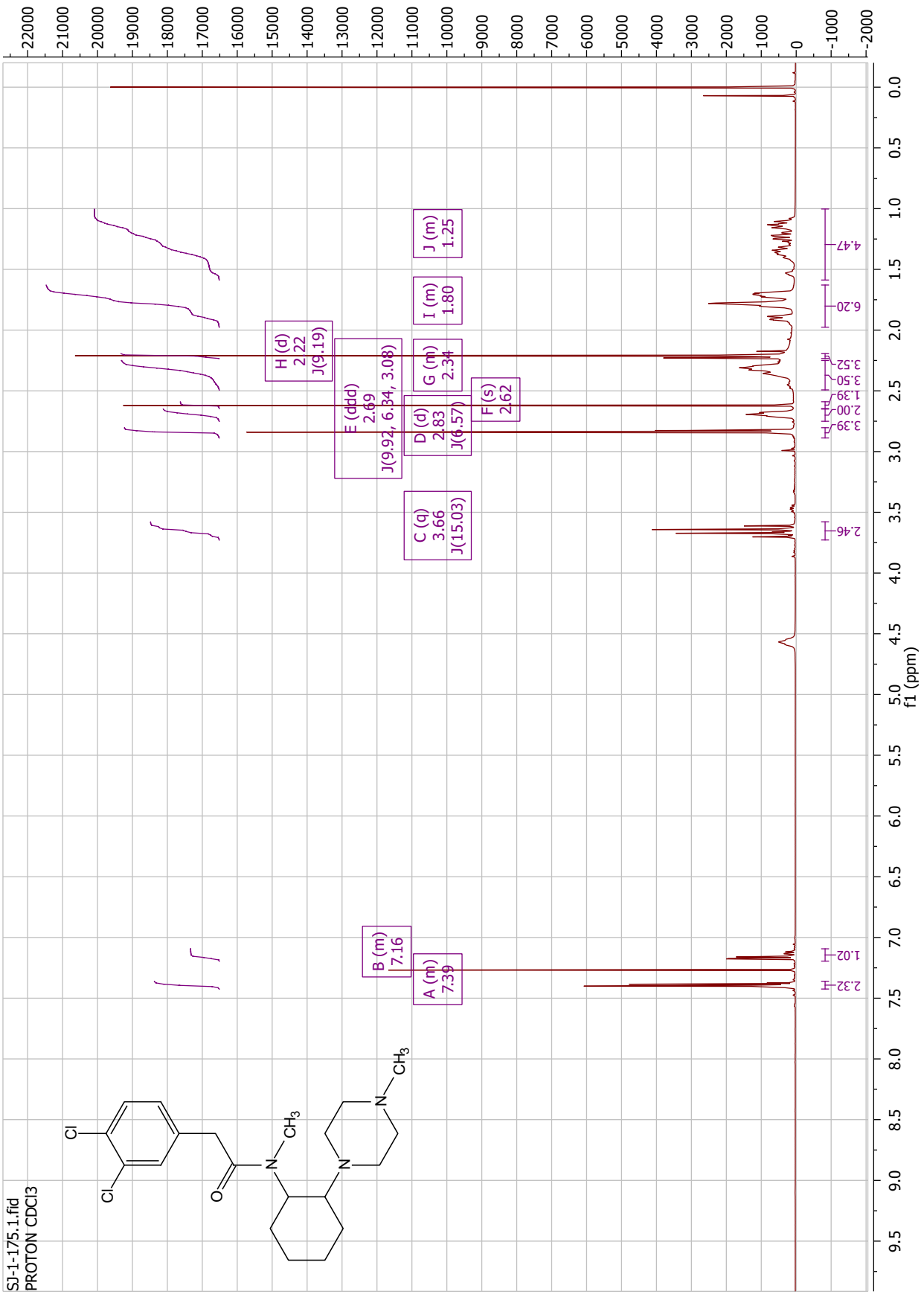
SJ-1-175.1.fid
PROTON CDCl3
A (m)
7.39
B (m)
7.16
C (q)
3.66
J(15.03)
D (d)
2.83
J(6.57)
E (ddd)
2.69
J(9.92, 6.34, 3.08)
F (s)
2.62
G (m)
2.34
H (d)
2.22
J(9.19)
I (m)
1.80
J (m)
1.25
4.47
6.20
3.52
3.50
1.39
2.00
3.39
2.46
1.02
2.32
f1 (ppm)

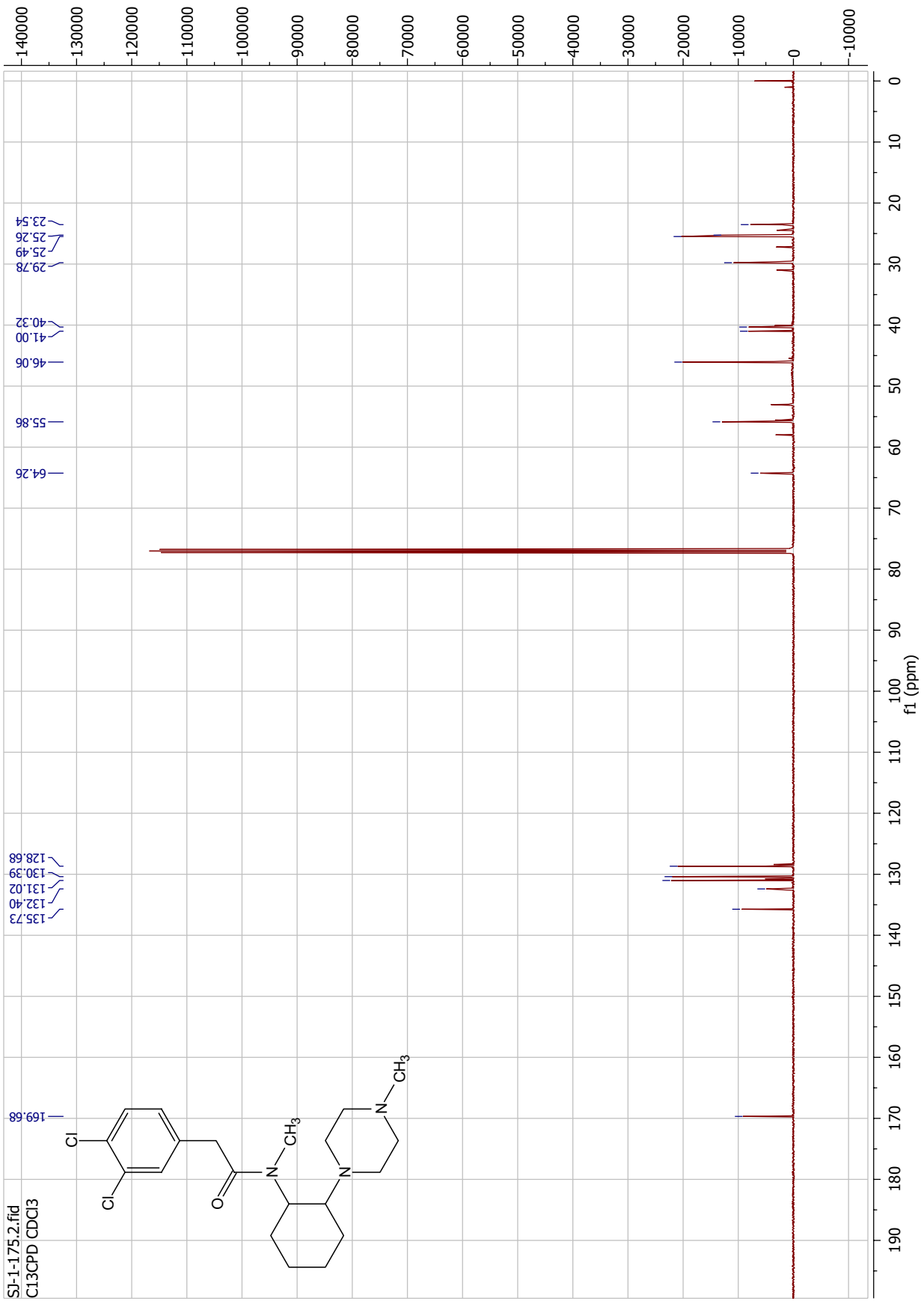
S3-1-175.2.fid
C13CPD CDCl3
169.68
135.73
132.40
131.02
130.39
128.68
64.26
55.86
46.06
41.00
40.32
29.78
25.49
25.26
23.54
Cl
Cl
O
N
CH3
N
N
CH3
f1 (ppm)

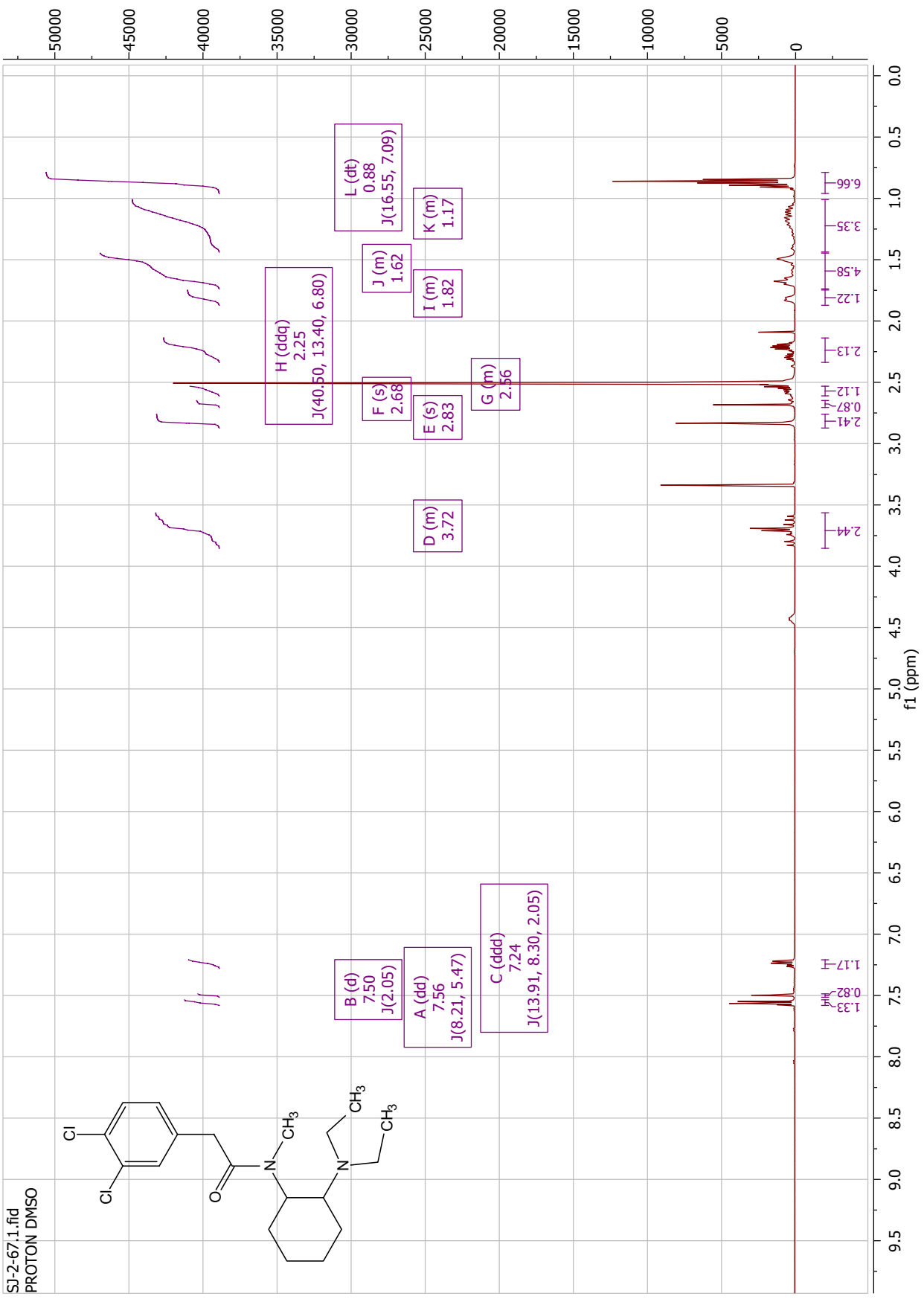
SJ-2-67.1.fid
PROTON DMSO
A (dd)
7.56
J(8.21, 5.47)
B (d)
7.50
J(2.05)
C (ddd)
7.24
J(13.91, 8.30, 2.05)
D (m)
3.72
E (s)
2.83
F (s)
2.68
G (m)
2.56
H (ddq)
2.25
J(40.50, 13.40, 6.80)
I (m)
1.82
J (m)
1.62
K (m)
1.17
L (dt)
0.88
J(16.55, 7.09)
6.66
3.35
4.58
1.22
2.13
1.12
0.87
2.41
2.44
1.17
0.82
1.33
f1 (ppm)

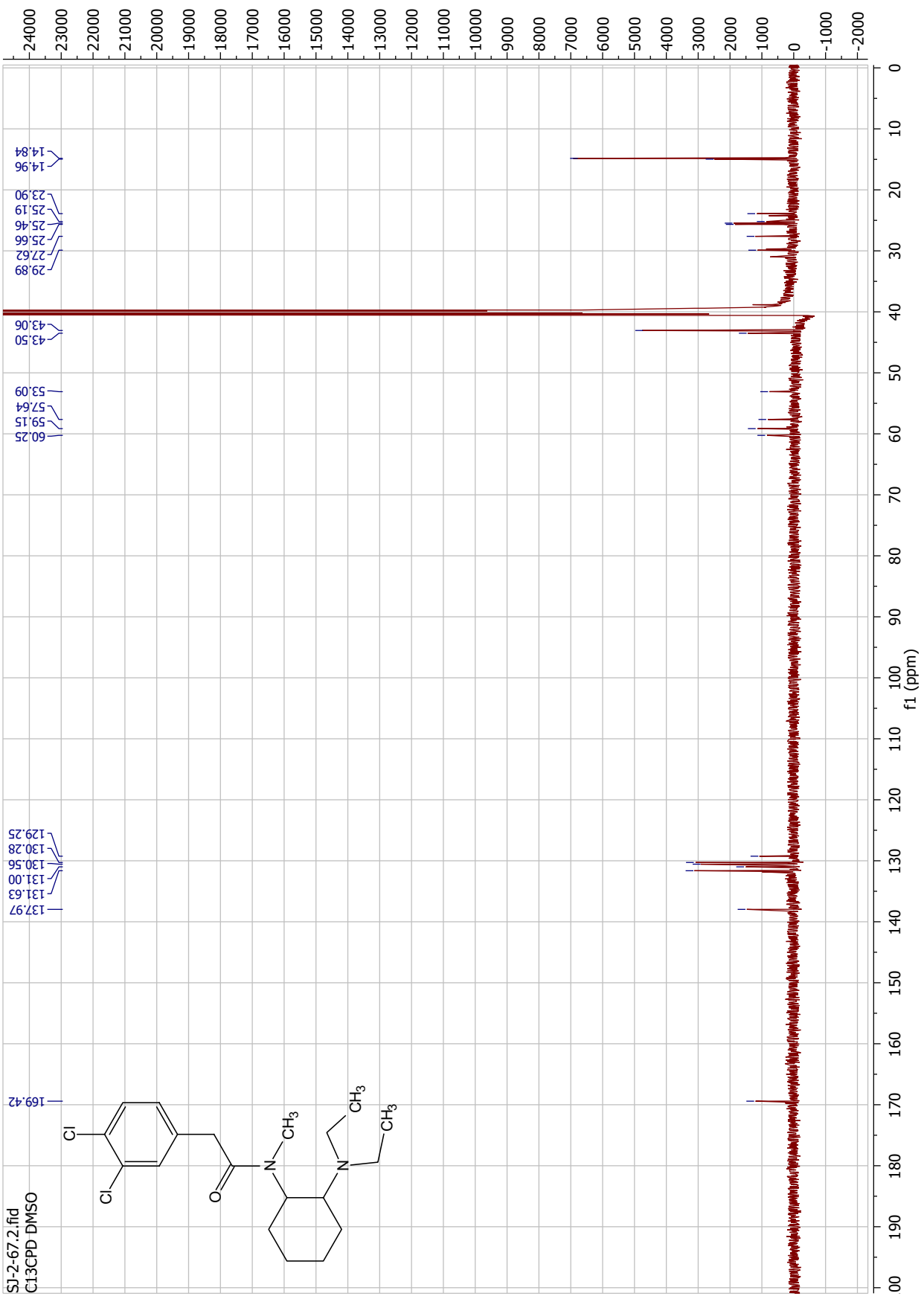
SJ-2-67.2.fid
C13CPD DMSO
f1 (ppm)
14.84
14.96
23.90
25.19
25.46
25.66
27.62
29.89
43.06
43.50
53.09
57.64
59.15
60.25
129.25
130.28
130.56
131.00
131.63
137.97
169.42
Cl
Cl
O
N
CH3
N
CH3
CH3


SJ-2-71.1.fid
PROTON DMSO
A (dd)
7.56
J(8.20, 2.43)
B (d)
7.47
J(2.06)
C (ddd)
7.23
J(13.59, 8.29, 2.04)
D (m)
3.70
E (s)
2.79
F (m)
2.66
G (m)
2.23
H (s)
2.05
I (m)
1.33
K (t)
0.69
J(7.35)
2.67
10.00
2.80
3.07
0.97
2.71
2.69
1.29
0.94
1.48
f1 (ppm)

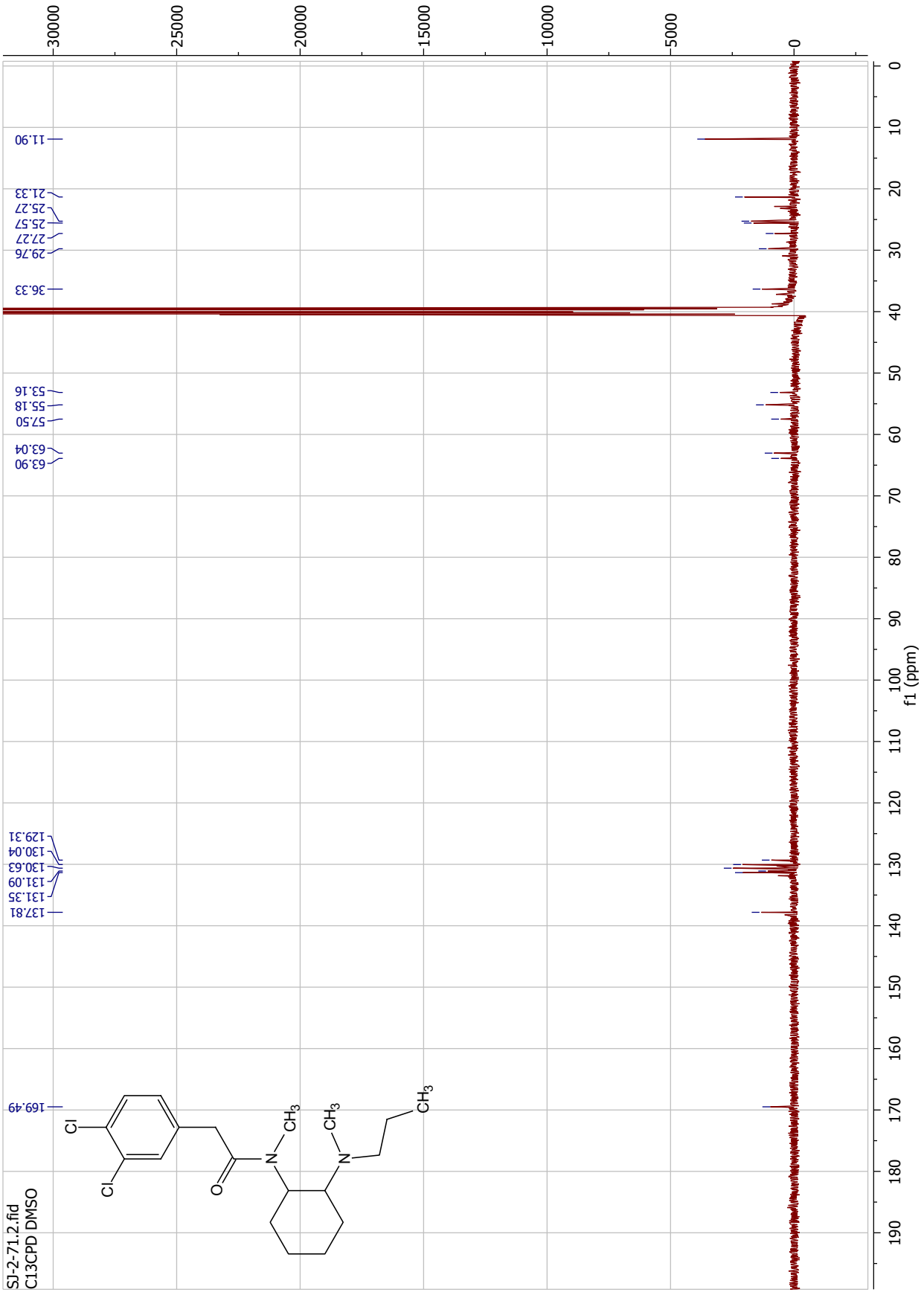
SJ-2-71.2.fid
C13CPD DMSO
169.49
137.81
131.35
131.09
130.63
130.04
129.31
63.90
63.04
57.50
55.18
53.16
36.33
29.76
27.27
25.57
25.27
21.33
11.90
Cl
Cl
O
N
CH3
CH3
N
CH3
f1 (ppm)


SJ-2-69.1.fid
PROTON DMSO
A (dd)
7.56
J(8.51, 4.54)
B (d)
7.48
J(2.06)
C (m)
7.18
D (q)
3.64
J(15.63)
E (s)
2.68
F (s)
2.55
G (m)
2.42
H (d)
2.19
J(18.69)
I (d)
1.79
J(7.15)
J (m)
1.67
K (tt)
1.46
J(12.29, 5.31)
L (m)
1.14
4.04
2.16
2.64
1.48
3.65
1.36
1.24
2.82
2.32
7.38
1.00
1.45
f1 (ppm)

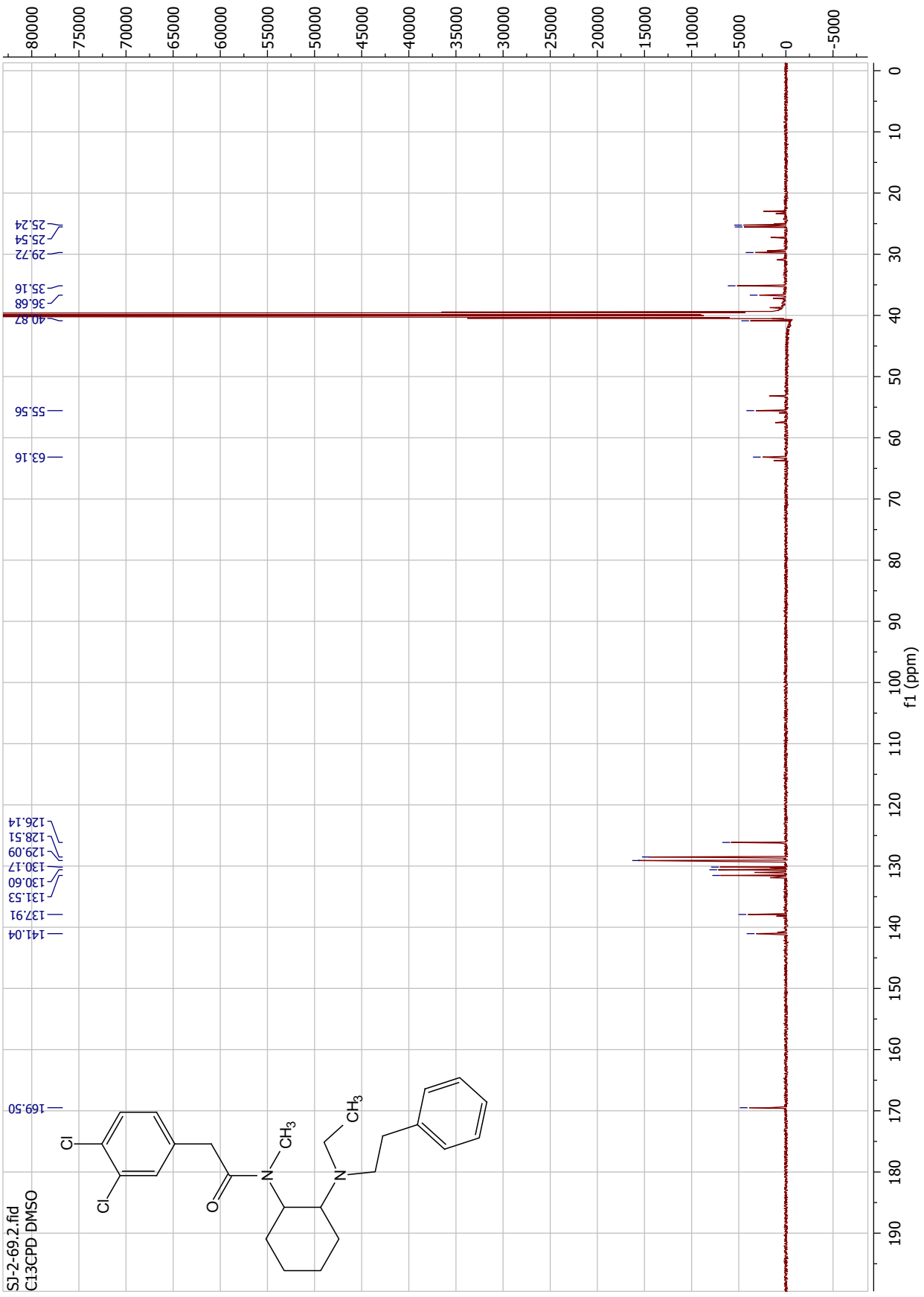
SJ-2-69.2.fid
C13CPD DMSO
169.50
141.04
137.91
131.53
130.60
130.17
129.09
128.51
126.14
63.16
55.56
40.87
36.68
35.16
29.72
25.54
25.24
f1 (ppm)

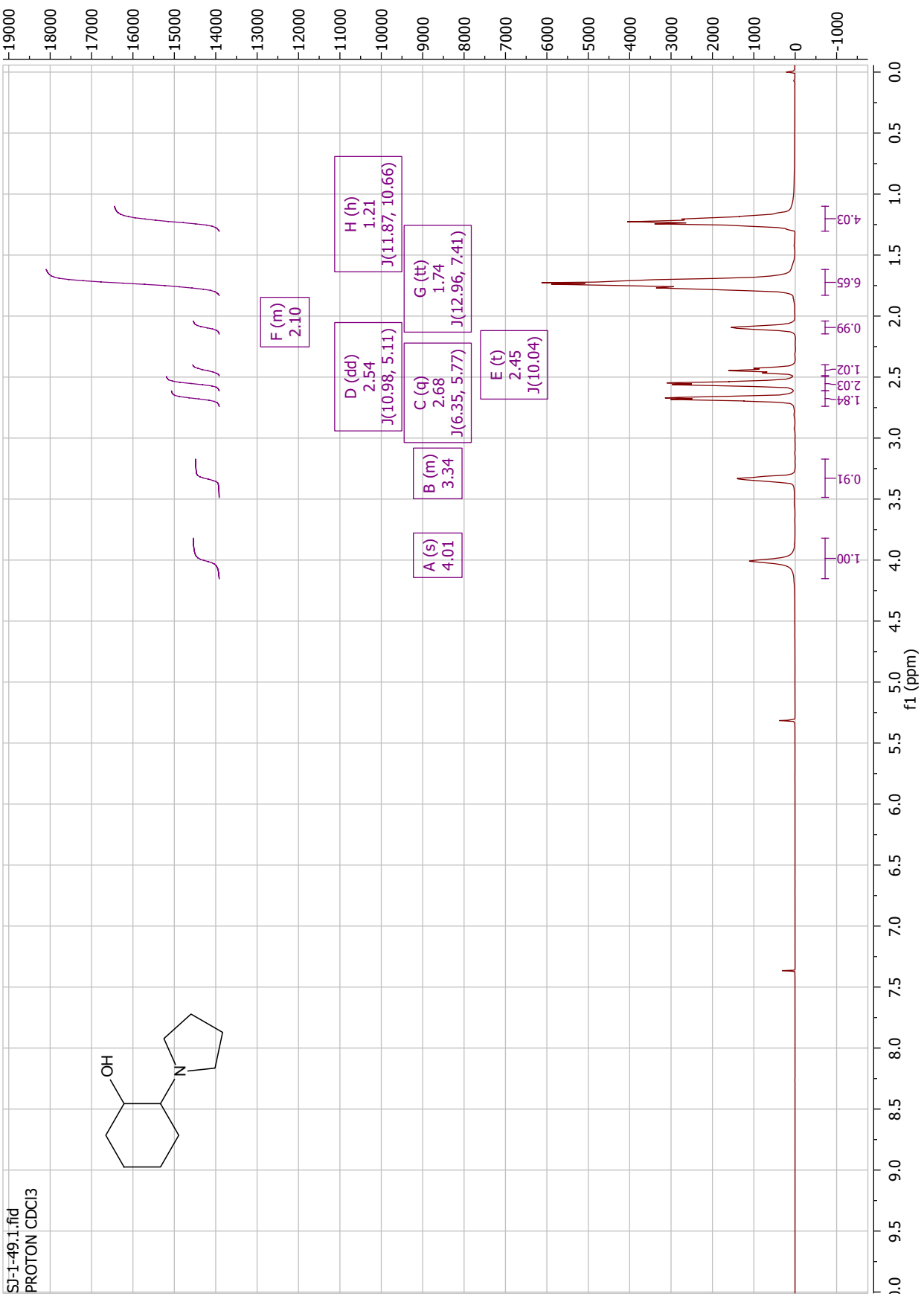
SJ-1-49.1.fid
PROTON CDCl3
A (s)
4.01
B (m)
3.34
C (q)
2.68
J(6.35, 5.77)
D (dd)
2.54
J(10.98, 5.11)
E (t)
2.45
J(10.04)
F (m)
2.10
G (tt)
1.74
J(12.96, 7.41)
H (h)
1.21
J(11.87, 10.66)
1.00
0.91
1.84
2.03
1.02
0.99
6.65
4.03
OH
N
f1 (ppm)

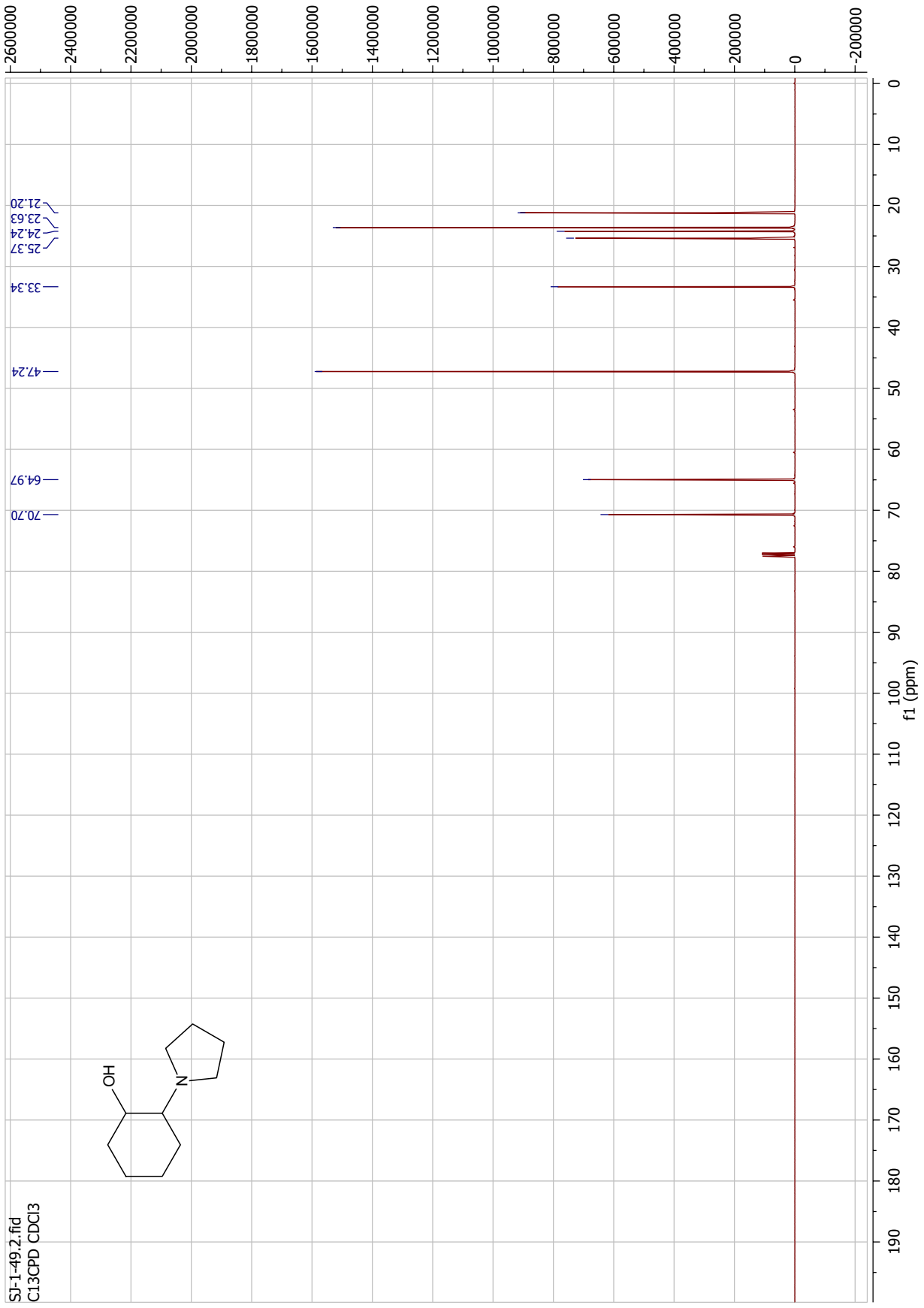
SJ-1-49.2.fid
C13CPD CDCl3
21.20
23.63
24.24
25.37
33.34
47.24
64.97
70.70
OH
N
f1 (ppm)

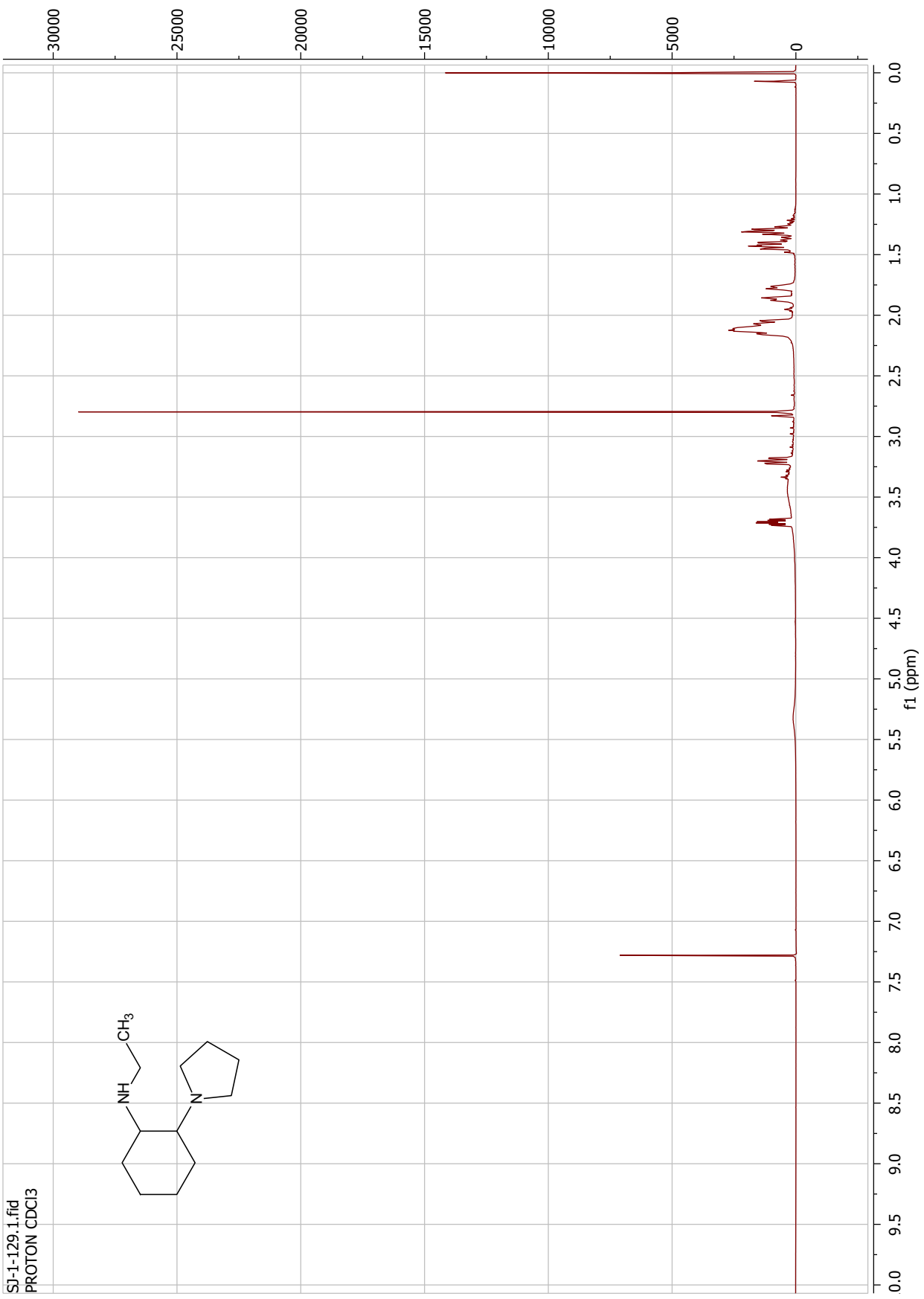
SJ-1-129.1.fid
PROTON CDCl3
NH
CH3
N
f1 (ppm)

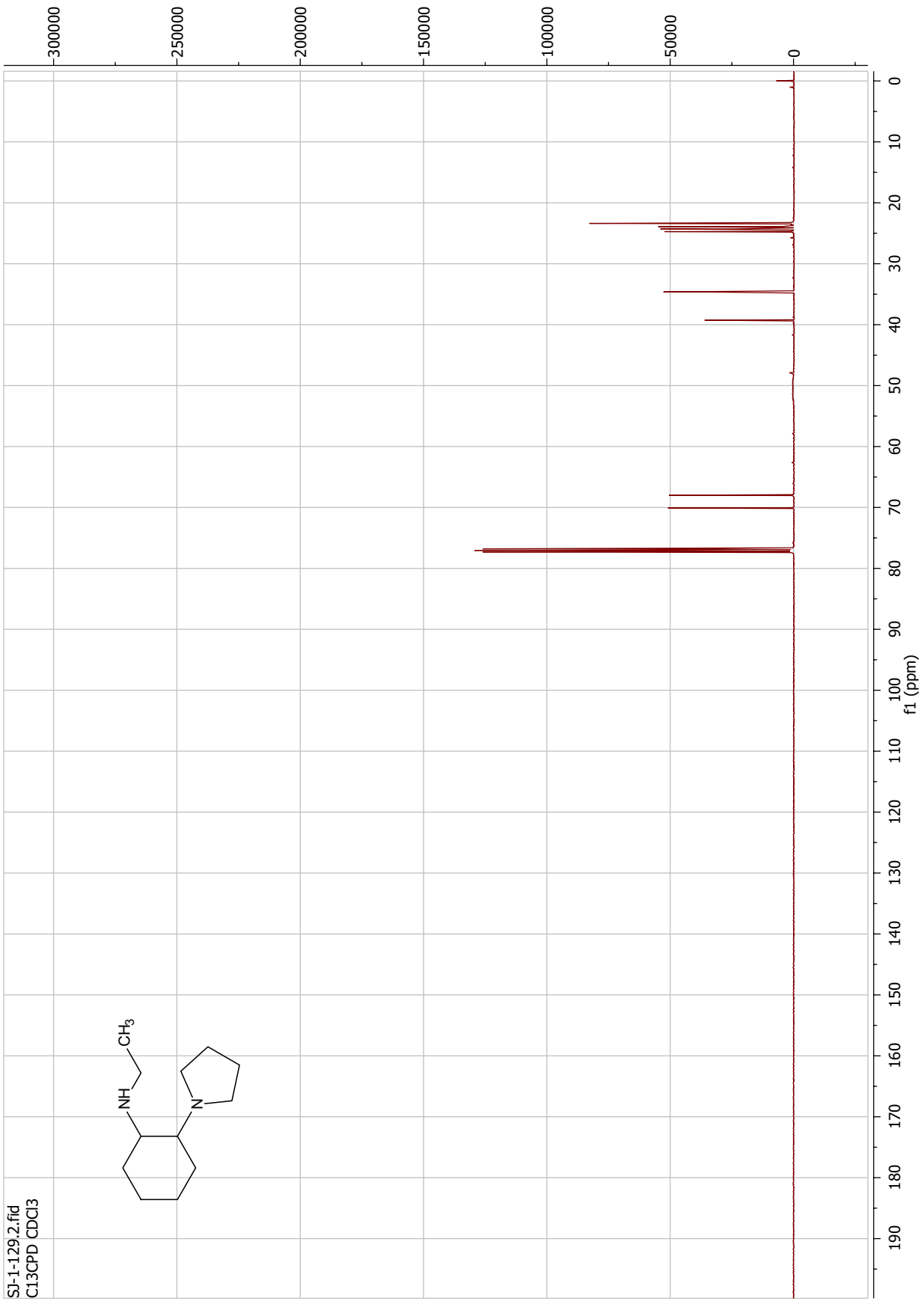
SJ-1-129.2.fid
C13CPD CDCl3
300000
250000
200000
150000
100000
50000
0
0
10
20
30
40
50
60
70
80
90
100
110
120
130
140
150
160
170
180
190
f1 (ppm)
NH
CH3
N

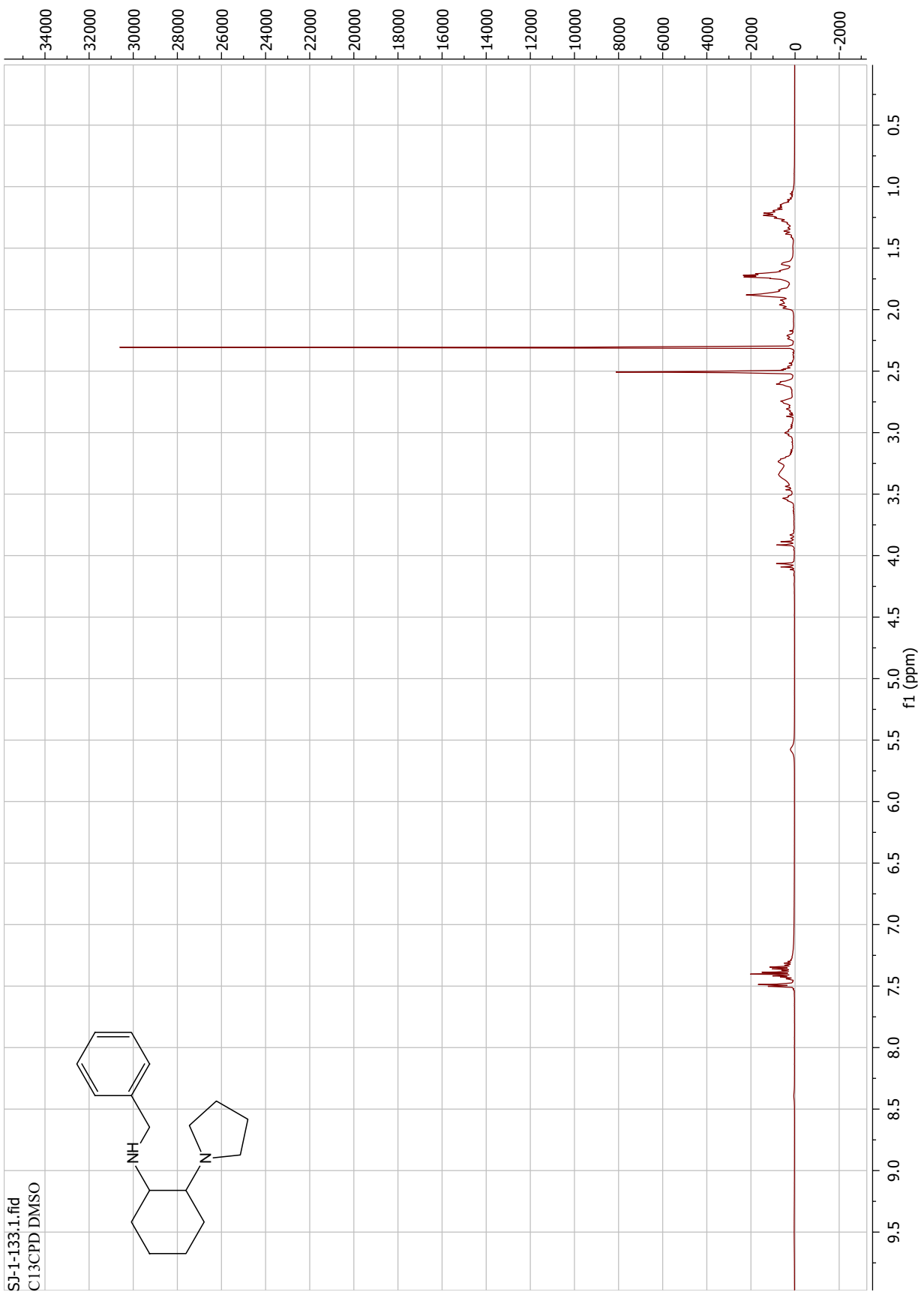
SJ-1-133.1.fid
C13CPD DMSO
NH
N
f1 (ppm)

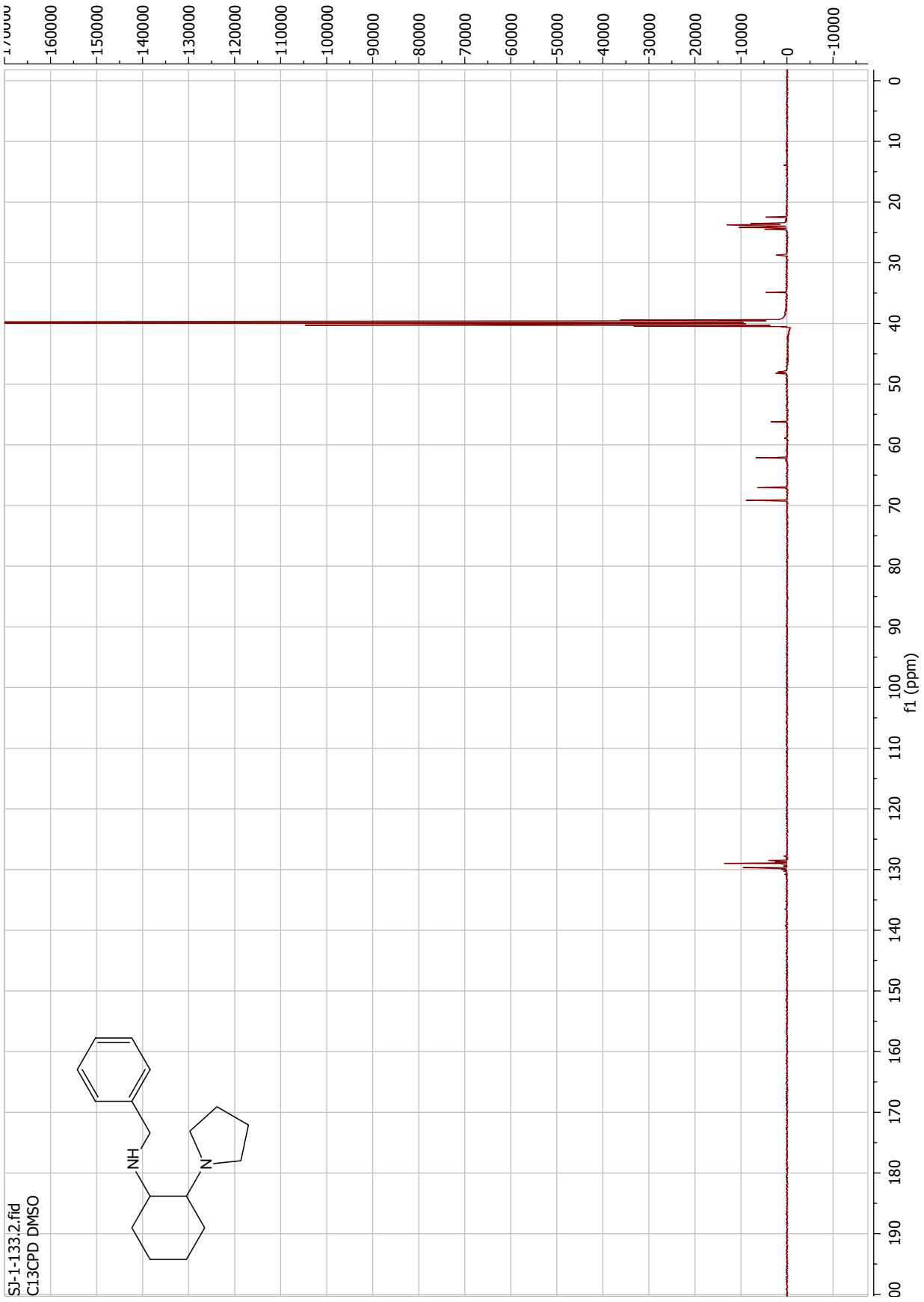
SJ-1-133.2.fid
C13CPD DMSO
NH
N
f1 (ppm)

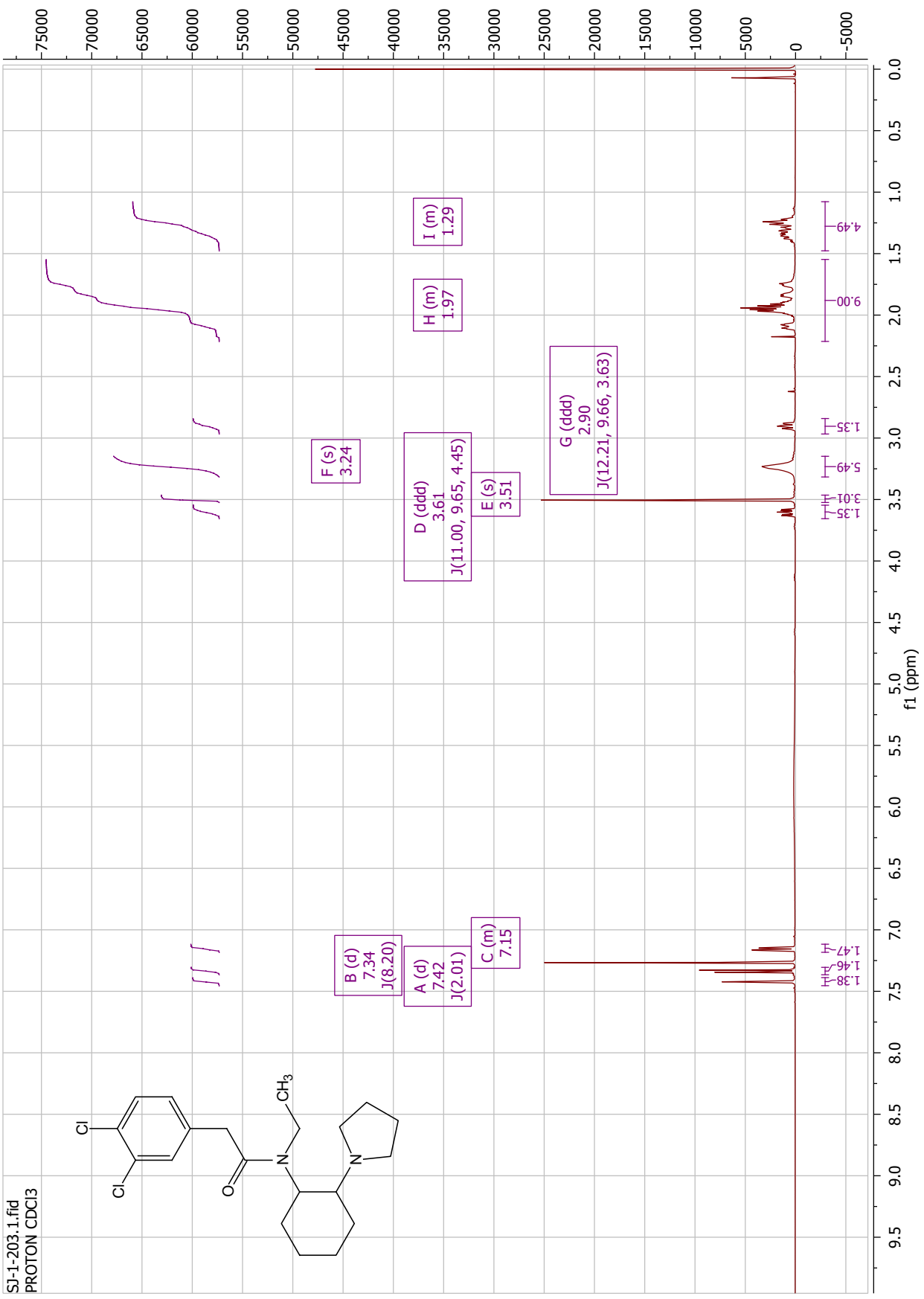
SJ-1-203.1.fid
PROTON CDCl3
B (d)
7.34
J(8.20)
A (d)
7.42
J(2.01)
C (m)
7.15
F (s)
3.24
D (ddd)
3.61
J(11.00, 9.65, 4.45)
E (s)
3.51
G (ddd)
2.90
J(12.21, 9.66, 3.63)
H (m)
1.97
I (m)
1.29
4.49
9.00
1.35
5.49
3.01
1.35
1.47
1.46
1.38
f1 (ppm)

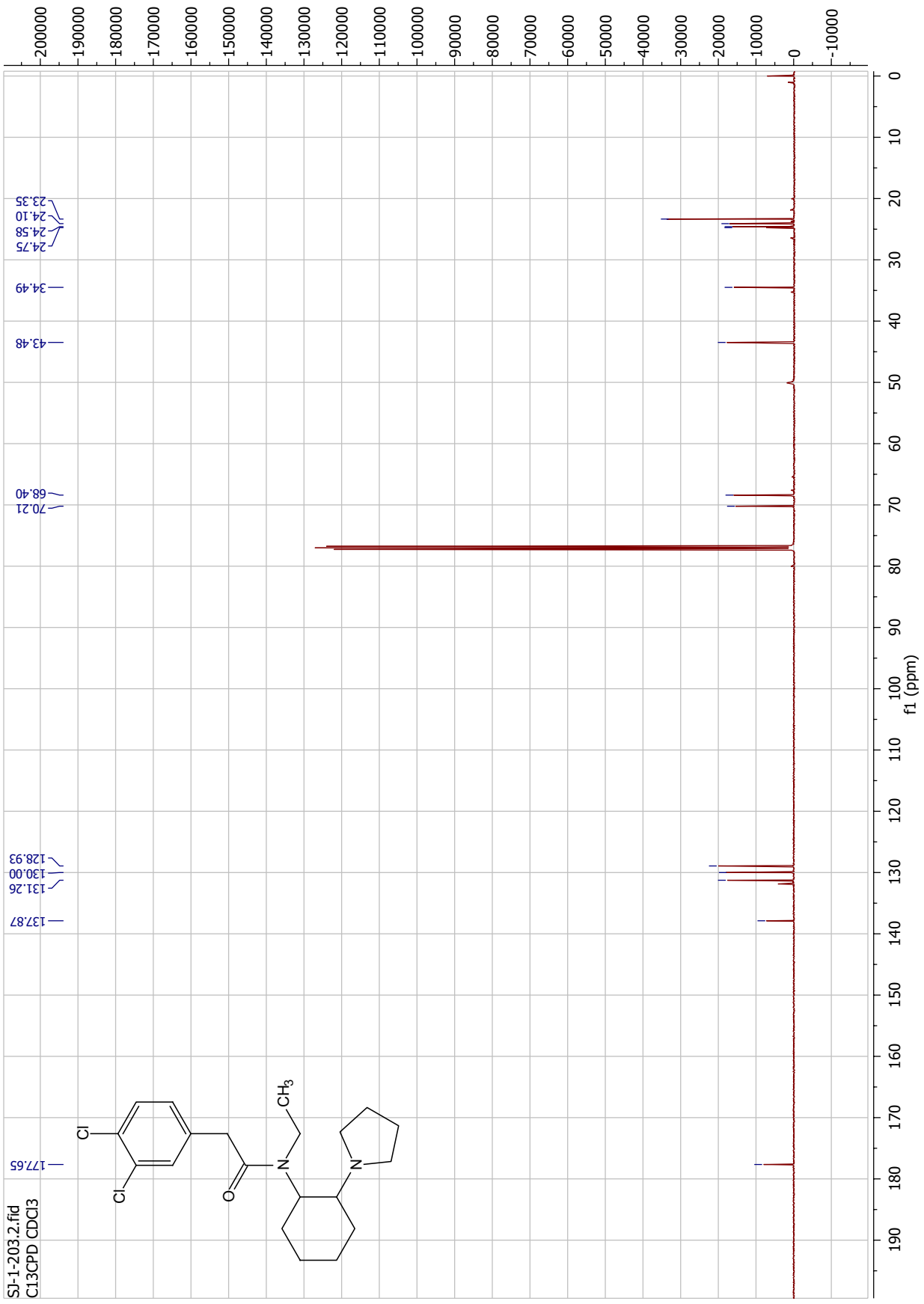
SJ-1-203.2.fid
C13CPD CDCl3
177.65
137.87
131.26
130.00
128.93
70.21
68.40
43.48
34.49
24.75
24.58
24.10
23.35
f1 (ppm)

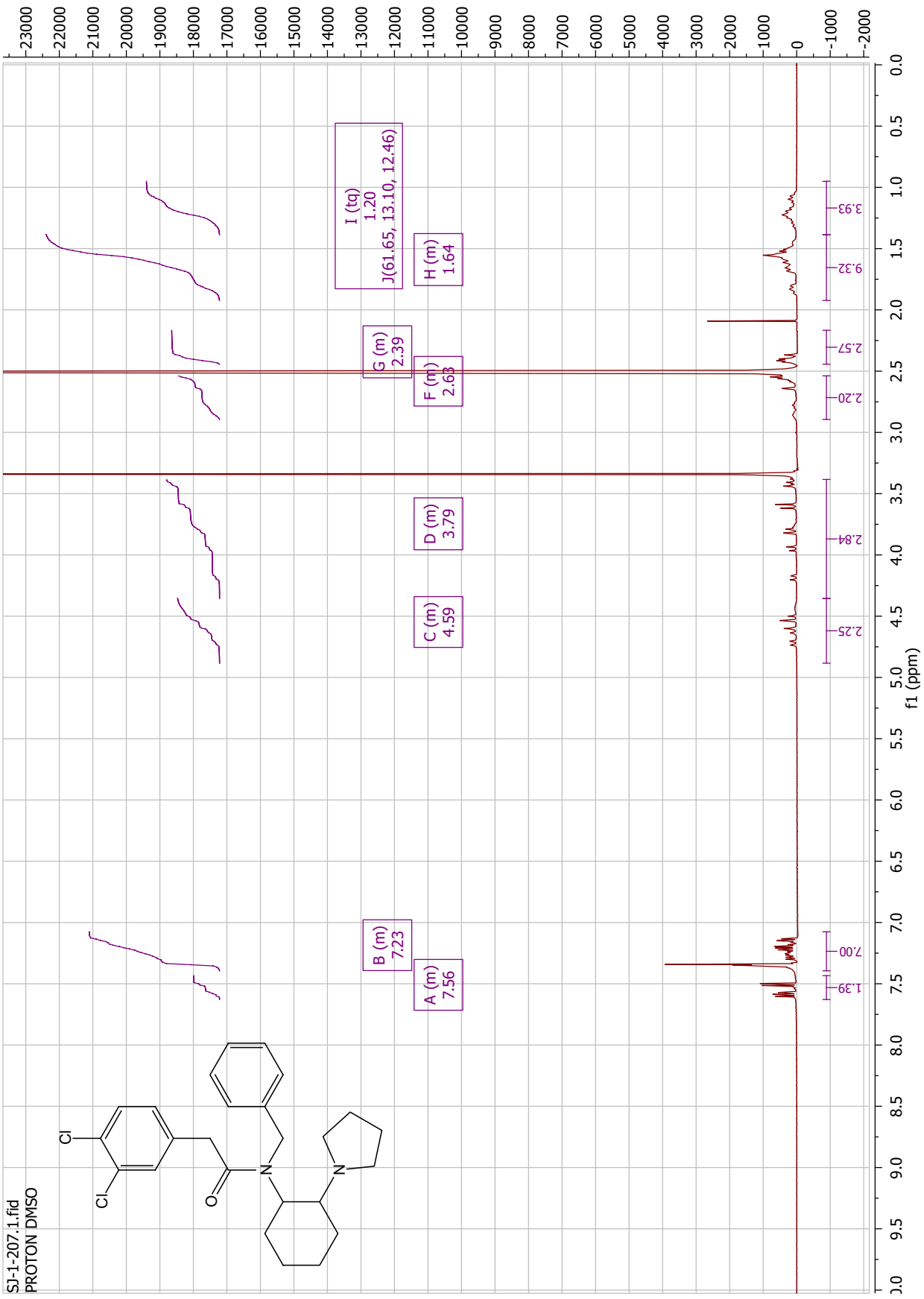
SJ-1-207.1.fid
PROTON DMSO
A (m)
7.56
B (m)
7.23
C (m)
4.59
D (m)
3.79
F (m)
2.63
G (m)
2.39
H (m)
1.64
I (tq)
1.20
J(61.65, 13.10, 12.46)
1.39
7.00
2.25
2.84
2.20
2.57
9.32
3.93
Cl
Cl
O
N
N
f1 (ppm)

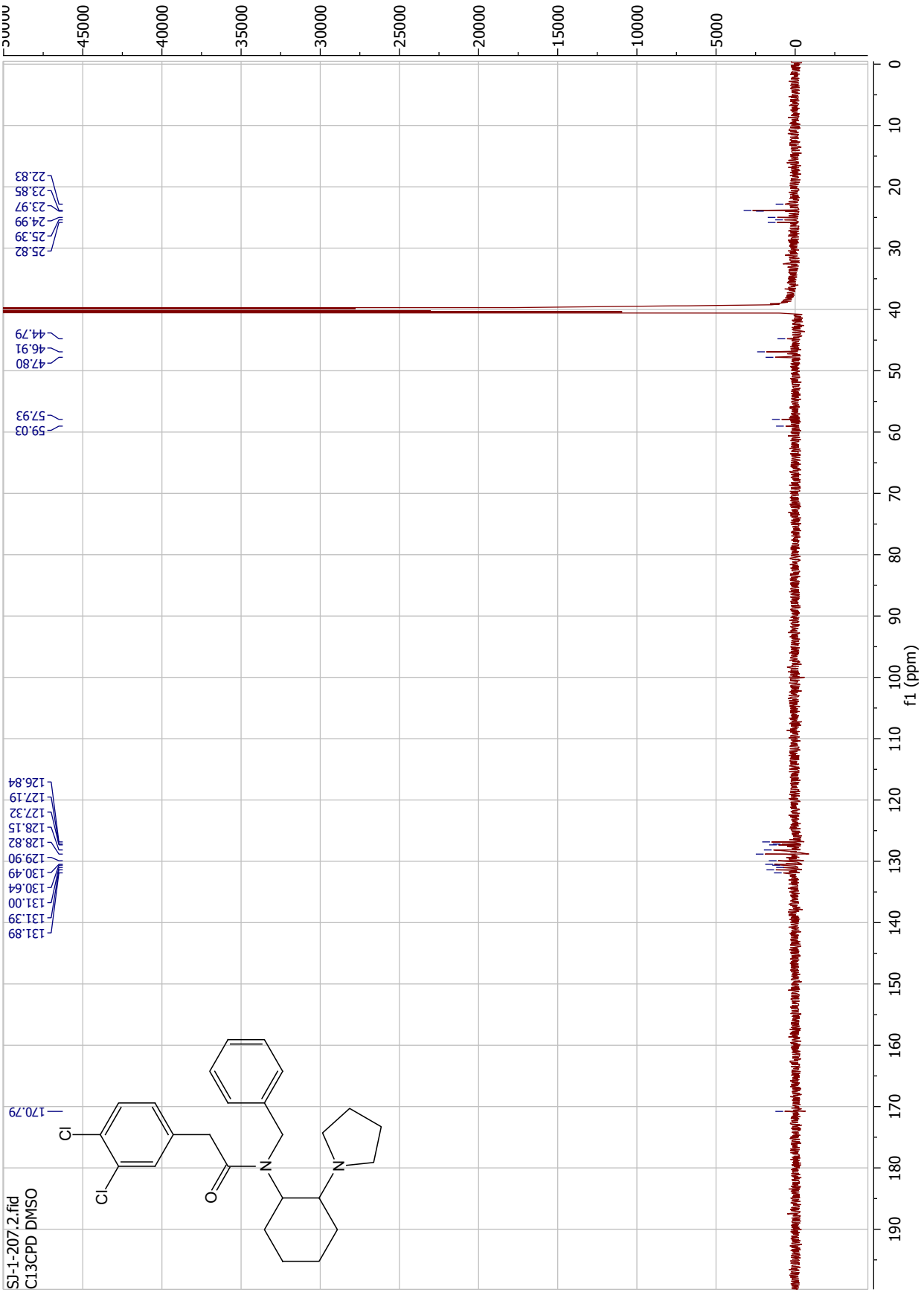
SJ-1-207.2.fid
C13CPD DMSO
f1 (ppm)
170.79
131.89
131.39
131.00
130.64
130.49
129.90
128.82
128.15
127.32
127.19
126.84
59.03
57.93
47.80
46.91
44.79
25.82
25.39
24.99
23.97
23.85
22.83
Cl
Cl
O
N
N

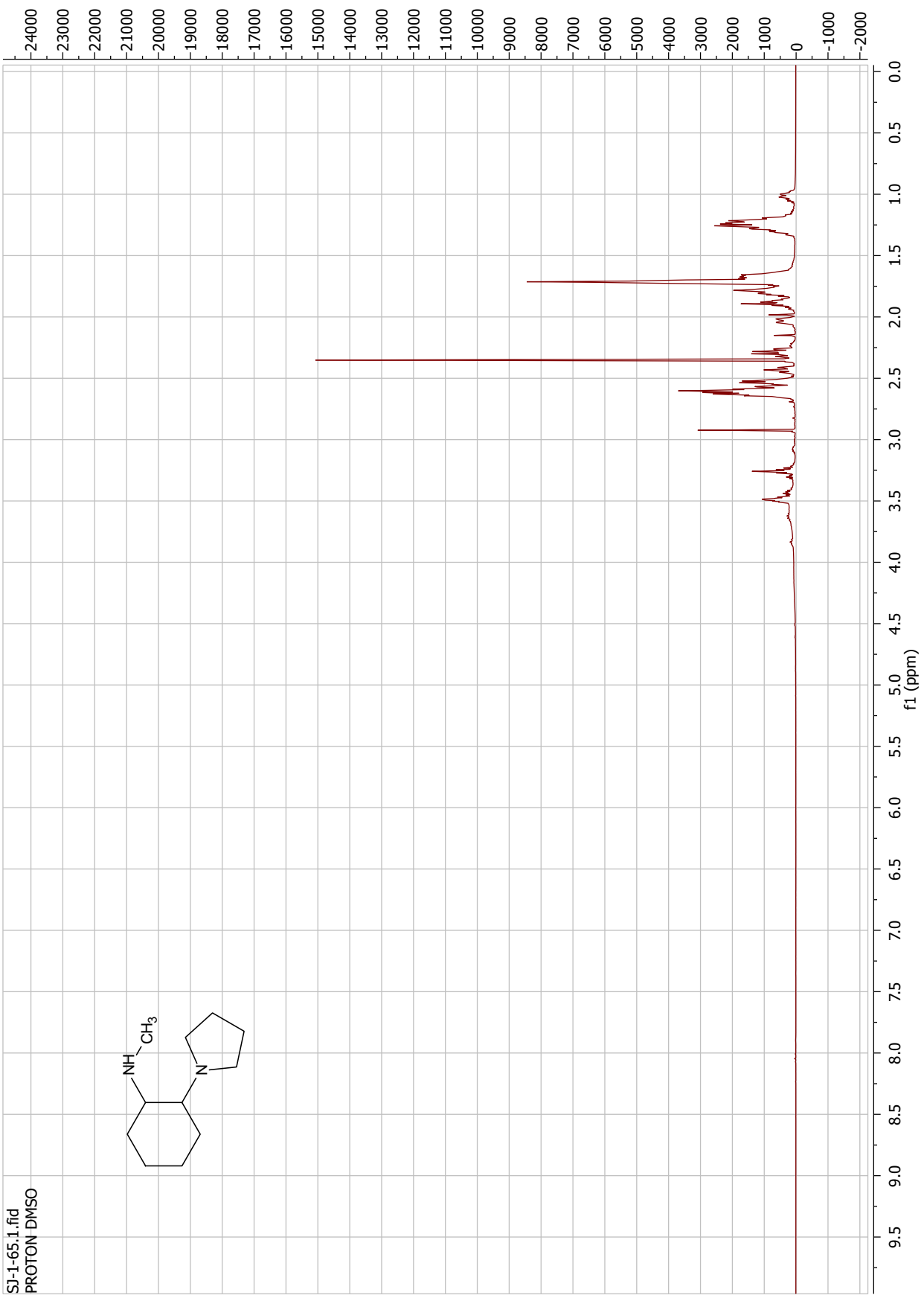
SJ-1-65.1.fid
PROTON DMSO
NH
CH3
N
f1 (ppm)

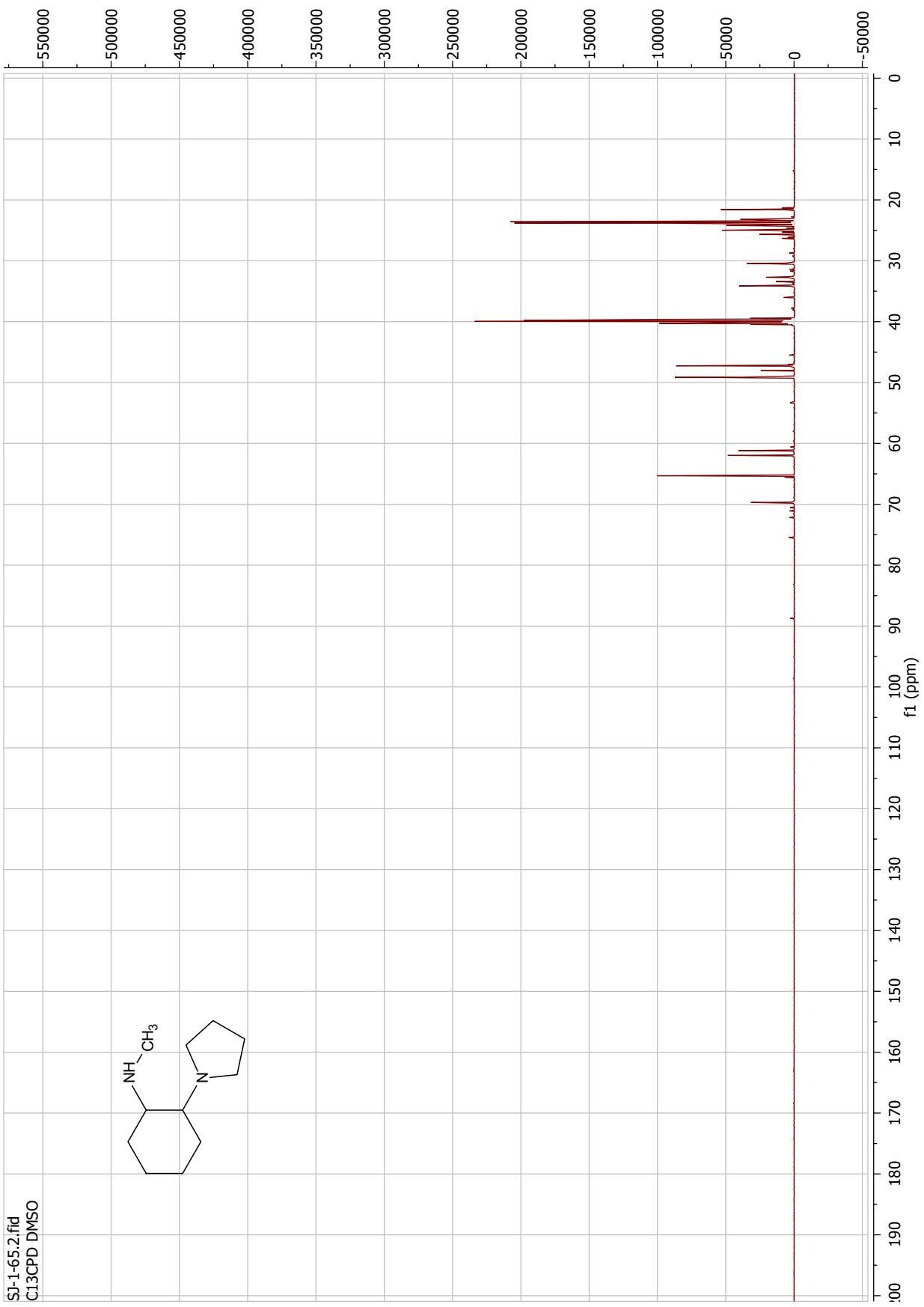
SJ-1-65.2.fid
C13CPD DMSO
NH
CH3
N
f1 (ppm)

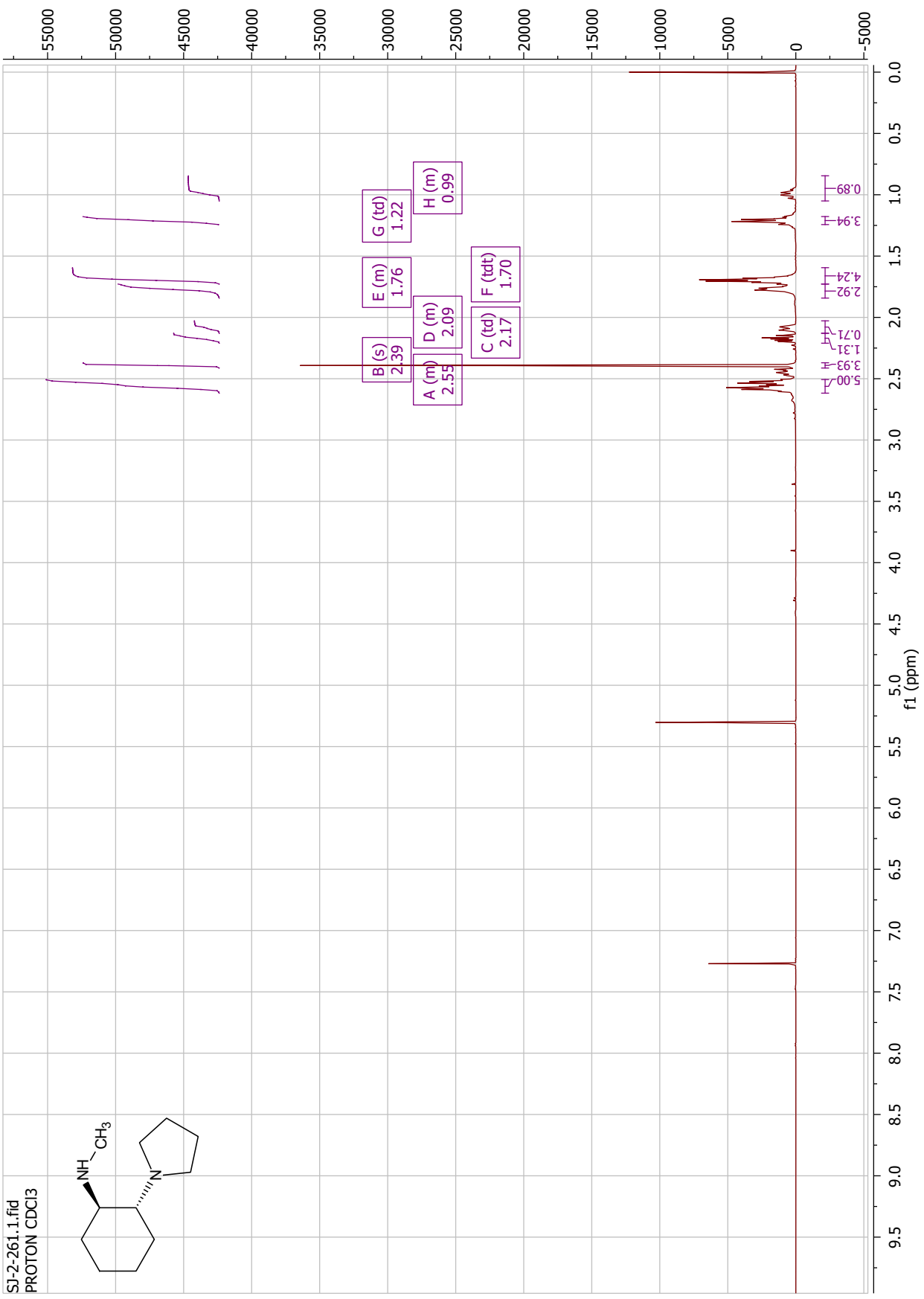
SJ-2-261.1.fid
PROTON CDCl3
NH
CH3
N
A (m) 2.55
B (s) 2.39
C (td) 2.17
D (m) 2.09
E (m) 1.76
F (tdt) 1.70
G (td) 1.22
H (m) 0.99
5.00
3.93
1.31
0.71
2.92
4.24
3.94
0.89
f1 (ppm)

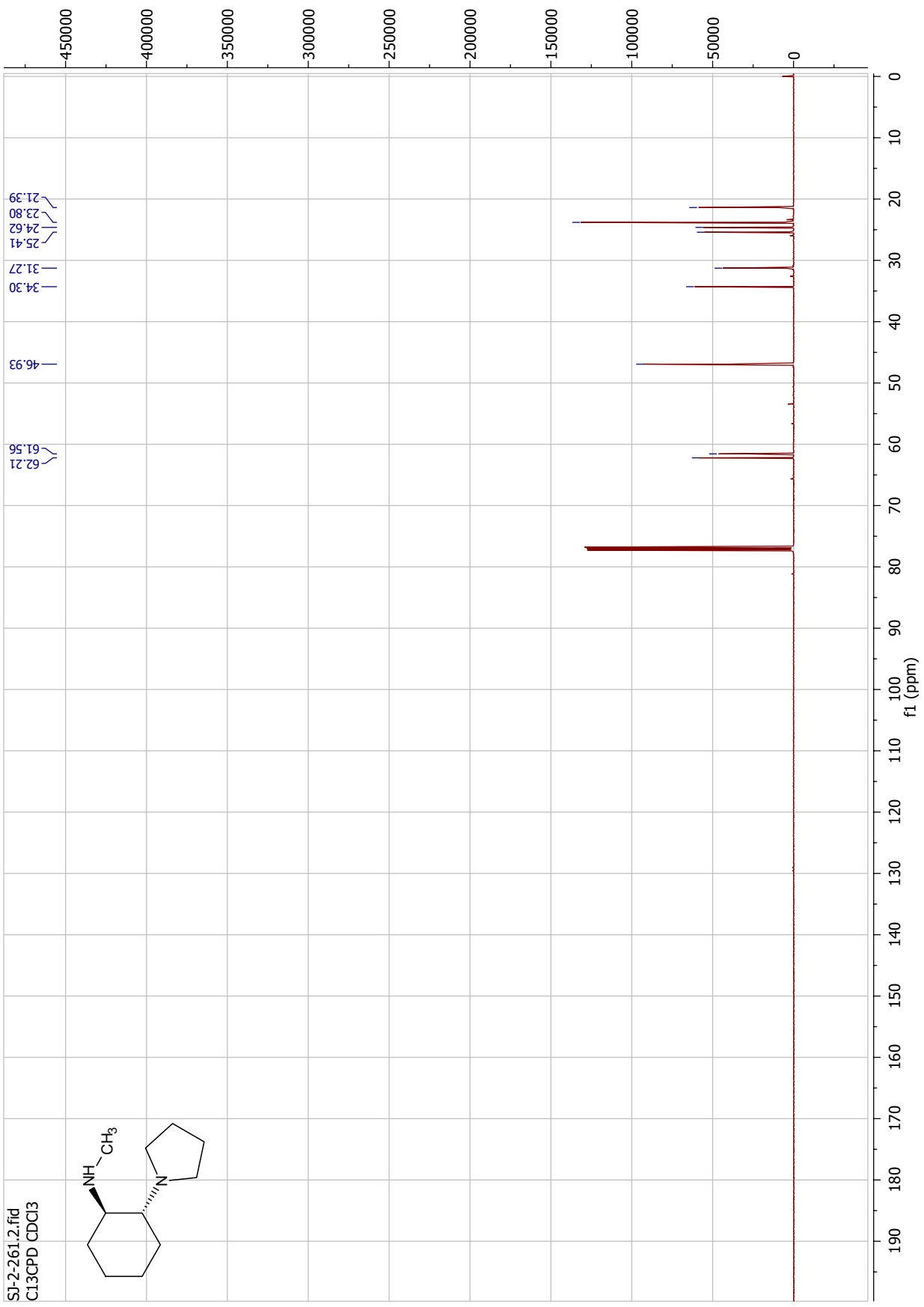
S1-2-261.2.fid
C13CPD CDCl3
21.39
23.80
24.62
25.41
31.27
34.30
46.93
61.56
62.21
NH
CH3
N
f1 (ppm)

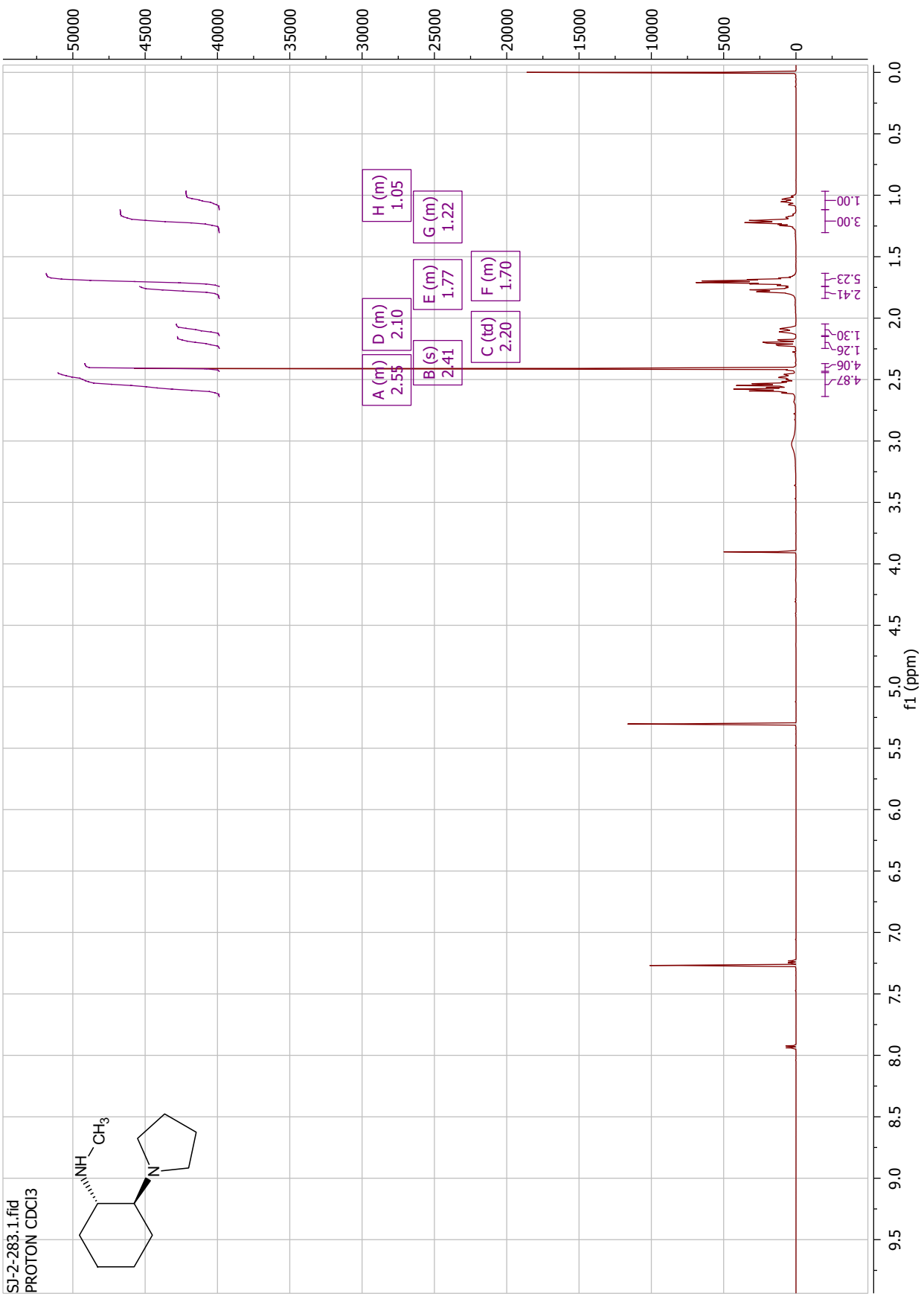
SJ-2-283.1.fid
PROTON CDCl3
NH
CH3
N
A (m) 2.55
B (s) 2.41
C (td) 2.20
D (m) 2.10
E (m) 1.77
F (m) 1.70
G (m) 1.22
H (m) 1.05
1.00
3.00
5.23
2.41
1.30
1.26
4.06
4.87
f1 (ppm)

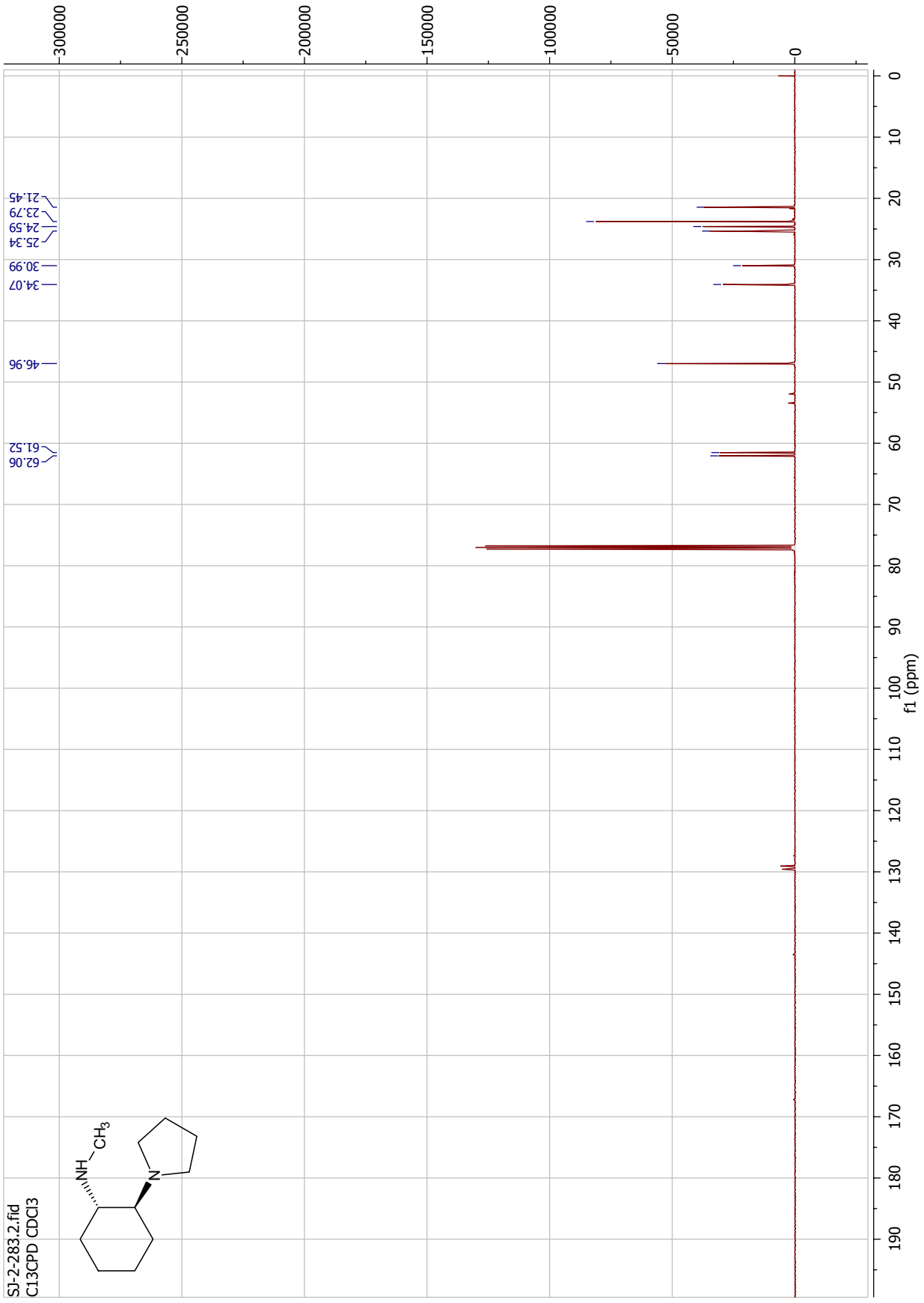
S1-2-283.2.fid
C13CPD CDCl3
21.45
23.79
24.59
25.34
30.99
34.07
46.96
61.52
62.06
f1 (ppm)


SJ-1-135.1.fid
PROTON DMSO
A (m) 7.25
B (m) 3.68
C (s) 3.34
D (m) 2.73
E (m) 2.39
F (d) 1.82
G (dq) 1.71
H (m) 1.52
I (m) 1.20
4.37
1.78
9.00
2.47
1.69
0.78
1.93
4.61
1.51
O
N
CH3
N
f1 (ppm)

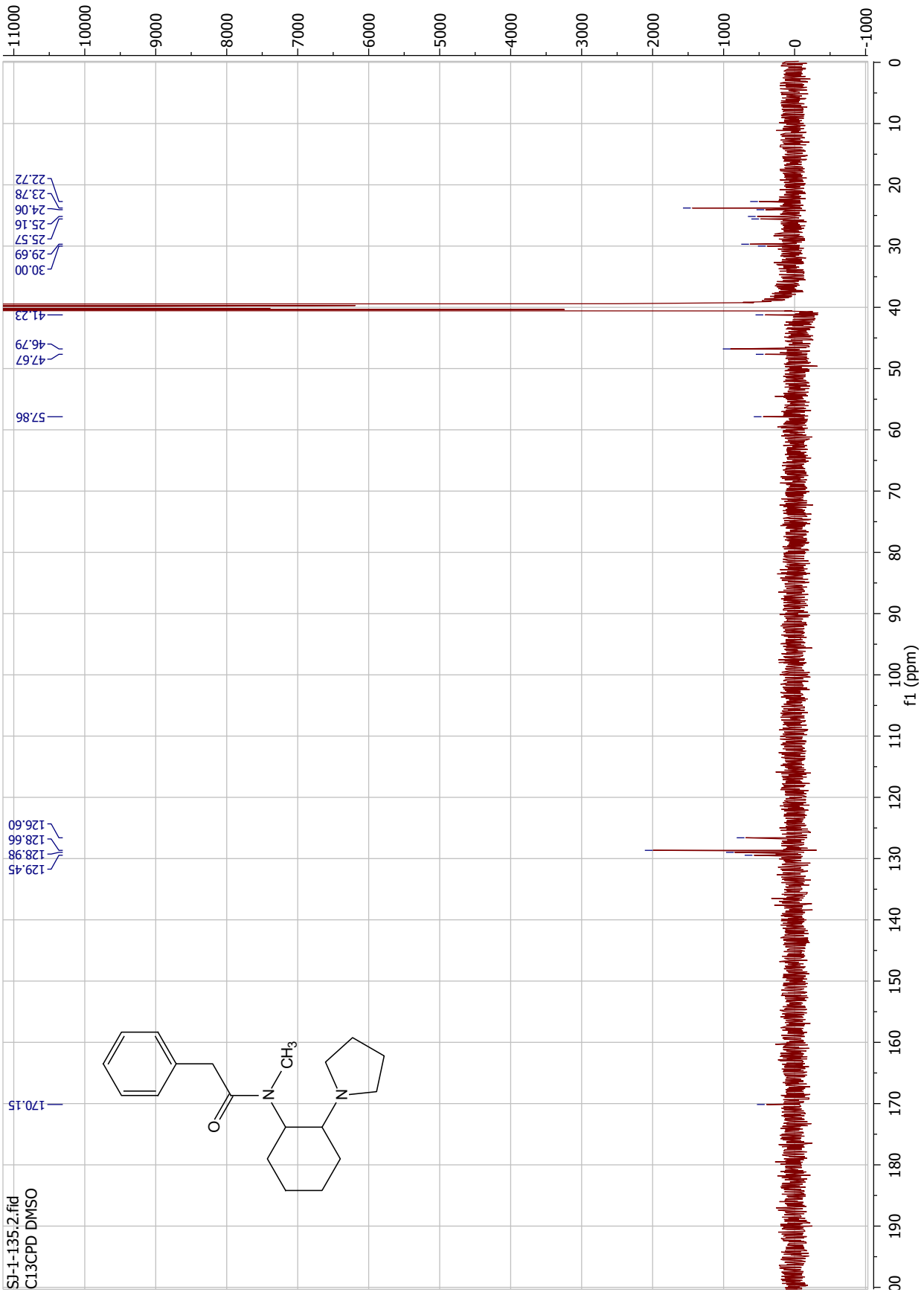
SJ-1-135.2.fid
C13CPD DMSO
170.15
129.45
128.98
128.66
126.60
57.86
47.67
46.79
41.23
30.00
29.69
25.57
25.16
24.06
23.78
22.72
f1 (ppm)

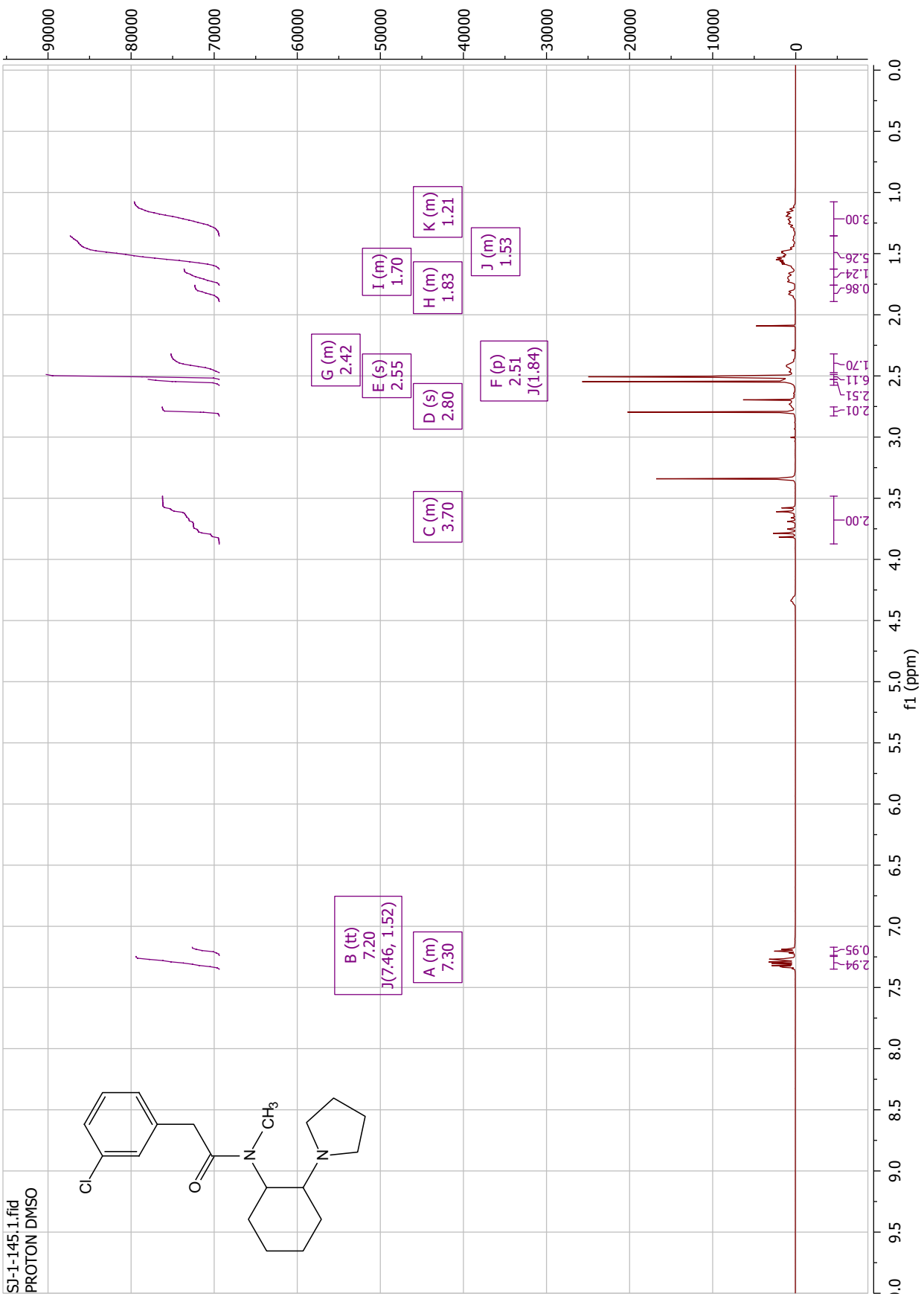
SJ-1-145.1.fid
PROTON DMSO
A (m)
7.30
B (tt)
7.20
J(7.46, 1.52)
C (m)
3.70
D (s)
2.80
E (s)
2.55
F (p)
2.51
J(1.84)
G (m)
2.42
H (m)
1.83
I (m)
1.70
J (m)
1.53
K (m)
1.21
2.94
0.95
2.00
2.01
2.51
6.11
1.70
0.86
1.24
5.26
3.00
f1 (ppm)

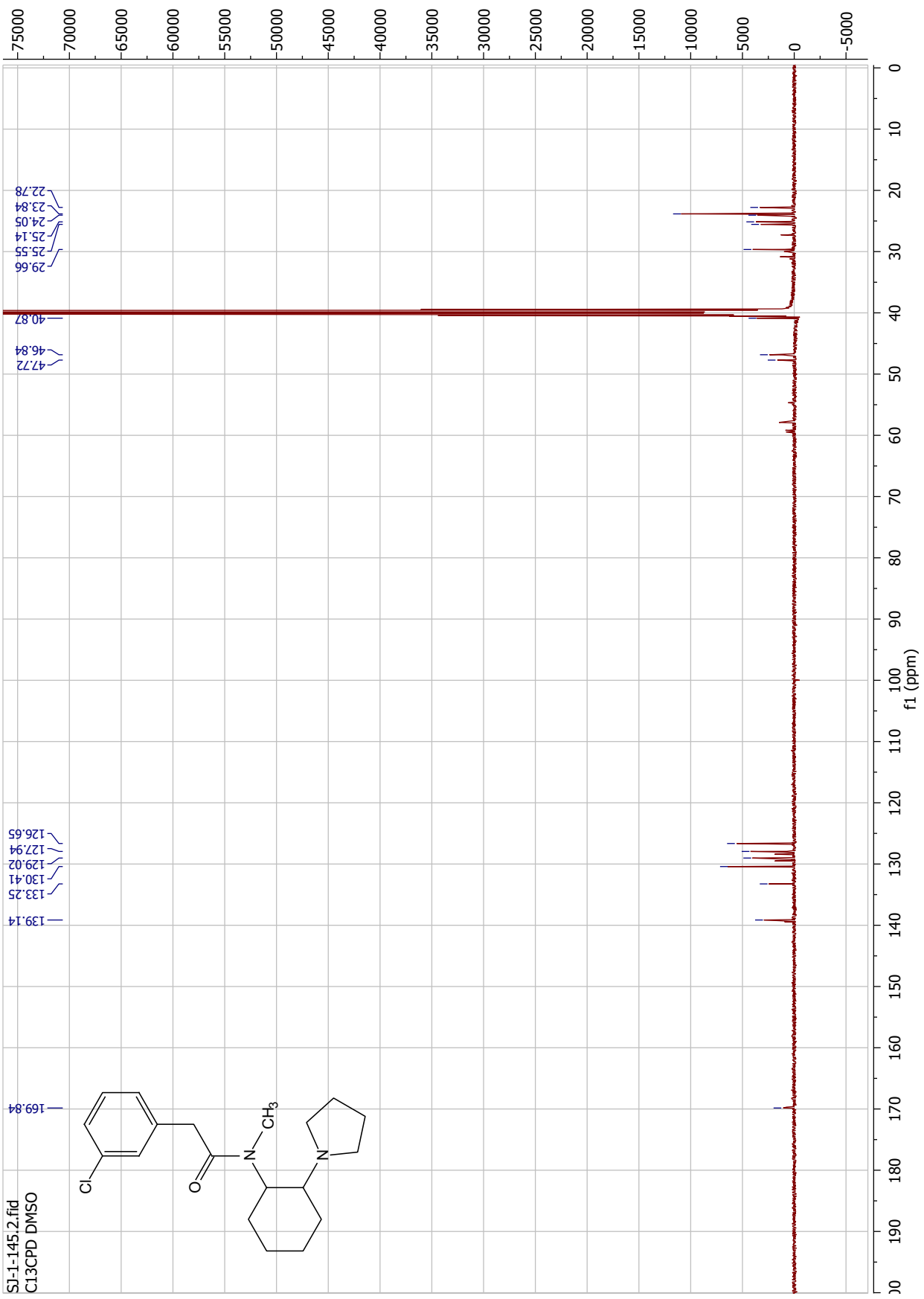
SJ-1-145.2.fid
C13CPD DMSO
f1 (ppm)
169.84
139.14
133.25
130.41
129.02
127.94
126.65
47.72
46.84
40.87
29.66
25.55
25.14
24.05
23.84
22.78
Cl
O
N
CH3
N

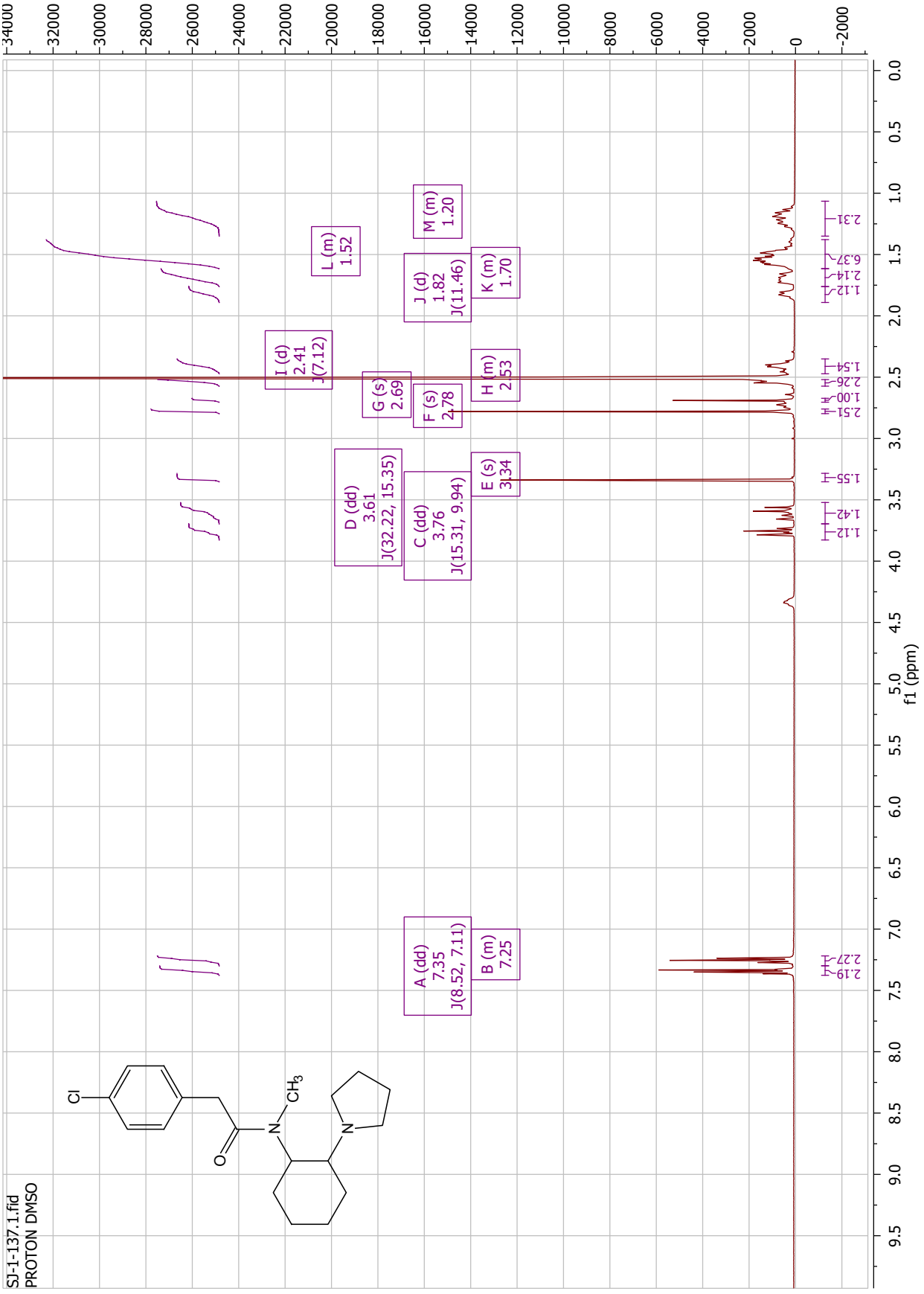
SJ-1-137.1.fid
PROTON DMSO
A (dd)
7.35
J(8.52, 7.11)
B (m)
7.25
C (dd)
3.76
J(15.31, 9.94)
D (dd)
3.61
J(32.22, 15.35)
E (s)
3.34
F (s)
2.78
G (s)
2.69
H (m)
2.53
I (d)
2.41
J(7.12)
J (d)
1.82
J(11.46)
K (m)
1.70
L (m)
1.52
M (m)
1.20
2.27
2.19
1.55
1.42
1.12
2.31
6.37
2.14
1.12
1.54
2.26
1.00
2.51
Cl
O
N
CH3
N
f1 (ppm)

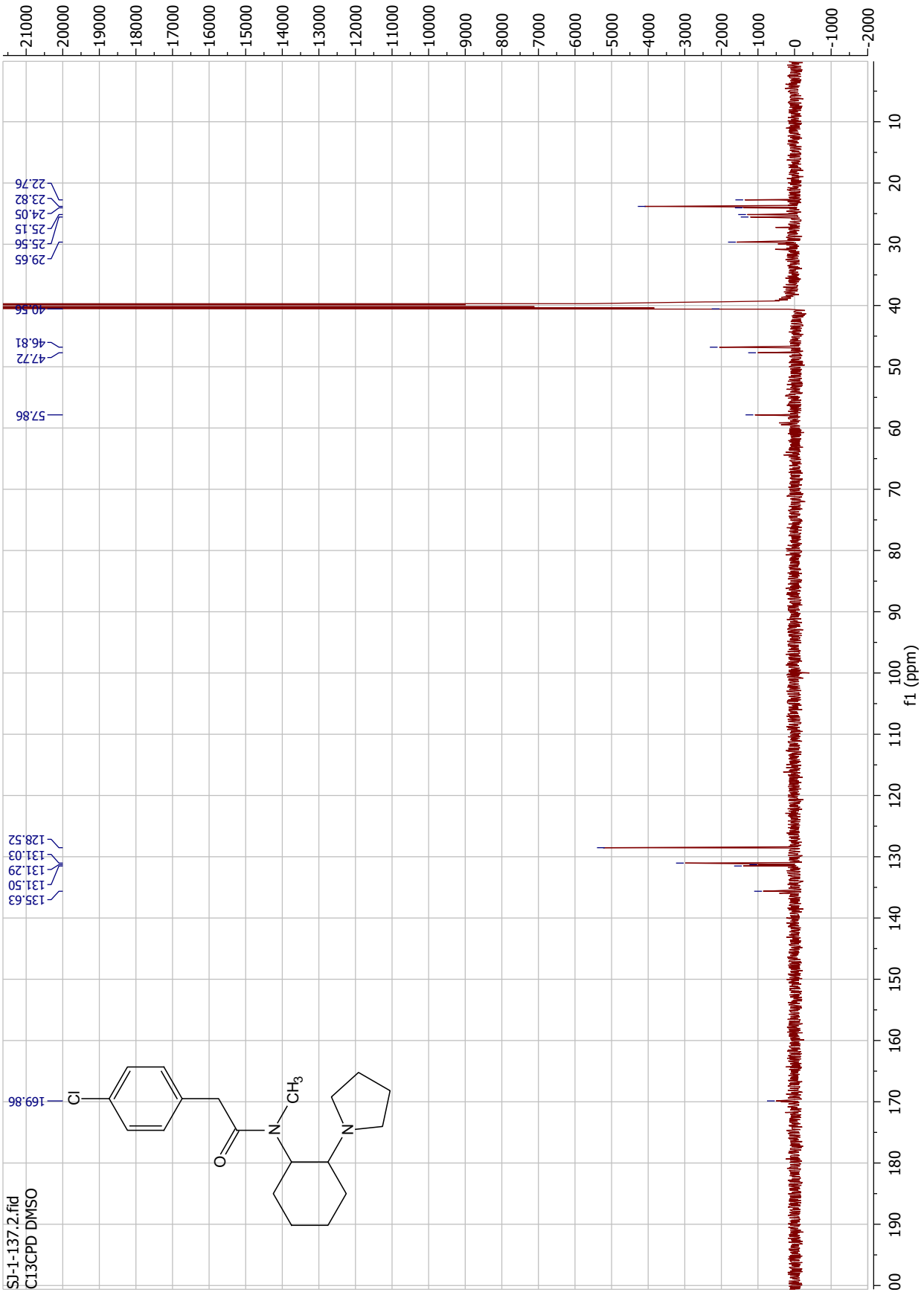
SJ-1-137.2.fid
C13CPD DMSO
169.86
135.63
131.50
131.29
131.03
128.52
57.86
47.72
46.81
40.56
29.65
25.56
25.15
24.05
23.82
22.76
Cl
O
N
CH3
N
f1 (ppm)

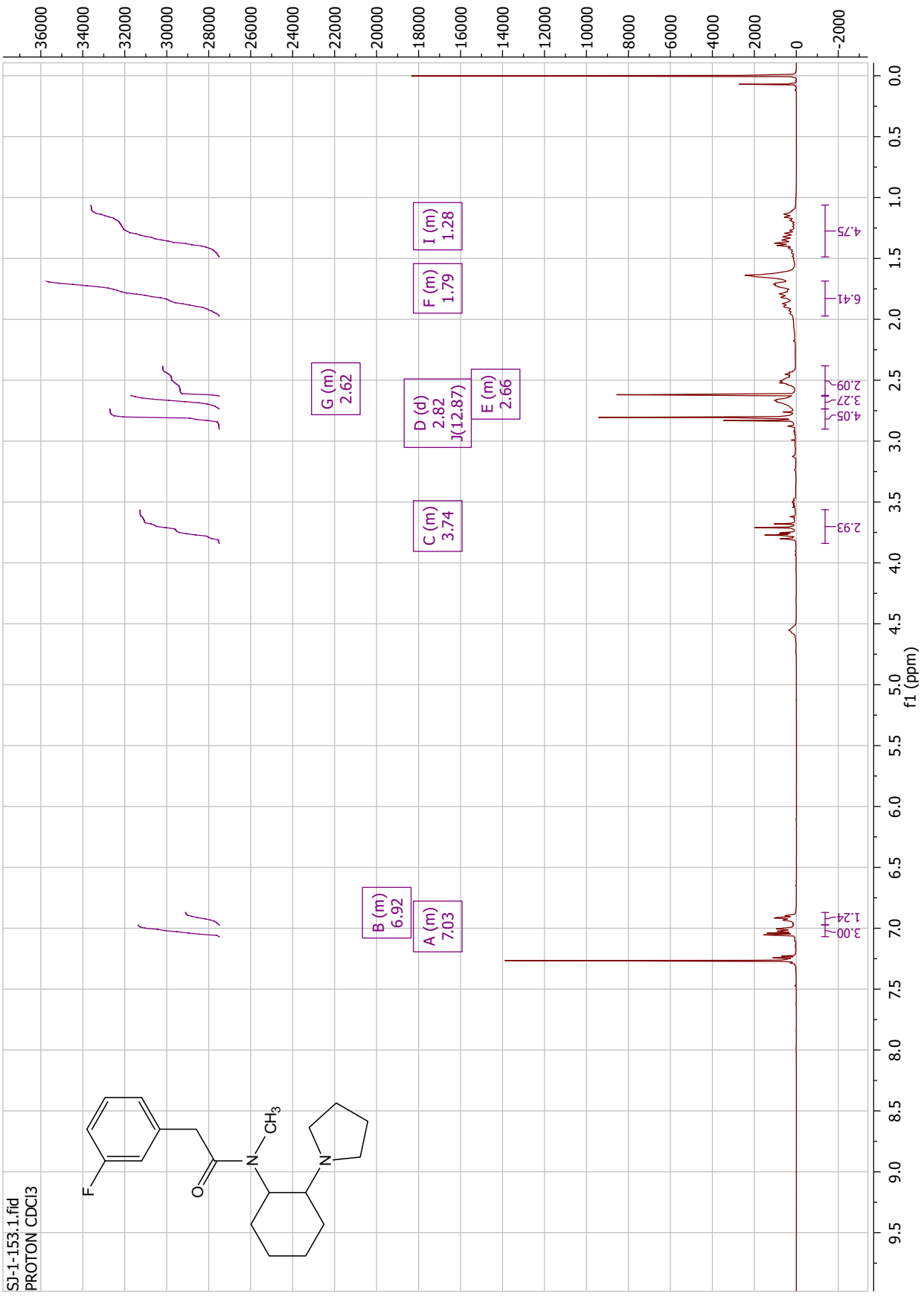
SJ-1-153.1.fid
PROTON CDCl3
A (m) 7.03
B (m) 6.92
C (m) 3.74
D (d) 2.82 J(12.87)
E (m) 2.66
F (m) 1.79
G (m) 2.62
I (m) 1.28
4.75
6.41
2.09
3.27
4.05
2.93
1.24
3.00
f1 (ppm)

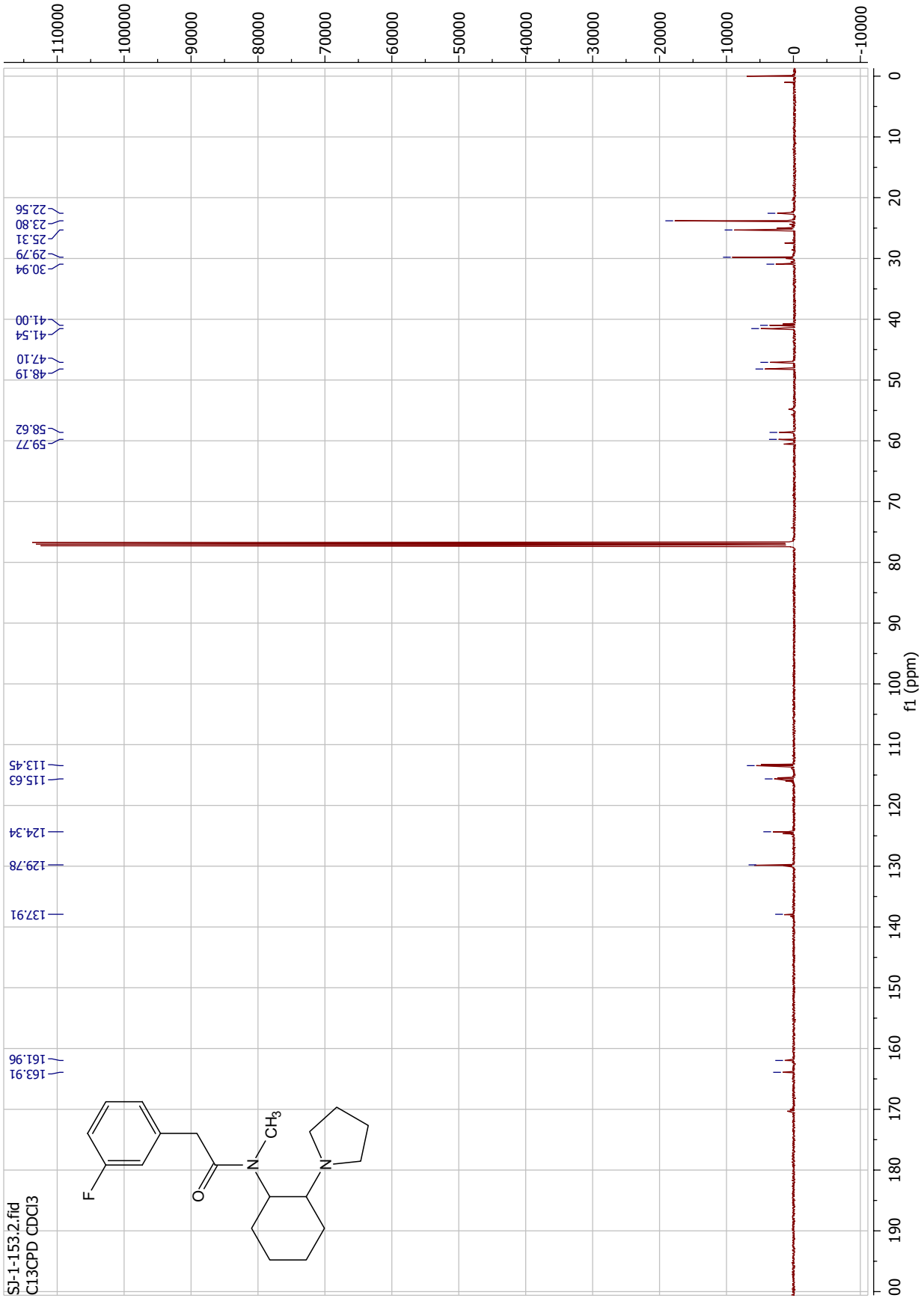
SJ-1-153.2.fid
C13CPD CDCl3
22.56
23.80
25.31
29.79
30.94
41.00
41.54
47.10
48.19
58.62
59.77
113.45
115.63
124.34
129.78
137.91
161.96
163.91
F
O
N
CH3
N
f1 (ppm)

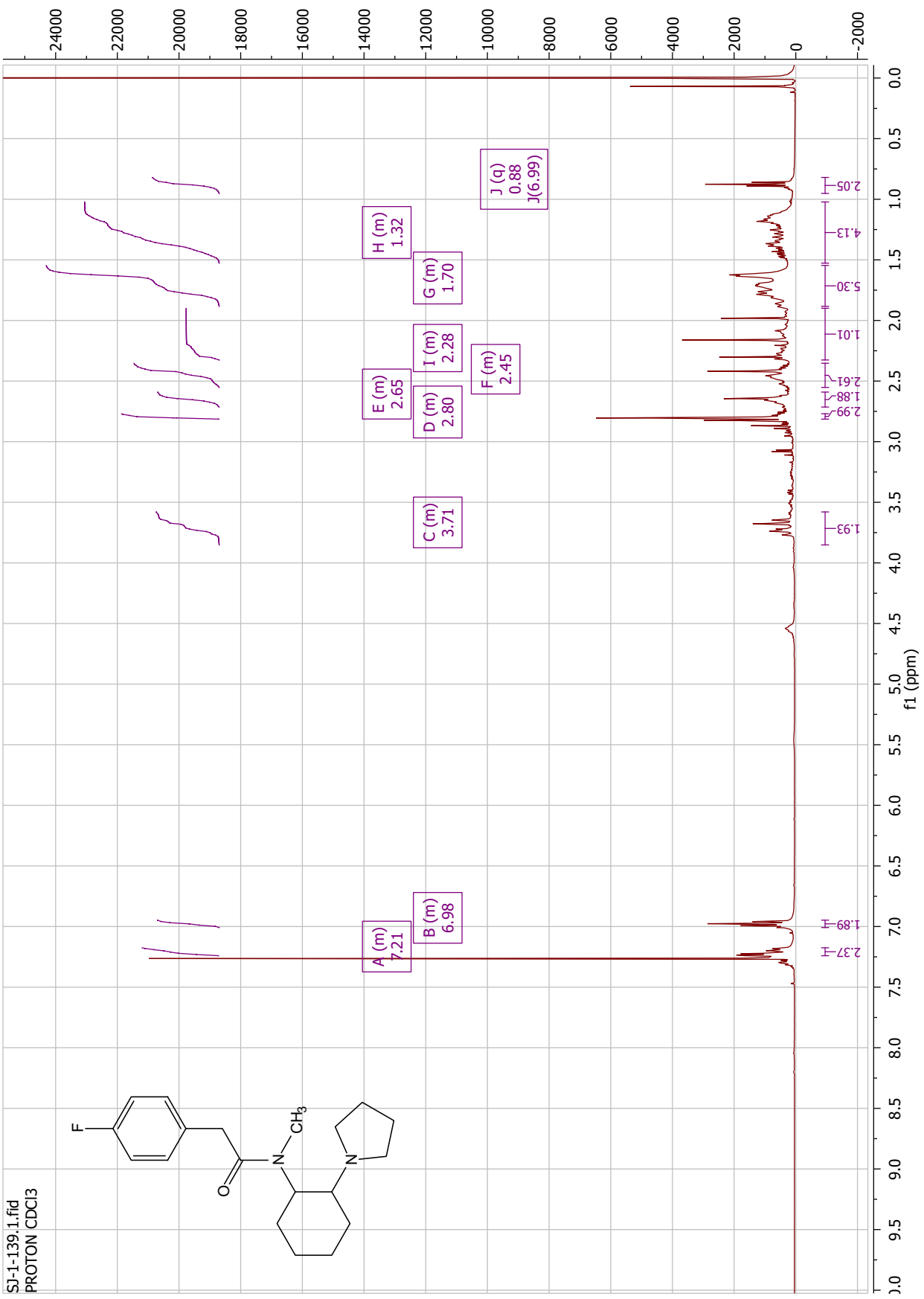
SJ-1-139.1.fid
PROTON CDCl3
A (m) 7.21
B (m) 6.98
C (m) 3.71
D (m) 2.80
E (m) 2.65
F (m) 2.45
G (m) 1.70
H (m) 1.32
I (m) 2.28
J (q) 0.88 J(6.99)
2.37
1.89
1.93
2.99
1.88
2.61
1.01
5.30
4.13
2.05
F
O
N
CH3
N
f1 (ppm)

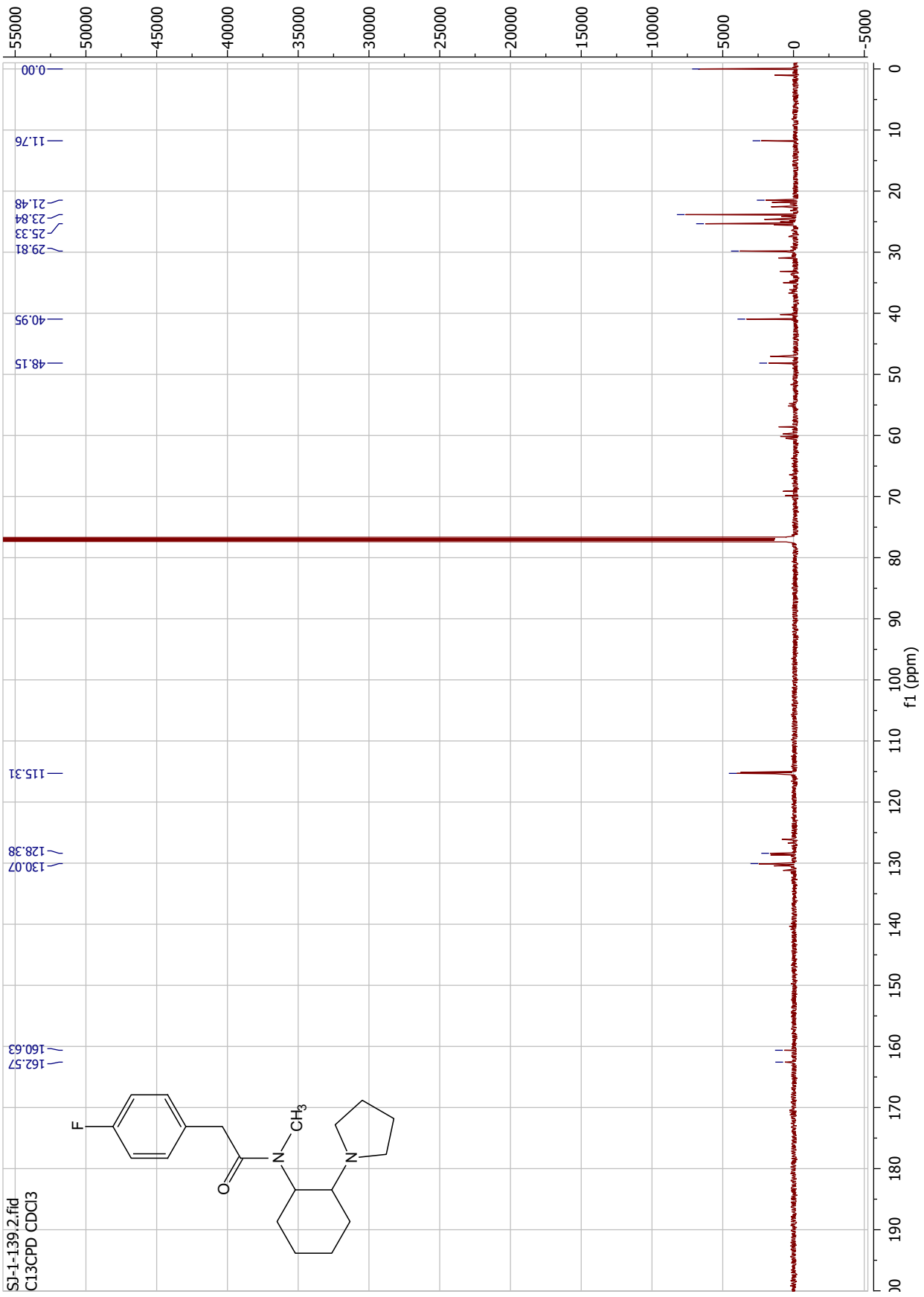
SJ-1-139.2.fid
C13CPD CDCl3
0.00
11.76
21.48
23.84
25.33
29.81
40.95
48.15
115.31
128.38
130.07
160.63
162.57
F
O
N
CH3
N
f1 (ppm)

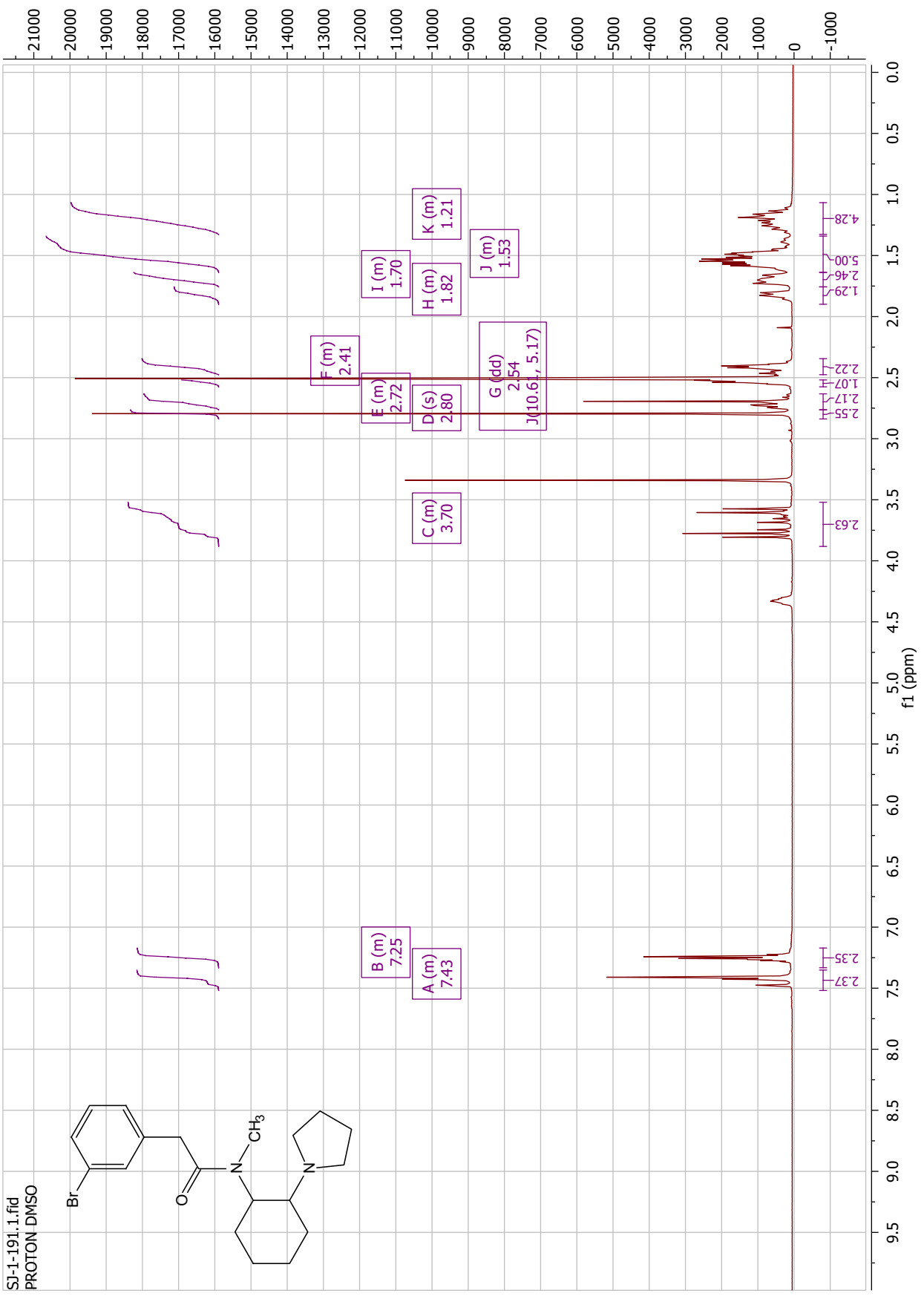
SJ-1-191.1.fid
PROTON DMSO
Br
O
N
CH3
N
A (m) 7.43
B (m) 7.25
C (m) 3.70
D (s) 2.80
E (m) 2.72
F (m) 2.41
G (dd) 2.54 J(10.6, 5.17)
H (m) 1.82
I (m) 1.70
J (m) 1.53
K (m) 1.21
2.37
2.35
2.63
2.55
2.17
1.07
2.22
4.28
5.00
2.46
1.29
f1 (ppm)

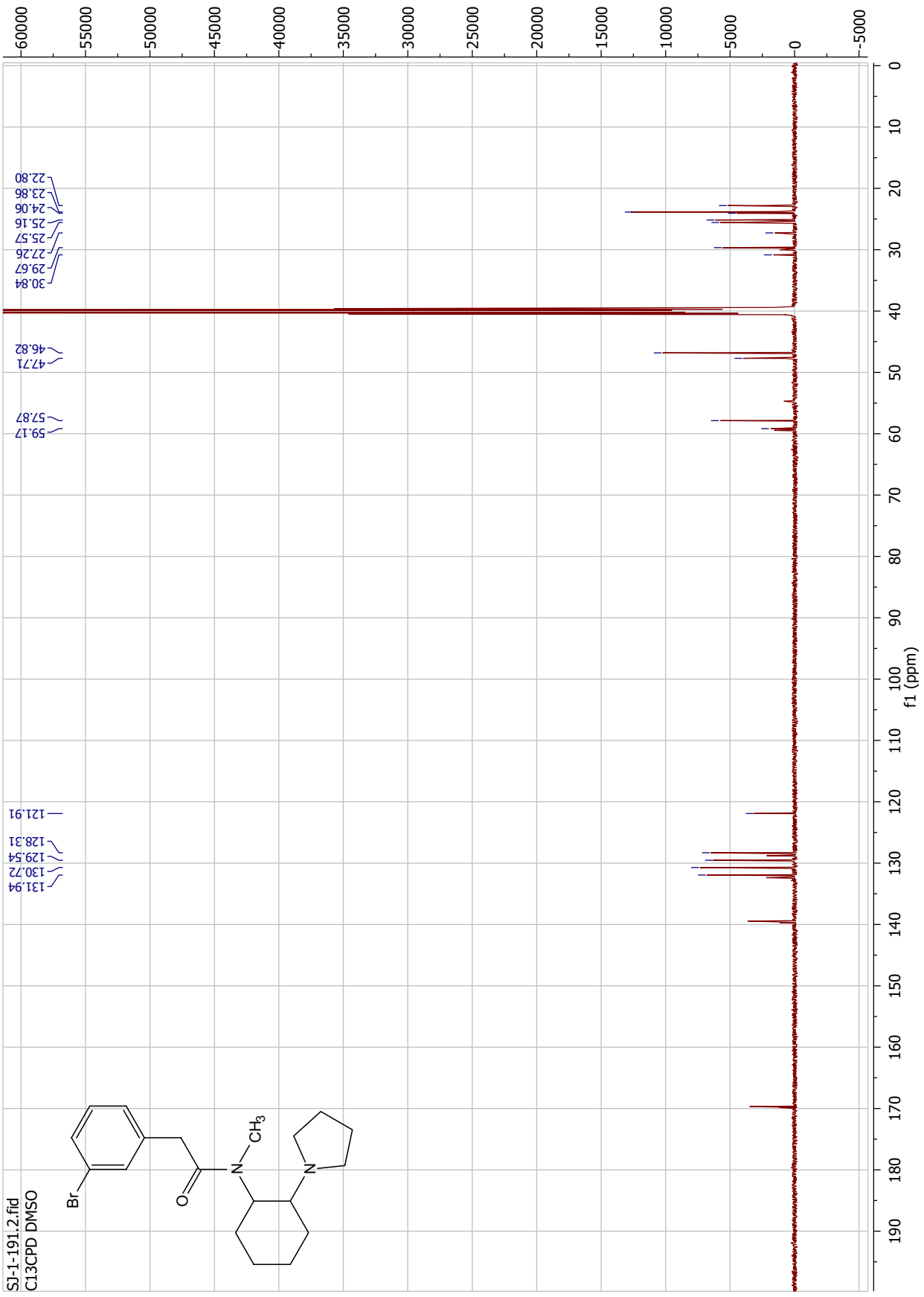
SJ-1-191.2.fid
C13CPD DMSO
Br
O
N
CH3
N
22.80
23.86
24.06
25.16
25.57
27.26
29.67
30.84
46.82
47.71
57.87
59.17
121.91
128.31
129.54
130.72
131.94
f1 (ppm)

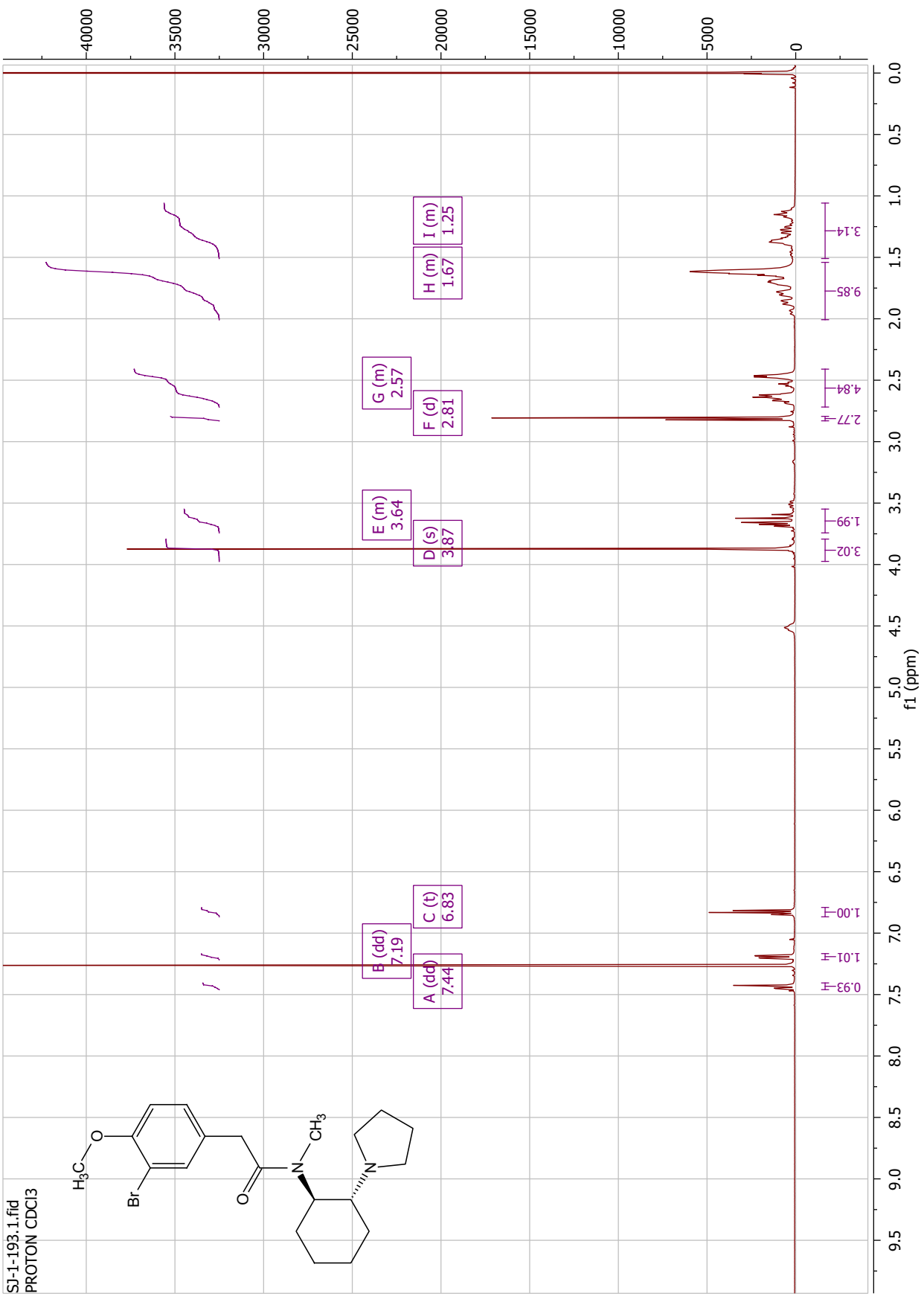
SJ-1-193.1.fid
PROTON CDCl3
A (dd) 7.44
B (dd) 7.19
C (t) 6.83
D (s) 3.87
E (m) 3.64
F (d) 2.81
G (m) 2.57
H (m) 1.67
I (m) 1.25
1.00
1.01
0.93
3.14
9.85
4.84
2.77
1.99
3.02
f1 (ppm)

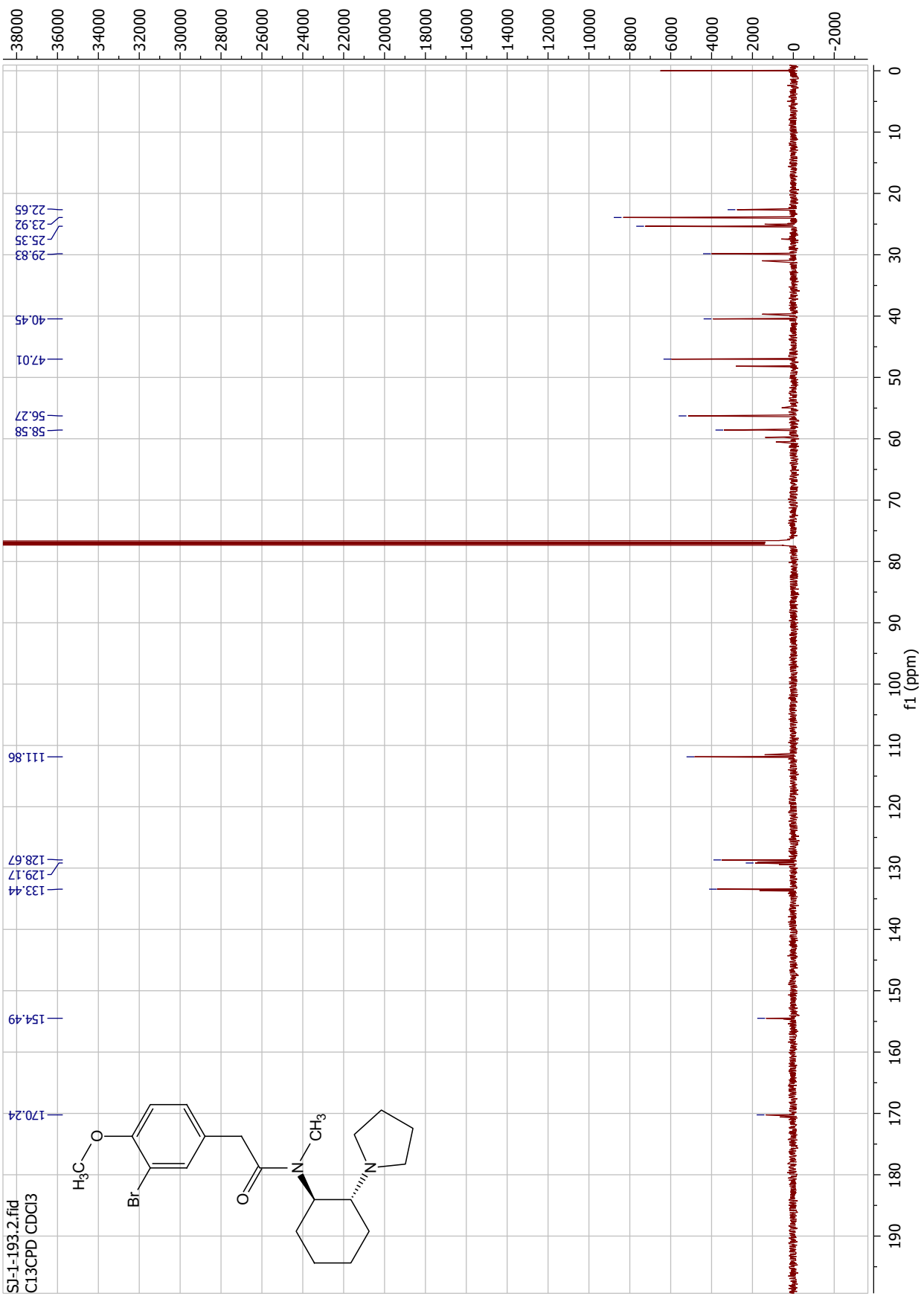
SJ-1-193.2.fid
C13CPD CDCl3
170.24
154.49
133.44
129.17
128.67
111.86
58.58
56.27
47.01
40.45
29.83
25.35
23.92
22.65
f1 (ppm)

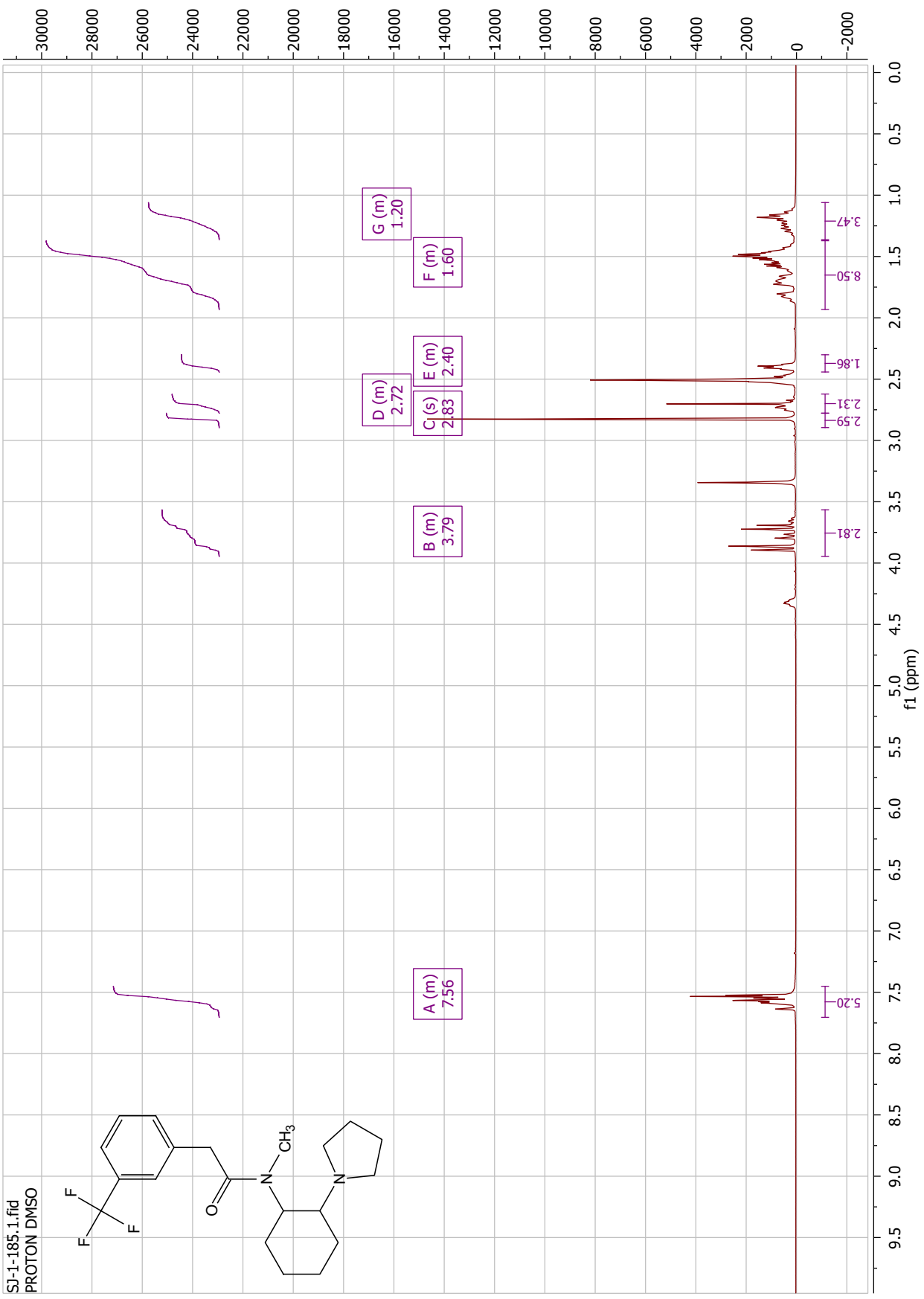
SJ-1-185.1.fid
PROTON DMSO
A (m) 7.56
B (m) 3.79
C (s) 2.83
D (m) 2.72
E (m) 2.40
F (m) 1.60
G (m) 1.20
5.20
2.81
2.59
2.31
1.86
8.50
3.47
f1 (ppm)

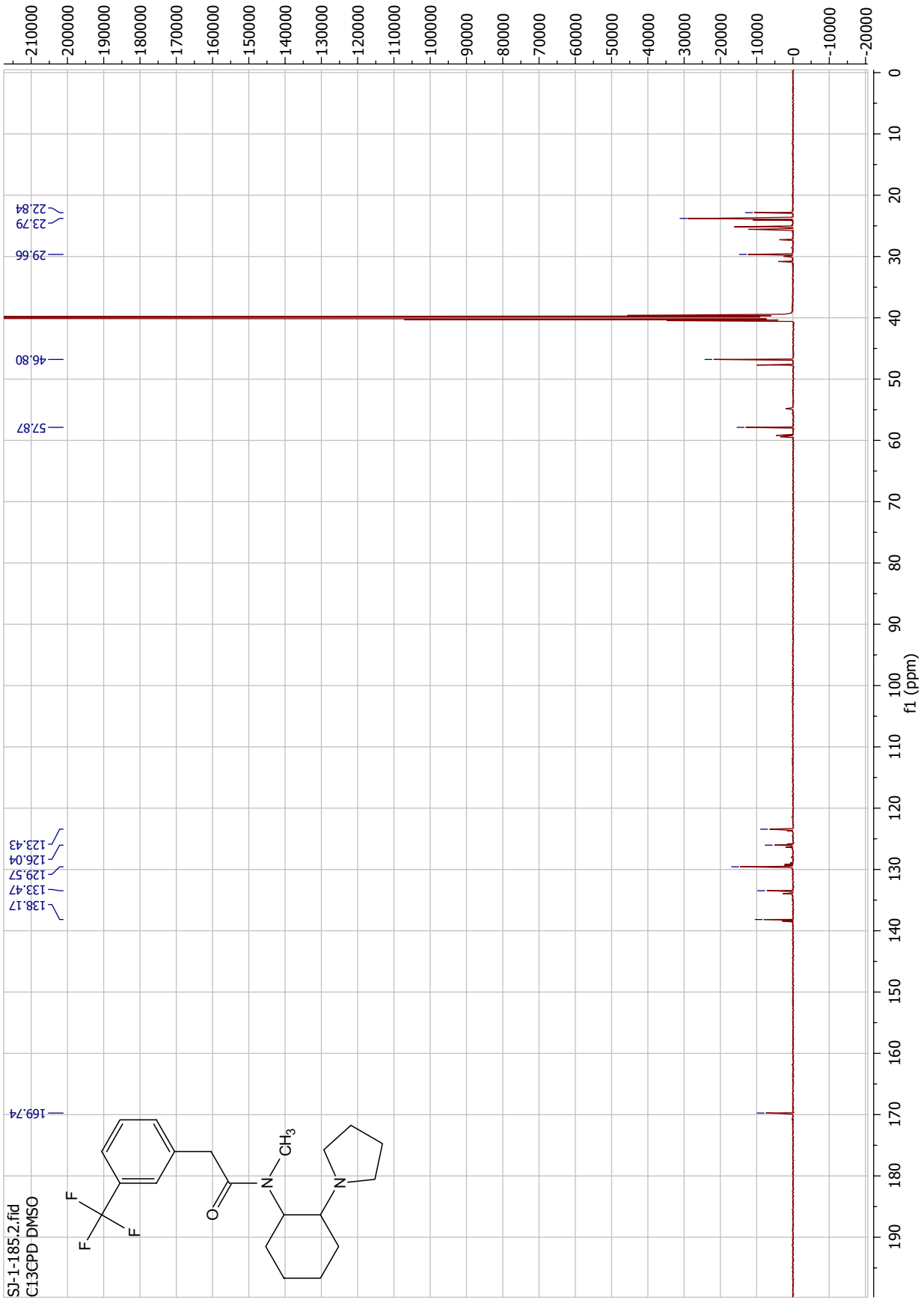
SJ-1-185.2.fid
C13CPD DMSO
169.74
138.17
133.47
129.57
126.04
123.43
57.87
46.80
29.66
23.79
22.84
f1 (ppm)

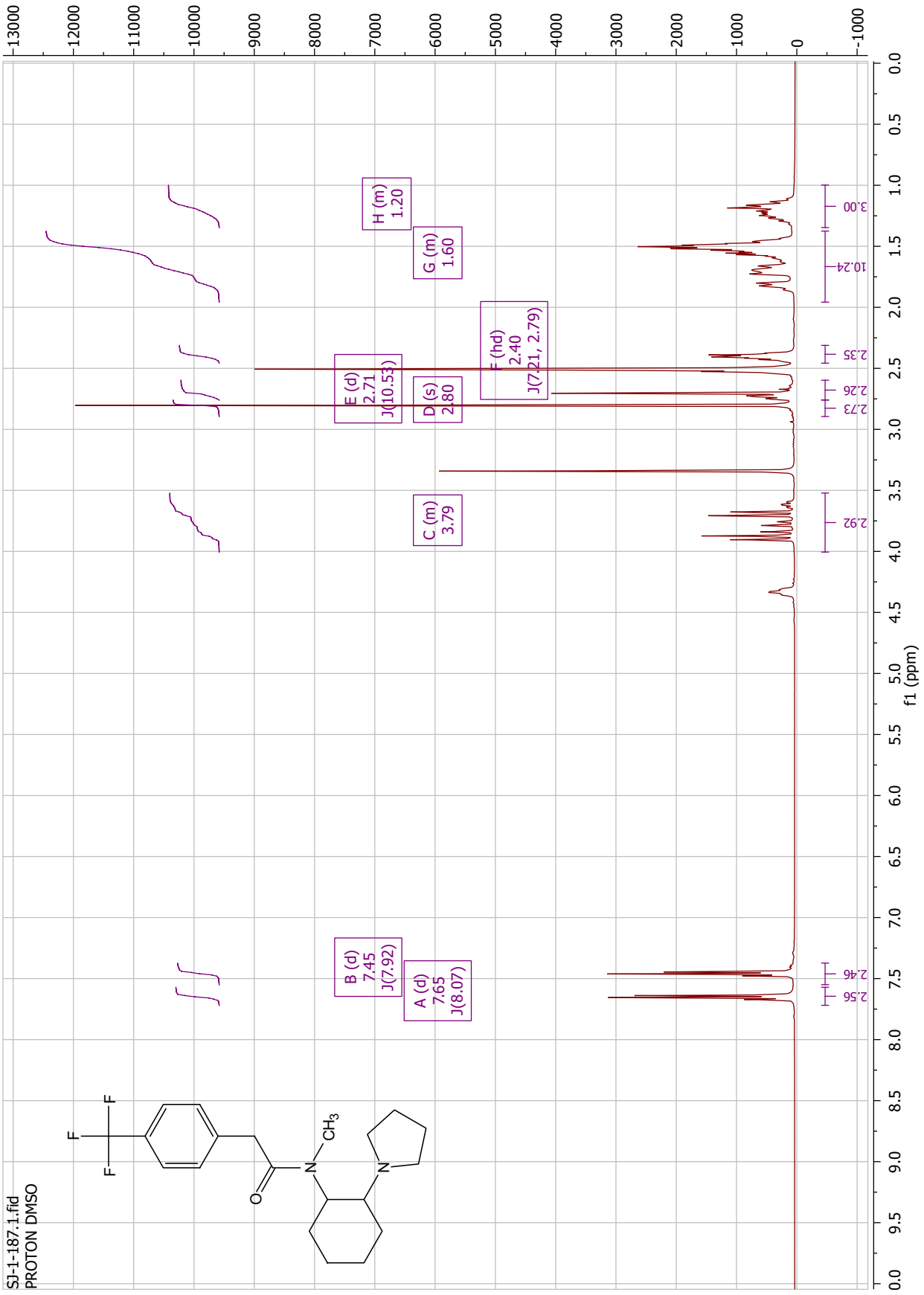
SJ-1-187.1.fid
PROTON DMSO
A (d)
7.65
J(8.07)
B (d)
7.45
J(7.92)
C (m)
3.79
D (s)
2.80
E (d)
2.71
J(10.53)
F (hd)
2.40
J(7.21, 2.79)
G (m)
1.60
H (m)
1.20
2.56
2.46
2.92
2.73
2.26
2.35
10.24
3.00
f1 (ppm)

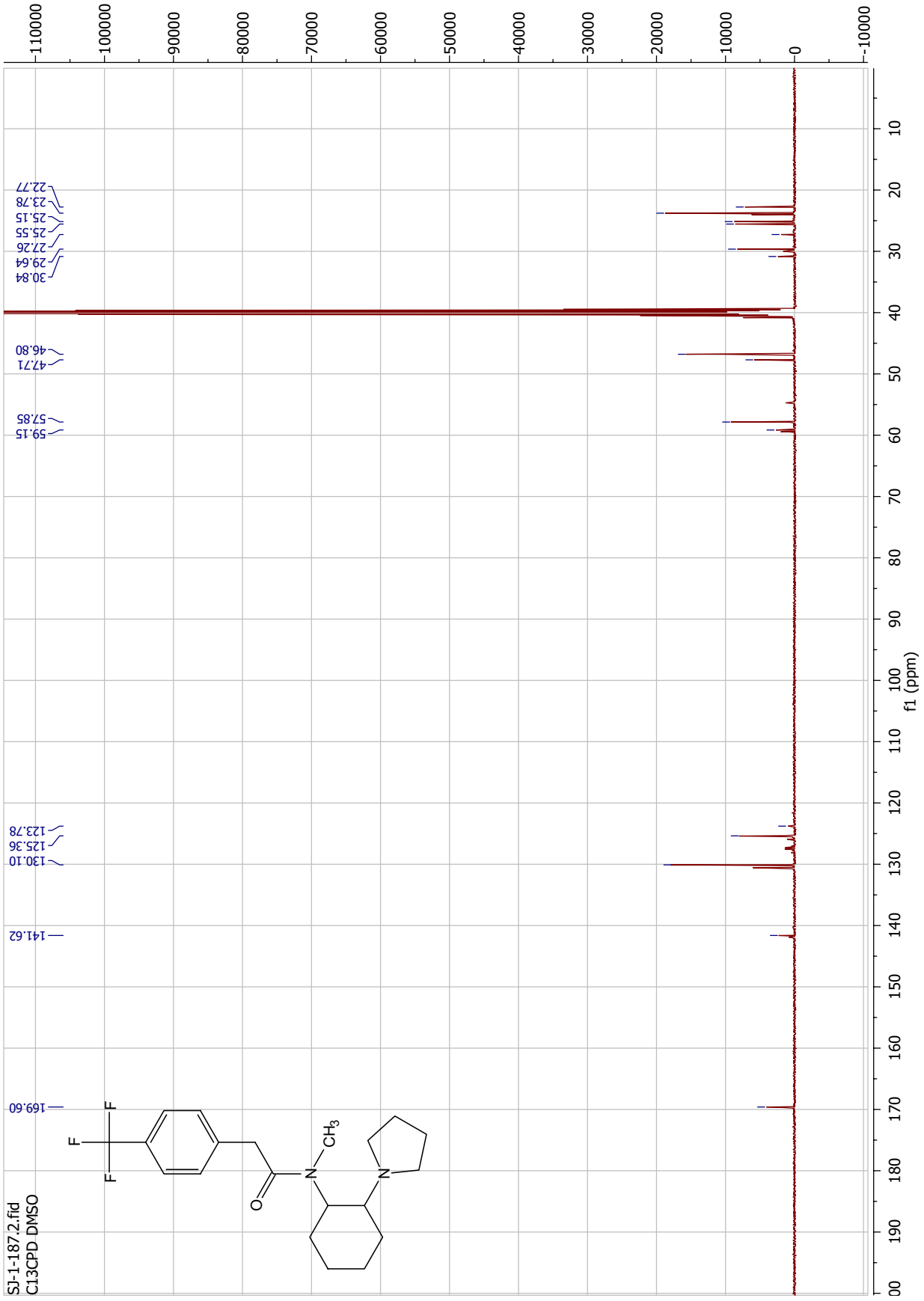
S3-1-187.2.fid
C13CPD DMSO
169.60
141.62
130.10
125.36
123.78
59.15
57.85
47.71
46.80
30.84
29.64
27.26
25.55
25.15
23.78
22.77
F
F
F
O
N
CH3
N
f1 (ppm)


SJ-2-23.1.fid
PROTON DMSO
A (m) 8.11
B (m) 7.65
C (m) 3.87
D (s) 2.84
E (m) 2.71
F (m) 2.46
G (m) 1.57
H (m) 1.19
2.30
2.52
2.11
2.23
2.03
3.13
8.07
3.00
f1 (ppm)

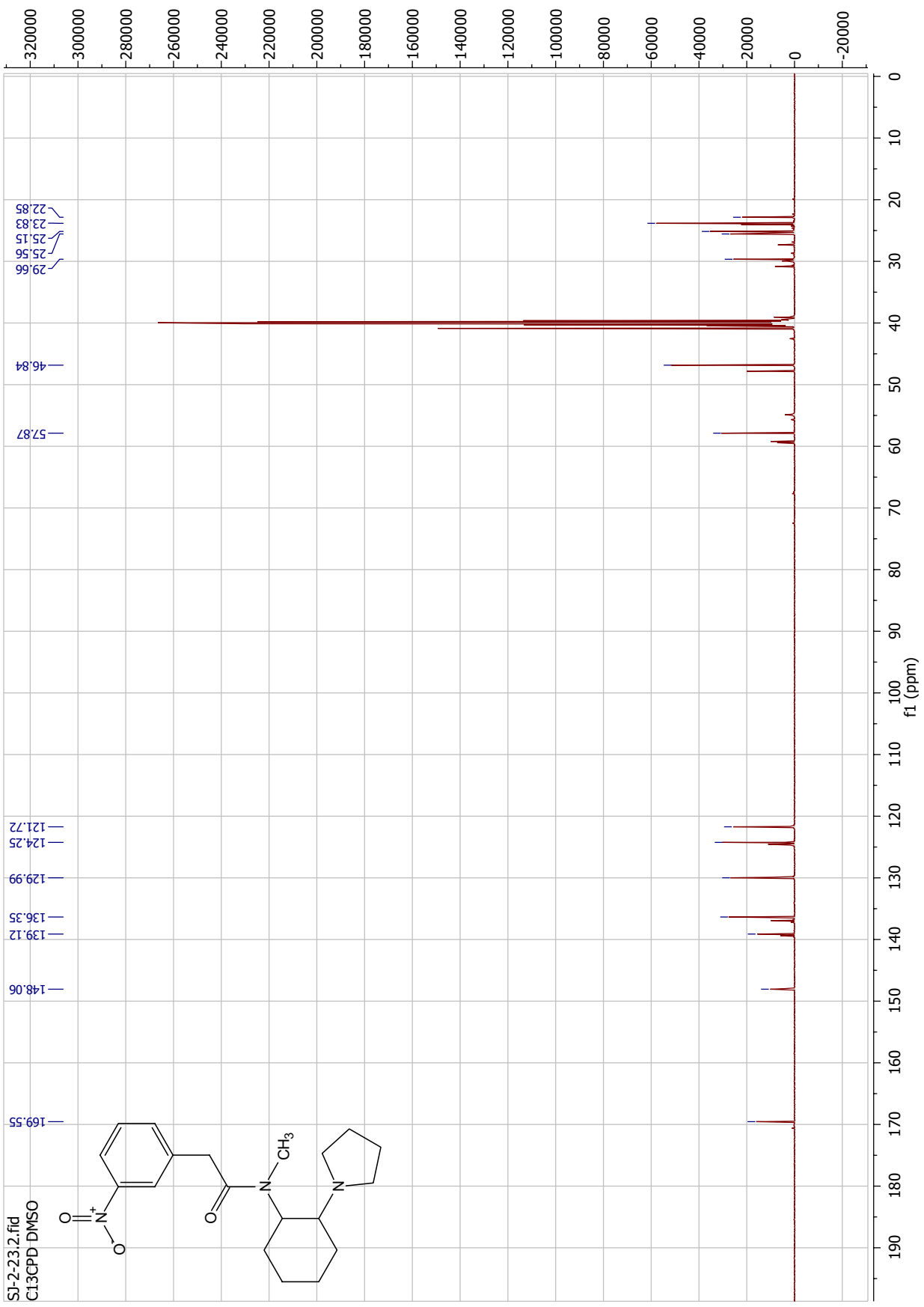
SJ-2-23.2.fid
C13CPD DMSO
169.55
148.06
139.12
136.35
129.99
124.25
121.72
57.87
46.84
29.66
25.56
25.15
23.83
22.85
f1 (ppm)

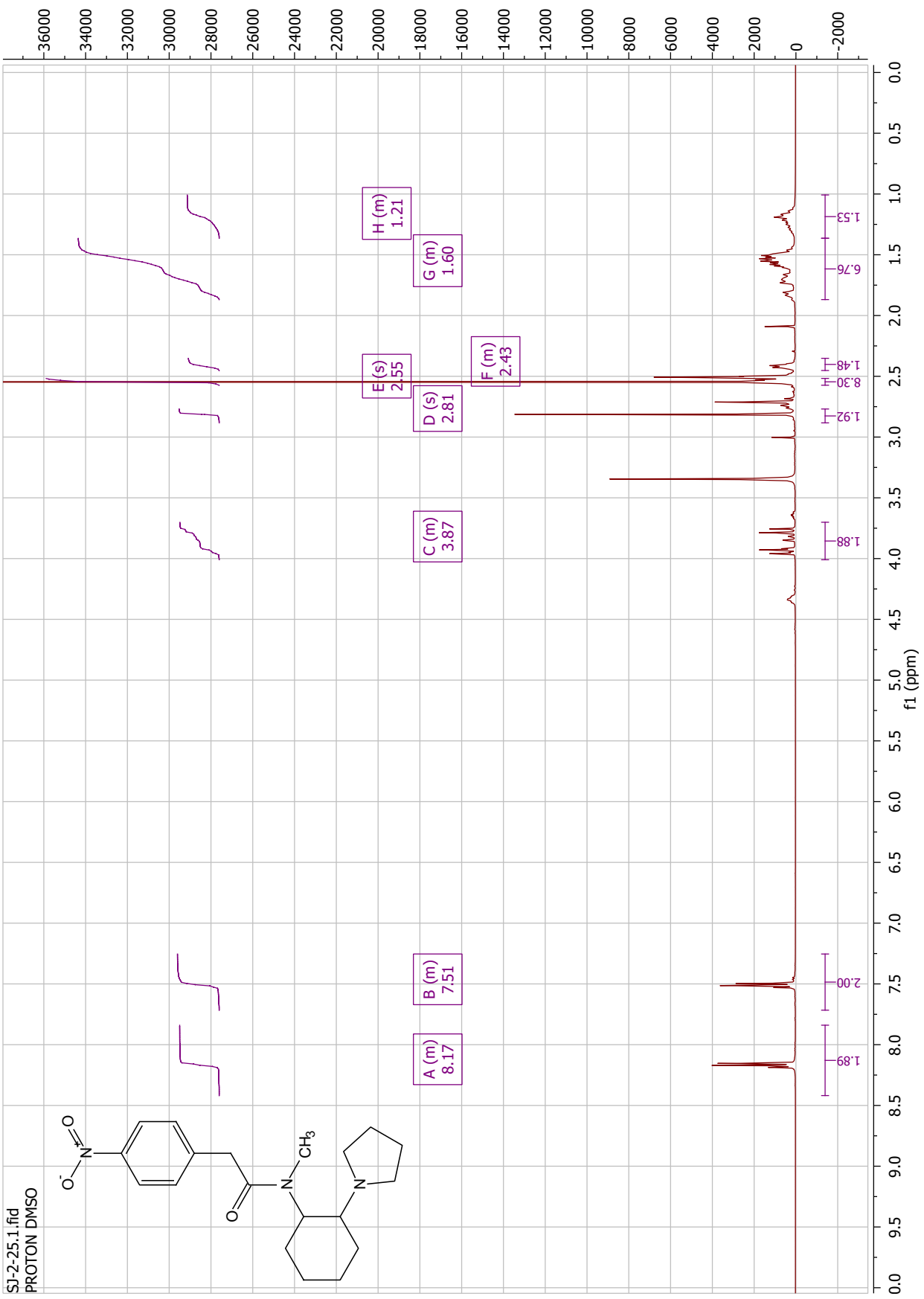
SJ-2-25.1.fid
PROTON DMSO
A (m) 8.17
B (m) 7.51
C (m) 3.87
D (s) 2.81
E (s) 2.55
F (m) 2.43
G (m) 1.60
H (m) 1.21
1.89
2.00
1.88
1.92
8.30
1.48
6.76
1.53
f1 (ppm)

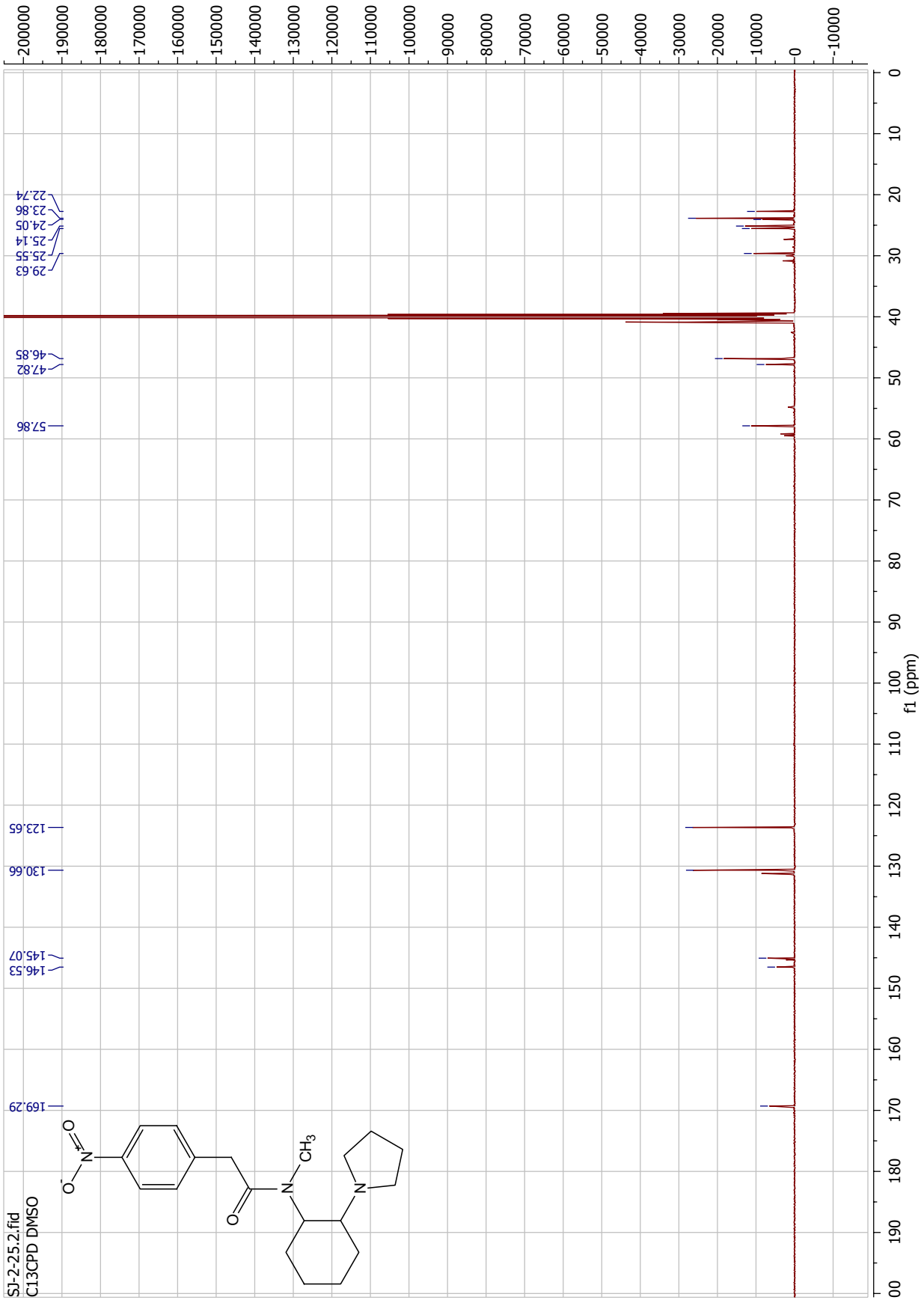
SJ-2-25.2.fid
C13CPD DMSO
169.29
146.53
145.07
130.66
123.65
57.86
47.82
46.85
29.63
25.55
25.14
24.05
23.86
22.74
f1 (ppm)


SJ-1-155.1.fid
PROTON DMSO
A (m)
7.11
B (m)
3.68
D (d)
3.51
J(16.23)
E (s)
2.80
F (s)
2.71
H (d)
2.46
J(7.68)
G (m)
2.62
I (s)
2.18
J (d)
1.84
J(11.49)
K (m)
1.63
L (ddd)
1.21
J(30.07, 17.67, 8.27)
4.90
0.87
1.34
2.58
0.66
0.92
1.50
3.00
1.20
8.35
3.85
f1 (ppm)

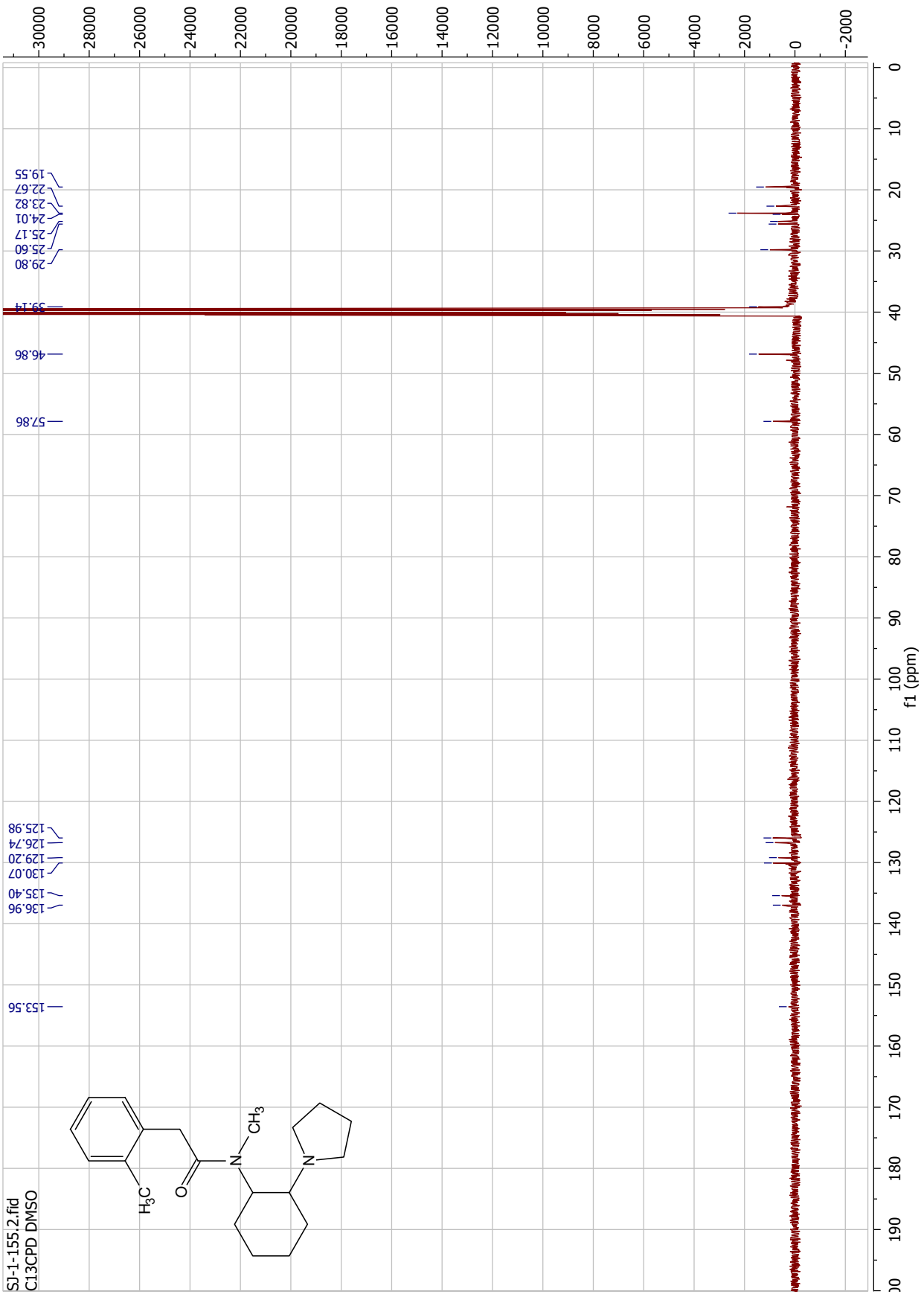
SJ-1-155.2.fid
C13CPD DMSO
f1 (ppm)
153.56
136.96
135.40
130.07
129.20
126.74
125.98
57.86
46.86
39.14
29.80
25.60
25.17
24.01
23.82
22.67
19.55
H3C
O
N
CH3
N

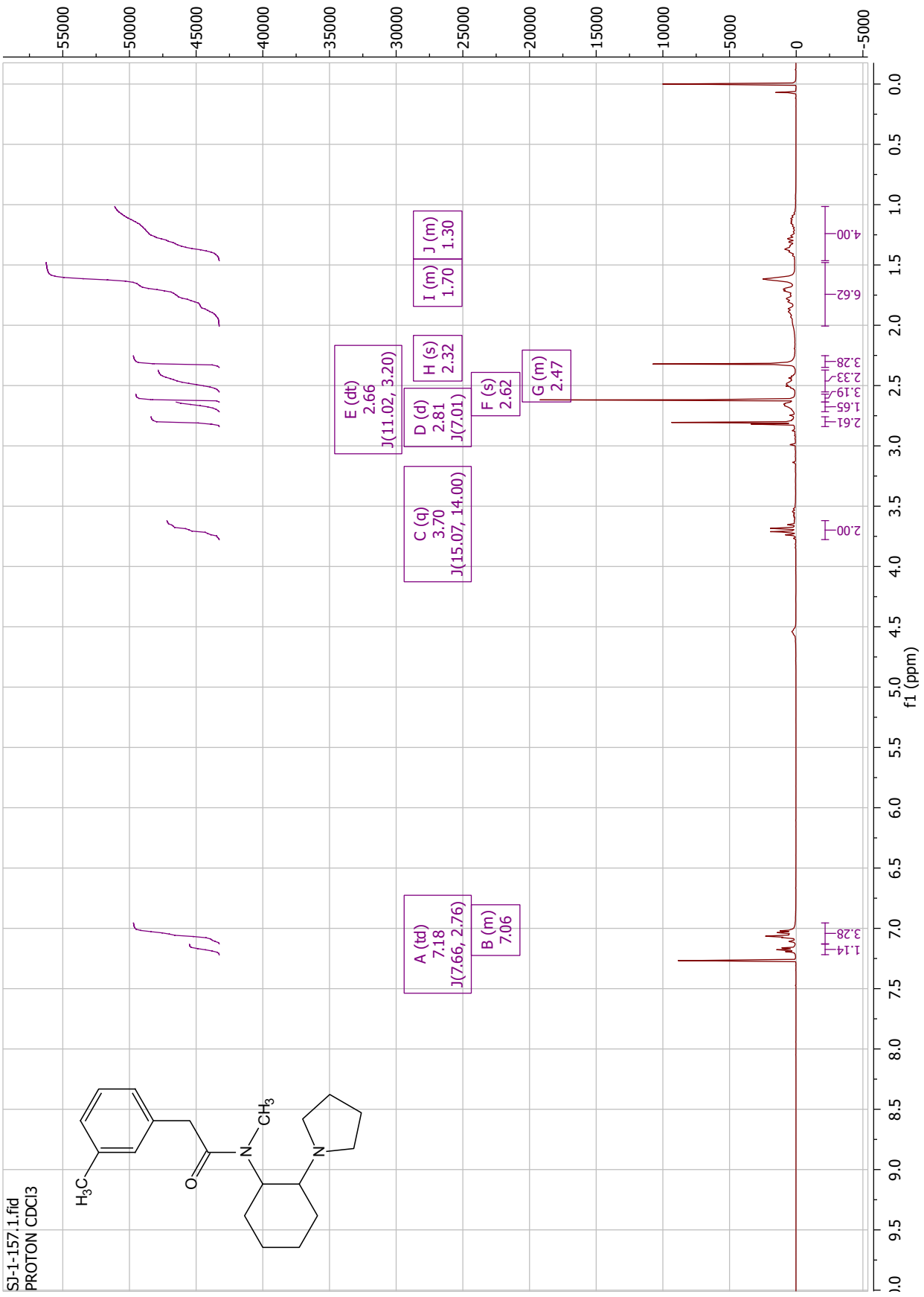
SJ-1-157.1.fid
PROTON CDCl3
A (td)
7.18
J(7.66, 2.76)
B (m)
7.06
C (q)
3.70
J(15.07, 14.00)
D (d)
2.81
J(7.01)
E (dt)
2.66
J(11.02, 3.20)
F (s)
2.62
G (m)
2.47
H (s)
2.32
I (m)
1.70
J (m)
1.30
4.00
6.62
3.28
2.33
3.19
1.65
2.61
2.00
3.28
1.14
f1 (ppm)

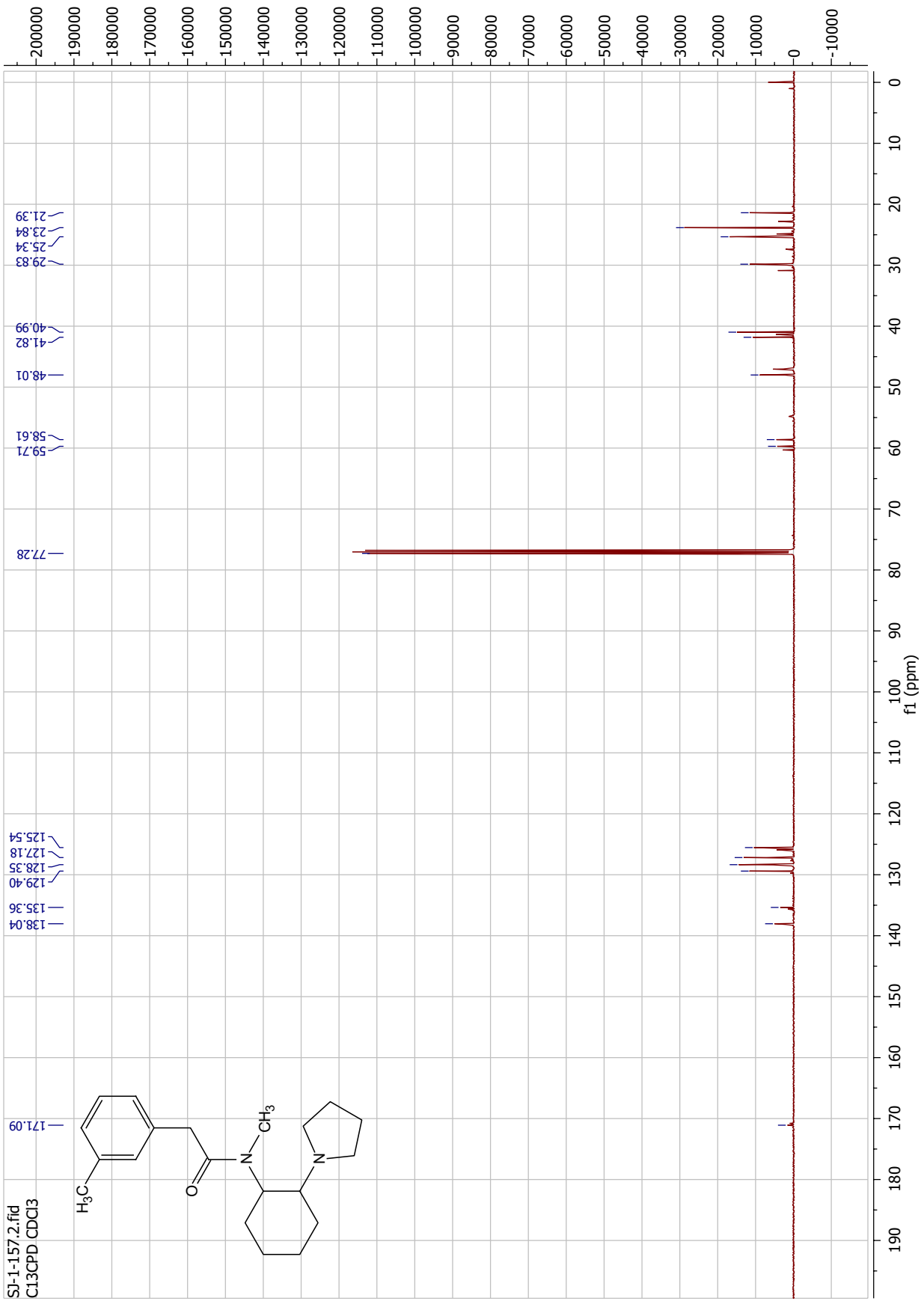
SJ-1-157.2.fid
C13CPD CDCl3
171.09
138.04
135.36
129.40
128.35
127.18
125.54
77.28
59.71
58.61
48.01
41.82
40.99
29.83
25.34
23.84
21.39
f1 (ppm)

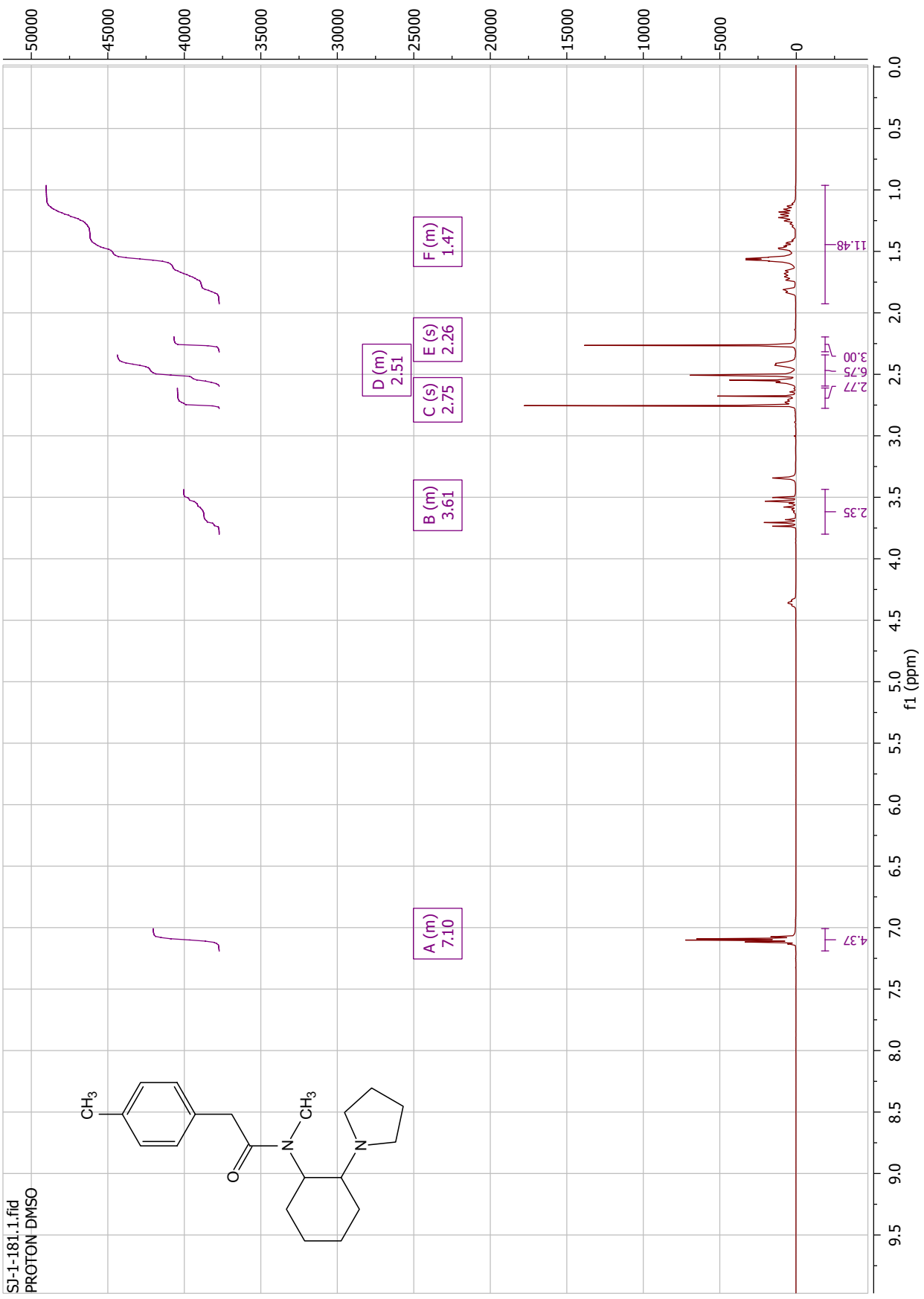
SJ-1-181.1.fid
PROTON DMSO
A (m)
7.10
B (m)
3.61
C (s)
2.75
D (m)
2.51
E (s)
2.26
F (m)
1.47
4.37
2.35
2.77
6.75
3.00
11.48
f1 (ppm)

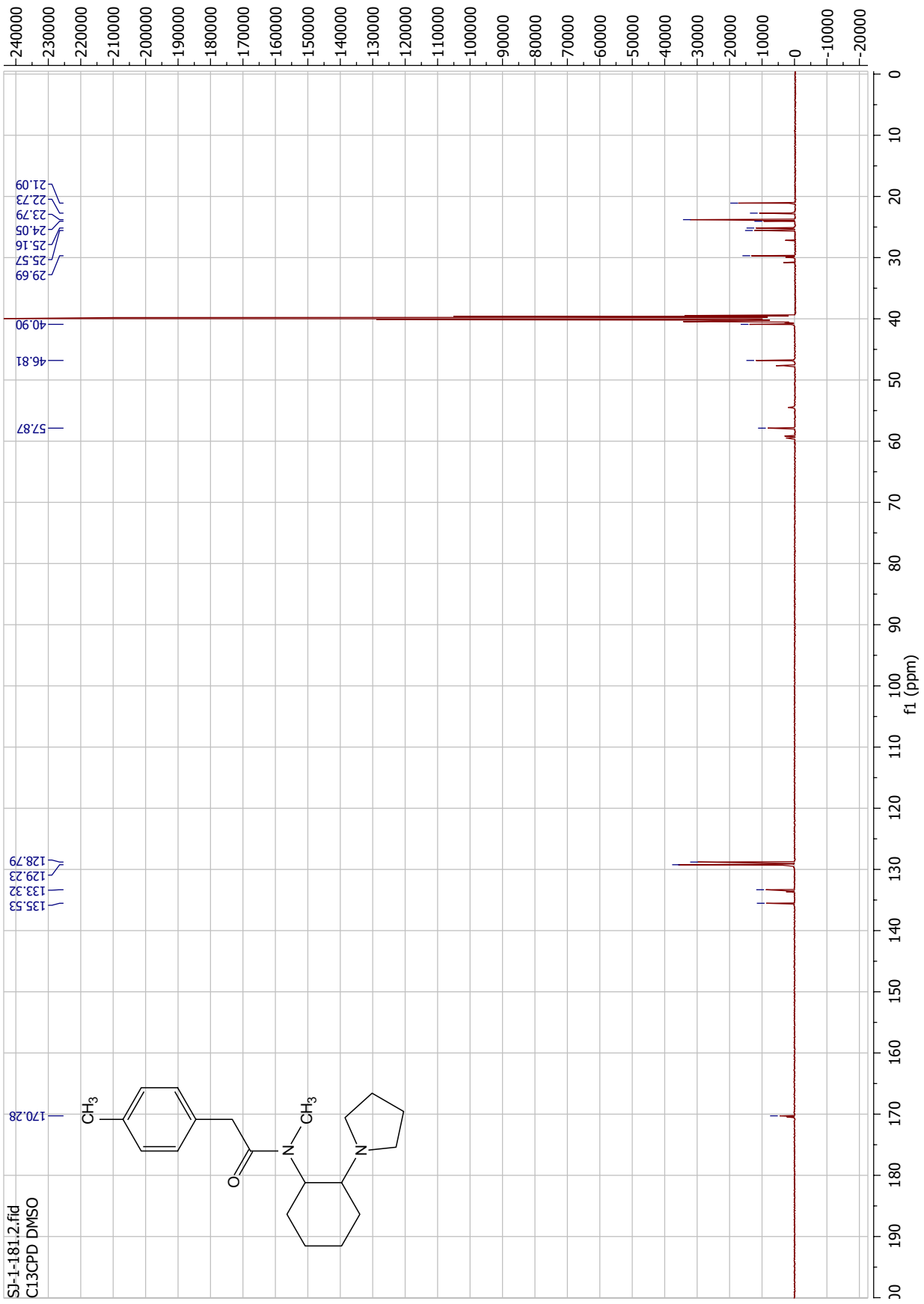
SJ-1-181.2.fid
C13CPD DMSO
170.28
135.53
133.32
129.23
128.79
57.87
46.81
40.90
29.69
25.57
25.16
24.05
23.79
22.73
21.09
f1 (ppm)


SJ-1-183.1.fid
PROTON DMSO
A (d)
7.15
J(8.42)
B (m)
3.61
C (pd)
2.85
J(6.92, 2.53)
D (s)
2.78
F (m)
2.39
E (m)
2.70
G (dt)
1.81
J(9.06, 3.09)
H (m)
1.69
I (m)
1.50
J (dd)
1.18
J(6.92, 3.21)
5.45
2.16
2.00
1.00
2.31
1.59
1.01
2.03
4.50
11.58
f1 (ppm)

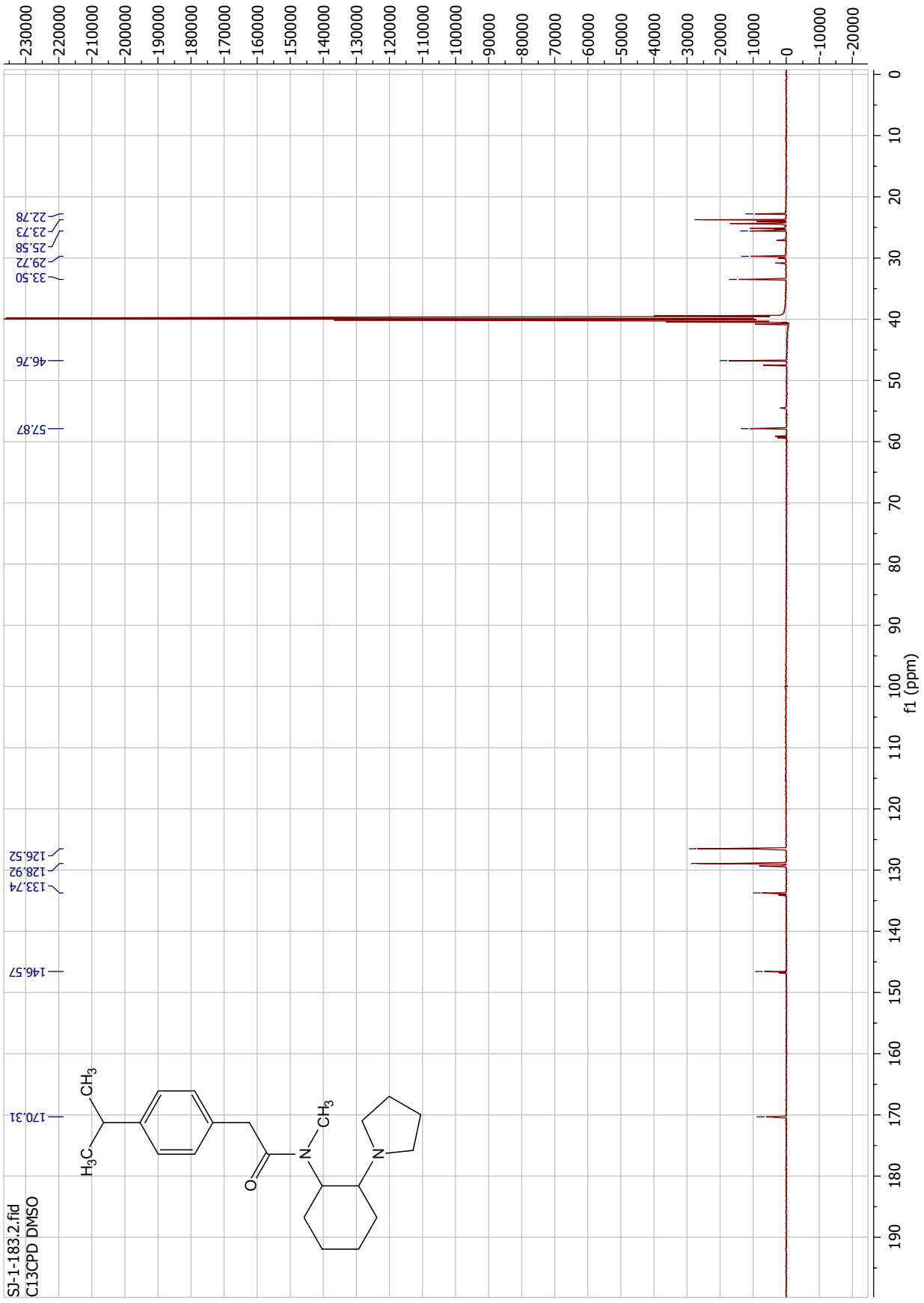
SJ-1-183.2.fid
C13CPD DMSO
170.31
146.57
133.74
128.92
126.52
57.87
46.76
33.50
29.72
25.58
23.73
22.78
f1 (ppm)

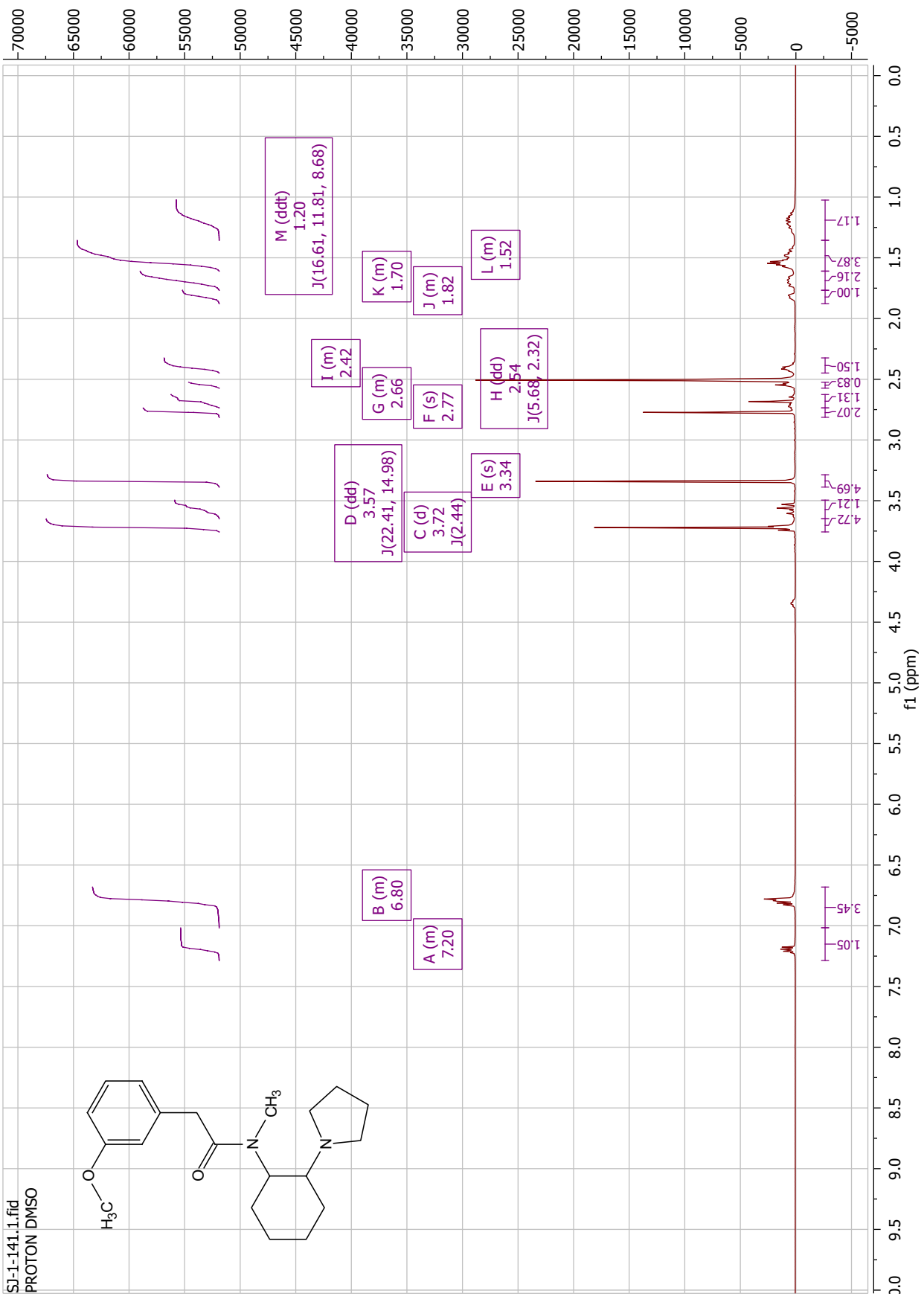
SJ-1-141.1.fid
PROTON DMSO
M (ddt)
1.20
J(16.61, 11.81, 8.68)
K (m)
1.70
J (m)
1.82
L (m)
1.52
I (m)
2.42
G (m)
2.66
F (s)
2.77
H (dd)
2.54
J(5.68, 2.32)
D (dd)
3.57
J(22.41, 14.98)
C (d)
3.72
J(2.44)
E (s)
3.34
B (m)
6.80
A (m)
7.20
1.17
3.87
2.16
1.00
1.50
0.83
1.31
2.07
4.69
1.21
4.72
3.45
1.05
f1 (ppm)

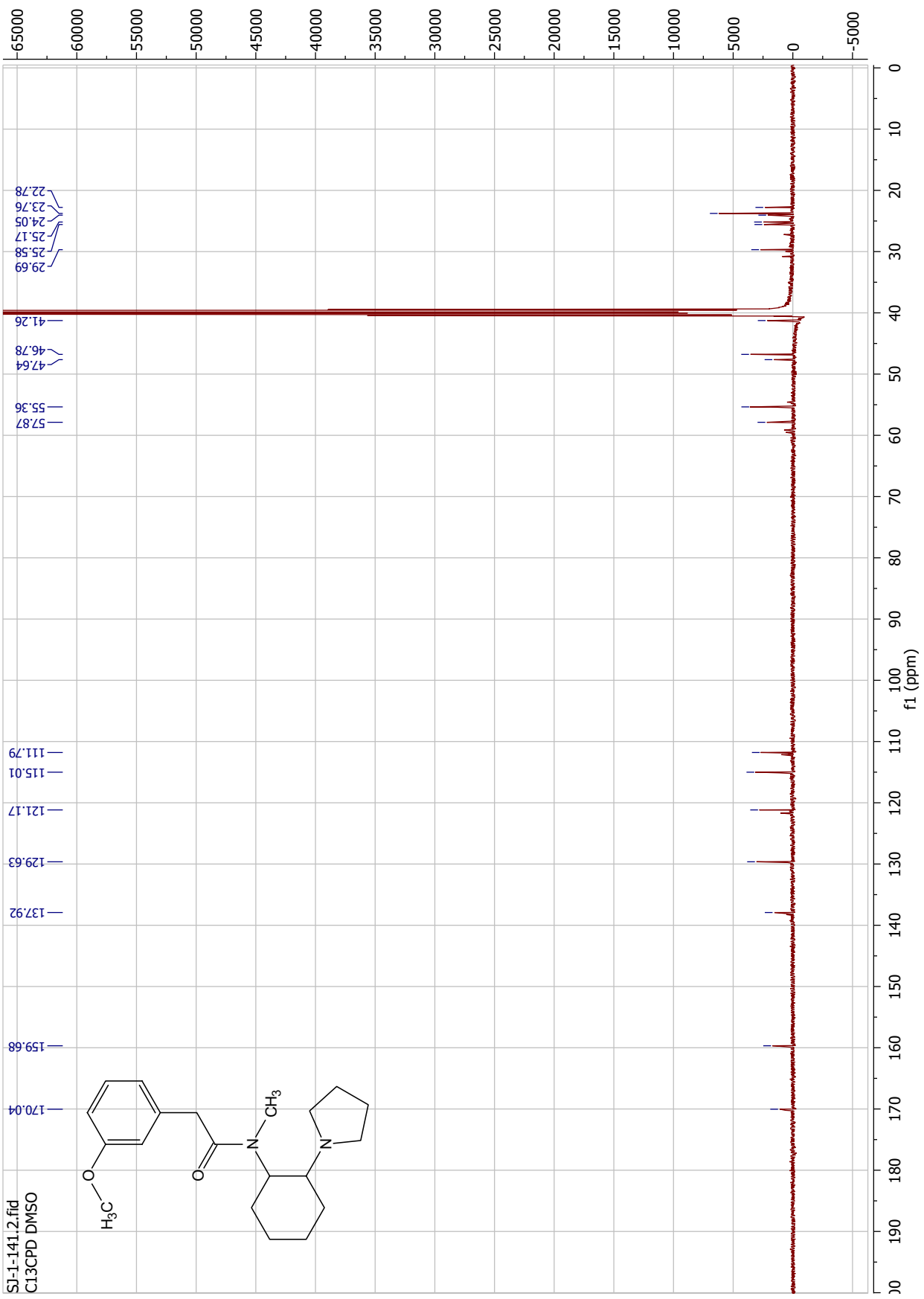
SJ-1-141.2.fid
C13CPD DMSO
22.78
23.76
24.05
25.17
25.58
29.69
41.26
46.78
47.64
55.36
57.87
111.79
115.01
121.17
129.63
137.92
159.68
170.04
f1 (ppm)


SJ-1-143.1.fid
PROTON CDCl3
A (m)
7.19
B (dq)
6.83
J(9.61, 3.06, 2.58)
C (d)
3.79
J(1.64)
D (m)
3.68
E (d)
2.80
J(11.18)
F (m)
2.59
G (m)
1.70
H (m)
1.28
2.22
2.51
4.10
2.06
2.99
5.54
7.05
3.00
f1 (ppm)

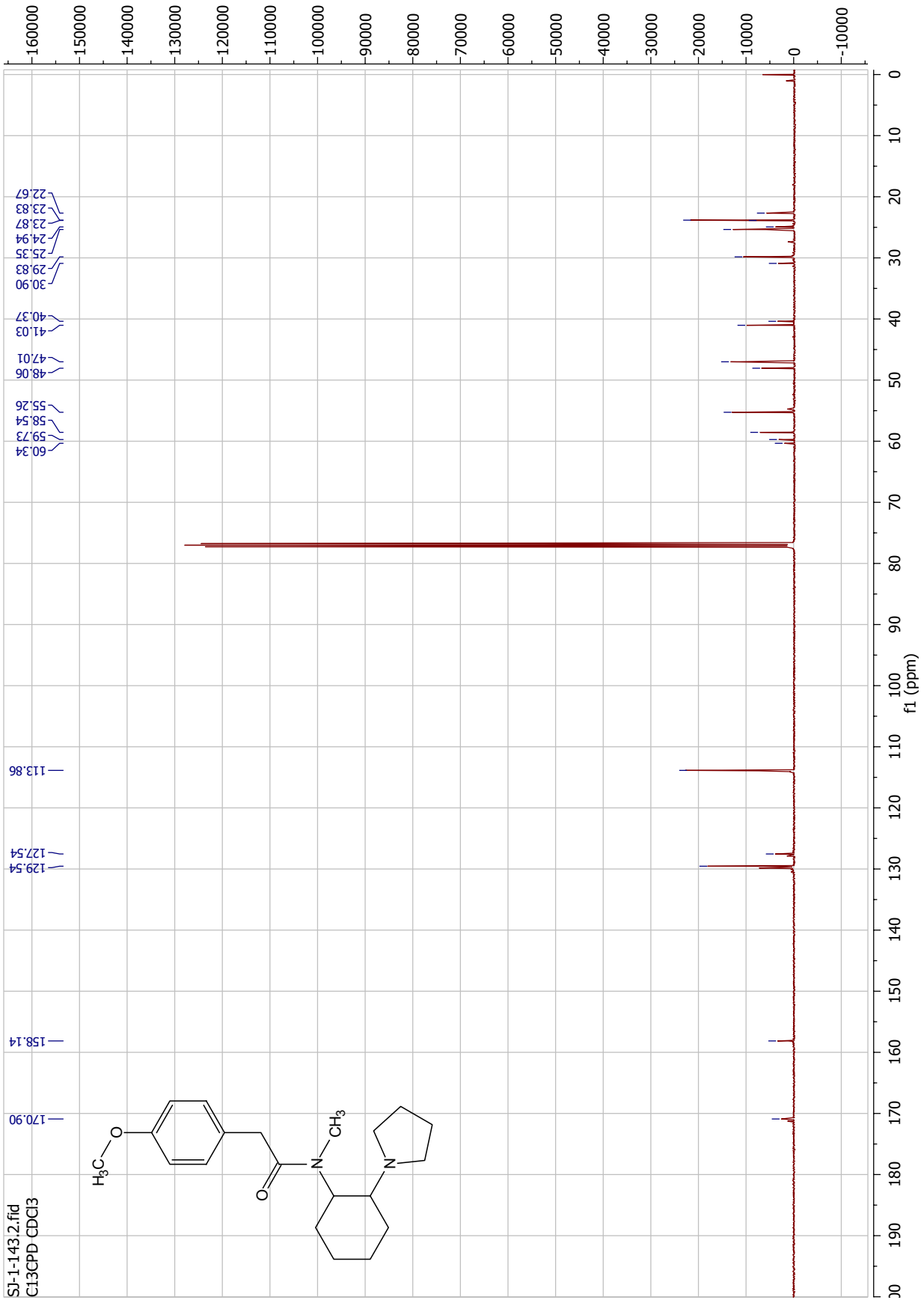
SJ-1-143.2.fid
C13CPD CDCl3
170.90
158.14
129.54
127.54
113.86
60.34
59.73
58.54
55.26
48.06
47.01
41.03
40.37
30.90
29.83
25.35
24.94
23.87
23.83
22.67
f1 (ppm)


SJ-1-189.1.fid
PROTON DMSO
A (m)
7.61
B (t)
7.46
J(7.68)
C (m)
7.34
D (m)
3.72
E (m)
2.61
F (m)
2.41
G (dd)
1.82
J(9.45, 4.11)
H (m)
1.71
I (m)
1.53
J (m)
1.21
4.59
3.20
3.53
2.47
3.57
2.27
1.30
2.60
6.20
1.81
f1 (ppm)

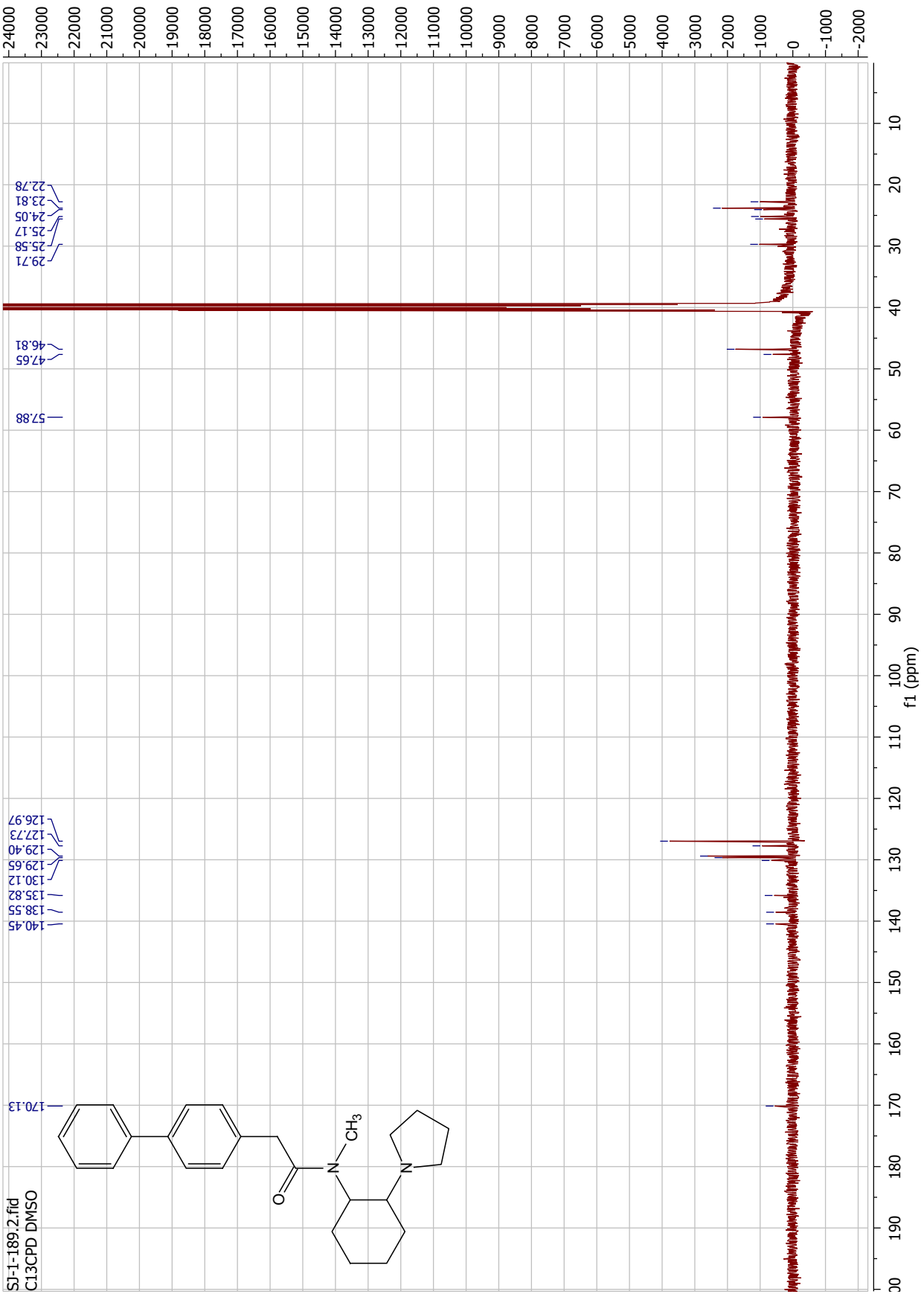
SJ-1-189.2.fid
C13CPD DMSO
170.13
140.45
138.55
135.82
130.12
129.65
129.40
127.73
126.97
57.88
47.65
46.81
29.71
25.58
25.17
24.05
23.81
22.78
f1 (ppm)

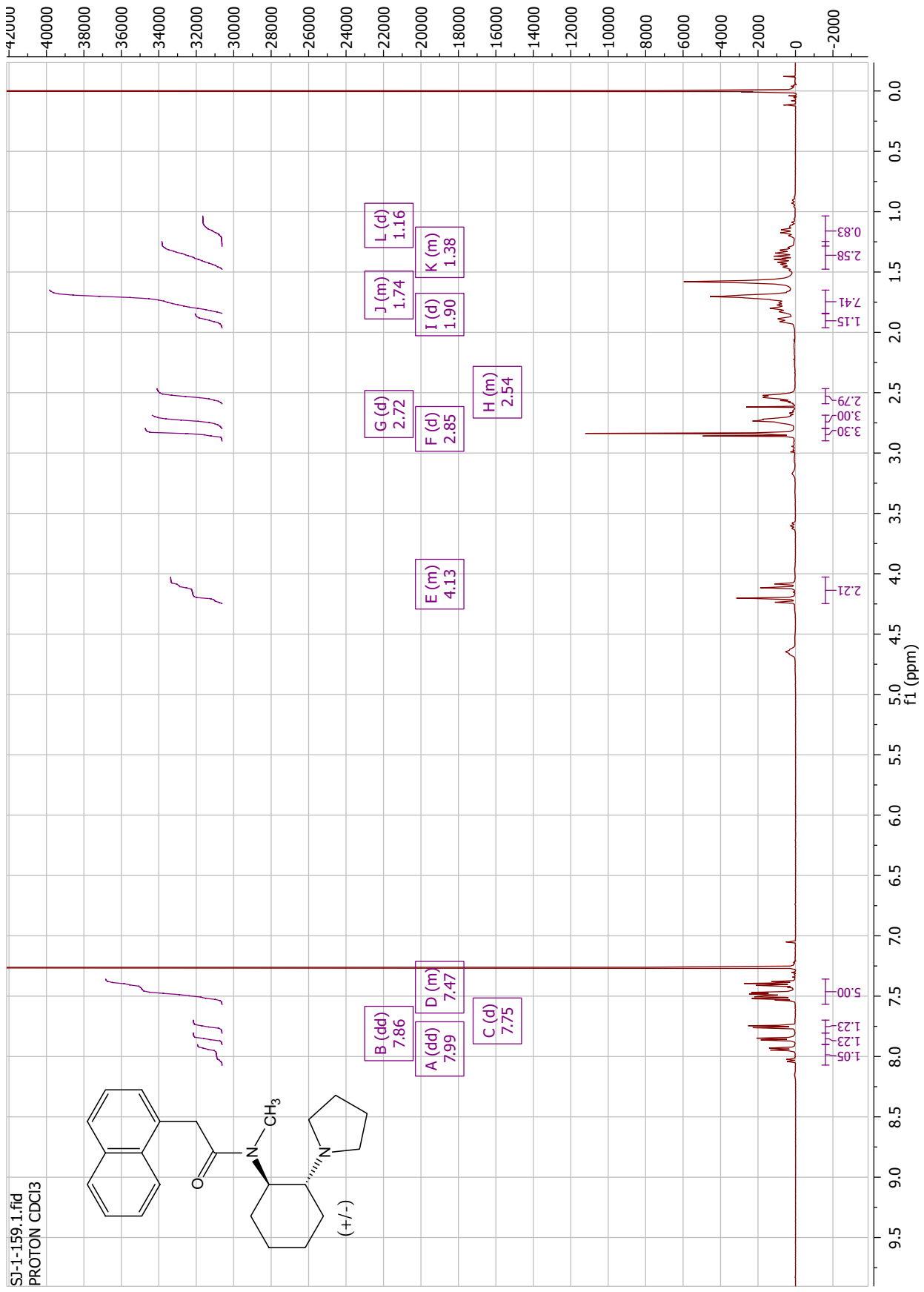
SJ-1-159.1.fid
PROTON CDCl3
(+/-)
A (dd) 7.99
B (dd) 7.86
C (d) 7.75
D (m) 7.47
E (m) 4.13
F (d) 2.85
G (d) 2.72
H (m) 2.54
I (d) 1.90
J (m) 1.74
K (m) 1.38
L (d) 1.16
5.00
1.05
1.23
1.23
2.21
3.30
3.00
2.79
1.15
7.41
2.58
0.83
f1 (ppm)

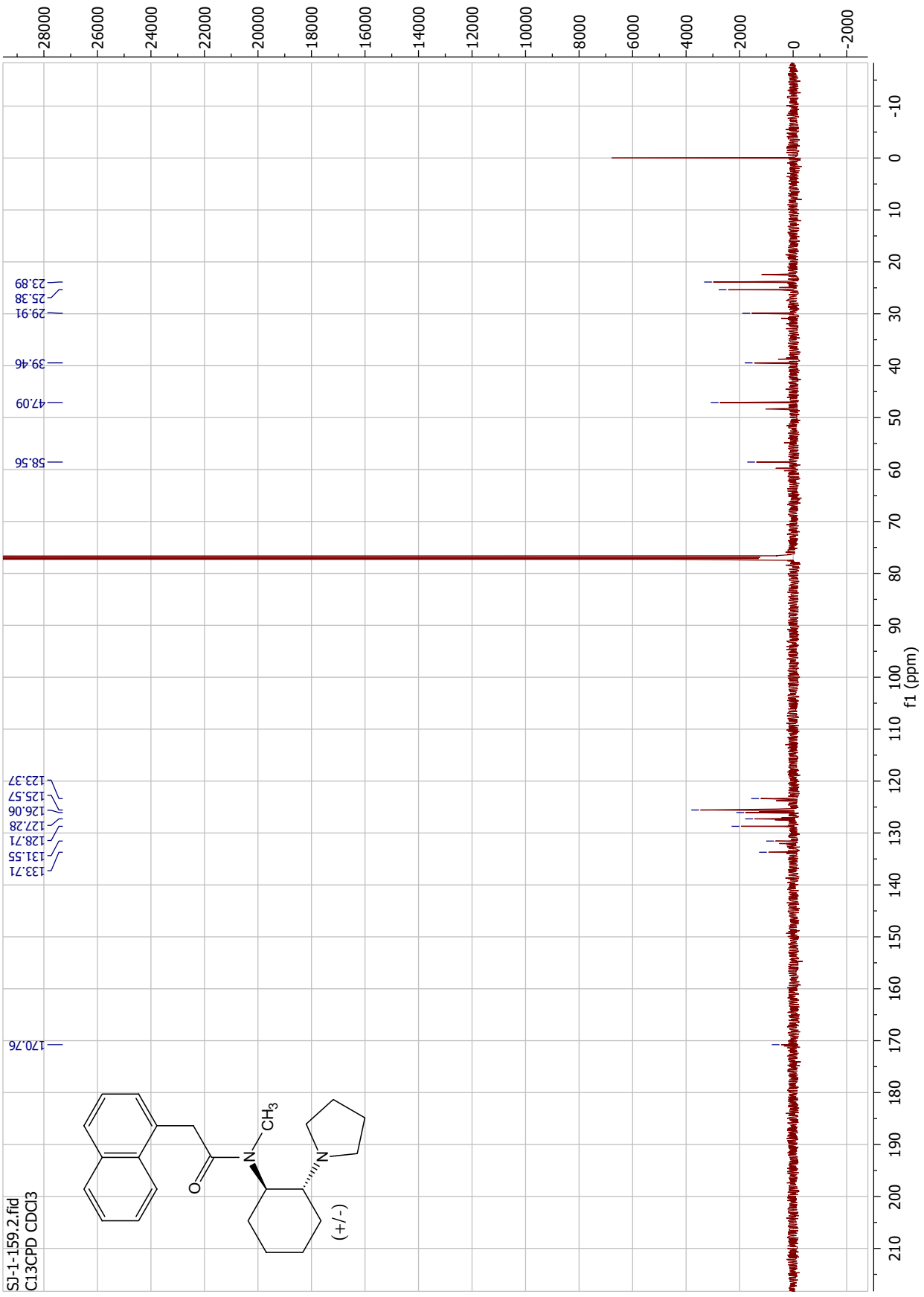
SJ-1-159.2.fid
C13CPD CDCl3
170.76
133.71
131.55
128.71
127.28
126.06
125.57
123.37
58.56
47.09
39.46
29.91
25.38
23.89
CH3
(+/-)
f1 (ppm)

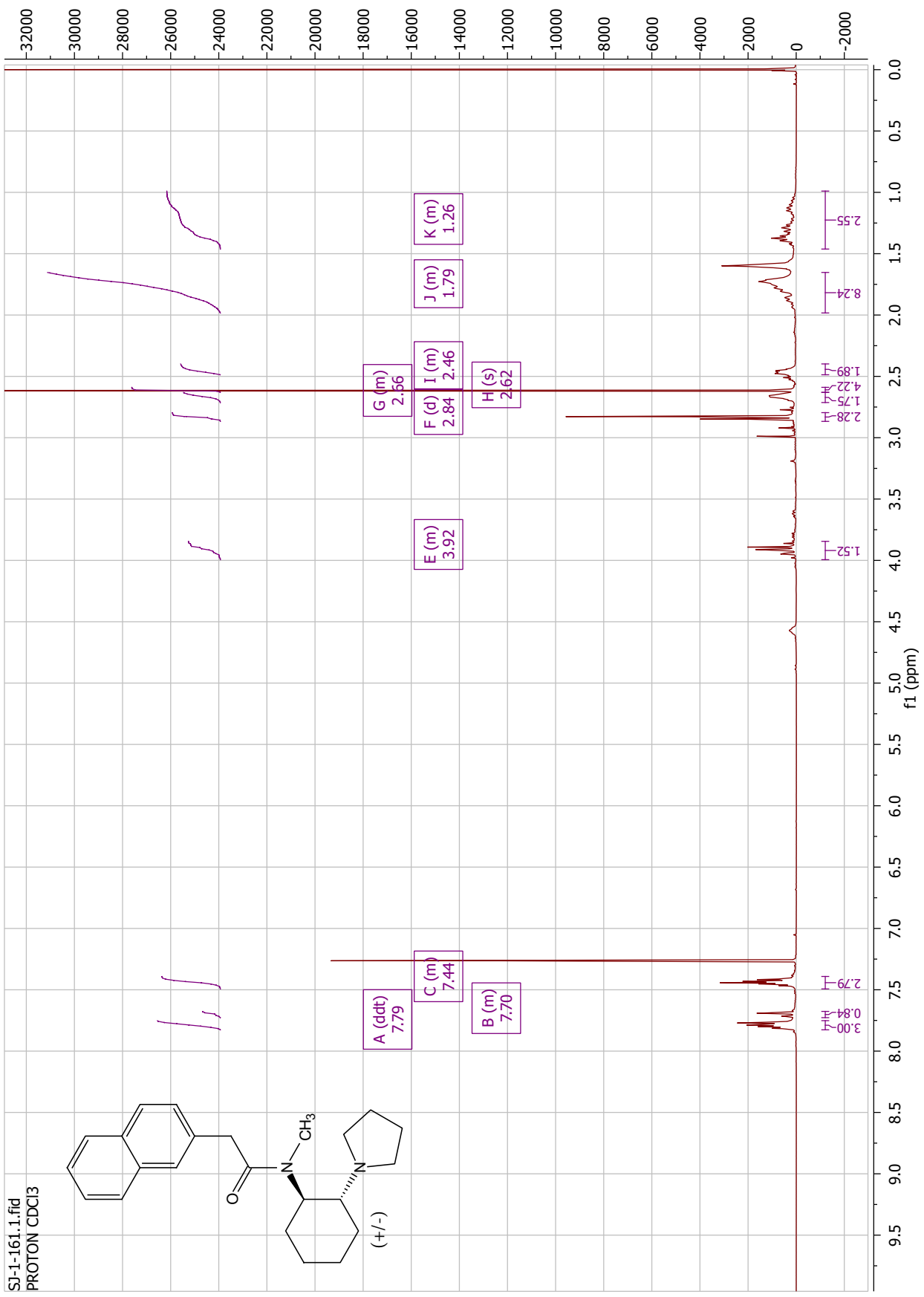
SJ-1-161.1.fid
PROTON CDCl3
A (ddt) 7.79
C (m) 7.44
B (m) 7.70
G (m) 2.56
F (d) 2.84
I (m) 2.46
H (s) 2.62
E (m) 3.92
K (m) 1.26
J (m) 1.79
2.55
8.24
1.89
4.22
1.75
2.28
1.52
2.79
0.84
3.00
(+/-)
f1 (ppm)

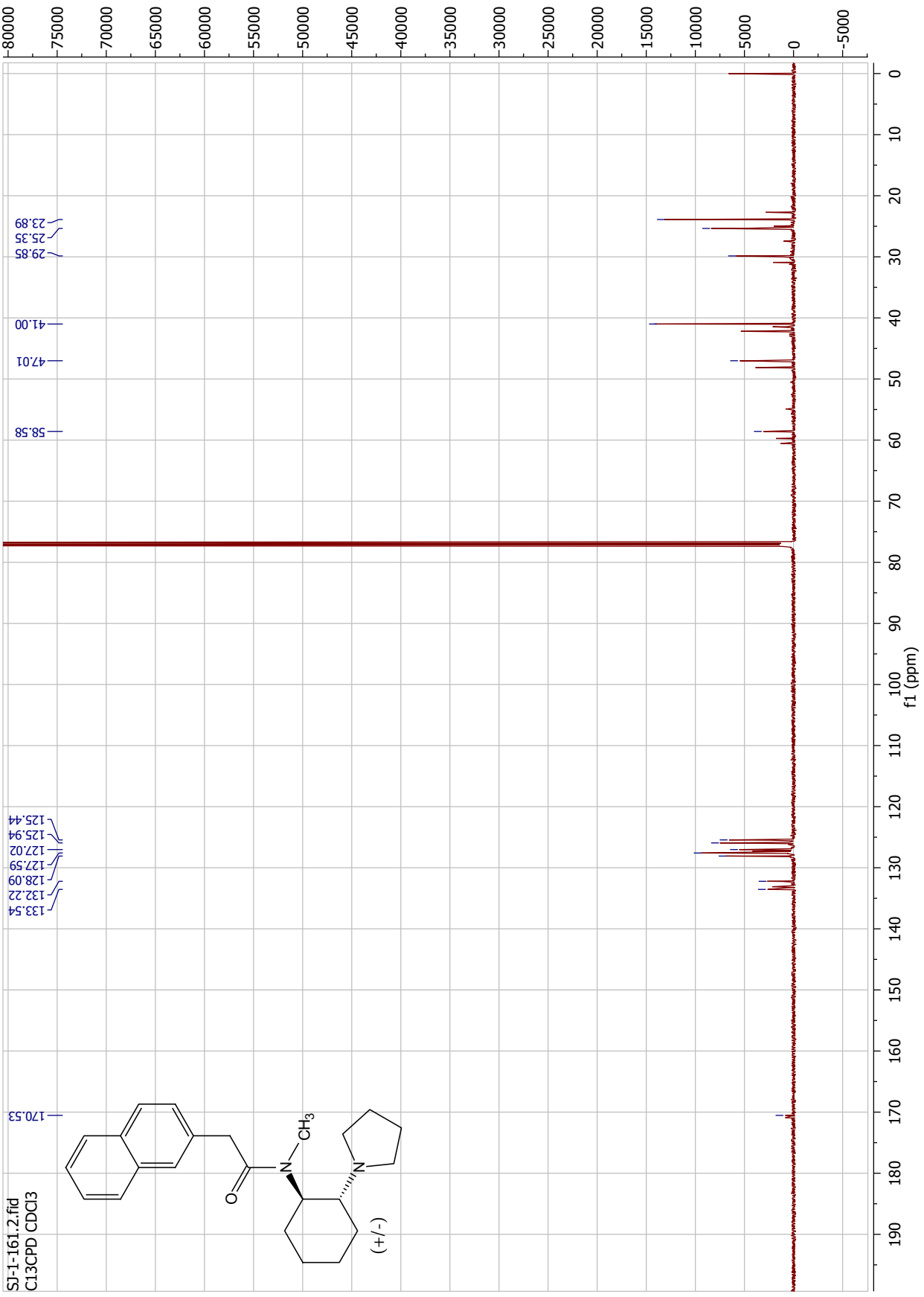
SJ-1-161.2.fid
C13CPD CDCl3
170.53
133.54
132.22
128.09
127.59
127.02
125.94
125.44
58.58
47.01
41.00
29.85
25.35
23.89
CH3
N
N
O
(+/-)
f1 (ppm)


SJ-1-147.1.fid
PROTON CDCl3
B (ddd)
7.13
J(8.46, 7.66, 5.95)
A (dd)
7.30
J(8.04, 3.79)
C (m)
4.01
D (s)
3.00
E (s)
2.87
F (m)
2.68
G (d)
2.50
J(6.57)
H (m)
1.68
I (m)
1.31
2.41
6.90
2.15
2.89
1.16
3.10
3.00
1.49
2.98
f1 (ppm)

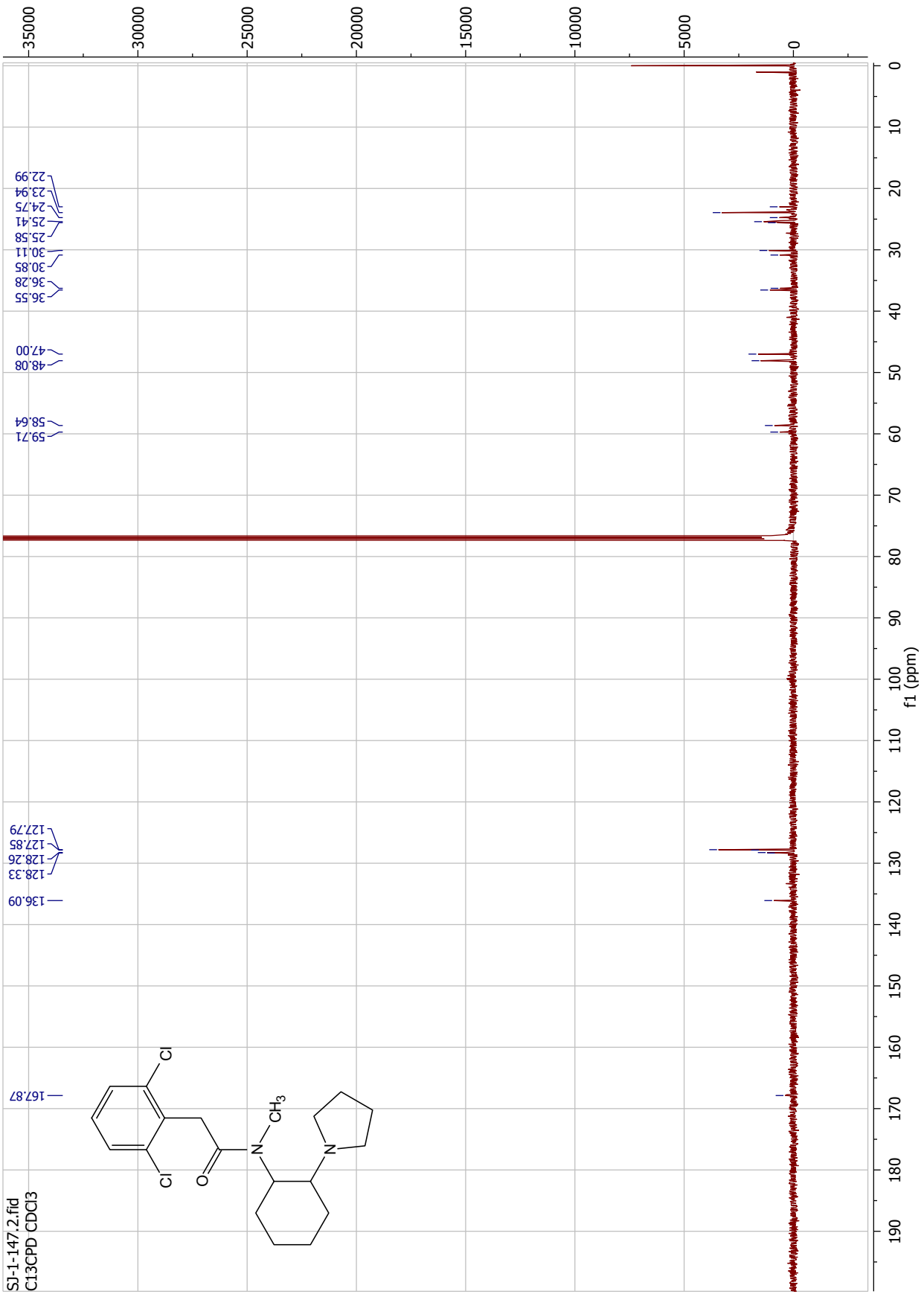
SJ-1-147.2.fid
C13CPD CDCl3
167.87
136.09
128.33
128.26
127.85
127.79
59.71
58.64
48.08
47.00
36.55
36.28
30.85
30.11
25.58
25.41
24.75
23.94
22.99
Cl
Cl
O
N
CH3
N
f1 (ppm)

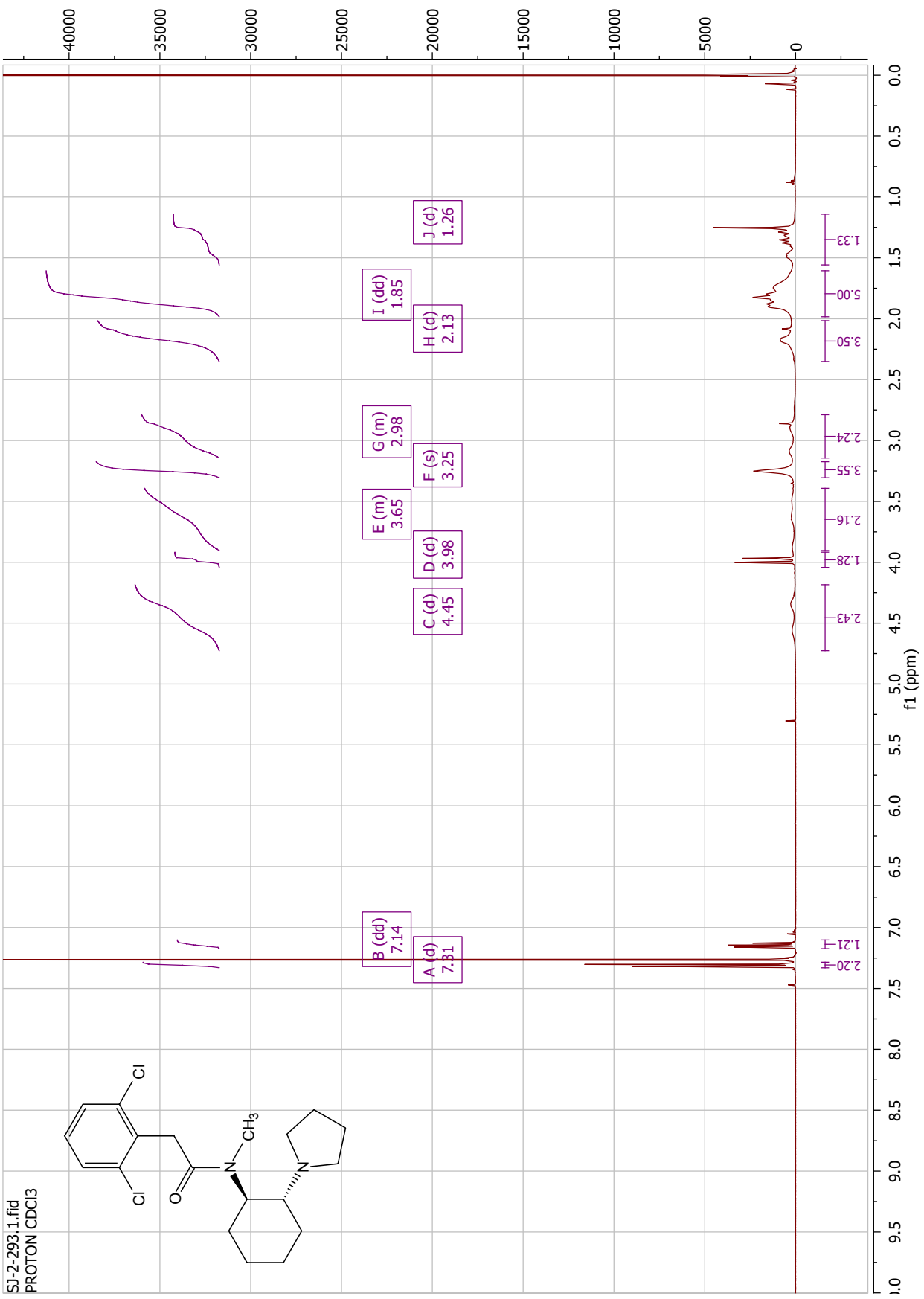
SJ-2-293.1.fid
PROTON CDCl3
A (d) 7.81
B (dd) 7.14
C (d) 4.45
D (d) 3.98
E (m) 3.65
F (s) 3.25
G (m) 2.98
H (d) 2.13
I (dd) 1.85
J (d) 1.26
1.21
2.20
2.43
1.28
2.16
3.55
2.24
3.50
5.00
1.33
f1 (ppm)

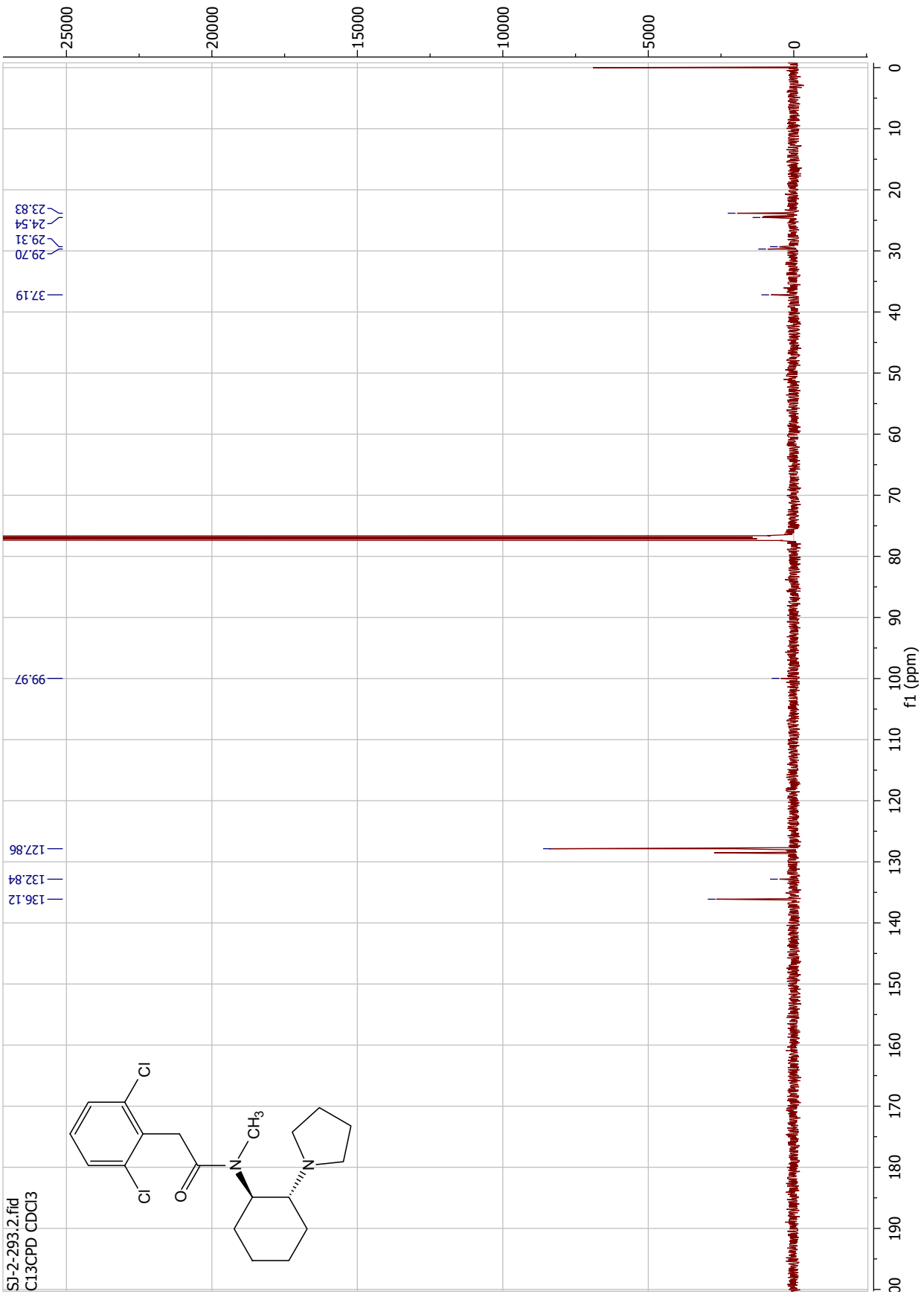
SJ-2-293.2.fid
C13CPD CDCl3
23.83
24.54
29.31
29.70
37.19
99.97
127.86
132.84
136.12
f1 (ppm)

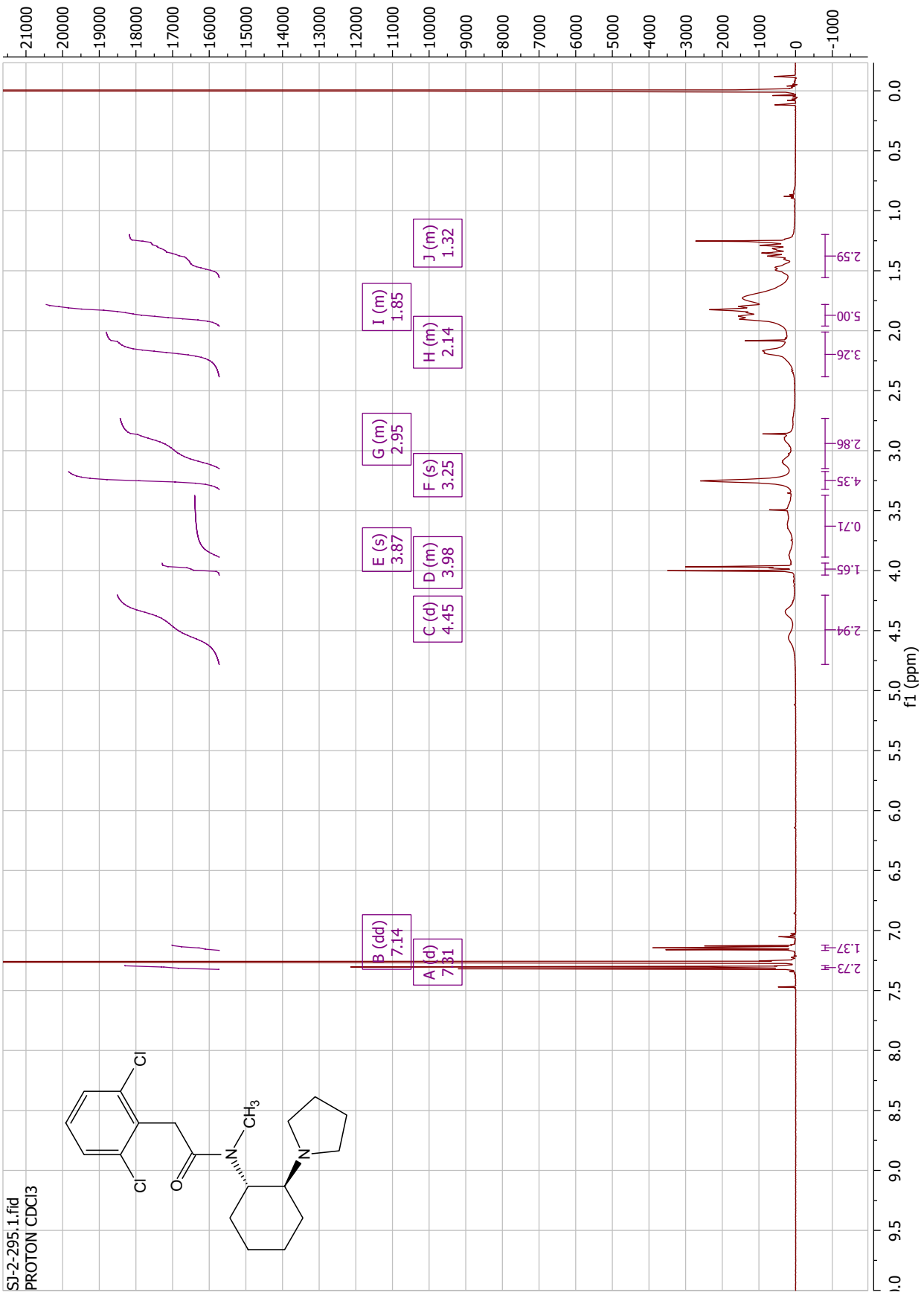
SJ-2-295,1.fid
PROTON CDCl3
A (d) 7.31
B (dd) 7.14
C (d) 4.45
D (m) 3.98
E (s) 3.87
F (s) 3.25
G (m) 2.95
H (m) 2.14
I (m) 1.85
J (m) 1.32
2.73
1.37
2.94
1.65
0.71
4.35
2.86
3.26
5.00
2.59
f1 (ppm)

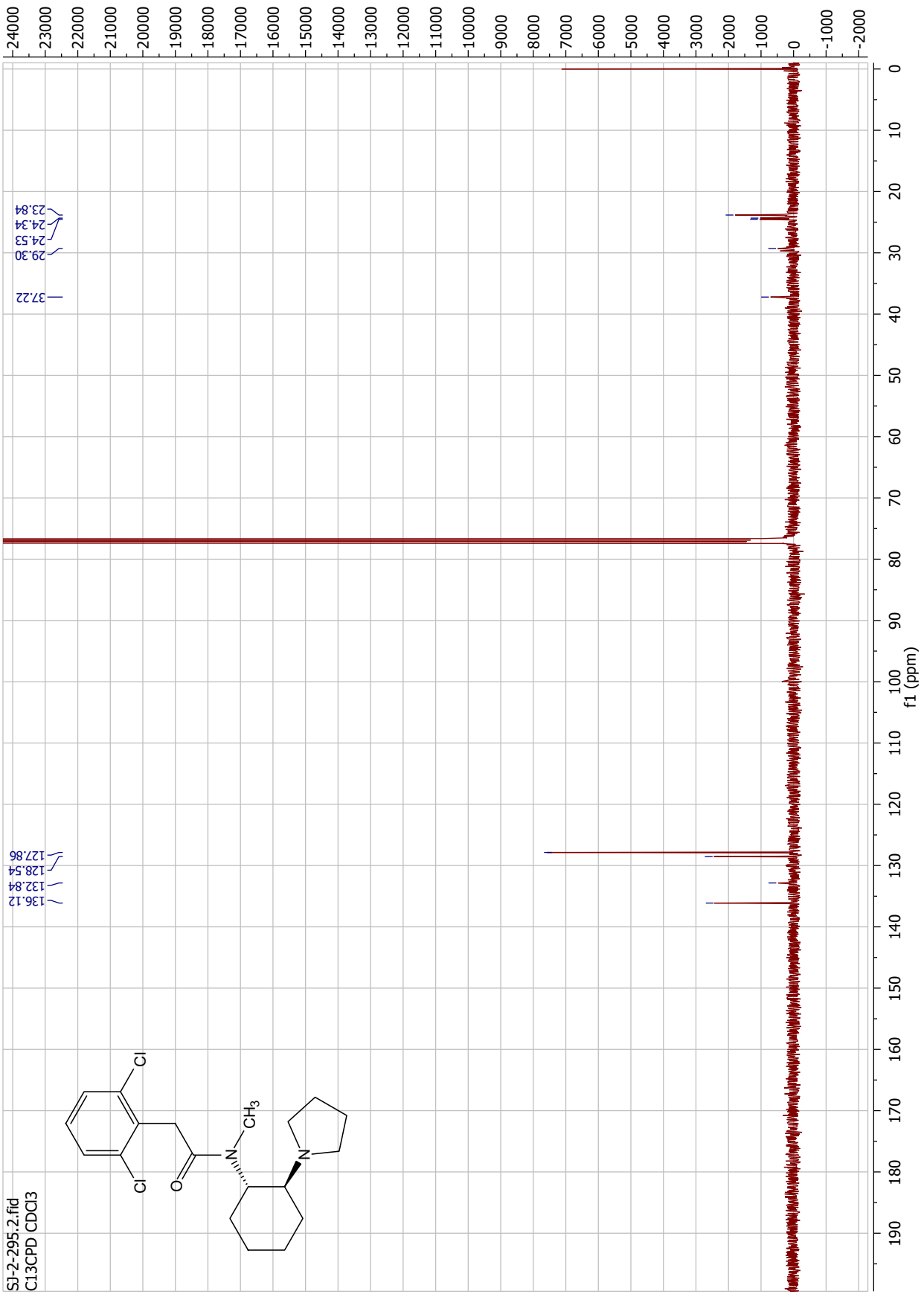
SJ-2-295.2.fid
C13CPD CDCl3
136.12
132.84
128.54
127.86
37.22
29.30
24.53
24.34
23.84
f1 (ppm)
Cl
Cl
O
N
CH3
N


SJ-1-149.1.fid
PROTON DMSO
A (m)
7.58
B (m)
7.35
C (m)
3.78
D (d)
2.78
J(72.00)
E (d)
2.56
J(15.37)
F (d)
2.45
J(7.38)
G (m)
1.64
H (m)
1.22
0.91
1.93
2.15
4.03
3.30
1.38
10.05
3.00
Cl
Cl
O
N
CH3
N
f1 (ppm)

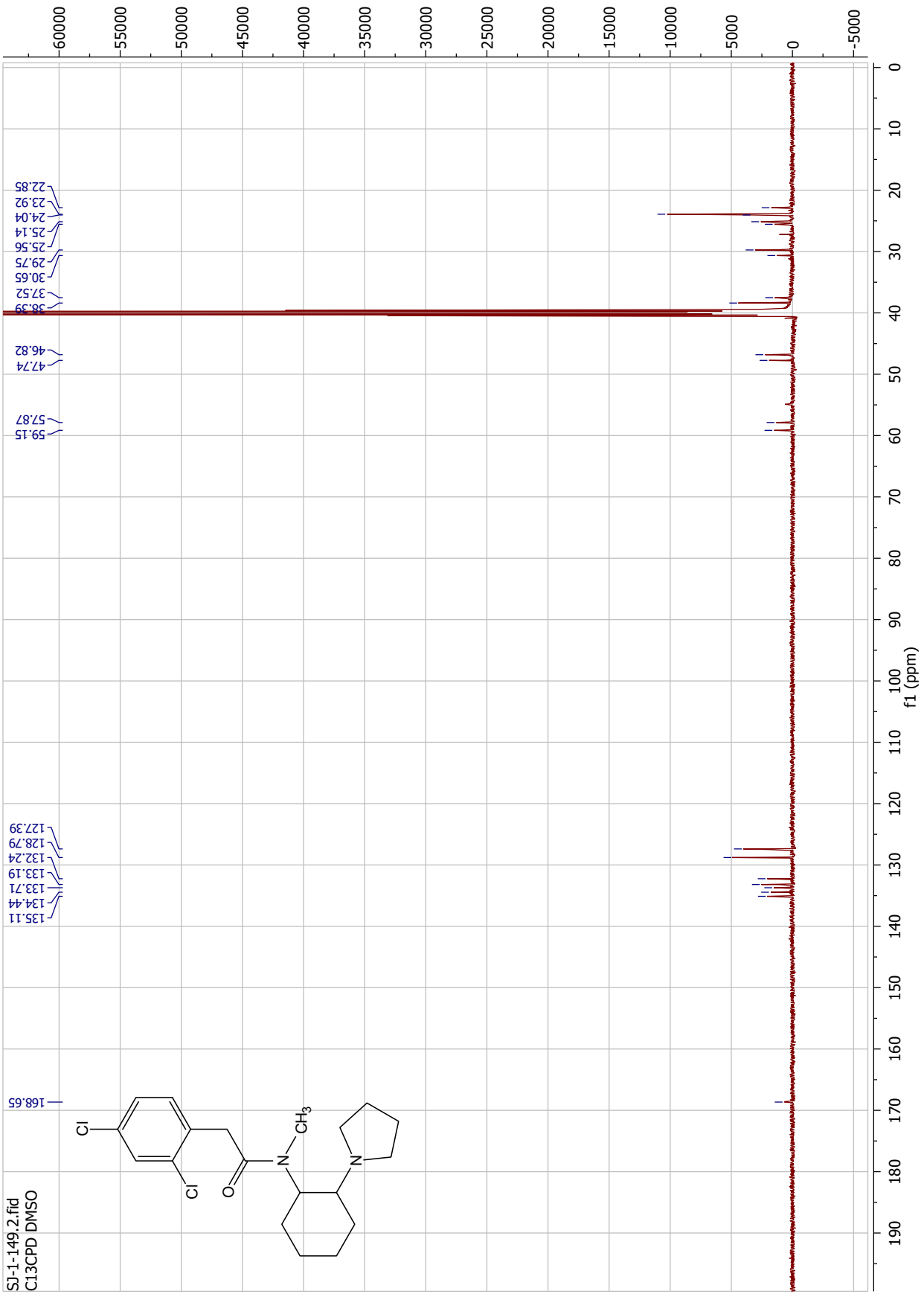
SJ-1-149.2.fid
C13CPD DMSO
168.65
135.11
134.44
133.71
133.19
132.24
128.79
127.39
59.15
57.87
47.74
46.82
38.39
37.52
30.65
29.75
25.56
25.14
24.04
23.92
22.85
Cl
Cl
O
N
CH3
N
f1 (ppm)

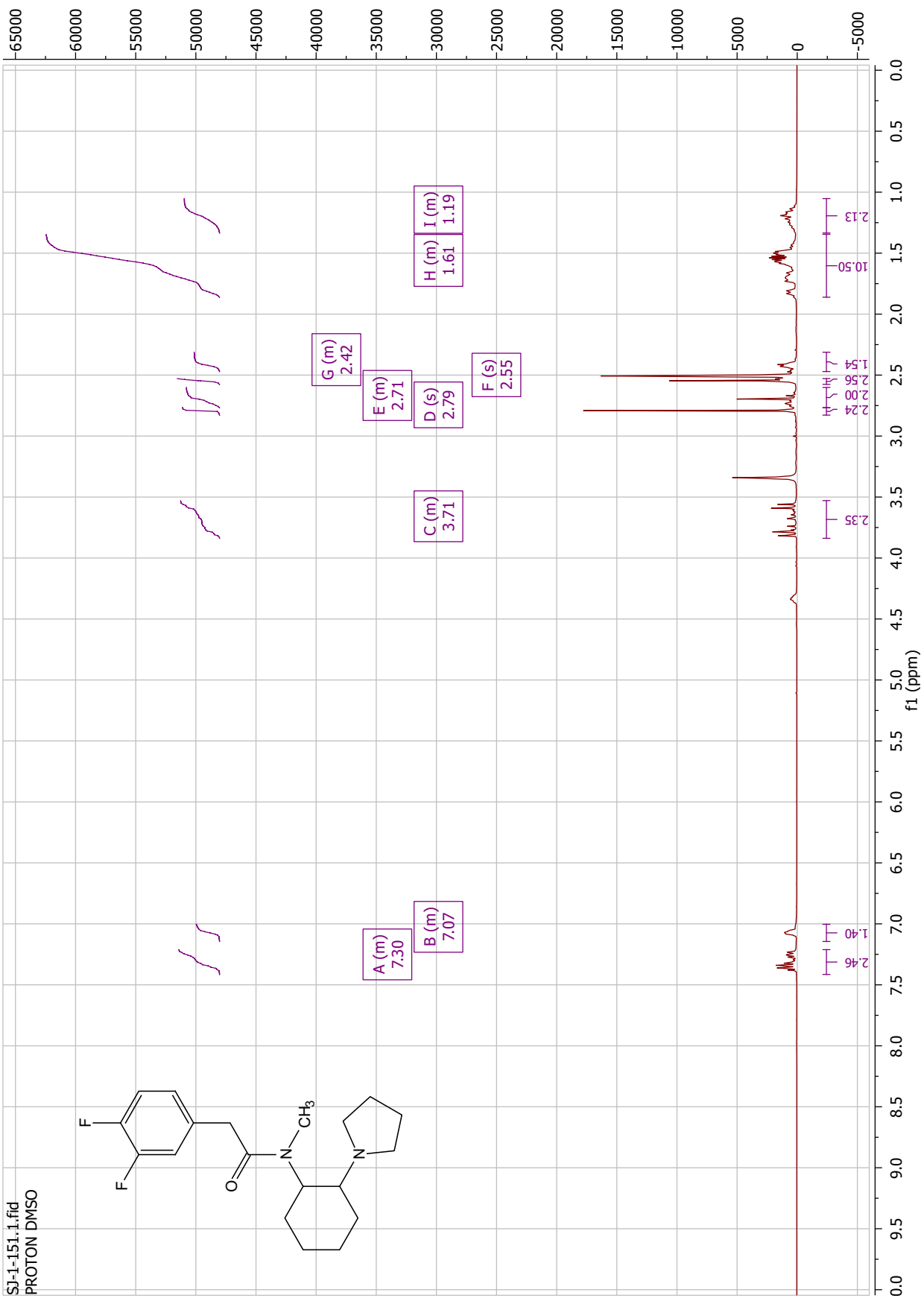
SJ-1-151.1.fid
PROTON DMSO
A (m) 7.30
B (m) 7.07
C (m) 3.71
D (s) 2.79
E (m) 2.71
F (s) 2.55
G (m) 2.42
H (m) 1.61
I (m) 1.19
2.46
1.40
2.35
10.50
2.13
1.54
2.56
2.00
2.24
F
F
O
N
CH3
N
f1 (ppm)

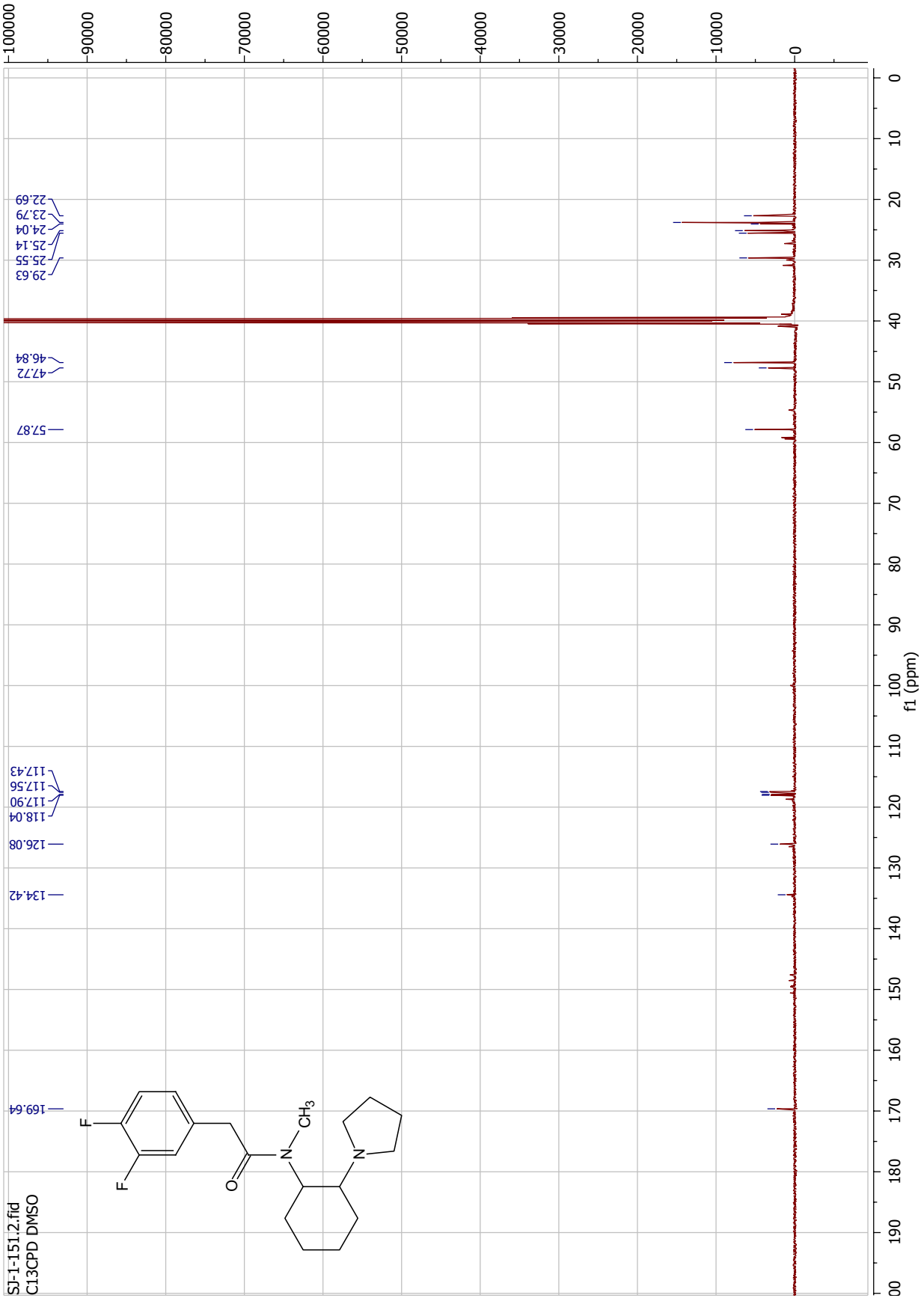
SJ-1-151.2.fid
C13CPD DMSO
169.64
134.42
126.08
118.04
117.90
117.56
117.43
57.87
47.72
46.84
29.63
25.55
25.14
24.04
23.79
22.69
F
F
O
N
CH3
N
f1 (ppm)

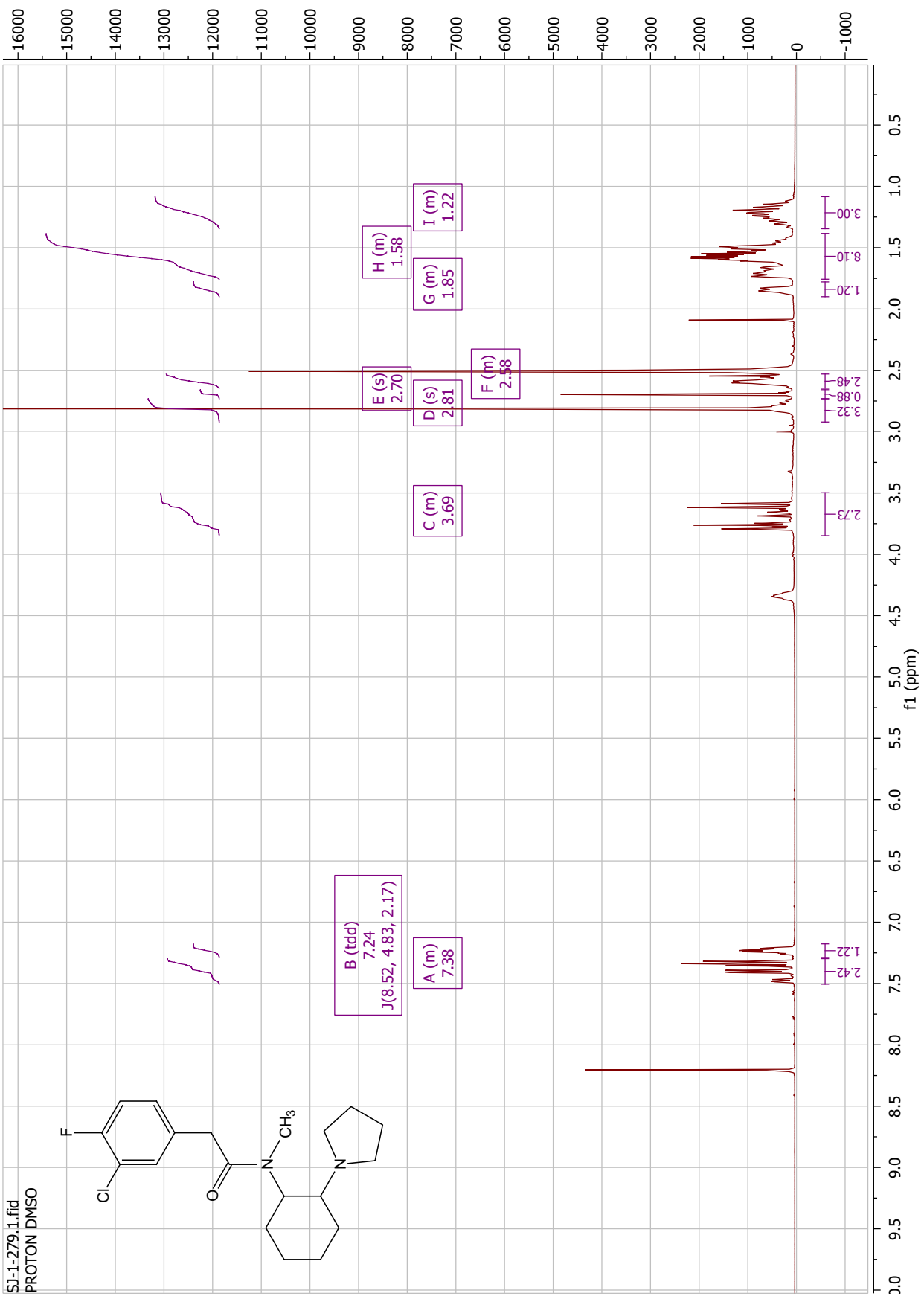
SJ-1-279.1.fid
PROTON DMSO
A (m)
7.38
B (tdd)
7.24
J(8.52, 4.83, 2.17)
C (m)
3.69
D (s)
2.81
E (s)
2.70
F (m)
2.58
G (m)
1.85
H (m)
1.58
I (m)
1.22
2.42
1.22
2.73
3.32
0.88
2.48
1.20
8.10
3.00
f1 (ppm)

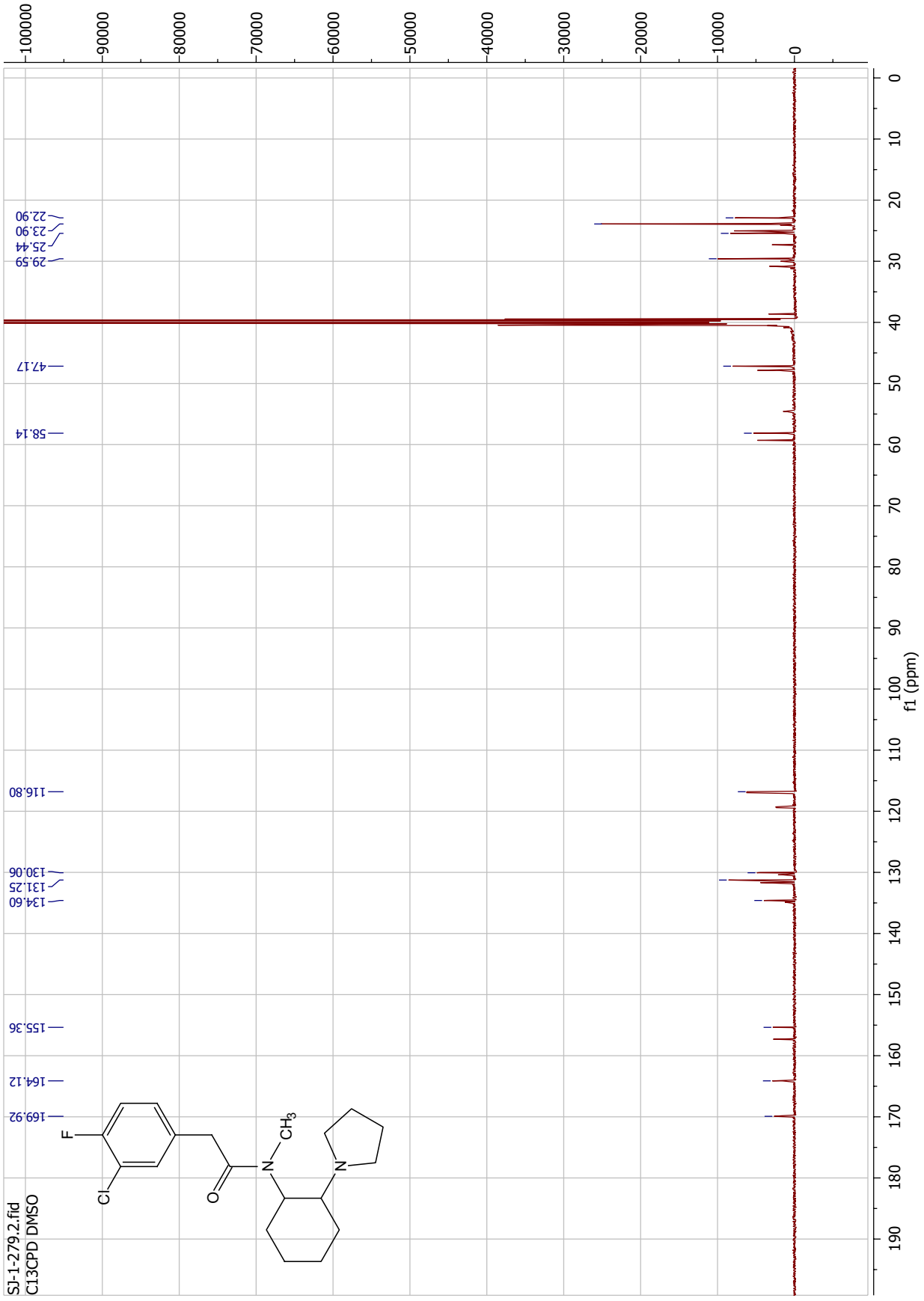
S3-1-279.2.fid
C13CPD DMSO
169.92
164.12
155.36
134.60
131.25
130.06
116.80
58.14
47.17
29.59
25.44
23.90
22.90
F
Cl
O
N
CH3
N
f1 (ppm)

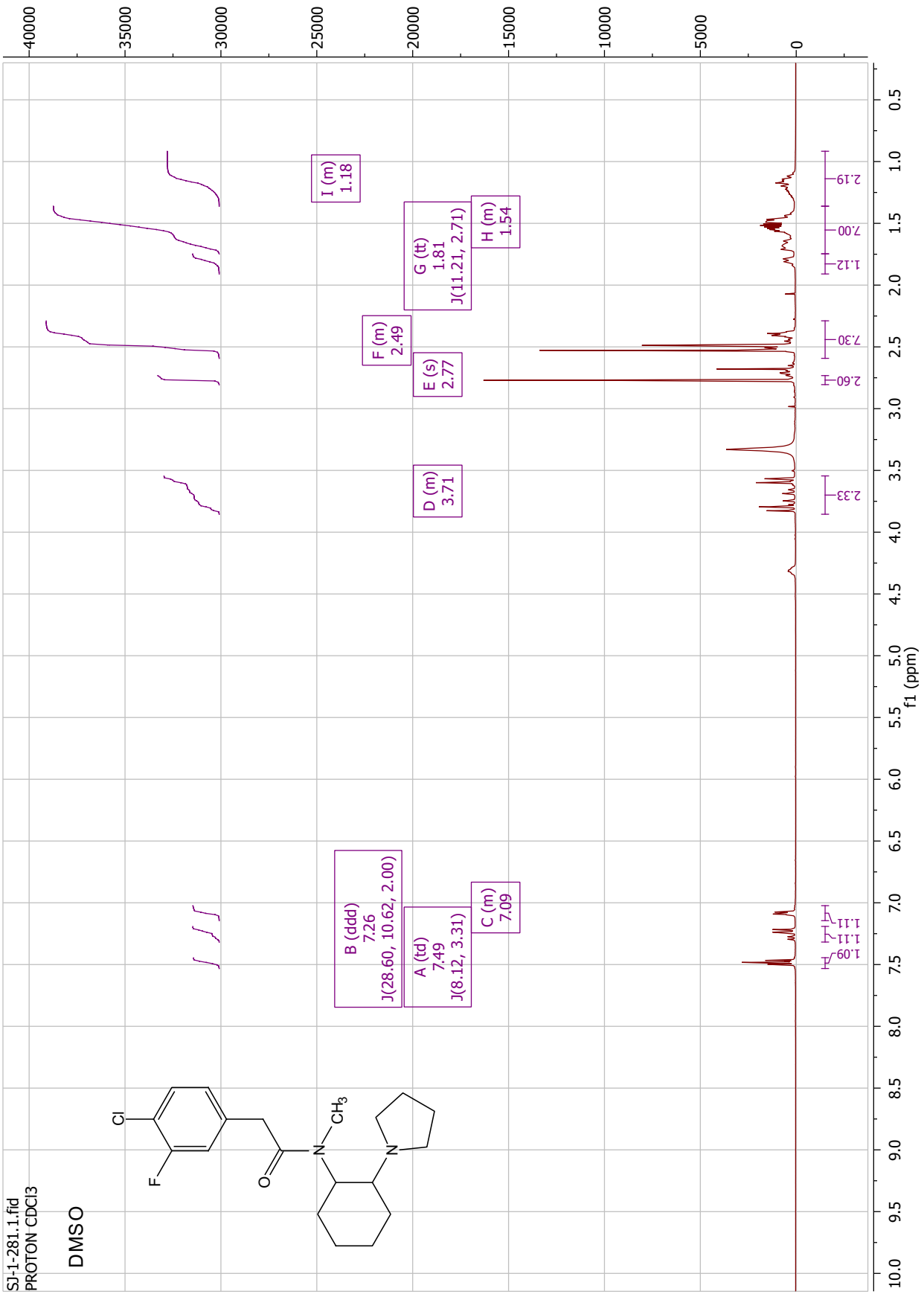
SJ-1-281.1.fid
PROTON CDCl3
DMSO
Cl
F
O
N
CH3
N
B (ddd)
7.26
J(28.60, 10.62, 2.00)
A (td)
7.49
J(8.12, 3.31)
C (m)
7.09
D (m)
3.71
E (s)
2.77
F (m)
2.49
G (tt)
1.81
J(11.21, 2.71)
H (m)
1.54
I (m)
1.18
1.09
1.11
1.11
2.33
2.60
7.30
1.12
7.00
2.19
f1 (ppm)

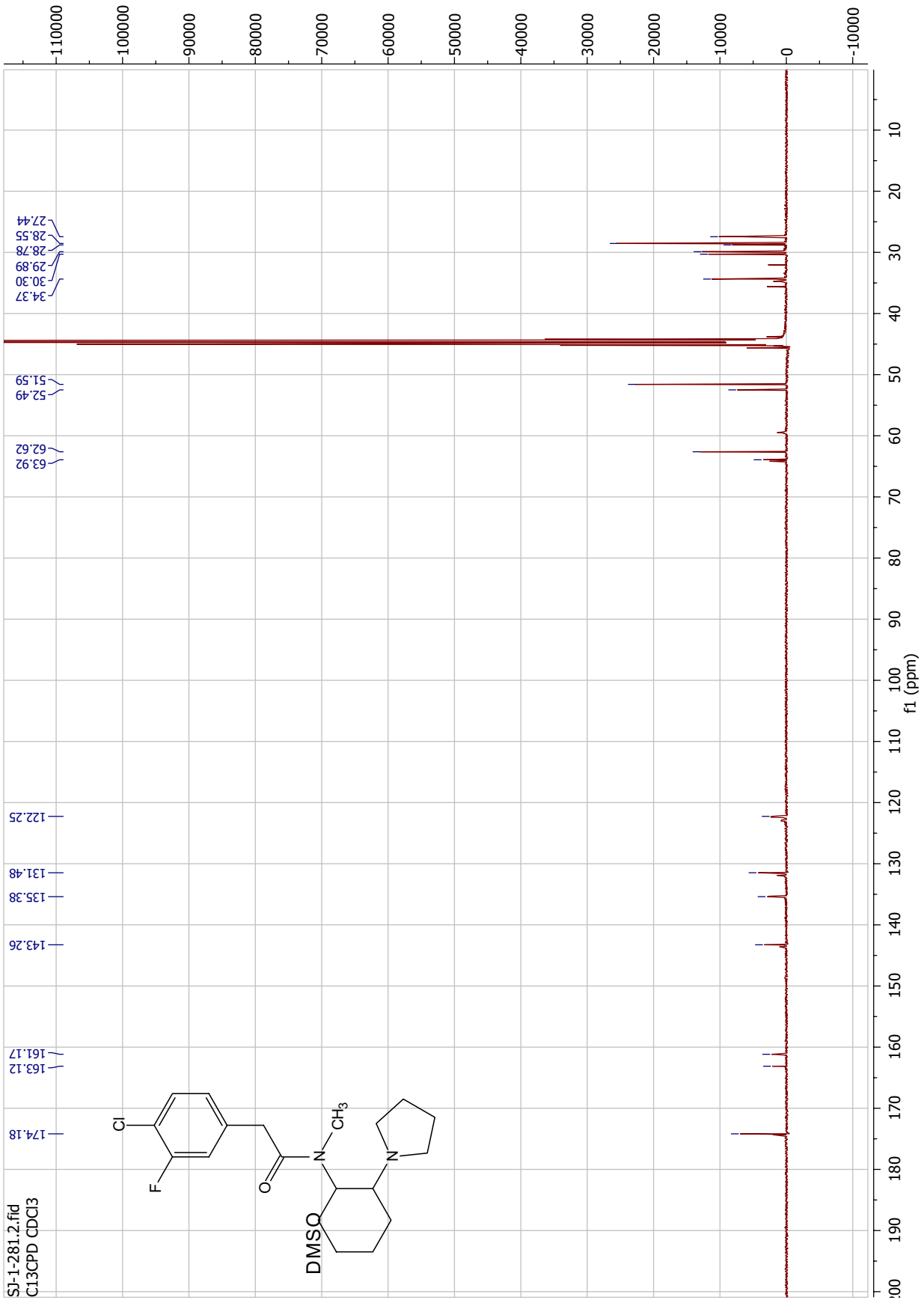
SJ-1-281.2.fid
C13CPD CDCl3
DMSO
Cl
F
O
N
CH3
N
174.18
163.12
161.17
143.26
135.38
131.48
122.25
63.92
62.62
52.49
51.59
34.37
30.30
29.89
28.78
28.55
27.44
f1 (ppm)

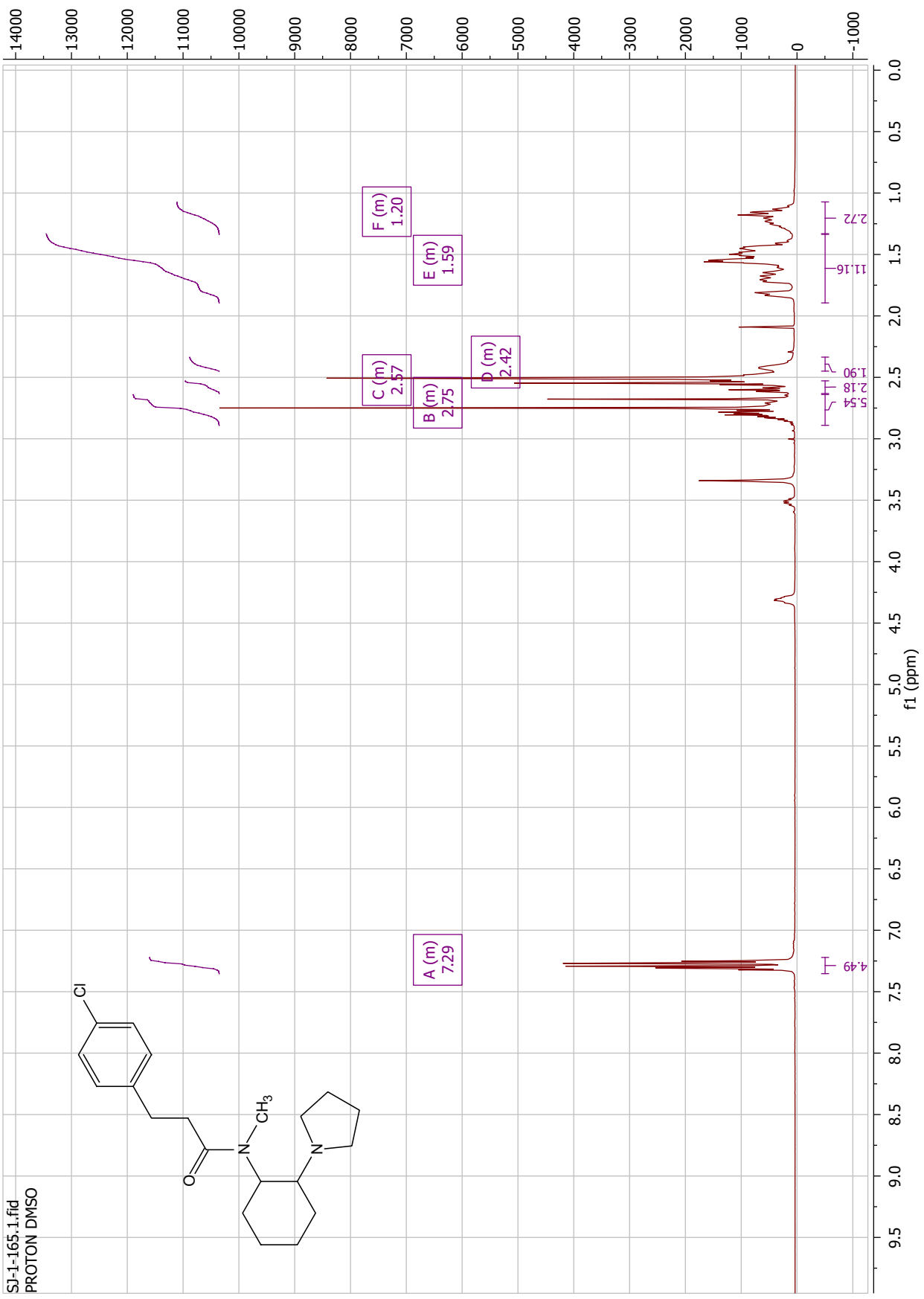
SJ-1-165.1.fid
PROTON DMSO
A (m) 7.29
B (m) 2.75
C (m) 2.57
D (m) 2.42
E (m) 1.59
F (m) 1.20
4.49
2.72
11.16
1.90
2.18
5.54
f1 (ppm)

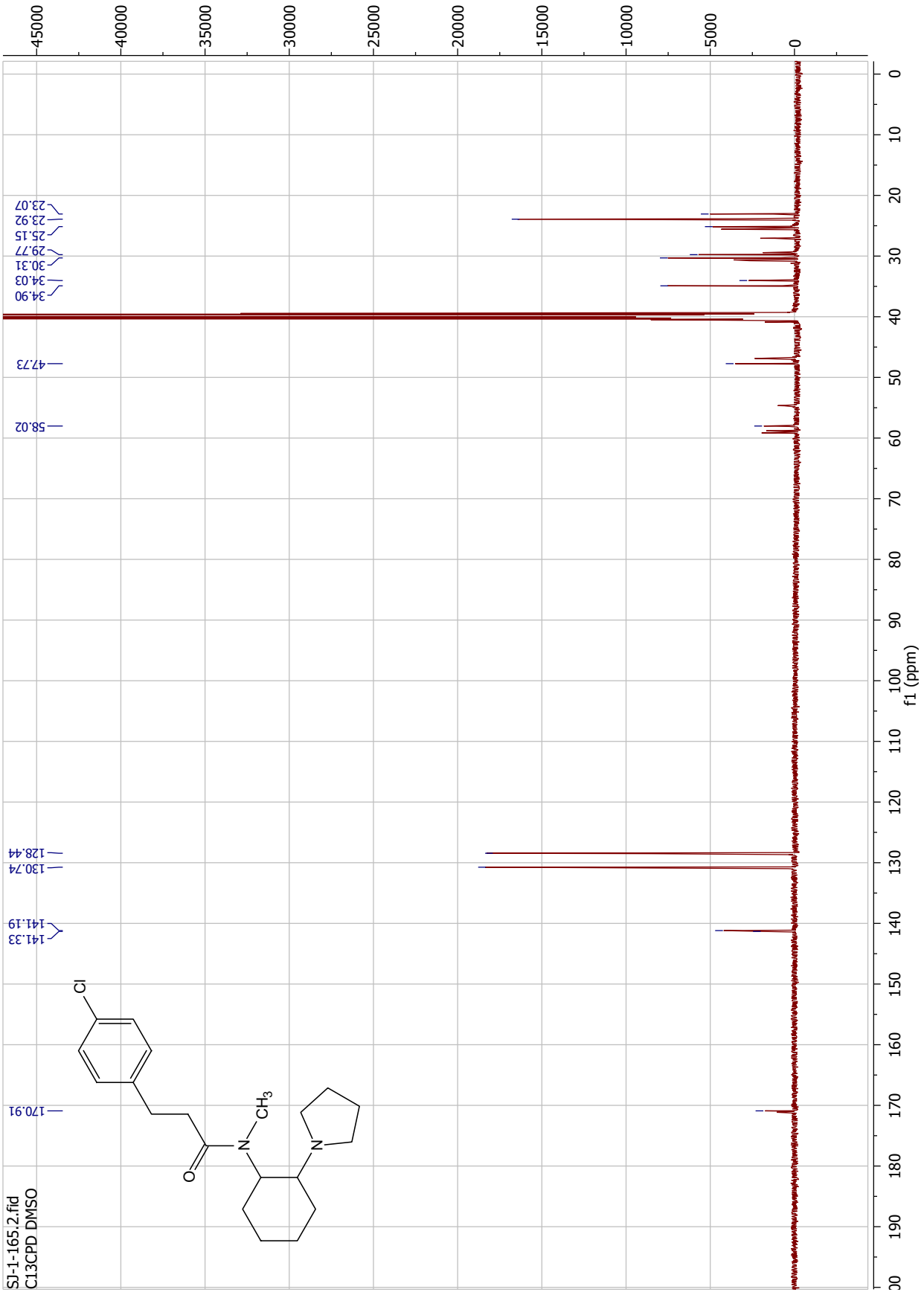
SJ-1-165.2.fid
C13CPD DMSO
170.91
141.33
141.19
130.74
128.44
58.02
47.73
34.90
34.03
30.31
29.77
25.15
23.92
23.07
Cl
O
N
CH3
N
f1 (ppm)

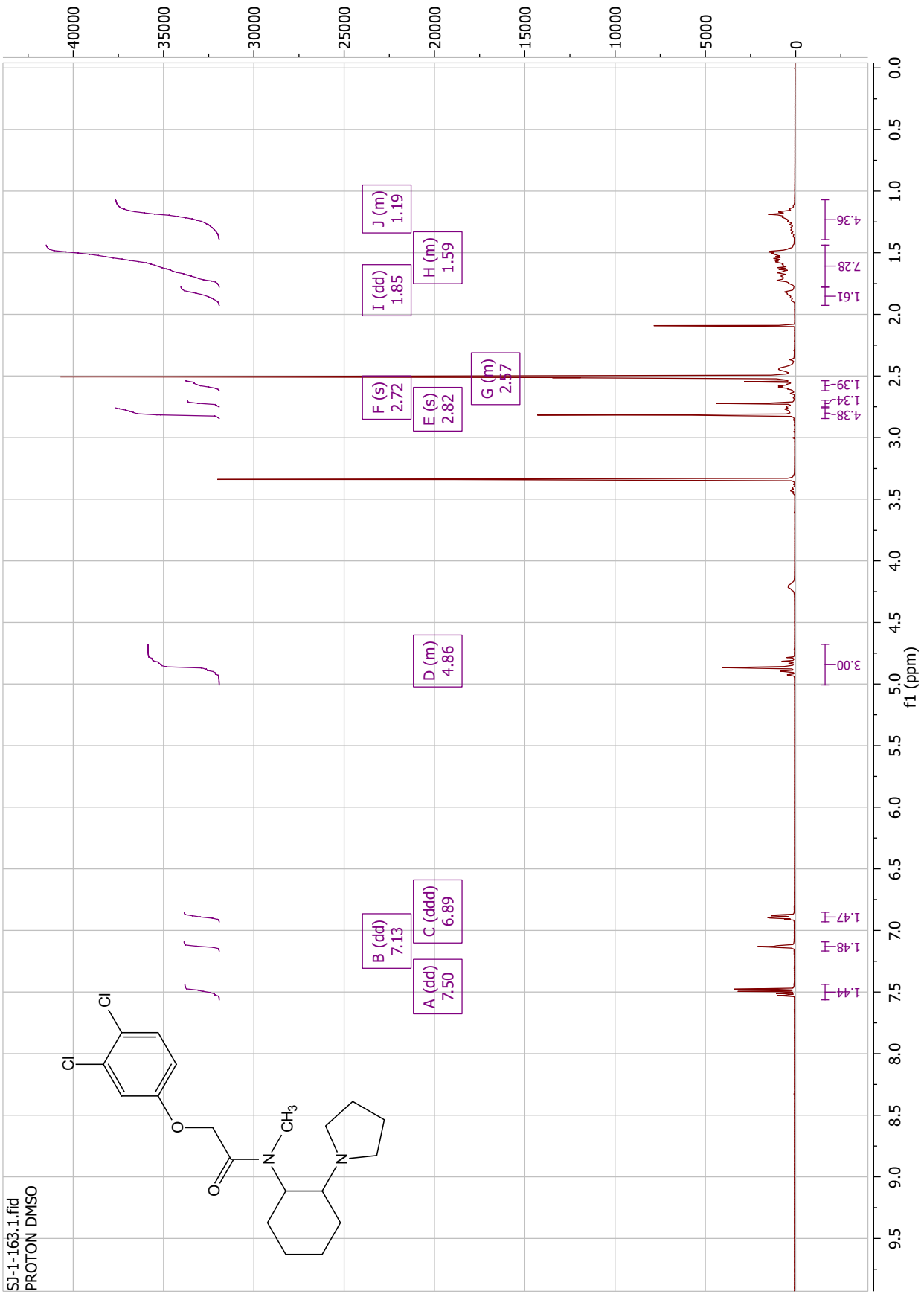
SJ-1-163.1.fid
PROTON DMSO
A (dd) 7.50
B (dd) 7.13
C (ddd) 6.89
D (m) 4.86
E (s) 2.82
F (s) 2.72
G (m) 2.57
H (m) 1.59
I (dd) 1.85
J (m) 1.19
4.36
7.28
1.61
1.39
1.34
4.38
3.00
1.47
1.48
1.44
f1 (ppm)

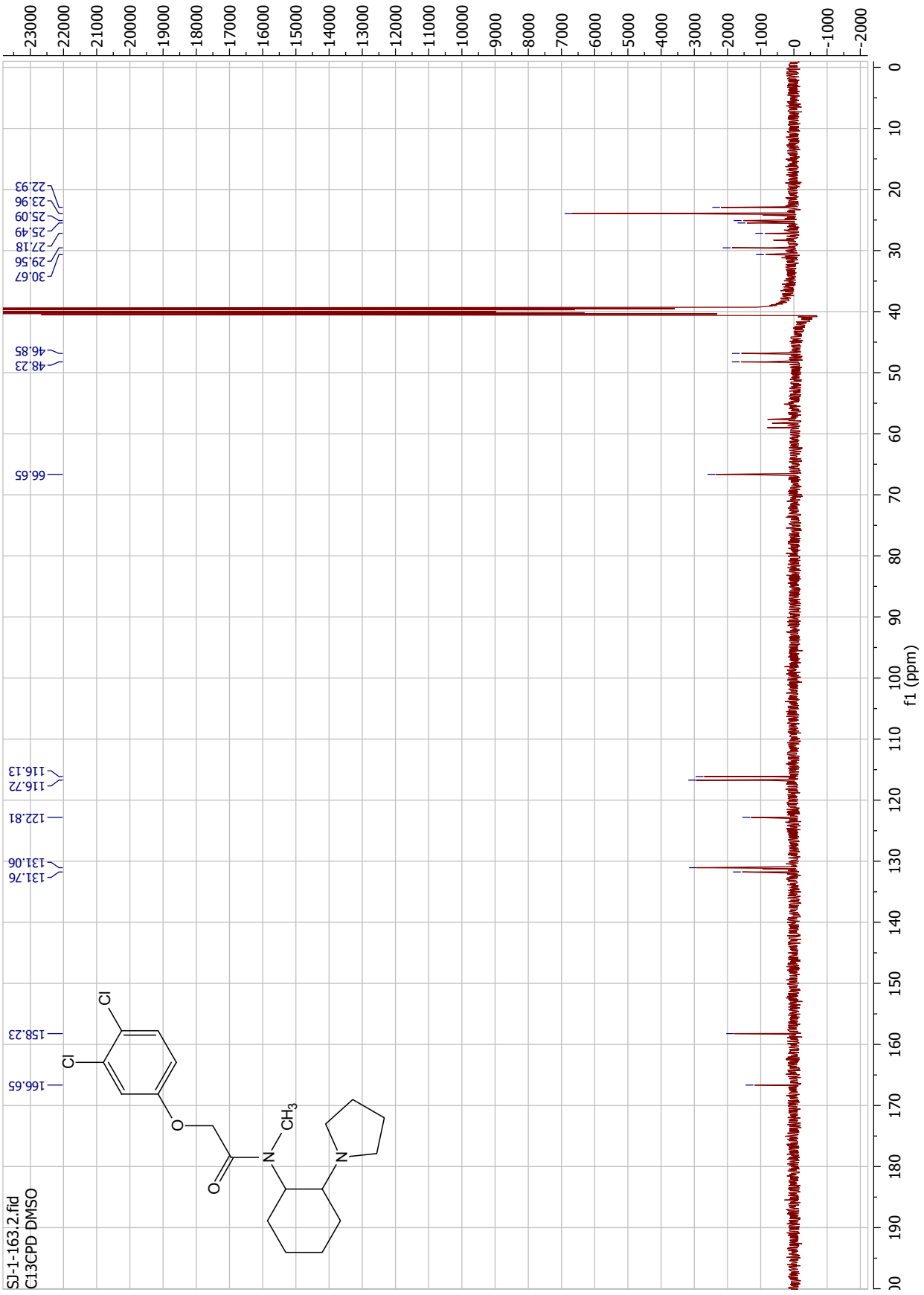
SJ-1-163.2.fid
C13CPD DMSO
166.65
158.23
131.76
131.06
122.81
116.72
116.13
66.65
48.23
46.85
30.67
29.56
27.18
25.49
25.09
23.96
22.93
f1 (ppm)
Cl
Cl
O
O
N
CH3
N

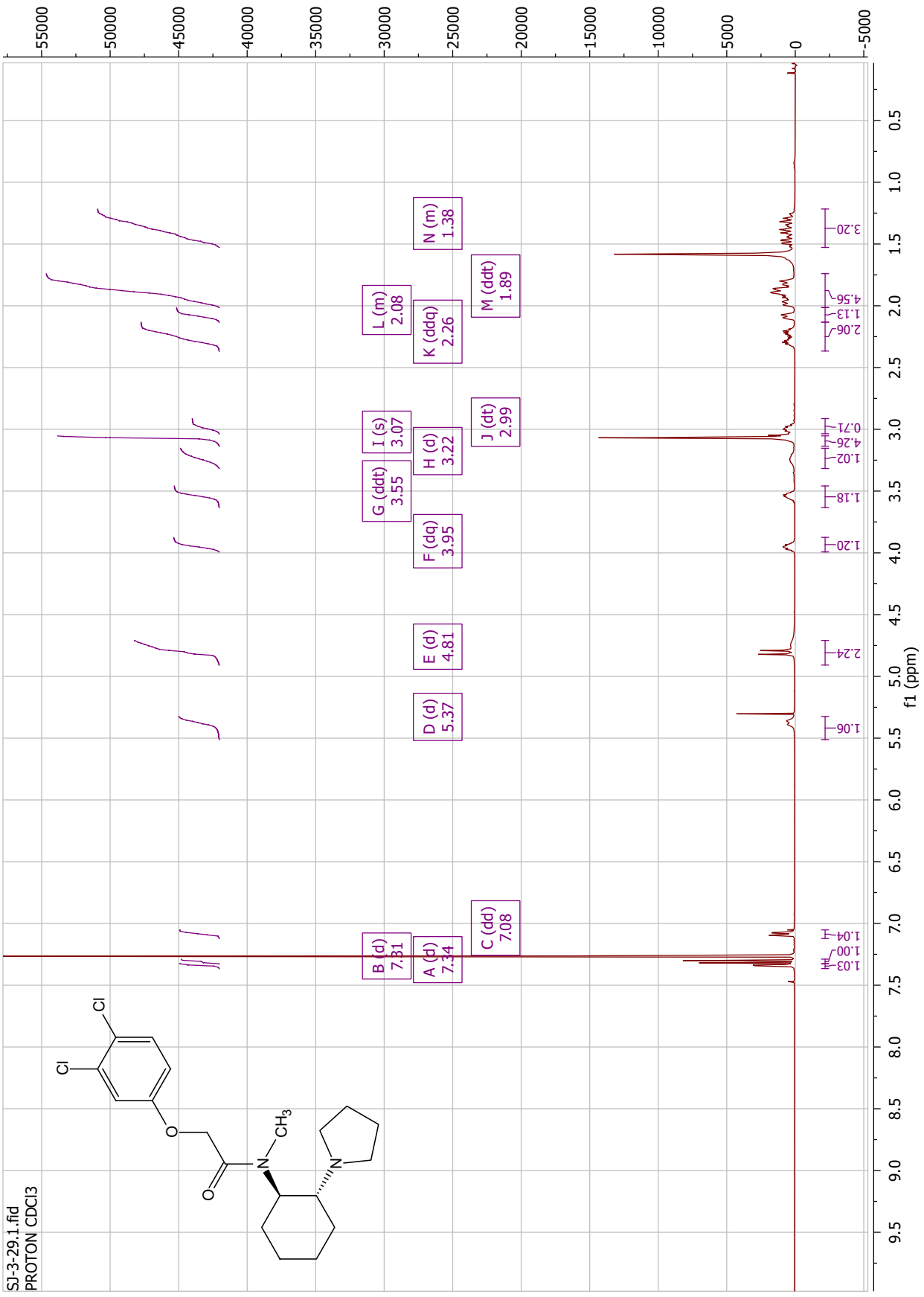
SJ-3-29.1.fid
PROTON CDCl3
A (d) 7.34
B (d) 7.31
C (dd) 7.08
D (d) 5.37
E (d) 4.81
F (dq) 3.95
G (ddt) 3.55
H (d) 3.22
I (s) 3.07
J (dt) 2.99
K (ddq) 2.26
L (m) 2.08
M (ddt) 1.89
N (m) 1.38
1.03
1.00
1.04
1.06
2.24
1.20
1.18
1.02
4.26
0.71
2.06
1.13
4.56
3.20
f1 (ppm)

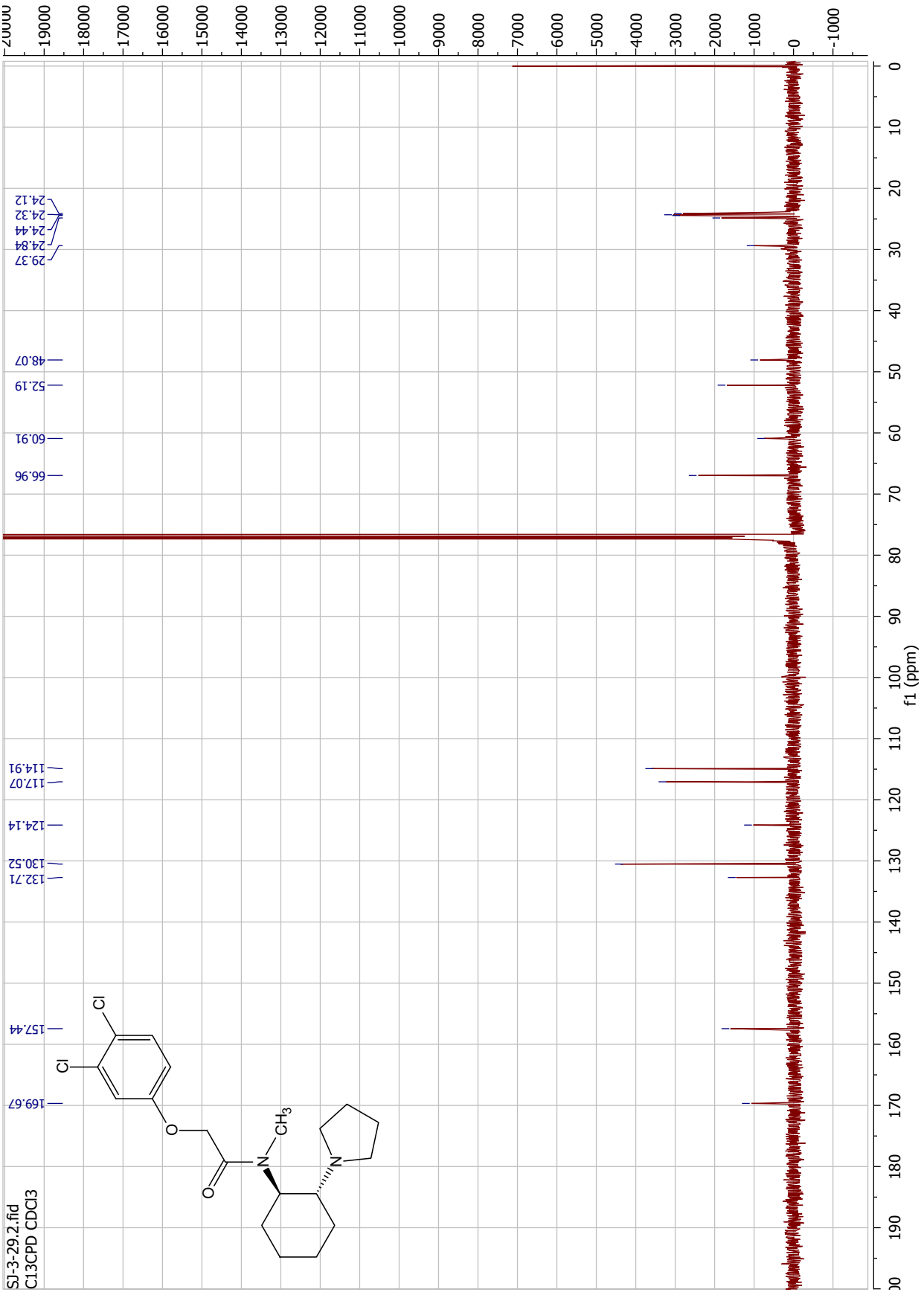
SJ-3-29.2.fid
C13CPD CDCl3
f1 (ppm)
24.12
24.32
24.44
24.84
29.37
48.07
52.19
60.91
66.96
114.91
117.07
124.14
130.52
132.71
157.44
169.67
Cl
Cl
O
O
N
CH3
N

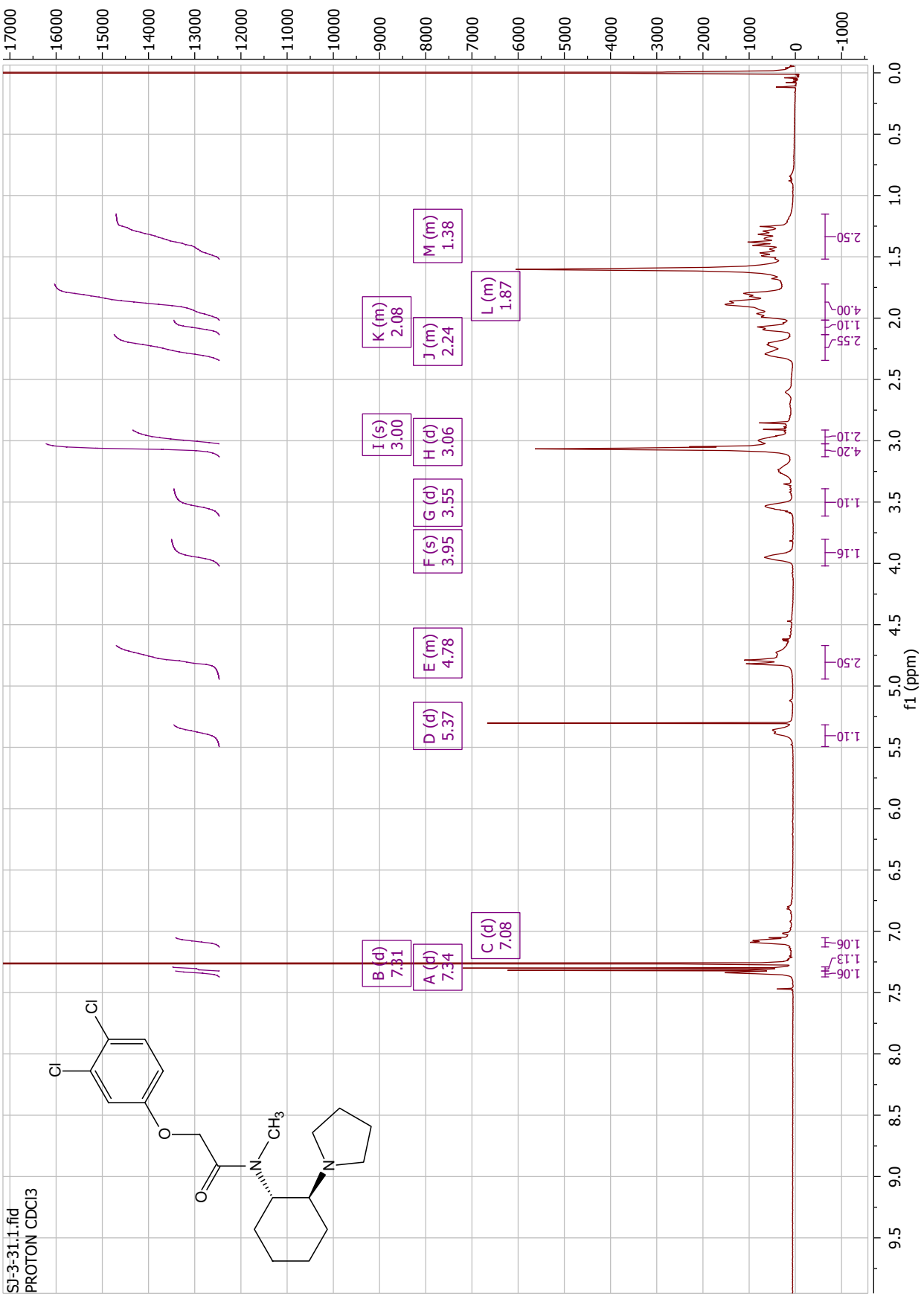
SJ-3-31.1.fid
PROTON CDCl3
B (d) 7.31
A (d) 7.34
C (d) 7.08
D (d) 5.37
E (m) 4.78
F (s) 3.95
G (d) 3.55
H (d) 3.06
I (s) 3.00
K (m) 2.08
J (m) 2.24
L (m) 1.87
M (m) 1.38
2.50
4.00
1.10
2.55
2.10
4.20
1.10
1.16
2.50
1.10
1.06
1.13
1.06
f1 (ppm)

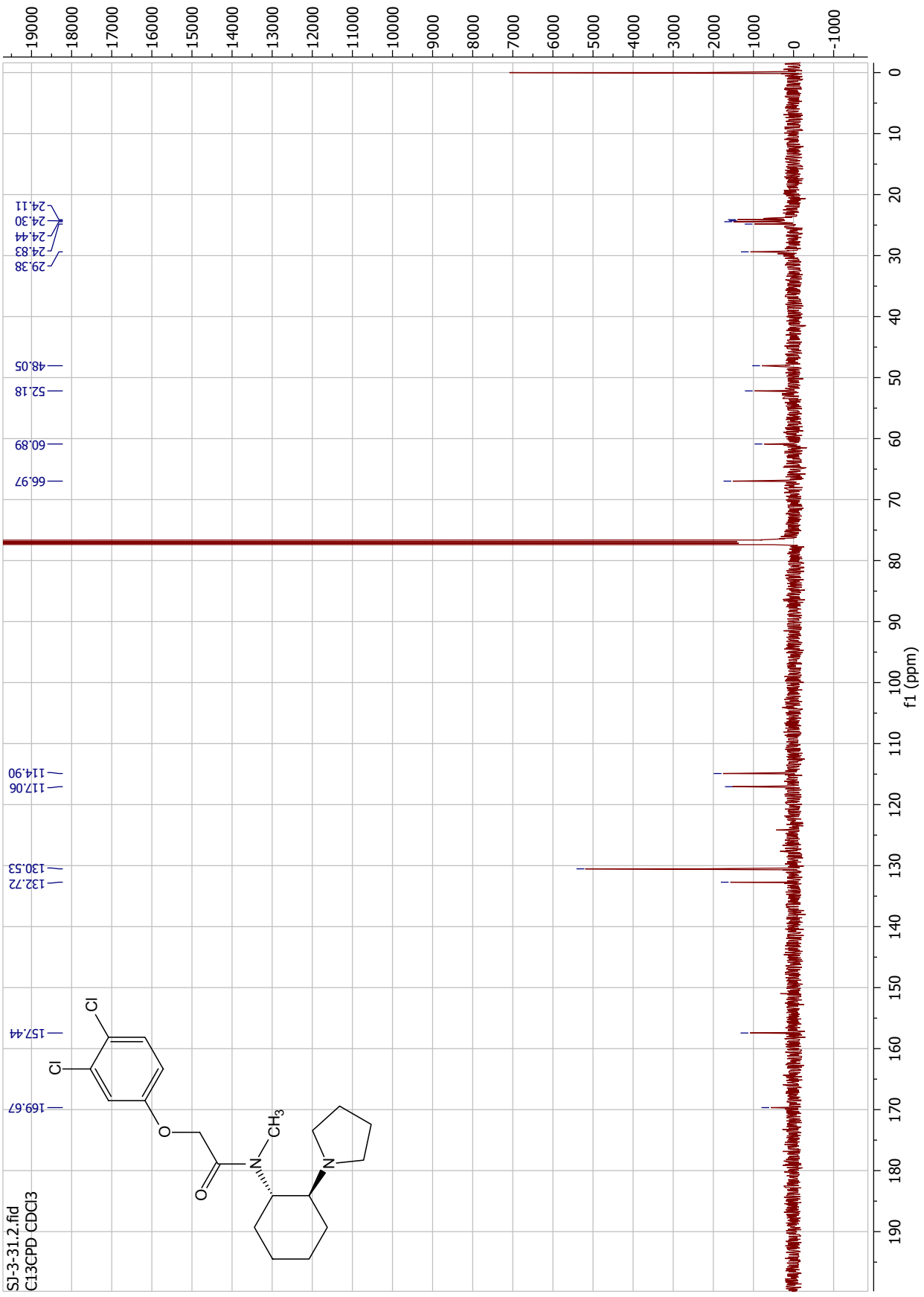
SJ-3-31.2.fid
C13CPD CDCl3
169.67
157.44
132.72
130.53
117.06
114.90
66.97
60.89
52.18
48.05
29.38
24.83
24.44
24.30
24.11
f1 (ppm)

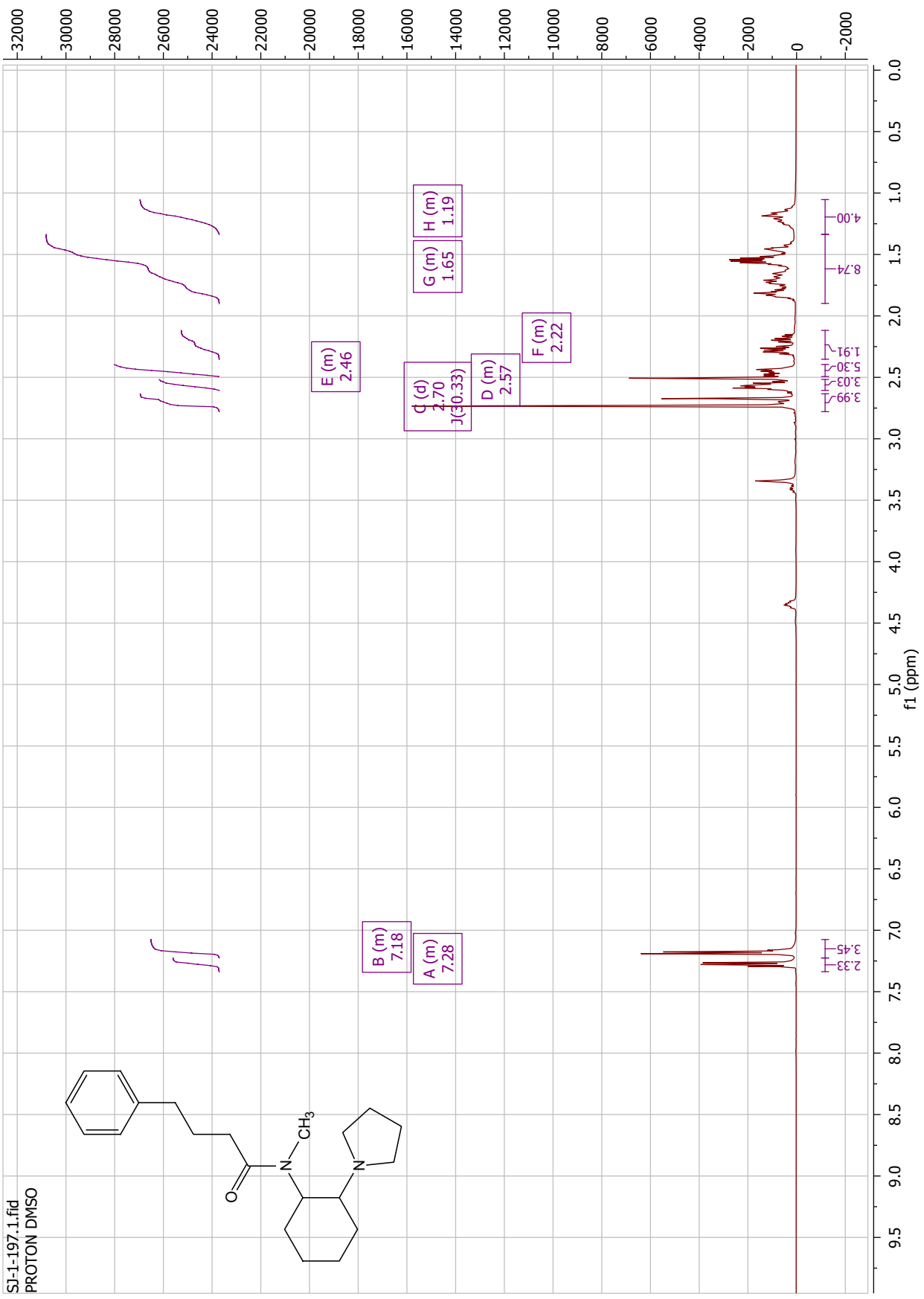
SJ-1-197.1.fid
PROTON DMSO
A (m) 7.28
B (m) 7.18
C (d) 2.70 J(10.33)
D (m) 2.57
E (m) 2.46
F (m) 2.22
G (m) 1.65
H (m) 1.19
4.00
8.74
1.91
5.30
3.03
3.99
2.33
3.45
f1 (ppm)

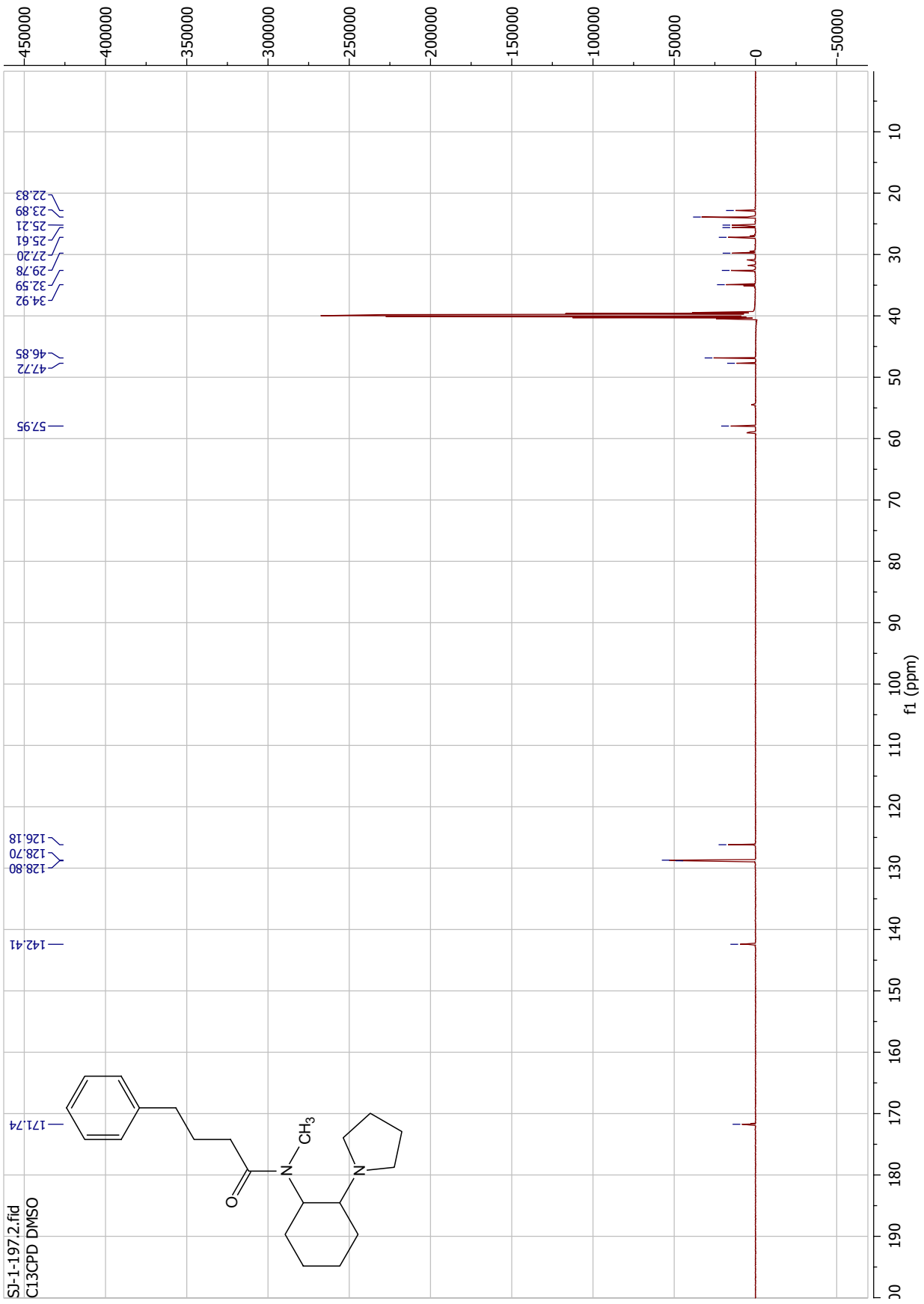
SJ-1-197.2.fid
C13CPD DMSO
171.74
142.41
128.80
128.70
126.18
57.95
47.72
46.85
34.92
32.59
29.78
27.20
25.61
25.21
23.89
22.83
f1 (ppm)

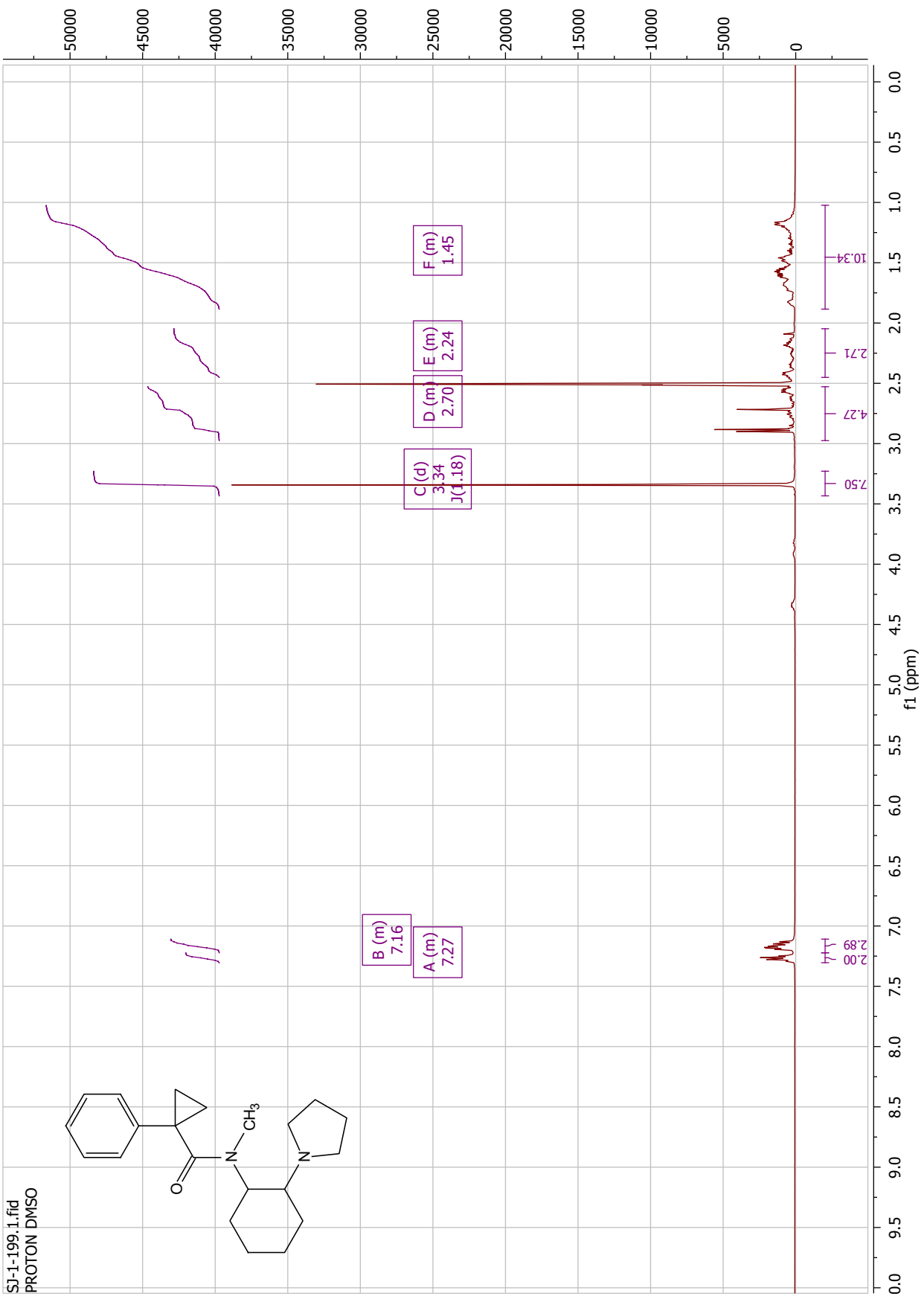
SJ-1-199.1.fid
PROTON DMSO
A (m)
7.27
B (m)
7.16
C (d)
3.34
J(1.18)
D (m)
2.70
E (m)
2.24
F (m)
1.45
2.89
2.00
7.50
4.27
2.71
10.34
f1 (ppm)


SJ-1-199.2.fid
C13CPD DMSO
f1 (ppm)
16.31
16.58
16.87
17.01
23.05
23.24
23.60
23.93
23.99
24.04
25.23
25.35
25.60
29.64
29.75
31.07
46.93
47.14
57.98
58.65
126.32
128.65
128.84
141.77
170.85
O
N
CH3
N


SJ-1-201.1.fid
PROTON DMSO
A (m) 7.30
B (m) 7.18
C (m) 2.62
D (m) 2.38
E (m) 1.81
F (m) 1.60
G (m) 1.38
H (m) 1.18
2.40
3.48
3.06
2.35
1.99
17.00
0.80
2.50
f1 (ppm)


SJ-1-201.2.fid
C13CPD DMSO
174.49
146.72
128.98
126.28
125.26
58.86
57.77
46.72
29.17
26.03
25.60
25.18
23.82
22.43
O
N
CH3
N
f1 (ppm)

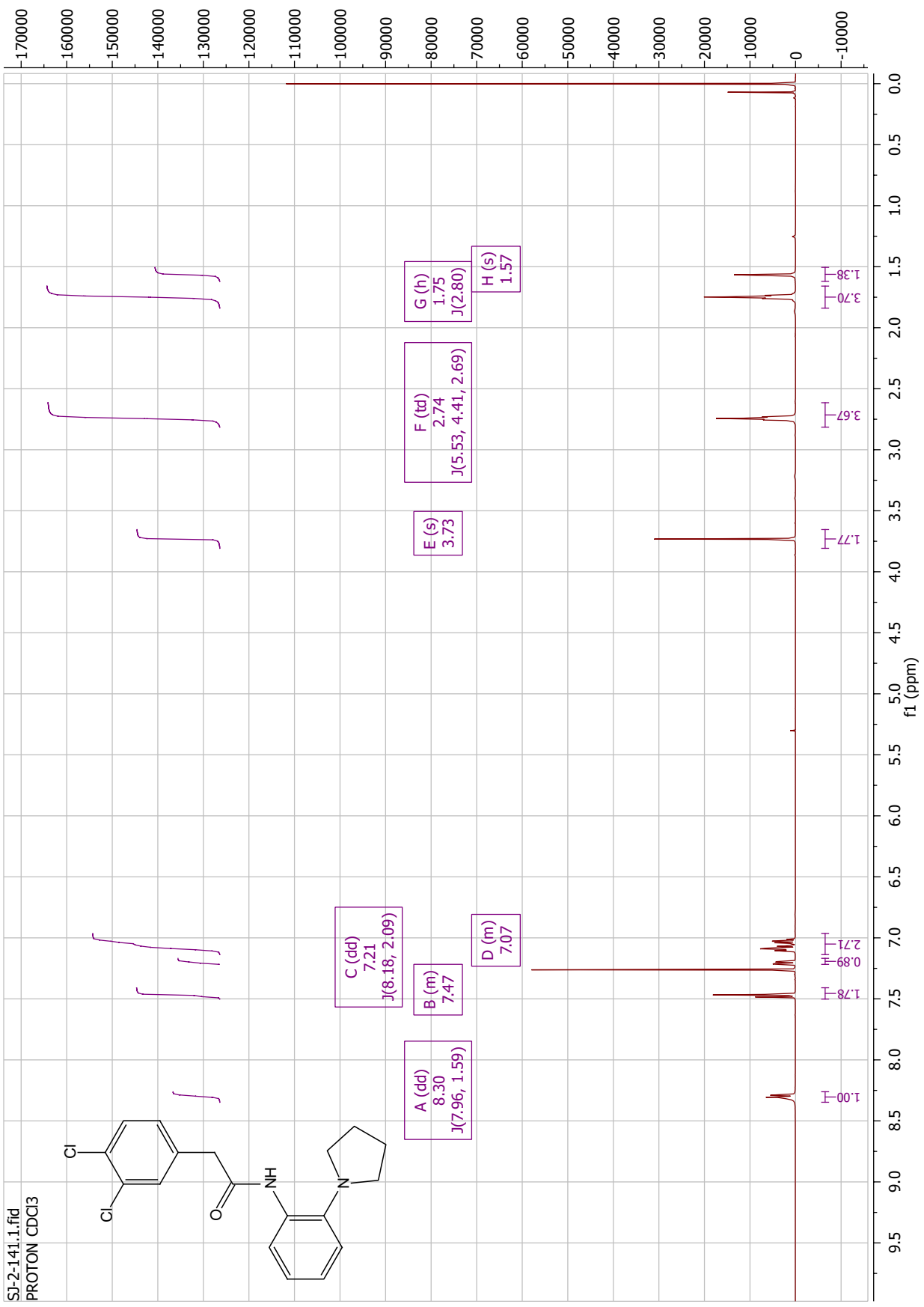
SJ-2-141.1.fid
PROTON CDCl3
A (dd)
8.30
J(7.96, 1.59)
B (m)
7.47
C (dd)
7.21
J(8.18, 2.09)
D (m)
7.07
E (s)
3.73
F (td)
2.74
J(5.53, 4.41, 2.69)
G (h)
1.75
J(2.80)
H (s)
1.57
1.00
1.78
0.89
2.71
1.77
3.67
3.70
1.38
f1 (ppm)

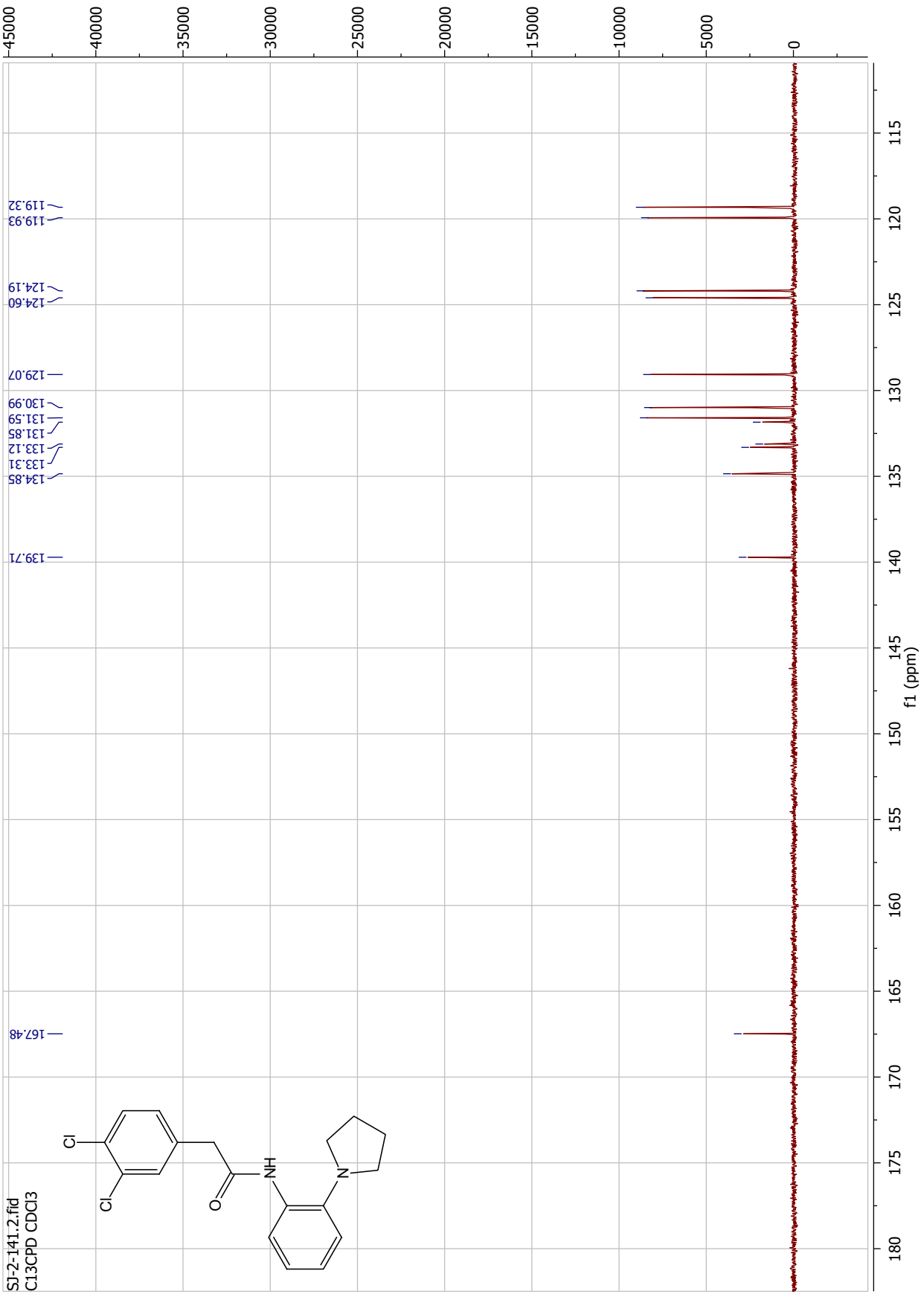
SJ-2-141.2.fid
C13CPD CDCl3
167.48
139.71
134.85
133.31
133.12
131.85
131.59
130.99
129.07
124.60
124.19
119.93
119.32
Cl
Cl
O
NH
N
f1 (ppm)


SJ-2-165.1.fid
PROTON CDCl3
Cl
Cl
O
N
CH3
N
F (td)
6.76
J(7.51, 1.36)
E (dd)
6.82
J(8.34, 1.36)
C (d)
7.29
J(8.22)
A (d)
7.09
J(2.06)
B (m)
7.23
D (m)
6.93
H (m)
3.20
G (s)
3.40
K (m)
1.89
4.05
7.17
1.98
0.92
0.87
1.00
2.01
1.03
0.96
f1 (ppm)

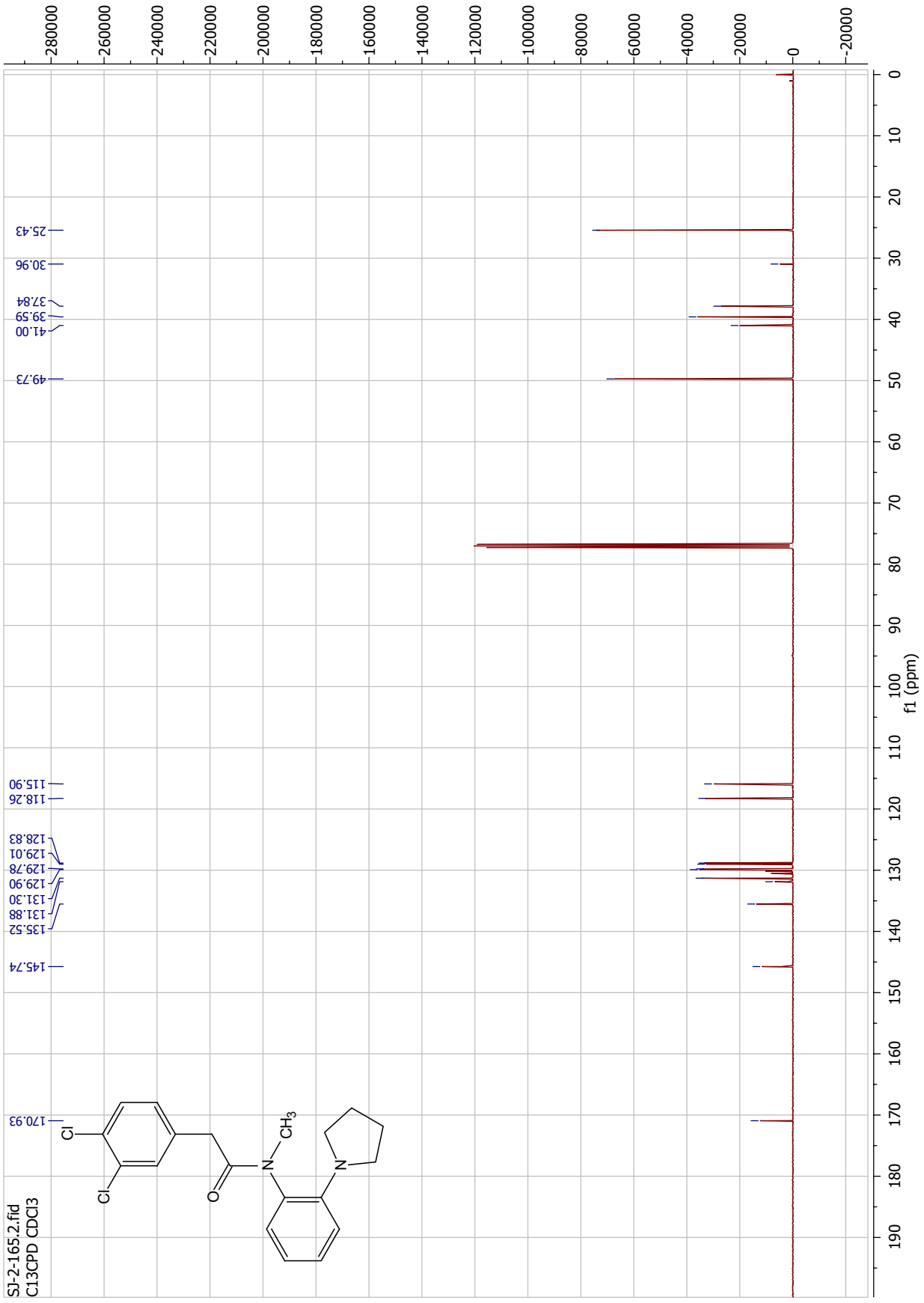
S1-2-165.2.fid
C13CPD CDCl3
25.43
30.96
37.84
39.59
41.00
49.73
115.90
118.26
128.83
129.01
129.78
129.90
131.30
131.88
135.52
145.74
170.93
Cl
Cl
O
N
CH3
N
f1 (ppm)

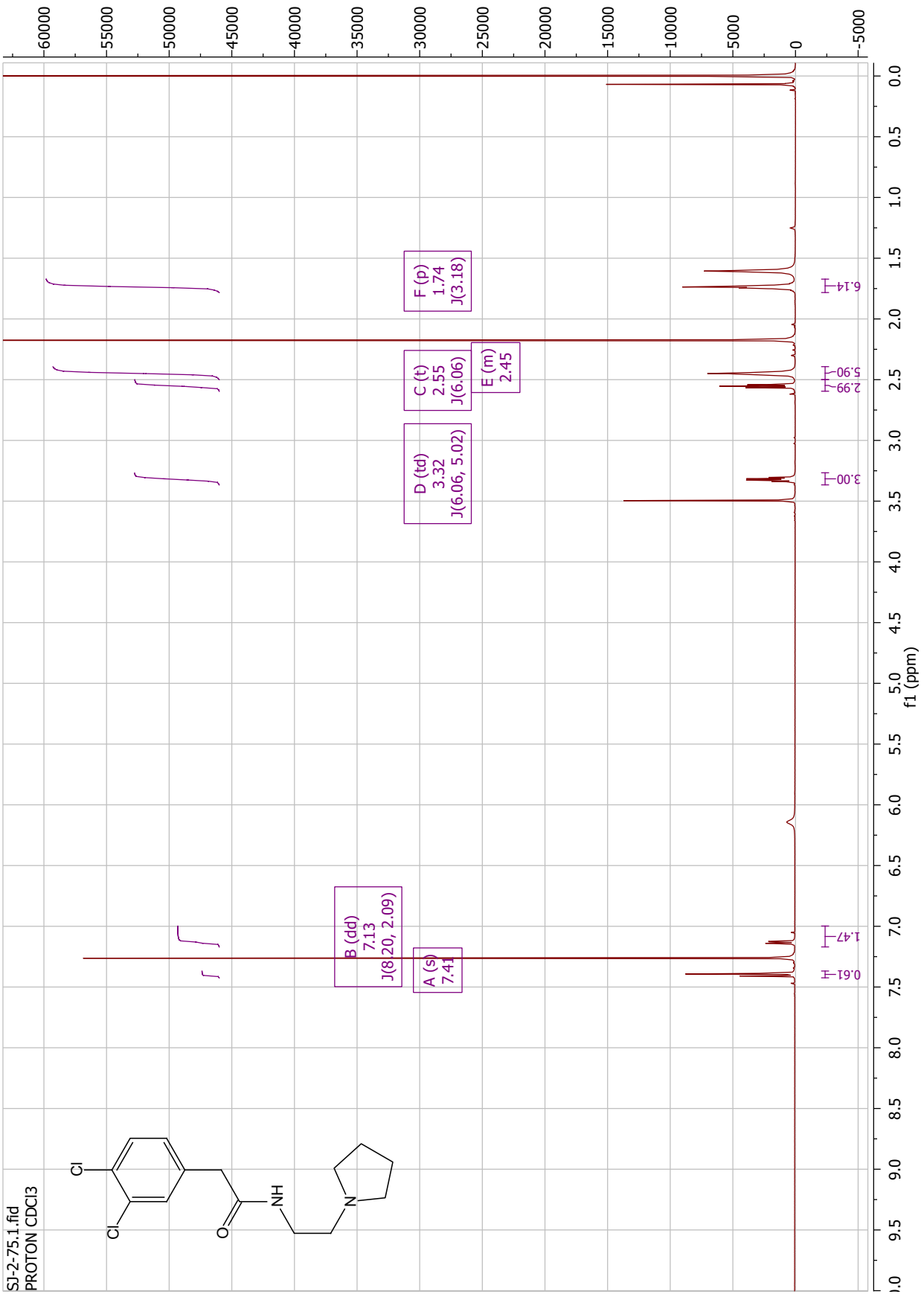
SJ-2-75.1.fid
PROTON CDCl3
A (s)
7.41
B (dd)
7.13
J(8.20, 2.09)
C (t)
2.55
J(6.06)
D (td)
3.32
J(6.06, 5.02)
E (m)
2.45
F (p)
1.74
J(3.18)
6.14
5.90
2.99
3.00
1.47
0.61
Cl
Cl
O
NH
N
f1 (ppm)

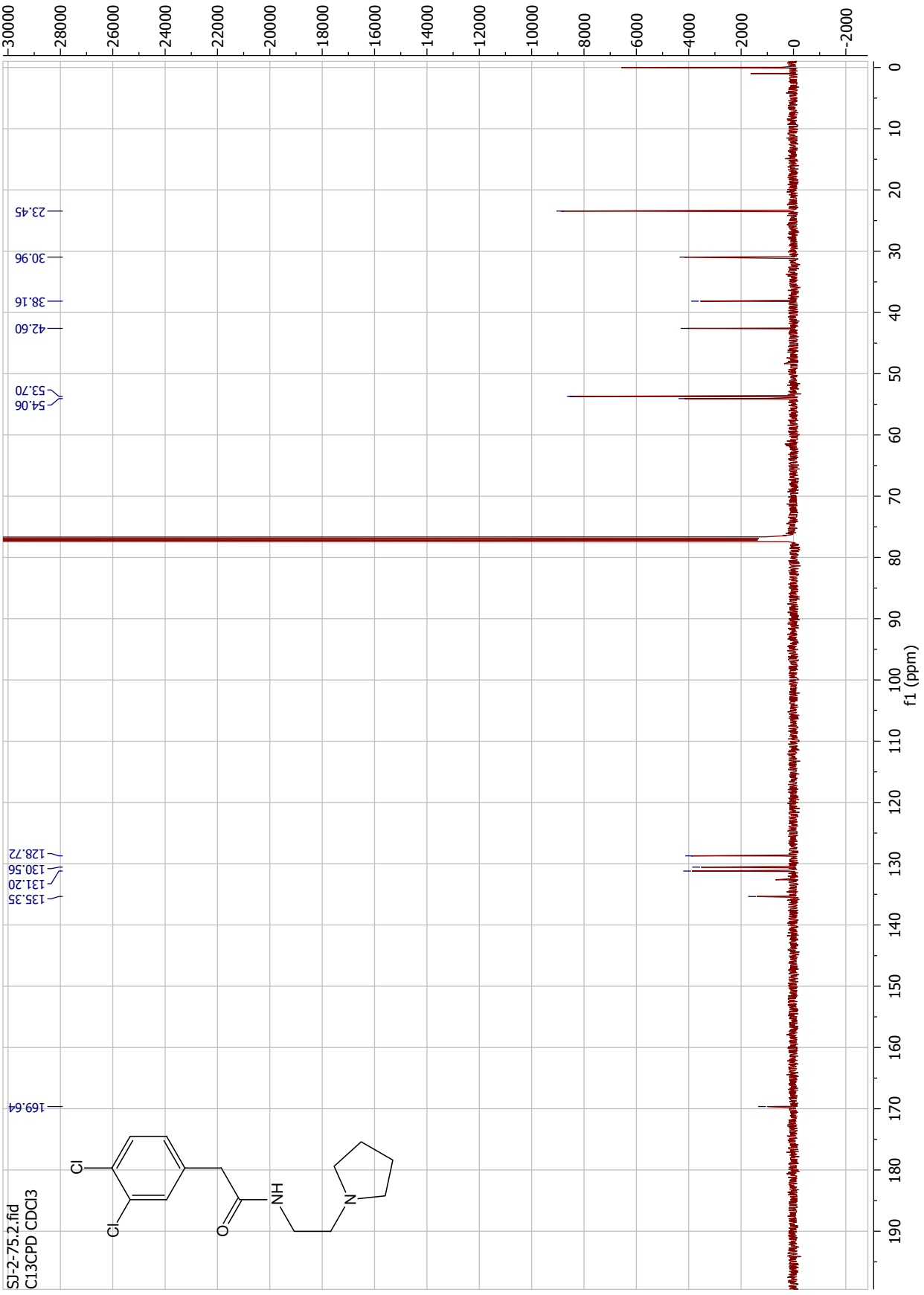
SJ-2-75.2.fid
C13CPD CDCl3
169.64
135.35
131.20
130.56
128.72
54.06
53.70
42.60
38.16
30.96
23.45
Cl
Cl
O
NH
N
f1 (ppm)

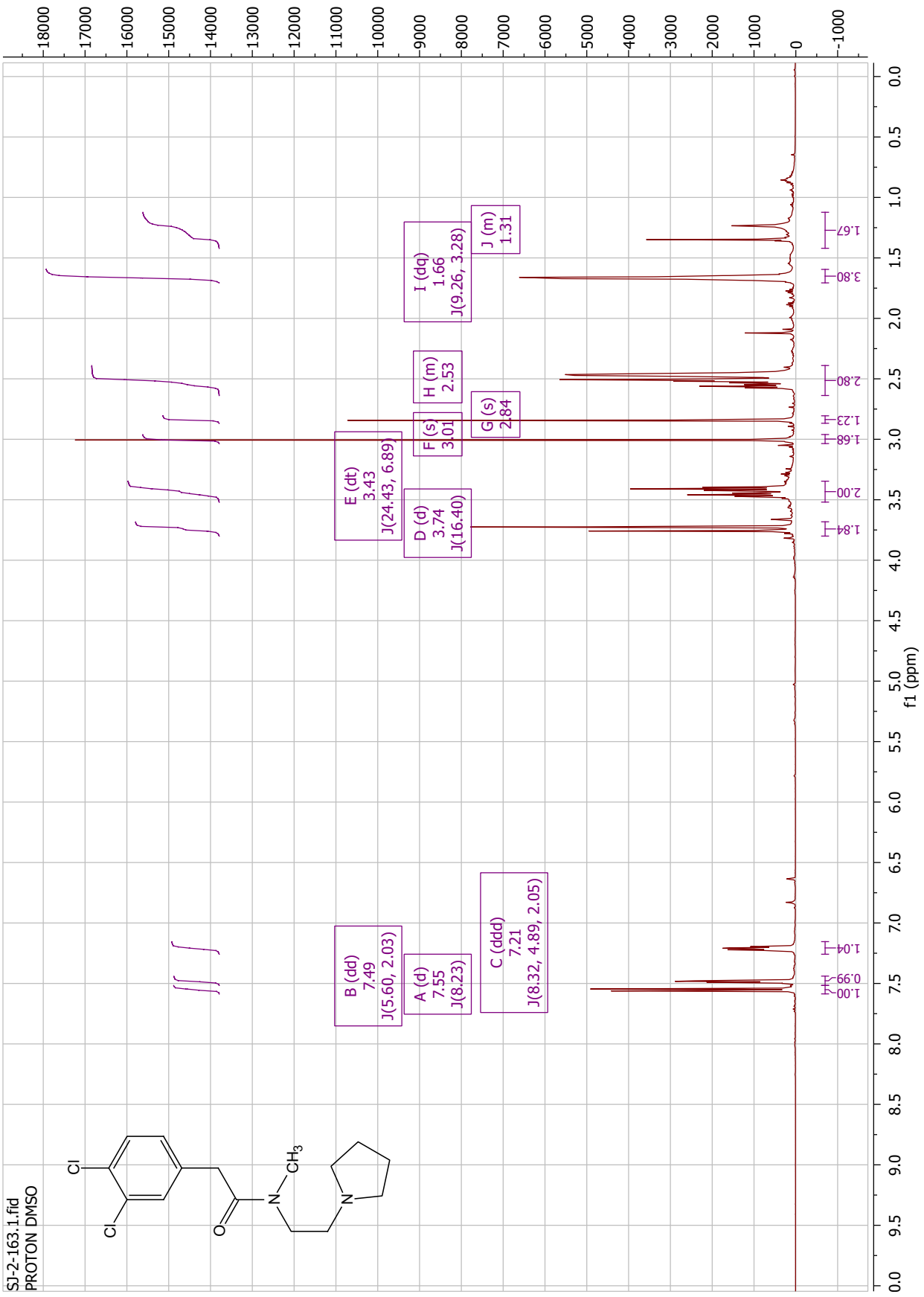
SJ-2-163.1.fid
PROTON DMSO
A (d)
7.55
J(8.23)
B (dd)
7.49
J(5.60, 2.03)
C (ddd)
7.21
J(8.32, 4.89, 2.05)
D (d)
3.74
J(16.40)
E (dt)
3.43
J(24.43, 6.89)
F (s)
3.01
G (s)
2.84
H (m)
2.53
I (dq)
1.66
J(9.26, 3.28)
J (m)
1.31
1.04
0.99
1.00
1.84
2.00
1.68
1.23
2.80
3.80
1.67
Cl
Cl
O
N
CH3
N
f1 (ppm)

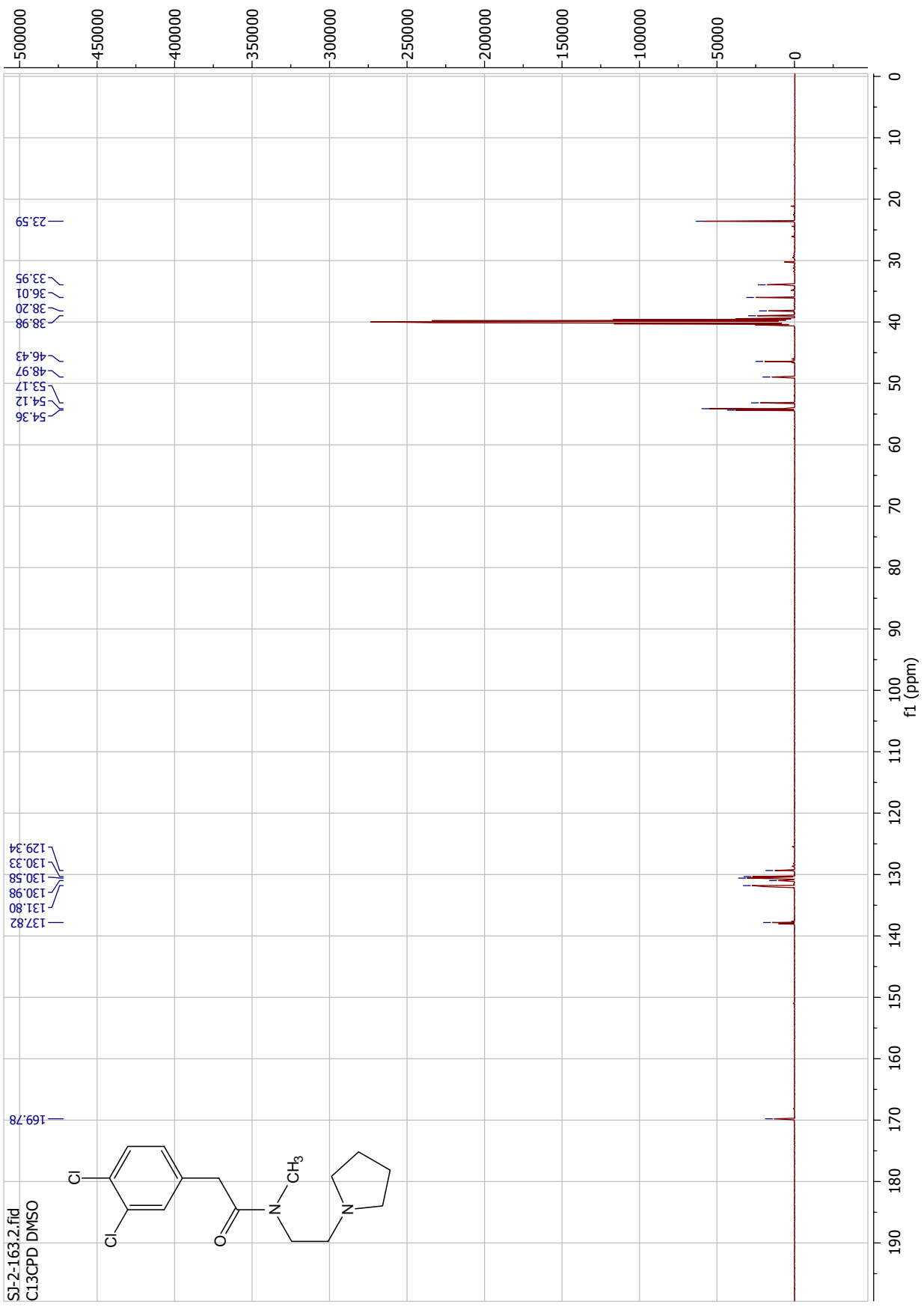
SJ-2-163.2.fid
C13CPD DMSO
169.78
137.82
131.80
130.98
130.58
130.33
129.34
54.36
54.12
53.17
48.97
46.43
38.98
38.20
36.01
33.95
23.59
Cl
Cl
O
N
CH3
N
f1 (ppm)

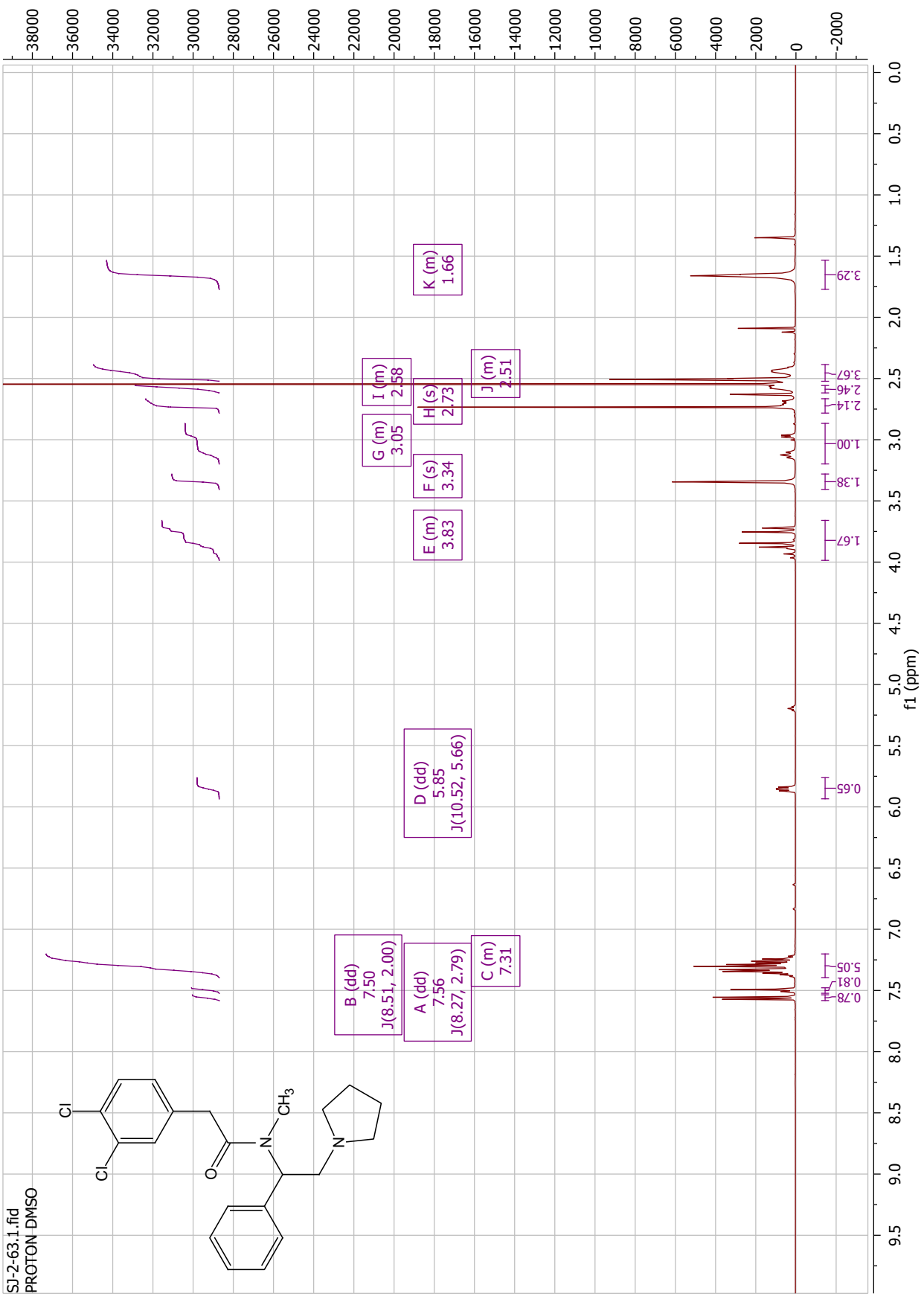
SJ-2-63.1.fid
PROTON DMSO
B (dd)
7.50
J(8.51, 2.00)
A (dd)
7.56
J(8.27, 2.79)
C (m)
7.31
D (dd)
5.85
J(10.52, 5.66)
E (m)
3.83
F (s)
3.34
G (m)
3.05
I (m)
2.58
H (s)
2.73
J (m)
2.51
K (m)
1.66
3.29
3.67
2.46
2.14
1.00
1.38
1.67
0.65
5.05
0.81
0.78
f1 (ppm)

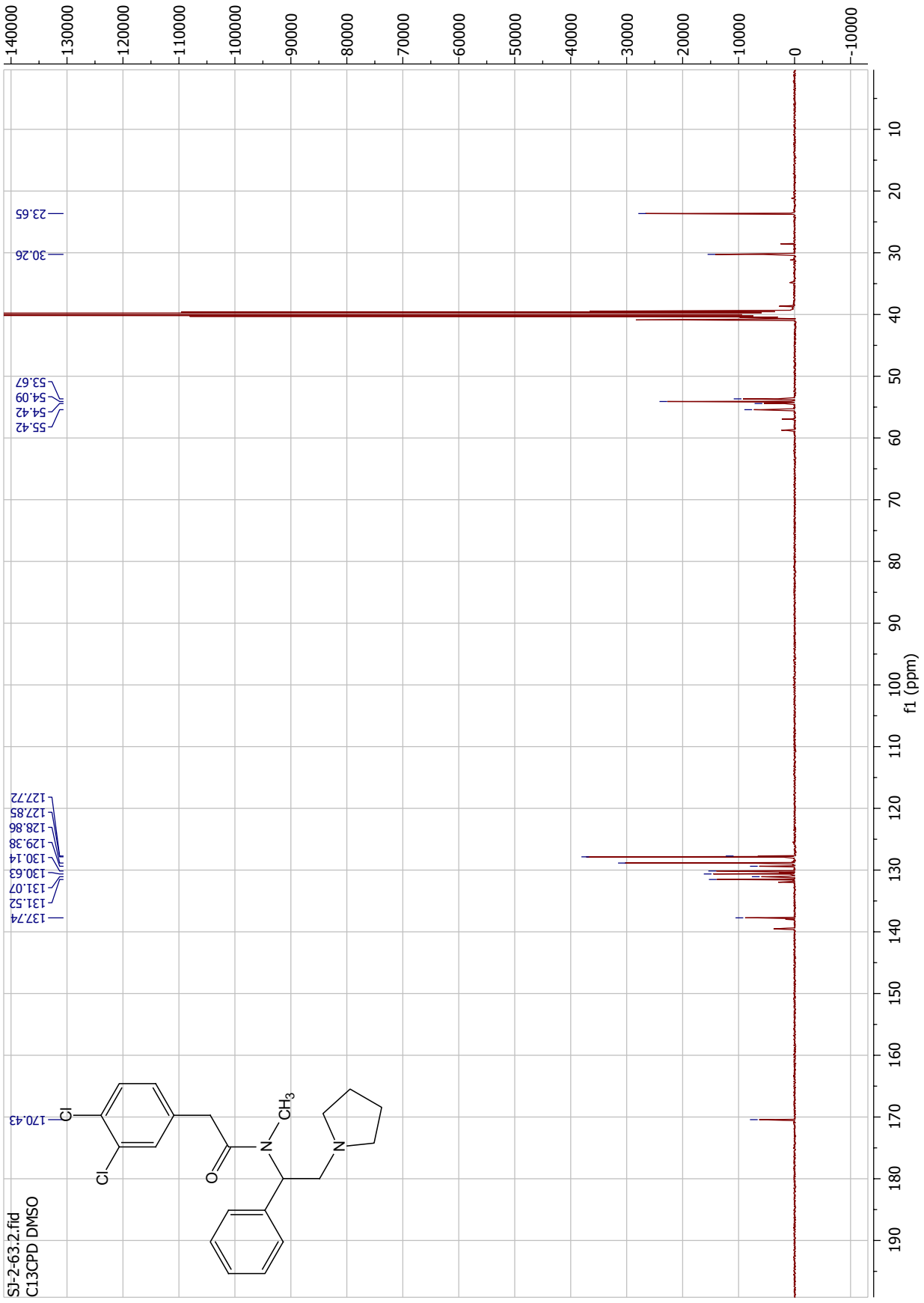
S1-2-63.2.fid
C13CPD DMSO
170.43
137.74
131.52
131.07
130.63
130.14
129.38
128.86
127.85
127.72
55.42
54.42
54.09
53.67
30.26
23.65
Cl
Cl
O
N
CH3
N
f1 (ppm)

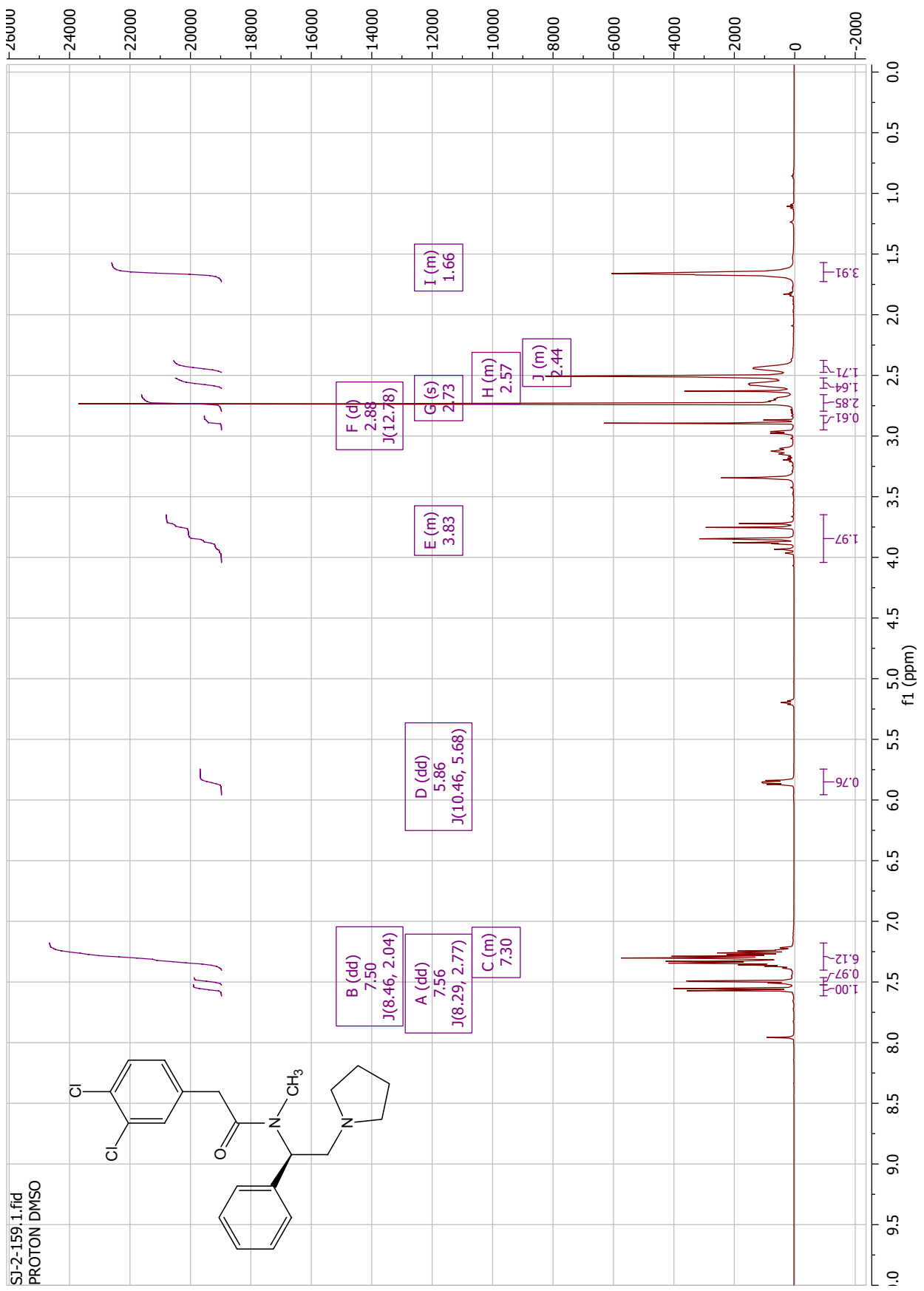
SJ-2-159.1.fid
PROTON DMSO
B (dd)
7.50
J(8.46, 2.04)
A (dd)
7.56
J(8.29, 2.77)
C (m)
7.30
D (dd)
5.86
J(10.46, 5.68)
E (m)
3.83
F (d)
2.88
J(12.78)
G (s)
2.73
H (m)
2.57
J (m)
2.44
I (m)
1.66
3.91
1.71
1.64
2.85
0.61
1.97
0.76
6.12
0.97
1.00
f1 (ppm)

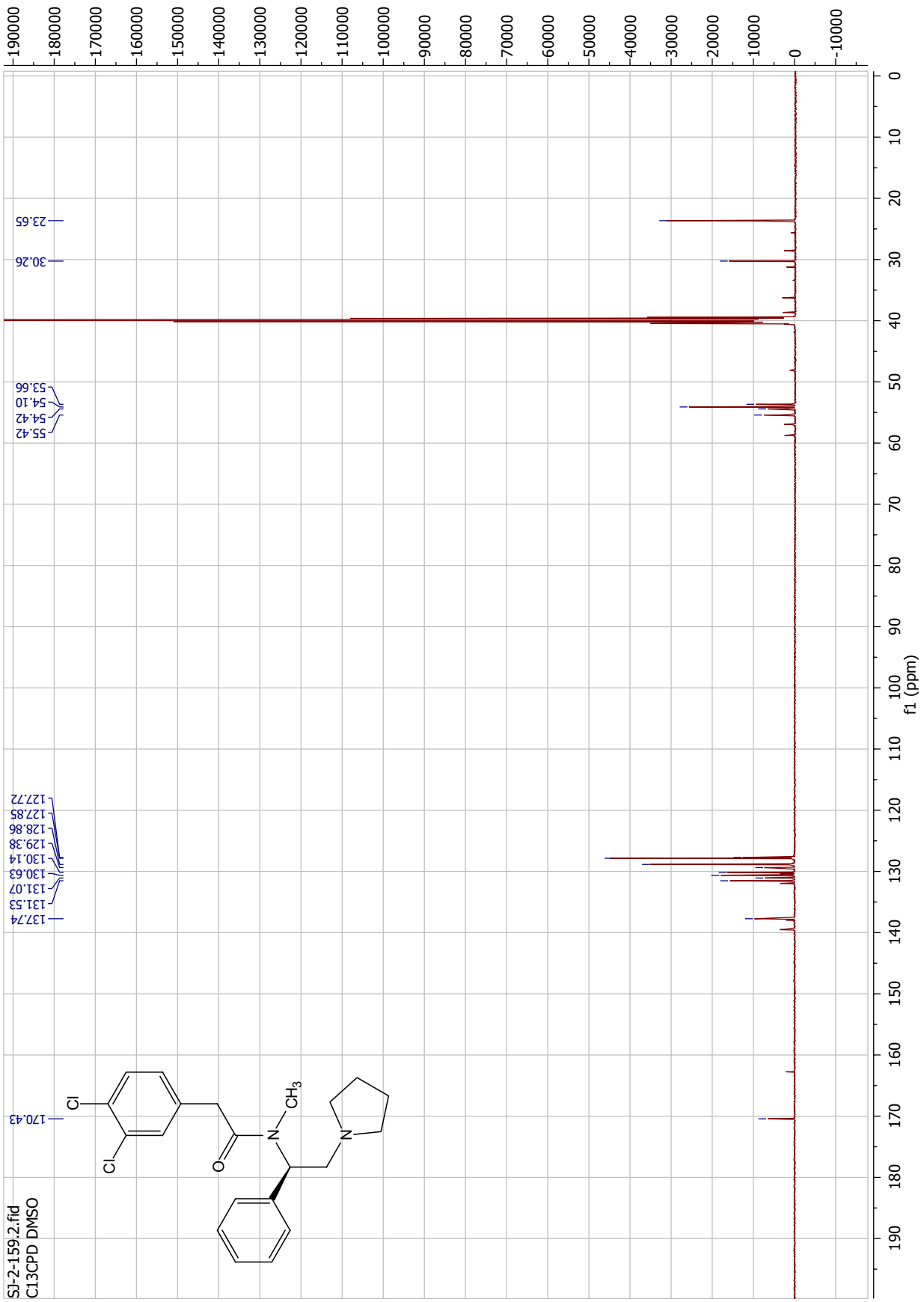
SJ-2-159.2.fid
C13CPD DMSO
23.65
30.26
53.66
54.10
54.42
55.42
127.72
127.85
128.86
129.38
130.14
130.63
131.07
131.53
137.74
170.43
Cl
Cl
O
N
CH3
N
f1 (ppm)

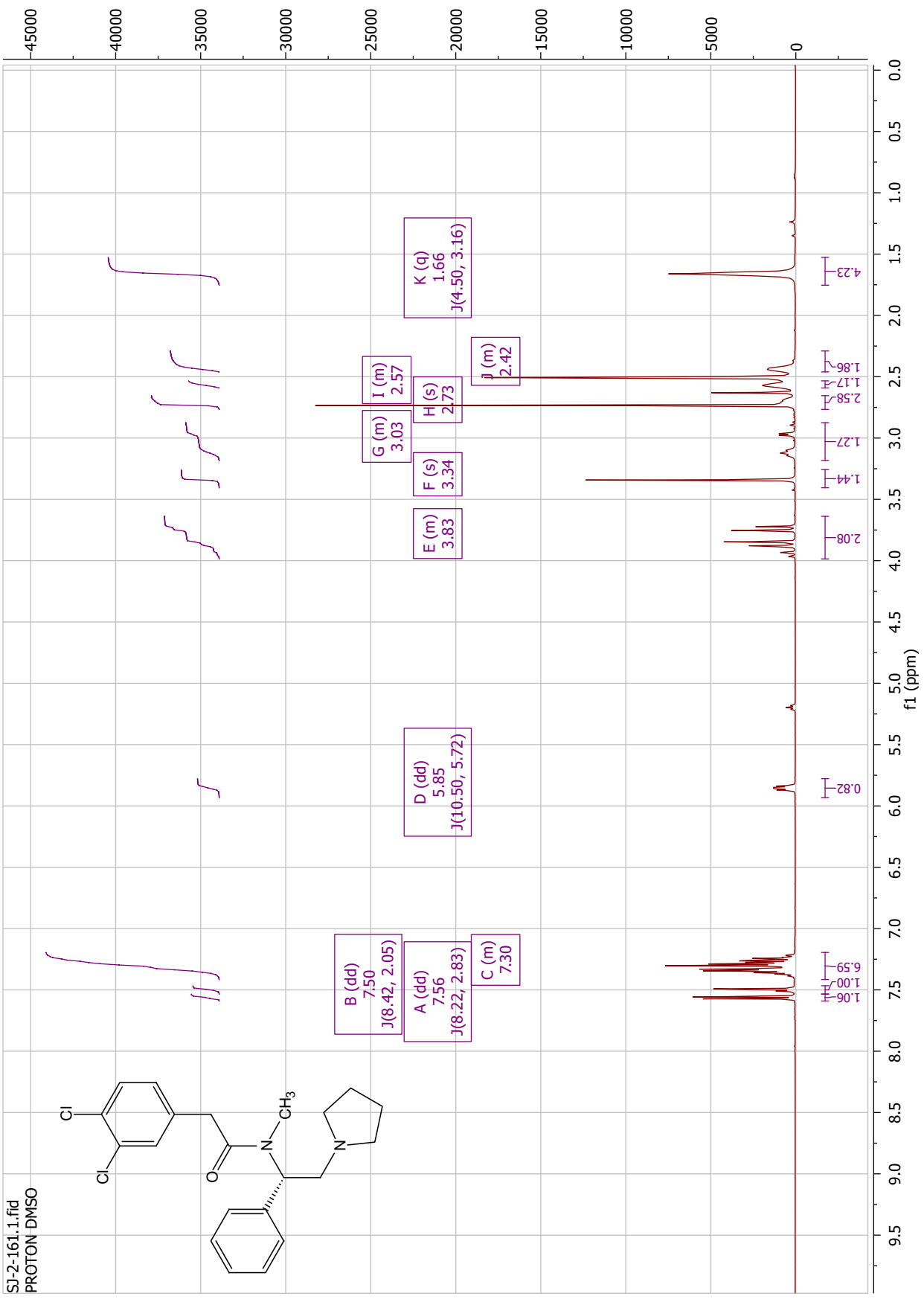
SJ-2-161.1.fid
PROTON DMSO
B (dd)
7.50
J(8.42, 2.05)
A (dd)
7.56
J(8.22, 2.83)
C (m)
7.30
D (dd)
5.85
J(10.50, 5.72)
E (m)
3.83
F (s)
3.34
G (m)
3.03
H (s)
2.73
I (m)
2.57
J (m)
2.42
K (q)
1.66
J(4.50, 3.16)
6.59
1.00
1.06
0.82
2.08
1.44
1.27
2.58
1.17
1.86
4.23
f1 (ppm)

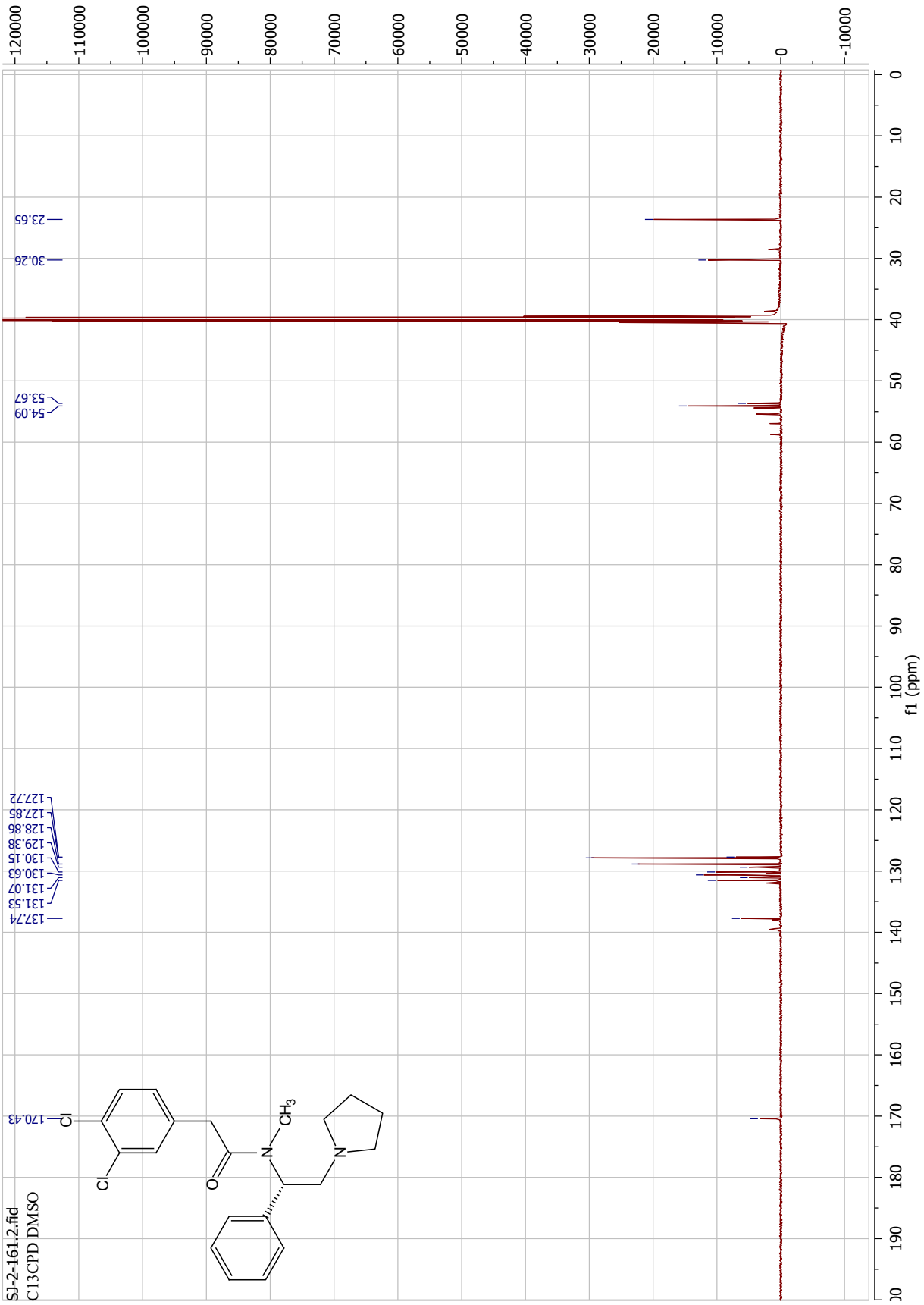
SJ-2-161.2.fid
C13CPD DMSO
23.65
30.26
53.67
54.09
127.72
127.85
128.86
129.38
130.15
130.63
131.07
131.53
137.74
170.43
Cl
Cl
O
N
CH3
N
f1 (ppm)

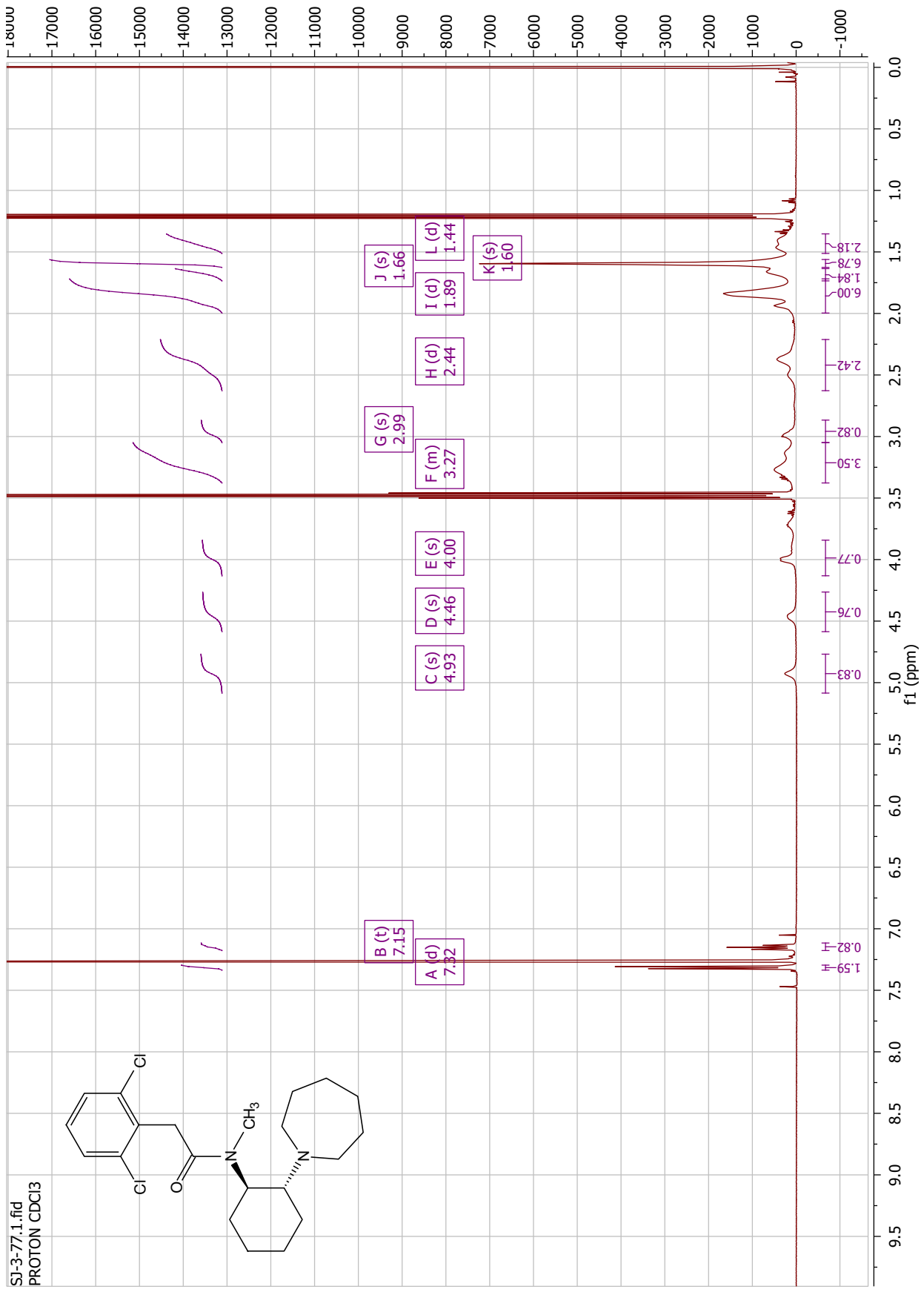
SJ-3-77.1.fid
PROTON CDCl3
A (d) 7.32
B (t) 7.15
C (s) 4.93
D (s) 4.46
E (s) 4.00
F (m) 3.27
G (s) 2.99
H (d) 2.44
I (d) 1.89
J (s) 1.66
K (s) 1.60
L (d) 1.44
f1 (ppm)

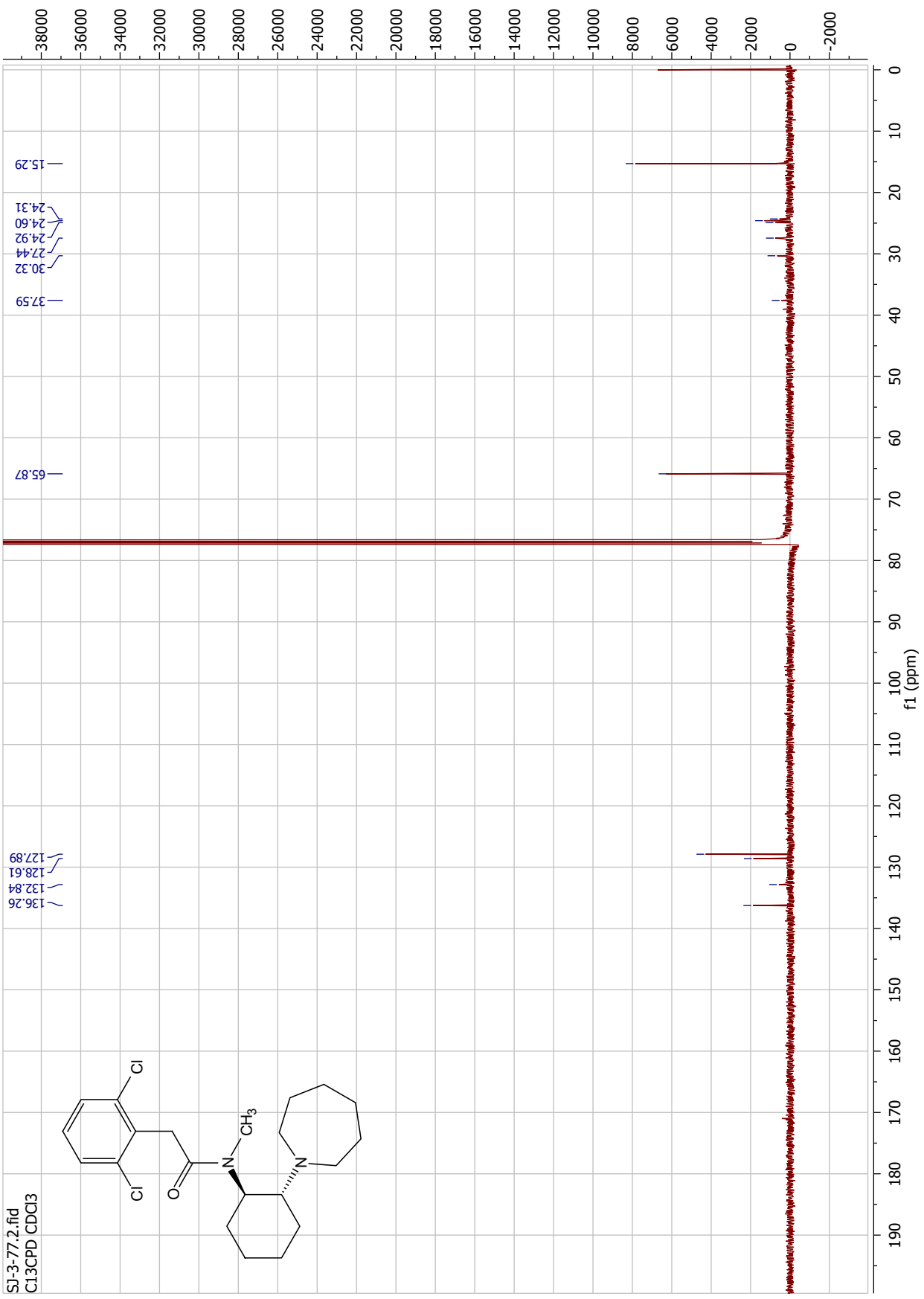
SJ-3-77.2.fid
C13CPD CDCl3
Cl
Cl
O
N
CH3
N
15.29
24.31
24.60
24.92
27.44
30.32
37.59
65.87
127.89
128.61
132.84
136.26
f1 (ppm)

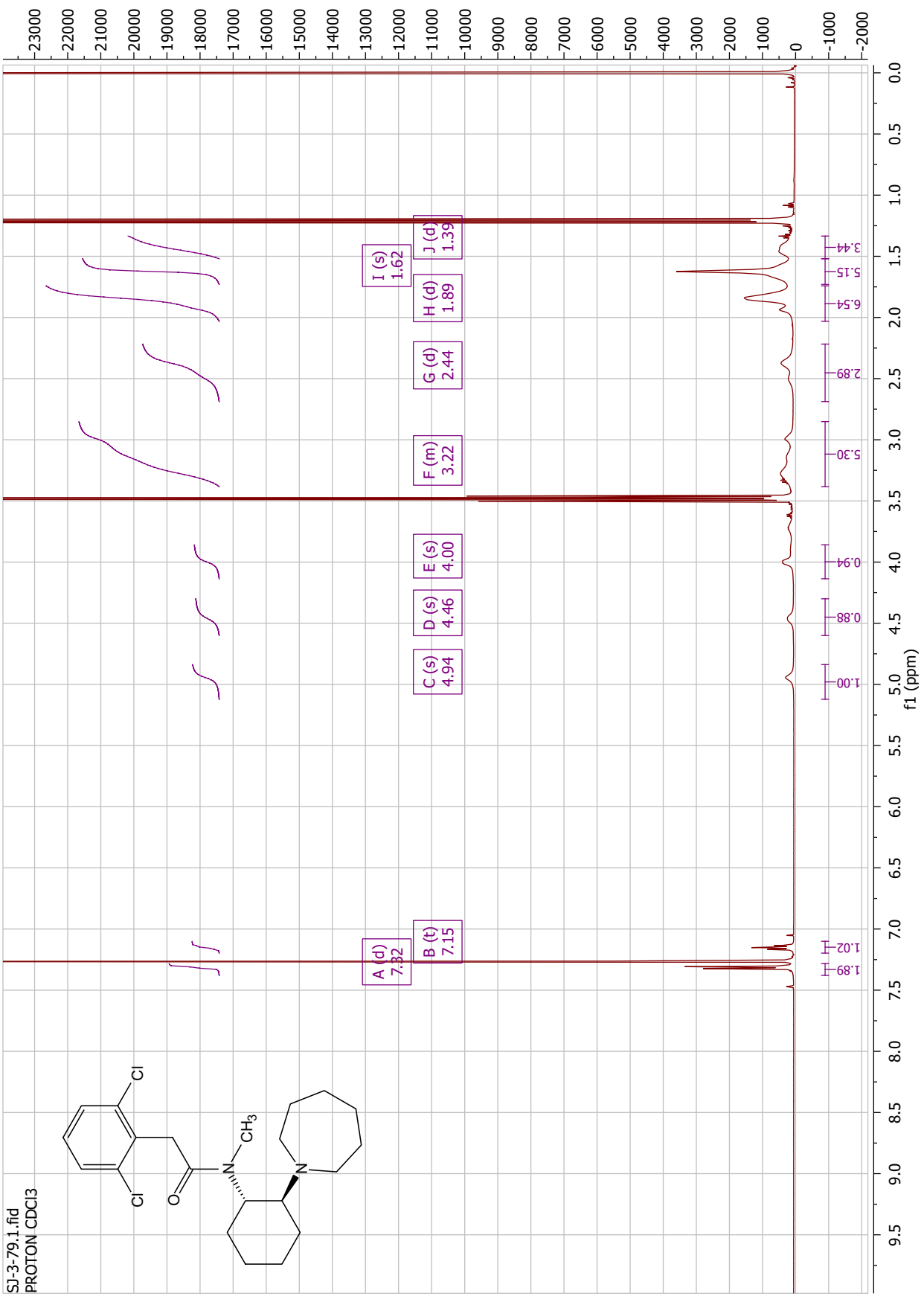
SJ-3-79.1.fid
PROTON CDCl3
A (d) 7.32
B (t) 7.15
C (s) 4.94
D (s) 4.46
E (s) 4.00
F (m) 3.22
G (d) 2.44
H (d) 1.89
I (s) 1.62
J (d) 1.39
3.44
5.15
6.54
2.89
5.30
0.94
0.88
1.00
1.02
1.89
f1 (ppm)


SJ-3-79.2.fid
C13CPD CDCl3
170.98
136.26
132.85
128.61
127.89
99.97
67.35
65.87
37.57
30.35
27.45
24.99
24.78
24.60
24.33
15.29
f1 (ppm)

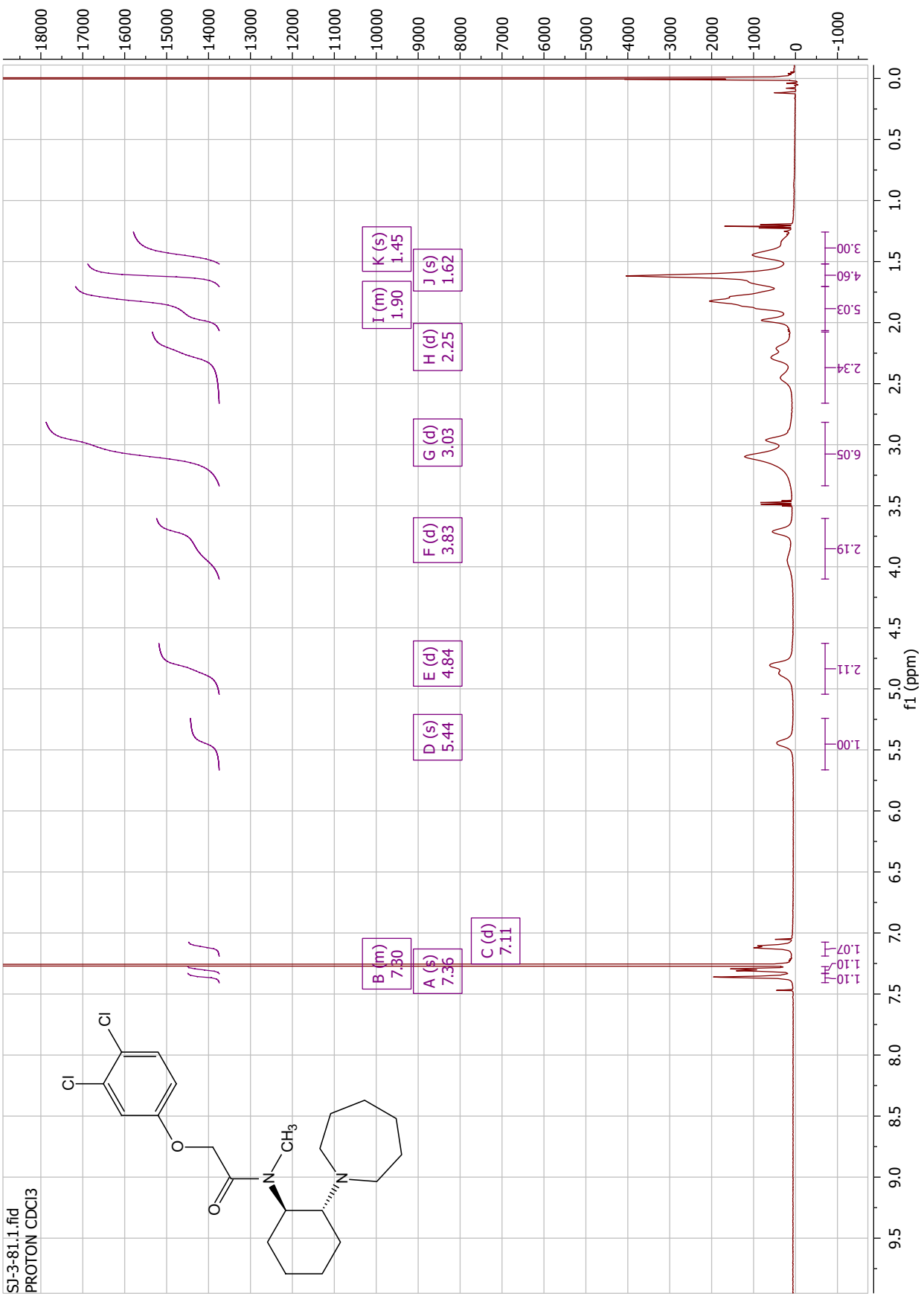
SJ-3-81.1.fid
PROTON CDCl3
A (s) 7.36
B (m) 7.30
C (d) 7.11
D (s) 5.44
E (d) 4.84
F (d) 3.83
G (d) 3.03
H (d) 2.25
I (m) 1.90
J (s) 1.62
K (s) 1.45
1.07
1.10
1.10
1.00
2.11
2.19
6.05
2.34
5.03
4.60
3.00
f1 (ppm)

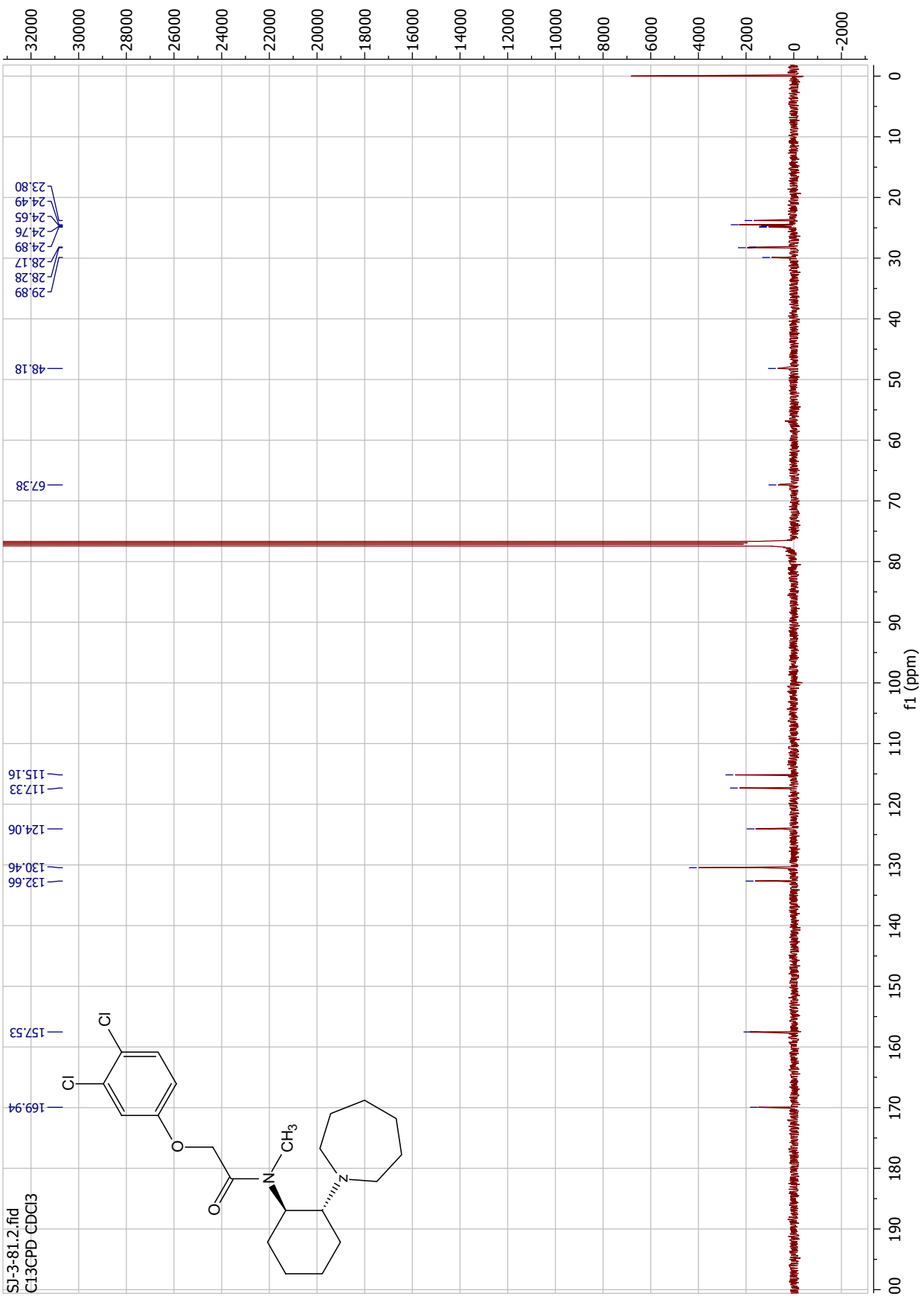
SJ-3-81.2.fid
C13CPD CDCl3
169.94
157.53
132.66
130.46
124.06
117.33
115.16
67.38
48.18
29.89
28.28
28.17
24.89
24.76
24.65
24.49
23.80
f1 (ppm)

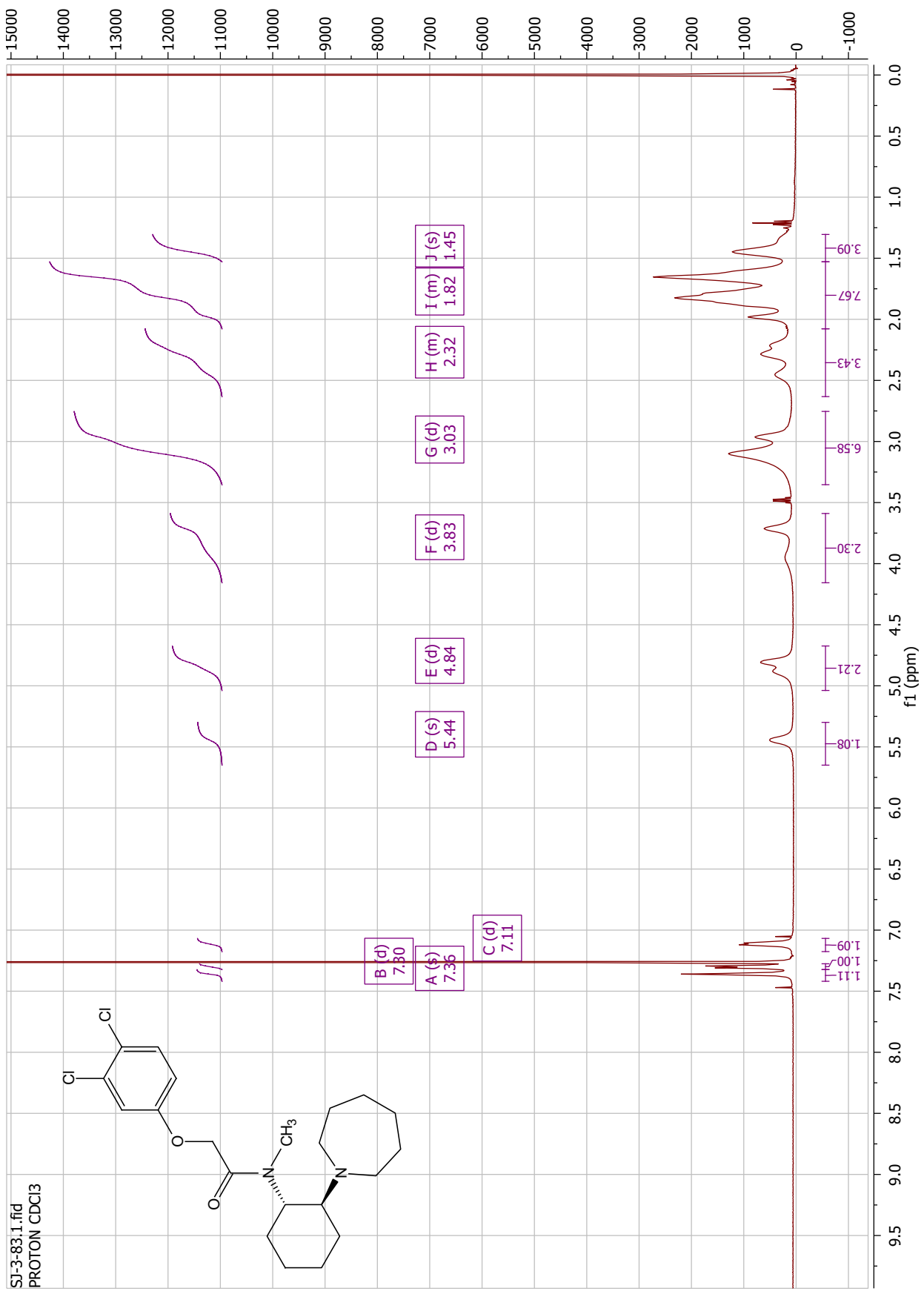
SJ-3-83.1.fid
PROTON CDCl3
B (d) 7.30
A (s) 7.36
C (d) 7.11
D (s) 5.44
E (d) 4.84
F (d) 3.83
G (d) 3.03
H (m) 2.32
I (m) 1.82
J (s) 1.45
1.09
1.00
1.11
1.08
2.21
2.30
6.58
3.43
7.67
3.09
f1 (ppm)

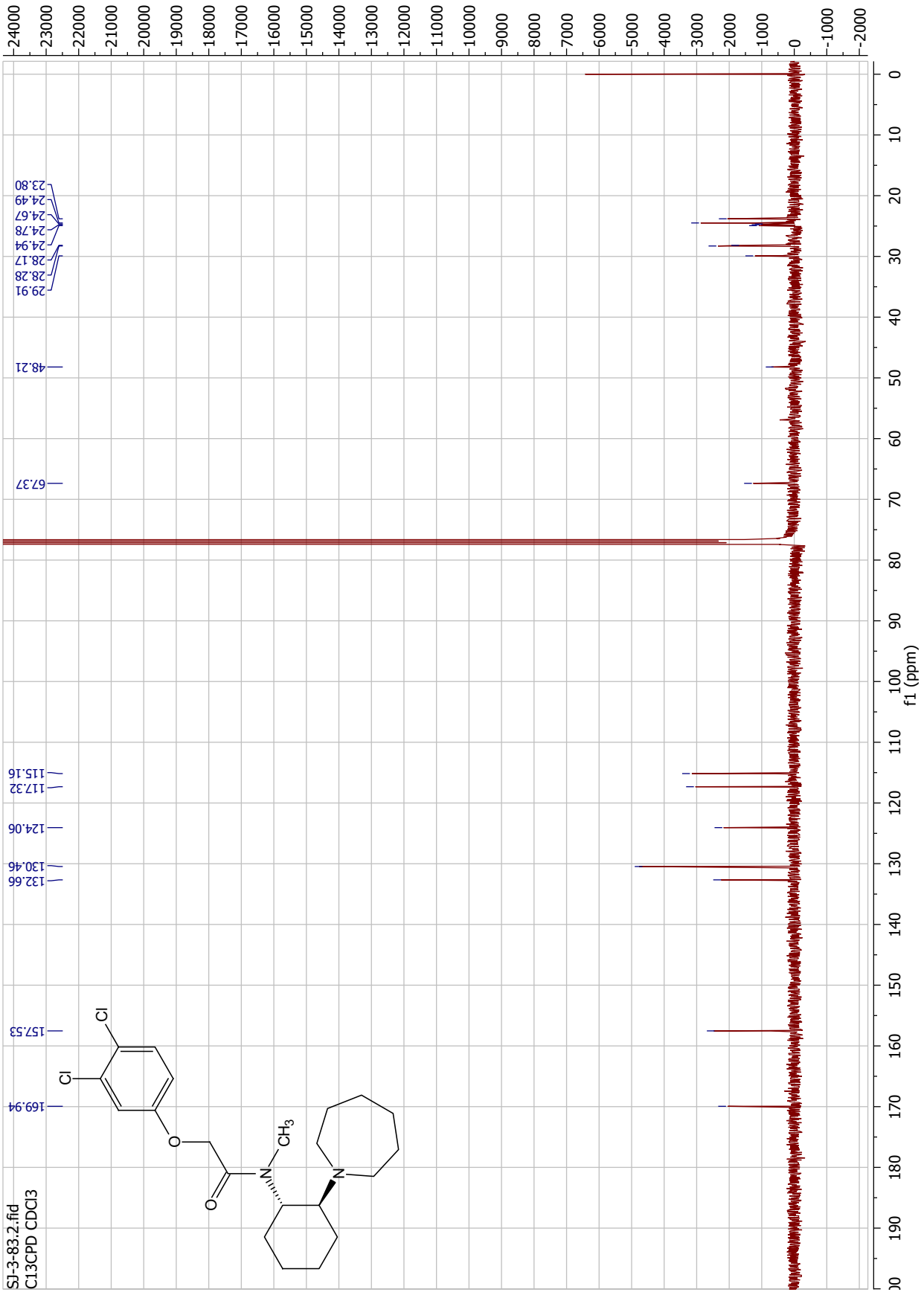
SJ-3-83.2.fid
C13CPD CDCl3
23.80
24.49
24.67
24.78
24.94
28.17
28.28
29.91
48.21
67.37
115.16
117.32
124.06
130.46
132.66
157.53
169.94
f1 (ppm)

Appendix B: HPLC Chromatograms

ID SJ-1-169 File SJ160212WT023 Date 18-Feb-2016 Time 7::1::5 Description MDF087649

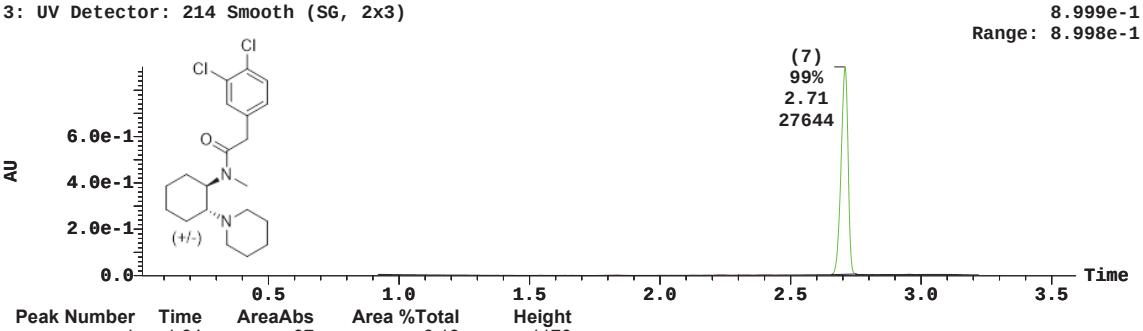

Peak Number	Time	AreaAbs	Area %Total	Height
1	1.84	37	0.13	1176
2	2.23	20	0.07	1053
3	2.33	15	0.05	673
4	2.40	25	0.09	856
5	2.57	18	0.06	909
6	2.61	23	0.08	1110
7	2.71	27644	99.38	894306
8	2.95	35	0.13	2117

Column: Waters XBridge C18, 19 × 150 mm, 5µm; w/ guard column Atlantis T3 19 × 50 mm
Gradient: 75% - 95% Acetonitrile/ pH 9.8 Aqueous Ammonium Hydroxide
Flow Rate: 20 mL/min over 3.5 minutes

ID SJ-1-171 File SJ160212WT025 Date 18-Feb-2016 Time 8::0::3 Description MDF087700

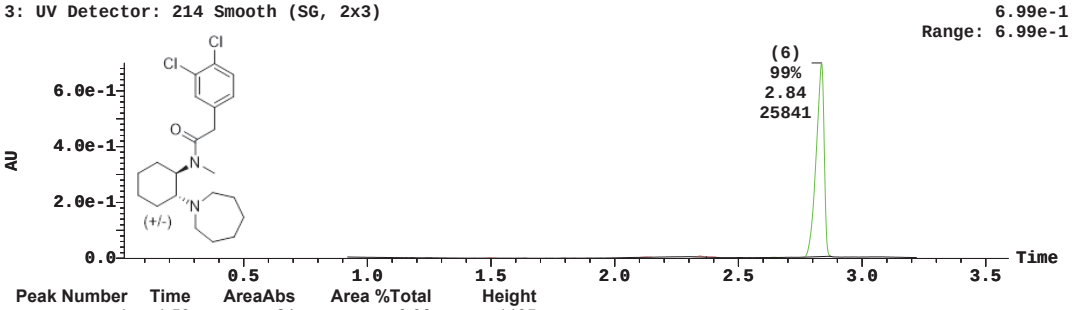

Peak Number	Time	AreaAbs	Area %Total	Height
1	1.50	21	0.08	1105
2	2.13	14	0.05	701
3	2.35	73	0.28	2893
4	2.38	34	0.13	666
5	2.64	15	0.06	758
6	2.84	25841	99.40	693045

Column: Waters XBridge C18, 19 × 150 mm, 5µm; w/ guard column Atlantis T3 19 × 50 mm
Gradient: 75% - 95% Acetonitrile/ pH 9.8 Aqueous Ammonium Hydroxide
Flow Rate: 20 mL/min over 3.5 minutes

ID SJ-3-73 File SJ170301WT001 Date 02-Mar-2017 Time 11:11:52 Description CCT138369

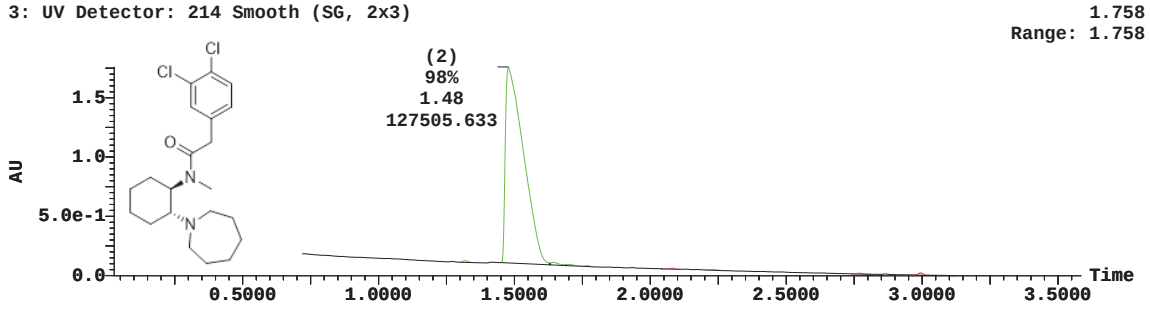

Peak Number	Time	AreaAbs	Area %Total	Height
1	1.32	320	0.25	15377
2	1.48	127506	98.07	1651757
3	1.64	810	0.62	22875
4	1.70	322	0.25	10128
5	1.77	150	0.12	7542
6	2.08	182	0.14	7106
7	2.23	133	0.10	3744
8	2.77	182	0.14	7286
9	2.99	404	0.31	18344

Column: Waters XBridge C18, 19 × 150 mm,
5µm; w/ guard column Atlantis T3 19 × 50 mm
Gradient: 85% - 100% Acetonitrile/ pH 9.8
Aqueous Ammonium Hydroxide
Flow Rate: 20 mL/min over 3.5 minutes

ID SJ-3-75 File SJ170301WT002 Date 02-Mar-2017 Time 11:16:15 Description CCT138372

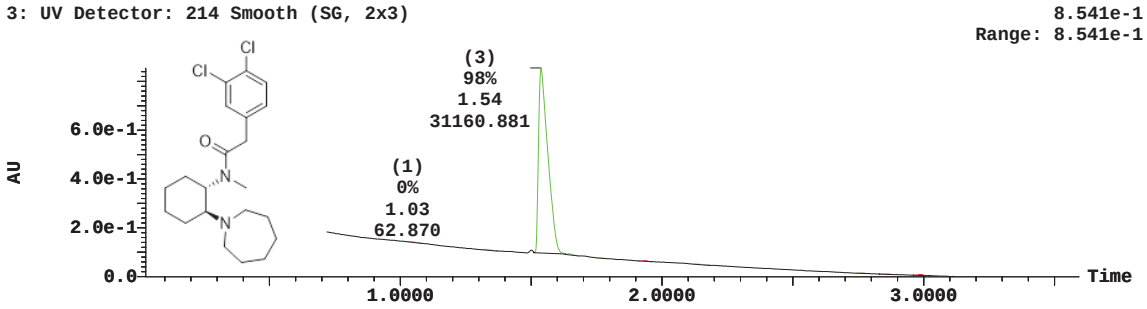

Peak Number	Time	AreaAbs	Area %Total	Height
1	1.03	63	0.20	1206
2	1.33	93	0.29	3285
3	1.54	31161	97.98	757351
4	1.64	93	0.29	3890
5	1.76	32	0.10	783
6	1.93	78	0.25	3558
7	2.13	77	0.24	1127
8	2.76	56	0.18	2313
9	2.86	43	0.14	1659
10	2.99	106	0.33	4307

Column: Waters XBridge C18, 19 × 150 mm,
5µm; w/ guard column Atlantis T3 19 × 50 mm
Gradient: 85% - 100% Acetonitrile/ pH 9.8
Aqueous Ammonium Hydroxide
Flow Rate: 20 mL/min over 3.5 minutes

ID SJ-1-173 File SJ160212WT026 Date 18-Feb-2016 Time 8::4::6 Description MDF087532

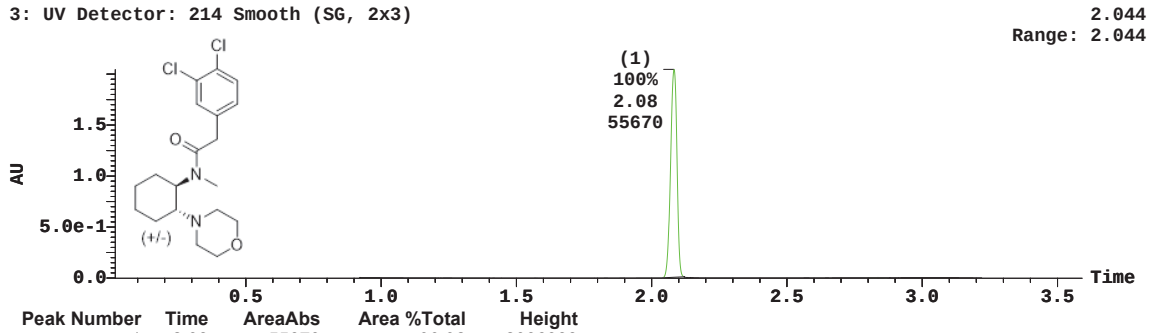

Peak Number	Time	AreaAbs	Area %Total	Height
1	2.08	55670	99.92	2036388
2	2.84	43	0.08	1294

Column: Waters XBridge C18, 19 × 150 mm, 5µm; w/ guard column Atlantis T3 19 × 50 mm
Gradient: 55% - 75% Acetonitrile/ pH 9.8 Aqueous Ammonium Hydroxide
Flow Rate: 20 mL/min over 3.5 minutes

ID SJ-1-175 File SJ160212WT027 Date 18-Feb-2016 Time 8::8::9 Description MDF087537

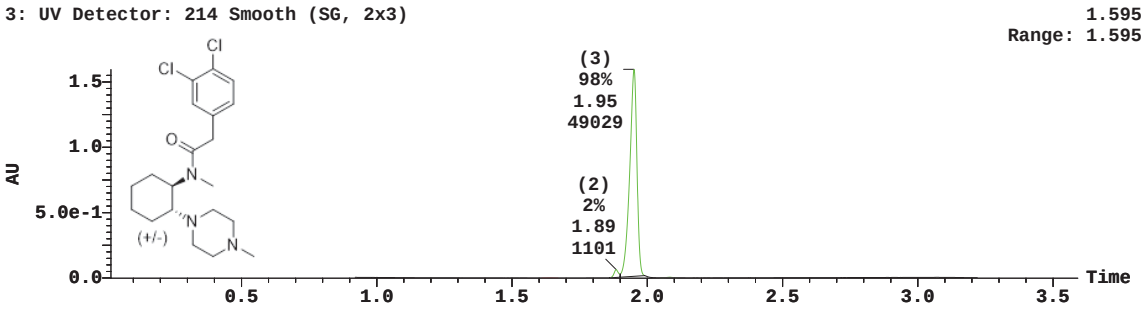

Peak Number	Time	AreaAbs	Area %Total	Height
1	1.64	53	0.10	1618
2	1.89	1101	2.19	58372
3	1.95	49029	97.51	1582017
4	2.08	99	0.20	4139

Column: Waters XBridge C18, 19 × 150 mm, 5µm; w/ guard column Atlantis T3 19 × 50 mm
Gradient: 50% - 70% Acetonitrile/ pH 9.8 Aqueous Ammonium Hydroxide
Flow Rate: 20 mL/min over 3.5 minutes

ID SJ-2-67 File SJ160712WT003 Date 12-Jul-2016 Time 10:50:48 Description MDF088619

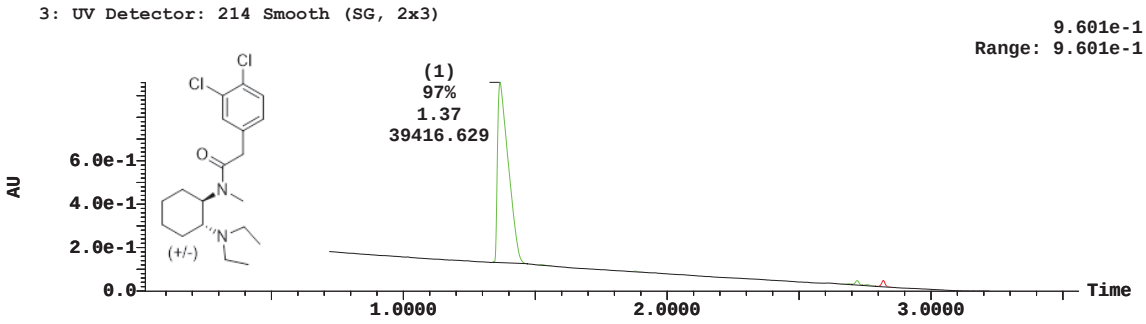

Peak Number	Time	AreaAbs	Area %Total	Height
1	1.37	39417	97.21	829485
2	1.52	61	0.15	3335
3	1.88	53	0.13	3074
4	2.69	62	0.15	3574
5	2.72	368	0.91	20468
6	2.76	130	0.32	4723
7	2.82	456	1.13	29005

Column: Waters XBridge C18, 19 × 150 mm, 5µm; w/ guard column Atlantis T3 19 × 50 mm
Gradient: 85% - 100% Acetonitrile/ pH 9.8 Aqueous Ammonium Hydroxide
Flow Rate: 20 mL/min over 3.5 minutes

ID SJ-2-71 File SJ160712WT006b Date 12-Jul-2016 Time 11:43:08 Description MDF088668

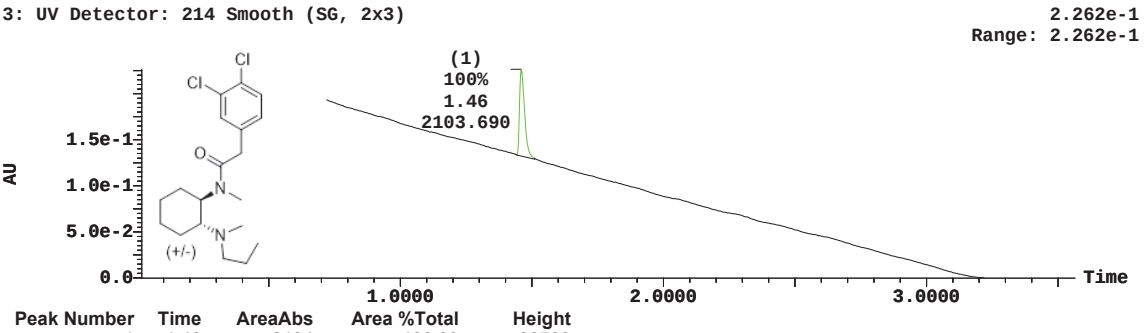

Peak Number	Time	AreaAbs	Area %Total	Height
1	1.46	2104	100.00	93783

Column: Waters XBridge C18, 19 × 150 mm, 5µm; w/ guard column Atlantis T3 19 × 50 mm
Gradient: 85% - 100% Acetonitrile/ pH 9.8 Aqueous Ammonium Hydroxide
Flow Rate: 20 mL/min over 3.5 minutes

ID SJ-2-69 File SJ160712WT005 Date 12-Jul-2016 Time 10:59:30 Description MDF088646

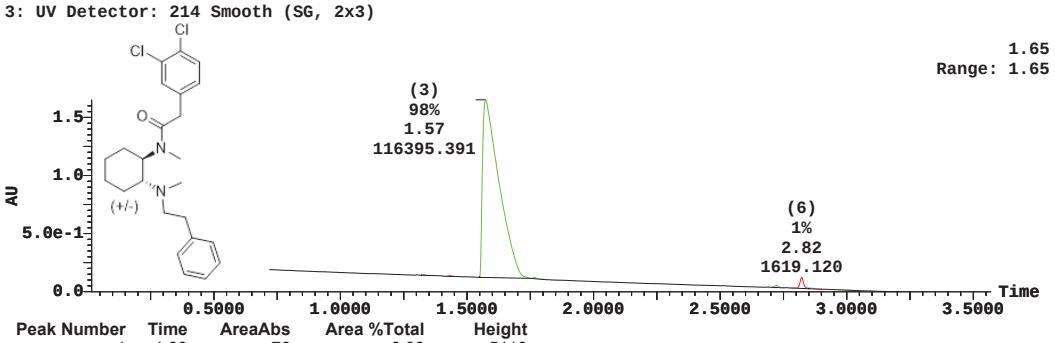

Peak Number	Time	AreaAbs	Area %Total	Height
1	1.33	76	0.06	5118
2	1.43	112	0.09	7546
3	1.57	116395	97.89	1528598
4	1.77	173	0.15	10070
5	2.72	319	0.27	18754
6	2.82	1619	1.36	95400
7	2.86	130	0.11	5267
8	3.00	76	0.06	2773

Column: Waters XBridge C18, 19 × 150 mm, 5µm; w/ guard column Atlantis T3 19 × 50 mm
Gradient: 85% - 100% Acetonitrile/ pH 9.8 Aqueous Ammonium Hydroxide
Flow Rate: 20 mL/min over 3.5 minutes

ID SJ-1-203-160308 File SJ160308WT003 Date 09-Mar-2016 Time 9::9::3 Description SMDF103748

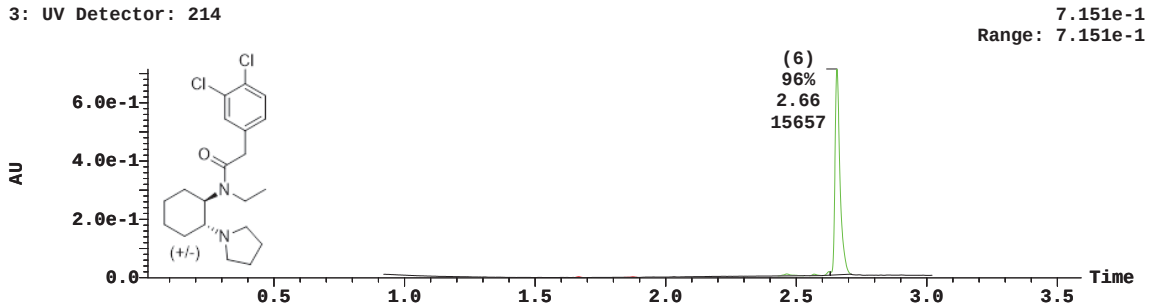

Peak Number	Time	AreaAbs	Area %Total	Height
1	1.67	46	0.28	2699
2	1.87	40	0.25	2088
3	2.46	227	1.40	6541
4	2.57	103	0.63	5086
5	2.63	215	1.32	12691
6	2.66	15657	96.12	705626

Column: Waters XBridge C18, 19 × 150 mm, 5µm; w/ guard column Atlantis T3 19 × 50 mm
Gradient: 75% - 95% Acetonitrile/ pH 9.8 Aqueous Ammonium Hydroxide
Flow Rate: 20 mL/min over 3.5 minutes

ID SJ-1-207-160308 File SJ160308WT004 Date 09-Mar-2016 Time 9::3::7 Description SMDF103747

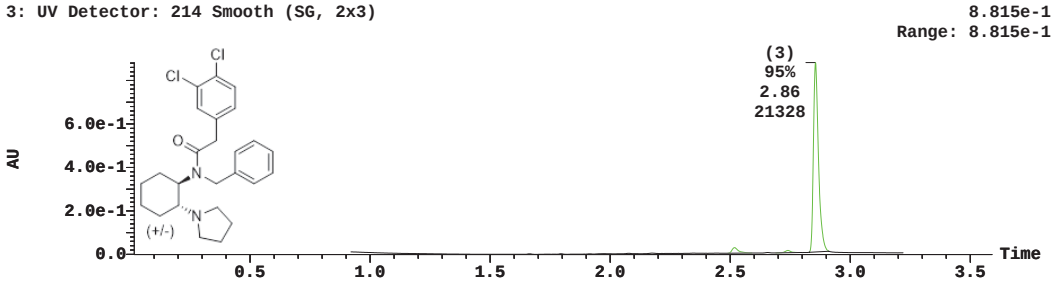

Peak Number	Time	AreaAbs	Area %Total	Height
1	2.52	800	3.57	25542
2	2.74	301	1.34	10703
3	2.86	21328	95.09	870646

Column: Waters XBridge C18, 19 × 150 mm, 5µm; w/ guard column Atlantis T3 19 × 50 mm
Gradient: 85% - 100% Acetonitrile/ pH 9.8 Aqueous Ammonium Hydroxide
Flow Rate: 20 mL/min over 3.5 minutes

ID SJ-1-135-160215 File SJ160215WT003 Date 16-Feb-2016 Time 11:56:58 Description SMDF103702

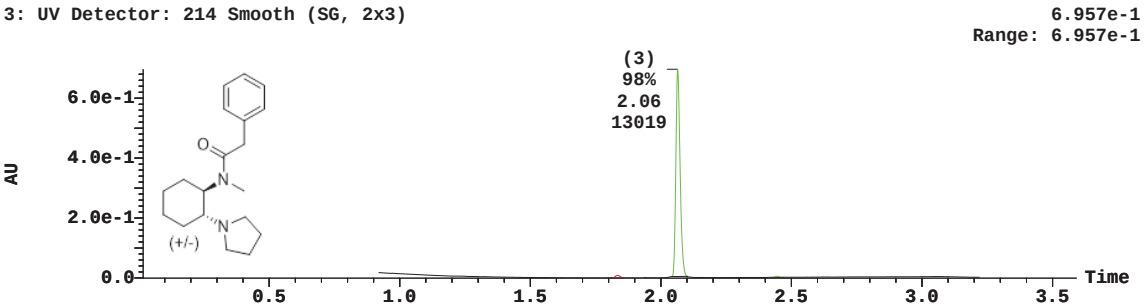

Peak Number	Time	AreaAbs	Area %Total	Height
1	1.83	174	1.31	8289
2	1.95	8	0.06	581
3	2.06	13019	98.11	690925
5	2.44	68	0.51	3588

Column: Waters XBridge C18, 19 × 150 mm, 5µm; w/ guard column Atlantis T3 19 × 50 mm
Gradient: 55% - 75% Acetonitrile/ pH 9.8 Aqueous Ammonium Hydroxide
Flow Rate: 20 mL/min over 3.5 minutes

ID SJ-1-145 File SJ160212WT001 Date 18-Feb-2016 Time 6::4::6 Description SMDF103689

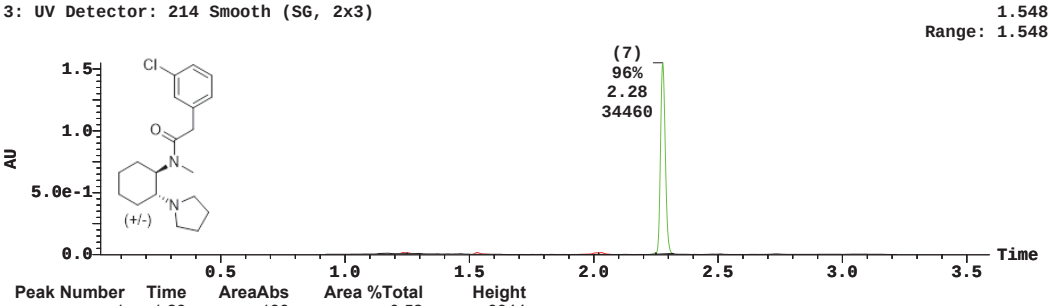

Peak Number	Time	AreaAbs	Area %Total	Height
1	1.23	188	0.52	8944
2	1.25	89	0.25	6351
3	1.53	365	1.01	14119
4	2.01	428	1.19	13292
5	2.03	429	1.19	15327
6	2.25	99	0.27	10409
7	2.28	34460	95.57	1542527

Column: Waters XBridge C18, 19 × 150 mm, 5µm; w/ guard column Atlantis T3 19 × 50 mm
Gradient: 60% - 80% Acetonitrile/ pH 9.8 Aqueous Ammonium Hydroxide
Flow Rate: 20 mL/min over 3.5 minutes

ID SJ-1-137 File SJ160213WT003b Date 12-Feb-2016 Time 3::0::4 Description MDF031838

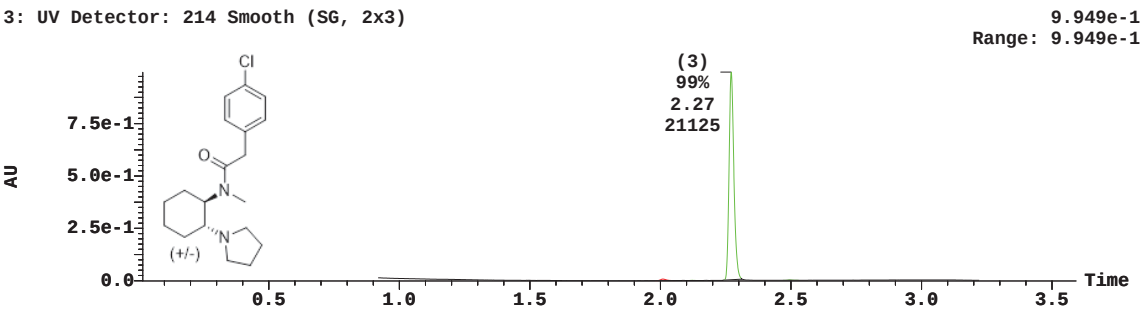

Peak Number	Time	AreaAbs	Area %Total	Height
1	2.01	179	0.84	7238
2	2.12	21	0.10	968
3	2.27	21125	98.81	990293
4	2.49	54	0.25	2708

Column: Waters XBridge C18, 19 × 150 mm, 5µm; w/ guard column Atlantis T3 19 × 50 mm
Gradient: 60% - 80% Acetonitrile/ pH 9.8 Aqueous Ammonium Hydroxide
Flow Rate: 20 mL/min over 3.5 minutes

ID SJ-1-153 File SJ160212WT009 Date 18-Feb-2016 Time 6::0::6 Description SMDF103718

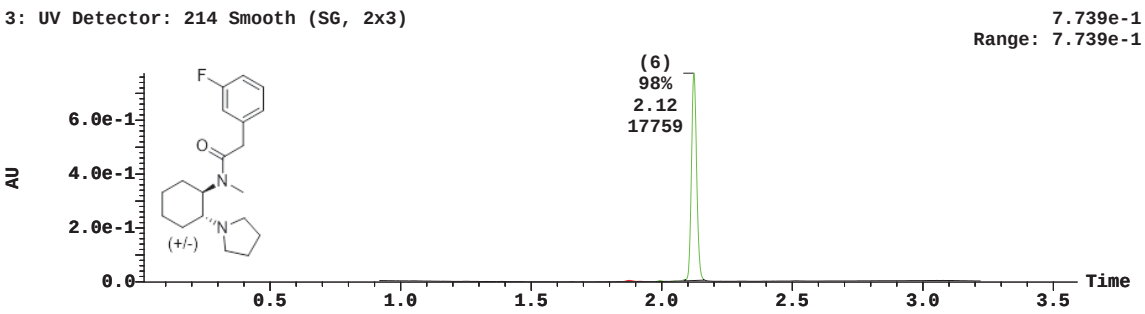

Peak Number	Time	AreaAbs	Area %Total	Height
1	1.88	140	0.78	4560
2	1.92	30	0.17	1246
3	1.99	56	0.31	3531
4	2.05	14	0.08	891
5	2.09	47	0.26	4426
6	2.12	17759	98.40	769063

Column: Waters XBridge C18, 19 × 150 mm, 5µm; w/ guard column Atlantis T3 19 × 50 mm
Gradient: 60% - 80% Acetonitrile/ pH 9.8 Aqueous Ammonium Hydroxide
Flow Rate: 20 mL/min over 3.5 minutes

ID SJ-1-139 File SJ160213WT004c Date 12-Feb-2016 Time 3::6::1 Description MDF031813

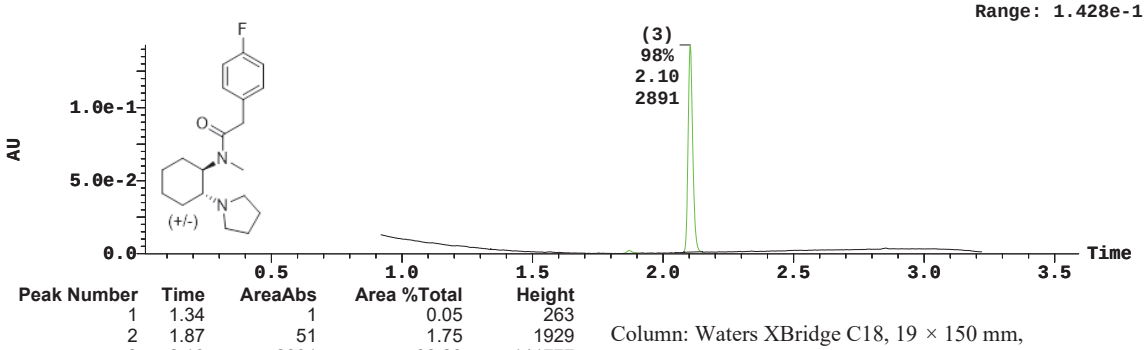

Peak Number	Time	AreaAbs	Area %Total	Height
1	1.34	1	0.05	263
2	1.87	51	1.75	1929
3	2.10	2891	98.20	141777

Column: Waters XBridge C18, 19 × 150 mm, 5µm; w/ guard column Atlantis T3 19 × 50 mm
Gradient: 55% - 75% Acetonitrile/ pH 9.8 Aqueous Ammonium Hydroxide
Flow Rate: 20 mL/min over 3.5 minutes

ID SJ-1-191 File SJ160307WT012 Date 07-Mar-2016 Time 12:54:20 Description MDF087792

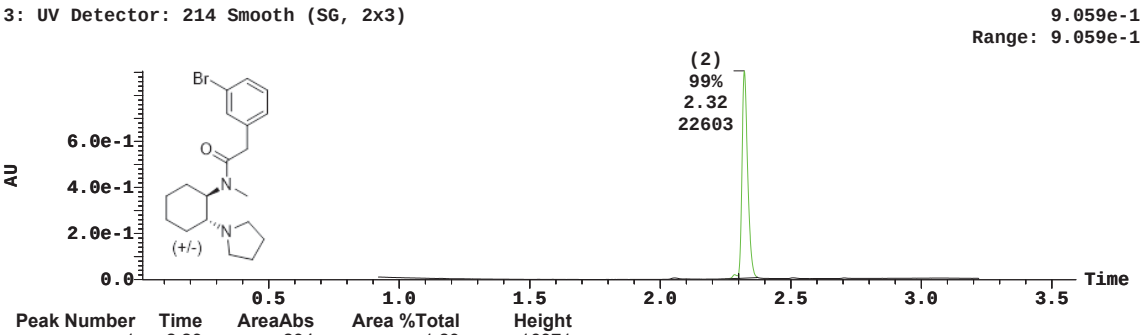

Peak Number	Time	AreaAbs	Area %Total	Height
1	2.29	294	1.29	16371
2	2.32	22603	98.71	899697

Column: Waters XBridge C18, 19 × 150 mm, 5µm; w/ guard column Atlantis T3 19 × 50 mm
Gradient: 70% - 90% Acetonitrile/ pH 9.8 Aqueous Ammonium Hydroxide
Flow Rate: 20 mL/min over 3.5 minutes

ID SJ-1-193 File SJ160307WT014 Date 07-Mar-2016 Time 1::3::3 Description MDF087800

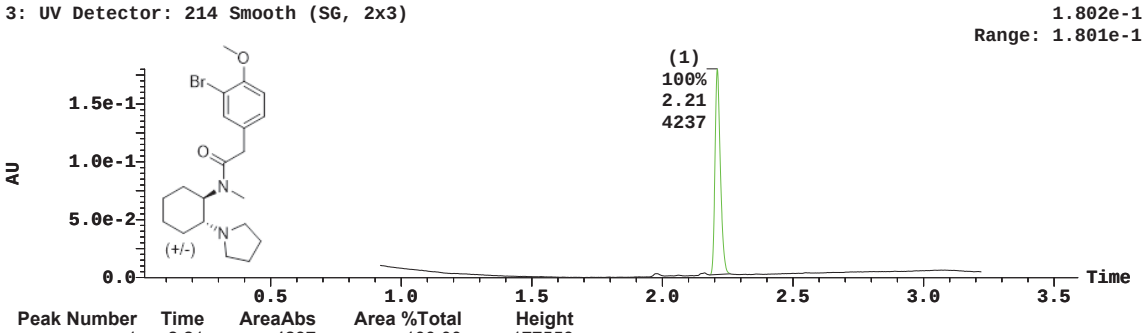

Peak Number	Time	AreaAbs	Area %Total	Height
1	2.21	4237	100.00	177558

Column: Waters XBridge C18, 19 × 150 mm, 5µm; w/ guard column Atlantis T3 19 × 50 mm
Gradient: 70% - 90% Acetonitrile/ pH 9.8 Aqueous Ammonium Hydroxide
Flow Rate: 20 mL/min over 3.5 minutes

ID SJ-1-185 File SJ160307WT006 Date 07-Mar-2016 Time 12:28:05 Description MDF087726

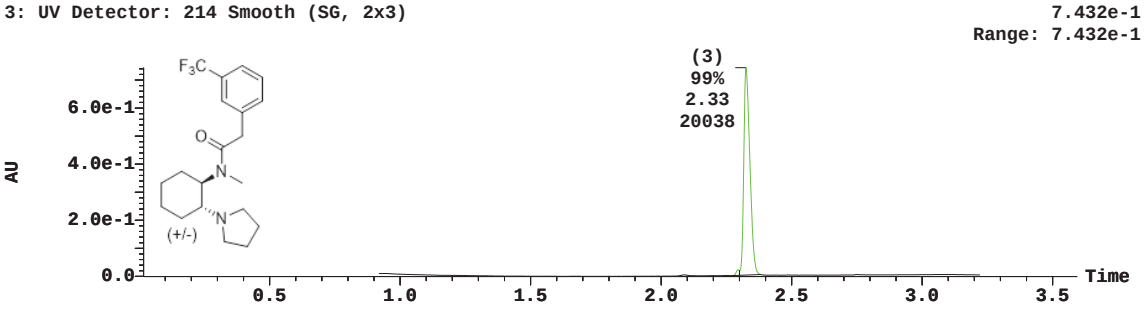

Peak Number	Time	AreaAbs	Area %Total	Height
2	2.29	263	1.30	19682
3	2.33	20038	98.70	738645

Column: Waters XBridge C18, 19 × 150 mm, 5µm; w/ guard column Atlantis T3 19 × 50 mm
Gradient: 65% - 85% Acetonitrile/ pH 9.8 Aqueous Ammonium Hydroxide
Flow Rate: 20 mL/min over 3.5 minutes

ID SJ-1-187 File SJ160307WT008 Date 07-Mar-2016 Time 12:36:54 Description MDF087723

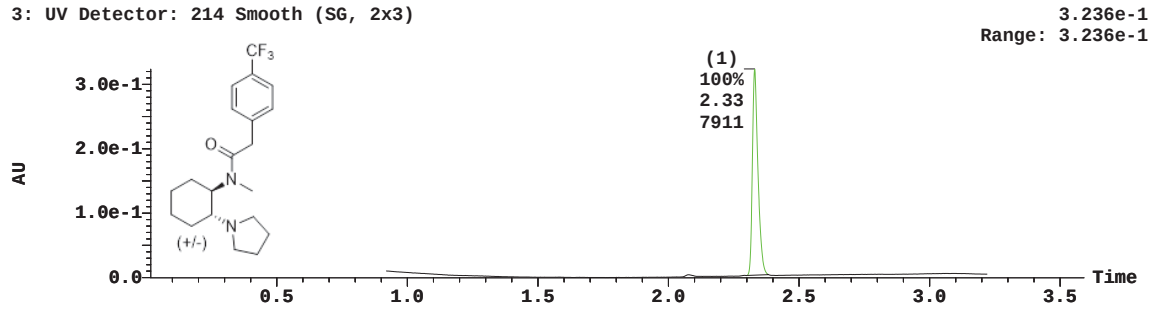

Peak Number	Time	AreaAbs	Area %Total	Height
1	2.33	7911	100.00	319834

Column: Waters XBridge C18, 19 × 150 mm, 5µm; w/ guard column Atlantis T3 19 × 50 mm
Gradient: 65% - 85% Acetonitrile/ pH 9.8 Aqueous Ammonium Hydroxide
Flow Rate: 20 mL/min over 3.5 minutes

ID SJ-2-23 File SJ160609WT003 Date 09-Jun-2016 Time 14:08:59 Description MDF088258

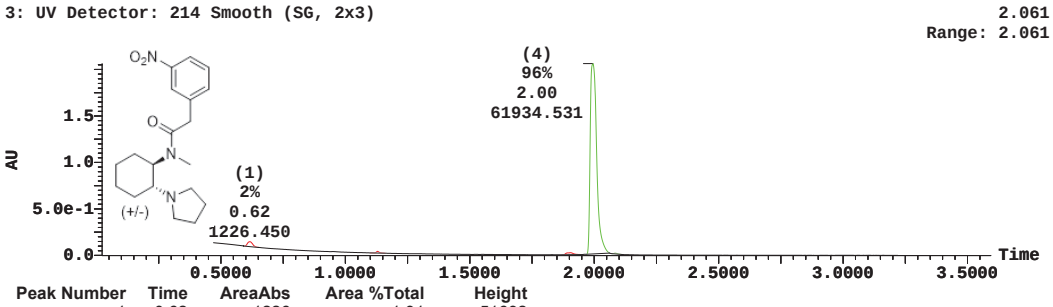

Peak Number	Time	AreaAbs	Area %Total	Height
1	0.62	1226	1.91	51692
2	1.13	256	0.40	18029
3	1.90	713	1.11	21183
4	2.00	61935	96.39	2046142
5	2.08	126	0.20	7656

Column: Waters XBridge C18, 19 × 150 mm, 5µm; w/ guard column Atlantis T3 19 × 50 mm
Gradient: 85% - 100% Acetonitrile/ pH 9.8 Aqueous Ammonium Hydroxide
Flow Rate: 20 mL/min over 3.5 minutes

ID SJ-2-25 File SJ160609WT004 Date 09-Jun-2016 Time 14:13:34 Description MDF088373

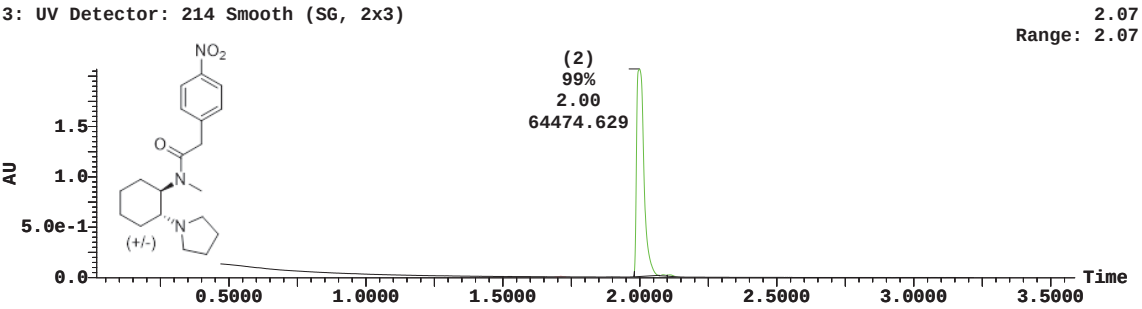

Peak Number	Time	AreaAbs	Area %Total	Height
1	1.71	71	0.11	4183
2	2.00	64475	99.08	2058476
3	2.09	180	0.28	11430
4	2.11	346	0.53	14739

Column: Waters XBridge C18, 19 × 150 mm, 5µm; w/ guard column Atlantis T3 19 × 50 mm
Gradient: 85% - 100% Acetonitrile/ pH 9.8 Aqueous Ammonium Hydroxide
Flow Rate: 20 mL/min over 3.5 minutes

ID SJ-1-155 File SJ160212WT011 Date 18-Feb-2016 Time 6::8::4 Description MDF087598

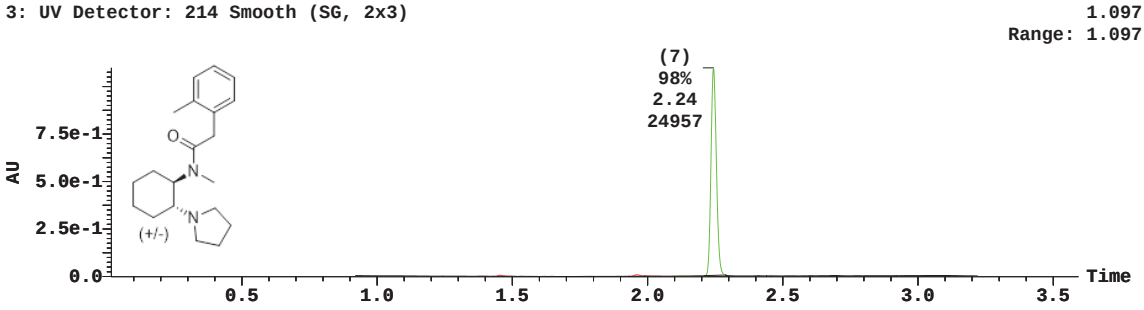

Peak Number	Time	AreaAbs	Area %Total	Height
1	1.38	20	0.08	984
2	1.46	146	0.57	5650
3	1.96	215	0.84	7517
4	2.00	71	0.28	2366
5	2.13	46	0.18	1746
6	2.18	54	0.21	2108
7	2.24	24957	97.62	1091294
9	2.46	55	0.22	2922

Column: Waters XBridge C18, 19 × 150 mm, 5µm; w/ guard column Atlantis T3 19 × 50 mm
Gradient: 60% - 80% Acetonitrile/ pH 9.8 Aqueous Ammonium Hydroxide
Flow Rate: 20 mL/min over 3.5 minutes

ID SJ-1-157 File SJ160212WT013 Date 18-Feb-2016 Time 7::7::2 Description MDF087576

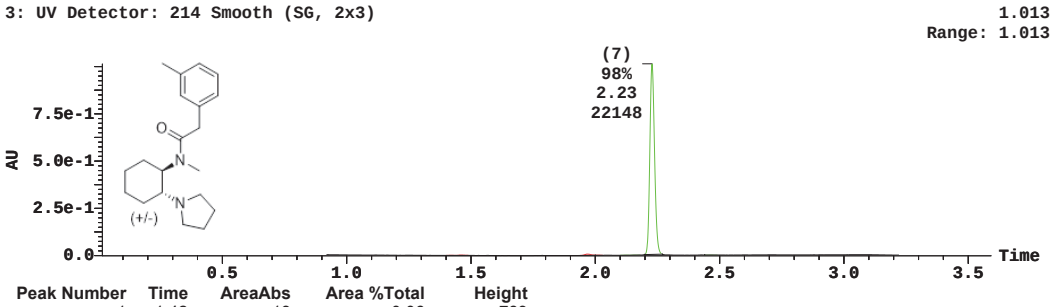

Peak Number	Time	AreaAbs	Area %Total	Height
1	1.42	13	0.06	789
2	1.46	41	0.18	1824
3	1.97	206	0.92	6682
4	2.01	24	0.11	1383
5	2.12	17	0.08	941
6	2.16	25	0.11	1172
7	2.23	22148	98.43	1007027
8	2.47	28	0.12	1326

Column: Waters XBridge C18, 19 × 150 mm, 5µm; w/ guard column Atlantis T3 19 × 50 mm
Gradient: 60% - 80% Acetonitrile/ pH 9.8 Aqueous Ammonium Hydroxide
Flow Rate: 20 mL/min over 3.5 minutes

ID SJ-1-181 File SJ160307WT002 Date 07-Mar-2016 Time 12:10:26 Description MDF087724

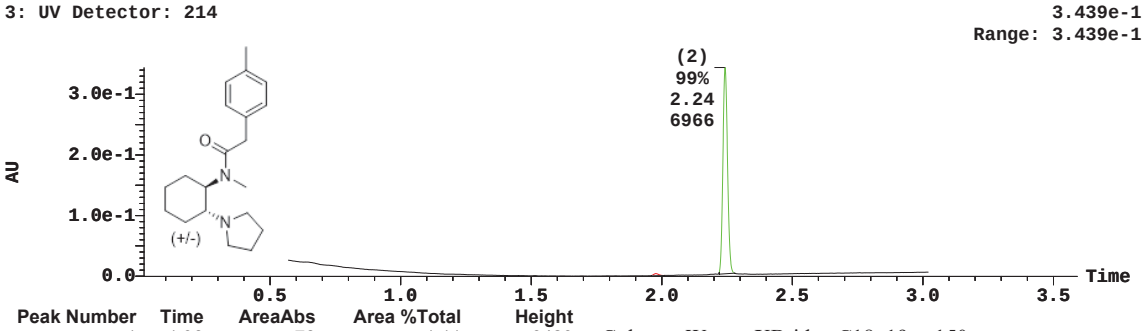

Peak Number	Time	AreaAbs	Area %Total	Height
1	1.98	78	1.11	3420
2	2.24	6966	98.89	339787

Column: Waters XBridge C18, 19 × 150 mm, 5µm; w/ guard column Atlantis T3 19 × 50 mm
Gradient: 60% - 80% Acetonitrile/ pH 9.8 Aqueous Ammonium Hydroxide
Flow Rate: 20 mL/min over 3.5 minutes

ID SJ-1-183 File SJ160307WT004 Date 07-Mar-2016 Time 12:19:14 Description MDF087737

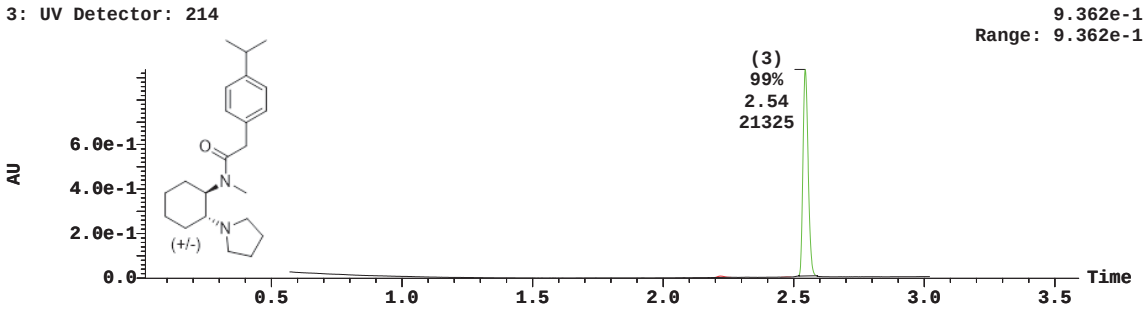

Peak Number	Time	AreaAbs	Area %Total	Height
1	2.22	184	0.85	6185
2	2.47	23	0.11	1356
3	2.54	21325	99.04	926435

Column: Waters XBridge C18, 19 × 150 mm, 5µm; w/ guard column Atlantis T3 19 × 50 mm
Gradient: 70% - 90% Acetonitrile/ pH 9.8 Aqueous Ammonium Hydroxide
Flow Rate: 20 mL/min over 3.5 minutes

ID SJ-1-141 File SJ160213WT005b Date 12-Feb-2016 Time 3::9::6 Description MDF031824

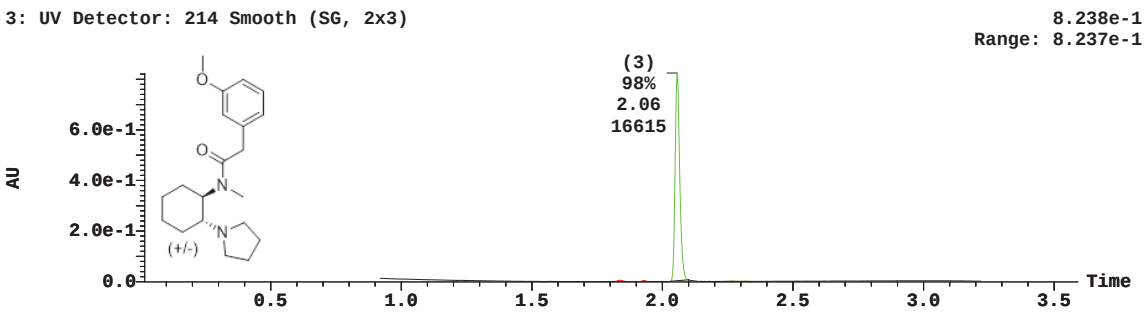

Peak Number	Time	AreaAbs	Area %Total	Height
1	1.84	138	0.82	5600
2	1.93	85	0.50	4782
3	2.06	16615	98.37	819777
5	2.27	41	0.24	2126
6	2.32	11	0.06	883

Column: Waters XBridge C18, 19 × 150 mm, 5µm; w/ guard column Atlantis T3 19 × 50 mm
Gradient: 55% - 75% Acetonitrile/ pH 9.8 Aqueous Ammonium Hydroxide
Flow Rate: 20 mL/min over 3.5 minutes

ID SJ-1-143 File SJ160213WT006b Date 12-Feb-2016 Time 3::4::1 Description SMDF103630

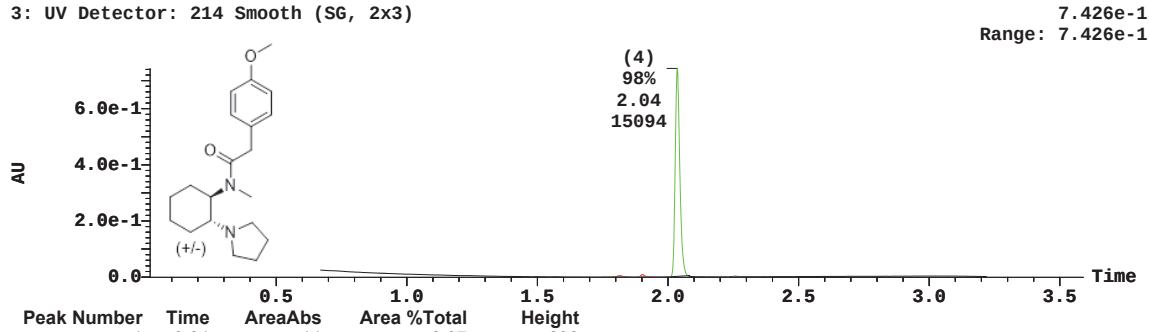

Peak Number	Time	AreaAbs	Area %Total	Height
1	0.91	11	0.07	698
2	1.82	113	0.73	4707
3	1.90	151	0.98	8791
4	2.04	15094	97.85	739813
5	2.26	56	0.36	2931

Column: Waters XBridge C18, 19 × 150 mm, 5µm; w/ guard column Atlantis T3 19 × 50 mm
Gradient: 55% - 75% Acetonitrile/ pH 9.8 Aqueous Ammonium Hydroxide
Flow Rate: 20 mL/min over 3.5 minutes

ID SJ-1-189 File SJ160307WT010 Date 07-Mar-2016 Time 12:45:37 Description MDF087735

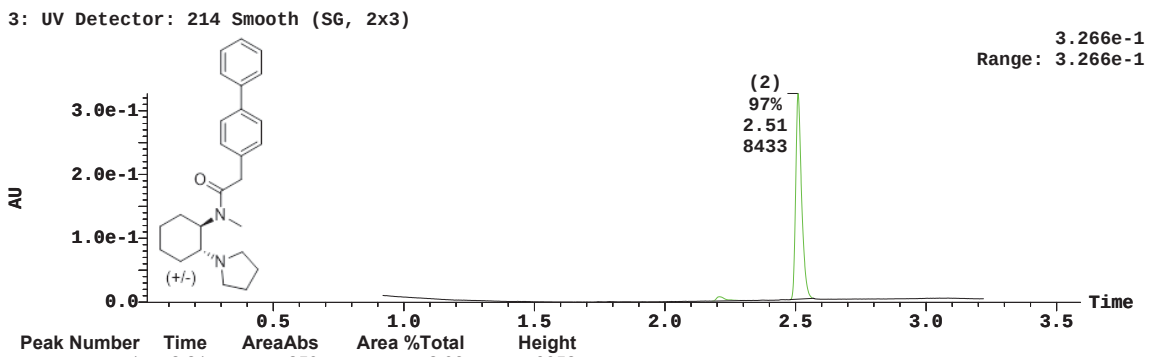

Peak Number	Time	AreaAbs	Area %Total	Height
1	2.21	259	2.98	6652
2	2.51	8433	97.02	321950

Column: Waters XBridge C18, 19 × 150 mm, 5µm; w/ guard column Atlantis T3 19 × 50 mm
Gradient: 70% - 90% Acetonitrile/ pH 9.8 Aqueous Ammonium Hydroxide
Flow Rate: 20 mL/min over 3.5 minutes

ID SJ-1-159 File SJ160212WT015 Date 18-Feb-2016 Time 7::6::4 Description MDF087574

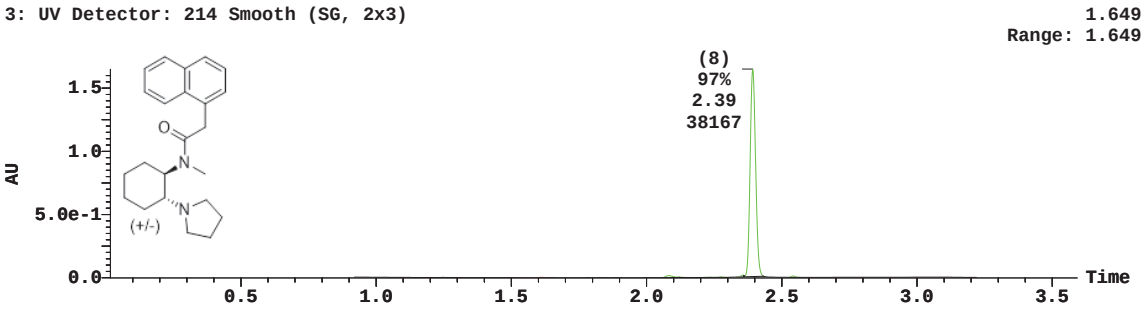

Peak Number	Time	AreaAbs	Area %Total	Height
1	1.55	30	0.08	1284
2	1.61	58	0.15	2514
3	2.08	470	1.20	15372
4	2.12	53	0.14	2907
5	2.23	46	0.12	1435
6	2.28	65	0.17	4023
7	2.36	218	0.56	14321
8	2.39	38167	97.16	1640113
9	2.54	176	0.45	10073

Column: Waters XBridge C18, 19 × 150 mm, 5µm; w/ guard column Atlantis T3 19 × 50 mm
Gradient: 65% - 85% Acetonitrile/ pH 9.8 Aqueous Ammonium Hydroxide
Flow Rate: 20 mL/min over 3.5 minutes

ID SJ-1-161 File SJ160212WT017 Date 18-Feb-2016 Time 7::5::1 Description MDF087583

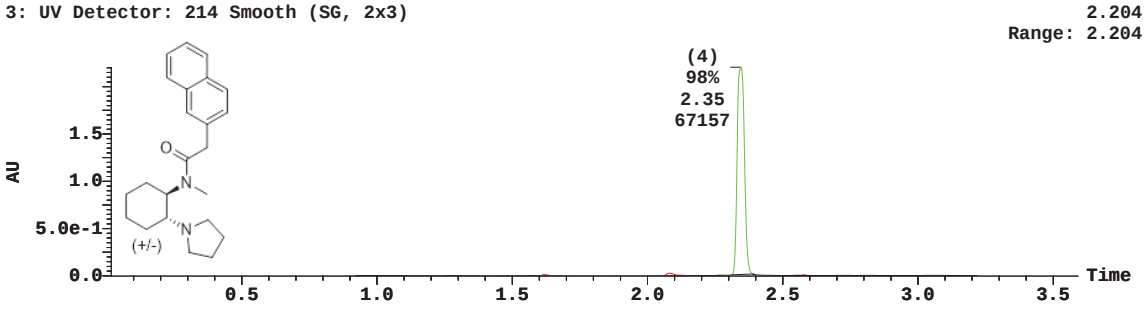

Peak Number	Time	AreaAbs	Area %Total	Height
1	1.62	295	0.43	12638
2	2.08	948	1.38	26494
3	2.27	96	0.14	4231
4	2.35	67157	97.73	2189060
5	2.55	72	0.10	3835
6	2.58	146	0.21	7281

Column: Waters XBridge C18, 19 × 150 mm, 5µm; w/ guard column Atlantis T3 19 × 50 mm
Gradient: 65% - 85% Acetonitrile/ pH 9.8 Aqueous Ammonium Hydroxide
Flow Rate: 20 mL/min over 3.5 minutes

ID SJ-1-147 File SJ160212WT004 Date 18-Feb-2016 Time 6::8::2 Description SMDF103697

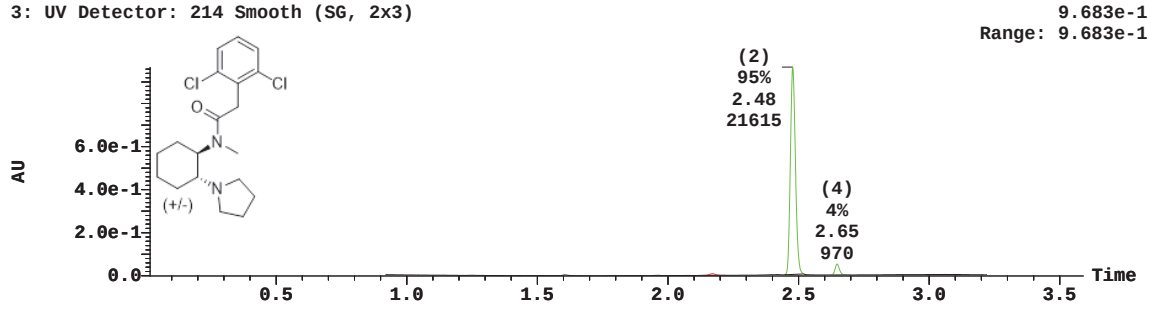

Peak Number	Time	AreaAbs	Area %Total	Height
1	2.17	211	0.93	7271
2	2.48	21615	94.82	962148
4	2.65	970	4.26	50406

Column: Waters XBridge C18, 19 × 150 mm, 5µm; w/ guard column Atlantis T3 19 × 50 mm
Gradient: 70% - 90% Acetonitrile/ pH 9.8 Aqueous Ammonium Hydroxide
Flow Rate: 20 mL/min over 3.5 minutes

ID SJ-2-293 File SJ170202WT004b Date 06-Feb-2017 Time 12:02:21 Description CCT138036

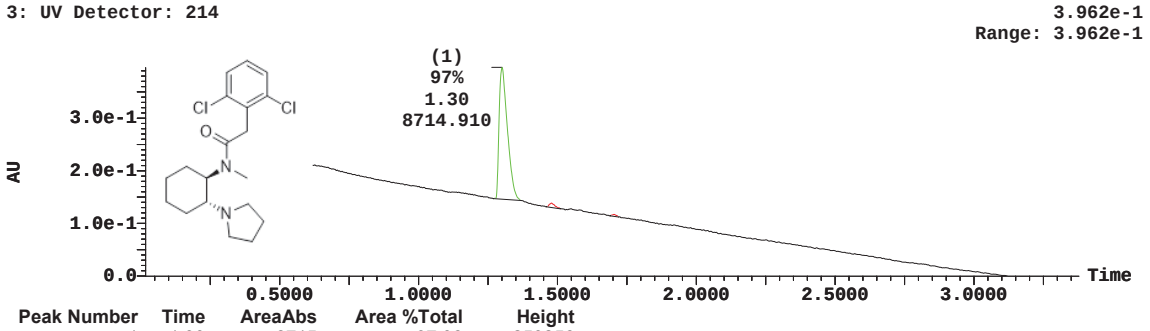

Peak Number	Time	AreaAbs	Area %Total	Height
1	1.30	8715	97.06	250256
3	1.48	196	2.18	8533
4	1.70	68	0.76	3716

Column: Waters XBridge C18, 19 × 150 mm, 5µm; w/ guard column Atlantis T3 19 × 50 mm
Gradient: 85% - 100% Acetonitrile/ pH 9.8 Aqueous Ammonium Hydroxide
Flow Rate: 20 mL/min over 3.5 minutes

ID SJ-2-295 File SJ170202WT005b Date 06-Feb-2017 Time 12:16:35 Description CCT138023

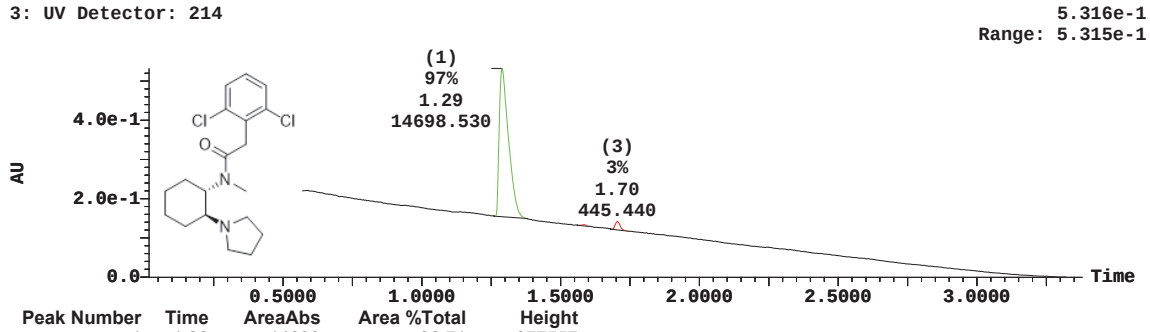

Peak Number	Time	AreaAbs	Area %Total	Height
1	1.29	14699	96.71	377557
2	1.58	54	0.35	2931
3	1.70	445	2.93	21153

Column: Waters XBridge C18, 19 × 150 mm, 5µm; w/ guard column Atlantis T3 19 × 50 mm
Gradient: 85% - 100% Acetonitrile/ pH 9.8 Aqueous Ammonium Hydroxide
Flow Rate: 20 mL/min over 3.5 minutes

ID SJ-1-149 File SJ160212WT006 Date 18-Feb-2016 Time 6::7::5 Description SMDF103723

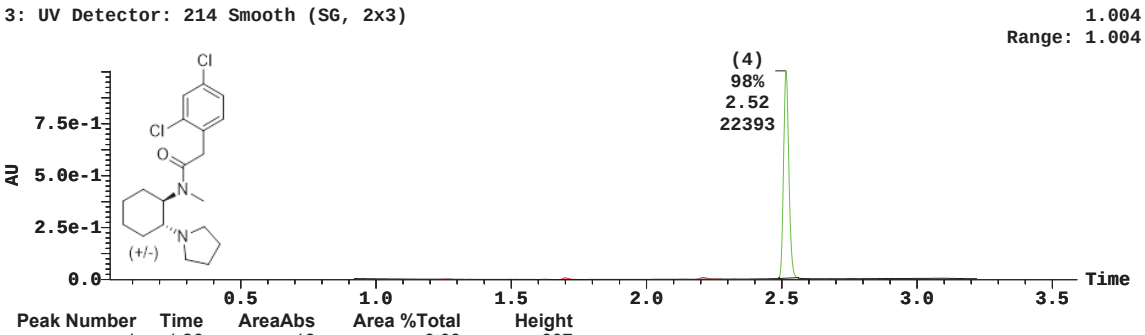

Peak Number	Time	AreaAbs	Area %Total	Height
1	1.26	18	0.08	907
2	1.70	199	0.87	7928
3	2.21	267	1.17	7699
4	2.52	22393	97.75	996923
5	2.68	31	0.14	1689

Column: Waters XBridge C18, 19 × 150 mm, 5µm; w/ guard column Atlantis T3 19 × 50 mm
Gradient: 70% - 90% Acetonitrile/ pH 9.8 Aqueous Ammonium Hydroxide
Flow Rate: 20 mL/min over 3.5 minutes

ID SJ-1-151 File SJ160212WT007 Date 18-Feb-2016 Time 6::1::9 Description SMDF103716

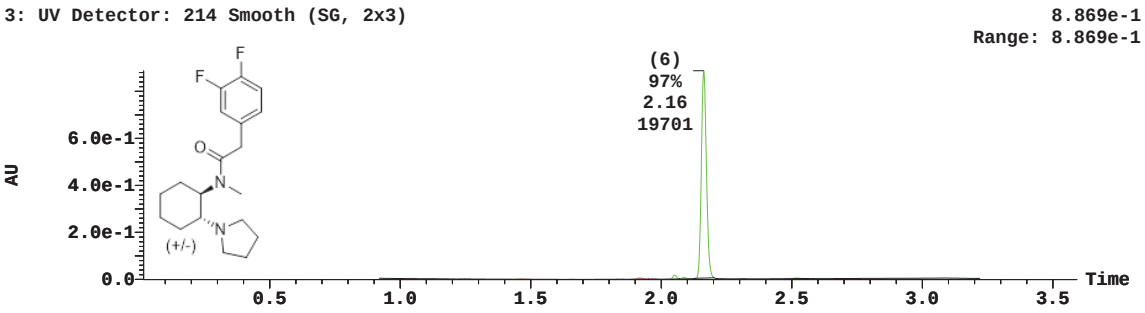

Peak Number	Time	AreaAbs	Area %Total	Height
1	1.46	23	0.12	1067
2	1.92	129	0.64	4529
3	1.96	11	0.06	701
4	2.05	274	1.35	16637
5	2.09	101	0.50	5416
6	2.16	19701	97.01	881318
7	2.52	69	0.34	2521

Column: Waters XBridge C18, 19 × 150 mm, 5µm; w/ guard column Atlantis T3 19 × 50 mm
Gradient: 60% - 80% Acetonitrile/ pH 9.8 Aqueous Ammonium Hydroxide
Flow Rate: 20 mL/min over 3.5 minutes

ID SJ-1-279 File SJ160520WT001 Date 20-May-2016 Time 3::3::4 Description MDF088110

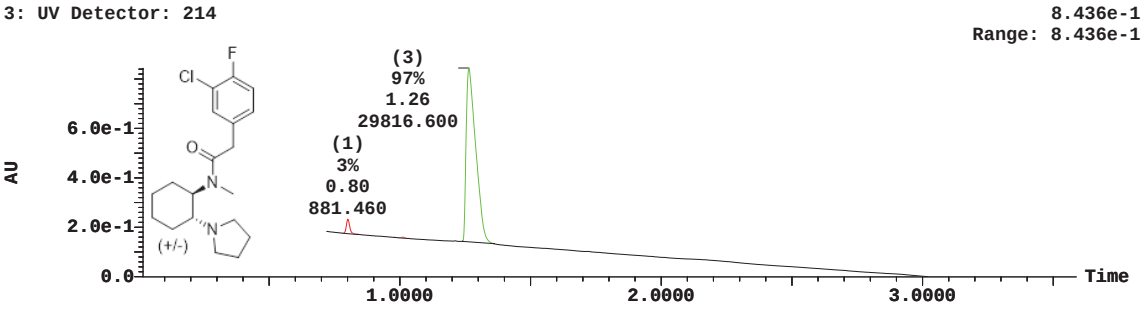

Peak Number	Time	AreaAbs	Area %Total	Height
1	0.80	881	2.87	58313
2	1.01	49	0.16	3270
3	1.26	29817	96.97	702662

Column: Waters XBridge C18, 19 × 150 mm, 5µm; w/ guard column Atlantis T3 19 × 50 mm
Gradient: 85% - 100% Acetonitrile/ pH 9.8 Aqueous Ammonium Hydroxide
Flow Rate: 20 mL/min over 3.5 minutes

ID SJ-1-281 File SJ160512WT002 Date 12-May-2016 Time 4::3::0 Description MDF088066

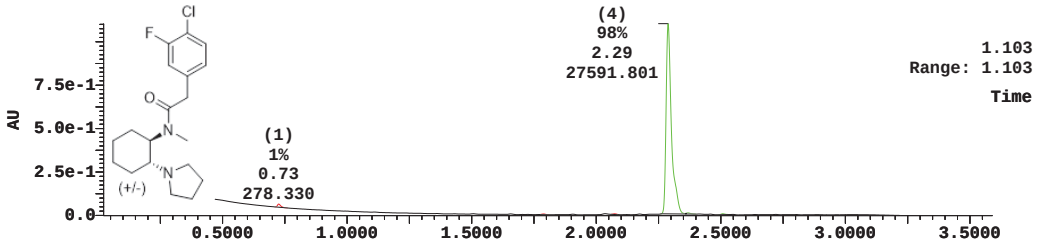

Peak Number	Time	AreaAbs	Area %Total	Height
1	0.72	278	0.99	18274
2	1.79	70	0.25	3709
3	2.07	68	0.24	3700
4	2.29	27592	97.70	1094099
5	2.37	139	0.49	6623
6	2.51	94	0.33	5167

Column: Waters XBridge C18, 19 × 150 mm, 5µm; w/ guard column Atlantis T3 19 × 50 mm
Gradient: 85% - 100% Acetonitrile/ pH 9.8 Aqueous Ammonium Hydroxide
Flow Rate: 20 mL/min over 3.5 minutes

ID SJ-1-165 File SJ160212WT021 Date 18-Feb-2016 Time 7::2::3 Description MDF087634

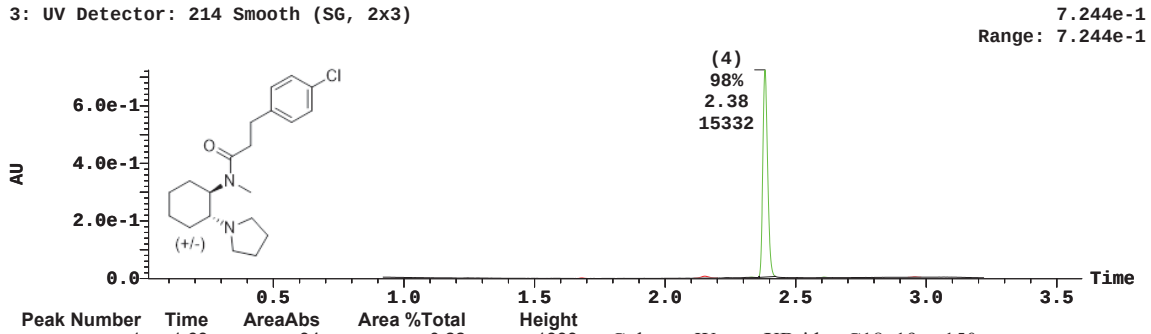

Peak Number	Time	AreaAbs	Area %Total	Height
1	1.68	34	0.22	1833
2	2.15	234	1.49	6669
3	2.33	19	0.12	1273
4	2.38	15332	97.74	719418
5	2.61	34	0.22	1811
6	2.96	35	0.22	1887

Column: Waters XBridge C18, 19 × 150 mm, 5µm; w/ guard column Atlantis T3 19 × 50 mm
Gradient: 65% - 85% Acetonitrile/ pH 9.8 Aqueous Ammonium Hydroxide
Flow Rate: 20 mL/min over 3.5 minutes

ID SJ-1-197 File SJ160307WT017 Date 07-Mar-2016 Time 1::6::4 Description MDF087809

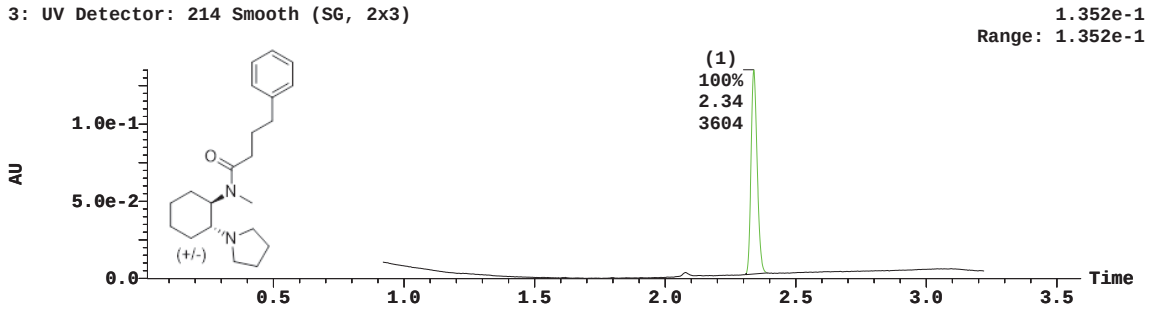

Peak Number	Time	AreaAbs	Area %Total	Height
1	2.34	3604	100.00	132291

Column: Waters XBridge C18, 19 × 150 mm, 5µm; w/ guard column Atlantis T3 19 × 50 mm
Gradient: 65% - 85% Acetonitrile/ pH 9.8 Aqueous Ammonium Hydroxide
Flow Rate: 20 mL/min over 3.5 minutes

ID SJ-1-163 File SJ160212WT019 Date 18-Feb-2016 Time 7::3::5 Description MDF087629

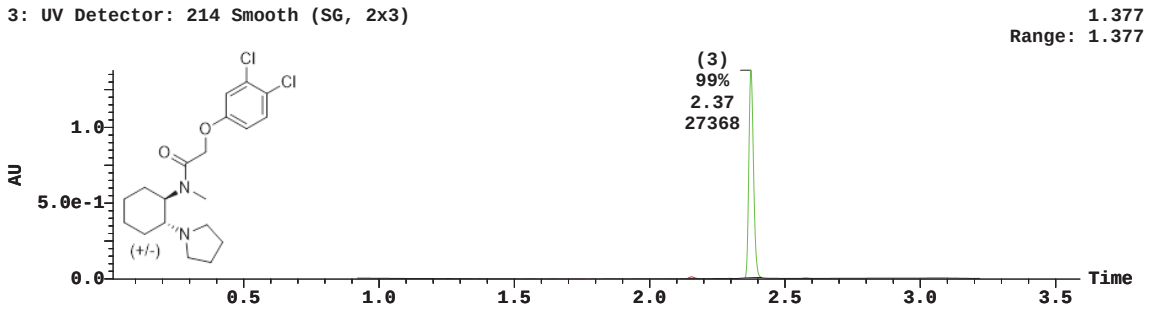

Peak Number	Time	AreaAbs	Area %Total	Height
1	1.74	38	0.14	1803
2	2.15	254	0.92	11788
3	2.37	27368	98.68	1369425
4	2.58	73	0.26	4049

Column: Waters XBridge C18, 19 × 150 mm, 5µm; w/ guard column Atlantis T3 19 × 50 mm
Gradient: 65% - 85% Acetonitrile/ pH 9.8 Aqueous Ammonium Hydroxide
Flow Rate: 20 mL/min over 3.5 minutes

ID SJ-3-29 File SJ170210WT001 Date 10-Feb-2017 Time 13:59:42 Description CCT137836

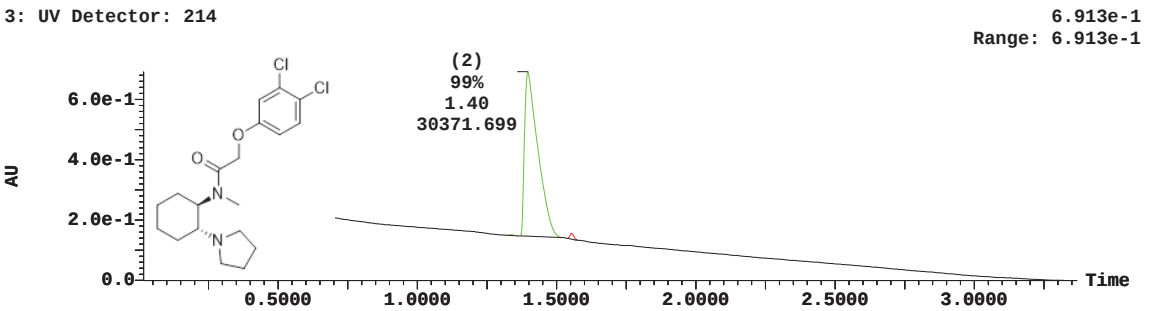

Peak Number	Time	AreaAbs	Area %Total	Height
1	1.34	57	0.18	2800
2	1.40	30372	98.81	545028
3	1.55	308	1.00	19056

Column: Waters XBridge C18, 19 × 150 mm, 5µm; w/ guard column Atlantis T3 19 × 50 mm
Gradient: 85% - 100% Acetonitrile/ pH 9.8 Aqueous Ammonium Hydroxide
Flow Rate: 20 mL/min over 3.5 minutes

ID SJ-3-31 File SJ170210WT002 Date 10-Feb-2017 Time 14:04:06 Description CCT137883

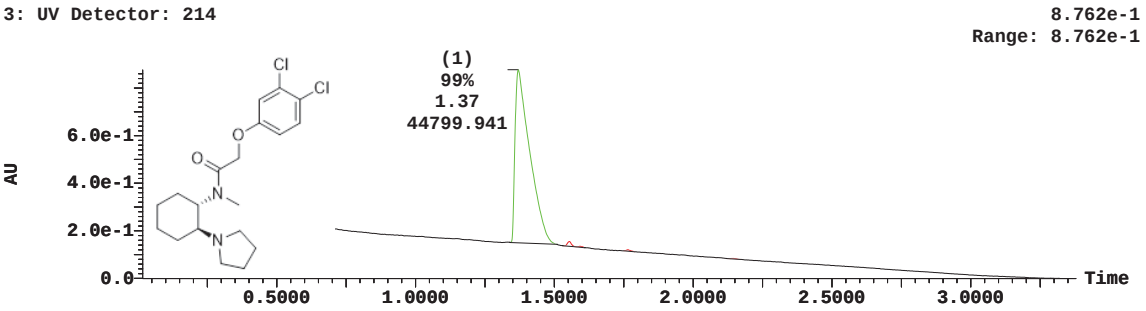

Peak Number	Time	AreaAbs	Area %Total	Height
1	1.37	44800	98.74	726896
2	1.55	334	0.74	20097
3	1.59	67	0.15	4068
4	1.76	116	0.26	6222
5	2.14	55	0.12	2514

Column: Waters XBridge C18, 19 × 150 mm, 5µm; w/ guard column Atlantis T3 19 × 50 mm
Gradient: 85% - 100% Acetonitrile/ pH 9.8 Aqueous Ammonium Hydroxide
Flow Rate: 20 mL/min over 3.5 minutes

ID SJ-1-199 File SJ160307WT019 Date 07-Mar-2016 Time 1::4::5 Description MDF087806

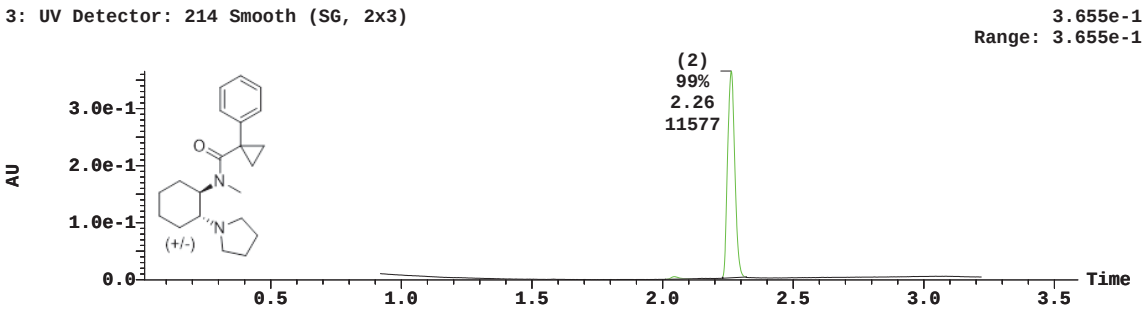

Peak Number	Time	AreaAbs	Area %Total	Height
1	2.05	161	1.37	4373
2	2.26	11577	98.63	362114

Column: Waters XBridge C18, 19 × 150 mm, 5µm; w/ guard column Atlantis T3 19 × 50 mm
Gradient: 60% - 80% Acetonitrile/ pH 9.8 Aqueous Ammonium Hydroxide
Flow Rate: 20 mL/min over 3.5 minutes

ID SJ-1-201-160308 File SJ160308WT002b Date 09-Mar-2016 Time 10:14:30 Description SMDF103745

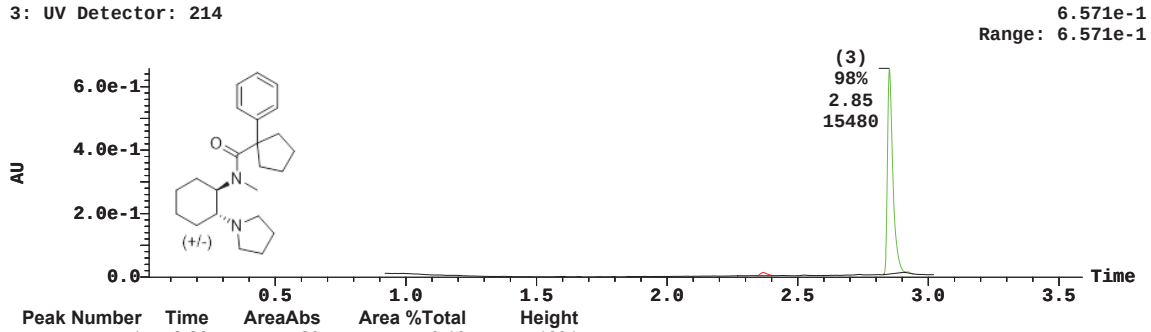

Peak Number	Time	AreaAbs	Area %Total	Height
1	2.28	29	0.18	1631
2	2.37	310	1.95	9754
3	2.85	15480	97.59	647389
4	2.92	44	0.28	2857

Column: Waters XBridge C18, 19 × 150 mm, 5µm; w/ guard column Atlantis T3 19 × 50 mm
Gradient: 80% - 100% Acetonitrile/ pH 9.8 Aqueous Ammonium Hydroxide
Flow Rate: 20 mL/min over 3.5 minutes

ID SJ-2-165 File SJ161021WT006 Date 21-Oct-2016 Time 16:43:51 Description MDF080079

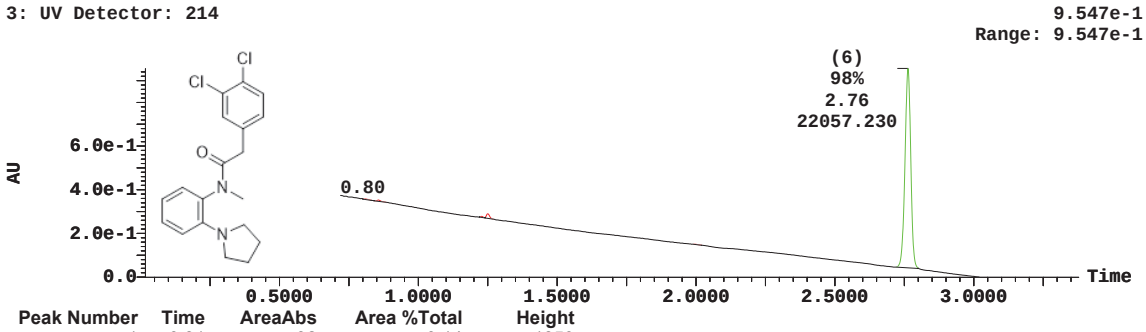

Peak Number	Time	AreaAbs	Area %Total	Height
1	0.81	32	0.14	1859
2	0.86	106	0.47	6141
3	1.23	63	0.28	5193
4	1.25	286	1.27	20810
5	1.99	32	0.14	711
6	2.76	22057	97.70	912242

Column: Waters XBridge C18, 19 × 150 mm, 5µm; w/ guard column Atlantis T3 19 × 50 mm
Gradient: 85% - 100% Acetonitrile/ pH 9.8 Aqueous Ammonium Hydroxide
Flow Rate: 20 mL/min over 3.5 minutes

ID SJ-2-75 File SJ160712WT008 Date 12-Jul-2016 Time 11:12:35 Description MDF088688

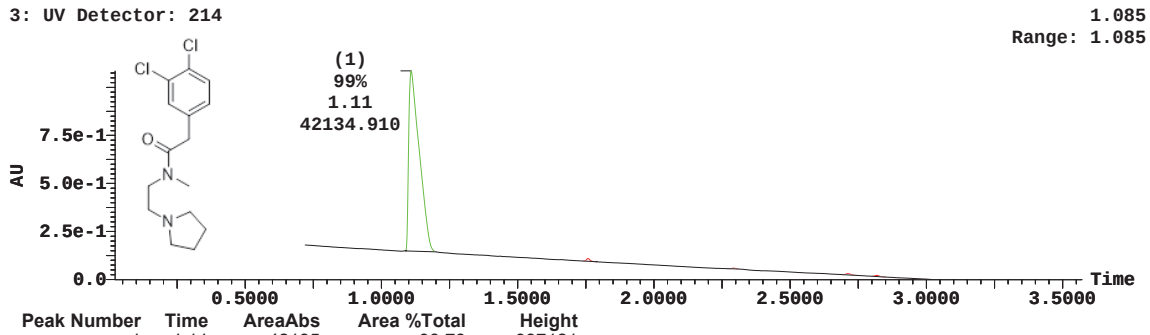

Peak Number	Time	AreaAbs	Area %Total	Height
1	1.11	42135	98.78	937121
3	1.76	216	0.51	14457
4	2.29	67	0.16	3837
5	2.71	131	0.31	6371
6	2.82	105	0.25	6333

Column: Waters XBridge C18, 19 × 150 mm, 5µm; w/ guard column Atlantis T3 19 × 50 mm
Gradient: 85% - 100% Acetonitrile/ pH 9.8 Aqueous Ammonium Hydroxide
Flow Rate: 20 mL/min over 3.5 minutes

ID SJ-2-63 File SJ161003WT009 Date 04-Oct-2016 Time 12:21:12 Description CCT133723

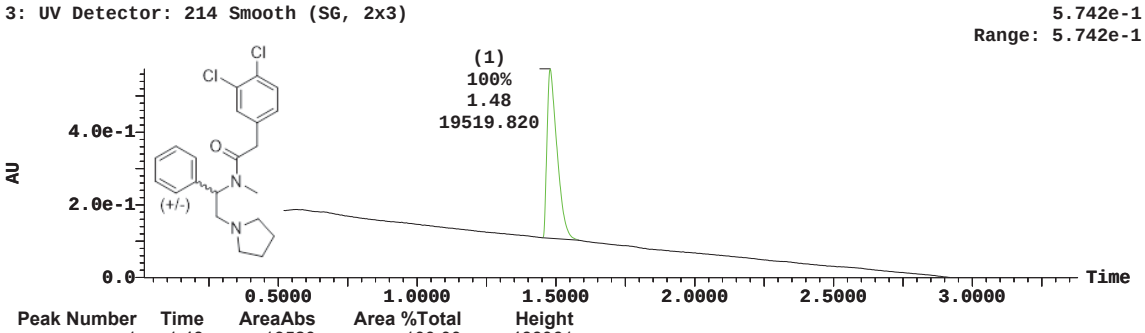

Peak Number	Time	AreaAbs	Area %Total	Height
1	1.48	19520	100.00	466061

Column: Waters XBridge C18, 19 × 150 mm, 5µm; w/ guard column Atlantis T3 19 × 50 mm
Gradient: 85% - 100% Acetonitrile/ pH 9.8 Aqueous Ammonium Hydroxide
Flow Rate: 20 mL/min over 3.5 minutes

ID SJ-2-159 File SJ161011WT012 Date 19-Oct-2016 Time 16:43:06 Description CCT133712

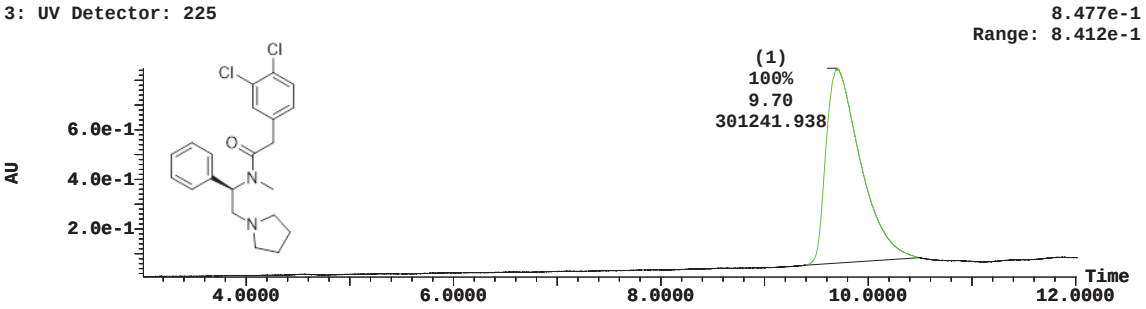

Peak Number	Time	AreaAbs	Area %Total	Height	Mass Found
1	9.70	301242	100.00	785412	390.13

Column: Waters XBridge C18, 19 × 150 mm, 5µm; w/ guard column Atlantis T3 19 × 50 mm
Gradient: 85% - 100% Acetonitrile/ pH 9.8 Aqueous Ammonium Hydroxide
Flow Rate: 20 mL/min over 3.5 minutes

ID SJ-2-161 File SJ161011WT013 Date 19-Oct-2016 Time 16:58:49 Description CCT137650

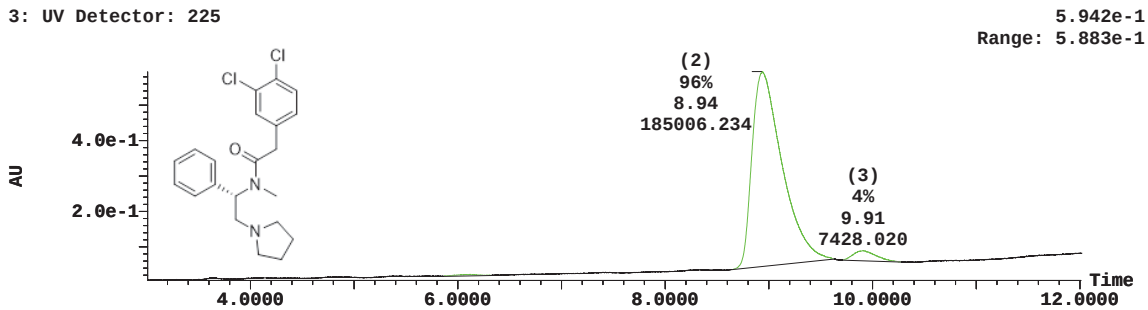

Peak Number	Time	AreaAbs	Area %Total	Height	Mass Found
1	6.12	956	0.49	4336	390.13
2	8.94	185006	95.66	549593	390.13
3	9.91	7428	3.84	29050	390.13

Column: Waters XBridge C18, 19 × 150 mm, 5µm; w/ guard column Atlantis T3 19 × 50 mm
Gradient: 85% - 100% Acetonitrile/ pH 9.8 Aqueous Ammonium Hydroxide
Flow Rate: 20 mL/min over 3.5 minutes

ID SJ-3-77 File SJ170301WT003 Date 02-Mar-2017 Time 11:20:40 Description CCT138371

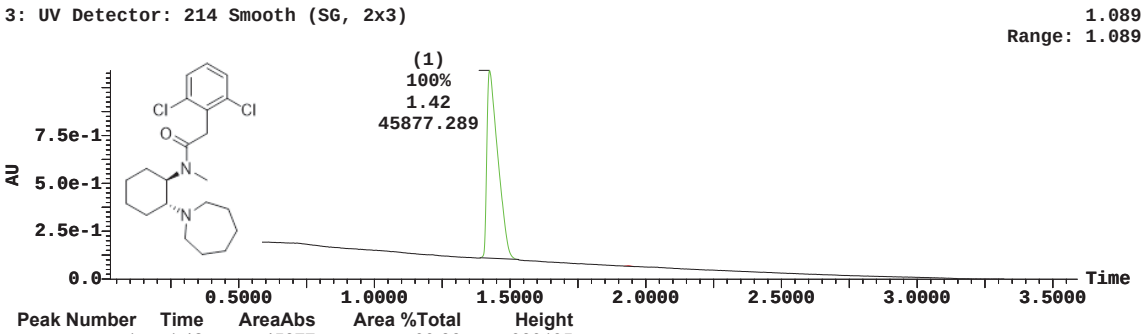

Peak Number	Time	AreaAbs	Area %Total	Height
1	1.42	45877	99.86	980195
2	1.94	66	0.14	3535

Column: Waters XBridge C18, 19 × 150 mm, 5µm; w/ guard column Atlantis T3 19 × 50 mm
Gradient: 85% - 100% Acetonitrile/ pH 9.8 Aqueous Ammonium Hydroxide
Flow Rate: 20 mL/min over 3.5 minutes

ID SJ-3-79 File SJ170301WT004 Date 02-Mar-2017 Time 11:25:00 Description CCT138370

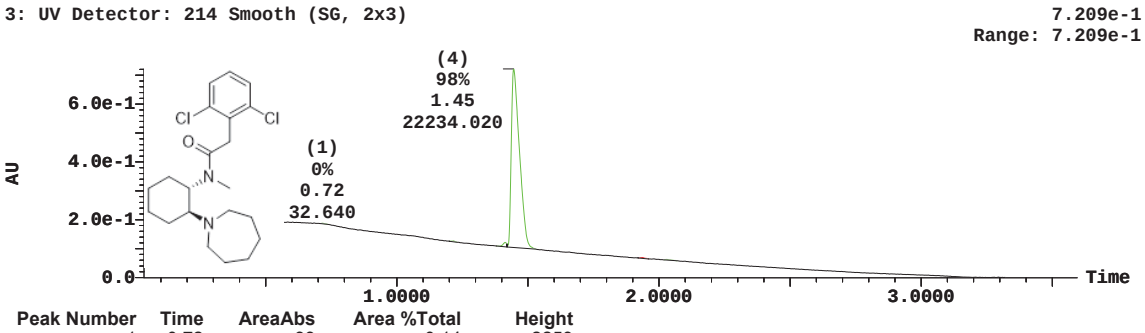

Peak Number	Time	AreaAbs	Area %Total	Height
1	0.72	33	0.14	2259
2	1.22	38	0.17	2887
3	1.41	265	1.17	14932
4	1.45	22234	98.02	616609
5	1.94	59	0.26	2946
6	2.03	55	0.24	2425

Column: Waters XBridge C18, 19 × 150 mm, 5µm; w/ guard column Atlantis T3 19 × 50 mm
Gradient: 85% - 100% Acetonitrile/ pH 9.8 Aqueous Ammonium Hydroxide
Flow Rate: 20 mL/min over 3.5 minutes

ID SJ-3-81 File SJ170301WT005 Date 02-Mar-2017 Time 11:29:19 Description CCT138365

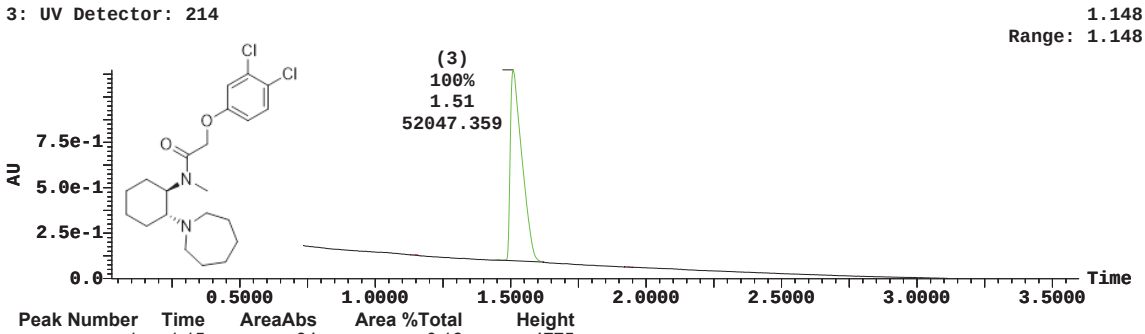

Peak Number	Time	AreaAbs	Area %Total	Height
1	1.15	84	0.16	4775
2	1.46	79	0.15	4501
3	1.51	52047	99.57	1049779
4	1.93	61	0.12	2933

Column: Waters XBridge C18, 19 × 150 mm, 5µm; w/ guard column Atlantis T3 19 × 50 mm
Gradient: 85% - 100% Acetonitrile/ pH 9.8 Aqueous Ammonium Hydroxide
Flow Rate: 20 mL/min over 3.5 minutes

ID SJ-3-83 File SJ170301WT006 Date 02-Mar-2017 Time 11:33:35 Description CCT138553

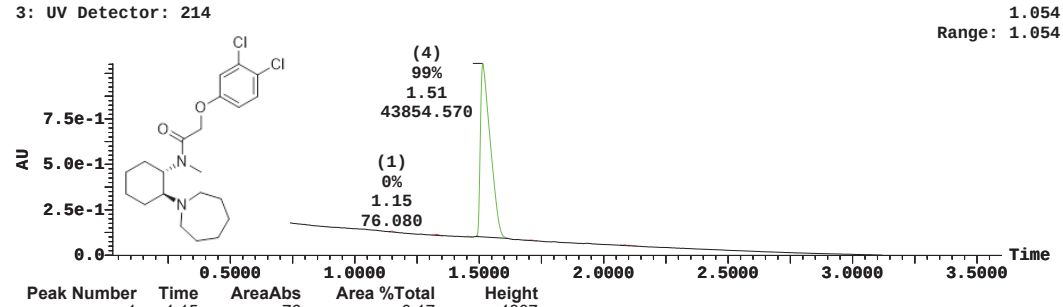

Peak Number	Time	AreaAbs	Area %Total	Height
1	1.15	76	0.17	4807
2	1.33	91	0.21	5566
3	1.45	56	0.13	3081
4	1.51	43855	99.12	953568
5	1.70	59	0.13	2408
6	2.09	60	0.14	3407
7	2.11	47	0.11	3027

Column: Waters XBridge C18, 19 × 150 mm, 5µm; w/ guard column Atlantis T3 19 × 50 mm
Gradient: 85% - 100% Acetonitrile/ pH 9.8 Aqueous Ammonium Hydroxide
Flow Rate: 20 mL/min over 3.5 minutes